DEPOSITIONAL ENVIRONMENTS AND DIAGENESIS OF THE DEVONIAN DAWSON BAY FORMATION IN SASKATCHEWAN AND NORTHWESTEN MANITOBA

A Thesis

Submitted to the Faculty of Graduate Studies and Research

in Partial Fulfilment of the Requirements for the Degree

of

Doctor of Philosophy

in the

Department of Geological Sciences

University of Saskatchewan

Saskatoon

by

Gu Chenggao

Spring, 1998

© Copyright Gu Chenggao, 1998. All rights reserved.

National Library of Canada
Bibliothèque nationale du Canada

Acquisitions and Bibliographic Services
Acquisitions et services bibliographiques

395 Wellington Street
Ottawa ON K1A 0N4
Canada

395, rue Wellington
Ottawa ON K1A 0N4
Canada

Your file Votre référence

Our file Notre référence

The author has granted a non-exclusive licence allowing the National Library of Canada to reproduce, loan, distribute or sell copies of this thesis in microform, paper or electronic formats.

L'auteur a accordé une licence non exclusive permettant à la Bibliothèque nationale du Canada de reproduire, prêter, distribuer ou vendre des copies de cette thèse sous la forme de microfiche/film, de reproduction sur papier ou sur format électronique.

The author retains ownership of the copyright in this thesis. Neither the thesis nor substantial extracts from it may be printed or otherwise reproduced without the author's permission.

L'auteur conserve la propriété du droit d'auteur qui protège cette thèse. Ni la thèse ni des extraits substantiels de celle-ci ne doivent être imprimés ou autrement reproduits sans son autorisation.

0-612-27411-X

Canada

The author has agreed that the Library, University of Saskatchewan, may make this thesis freely available for inspection. Moreover, the author has agreed that permission for extensive copying of this thesis for scholarly purposes may be granted by the professor or professors who supervised the thesis work recorded herein or, in their absence, by the head of the Department or the Dean of the College of Graduate Studies in which this thesis work was done. It is understood that due recognition will be given to the author of this thesis and to the University of Saskatchewan in any use of the material in this thesis. Copying or publication or any other use of the thesis for financial gain without approval by the University of Saskatchewan and the author's written permission is prohibited.

Requests for permission to copy or to make any use of material in this thesis in whole or in part should be addressed to:

Head of the Department of Geological Sciences
University of Saskatchewan
Saskatoon, Saskatchewan
S7N 5E2

ABSTRACT

The Devonian Dawson Bay Formation has been divided into the Second Red Bed, Burr, Neely and Hubbard Evaporite members from base to top. The purpose of this thesis is (1) to describe the sedimentary rocks of the formation from Saskatchewan and northwestern Manitoba, (2) to interpret the depositional environments and diagenesis, and (3) to discuss the implications of the new results.

The Second Red Bed Member (SRBM) comprises mudstone and dolostone. This study shows that the mudstone was deposited in environments that ranged from saline- and dry-mudflat to distal alluvial-eolian plain, and that the dolostone formed in a Coorong-like environment. New evidence indicates that the SRBM was affected by pedogenesis, with the paleosol better developed in central Saskatchewan than in southeastern Saskatchewan. This suggests that the paleorelief in the former part of the basin was higher than in the latter, and that the marine waters came from the southeast. This conclusion not only has a scientific significance in reconstructing the paleogeography of the Williston Basin, but also sheds light on the future exploration of petroleum and other economic minerals in the basin.

Three paleokarst horizons have been recognized in the contact zone between the SRBM and the Burr Member. The presence of the paleokarsts indicates that before the Williston Basin was completely flooded by seawater during early Burr time, two minor marine transgressions took place in the basin.

New evidence shows that the lower Burr Member was deposited in an oxygen-restricted environment. In central Saskatchewan, parts of the lower Burr Member contain fine laminations, but the equivalent units in southeastern Saskatchewan lack these laminations. This indicates that the environment in central Saskatchewan was more oxygen-restricted. Thus, from central to southeastern Saskatchewan, the environment became less oxygen-restricted with increasing water depth. This contradicts the Rhoads-Morse-Byers model, which predicts that oxygen decreases with increasing water depth.

In southeastern Saskatchewan, the upper Burr Member consists mainly of wackestone and lime mudstone, with a few thin packstone and grainstone interbeds. This reflects a low energy, relatively deep water environment. In contrast, the proportion of packstone and grainstone increases significantly in the upper Burr Member of central Saskatchewan and

northwestern Manitoba. This suggests that the depositional environments in those regions had higher energy and shallower water conditions.

From base to top, the depositional environment of the Neely Member changed from relatively deep, offshore settings, through higher energy, shallower water conditions represented by domical stromatoporoids, to intertidal and supratidal conditions.

The Hubbard Evaporite Member was deposited in salt pan to saline mudflat environment, and the overlying First Red Bed formed in environments that ranged from saline mudflat, dry mudflat to distal floodplain. New evidence also shows that no significant sedimentary break is present between the Hubbard Evaporite Member and the First Red Bed, and that they belong to a single upward-shallowing succession.

ACKNOWLEDGEMENTS

First of all, I would like to express my sincere gratitude to my supervisor Robin W. Renaut for his guidance, his encouragement, his patience and his financial assistance. Without all these, this study would have been impossible.

I would like also to express my appreciation to my committee members, Dr. B. R. Pratt, Dr. J. F. Basinger, Dr. K. Ansdell, Dr. D. Stead and Dr. D. De Boer for their kindness and guidance. Special thanks are extended to the late Prof. H. Hendry, former Chairman of Advisory Committee.

Many thanks go to Terry Danyluk, the Saskatchewan Potash Producers Association, and Dr. D. Paterson and Kim Kreis, for their help and cooperation throughout the course of the study.

Financial support was partially provided by the Saskatchewan Potash Producers Association and a University of Saskatchewan graduate scholarship, which is gratefully acknowledged.

TABLE OF CONTENTS

LIST OF TABLE

LIST OF FIGURES

LIST OF PLATES

CHAPTER 1

INTRODUCTION

1.1 Introduction and Aims

The Devonian Dawson Bay Formation has a widespread subsurface distribution extending from eastern Alberta, across southern Saskatchewan to western Manitoba, where it crops out along the western shores of Lake Winnipegosis and Lake Manitoba. A structural contour map of the top of the Dawson Bay Formation in Saskatchewan shows a gentle, regional dip of approximately 4 m/km to the south and southwest, with a strike in a northwesterly direction. It reaches a maximum thickness of more than 60 meters in southeastern Saskatchewan, with the thickness gradually thinning towards the northwestern portion of southern Saskatchewan and wedging out in eastern Alberta. In the United States, the formation is present in the subsurface of Montana and North Dakota (Fig. 1-1).

The Dawson Bay Formation is composed dominantly of shallow marine carbonate rocks, with subsidiary evaporites, mudstones and sandstones. The formation is directly underlain by the Prairie Evaporite Formation, which contains one of the richest potash deposits in the world. Although the formation was first described more than 100 years ago, it has been generally overlooked. However, recent flooding of several potash mines by brines flowing through and from the Dawson Bay Formation, and oil discoveries from the formation in North Dakota and Montana, have aroused considerable interest.

The purpose of this thesis is (1) to describe the sedimentary rocks of the Dawson Bay Formation, (2) to interpret the depositional environments and diagenesis, with emphasis on pedogenesis and karstification, and (3) to discuss the implications of the new results. A better understanding of the formation will not only have scientific significance but also

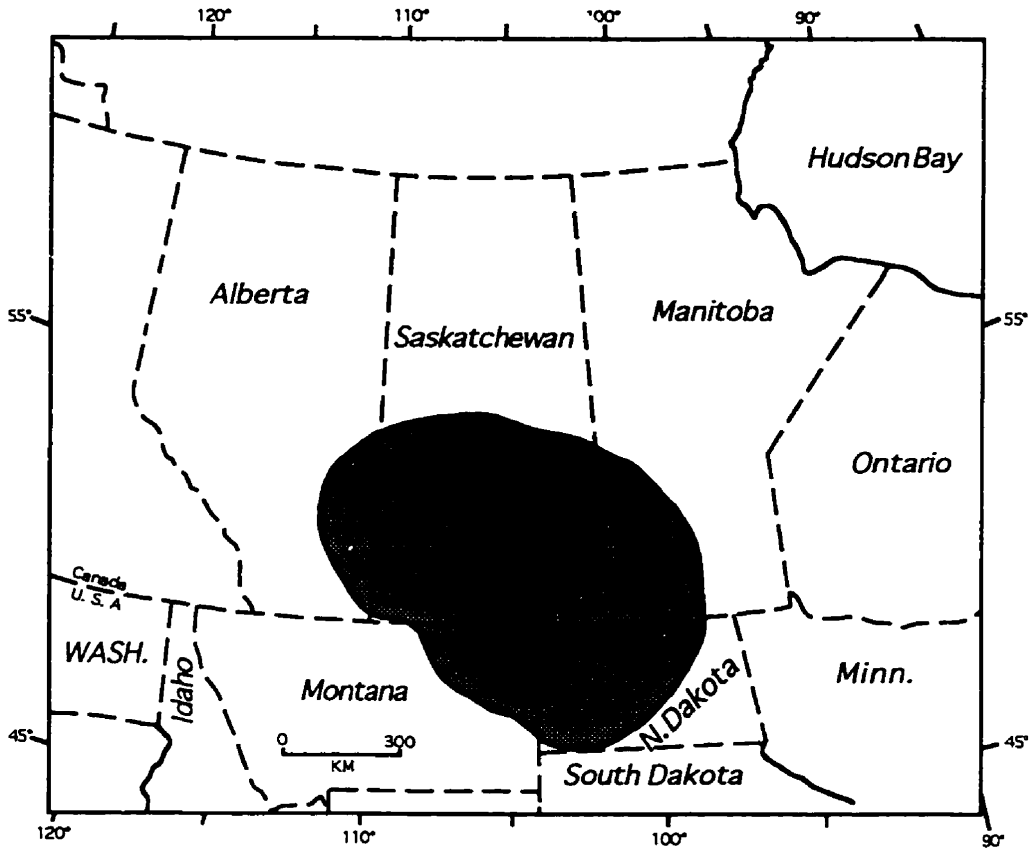

Fig. 1-1. Map showing the Williston Basin and extent of the Dawson Bay Formation (modified after Braun and Mathison, 1986).

shed light on the future petroleum exploration and development of potash in the Williston Basin.

1.2 Study Area

This project covers almost the entire subsurface distribution of the Dawson Bay Formation in Saskatchewan (except the southwest portion of the Province) (Fig. 1-2). Additionally, field work has been carried out in the outcrop belt of the formation in western Manitoba.

1.3 Previous Work

Voluminous literature has been published detailing various geological aspects of the Dawson Bay Formation. It has contributed information that has significantly increased our understanding of the formation. However, most published papers dealt with the geology of the formation in the Canadian portion of the Williston Basin and only few papers were concerned with the geology of the formation in the United States portion of the Williston Basin.

In Canada, the Dawson Bay Formation was probably first studied by Prof. H. Y. Hinde as early as 1858 (Kindle, 1914). He collected fossils on Snake Island near the southern end of Lake Winnipegosis and determined the presence of Devonian rocks in Manitoba (Kindle, 1914). However, no detailed research work was carried out until the late nineteenth century. Whiteaves (1891), Tyrrell (1892), and Kindle (1914) were among early geologists who carried out research work on the Dawson Bay Formation during that period. In 1890, Whiteaves (1891) described brachiopod species of *Stringocephalus burtini* from the shore of Dawson Bay in western Manitoba and assigned a Middle Devonian age for the rocks containing this species. In the following years, Tyrrell (1892) introduced the term `Manitoban´ for the shales and limestones of Devonian age that overlie the Winnipegosis Formation. The term `Manitoban Formation´, as applied by Tyrrell, includes all of the Devonian strata above the `Winnipegosan Formation´. Kindle (1914) found that the fauna in the lower part of the Manitoban Formation was different from that in the upper part.

After Kindle's work, the Dawson Bay Formation was generally overlooked by geologists until 1950's, when the second surge of interest in the Devonian strata was aroused by the discovery of Paleozoic oil on the large Nesson anticline in the Williston Basin. During this period, several geologists, including Baillie (1951, 1953, 1955), Andrichuk (1951),

Fig. 1-2. Map showing well and potash mine locations of this study.*

(1) 14-19-41-23W3;
(2) 4-18-35-8W3;
(3) 1-2-39-8W3;
(4) 1-18-36-6W3, 6-18-36-6W3;
(5) 10-7-32-5W3;
(6) 9-22-23-6W3;
(7) 3-30-37-2W3;
(8) 5-22A-34-1W3, 9-33-34-1W3, 41-1-12-34-1W3;
(9) 16-21-34-27W2;
(10) 3-27-38-27W2;
(11) 4-19-48-24W2;
(12) 13-11-33-23W2;
(13) 5-18-34-25W2;
(14) 15-36-32-29W2;
(15) 8-20-33-20W2;
(16) 13-21-29-20W2;
(17) 1-28-24-20W2;
(18) 09-22-23-06W2;
(19) 7-10-25-6W2;
(20) 4-10-24-7W2;
(21) 9-26-22-33W1;
(22) 9-14-23-33W1;
(23) 13-12-22-32W1;
(24) 16-11-21-31W1, 01-02-021-31W1, 16-4-21-31W1;
(25) 13-34-22-31W1, 4-2-22-31W1;
(26) 8-14-20-31W1;
(27) 8-14-20-30W1, 14-32-20-30W1, 11-2-20-30W1, 4-25-20-30W1, 10-32-20-30W1;
(28) 9-14-19-30W1;
(29) 09-24-21-30W1, 4-2-21-30W1;
(30) 16-29-22-30W1, 13-6-22-30W1;
(31) 2-5-52-6W2;
(32) 8-3-40-14W3;
(33) 1-27-31-16W2;
(34) 14-27-5-14W2;
(35) 8-23-3-24W2;
(36) 8-36-3-29W2;
(37) 12C-20-4-8W2.

* All well locations in this thesis refer to Fig. 1-2.

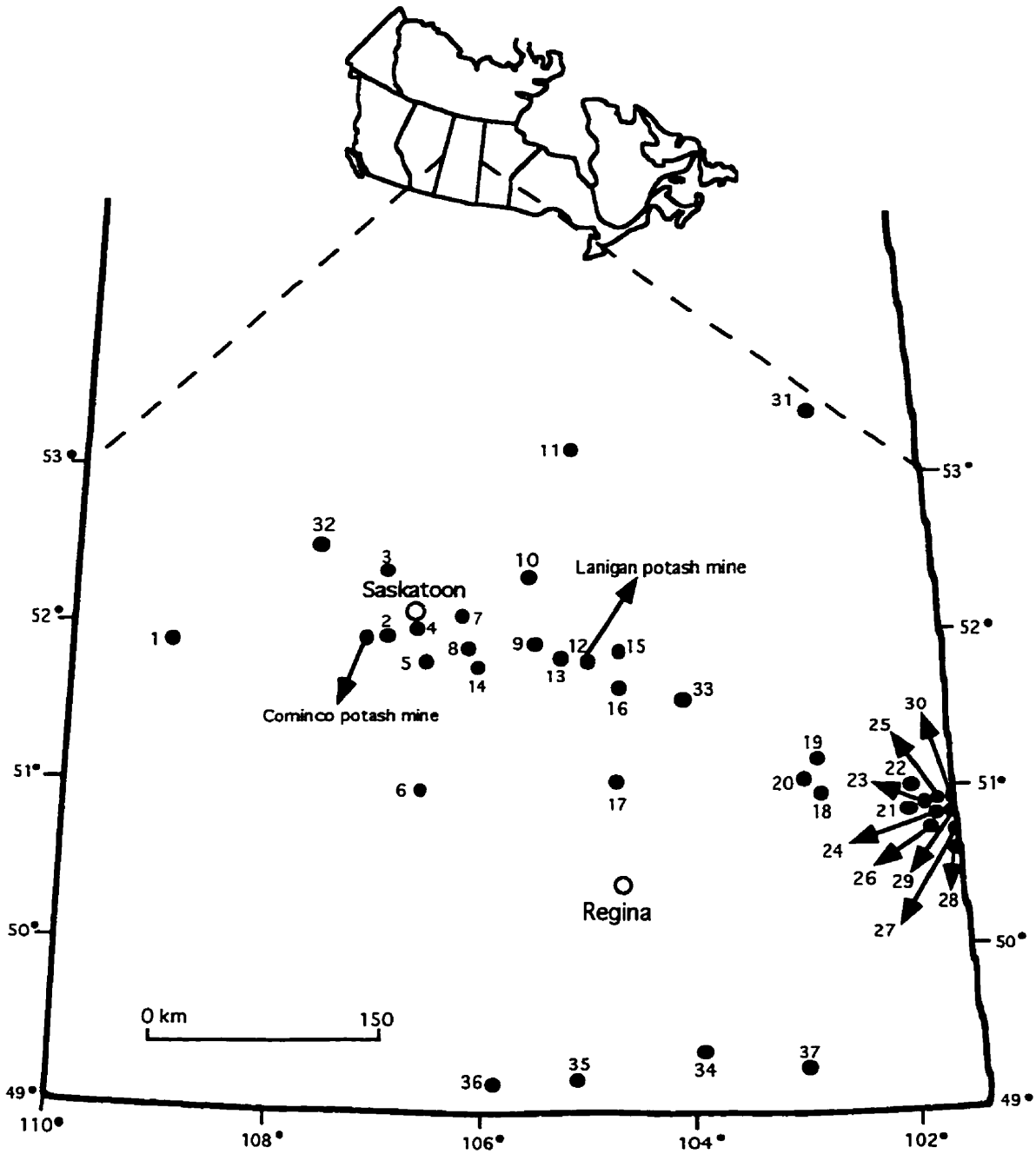
Saskatoon
Regina
Lanigan potash mine
Cominco potash mine
0 km
150
53°
52°
51°
50°
49°
110°
108°
106°
104°
102°

Powley (1951), Crickmay (1954, 1960, 1961), Warren and Stelk (1956), Walker (1957), Edie (1958, 1959) and Lane (1959), contributed much to the understanding of the stratigraphy, sedimentology and paleontology. Baillie (1951) divided the Devonian strata of the Williston Basin into, in ascending order: Elk Point, Manitoba, Saskatchewan and Qu'Appelle groups. He proposed the term `Dawson Bay Formation' for the lowest sequence of strata of the Manitoba group. Initially, Baillie described the Dawson Bay Formation from outcrops along Lake Winnipegosis and then traced the formation into the subsurface of Saskatchewan. He suggested that the formation was deposited in a normal marine environment in the lower part, becoming a restricted evaporitic environment at the top. Walker (1957) described the formation from western Saskatchewan. He found that the Dawson Bay Formation thinned toward the western boundary of Saskatchewan, and in many wells of eastern Alberta it was very thin or absent, which led him to believe that during Dawson Bay times there was a barrier in eastern Alberta. Lane (1959) published a detailed account of the subsurface sequence of the Dawson Bay Formation in southeastern Saskatchewan and divided the formation into six members (Fig. 1-6). Edie (1959) divided the upper part of the Dawson Bay carbonate unit into three facies. Based on the distribution of these facies, he suggested that the open sea lay in the direction of the Canadian shield. However, study of the Dawson Bay Formation was again overlooked in 1960's and early 1970's.

The third surge of interest in the Dawson Bay Formation was aroused by the discovery of oil in the formation in the United States part of the Williston Basin and potash mine flooding in Saskatchewan. During this period, the major research work on the formation was carried out by Dunn (1982a), Norris *et al.* (1982) and Ahlstrom (1992). Other geologists who have contributed to the understanding of the Dawson Bay Formation include Bannatyne (1975), Braun and Mathison (1982, 1986), and Lane (1987). Bannatyne (1975) informally divided the Dawson Bay Formation in western Manitoba into four units. He suggested that the depositional environment of the formation evolved from subaerial to shallow marine, then to deep marine conditions, followed by gradual shallowing and evaporitic conditions. Based on a study of the formation in central Saskatchewan, Dunn (1982a) formally divided the Dawson Bay Formation in the subsurface of Saskatchewan into the Second Red Bed, Burr, Neely, and Hubbard Evaporite members. He also found an unconformity between the Second Red Bed and Burr members. He proposed that the Second Red Bed Member was genetically more closely related to the underlying Prairie Evaporite Formation. Norris *et al.* (1982) gave a detailed description of the Dawson Bay Formation from both surface and subsurface

sections of western Manitoba. They formally divided the Dawson Bay Formation into four members. Ahlstrom (1992) gave a detailed description of the lithology, diagenesis and depositional environments of the Dawson Bay Formation in the Saskatoon area. Braun and Mathison (1982) identified an ostracod fauna in the Burr Member that is typical of the Michigan area, suggesting the incursion of a seaway from the southeast. A similar point of view was shared by Meijer Drees (1994), who suggested that the presence of the Dawson Bay carbonates in southern Saskatchewan points to an additional connection with the sea in the southeast. This viewpoint was further supported by Williams' assumption (1984) that the timespan represented by the Second Red Bed-Watt Mountain Formation hiatus increases from the southern to northern parts of the Elk Point Basin, and that the Dawson Bay sea encroached from the east. However, no previous studies have treated the formation systematically. They have been concerned either with the outcrops in western Manitoba or relatively small areas in the subsurface of the Williston Basin.

In the United States, scientists began to study the Dawson Bay Formation in the 1950's. Sandberg and Hammond (1958) believed that the Dawson Bay Formation was deposited during a single sedimentary cycle and divided the formation into four units. From the base to the top, they are (1) dolomitic siltstone or silty argillaceous dolomite, (2) thin-bedded argillaceous dolomite, (3) thick-bedded crystalline limestone or dolomite, (4) anhydrite or anhydritic limestone and dolomite. They found that the Dawson Bay Formation was conformably overlain by the Souris River Formation in North Dakota where deposition was probably continuous from Middle to Late Devonian, and that the contact between the Dawson Bay and overlying Souris River formations is disconformable in parts of northeastern Montana.

In recent years, the Dawson Bay Formation in North Dakota was studied by Dean (1982), Pound (1985), and Inden and Burke (1995). Dean (1982) found that much of the original depositional texture in the Dawson Bay Formation was obliterated by dolomitization. He suggested that the depositional environment of the formation in that area was a restricted platform exhibiting subtidal to supratidal conditions. He also proposed that the Dawson Bay Formation was deposited during a tectonically stable period. Pound (1985) suggested that the Dawson Bay Formation in North Dakota consisted of a shallowing-upward carbonate sequence, ranging from subtidal carbonate facies to supratidal anhydrite facies. Inden and Burke (1995) discussed the reservoir quality of the Dawson Bay Formation from central and northwestern North Dakota. They suggested that low energy, restricted marine conditions dominated the deposition of the Dawson bay Formation.

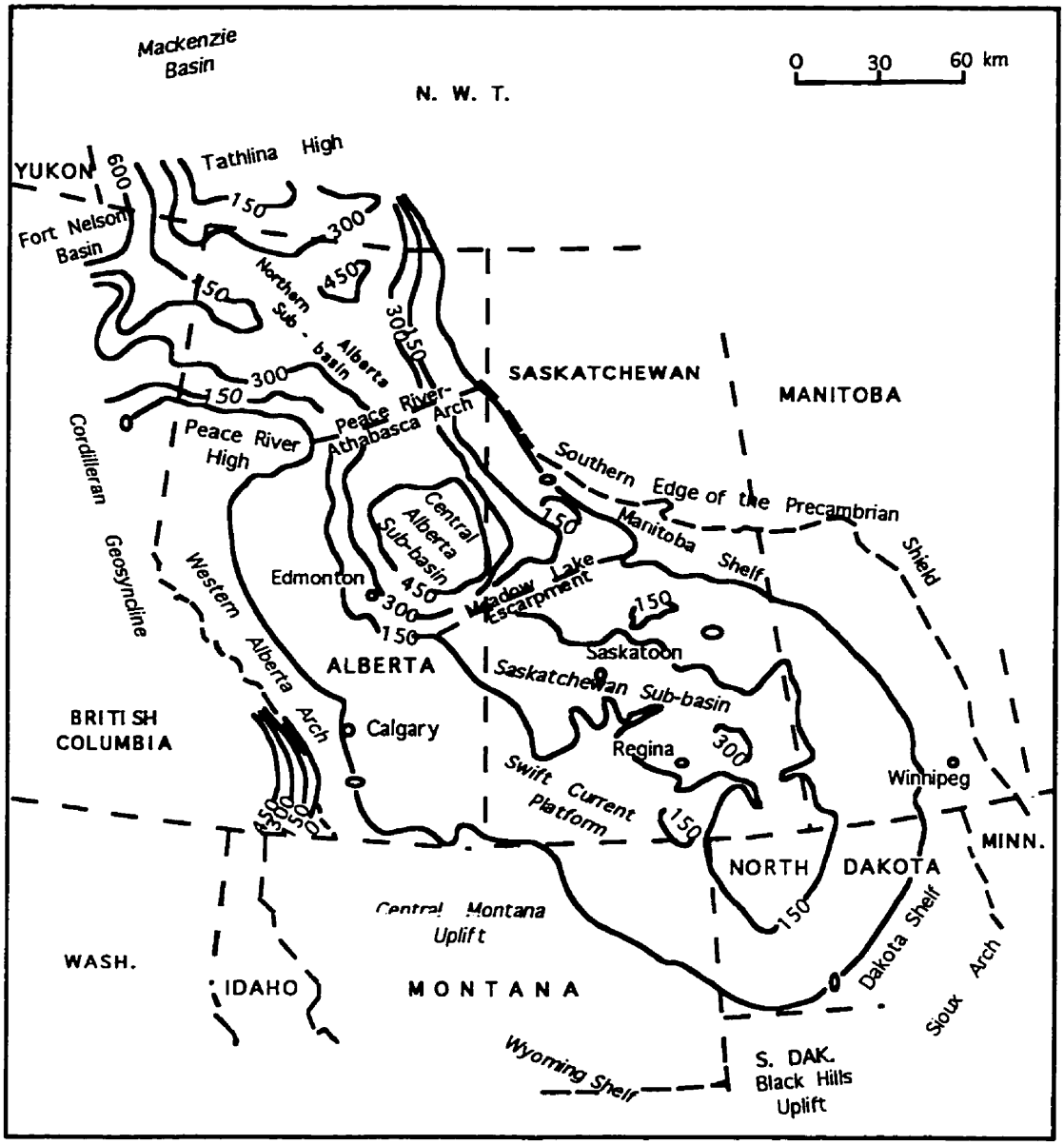

Fig. 1-3. Map showing the Elk Point Basin and isopach map of Elk Point Group (after Holter, 1969).

1.4 Regional Geology and Stratigraphy of the Williston Basin

1.4.1 Regional Geology

The Dawson Bay Formation is preserved as part of the thick sedimentary package deposited in the Williston Basin, which is a subcircular Phanerozoic sedimentary basin roughly 1000 km in diameter and 345,000 km^2 in area (Gerhard *et al.*, 1990). The sediments in the basin have a maximum thickness of 5 km in the U.S.A. and about 3 km in southern Saskatchewan. The main part of the basin lies Saskatchewan, Manitoba, Montana and North Dakota (Fig. 1-1). The southern boundary of the basin is characterized by thinning of the sedimentary section onto the Colorado-Wyoming shear zone. The northeastern boundary is drawn along the edge of the Canadian Shield (Fig. 1-3). The northwestern flank of the basin is marked by the Meadow Lake Escarpment (Aitken, 1993), which extends from the south La Ronge area westward through the Lloydminster region to eastern Alberta. Its east end coincided with a linear shear zone in the Canadian Shield. The Meadow Lake Escarpment may have been a significant topographic structural feature in the northwestern part of the Williston Basin during the early Paleozoic time (Belyea *et al.*, 1970). Isopach and paleogeological mapping by Porter and Fuller (1959) suggested that the escarpment may have been uplifted at the end of the Tippecanoe time. The western boundary of the Williston Basin is marked by Sweetgrass Arch, a northeasterly trending structure extending from Montana through Alberta into Saskatchewan. The basin is separated from the Hudson Platform by the Severn Arch and from the Michigan Basin by the Transcontinental Arch.

The origin of the Williston Basin is not well understood (Ahern and Mrkvicka, 1984; Fowler and Nisbet, 1985). Recent studies (Green *et al.*, 1985) indicate that an assemblage of several small Archean and early Proterozoic plates may constitute the basement of the Williston Basin. The basin began to take shape as a distinct area of increased subsidence during Middle Ordovician time (Carlson and Anderson, 1965; Gerhard *et al.*, 1982; Aitken, 1993) although there also is evidence for increased thickness of Cambrian and Lower Ordovician rocks in the basin center (Peterson and MacCary, 1987). Sedimentation in the basin was relatively continuous through Phanerozoic time, with carbonate deposition dominating the Paleozoic, and clastics dominating the Mesozoic and Cenozoic eras.

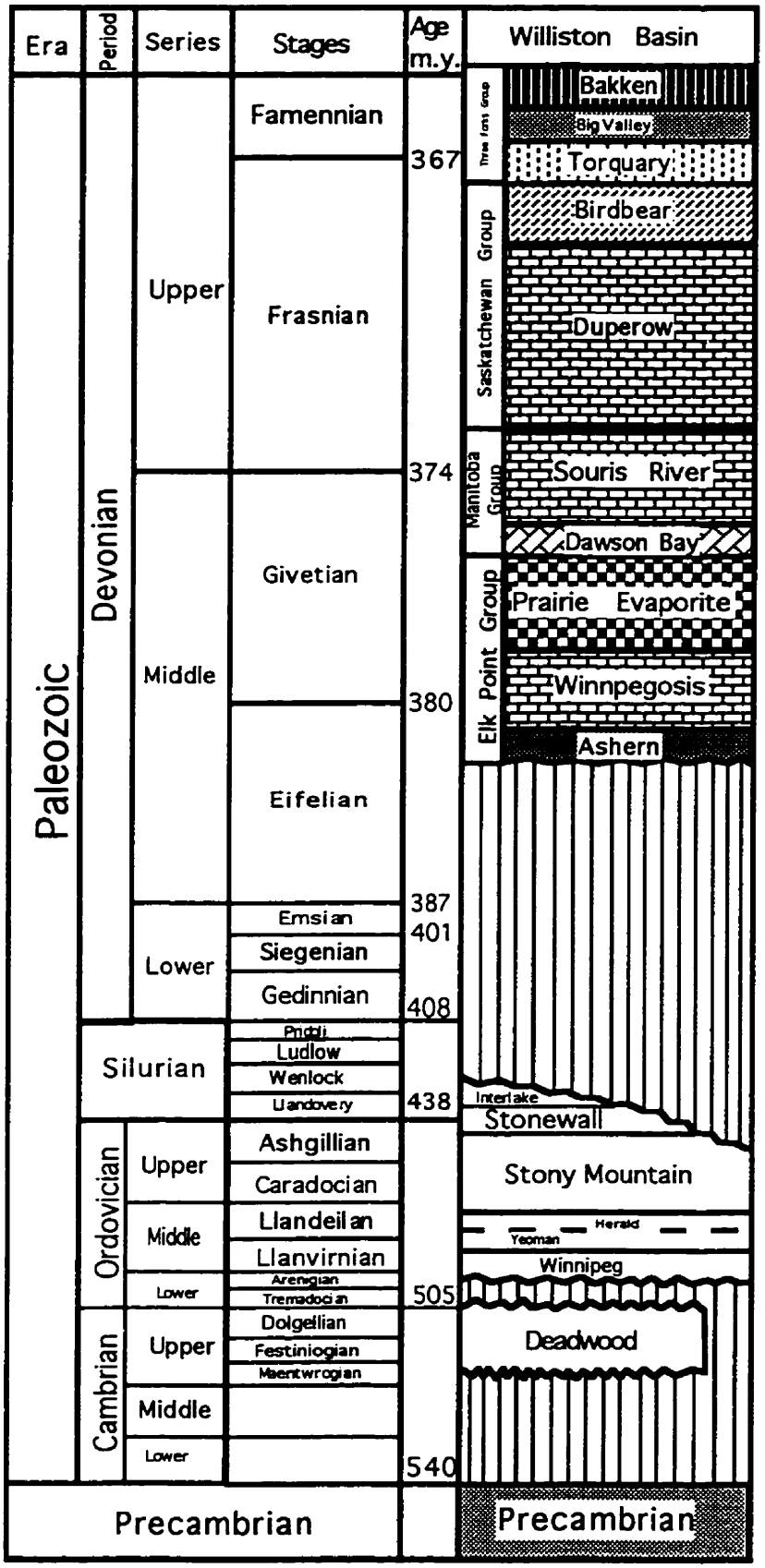

Fig. 1-4. Lower Paleozoic and Devonian stratigraphy of the Williston Basin (modified after Western Atlas International).

In the Paleozoic, the Williston Basin was first transgressed by marine waters during Upper Cambrian time (Gerhard *et al.*, 1990). The strata that formed during that time are called the Deadwood Formation (Fig. 1-4), which ranges from Late Cambrian to Early Ordovician in age (Carlson, 1960; Lochman-Balk and Wilson, 1967). This formation comprises a sequence of marine sandstones, shales, and some limestones, deposited as shoreward facies during the eastward transgression of the Cambrian seaway across the Cordilleran shelf. The Deadwood Formation is overlain unconformably by interbedded sandstones, shales and siltstones of the Middle to Late Ordovician Winnipeg Formation. The Winnipeg Formation is, in turn, overlain conformably by the Red River Strata of Late Ordovician age. The Red River Strata are characterized by cyclic sedimentation. Each complete cycle begins with a fossiliferous, burrow-mottled mudstone and wackestone unit, passes through a middle laminated dolostone unit, and culminates in evaporites. In Saskatchewan, the Red River Strata have been divided into the Yeoman Formation and the Herald Formation. The strata directly overlying the Red River Strata are called the Stony Mountain Formation, which is composed of fossiliferous mudstones, wackestones and locally packstones. This formation is, in turn, overlain by the Upper Ordovician Stonewall Formation, which grades upward into the Interlake Formation. The Interlake Formation includes rocks of latest Ordovician and Silurian age. Silurian deposition was followed by a widespread marine regression that affected most of the interior of the North America. During this time, pre-Devonian rocks in western Canada underwent widespread epeirogenic uplift and erosion. The surface relief produced by the uplift not only controlled the distribution, thickness and character of the initial deposits of the Devonian sequence (Porter *et al.*, 1982), but also forced epeiric seas to transgress from the northwest (Porter *et al.*, 1982) into the Elk Point Basin.

The Elk Point Basin (Fig. 1-3) extended from the Northwest Territories through northeast British Columbia, Alberta, southern Saskatchewan, western Manitoba and into Montana, North and South Dakota. It was bounded by the West Alberta Arch and the Peace River High in the west, the Tathlina Arch in the north, and the Canadian Shield to the east. Based on changes in the thickness and structure of Devonian sedimentary strata in the Elk Point Basin, the following tectonic elements can be distinguished (from south to north): (1) Saskatchewan sub-basin, which is often subdivided into the main Saskatchewan Depression and the southern Williston Depression to the southwest, with the Swift Current Platform between them; (2) Meadow Lake Escarpment; (3) Central Alberta sub-basin; (4) Peace River-Athabasca Arch; (5) Northern Alberta sub-basin or Peace River sub-basin; (6) Tathlina High. The Saskatchewan and Central Alberta sub-basins were

separated by the Meadow Lake Escarpment, which forms the southern boundary of the Central Alberta sub-basin.

The Lower to Middle Devonian clastics, redbeds, evaporites and carbonates in the Elk Point Basin overlie Precambrian or lower Paleozoic rocks with an erosional unconformity that has up to 1400 m of relief. Moore (1989) has shown that the Devonian rocks of Western Canada can be divided into five major sequences bounded by discontinuities. The region south of the Meadow Lake Escarpment (the Williston Basin) was a broad upland while the first two major sequences were deposited to the north of it. It became a region of negative relief during the early part of the Middle Devonian. The sediments deposited in the Elk Point Basin during early and middle Devonian times (except the Dawson Bay Formation) are called the Elk Point Group (Fig. 1-4). The base of the Elk Point Group coincides with the pre-Devonian erosional unconformity. Its top is defined at the top of a thin, green or reddish brown shale unit (the Watt Mountain Formation - Second Red Bed Member) that overlies an unconformity. The Elk Point Group is divided into the Lower Elk Point Subgroup and the Upper Elk Point Subgroup. The Lower Elk Point Subgroup is that part of the Devonian that is found below the Ashern Formation and above the sub-Devonian unconformity (Van Hees, 1956), which is found only in the region north of the Meadow Lake Escarpment. The Upper Elk Point Subgroup is more widespread, and includes the basal red beds of the Ashern Formation, the Winnipegosis Formation, which is mainly dolomitized and composed of patch reef deposits and laminated inter-reef carbonate muds, and the Prairie Evaporite Formation. During Prairie Evaporite times, the Saskatchewan Sub-basin may have been partially isolated from the central Alberta sub-basin by the structural feature associated with the Meadow Lake Escarpment (Kent, 1987).

1.5 Stratigraphy and Correlation of the Dawson Bay Formation

1.5.1 Stratigraphy

The Dawson Bay Formation is Middle Devonian in age because it contains the brachiopod *Stringocephalus*, the guide fossil for the Givetian. Although the fossil has not been found in the Dawson Bay Formation in the outcrop belt, it has been reported by Brindle and Lane (1963) from the correlative subsurface unit in several localities in Saskatchewan. The Dawson Bay Formation is normally underlain by the Prairie Evaporite Formation (Fig. 1-5). In areas where the Prairie Evaporite Formation is absent, it is in direct contact with the underlying Winnipegosis Formation. Authors of the early reports on the

Well 13-12-22-32W1

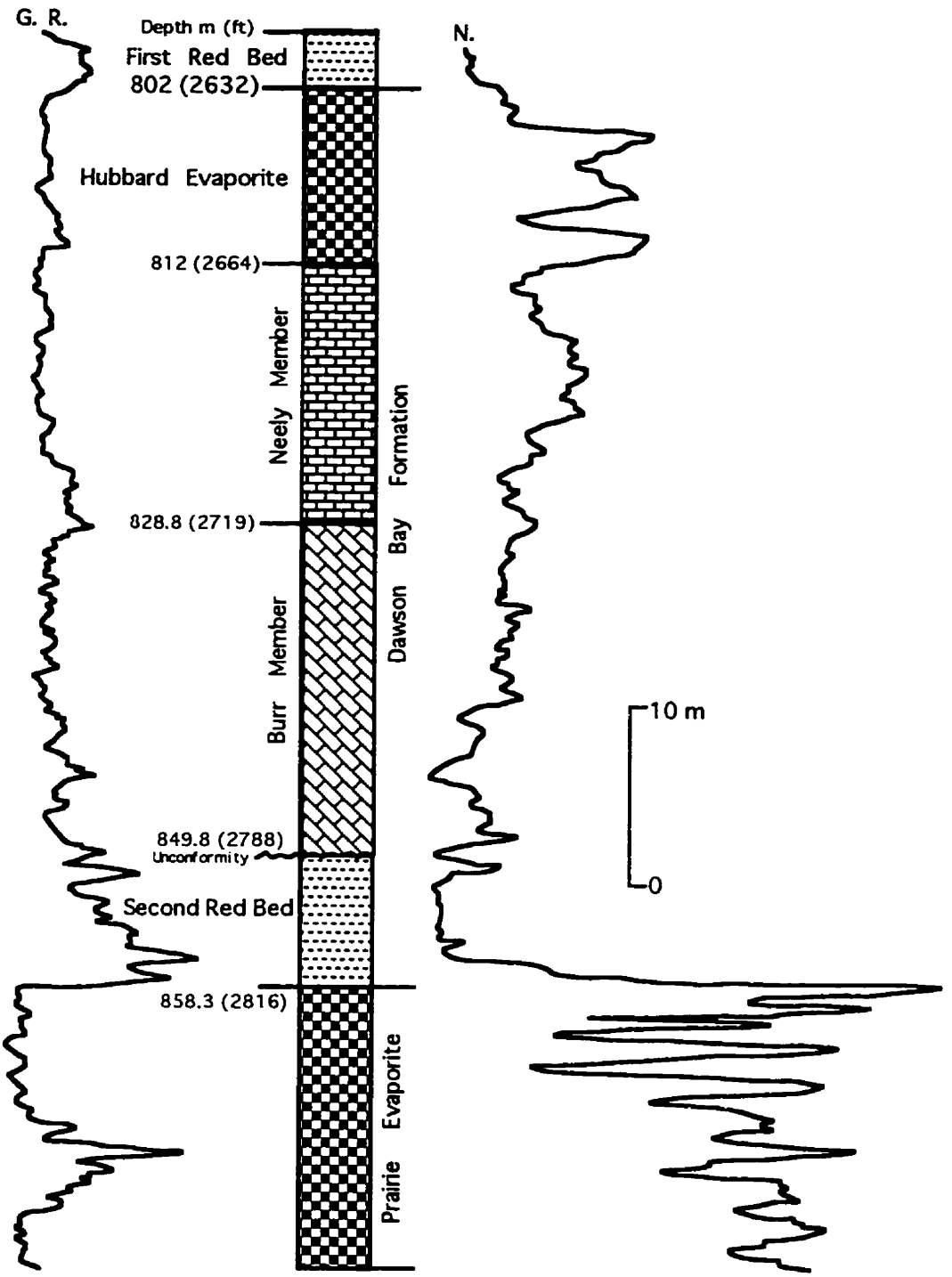

Fig. 1-5. Stratigraphy of the Dawson Bay Formation

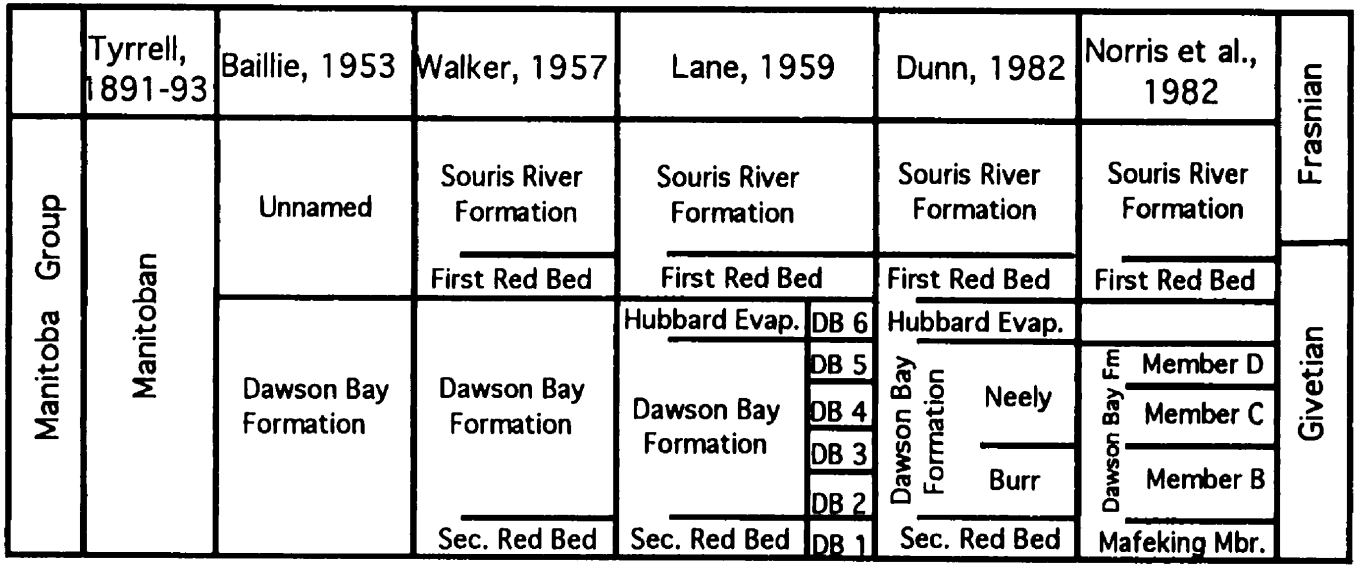

Fig. 1-6. Development of lithostratigraphic framework and nomenclature of Dawson Bay Formation (after Dunn, 1982a).

subsurface geology favoured a conformable transition from the Prairie Evaporite Formation (Baillie, 1955; Sandberg and Hammond, 1958; Edie, 1959; Jones, 1965; Peterson and MacCary, 1987). Baillie (1953) stated that the fauna of the Dawson Bay Formation includes many species which are present in the underlying Winnipegosis Formation and no faunal break is present between the Elk Point Group and the Manitoba Group. More recently, however, geologists have inferred that at least some erosion took place at the contact (Klingspor, 1969; Fuzesy, 1982; Dunn, 1982a; Williams, 1984). The upper boundary of the Dawson Bay Formation is placed beneath the First Red Bed of the Souris River Formation (Fig. 1-5) and may be disconformable (Moore, 1993).

Although the Dawson Bay Formation was named by Baillie (1953), he did not subdivide the formation. Walker (1957) was the first to divide the Dawson Bay Formation, recognizing the Second Red Bed in the lower part and carbonate and evaporitic rocks in the upper part (Fig. 1-6). Lane (1959) divided the sequence into six members, DB1 to DB6, in ascending order. The term DB-1 was used for the basal argillaceous zone, called the Second Red Bed. Succeeding lithologic units were designated by DB-2, DB-3, DB-4 and DB-5 in upward vertical sequence. The name Hubbard Evaporite was proposed for the DB-6 member. Lane's divisions, unfortunately, cannot be recognized in the more marginal areas to the northwest (Braun and Mathison, 1986), and the sequence can rarely be divided on the basis of geophysical well log responses, which forced Dunn (1982a, 1982b) to propose an alternative scheme for the Dawson Bay Formation. He formally divided the Dawson Bay Formation into four members (Fig. 1-6). They are named the Second Red Bed, Burr, Neely and Hubbard Evaporite members. The Second Red Bed Member corresponds to Lane's DB1 Member or the Second Red Bed. It ranges from 3 to 12 m and is characterized by a well-defined positive reponse on gamma-ray logs (Fig. 1-5). The Burr Member includes the DB2 and most of the DB3 members of Lane (Fig. 1-6). It has an average thickness of 20 m. The lower limit of the Burr Member is defined by a basal unconformity with the Second Red Bed Member (Fig. 1-5). Its upper limit is defined by a sharp gamma-ray response, the presence of a pronounced hiatus, and by a faunal change from dominantly corals, bryozoans and pelmatozoans beneath the diastem to sparse brachiopods and stromatoporoids above. The Neely Member comprises Lane's DB4 and DB5, and the argillaceous carbonate at the top of DB3. It maintains a thickness of 15 m to 18 m from central Saskatchewan to Manitoba. The uppermost member is the Hubbard Evaporite. It is composed of a relatively thin rock-salt unit alternating with anhydrite and mudstone, with a thickness attaining 19 m. The member is limited to a depocenter east of the third meridian.

At about the same time, Bannatyne (1975) informally defined four rock units for the Dawson Bay Formation in the outcrop belt of western Manitoba - A) basal red shale, or Second Red Bed, B) a lower carbonate unit of argillaceous limestone or dolostone, and high-calcium brachiopod biomicrite, C) a middle calcareous shale unit, with some argillaceous limestone, and D) an upper carbonate unit of dolomite and, in places, high-calcium stromatoporoid limestone. Norris *et al.* (1982) formally named the Second Red Bed the Mafeking Member; the lower carbonate unit, Member B; the middle calcareous shale, Member C; and the upper carbonate unit, Member D (Fig. 1-6).

1.5.2 Stratigraphic Correlation

Lithologically, the Dawson Bay Formation can be traced only a short distance into Alberta. There it thins rapidly and contains ever-increasing amounts of dolomitic mudstones and anhydrites. For this reason the stratigraphic equivalence of the Dawson Bay Formation within Alberta has not been satisfactorily resolved because of the limited biostratigraphic control within the time period (Braun *et al.*, 1988). The Dawson Bay Formation has been correlated with the Slave Point Formation (Baillie, 1951), the upper part of the Muskeg Formation (Graystone *et al.*, 1964; Bassett and Stout, 1968), either part or all of the Watt Mountain sequence (Kramers and Lerbekmo, 1967), or all of the Watt Mountain Formation (Dunn, 1982b), and with the Bistcho Formation (Moore, 1989, 1993). Williams (1984) proposed that the Second Red Bed Member is equivalent to the Watt Mountain Formation, but did not discuss the equivalence of the remainder of the Dawson Bay Formation.

Braun and Mathison (1986) have recently identified problems in the traditional correlations of the Dawson Bay sediments with other formations. There is a problem with correlating the open marine limestones of the Dawson Bay Formation with the Muskeg anhydrites of northern Alberta because the opening of the basin is usually considered to have been located in the northwest. Correlation with the Slave Point Formation is also a problem in that both the megafauna and microfauna of these rock units are younger than the Dawson Bay Formation (Braun and Mathison, 1986). Based on ostracod biostratigraphy, Braun and Mathison suggested that the basal unit of the Watt Mountain Formation is laterally equivalent to the Second Red Bed Member, and that the Burr Member is equivalent to most of the Watt Mountain Formation. The Neely Member has been correlated with the Fort Vermilion Formation. The Hubbard Evaporite Member is then correlated with the Slave Point Formation.

1.6 Methods of Study

1.6.1 Core Examination and Field Work

The materials for this study were mostly derived from the Dawson Bay Formation in the subsurface of Saskatchewan. Data presented here are based on extensive subsurface-stratigraphic analysis, involving geophysical logs, core logs and sample collection. Altogether, 70 cores have been logged. Several of them have been studied in great detail, which includes slabbing, photographing and sampling of the complete core interval of the Dawson Bay Formation. Some cores were re-examined in greater detail to delineate significant depositional and diagenetic features as an aid for interpretation. Samples were taken from all lithologies in these cores. In each core, samples were collected at vertical intervals from 5 to 50 cm apart. Most cores examined are stored at the Subsurface Geological Laboratory, Saskatchewan Energy and Mines, in Regina. Several cores donated by the Cominco potash mine are stored at the Department of Geological Sciences, University of Saskatchewan.

Additionally, field work was carried out on the Dawson Bay Formation in the outcrop area along the northwestern shore of Lake Winnipegosis. Data collection involved selection, logging and sampling of vertical sections of the formation.

1.6.2 Polishing, Thin Sections and Staining

In the laboratory, samples of oriented carbonate rocks were polished for analysis of their physical and biogenic sedimentary structures.

Two hundred thin sections were made for petrographic study. These samples were mounted on 5 x 7.5 cm glass slides with cold epoxy resin. Each chip was left to dry and ground to a standard thickness of 0.03 mm.

Some of the thin-sections were stained according to the method outlined by Dickson (1965). Potassium ferricyanide and alizarin red S were used for distinguishing between carbonate minerals. Before the thin sections were stained, they were etched first for 10-15 seconds by using 1.5 per cent hydrochloric acid. The etched thin sections were then immersed in an acidified mixture of the two stains. Each stain worked independently, and there was no mutual interference. Then, the thin sections were carefully washed in running water for a few seconds and left to dry.

1.6.3 Scanning Electron Microscope and Electron Microprobe Analysis

Some samples were prepared for scanning electron microscope (SEM) and electron microprobe analysis (EMPA) examination. Rock chips, polished samples and polished thin sections were used for the examination. Freshly broken surfaces of the rock chips were acquired for SEM examination. Samples were put into distilled water to remove soluble salts. These samples were left to dry by gentle heating in air. Any fine debris on the surface was dislodged with a Freon duster. Each sample used for the SEM analysis was coated with approximately 100 nm of gold or carbon. Samples were handled with disposable gloves. The cut sample was attached to a SEM specimen plug with epoxy or Silpaste and dried overnight in a low-temperature drying oven. The sample was then coated with a conductive metal, such as carbon, gold, or palladium in either a sputter or evaporative coater. After coating, the sample was ready for SEM analysis. Some polished thin-sections were analysed using energy-dispersive (EDS) methods on a JEOL JXA 8600 electron microprobe. Those thin-sections were coated with approximately 400 nm of carbon.

1.6.4 ICP-MS

Trace elements from the black shales at the base of the Burr Member were analyzed by inductively coupled plasma mass spectrometry (ICP-MS) following the techniques discussed by Jenner *et al.* (1990) and Longerich *et al.* (1990), using a Perkin Elmer Elan 5000 at the Department of Geological Sciences, University of Saskatchewan. All samples were hand crushed and comminuted to a powder using an agate mill. Powdered samples (normally 0.1 g) were dissolved in a screw-top Teflon® bomb (Savillex®) using HF-HNO_3. After evaporation of the HF-HNO_3, the sample was evaporated to dryness, taken up in 2-3 ml of 8 *N* HNO_3, transferred to a 125-ml bottle, and diluted with water to 90 g. The solutions were then analysed by ICP-MS with detection limits of 10% for most trace elements.

CHAPTER 2

THE SECOND RED BED MEMBER

2.1 Introduction

The Second Red Bed Member (SRBM) is one of three argillaceous stratigraphic units recognized in the subsurface Devonian strata in western Canada. It constitutes the lowest member of the Dawson Bay Formation and was formally defined by Dunn (1982a). The SRBM is normally underlain by the halite of the Prairie Evaporite Formation and overlain by the carbonate rocks of the Burr Member (Dawson Bay Formation) (Fig. 1-5). Where the Prairie Evaporite Formation is absent, due to erosion or non-deposition, the Second Red Bed Member lies unconformably upon carbonate rocks of the Winnipegosis Formation. In western Manitoba, the time-equivalent stratigraphic interval is called the Mafeking Member (Norris *et al.*, 1982).

The significance and origin of the Second Red Bed Member have long been unclear. These rocks either represent the very last phase of a regression or the initiating phase of a transgression (Braun and Mathison, 1986). Lane (1959) postulated that the red mudstones that form the lower part of the Second Red Bed Member were deposited under continental conditions, whereas the grey and green mudstones that comprise the upper part of the member were laid down under marine conditions. Edie (1959) concluded that the mudstones formed by the slow accumulation of terrestrial clastics, at or near sea level, under evaporitic conditions. Dunn (1982a) proposed that the Second Red Bed Member is a transgressive deposit that formed when the sea advanced across the saline-pan evaporites of the Prairie Evaporite Formation. Norris *et al.* (1982) and Day *et al.* (1996) suggested that the equivalent Mafeking Member in Manitoba accumulated under continental or very shallow water intertidal conditions. However, no conclusive evidence has ever been presented to support these interpretations.

The purpose of this chapter is (1) to describe sedimentary rocks of the Second Red Bed Member, (2) to interpret the depositional and diagenetic environments, and (3) to discuss the implications of the new results. Results are based on a detailed examination of more than 70 cores from sites across Saskatchewan, and are based on studies of thin sections, and SEM, and microprobe analysis of core samples.

2.2 Stratigraphy

The Second Red Bed Member is 3-9 m thick in Saskatchewan, increasing in thickness gradually from northwest to southeast (Fig. 2-1). In Alberta, the Second Red Bed Member merges with the First Red Bed of the Souris River Formation (Williams, 1984) and pinches out into the lower part of the Watt Mountain Formation (Grayston *et al.*, 1964) (Fig. 2-2). The Second Red Bed Member is characterized by a colour change from alternating red and green in the lower part, through red-brown in the middle part, to dark-grey and olive-green in the upper part.

Based on lithological variations observed throughout Saskatchewan, the Second Red Bed Member is here divided into four informal units -- A, B, C and D (Fig. 2-3), from top to bottom (because the Second Red Bed Member is rich in paleosol features, a soil-stratigraphic description from top to base is used). Unit A is a thin dolostone. It is separated from underlying Unit B by a sharp, angular contact. In contrast, the contacts between each of the lower three units are gradational. Unit B consists of argillaceous dolomitic rocks. Units C and D constitute a mudstone-dominated succession.

2.3 Gamma Ray Features of the Second Red Bed Member

Throughout the subcrops of the Dawson Bay Formation in Saskatchewan, the Second Red Bed Member is characterized by a strong gamma-ray response (Fig. 2-4), which is sharply different from that of the rest of the Dawson Bay Formation. Throughout the Second Red Bed Member, the strength of the gamma ray response decreases gradually from the lower to the upper part. However, a narrow, isolated peak is present at the top of the member (Fig. 2-4).

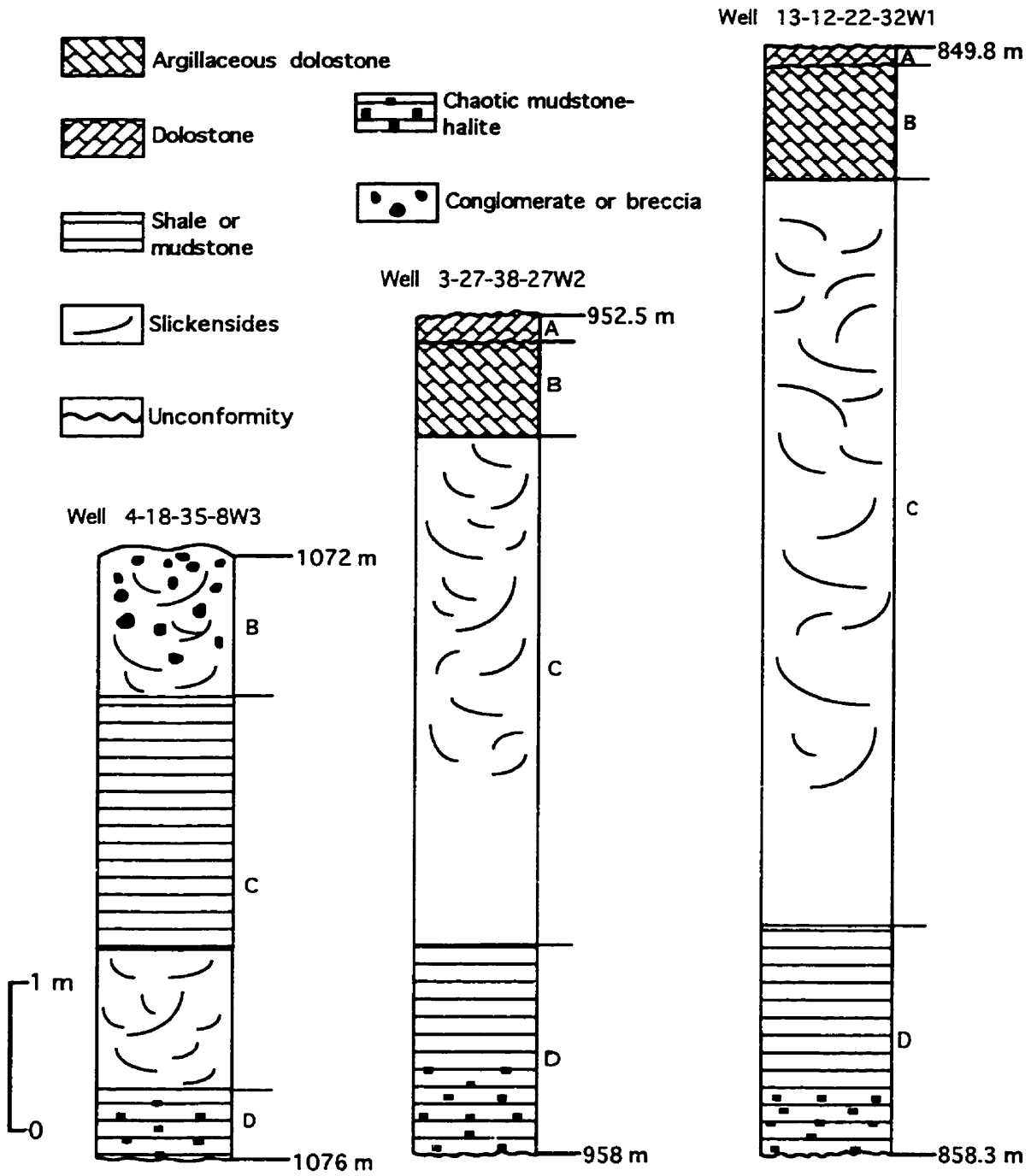

Fig. 2-1. Lateral thickness and lithological facies changes of the Second Red Bed Member.

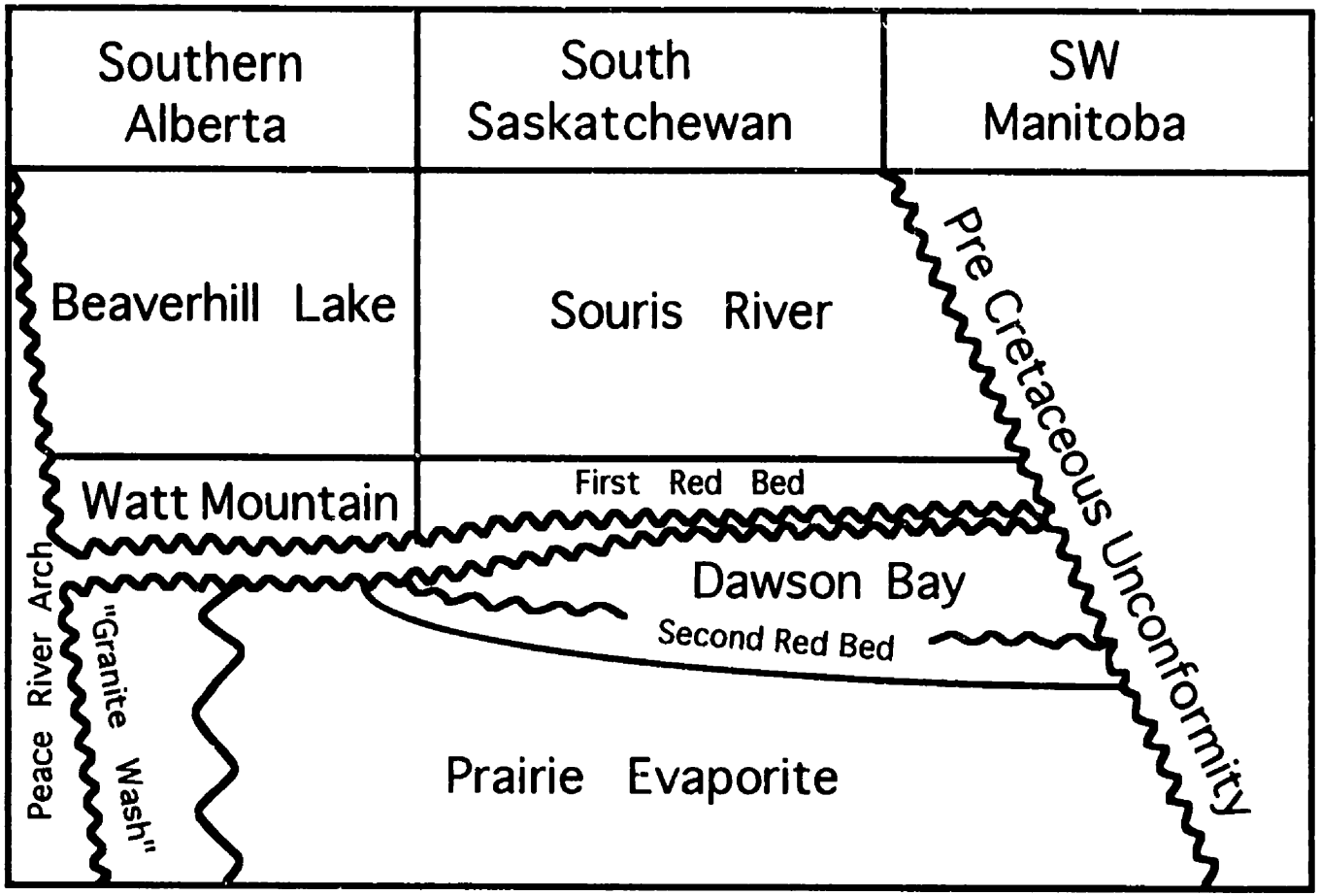

Fig. 2-2. Diagram showing the mergence of the Second Red Bed Member with the First Red Bed in eastern Alberta (after Meijer Drees, 1994).

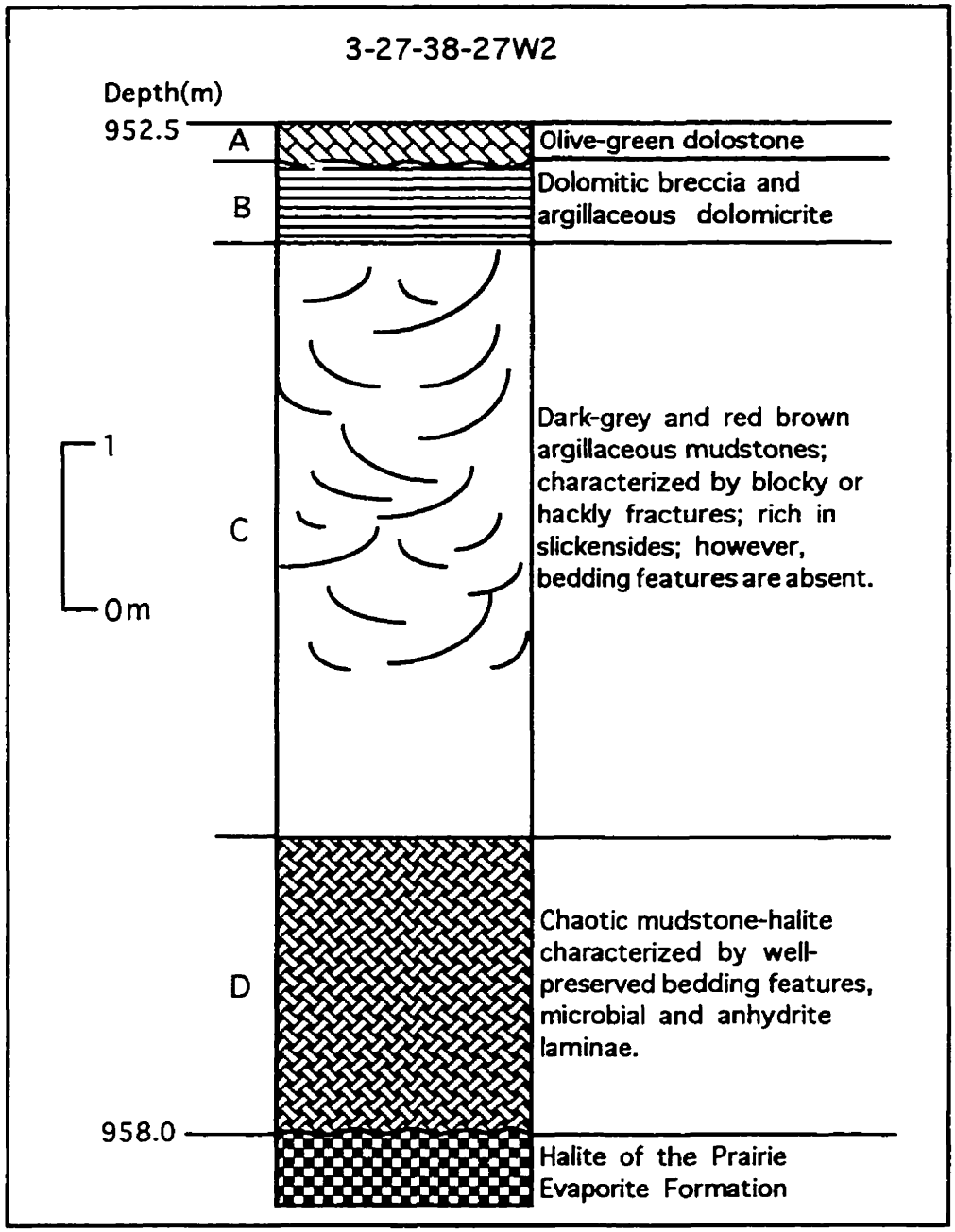

Fig. 2-3. Stratigraphic section of the Second Red Bed Member.

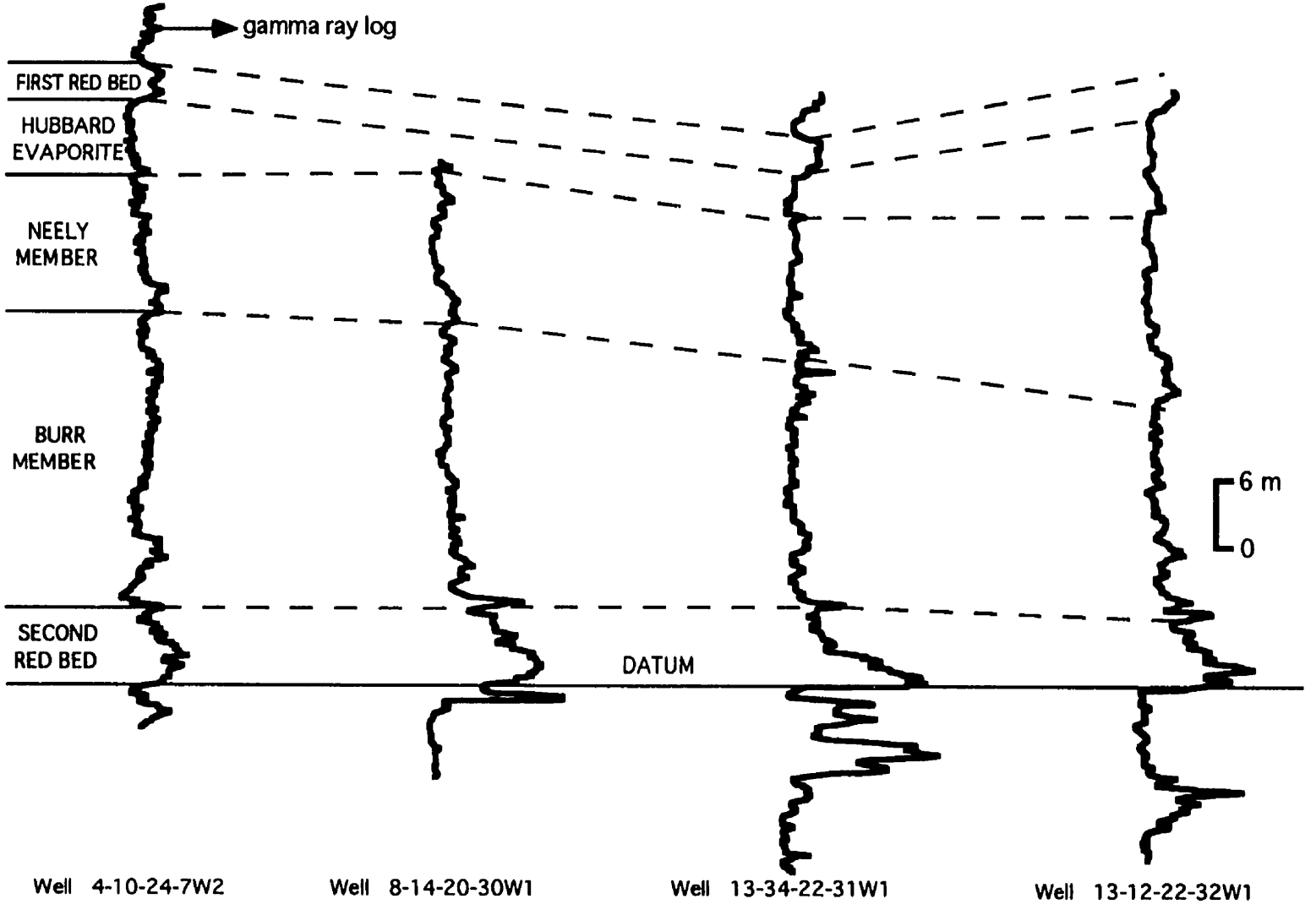

Fig. 2-4. Cross section of the Dawson Bay Formation in southeastern Saskatchewan.

2.4 Lithological and Sedimentological Features of the Second Red Bed Member

2.4.1 Unit A

Unit A (the dolomitic unit) is significantly different from the rest of the Second Red Bed Member by its predominant dolomitic composition and well-preserved sedimentary structures. It is present in southeastern Saskatchewan and in some areas of central Saskatchewan. In the rest of central Saskatchewan, it is absent. This unit represents the uppermost part of the Second Red Bed Member (Plate 2-1A & B). It is olive-green, and up to 20 cm thick. The dolomitic unit is in sharp contact with both the overlying Burr Member and the underlying Unit B. The unit is composed of dolomite, with subsidiary illite, chlorite, potassium feldspar, and quartz. Locally, silt-grade, detrital quartz is a major component. Scanning electron microscopy (SEM) shows that most of the dolomite is present as small (1-4 μm), euhedral crystals (Plate 2-1D). However, in some samples, the dolomite crystals are bimodal in size. Some are smaller than 5 μm; others are about 10 μm in length. Qualitative microprobe analyses (EDS) of the dolomite showed them to be calcium-rich (up to ~60% $CaCO_3$) and, therefore, non-stoichiometric (Fig. 2-5). Previous studies reported that these dolomites are slightly ferroan (Dunn, 1982a; Ahlstrom, 1992).

The dolostones in Unit A can be divided into three facies: massive dolostone, laminated dolostone, and dolomite intraclast breccia.

Massive Dolostone

The massive dolostone (Plate 2-2B) is composed of microcrystalline dolomite that lacks distinctive features. This facies is underlain sharply by argillaceous dolomitic conglomerate of Unit B. In places, the contact between the massive dolostone and dolomitic conglomerate displays a slight upward doming (Plate 2-2B). The massive dolostone ranges in thickness from several centimetres to tens of centimetres. Some examples are mottled, with black spots or patches of argillaceous sediment unevenly distributed in the rock. Small indistinct burrows are present in the massive dolostone, but they cannot be identified with confidence.

Laminated Dolostone

Two types of laminated dolostone are present in Unit A. They are termed Types A and B

PLATE 2-1

Plate 2-1 A: Core photograph of the uppermost part of the Second Red Bed Member (s) and the base of the Burr Member (b). The top (T) of the Second Red Bed Member is characterized by a thin laminated dolostone (Unit A) that is in sharp but planar contact with the Burr Member. Lsd. 4-25-20-30W1. (One core box is 0.76 m long and core diameter is 10.1 cm.)

Plate 2-1 B: Slabbed core photograph showing Unit A and B of the Second Red Bed Member. The contact (c) between Unit A (top half) and B (bottom half) displays a slight upward doming. Unit B contains pillar structure that is characterized by numerous irregularly spaced vertical to subvertical streaks. Lsd. 16-4-21-31W1. Coin diameter: 1.7 cm.

Plate 2-1 C: Slabbed core photograph of dolomitic intraclast breccia from Unit A of the Second Red Bed Member. Lsd. 8-20-33-20W2. Coin diameter: 1.7 cm.

Plate 2-1 D: SEM photomicrograph showing well-crystallized dolomite rhombs. Most rhombs are smaller than 5 μm. Unit A, the Second Red Bed Member. Lsd. 4-2-21-30W1.

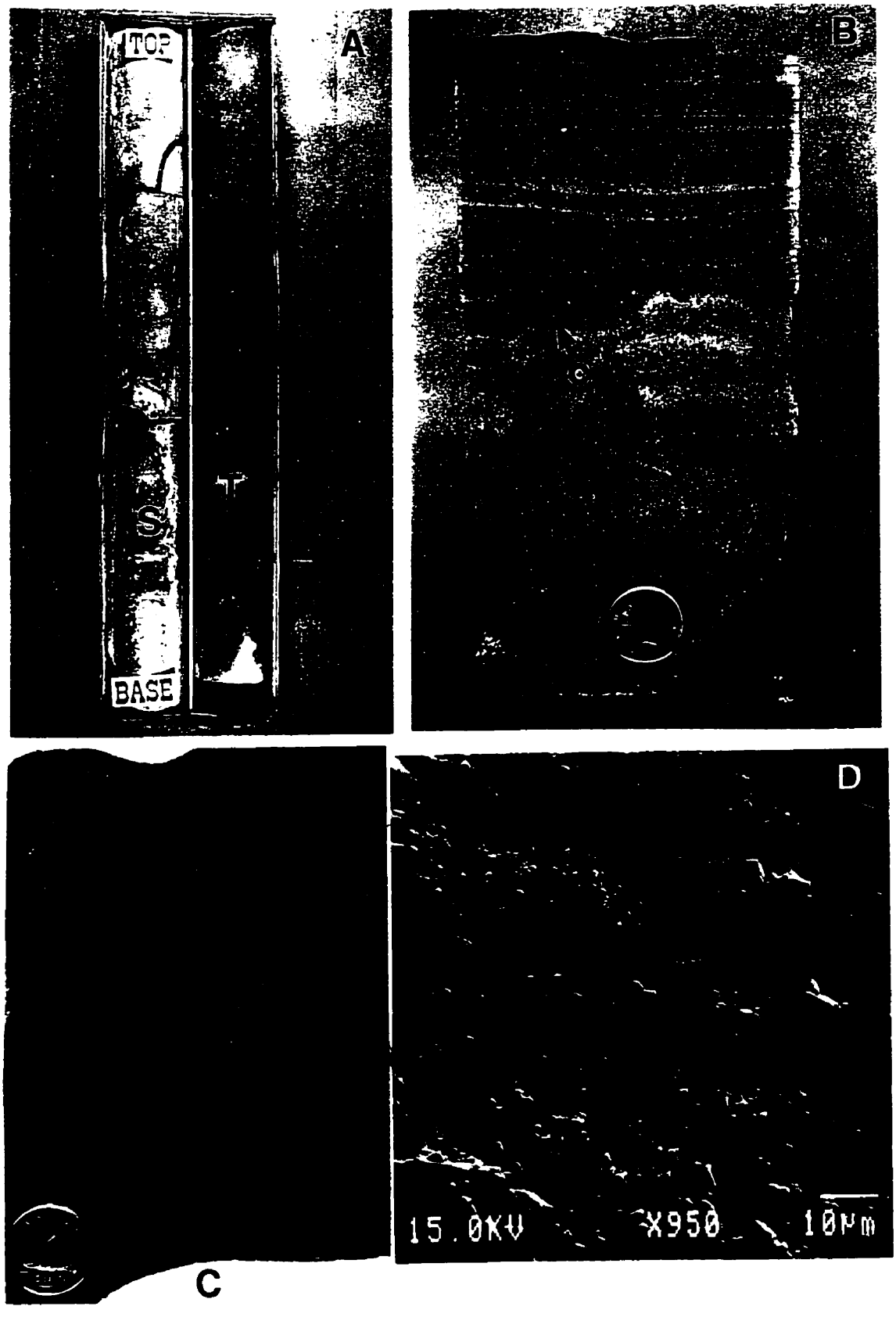
TOP
BASE
A
B
C
D
15.0KV
X950
10µm

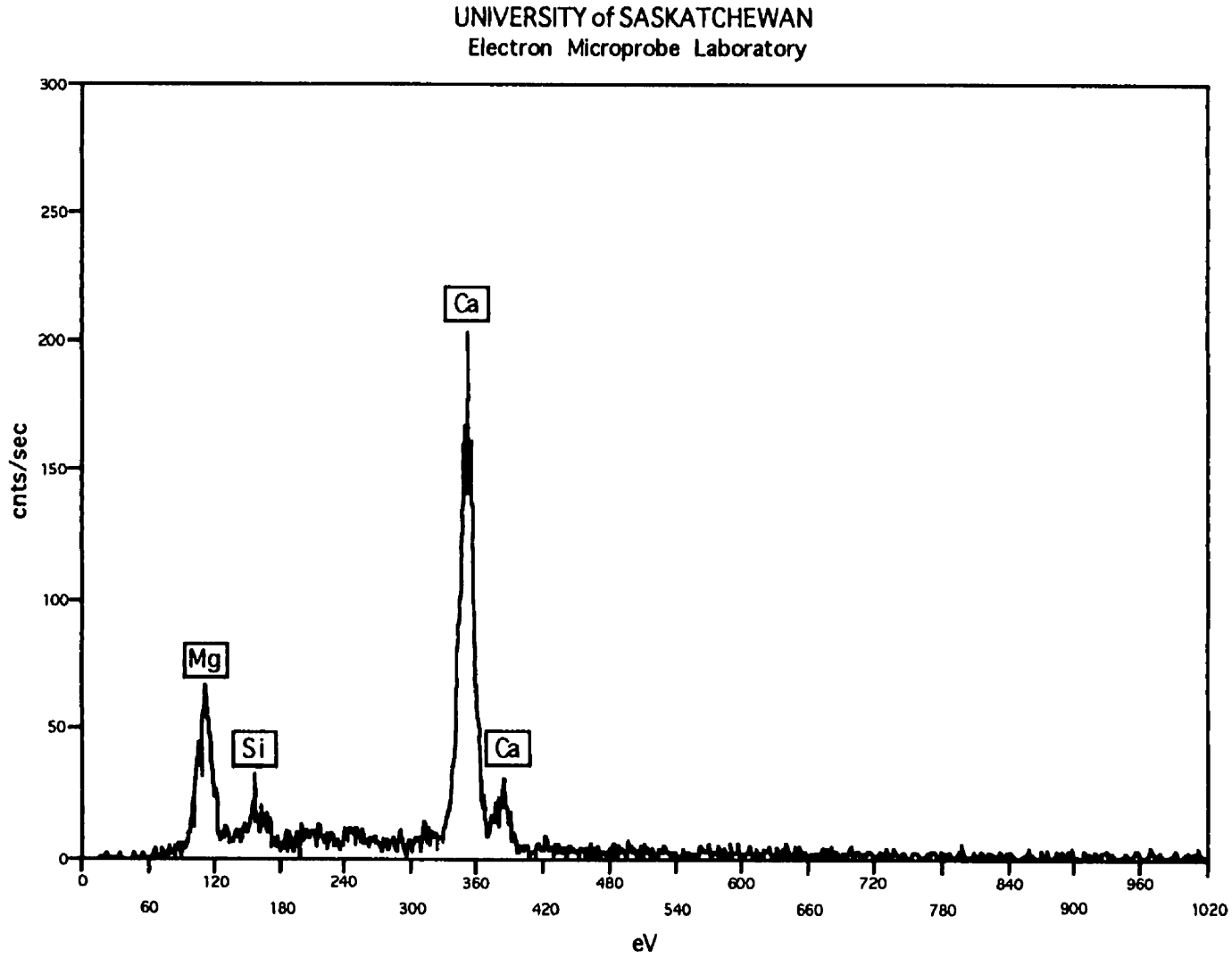

Fig. 2-5. EDS element pattern of the dolomite from Unit A of the Second Red Bed Member.

PLATE 2-2

Plate 2-2 A: Slabbed core section showing truncation (t) of lamination at the top, horizontal lamination in the upper part, a small symmetrical wave-ripple (r) in the middle part, and convolute bedding (c) in the lower part. Lsd. 8-14-20-30W1. Scale bar is 2 cm.

Plate 2-2 B: Slabbed core photograph showing a sharp, concave contact (c) between the Second Red Bed and Burr members; the massive dolostone of unit A, and the slightly upward doming structure (d) between Units A and B of the Second Red Bed Member. Lsd. 1-12-34-1W3. Scale bar is 2 cm.

Plate 2-2 C: Slabbed core photograph showing Type A laminated dolostone, which is characterized by horizontal to slightly wavy lamination, a sharp erosional structure (e), anhydrite nodules (a), and a microfault (f). The top of the dolostone is overlain by a very thin black shale that is characterized by fine lamination and mudcracks. Lsd. 1-2-21-31W1. Scale bar is 2 cm.

Plate 2-2 D: Plane-polarized light photomicrograph of laminated dolostone, consisting of alternating peloid-rich laminae and peloid-poor laminae. Lsd. 4-2-21-30W1. Scale bar is 0.5 mm.

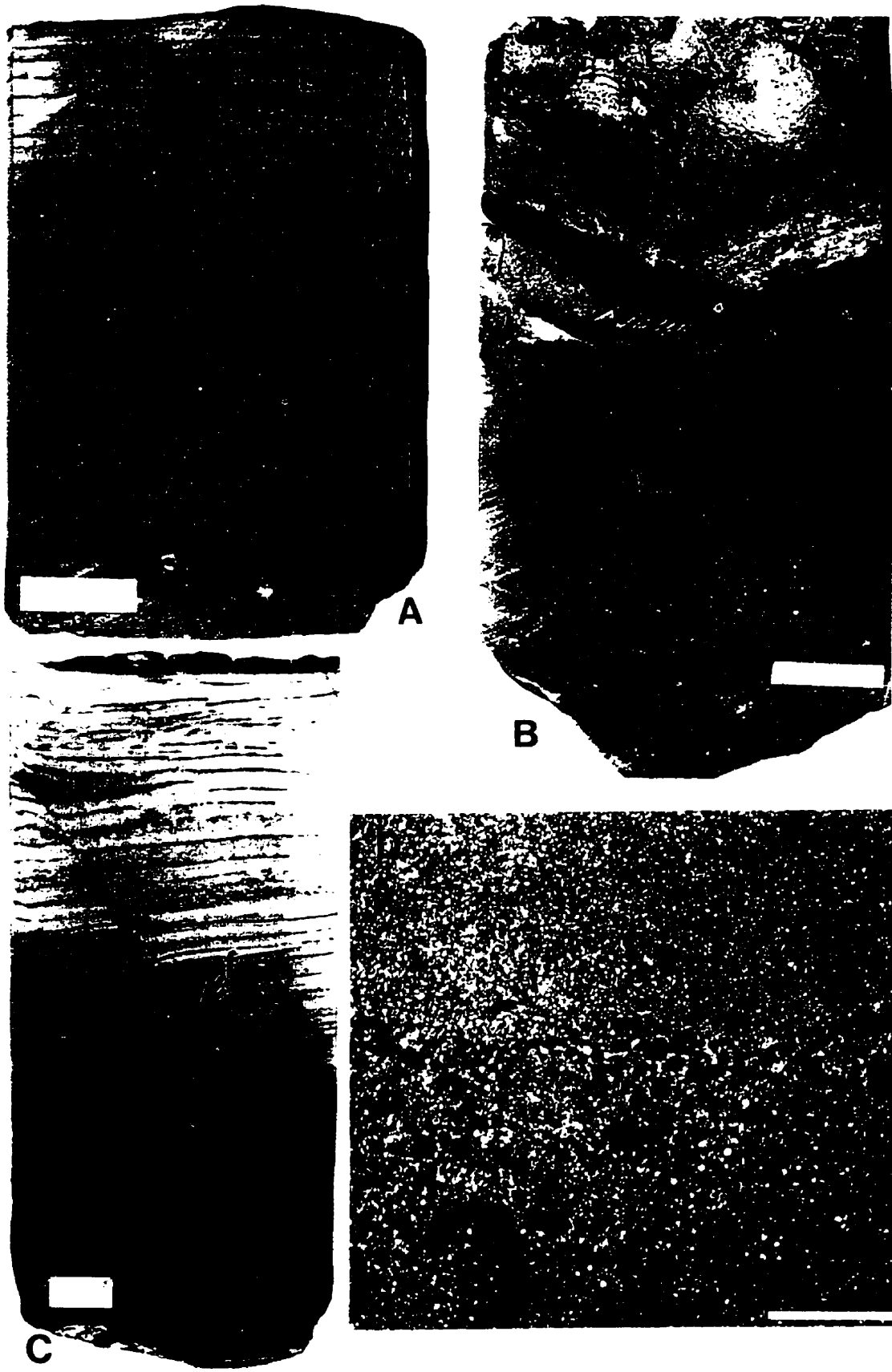
A
B
C

laminated dolostones, respectively.

Type A laminated dolostone

Type A laminated dolostone, which is characterized by parallel to slightly wavy laminae (Plate 2-2A), is interlayered with massive dolostone (Plate 2-2A) or Type B laminated dolostone. In hand specimen, Type A laminated dolostone is composed of alternating light grey and dark grey laminae ranging from 2 to 3 mm thick. These laminae are more or less laterally continuous. The rock lacks mudcracks, doming, bioerosion or other evidence of subaerial exposure. This indicates that the laminated dolostone probably formed under perennial subaqueous conditions. Commonly, a third group of laminae is present (Plate 2-2A & C). These laminae are laterally discontinuous and variable in thickness. They are composed either of black, sand-sized, discrete argillaceous grains or black muddy sediment. The laminae composed of muddy sediment are generally thicker, lighter and more laterally continuous than the laminae composed of discrete argillaceous grains. The black argillaceous laminae are normally less than 2 mm thick.

In thin section, the laminated dolostone is composed of peloid-rich and peloid-poor layers (Plate 2-2D). The peloid-poor layers are composed of microcrystalline dolomite. The peloid-rich layers consist of peloids and microcrystalline dolomite. The peloids themselves are, in turn, composed of microcrystalline dolomite. The peloids are irregular to elliptical in shape, and are probably reworked intraclasts. However, all the peloids are rounded with little difference in individual sizes. Sparse argillaceous grains with diffuse margins can be also seen in the peloid-rich layers (Plate 2-2D).

The black laminae in thin section are composed of argillaceous grains (Plate 2-3A). They are laterally discontinuous, indicating that the argillaceous sediment was not sufficient to form a laterally continuous lamina. The boundaries of the argillaceous grains are obscured and diffuse. Some grains have disintegrated into small patches of argillaceous sediment without definite shapes (Plate 2-3B). This suggests that the argillaceous grains were weakly lithified when they were deposited. Similar laminae are present in the sedimentary rocks described by Lowe (1975) and Lowe and LoPiccolo (1974), where they are associated with groundwater escape structures. This suggests that these argillaceous sediments could have been brought up to the depositional substrate by groundwaters through water escape structures, where they were reworked by waves or currents in the depositional environment. This interpretation is strongly supported by vertically aligned

PLATE 2-3

Plate 2-3 A: Plane-polarized light photomicrograph of laminated dolostone showing black argillaceous grains (b), which are characterized by irregular shape, and obscured and diffuse boundaries. Lsd. 4-2-21-30W1. Scale bar is 0.5 mm.

Plate 2-3 B: Plane-polarized light photomicrograph showing an indistinct lamina (l) in the laminated dolostone. The lamina was probably formed by dissolution of black argillaceous grains. Lsd. 4-2-21-30W1. Scale bar is 0.5 mm.

Plate 2-3 C: Slabbed core photograph showing paleokarst at the base of the Burr Member and laminated dolostone at the top of the Second Red Bed Member. The laminated dolostone contains black vertical streaks that cross-cut the horizontal lamination. Lsd. 13-12-22-32W1. Scale bar is 3 cm.

Plate 2-3 D: Plane-polarized light photomicrograph showing a vertical streak (s) that is composed of dolomitic peloids and cross-cuts horizontal laminations. Lsd. 13-12-22-32W1. Scale bar is 0.5 mm.

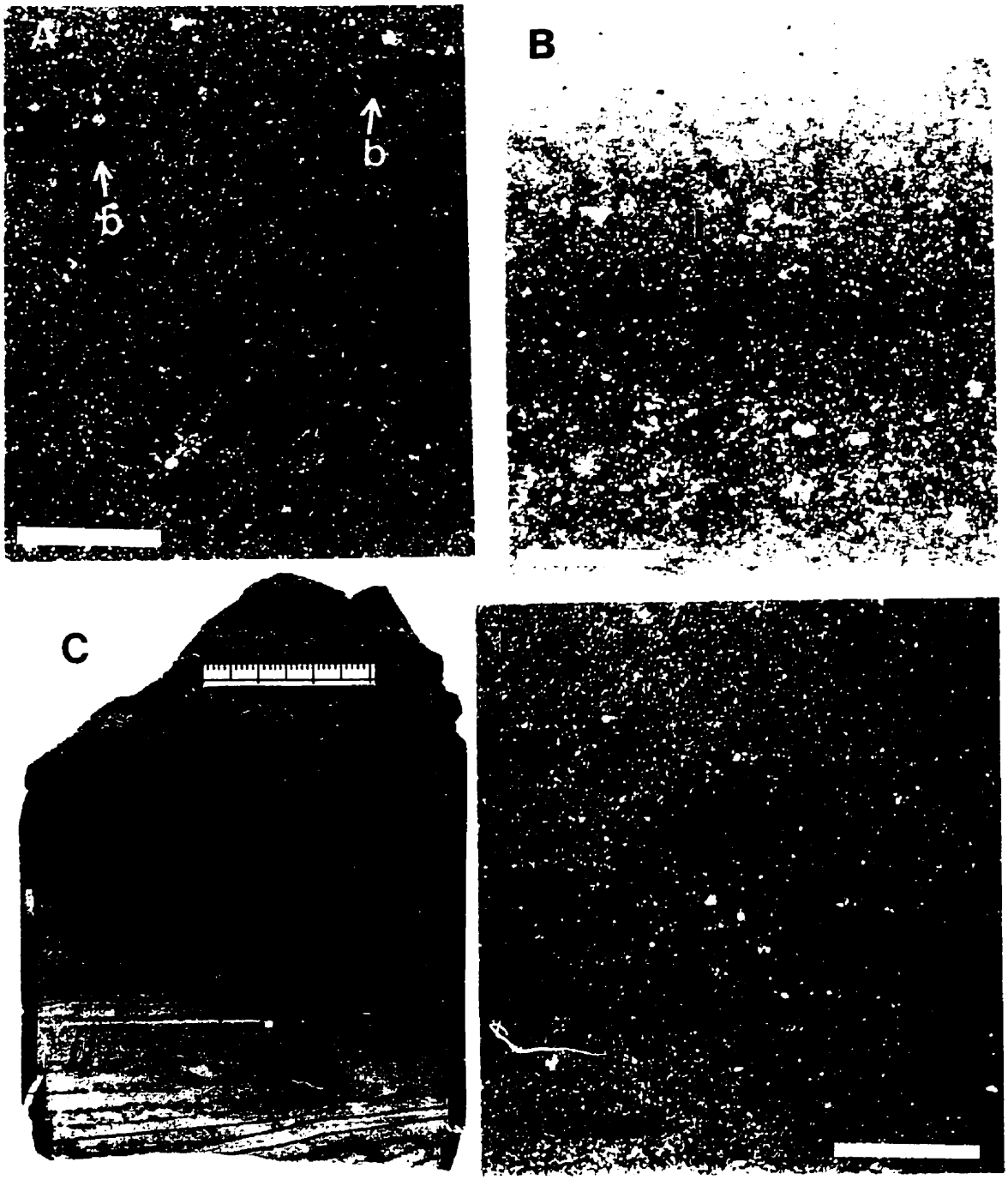
A
b
b
B
C

argillaceous grains in Core 13-12-22-32W1 (Plate 2-3C & D). These black argillaceous grains form vertical streaks that cross cut horizontal laminations. The vertical streaks were emplaced after the surrounding sediment was deposited. Thus, the argillaceous sediment was probably carried upward to the surface by groundwaters. Because the source and amount of this sediment were restricted, they could not form a laterally continuous lamina.

Type B laminated dolostone

Type B laminated dolostone is confined to central Saskatchewan. It lies on Type A laminated dolostone or the massive dolostone of Unit A, or rests on argillaceous dolomitic conglomerate of Unit B. The rock is characterized by wavy-crinkly laminae (Plate 2-4A). These laminae are less than 1 mm to a few millimetres in thickness. Petrographic study shows that the laminae are composed of extremely fine dolomite. They are clotted in places, with dark brown organic filaments, probably remains of microbial mats, present throughout the rock (Plate 2-4B). Additionally, the black argillaceous grains that have been described above are highly concentrated in some laminae. They are also present as pockets in a dolomitic matrix (Plate 2-4D). Some argillaceous grains are oriented with their long axes perpendicular to bedding plane (Plate 2-4D). Moreover, sand-grade dolomitic intraclasts are locally present. The wavy, crinkly laminae and the presence of probable microbial filamentous remains indicate that microbial mats may have played a significant role in the deposition of Type B laminated dolostone.

Dolomite Intraclast Breccia

Dolomitic intraclast breccia is composed of dolomitic intraclasts and matrix (Plate 2-1C, 2-4C). This lithology is mainly distributed in northwestern and central Saskatchewan. Only rarely was this facies observed in southeastern Saskatchewan (Core 9-14-23-33W1). The colour and composition of the intraclasts are identical to the matrix. In some examples, the intraclasts cannot be distinguished from the matrix without careful examination (Plate 2-4C). The intraclasts are present in many shapes and sizes, ranging from a few millimetres to centimetres in length. Some clasts can be fitted back together, indicating *in situ* brecciation. The margins of the intraclasts are sharp and undistorted; most intraclasts are characterized by wavy-crinkly microbial laminae. The angular clasts lie at random angles to the bedding.

The intraclasts in the breccia were previously interpreted as products of rip-up associated

PLATE 2-4

Plate 2-4 A: Slabbed core photograph of Type B laminated dolostone. It is characterized by crinkly, wavy microbial laminae. Lsd. 13-11-33-23W2. Scale bar is 3 cm.

Plate 2-4 B: Plane-polarized light photomicrograph of Type B laminated dolostone showing dark brown organic filaments (f) in a micritic-microspar matrix. Patches of black argillaceous sediment (b) are also present. Lsd. 3-27-38-27W2. Scale bar is 0.25 mm.

Plate 2-4 C: Slabbed core photograph of dolomitic breccia, which is composed of subhorizontally- to vertically-oriented angular intraclasts. Lsd. 9-14-23-33W1. Coin diameter is 1.7 cm.

Plate 2-4 D: Plane-polarized light photomicrograph of Type B laminated dolostone showing black argillaceous grains with their longest axis oriented vertically. Lsd. 3-27-38-27W2. Scale bar is 0.25 mm.

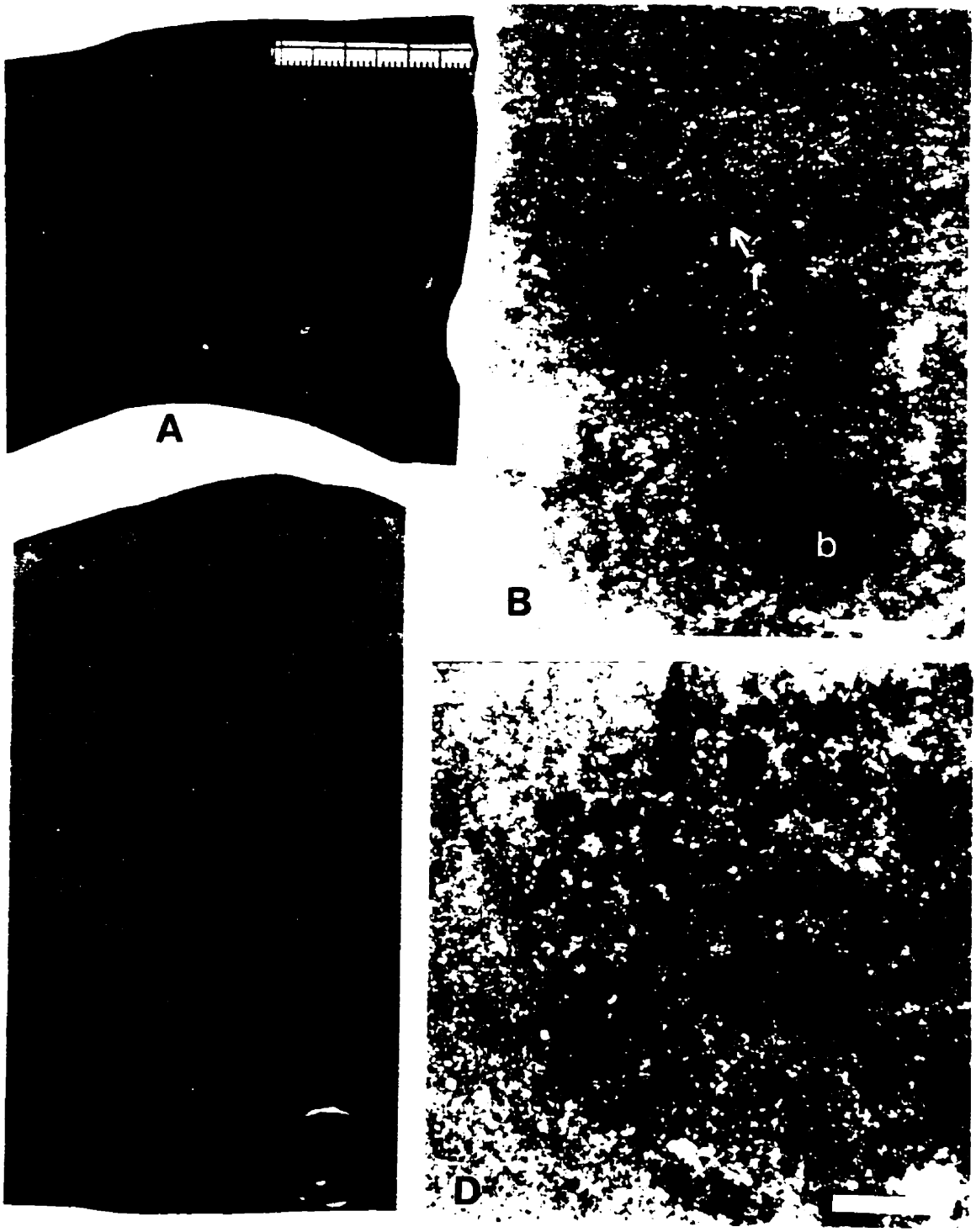
A
B
b
D

with storms (Dunn, 1982a; Braun and Mathison, 1986). However, the margins of almost all the clasts are sharp, lacking evidence of soft sediment deformation. This suggests that their parent sediments were well lithified before the clasts formed. If the clasts were formed by storm action, some plastically deformed clasts would also likely be present because it is easier for storm processes to disrupt soft subaqueous sediments than lithified rocks. Additionally, no associated storm- or current-related sedimentary structures were observed. Thus, the evidence does not support storms as the main agents to produce the intraclasts. These intraclasts are found at the top of the Second Red Bed Member, which is truncated by a subaerial erosional surface, and may indicate that they formed in a very shallow to subaerial environment, probably by the spalling of tepee carbonates.

Primary Sedimentary and Penecontemporaneous Deformation Structures

Primary sedimentary and penecontemporaneous deformation structures are well preserved in Unit A. The former include micro-scale ripples, parallel- and cross-laminations, microbial structures. The latter include tepee structures, convolute bedding, microfaults, water escape structures and broken stromatoids. In the following sections, each of the structures will be described in detail.

Tepee structures

A small tepee structure is found at the top of the dolomitic unit in Core 41-1-12-34-1W3 (Plate 2-5A). It is composed of overthrust layers of laminated dolostone, with a thickness of about 2 cm. This grades downward into dolostone with indistinct laminations and intraclasts. No large tepee structures were recognized in the cores of the dolostone. This is not surprising, because tepee structures are normally too large to be revealed within the narrow diameter of core samples. Where present, large tepee structures might be recognized in core by carbonate layers that are discordant with respect to the general bedding planes in a sedimentary succession; they may also show evidence for early cementation and physical breakage and erosion before the overlying sediments were deposited. Such discordant layers are common in the dolostone of Unit A. For example, in Plate 1 (2) of Dunn (1982a), the contact between the Second Red Bed and Burr members is planar. However, a dolostone layer composed of laminated sediments near the contact is discordant with respect to the planar surface. The upper bedding surface of the laminated dolostone was clearly eroded before the uppermost massive dolostone was deposited. The erosional surface is sharp and irregular, and the fractures in the discordant carbonate layer

PLATE 2-5

Plate 2-5 A: Slabbed core photograph showing a small tepee structure (t) at the top. Lsd. 41-1-12-34-1W3. Scale bar is 2 cm.

Plate 2-5 B: Slabbed core photograph showing cross-lamination with foreset laminae dipping in the same direction. Convolute lamination (c) can be seen in the middle portion of the slabbed core. Lsd. 4-19-48-24W2. Scale bar is 3 cm.

Plate 2-5 C: Slabbed core photograph showing erosive form of micro-ripples (r) in the middle part of the slabbed core. Lsd. 13-11-33-23W2. Scale bar is 3 cm.

Plate 2-5 D: Lower part of slabbed core photograph displaying a microbial structure (m) with evidence of penecontemporaneous erosion. Lsd. 3-30-37-2W3. Coin diameter is 1.7 cm.

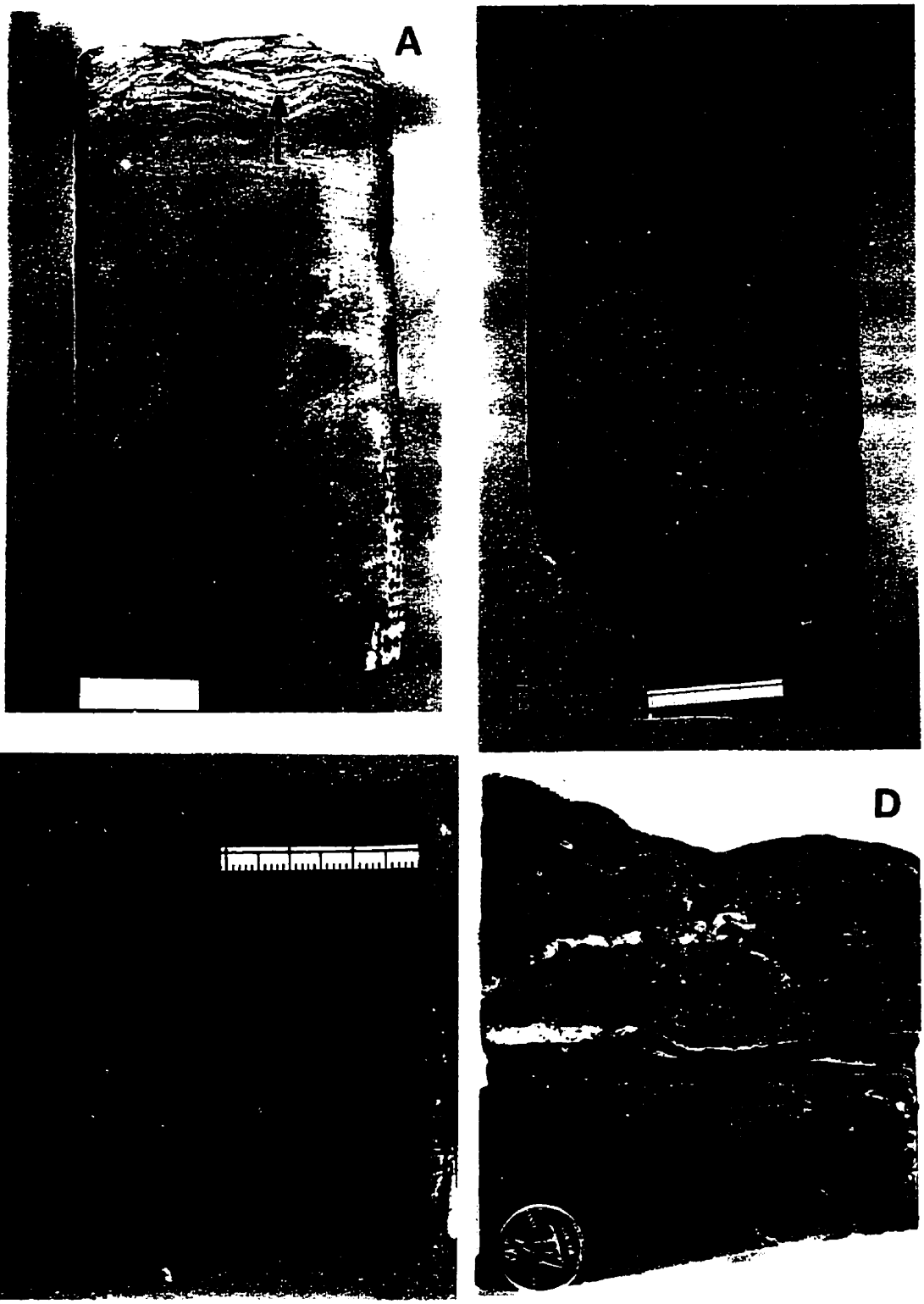
A
D

were truncated by the overlying dolostone. All these features suggest that the discordant carbonate layer underwent early lithification, and that the physical breakage and erosion took place before the overlying sediment accumulated. Thus, this feature may also represent part of a tepee structure.

Parallel- and cross-laminations

Parallel lamination is characteristic of Type A laminated dolostone and has been described previously. Cross-lamination is locally present in the dolomitic rocks. It is well developed in Core 4-19-48-24W2 (Plate 2-5B), which is composed of individual sets less than 5 mm thick. Both planar and trough-shaped units are present. The foreset laminae of the different sets are dipping in only one direction. This cross-lamination is mostly a result of deposition from migrating small-current and wave ripples (Reineck and Singh, 1980). Additionally, small, symmetrical wave ripples are observed in Core 8-14-20-30W1 (Plate 2-2A). Erosive forms of micro-ripples have been observed in Core 13-11-33-23W2 (Plate 2-5C). These ripple forms were produced by scouring of sediment from the ripple troughs (Reineck and Singh, 1980). Hummocky-like cross-lamination is present in some cores.

Microbial structures

Microbial structures are common in the dolomitic facies of central and northwestern Saskatchewan. In contrast, no stromatolites or microbial laminites were observed in southeastern Saskatchewan. They are normally present at the top of the dolomitic unit. Their upper surface was commonly truncated by a paleokarstic surface. They grade downward into dolomite breccia or laminated dolostone. The commonest microbial structures are planar microbial laminites (Plate 2-5D), but domal stromatolites (Plate 2-6A) are locally present in central Saskatchewan. The thickness of the microbialite units ranges from less than 1 cm to 11 cm.

The microbialites are composed of alternating light grey and dark grey laminae. The laminae are from less than 1 mm to more than 2.5 cm thick. In hand specimen, microbial structures show slightly to moderately wavy laminations. In the domal stromatolites, a third type of lamination is present. These laminae are brown and less than 1 mm thick. They are sparse in the lower part of the stromatolite, increasing in abundance toward the top. Such laminae probably record brief periods of exposure and oxidation. However, neither mudcracks nor intraclasts are observed in the [illegible]

PLATE 2-6

Plate 2-6 A: Slabbed core section of Type B laminated dolostone showing a domal stromatolite. Its lower part is characterized by broken stromatoids, which are filled with sand- and pebble-grade dolomitic intraclasts. Lsd. 3-27-38-27W2. Coin diameter is 1.7 cm.

Plate 2-6 B: Slabbed core photograph showing disrupted microbial structures. These are mainly composed of intraclasts with original microbial structure and mudcracks preserved, in the upper right part of the photograph (arrow). Unit A, the Second Red Bed Member. Lsd. 14-19-41-23W3. Coin diameter is 1.7 cm.

Plate 2-6 C: Slabbed hand-specimen photograph showing a sharp contact (c) between Unit A and Unit B of the Second Red Bed Member, water escape structures (w) and microfaults in Unit A, and pockets (p) of clayey sediment in Unit B. The Second Red Bed Member, from the Lanigan potash mine. Scale bar is 3 cm.

Plate 2-6 D: Core photograph showing convolute bedding in the upper part of the core, and Type B brecciated dolomicrite in the lower part. The middle part is composed of dolomitic conglomerate with a sharp erosional surface in the middle. Lsd. 4-2-22-31W1. Coin diameter is 2.3 cm.

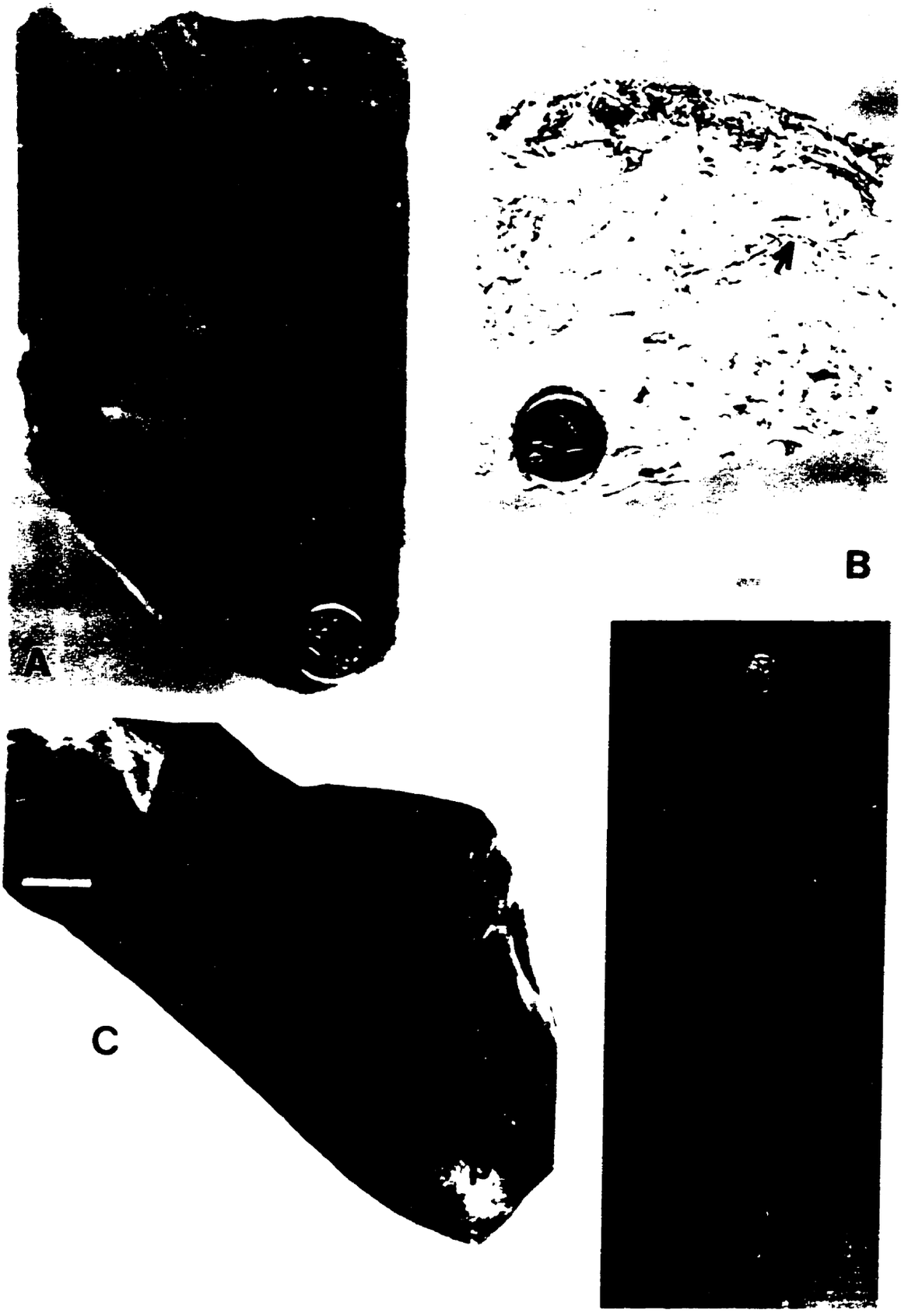
A
B
C

they formed mainly in a perennial subaqueous environment.

In contrast, the predominant microbial laminites are characterized by mudcracks and intraclasts. In Core 14-19-41-23W3, for example, the microbial laminites are represented mainly by intraclasts (Plate 2-6B). Only a small part of the core sample contains original microbial structures. These consist of laminated sediments, a few mm thick, with well-preserved mudcracks. The associated intraclasts are composed of elongate, flattened clasts. They are only about 2-3 mm thick, but up to 15 mm long. They increase in sphericity with decreasing grain size due to a shortening of the long axis, whereas the thickness of the clasts remains similar. These intraclasts are chaotically mixed, but a few are found with vertical to subvertical orientations. They do not appear to be products of storm processes, as suggested by Dunn (1982a). The close association of the intraclasts with the eroded microbial structures implies that these intraclasts are desiccated fragments of microbial mats.

In Core 3-30-37-2W3, a microbial mat is present in the uppermost part of the Second Red Bed Member, where it overlies a dolomitic wackestone containing mat debris (Plate 2-5D). These mats are laterally discontinuous, showing evidence of penecontemporaneous erosion. The microbial debris is very small, mostly of sand grade. The fragments are brown, which distinguishes them from the dark grey dolomitic matrix. Some relatively large intraclasts, up to 1 cm in diameter, are also present.

Microfaults

Minor faulting structures were frequently observed in the dolostone (Plates 2-2C, 2-6C). They were first reported by Dunn (1982a), but no explanation was presented. These microfaults are confined to the dolostone and they did not develop in the directly overlying or underlying sedimentary rocks. They are most obvious in the laminated dolostone, and are clearly syndepositional features because they are intrastratal. Both normal and thrust faults are present. Beds show displacement of up to 1.5 cm. Most fault planes dip at more than 60°; some are vertical. In southeastern Saskatchewan, single fault planes usually cross cut the entire dolostone unit (Plate 2-2C), whereas in central Saskatchewan, the microfaults usually cross cut mm-thick layers of the dolostone. Different layers are displaced by microfaults, indicating multiple phases of faulting.

Similar microfaults were described by Pratt (1994) from the

Formation of Montana and were considered to indicate synsedimentary seismic activity. This interpretation may also be applicable to the formation of the microfaults in the present study. This implies that during the deposition of the dolomitic sediments, central Saskatchewan was more frequently affected by earthquakes than southeastern Saskatchewan. An alternative explanation is that the microfaults were produced by thermal expansion when the sediment was subaerially exposed. Because the dolomitic sediments in central Saskatchewan experienced more frequent subaerial exposure than the sediments in southeastern Saskatchewan (see below), there are more microfaults in the former region than in the latter. This implies that the depositional environment in central Saskatchewan had shallower water than that in southeastern Saskatchewan. This implication is supported by the fact that the microbial mats and tepee structures are well developed in central Saskatchewan, but they are absent in the dolostones of southeastern Saskatchewan. The presence of abundant, thin layer-confined microfaults in central Saskatchewan indicates that the dolomitic sediments underwent early lithification and experienced more microfaulting than those in southeastern Saskatchewan. This, in turn, suggests that the sediments were subaerially exposed more frequently in central Saskatchewan than in southeastern Saskatchewan.

Convolute bedding

Convolute bedding is common in the laminated dolostone within the few cm directly above Unit B (Plates 2-2A, 2-5B, 2-6D). It is characterized by complex recumbent folds, but faulting and slipping are normally absent, indicating a predominantly plastic deformation. Above the rocks with convolute bedding lies the laminated dolostone with well-preserved parallel laminae (Plate 2-1B). No truncation surface is present between the convoluted dolostone and laminated dolostone. Locally, cups are developed at the base of the laminated dolostone, but the laminae are only slightly compressed and disrupted. The top of the underlying sediment of Unit B is slightly injected upward into the laminated dolomitic sediment (Plate 2-1B). Pillar structures (described below) are present directly below the convoluted dolostone.

Several explanations have been proposed for the genesis of convolute bedding. Liquefaction is generally believed to be the most important factor (Reineck and Singh, 1980). The smoothly deformed laminae that lack faults are typical of deformation by liquefaction and fluidization as opposed to localized intergranular shear, which occurs along discrete shear planes (Maltman, 1987a, 1987b; [illegible], 1987). Some

that liquefaction of a sediment can be achieved by earthquakes (e.g., Allen and Banks, 1972; Pratt, 1994); others have proposed that groundwater movements are responsible (e.g., Williams, 1970). The origin of the convolute bedding in the dolostones of Unit A is not clear. The well-preserved parallel laminae in the upper part of the dolostone indicate that the liquefaction took place when the upper part of the laminated dolostone was already lithified. Early cementation and lithification of carbonate sediment are commonly associated with subaerial exposure. It is likely that, because of early cementation of surficial carbonate sediment, a layer of low permeability was formed, which impeded the upward movement of groundwater.

Three types of liquefaction can be distinguished (Allen, 1982). Of these, static liquefaction is induced by an increase in pore-fluid pressure that is related to groundwater movement in a permeable layer beneath an impermeable or low permeability cap. Triggers that directly influence pore-fluid pressures include artesian groundwater movement and the escape of excess pore-water from underlying sediment that is compacting or has liquefied.

Pillar structure

Pillar structure (Lowe and LoPiccolo, 1974) is locally present in the dolomitic conglomerate directly below the laminated dolostone (Plate 2-1B). It slices steeply through the conglomerate. In cross section it is characterized by numerous, regularly spaced, vertical to sub-vertical streaks, with numerous bifurcations. Three-dimensional exposures indicates that it is oriented perpendicular to bedding and is tubular to sheetlike in shape.

Broken stromatoids

Broken stromatoids are present in Core 3-27-38-27W2 (Plate 2-6A). They are present in the lower part of a domal stromatolite and overlie dolomitic sediment composed of coarse sand- and pebble-grade intraclasts. These stromatoids exhibit crumpled laminae that are broken and cross-cut by small fractures. Originally coherent laminae are now split. They are now separated by irregular pockets of intraclasts that are identical in composition to the directly underlying sediment, which suggests that they were derived from below by injection.

PLATE 2-7

Plate 2-7 A: Photomicrograph showing gypsum crystals floating in microcrystalline dolomite, plane-polarized light. Unit A, the Second Red Bed Member. Lsd. 41-1-12-34-1W3. Scale bar is 0.5 mm.

Plate 2-7 B: Photomicrograph showing silicified microfossils -- probably ostracods (o) -- in microcrystalline dolomite. Unit A, the Second Red Bed Member. Lsd. 13-11-33-23W2. Scale bar is 0.5 mm.

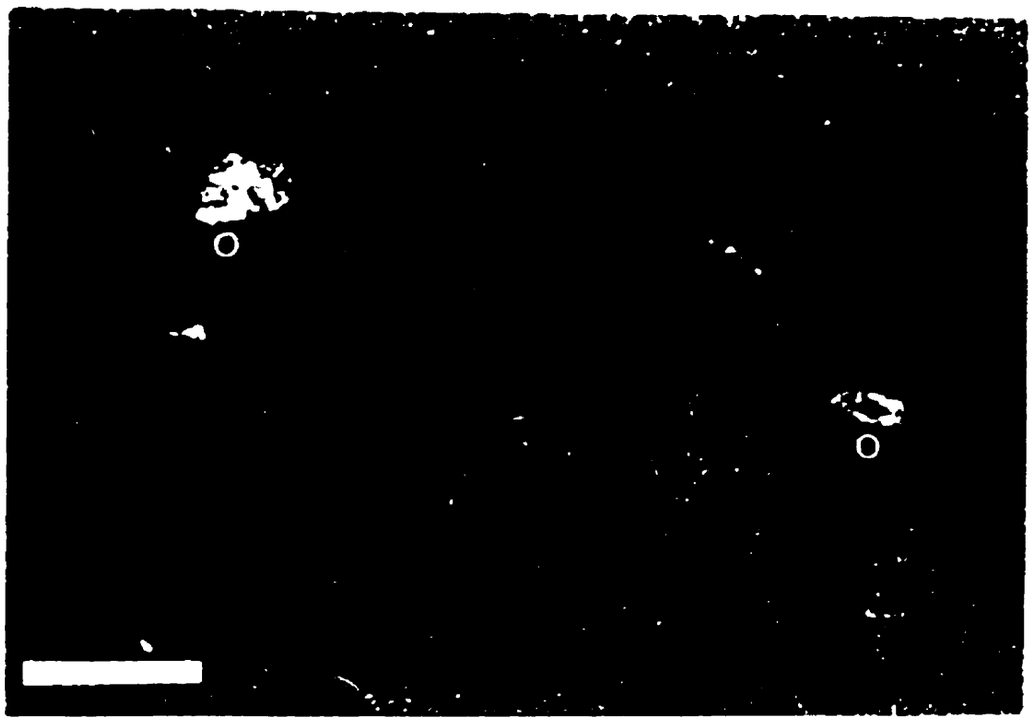

Evaporite minerals

Small amounts of evaporite minerals are present in the dolostone. They typically form small crystal aggregates within the dolomitic rocks and are never preserved as distinct evaporite layers. Halite is the most common evaporite mineral, but a few gypsum crystals (Plate 2-7A) were also observed. The cubic halite crystals are generally smaller than 5 µm. Additionally, sparse anhydrite nodules are present in the dolostone (Plate 2-2C). The anhydrite nodules, which have a diameter less than 1 cm, cross-cut the laminations, showing that they are probable secondary. Similar anhydrite nodules are very common in normal marine limestones of the Burr and Neely members of the Dawson Bay Formation, where they clearly are diagenetic.

Biota

The dolomitic rocks of the Second Red Bed Member have only very rare fossils. No normal marine fossils are present. Rare ostracods were first reported by Dunn (1982), and a few examples were found in this study (Plate 2-7B). The restricted ostracod fauna and absence of normal marine fossils indicate that the depositional environment was either brackish or hypersaline.

2.5 Discussion

The dolomitic rocks in Unit A are composed of microcrystalline dolomite. Although the directly underlying sedimentary rocks experienced pedogenesis (as described and discussed in the following sections), these dolomitic rocks contain well-preserved sedimentary structures and lack calcrete or other pedogenic features. This indicates that they are depositional in origin and were deposited after the major phases of pedogenesis. This interpretation is supported by the sharp, disconformable contact between the dolostone unit and the underlying paleosol profile. The presence of well-preserved sedimentary and penecontemporaneous structures, the absence of replacive features in the dolostone, and the contemporary erosional surface at the top of the dolostone unit, all indicate that the dolomite was primary or penecontemporaneous in origin.

The significance of the halite, gypsum and anhydrite is more difficult to assess, because there is evidence for several stages of salt precipitation, some postdating burial. For

the Burr and Neely members. The anhydrite nodules in the fossiliferous limestones of the overlying Burr and Neely members are also clearly unrelated to the depositional environment. However, the presence of halite and gypsum, though ambiguous in interpretation, is not incompatible with the environments proposed for the Second Red Bed sedimentation. Indeed, given proximity to the underlying Prairie Evaporite Formation salts, saline groundwater would likely have existed close to the sediment surface throughout the time-period represented by the Second Red Bed Member. Thus some interstitial precipitation of salts, during or shortly after sedimentation, would be probable, especially at times of subaerial exposure.

Most dolomite grains in the Second Red Bed Member are very small, with diameters ranging from 1 to 4 μm. In modern environments, similar dolomite grains have been found in (1) the marine supratidal environments of the Persian Gulf (Illing *et al.*, 1965), the Florida Keys (Carballo *et al.*, 1987), the Bahamas (Shinn *et al.*, 1965), and elsewhere in the Caribbean (Deffeyes *et al.*, 1965); (2) the marine-marginal lakes of the Coorong region (von der Borch, 1965; von der Borch and Lock, 1979; Rosen *et al.*, 1988; Rosen and Coshell, 1992); (3) hypersaline marine lagoons (Gunatilaka *et al.*, 1984), and (4) several continental saline lakes, such as those of western Victoria, Australia (De Deckker and Last, 1988).

Today, dolomite in the supratidal environment of the Persian Gulf is associated with microbial mats, nodular anhydrite, carbonaceous bands and marine fossils. Both laterally and vertically it grades into intertidal and subtidal sediments. This type of dolomite forms under high aridity and has been widely used as a model for many ancient microcrystalline dolomites. Dolomite in marine marginal lagoons forms in organic-rich muds, commonly where sulfate reduction is taking place. The dolomite forming in the Coorong region is considered primary (Warren, 1990), and is characterized by tepee structures, tepee breccias, stromatolites, thin depositional units and a lack of evaporites. This dolomite is forming in a relatively humid climate (Muir *et al.*, 1980). However, Coorong-type dolomite has rarely been recognized in the geological record (Tucker, 1990).

The dolomitic rocks in the Second Red Bed Member have features similar to those in the Coorong region. Both of them occur as thin capstones on the top of successions. Both are composed of massive to laminated dolostone and intraclast breccias. Warren (1988) suggested that the presence of this capstone unit, in conjunction with laminated sediments,

Additionally, although the dolostone in the Second Red Bed Member extends hundreds of kilometers across the Canadian part of the Williston Basin, it does not appear to grade directly into intertidal and subtidal marine sediments either laterally or vertically. Furthermore, these dolomitic rocks lack the evaporite layers, black carbonaceous bands and marine fossils that characterize the dolomite forming in modern and ancient sabkha environments (e.g., Amiri-Garroussi, 1988).

From the sedimentological evidence, it can be concluded that the dolomite in the Second Red Bed Member was probably deposited in a setting with characteristics more similar to a Coorong-like environment than a typical marginal-marine sabkha. The presence of only small amounts of possible primary evaporites in the dolomitic sediment suggests that hypersaline waters were only briefly present. However, like dolomite in the Coorong region, the abundant evidence for subaerial exposure but a paucity of evaporites may indicate that the basin had seasonally alternating, arid and humid climatic conditions. This conclusion is strongly supported by the presence of the vertisol profile in the directly underlying sediments, which also implies a seasonally alternating, arid and humid climate (Gu and Renaut, 1995).

The paleogeography of the basin during the period of the SRBM sedimentation is very difficult to reconstruct. The local presence of domal stromatolites in central Saskatchewan may indicate that the water was slightly deeper in that area than that in northwestern Saskatchewan, where only flat microbial mats are present. In southeastern Saskatchewan, the dolostone is composed only of laminated and massive dolomitic sediments with sparse intraclasts. Neither stromatolites nor mudcracks were observed. Except in Core 9-14-23-33W1, tepee breccias are absent. These features suggest that the dolomite deposition in southeastern Saskatchewan took place in a body of water that was perennial for most of the period of sedimentation. From this evidence, it can be concluded that the depositional environment changed from mainly ephemeral water bodies in the northwest to nearly perennial submergence in southeastern Saskatchewan.

While the dolostones share many attributes of Coorong-type dolomites, with present evidence it is difficult to determine whether sedimentation took place in a Coorong-like environment, mostly isolated from the sea, or from waters of mixed continental-marine derivation that periodically inundated the vast, often emergent, plain. The common presence of black argillaceous grains in the dolomitic rocks, which are believed to have

played a major role in the deposition of dolomitic sediments. However, it is unclear if the depositional environment was affected by marine water. Further research must be carried out to answer this question. The scale difference between the two basins is vast, thus the analogies are more process oriented than for depositional setting.

2.6 Argillaceous Dolomitic Rocks and Mudstones in Units B, C and D

2.6.1 Unit B

Unit B is widespread in the subsurface of Saskatchewan. It consists of argillaceous dolomitic rocks, with a thickness up to 80 cm. The top of Unit B is truncated by an erosional surface (Plate 2-8B). The erosional surface is locally characterized by a `gilgai' microrelief (Plate 2-9C). It is sharply and unconformably overlain by Unit A (Plate 2-8B) or by the Burr Member (Plate 2-9C) where Unit A is absent.

In central Saskatchewan, where Unit A is absent, Unit B represents the top of the Second Red Bed Member. It is massive and characterized by numerous fractures (such as in Well 4-18-35-8W3) (Plate 2-9C), which cause the rocks to take the form of rhombohedral or angular to blocky aggregates. Most fractures are arcuate or bowl-shaped. They vary from subhorizontal to subvertical. The fractures close to the top of the unit are filled with black argillaceous sediment identical to the black shale that rests directly on the top of the Second Red Bed Member (Plate 2-9D), which indicates that the fractures have a penecontemporaneous origin. In central and southeastern Saskatchewan, where Unit A is present, Unit B is more cohesive and less severely brecciated (Plate 2-10C & F). In these regions, it is composed of both brecciated and well-consolidated dolomitic rocks.

Petrographically, Unit B is composed of dolomitic conglomerate, dolomitic breccia, massive dolomicrite and brecciated dolomicrite. In the following sections, each of the rock types is described in detail.

Dolomitic Conglomerate

Dolomitic conglomerate is the predominant rock type in Unit B. In central Saskatchewan where Unit A is absent, entire Unit B is composed of dolomitic conglomerate, which is up to 80 cm thick (such as in Well 4-18-35-8W3 and 10-7-32-5W3) (Plates 2-9C, E & F, 2-11D). The dolomitic conglomerate grades downward into argillaceous mudstone with

PLATE 2-8

Plate 2-8 A: Photomicrograph of dolomitic conglomerate showing a large dolomitic intraclast that is composed of smaller ones, probably indicating multi-cycles of fracturing and recementation. Unit B, the Second Red Bed Member. Lsd. 4-18-35-8W3. Scale bar is 0.5 mm.

Plate 2-8 B: Slabbed core photograph showing sharp truncation of Unit B (b) by Unit A (a). Unit B, which is composed of dolomitic conglomerate, contains vertical cracks (v) filled with dolomite. Lsd. 6-18-36-6W3. Scale bar is 3 cm.

Plate 2-8 C: BSE micrograph of dolomitic conglomerate that consists predominantly of broken dolomite, with minor K feldspar, quartz and clay minerals. Lsd. 4-18-35-8W3.

Plate 2-8 D: SEM photomicrograph of the dolomitic veins in Plate 2-8 B. These are composed of well-crystallized dolomite rhombs. Lsd. 6-18-36-6W3.

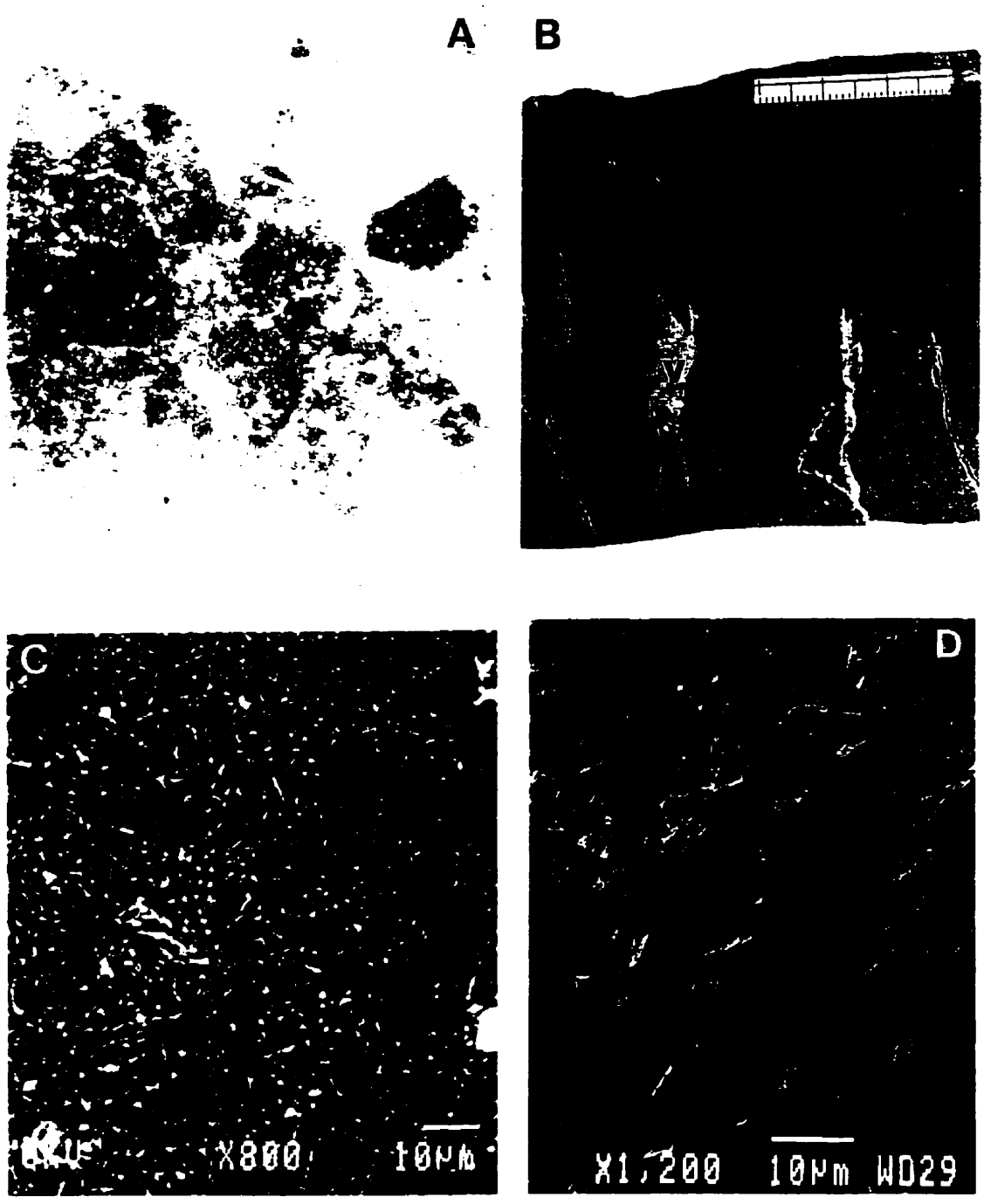
A
B
C
X800 10µm
D
X1,200 10µm WD29

PLATE 2-9

Plate 2-9 A, B and C: Detail core photograph showing the Second Red Bed Member from base to top. The top of the Second Red Bed Member is sharply overlain by black shale B (b) of the Burr Member. Lsd. 4-18-35-8W3. (One core box is 0.76 m long and core diameter is 10.1 cm.)

Plate 2-9 D: Slabbed core photograph showing the top of the Second Red Bed Member. This is characterized by fractures filled with black shale identical to that of black shale B. See also Plate 2-9 C. Lsd. 4-18-35-8W3. Coin diameter is 1.7 cm.

Plate 2-9 E: Slabbed core photograph of dolomitic conglomerate showing intraclasts with colour variation from light grey, olive green to black. Lsd. 4-18-35-8W3. Scale bar is 3 cm.

Plate 2-9 F: Slabbed core photograph of dolomitic conglomerate showing clay stringers (s). Lsd. 4-18-35-8W3. Coin diameter is 1.7 cm.

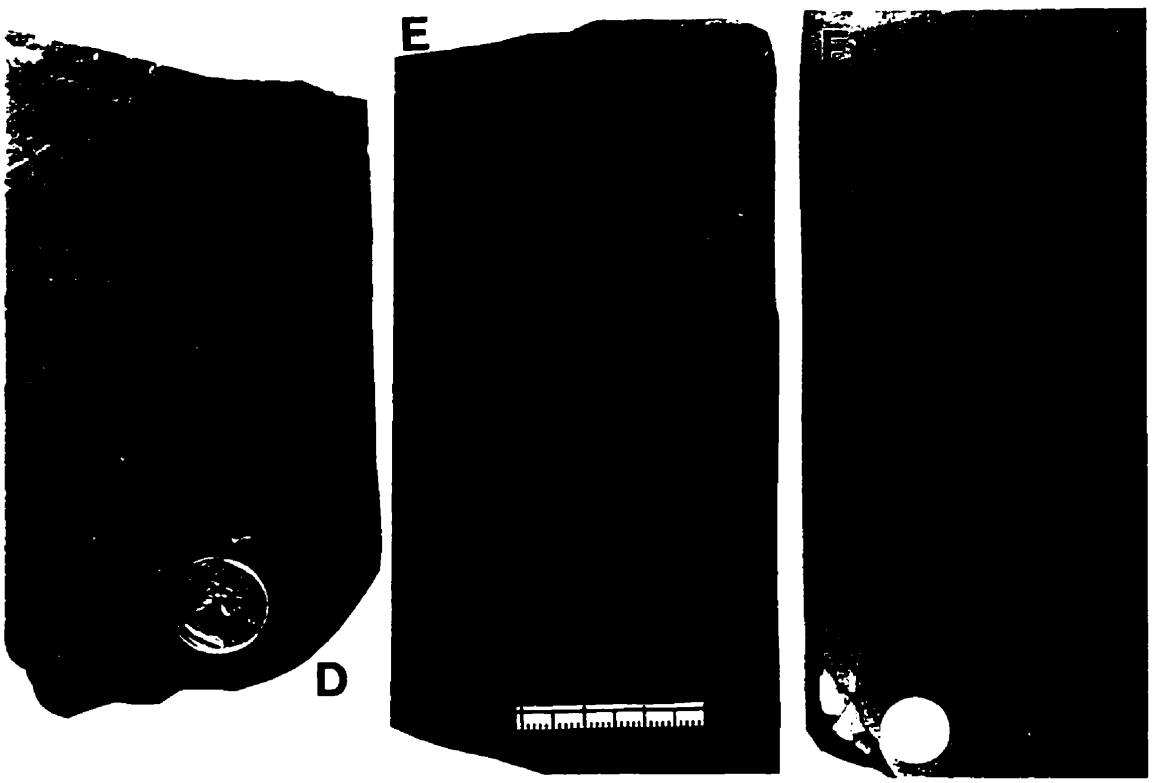
E
D

PLATE 2-10

Plate 2-10 A, B and C: Core photograph showing the Second Red Bed Member from base to top. Lsd. 13-12-22-32W1. (One core box is 0.76 m long and core diameter is 10.1 cm.)

Plate 2-10 E, F and G: Core photograph showing the Second Red Bed Member from base to top. Lsd. 3-27-38-27W2. (One core box is 0.76 m long and core diameter is 10.1 cm.)

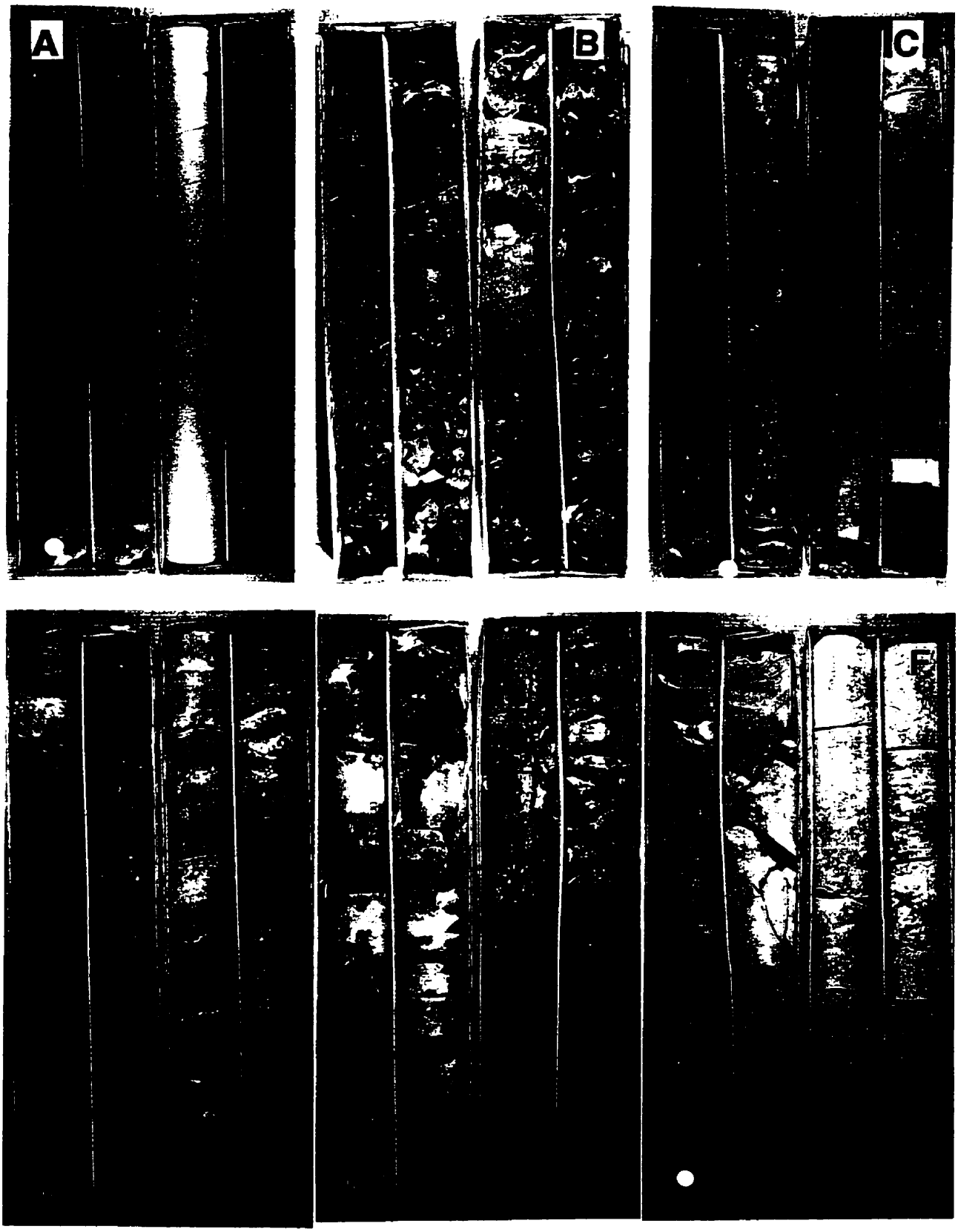
A
B
C
F

PLATE 2-11

Plate 2-11 A: Core photograph showing dolomitic conglomerate (d) in Unit B of the Second Red Bed Member underlain by brecciated dolomicrite (b), which in turn overlies massive dolomicrite (m). Lsd. 8-14-20-30W1. (One core box is 0.76 m long and core diameter is 10.1 cm.)

Plate 2-11 B: Hand specimen photograph showing a sharp contact (c) between dolomitic conglomerate and massive dolomicrite of Unit B, the Second Red Bed Member. Clayey sediment (s) is highly concentrated directly above the contact, which shows wavy lamination. The Lanigan potash mine. Scale bar is 3 cm.

Plate 2-11 C: Slabbed core photograph showing the sharp contact (c) between Unit A and B of the Second Red Bed Member. Unit B consists of dolomitic conglomerate (d), containing intraclasts that display a jigsaw fit, which suggests *in situ* brecciation. The Cominco potash mine. Scale bar is 3 cm.

Plate 2-11 D: Optical micrograph of dolomitic conglomerate. Unit B, the Second Red Bed Member. Lsd. 4-18-35-8W3. Scale bar is 0.5 mm.

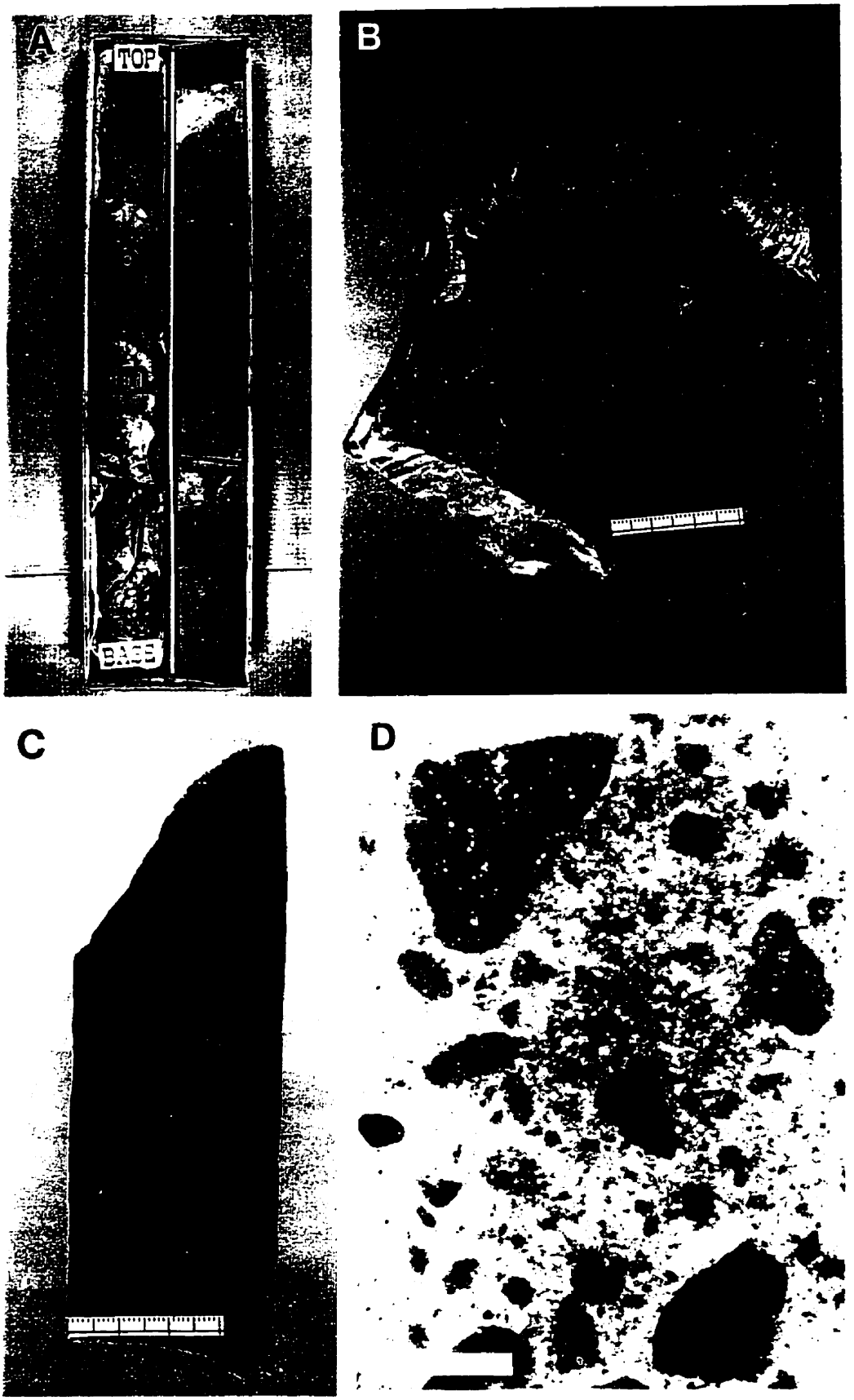
A
TOP
BASE
B
C
D

blocky fractures that, in turn, is underlain by completely disintegrated, olive-green mudstone of Unit C (Plate 2-9B).

Where Unit A is present in central and southeastern Saskatchewan, the dolomitic conglomerate is present as two relatively thin horizons in Unit B (Plate 2-11A). They are separated by dolomitic breccia, massive dolomicrite and brecciated dolomicrite. Each horizon is less than 20 cm thick. Vertically, the dolomitic conglomerate is underlain by massive dolomicrite or brecciated dolomicrite. The contact between them is sharp and irregular (Plate 2-11B).

Petrographically, the dolomitic conglomerate is composed of sand- to pebble-grade, monotonous dolomitic intraclasts, with a mixed argillaceous and carbonate matrix (Plates 2-9E & F, 2-11C & D). It is structureless and has a fabric varying from mud- to grain-supported. The dolomitic intraclasts are poorly sorted, randomly oriented, and angular to well-rounded. Some intraclasts consist of nearly structureless dolomicrite; others contain crenulate microbial laminae. Most intraclasts show some rotation, but a few show a jigsaw fit (Plate 2-11C). The latter indicate *in situ* brecciation. The colour of the intraclasts varies from light grey, through olive-green, to dark grey and black (Plate 2-9E). Mixing of differently coloured intraclasts indicates that they are probably derived from different parent sediments (or rocks). In addition, a few intraclasts in the dolomitic conglomerate from central Saskatchewan appear to be multicyclic, exhibiting multiple fracturing and recementation (Plate 2-8A). Detailed thin-section study shows that although intraclasts are all dolomitic in composition, their subsidiary mineral composition is variable. Some contain a significant amount of detrital grains of silt- to fine sand-grade anhydrite. Others do not. SEM study shows that the intraclasts consist predominantly of dolomite, with subordinate clay minerals, pyrite, potassium feldspar and quartz (Plate 2-8C). Dolomite grains are generally less than 10 μm in diameter. Some are euhedral, whereas others are worn and abraded. Pyrite is present both as single microcrystals and as framboidal aggregates.

The matrix of the dolomitic conglomerate is composed of dolomite, illite, chlorite, with subsidiary silt-grade quartz and potassium feldspar. The clay content of the sediment increases significantly downward. Additionally, stringers of olive-green to dark grey clay sediment are very common in the conglomerate (Plates 2-9F, 2-6C), and are locally characterized by fine laminae (Plate 2-11B). Moreover, the clay sediment is also found to rest only on the upper surface of some intraclasts. Similar features have been termed shelter

fabrics (Ettensohn *et al.*, 1988). They form when descending vadose waters encounter locally impermeable barriers during eluviation. These barriers prevent further downward movement of soil water, resulting in the buildup of vadose sediment only on the upper surface of particles (Ettensohn *et al.*, 1988).

No primary sedimentary structures have been found in the dolomitic conglomerate. However, small secondary, vertical cracks that are filled with carbonate sediment are locally present (in Core 6-18-36-6W3) (Plate 2-8B). These cracks are sharply truncated by the dolostone of Unit A, indicating that they formed before the deposition of Unit A. Scanning electron microscopy (SEM) study shows that the carbonate sediment filling the cracks consists of pure, well-crystallized dolomite rhombs, less than 10 microns in diameter (Plate 2-8D).

Additionally, a large vertical crack is present in Core 9-22-23-6W2 (Plate 2-12A). It has a measurable width of 2 cm and a height of 12 cm (the real width and height of the crack cannot be measured because it extends beyond limit of the core). The crack is filled with a mixture of clay, and dolomitic silts, sands and pebbles. The filling sediment disintegrates readily if wetted. In contrast, the wall rock of the crack consists of well-lithified dolomitic conglomerate. The contact between the filling materials and wall rock is sharp and vertical. The top of the fracture is truncated by the laminated dolostone of Unit A, showing that the crack predates the latter.

Interpretation

The dolomitic conglomerate is the dominant rock type in Unit B. It was previously interpreted as a product of rip-up disruption associated with storms (Dunn, 1982a; Braun and Mathison, 1986). However, no storm- or current-related sedimentary structures are found in the dolomitic conglomerate. Instead, the rock is massive and structureless. It is characterized by a sharp erosional surface, gilgai micro-lows, *in situ* brecciation, vertical cracks, arcuate- to bowl-shaped fractures, angular to blocky aggregates, and a downward increase in the amount of clay. These features cannot be attributed to storm processes, but they are typical of soils. This suggests that the dolomitic conglomerate probably formed by pedogenesis, or that the conglomerate was at least reworked by pedogenesis. Similar rocks, described by Rizzi and Braithwaite (1996), were interpreted to reflect subaerial exposure.

PLATE 2-12

Plate 2-12 A: Core photograph showing dolomitic conglomerate of Unit B truncated by laminated dolostone of Unit A. The right part of the core is composed of well-lithified dolomitic conglomerate. Although the left part also consists of dolomitic conglomerate, the rock disintegrated readily when wetted. The latter probably represents material infilling a vertical crack. Lsd. 9-22-23-6W2. Coin diameter is 1.7 cm.

Plate 2-12 B: Slabbed core photograph showing Type A brecciated dolomicrite of Unit B, the Second Red Bed Member. The rock is characterized by intraclasts formed by *in situ* brecciation (b) and channel-like voids (c). The Cominco Potash mine. Scale bar is 3 cm.

Plate 2-12 C: Slabbed core photograph showing Type B brecciated dolomicrite. Unit B, the Second Red Bed Member. Lsd. 13-34-22-31W1. Scale bar is 3 cm.

Plate 2-12 D: Slabbed core photograph showing dolomitic breccia. Unit B, the Second Red Bed Member. Lsd. 13-34-22-31W1. Scale bar is 3 cm.

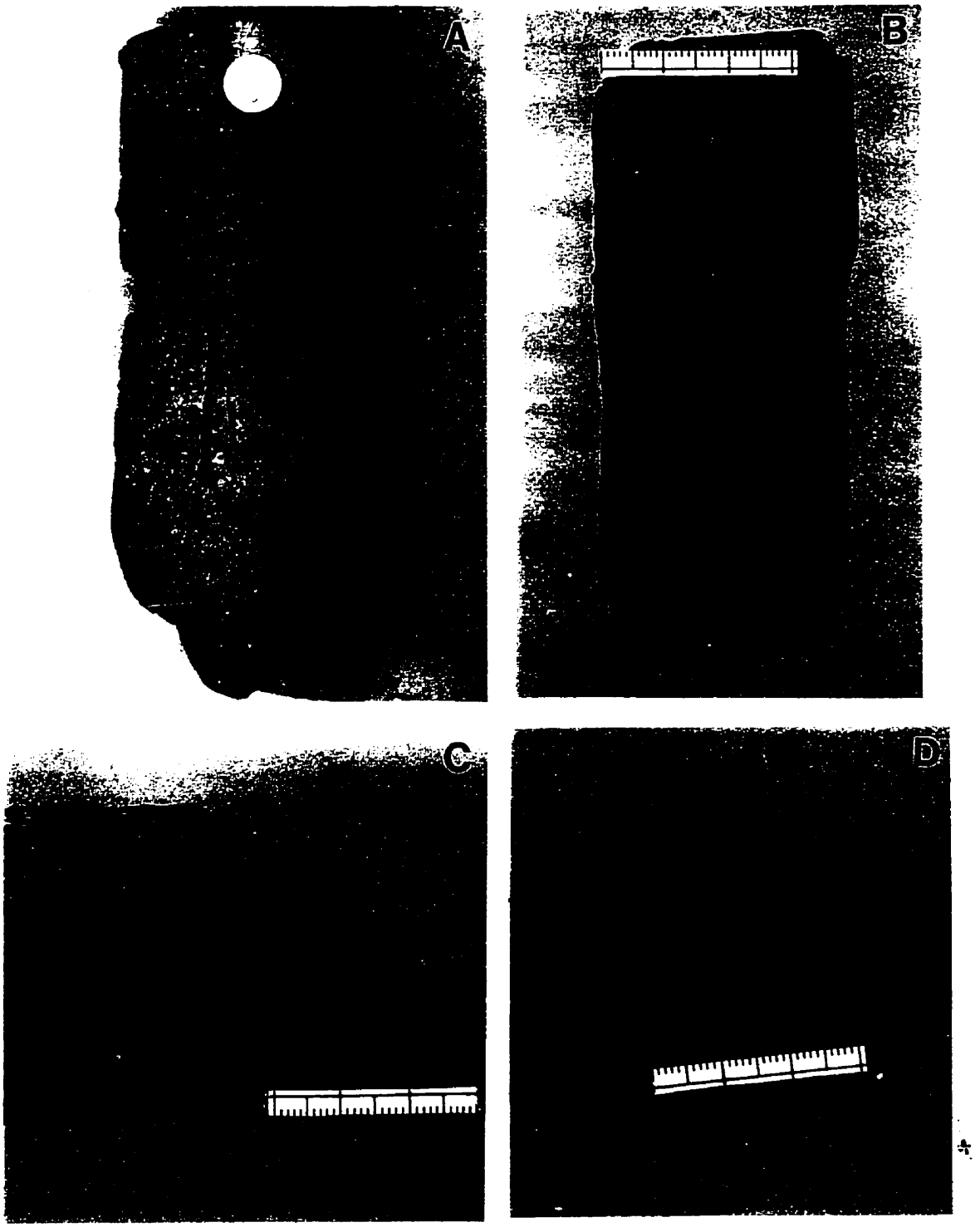
A
B
C
D

Brecciated Dolomicrite

The brecciated dolomicrite is only present in those cores that contain Unit A. It can be subdivided into Types A and B brecciated dolomicrite.

Type A brecciated dolomicrite

Type A brecciated dolomicrite lies directly below the dolomitic conglomerate (Plate 2-11A). It is composed of dolomitic intraclasts and characterized by fractures and channel-like voids (Plate 2-12B). The intraclasts are angular, irregular, and have the same composition and colour as the intraclasts in the directly overlying dolomitic conglomerate. Almost all of the adjacent intraclasts can be fitted back together, indicating *in situ* brecciation. The channel-like voids are mostly vertical to subvertical with a width of several millimetres. They are filled with olive-green clay to light grey carbonate sediments. Fine laminae can be observed in the infilling sediments, which are parallel to the channel walls. Some voids also contain subangular to well-rounded, sand- to pebble-grade intraclasts (Plate 2-12B), which were probably washed in from above. The brecciated dolomicrite grades downward into well-consolidated massive dolomicrite.

Interpretation

The filling of the fractures and channel-like voids of the brecciated dolomicrite by olive-green to light-grey clay and carbonate sediment indicates a primary or penecontemporaneous origin for these cracks. The irregularity of the cracks precludes the possibility that they are simply compacted mudcracks formed by desiccation when sediment was subaerially exposed. Similar channel-like voids in the Upper Pennsylvanian Iatan Limestone of southwestern Iowa were interpreted to form by periodic wetting and drying during pedogenesis, and by plant rooting activity (Goebel *et al.*, 1989). Because the brecciated dolomicrite is directly overlain by the dolomitic conglomerate that had experienced pedogenesis, it is likely that the channel-like voids in the brecciated dolomicrite also formed by pedogenesis, and that Type A brecciated dolomicrite represents a transition between fresh bedrock and a soil horizon.

Type B brecciated dolomicrite

Type B brecciated dolomicrite is olive-green and has a thickness ranging from a few

centimetres to tens of centimetres. It is composed of dolomitic intraclasts and matrix. The rock is characterized by narrow, jagged cracks or sinuous cracks with indistinct edges (Plate 2-12C). Most cracks are mm in width and are filled with internal sediments of olive-green clay and carbonate. The intraclasts are several cm in length, with their long axis parallel to the bedding plane. They are angular to subangular in shape. These intraclasts show little or no evidence of displacement or rotation and most adjacent intraclasts can be fitted back together, indicating *in situ* brecciation.

Interpretation

Rocks with similar structures have been described by Smoot and Olsen (1988). The brecciated dolomicrites are interpreted as sediments that were disrupted by repeated desiccation and rewetting over long periods of very slow deposition, by analogy to processes occurring on modern playa flats (Smoot, 1981; Smoot and Katz, 1982).

Dolomitic Breccia

Dolomitic breccia is interbedded with Type B brecciated dolomicrite, with a thickness generally less than 10 cm. It is composed of subangular to subrounded intraclasts in a dolomitic matrix and has a grain-supported fabric (Plate 2-12D). The intraclasts are light grey to olive-green, dolomitic and moderately sorted. They are normally less than 1 cm in length. Most intraclasts have their long axis parallel to bedding plane, with imbricate structure locally present. Most of the adjacent intraclasts cannot be fitted together. The dolomitic matrix has a slightly lighter hue than the adjacent intraclasts.

Interpretation

The association of the dolomitic breccia with Type B brecciated dolomicrite indicates that they are closely related in origin. This is supported by the identical colour and composition of the intraclasts in the breccia to those of the brecciated dolomicrite. However, the greater roundness of the intraclasts in the breccia suggests that they were reworked by physical processes. This interpretation is supported by the presence of imbricate structure. Thus, the origin of the breccia may be due to the reworking of Type B brecciated dolomicrite by currents during periods of submergence.

PLATE 2-13

Plate 2-13 A: Slabbed core photograph showing massive dolomicrite from Unit B of the Second Red Bed Member. Parts of the slabbed core contain indistinct horizontal lamination and small burrows. Lsd. 13-34-22-31W1. Scale bar is 3 cm.

Plate 2-13 B: Optical micrograph of massive dolomicrite composed of micritic to microspar dolomite and minor black argillaceous sediment. Lsd. 13-34-22-31W1. Scale bar is 0.25 mm.

Plate 2-13 C: Slabbed core photograph of massive dolomitic mudstone from Unit C of the Second Red Bed Member that is characterized by jagged, sinuous cracks. Lsd. 14-32-20-30W1. Scale bar is 3 cm.

Plate 2-13 D: Optical micrograph of massive dolomitic mudstone that contains an abraded anhydrite crystal. Unit C of the Second Red Bed Member. Lsd. 14-32-020-30W1. Scale bar is 0.25 mm.

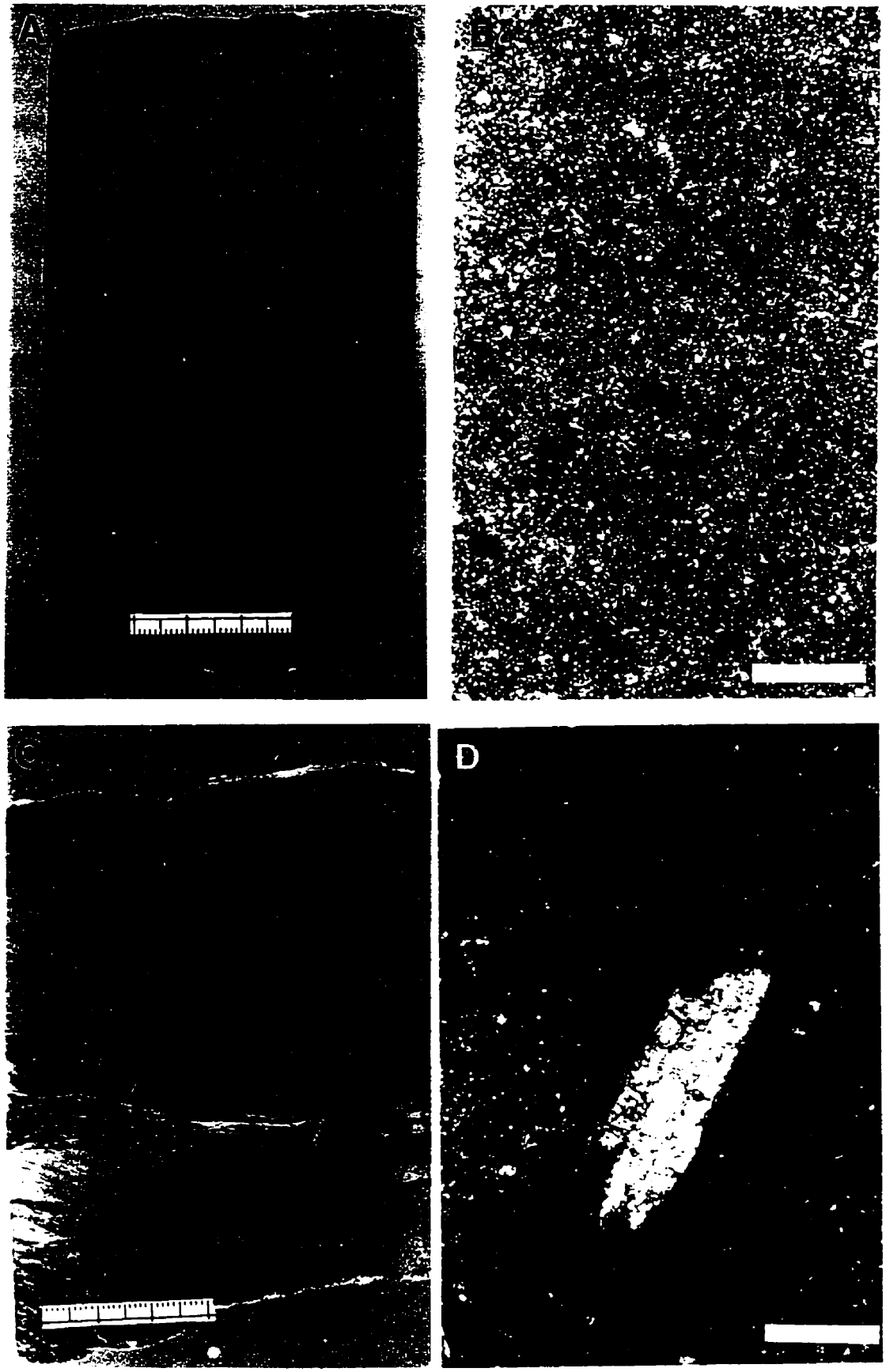
A
B
C
D

Massive Dolomicrite

Massive dolomicrite is present in Unit B in central and southeastern Saskatchewan where Unit A is present. It lies below brecciated dolomicrite. The rock is well consolidated, olive green and massive. Locally, remains of indistinct horizontal laminations are present (Plate 2-13A). Small, indistinct burrows can be observed in places (Plate 2-13A), but they cannot be identified with confidence. Petrographic study shows that the rock is composed of dolomite, clay minerals and silt-grade quartz and potassium feldspar (Plate 2-13B).

Locally, very abundant silt-grade, detrital anhydrite grains are dispersed in the dolomitic matrix. They are well rounded. However, no *in situ* preserved evaporites or fossils are present in the rock.

Interpretation

The well-consolidated nature of the rock and the preservation of physical sedimentary structures indicate that this rock experienced little pedogenesis. The depositional environment of the massive dolomicrite is difficult to reconstruct. However, the similarity of this rock to the massive dolostone in Unit A may indicate that they were deposited in similar environments, in which salinity of the waters was not too high for animals to live. The absence of mudcracks may indicate a perennially aqueous depositional environment.

2.6.2 Unit C

Unit C ranges from 2 to 6 m thick. It is normally overlain by Unit B and underlain by Unit D. Where Unit A is present, Unit C is composed of massive dolomitic mudstones, with a colour change from red-brown in the lower part to dark grey in the upper part. Boundaries between different coloured horizons are gradational. Slickensides and arcuate fractures are highly developed, which cause the dolomitic mudstones to disintegrate into angular blocky to wedge-shaped aggregates (Plate 2-10B, C, E & F). There are generally more slickensides and arcuate fractures in the upper part than in the lower part of Unit C. Where Unit A is absent, Unit C consists predominantly of a black to olive green, fissile argillaceous mudstone (shale) that is completely disintegrated into small pieces 1-2 cm long (Plate 2-9A & B). The rock is massive and lacks primary sedimentary structures. No slickensides are observed in the black argillaceous mudstone, but close to the bottom of this unit, slickensides are present in the red-brown massive mudstone. Scattered halite

chips are present throughout this unit.

Petrographically, the red-brown to dark-grey dolomitic mudstones in Unit C are characterized by blocky or hackly fractures that make the rocks break up easily into small blocks with curved faces. Some mudstone horizons have crumbled almost completely into small fragments. The mudstones are generally massive and structureless. However, horizons composed of mudstone intraclasts and characterized by narrow, jagged cracks or sinuous cracks are locally present. The cracks are filled with brown argillaceous sediment (Plate 2-13C). The mudstone intraclasts vary from mm to cm in length, with their longest axes parallel or sub-parallel to bedding plane. Most intraclasts can be fitted back together, indicating *in situ* brecciation and little displacement or rotation. A similar type of mudstone was described by Smoot and Olsen (1988). It was named a "mud-cracked massive mudstone" and formed by repeated desiccation and rewetting over long periods of very slow deposition (Smoot and Olsen, 1988). The mudstone intraclasts are sediments displaced by superimposed polygonal cracks that were filled with sediment during flooding events. These then recracked, while no new sedimentary layers were deposited. The preservation of the mud-cracked massive mudstone indicates that the pedoturbation was incomplete. The red-brown mudstones that form the lower part of Unit C are normally more cohesive and less fractured. The red colour of the mudstone is probably due to the presence of hematite, which was confirmed by X-ray diffraction analysis by Ahlstrom (1992).

Thin sections of the mudstones show a massive fabric (Plate 2-13D). The absence of stratification in thin sections may indicate that original sedimentary fabrics were destroyed. The mudstones are composed of mixed clay and dolomitic minerals, with scattered silt- to sand-grade anhydrite and silt-grade quartz dispersed throughout the rocks (Plate 2-13D). However, the amount of detrital anhydrite in the dark grey dolomitic mudstone is generally less abundant than that in the reddish-brown dolomitic mudstone. In addition, anhydrite grains are smaller in the former than in the latter. The detrital anhydrite crystals are broken, worn or abraded (Fig 2-13D), showing that they were mechanically transported to the depositional site. SEM study shows that clay minerals and dolomite are major components, with subsidiary detrital anhydrite, quartz and potassium feldspar (Plate 2-14A).

Slickensides are well developed in this unit. The presence of slickensides in the Second Red Bed Member was previously mentioned by Lane (1959), Dunn (1982a), Norris *et al.* (1982) and Ahlstrom (1992). They are macroscopic, shiny, grooved, planar fractures that

PLATE 2-14

Plate 2-14 A: SEM photomicrograph of massive dolomitic mudstone that consists of clay minerals (c), dolomite (d) and minor anhydrite (a). Unit C, the Second Red Bed Member. Lsd. 8-14-20-30W1.

Plate 2-14 B: Core photograph of a slickenside from Unit C of the Second Red Bed Member. Lsd. 4-2-22-31W1. Coin diameter is 1.7 cm.

Plate 2-14 C: Core photograph showing root-like green mottles. Unit C, the Second Red Bed Member. Lsd. 4-2-22-31W1. Coin diameter is 2.3 cm.

Plate 2-14 D: Core photograph showing raindrop imprints (r) that are circular to elliptical in shape. Unit C, the Second Red Bed Member. Lsd. 15-36-32-29W2. Scale bar is 3 cm.

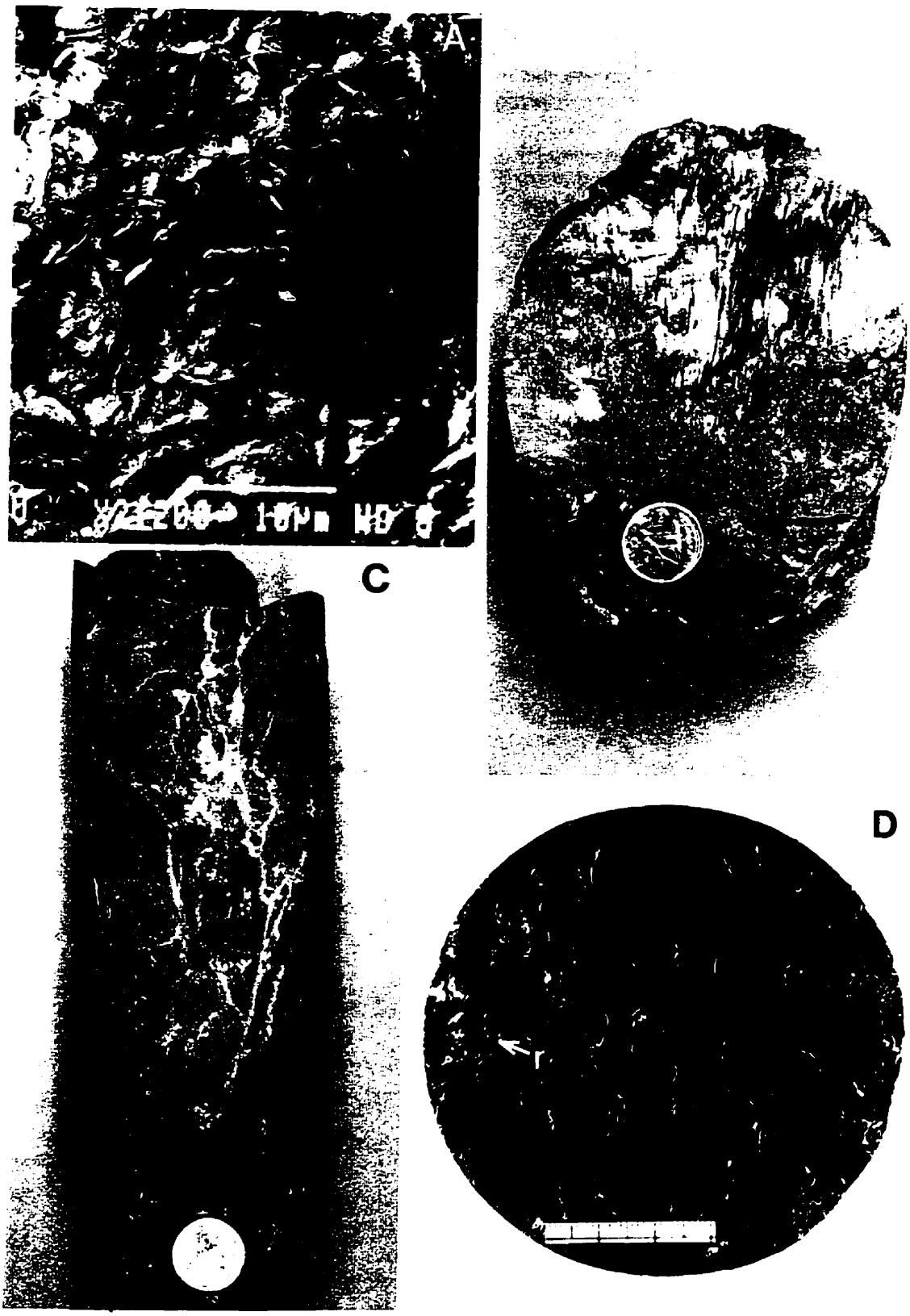
A
C
D

intersect to form concave-up, dish-shaped structures (Plate 2-14B). Most slickensides are single but some are cross-cutting, with dip-angles varying from 45° to nearly horizontal. They are arcuate to bowl-shaped, randomly oriented, and locally form pseudo-anticlines.

Green mottling is also common in the red-brown mudstones. It is developed as irregular grey to green patches on a centimetre to decimetre scale. The boundaries between the green mottles and red-brown mudstone are diffuse. In Well 4-2-22-31W1 (Plate 2-14C), the mottling has a vertical, sinuous, and string-like morphology, and is characterized by irregular branching with variable diameter. This type of mottling is typical of root activity (Joeckel, 1989; Platt and Keller, 1992).

Apart from slickensides and green mottling, other large sedimentary or synsedimentary structures are generally absent. However, raindrop imprints are common in both the red-brown and dark-grey to olive-green mudstones. Individual imprints are circular to slightly elliptical in shape, 1-3 mm in diameter (Plate 2-14D), and vary greatly in abundance on bedding plane surfaces. Where abundant, bedding planes are covered with irregular, partly connected depressions that are separated by narrow ridges (Plate 2-15A).

Although present throughout the Second Red Bed Member, chips of orange halite are particularly common in this unit. Most are tabular and arcuate, although wedge-shaped chips are locally present. Halite chips are mainly subhorizontal to subvertical in orientation. They range from mm up to 1 cm in thickness and are composed of acicular halite crystals that are oriented normally to the host fracture walls. Dunn (1982a) attributed their formation to the poorly consolidated nature of the Second Red Bed mudstones, which rendered them readily susceptible to fracturing and wedging apart by halite. However, most halite chips are not wedge-shaped but are tabular. Some chips are attached to slickensides and bear the imprints of the striated surface. This shows that the halite grew on slip surfaces that were already present before the precipitation of the halite. This, in turn, suggests that the high concentration of the halite chips in this unit is probably due to the abundance of slickensides.

Interpretation

Unit C is composed of dolomitic mudstones that are characterized by intersecting slickensides. The origin of the slickensides was previously attributed to the collapse of the Second Red Bed Member (Ahlstrom, 1992), which was associated with salt dissolution in

PLATE 2-15

Plate 2-15 A: Core photograph showing abundant rain imprints that are characterized by partly connected depressions which are separated by narrow ridges. Unit C, the Second Red Bed Member, Lsd. 10-7-32-5W3. Scale bar is 3 cm.

Plate 2-15 B: Core photograph showing chaotic mudstone-halite from Unit D of the Second Red Bed Member. The upper left part of the core is composed of cloudy orange halite. In the central part, a relatively large clear halite crystal is present. Lsd. 1-12-34-1W1. Scale bar is 3 cm.

Plate 2-15 C: Core photograph showing the sharp contact between the Second Red Bed Member and the Prairie Evaporite Formation, with Unit D and C of the Second Red Bed Member. The lower part of Unit D is composed of brick-red chaotic mudstone-halite. Lsd. 9-22-23-6W2. (One core box is 0.76 m long and core diameter is 10.1 cm.)

Plate 2-15 D: Core photograph of chaotic mudstone-halite from Unit D of the Second Red Bed Member. Lsd. 14-32-20-30W1. Scale bar is 2 cm.


A
B
C

the Prairie Evaporite Formation. However, the following evidence precludes this mechanism and tectonism as a factor in their genesis: (1) the slickensides curve through arcs of more than 90°; (2) they are present in undeformed rocks; (3) they are restricted to Unit C; and (4) they are widespread from northwestern Saskatchewan to western Manitoba.

The widespread distribution of the slickensides from northwestern Saskatchewan to northwestern Manitoba and their restriction to Unit C indicate that they are pedogenic in origin and not due to tectonism, which would have affected the entire Second Red Bed Member. Unlike slickensides associated with faults, those associated with pedogenic features are restricted to particular horizons (Retallack, 1988). Slickensides in contemporary soils commonly form in smectite-rich soils that experience seasonal wetting and drying, which induces shrink-swell phenomena (e.g., Brewer, 1976; Yaalon and Kalmar, 1978; Fanning and Fanning, 1989). Intersecting slickensides of this type are typical features of vertisols (Buol *et al.*; 1980, Forth and Schafer, 1980) and similar slickensides have been described from paleovertisols (e.g., Joeckel, 1989; Goebel *et al.*, 1989). From these features and their widespread development, it can be concluded that Unit C is a part of paleosol with strong similarities to modern vertisols.

The depositional environments of the mudstones were discussed by Lane (1959). He believed that the red mudstones in the lower part of the Second Red Bed Member were deposited under continental conditions, and that the overlying grey and green mudstones were deposited under marine conditions. The common development of raindrop imprints and possible root traces in the red-brown mudstones support his interpretation. Both features indicate subaerial exposure and are most likely to be preserved in continental beds (e.g., Pettijohn, 1975; Reineck and Singh, 1973). However, raindrop imprints are also common in the dark-grey and olive-green mudstones, which precludes sedimentation in permanently subaqueous environments. The dark-grey and olive-green mudstones were also probably deposited in a continental setting. The different colours of the mudstones probably reflect marine hydromorphism, as discussed below. The detrital anhydrite crystals in the red-brown mudstones may indicate that efflorescent anhydrite crusts once formed in contemporaneous lateral environments, but were subsequently disrupted and eroded during subaerial exposure.

The lower part of this unit is composed of red mudstone. Green mudstone is almost absent, indicating well-drained conditions. The reddish colour of the mudstone is probably

due to subaerial ageing of fine-grained iron hydroxide to hematite under a warm, well-drained, subaerial regime during the Middle Devonian. Similar redbed facies are deposited in continental environments on the landward side of saline mudflats. Thus, it may be concluded that the red mudstone in Unit C was probably deposited in a desert alluvial-eolian plain, and mudflat environment. However, unlike the sediments in wadi plains of the Permian and Holocene ages (Handford, 1981; Handford, 1982), which are composed of both clay and sand sediments, sandstone layers are absent in Unit C in central and southeastern Saskatchewan. This may indicate that the red mudstone in these regions formed in a distal wadi plain. In contrast, sandstone layers are present in the outcrop area of western Manitoba (Norris *et al.*, 1982). The presence of sandy sediments in that area may indicate that it was deposited in more proximal alluvial environments. Thus, the redbed facies pass from proximal braided-alluvial deposits into distal wadi plain and inner-sabkha mudflat deposits in a southwesterly direction. This, in turn, suggests that from southeastern Saskatchewan to the outcrop area of northwestern Manitoba, the depositional environment of the Second Red Bed Member became progressively more continental.

2.6.3 Unit D

Unit D is 0.5-2 m thick. It is distinguished from Unit C by the absence of slickensides (although pseudo-anticlines are locally observed in the upper part of Unit D in Core 3-27-38-27W2), the presence of bedding features in the upper part, and better induration in core sections. Its basal contact with the Prairie Evaporite Formation is either transitional or erosional. Normally, Unit D consists of brick-red, chaotic mudstone-halite in the lower part and alternating reddish and olive-green mudstones in the upper part (Plate 2-15C). It may also consist wholly of brick-red chaotic mudstone-halite (Plate 2-10A) or alternation of brick-red, chaotic mudstone-halite and reddish-olive green mudstones (Plate 2-10D).

Chaotic Mudstone-Halite

The chaotic mudstone-halite has a thickness ranging from tens of centimetres to over 1 meter. It is predominantly brick-red, but green-coloured banding parallel to bedding on a 1 to 10 cm scale is also present locally. The rock is massive and structureless. It comprises a disorganized mixture of halite crystals and mudstone (Plate 2-15D), with the evaporite content gradually decreasing upward. Mudstone forms irregularly shaped masses between the halite crystals. The amount of halite is highly variable, ranging from isolated crystals in the mudstone, to crystal aggregates in a mudstone matrix, to displacive halite that exceeds

mudstone by volume. Based on its colour difference, two different types of halite are present in the rock. They are called here `clear halite´ and `orange-coloured halite´, respectively.

Clear halite is present either as isolated euhedra or interlocking aggregates of cubes in mudstones (Plate 2-15B). Crystals are typically coarse (up to 2 cm long), euhedral to subhedral, and lack preferred crystal orientation, preferential growth direction, or elongation with respect to bedding. These crystals normally lack many fluid inclusions, which indicates slow growth in a relatively stable environment (Handford, 1981).

The orange halite crystals are smaller than the clear halite. They are cloudy in appearance (Plate 2-15B), pyramidal in shape, and are separated by clear halite. Moreover, halite moulds are present in some mudstone beds. Locally, the halite moulds are so abundant that the rock appears spongy.

In thin section, the chaotic mudstone-halite is strongly impregnated with iron oxide. The iron oxide commonly has a patchy distribution. The rock consists of clay minerals and dolomite, with abundant acicular anhydrite crystals (Plate 2-16A). These anhydrite crystals are well preserved, but are randomly distributed in the argillaceous matrix. They probably grew displacively in the sediment. Additionally, irregular voids are common in the reddish mudstones; most resulted from by dissolution of halite during thin section preparation. SEM and XRD study show that the mudstone part of the rock is composed of illite, chlorite, dolomite, anhydrite, halite, quartz and potassium feldspar.

Alternating Reddish- to Olive-Green Mudstone

The alternating reddish to olive-green mudstone is thinly-bedded, ranging in thickness from centimetres to decimetres (Plates 2-10D, 2-16B). The rock is characterized by well-preserved bedding features. The contact between individual beds is sharp and erosional. Individual beds have either a massive or a brecciated fabric. Where massive, clear halite crystals may be present in the mudstone, but they are significantly less abundant than in the chaotic mudstone-halite. As in the latter mudstone, the halite in the alternating reddish to olive-green mudstone is present as isolated, randomly oriented crystals. Where the rock has a brecciated fabric, it is characterized by a series of superimposed polygonal cracks and is composed of mudstone intraclasts (Plate 2-16C). The intraclasts are subrounded to angular, mm to cm in size, and poorly sorted. Some intraclasts show rotation and

PLATE 2-16

Plate 2-16 A: Plane-polarized light photomicrograph of chaotic mudstone-halite. The rock is characterized by abundant acicular anhydrite crystals. Lsd. 01-02-021-31W1. Scale bar is 0.25 mm.

Plate 2-16 B: Core photograph showing alternation of reddish and olive green-mudstone from the upper part of Unit D, the Second Red Bed Member. Lsd. 3-27-38-27W2. Coin diameter is 2 cm.

Plate 2-16 C: Slabbed core photograph of alternating reddish and olive-green mudstone that shows mudcracks and halite remains. Lsd. 3-27-38-27W2. Scale bar is 3 cm.

Plate 2-16 D: Slabbed core photograph of alternating reddish and olive-green mudstone that is characterized by crinkly, undulating laminae in the upper part. Unit D, the Second Red Bed Member. Lsd. 3-27-38-27W2. Scale bar is 3 cm.

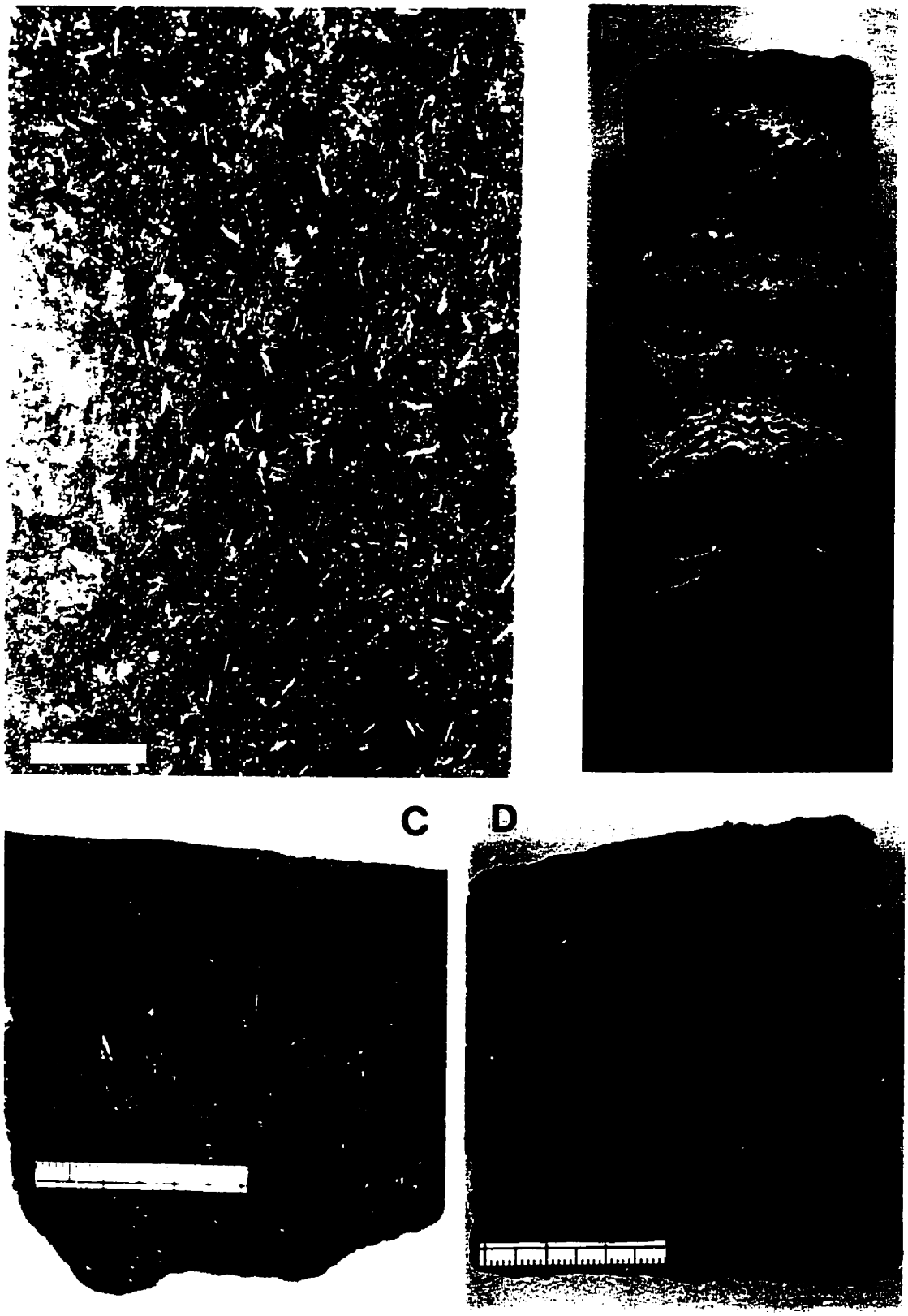
A
C
D

displacement, but most adjacent intraclasts can be fitted back together, indicating *in situ* brecciation. At the surface of some beds, the intraclasts are reduced to silt- and sand-sized sediment. The matrix between intraclasts is composed of fine-grained argillaceous sediment and silt- to sand-grade intraclasts. SEM, XRD and thin section studies show that the alternating reddish- to olive-green mudstone is also composed of illite, chlorite, dolomite, anhydrite and halite, with subsidiary quartz and potassium feldspar.

Unlike the chaotic mudstone-halite, which is structureless, the alternating reddish and olive-green mudstone contains laminated structures (Plate 2-16B & D) with a thickness of less than 1 cm. These laminated structures are present mainly in green mudstone or in the sediment directly overlying a sharp, erosional surface. They are characterized by crinkly, undulating laminae, probably signifying a microbial origin. Thin section study shows that they are composed of olive-green argillaceous sediment and white felted anhydrite. The microbial laminae are usually intercalated with, or overlain by, olive-green to white anhydrite laminae.

Interpretation

Unit D is normally composed of brick-red, chaotic mudstone-halite in the lower part and alternating reddish- to olive-green mudstone in the upper part. The former is massive, rich in displacive halite and the residue of probable primary halite, and lacks primary sedimentary structures. Similar rocks were termed "Haselgebirge facies" by Arthurton (1973) and Smith (1971), or "chaotic mudstone-halite" by Handford (1981). They were interpreted as deposits formed in saline mudflat environments. The same depositional environment is suggested here for the chaotic mudstone-halite in Unit D. The massive, chaotic structure of the rock is caused by disruption due to displacive growth of evaporite minerals within the sediments, which are known to destroy sedimentary structures in saline mudflats (Hardie *et al.*, 1978; Renaut and Long, 1989). The clear halite in this facies may have formed in brine-soaked sediment in a phreatic zone at, or just below, a sabkha surface. The vadose zone is less suited for this type of salt deposition because of the rapid rate of crystallization and alternating periods of precipitation and dissolution, induced by surface runoff, infiltration, and evaporation (Handford, 1981). Supporting evidence for halite crystallization in the saturated zone is the green colour of some mudstone horizons, which probably indicates reduction of ferric iron in reducing, water-logged environments.

Similar chaotic mudstone-halite facies were reported from Holocene saline sediments of

Bristol Dry Lake, California, and from Permian evaporites in the Permian Basin of Texas (Handford, 1981, 1982). Regional subsurface mapping of the Permian evaporites and the facies distribution of the Holocene saline sediments of Bristol Dry Lake showed that the chaotic mudstone-halite formed in a facies belt between continental red beds (desert alluvial-aeolian) and saline pan beds of banded halite (Handford, 1981, 1982). Smith (1971) observed a similar facies progression in the Permian Upper Halite Group of England. Likewise, Poborski (1970) described a lateral facies change of red beds through a lagoonal-continental belt of red clastics and halite, into a basin-center zone of lagoonal halite in the Zechstein (Z4) evaporites of Poland.

In contrast, the alternating reddish to olive-green mudstone is thinly-bedded and is characterized by well-preserved bedding features, such as microbial mat-like structures. This indicates that the sediments experienced little internal disruption after they were deposited. The numerous mudcracks indicate that the sediments were often subaerially exposed, a conclusion supported by micro-erosional surfaces between individual layers. Similar sediments have been interpreted as deposits that formed in dry mudflat environments (Smoot and Lowenstein, 1991; Handford, 1991; Kendall, 1992; Renaut, 1994). The same interpretation can be applied to the alternating reddish to olive-green mudstone in Unit D.

The abundant displacive halite, saline crusts, and the absence of fauna reflect a hypersaline environment under an arid climate. However, the thin microbial mats above erosional surfaces and saline crusts imply that the depositional environment was periodically flooded either by marine or non-marine waters to form ephemeral bodies of water. The thinness of the microbial mats and evaporite crusts implies that these water bodies were very shallow and short-lived. Such mats commonly form after flooding of a saline pan or salina, and are common in modern and ancient saline environments (cf. Lowenstein and Hardie, 1985).

By analogy with similar facies elsewhere, the halite at the top of the Prairie Evaporite Formation probably formed in a saline-pan environment, as shown by Utha-Aroon (1990). The new evidence from Unit D accords with sedimentation in a saline mudflat - dry mudflat flanking a shallow saline-pan complex. The saline-pan evaporites, saline mudflat and dry mudflat sediments are laterally adjoining facies. This suggests that the depositional environments of the halite at the top of the Prairie Evaporite Formation and the chaotic mudstone-halite at the base of the Second Red Bed Member may have been laterally transitional facies. If this interpretation is correct, it implies that the sediments deposited at

the latest stage of the Prairie Evaporite Formation period and earliest stage of the Second Red Bed Member period belong to a single upward-shallowing sedimentary cycle. This conclusion differs from that of Dunn (1982a), who suggested that the Second Red Bed Member was deposited during a later marine transgression.

This interpretation also implies that the contact between the Second Red Bed Member and the Prairie Evaporite Formation is not a major unconformity, as inferred in previous studies. A sharp erosional contact is indeed present between the Second Red Bed Member and the Prairie Evaporite Formation in some wells, but such an erosional surface could have formed readily on the exposed salt surface; there may have been very little time between deposition of the salt at the top of the Prairie Evaporite Formation and the deposition of the overlying mudstone of the Second Red Bed Member (Dunn, 1982a).

2.7 Discussion

From the new evidence presented, it is clear that Units B and C of the Second Red Bed Member are rich in pedogenic features that include subangular to angular blocky soil aggregates, pseudo-anticlines, slickensides, vertical cracks, carbonate veins, colour horizonation and mottling, and a general absence of bedding features. Furthermore, the downward gradation in colour from low-chroma mudstones into high-chroma mudstones is typical of many soils (Retallack, 1988; Joeckel, 1995). The persistence of slickensides in Unit C from Saskatchewan to northwestern Manitoba suggests that they are pedogenic in origin. This type of slickensides forms in clay-rich soils when swelling pressures exceed shear strength, at depths where vertical movement of sediments is confined. They are produced by shrinkage and expansion of clay-rich soils, typically associated with seasonal wetting and drying (Birkeland, 1984; Blokhuis *et al.*, 1990; Soil Survey Staff, 1992). They characterize Holocene vertisols and have also been described from paleovertisols (e.g., Allen, 1986; Joeckel, 1989; Gustavson, 1991; Vanstone, 1991; Wright *et al.*, 1991; Driese and Forman, 1992). In modern soil profiles, the optimum depth for slickenside formation is just below the level of cracking, at the depth of seasonal wetting (Yaalon and Kalmar, 1978). Most pedogenic slickensides are found at a soil depth of 0.7-0.8 m, and all are normally found between 0.3 and 1.3 m below the land surface (Gray and Nickelsen, 1989).

Based on the macro- and micro-features discussed, the paleosol in the Second Red Bed Member resembles several Holocene vertisols. The climatic requirements for development

of Holocene vertisols are seasonally moist and typically tropical to warm temperate conditions, with 4-8 dry months each year (Ahmad, 1983; Dudal and Eswaran, 1988). Thus, during development of the paleovertisol in the Second Red Bed Member, the Saskatchewan part of the Williston Basin had a seasonally alternating arid and humid climate. Gu and Renaut (1995) reached this conclusion in a study of the dolostone unit (Unit A) at the top of the Second Red Bed Member. This, in turn, suggests that from the early stages during which the lower part of the Second Red Bed Member was forming to the late stages during which the paleovertisol was developing, the paleoclimate in the Saskatchewan part of the Williston Basin changed from predominantly arid to seasonally alternating arid and humid.

Although the Second Red Bed Member in both central and southeastern Saskatchewan has evidence of pedogenesis, the maturity of the paleosol development in these two areas is significantly different. In central Saskatchewan, where Unit A is absent, the dolostone throughout Unit B is completely brecciated. In contrast, in central and southeastern Saskatchewan, where Unit A is present, the dolomitic conglomerate that has pedogenic features comprises only parts of Unit B, with dolomitic conglomerate horizons separated by dolostones that are well consolidated and contain bedding features. This indicates that (1) the paleosol development in southeastern Saskatchewan is less mature than that in central Saskatchewan (where Unit A is absent); and (2) the pedogenic development in the former area was interrupted by contemporaneous sedimentation. This, in turn, implies that relatively, central Saskatchewan was located in a paleogeographic high whereas southeastern Saskatchewan was situated in a paleogeographic low.

To explain why the dolostones of Unit A are absent in the cores that contain a more mature paleovertisol, there are two alternatives: (1) either Unit A was not deposited in these areas because they were situated in paleogeographically high places, or (2) Unit A was deposited, but was completely reworked by pedogenesis during long periods of subaerial exposure.

As noted, the colour of the rocks in the Second Red Bed Member changes upward from predominantly red through brown to dark-grey and olive-green. This probably indicates a change in the oxidation state of iron within the sediments, from ferric to ferrous. Following Lane (1959), Ahlstrom (1992) suggested that this colour change resulted from a change from strongly oxidizing conditions to reducing conditions, associated with an increase in water depth. However, the upper part of the Second Red Bed Member contains sediments

with raindrop imprints, *in situ* brecciation and other soil features, and the top of the Second Red Bed Member is a paleokarstic surface (Gu and Renaut, 1996). These features indicate that the sediments were subaerially exposed frequently, which is incompatible with the interpretation proposed by Lane (1959) and Ahlstrom (1992). Instead, the top of the Second Red Bed Member is directly overlain by marine strata. Marine hydromorphism (Wright *et al.*, 1997) occurred before and during the deposition of the overlying marine sediments, as shown by the presence of pyritic crusts and framboids in the olive- to dark-grey mudstones and at the top of the Second Red Bed Member. Periodic waterlogging may create localized iron reduction within a soil profile. Thus it is more likely that the colour change in the Second Red Bed Member was induced by marine hydromorphism rather than by more permanent submergence. This interpretation is also supported by the fact that the colour change between the different units is gradational and that mottling is common. Similar colour changes, ascribed to marine hydromorphism, have been described from other paleovertisols overlain directly by marine strata (e.g., Joeckel, 1991; Driese and Foreman, 1992; Driese *et al.*, 1992).

In contrast to Units B and C, Unit D is composed of stratified mudstones. Although its lower part is usually characterized by massive chaotic mudstone, its upper part contains well-preserved bedding features and other sedimentary structures. This suggests that they experienced little pedogenesis. However, where the Second Red Bed Member is relatively thin, Unit D is completely absent. This may indicate that the presence or absence of Unit D is strongly controlled by the total thickness of the Second Red Bed Member.

2.8 Summary

The Second Red Bed Member differs significantly in lithology from the rest of the Dawson Bay Formation by being dominated by dolomitic argillaceous mudstones. This study shows that the lower (Unit D) and the middle parts (Unit C) of the member were deposited in an environment that ranged from saline-mudflat and dry-mudflat to distal alluvial-eolian plain, and that the upper part (Units A and B) of the member formed in a Coorong-like environment. The new evidence shows that the Second Red Bed Member was affected by development of a paleovertisol during and after its formation, and that the paleosol became better developed in central Saskatchewan than in southeastern Saskatchewan. This, in turn, suggests that the paleorelief in central Saskatchewan was higher than that in southeastern Saskatchewan, and that the marine waters entered the basin from the southeast. The presence of the paleovertisol also indicates a seasonally alternating, arid and humid climate.

Thus, it can be concluded that from the early stages during which the lower part of the Second Red Bed Member was forming, to the late stages during which the paleovertisol was developing, the paleoclimate in the Saskatchewan part of the Williston Basin changed from predominantly arid to alternating arid and humid. Additionally, new evidence also shows that no significant disconformity is present between the Second Red Bed Member and the Prairie Evaporite Formation, and that the sediments deposited at the latest stage of the Prairie Evaporite Formation period and the earliest stage of the Second Red Bed period are laterally adjoining facies, belonging to a single upward-shallowing succession.

CHAPTER 3

PALEOKARSTS AND BLACK SHALES IN THE CONTACT ZONE BETWEEN THE SECOND RED BED AND BURR MEMBERS

3.1 Introduction

Detailed core examination has shown that there are three, previously unrecognized paleokarst horizons in the Dawson Bay Formation of Saskatchewan (Fig. 3-1). One is the contact between the Second Red Bed Member and the Burr Member. This is characterized by small-scale solution basins, fractures, and discolored dolostone directly beneath the contact. The two other paleokarst horizons are at the base of the Burr Member. These are characterized by familiar karst features, including solution vugs and pipes, fossil molds, terra rossa, *in situ* breccias, collapse breccias and erosional surfaces.

Core examination has also revealed that there are two black shales in the basal part of the Burr Member (Fig. 3-1). One lies above the top of the Second Red Bed Member; the other overlies the paleokarst(s) of the Burr Member or rests upon the top of the Second Red Bed Member, where the paleokarst(s) of the Burr Member is absent. In the following sections, these paleokarsts and black shales are described and interpreted, respectively.

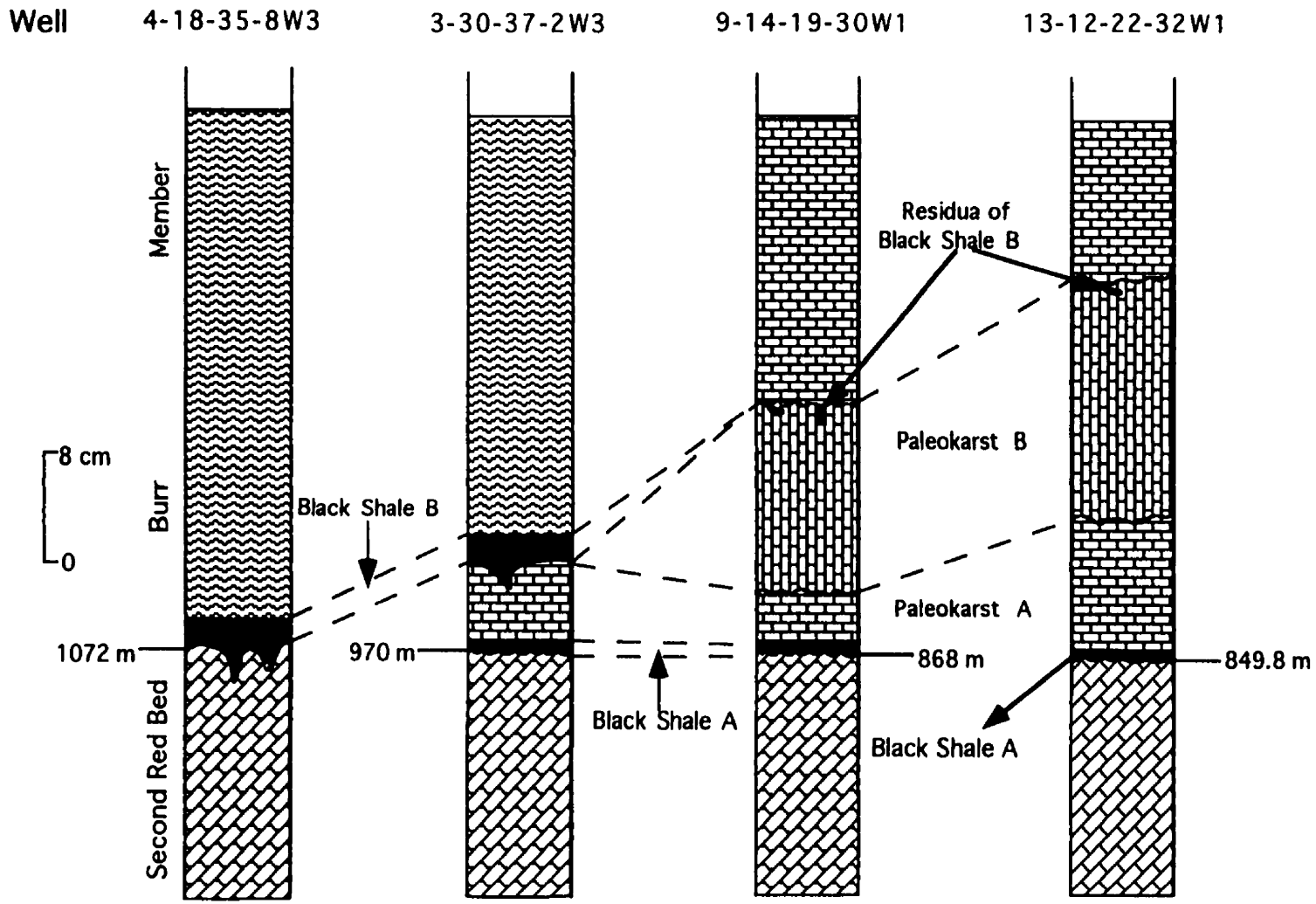

Fig. 3-1. Paleokarsts and black shales in the contact zone between the Second Red Bed and Burr members.

3.2 Paleokarsts

3.2.1 Paleokarst at the Top of the Second Red Bed Member

Description

The contact between the Second Red Bed Member and the Burr Member is everywhere sharp. It can be separated into two types: planar and discordant.

The planar contacts between the Second Red Bed Member and the Burr Member are flat and smooth, with little or no relief (Plate 3-1A). Although the contact is generally planar, in some cores, the surface is inclined slightly downward or upward, and the dolomite laminae of the SRBM are clearly truncated (Plate 3-1B, 2-2A), providing strong evidence of erosion. A thin black shale is present directly upon the surface (Plate 3-1C). The shale is finely laminated and contains small mudcracks (Plate 3-1C), indicating that the shale is of primary origin, which shows in turn that the planar erosional surface below the shale formed before deposition of the shale. The mudcracks are confined to the shale and never penetrate the underlying dolostone (Plate 3-1C). This suggests that the dolomitic sediment was already well lithified when the mudcracks formed.

Where in angular discordance with the overlying Burr Member, the maximum relief observed on the surface is 4 cm. In places, the contact is characterized by basin-like forms, with flat bases and smooth upward-inclined margins (Plate 3-1D). The dolostone directly below the surface is discolored, changing from normal olive-green to light brown. The thin black shale covers the inclined surface conformably (Plate 3-1D). No coarse clasts are present in the basins. The mudcracks are also present in the shale (Plate 3-2A), faithfully following the micro-topography of the substrate, which indicates that the shale is primary. This, in turn, shows that the discordant surface was formed before the black shale was deposited, rather than being formed by intrastratal dissolution after burial. The shale is less than 1 cm thick and it did not fill the solution basins completely. Thus, the carbonate sediment of the Burr Member filled the remainder of the basins first. Consequently, the base of the Burr Member is undulatory, and concordant with the irregular top of the Second Red Bed Member (Plate 2-2B). This supports the contention that the basin-like forms at the top of the Second Red Bed Member formed before burial by the overlying sediments.

PLATE 3-1

Plate 3-1 A: Core photograph showing the upper part of the Second Red Bed Member (s) and the basal part of the Burr Member (b). The upper surface of the Second Red Bed Member is slightly undulating. The base of the Burr Member contains two superimposed paleokarst horizons (k) that are overlain by a dark brown argillaceous limestone containing small *Chondrites*. Lsd. 8-14-20-30W1. (One core box is 0.76 m long and core diameter is 10.1 cm.)

Plate 3-1 B: Core photograph of the uppermost part of the Second Red Bed Member and the basal part of the Burr Member. The contact between the Second Red Bed Member and the Burr Member (c), which is sharp and undulating, represents a paleokarstic surface. The basal carbonate rock of the Burr Member overlies the undulating paleokarstic surface conformably. Lsd. 16-11-21-31W1. (One core box is 0.76 m long and core diameter is 10.1 cm.)

Plate 3-1 C: Slabbed core photograph showing the top of the Second Red Bed Member, which is slightly inclined upward to the left and is overlain by a thin black shale (s). The black shale contains mudcracks that are confined to the shale. Lsd. 01-02-021-31W1. Scale bar is 2 cm.

Plate 3-1 D: Slabbed core section showing a small dissolution basin (b) at the top of the Second Red Bed Member. The basin has a relatively flat bottom and smooth upward inclined margins. The massive dolostone below the surface is discoloured (d). Lsd. 1-12-34-1W3. Scale bar is 2 cm.

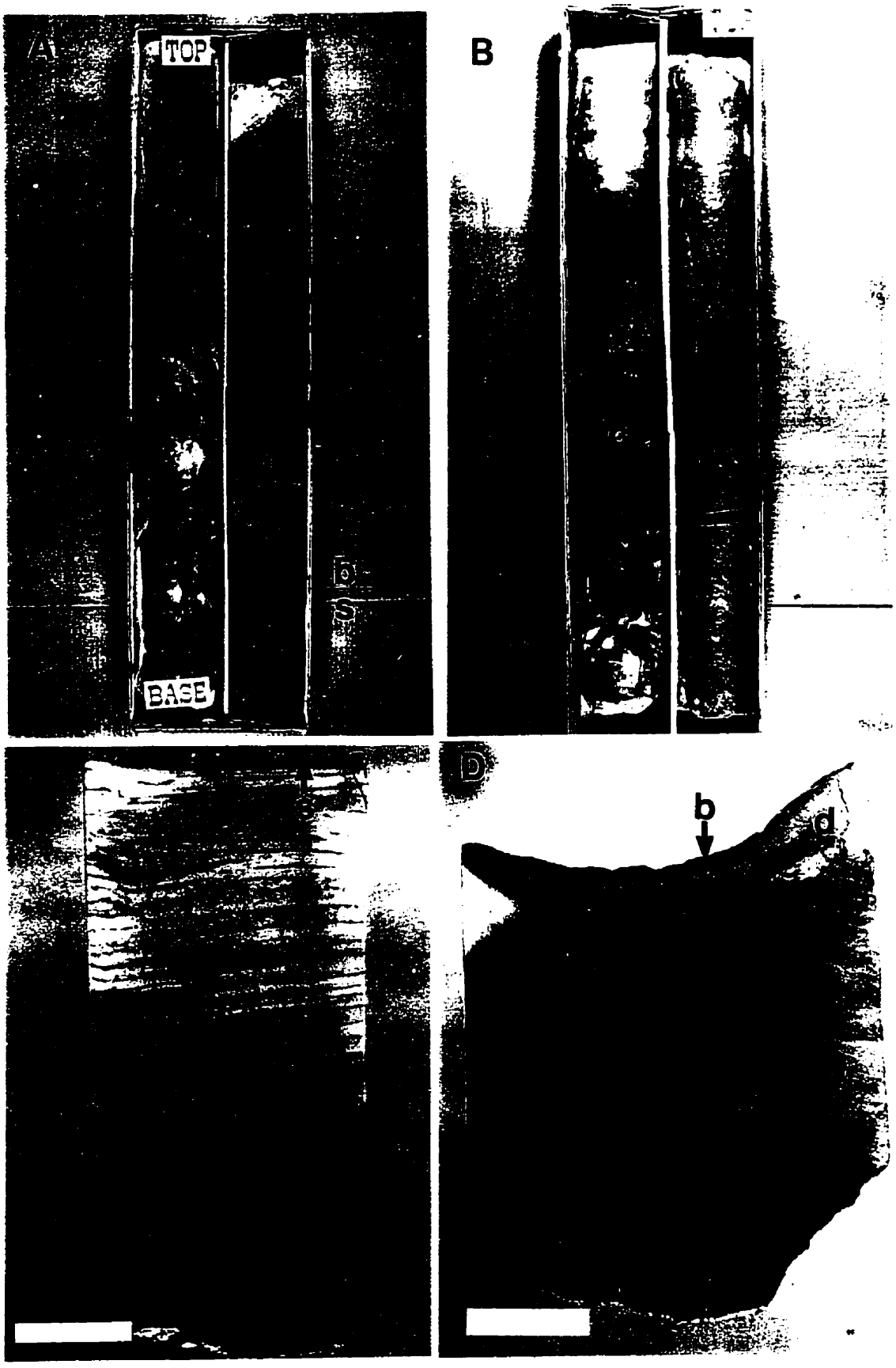
A
TOP
BASE
B
C
D
b
d

PLATE 3-2

Plate 3-2 A: Core photograph showing mudcracks in the black shale directly above a dissolution basin at the top of the Second Red Bed Member. Lsd. 16-29-22-30W1. Scale bar is 2 cm.

Plate 3-2 B: Core photograph showing a single paleokarst horizon (p) at the base of the Burr Member. The paleokarst is underlain by a thin black shale and overlain by carbonate rock with indistinct horizontal lamination. Lsd. 15-36-32-29W2. (One core box is 0.76 m long and core diameter is 10.1 cm.)

Plate 3-2 C: Slabbed core photograph showing the single paleokarst horizon of Plate 3-2 B that is characterized by an irregular upper surface and solution channels. The latter are filled with dolomitic clasts. Lsd. 15-36-32-29W2. Scale bar is 3 cm.

Plate 3-2 D: Slabbed core photograph showing the top (t) of the Second Red Bed Member and the base of the Burr Member. The paleokarst (p) at the base of the Burr Member has an irregularly undulating upper surface that is conformably overlain by a thin black shale (s). The karstic rock is characterized by fossil molds, solution vugs and fractures that are also filled with the black shale. Lsd. 3-30-37-2W3. Coin diameter is 1.7 cm.

A

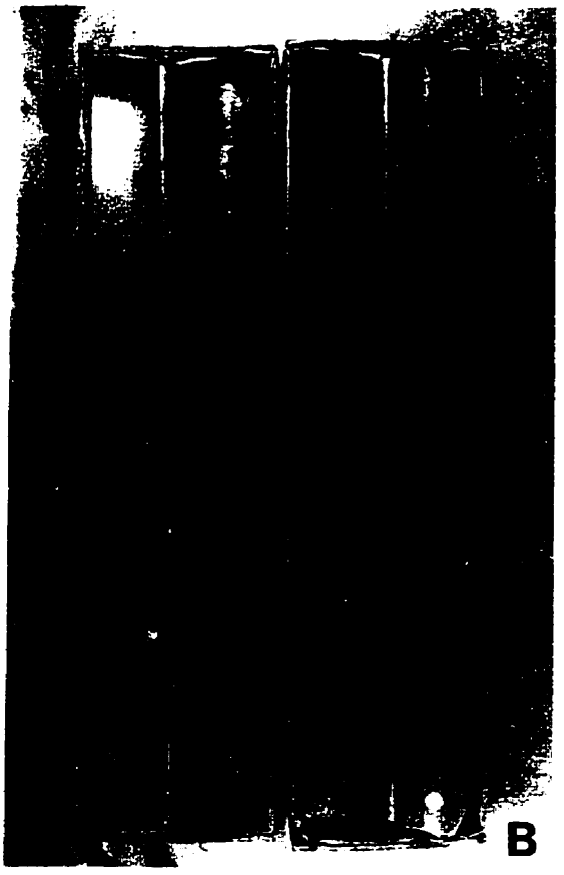

B

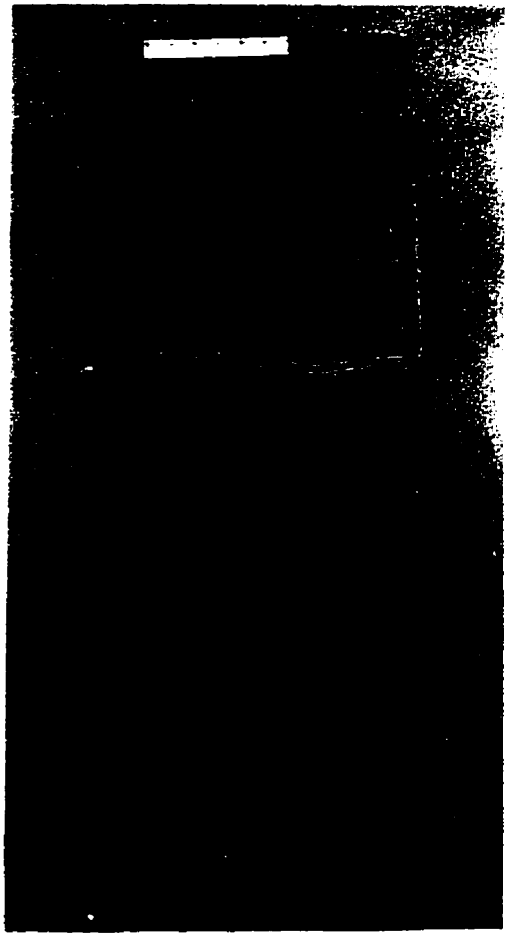

D

Interpretation

Although individual cores reveal a very small area of a bedding plane, based on the examination of cores over a large area, it can be concluded that the top of the Second Red Bed Member has a gently undulating surface. Where drill holes penetrate the center of the small basins, the cores show a characteristic basinal morphology. Where drill holes penetrate the edges of the basins, a discordant contact will be seen. Where they strike areas between the basins, the surface will be planar.

This undulating surface was first reported by Dunn (1982a), who recognized that it is an unconformity, but attributed its formation to widespread dissolution of the upper beds of the Prairie Evaporite Formation. This, he suggested, caused the partially lithified Second Red Bed Member to drape the low relief of the irregular surface conformably, resulting in the undulatory surface on the top of the Second Red Bed Member. If his explanation is correct, then undulating bedding planes might be expected throughout the Second Red Bed Member. However, these are not observed. Even the bedding plane directly below the discordant surface is generally horizontal (Plate 3-1D), providing strong evidence that the undulating upper surface of the Second Red Bed Member did not form by evaporite dissolution.

The smoothly curved erosional basins, the discolored dolostone directly beneath the surface, and the absence of coarse clasts above it all indicate that the undulating surface was probably formed by chemical dissolution in a subaerial environment. It is, therefore, a paleokarst surface. This hypothesis is supported by the fact that the top of the Second Red Bed Member was deposited in very shallow water, as shown by the presence of the tepee structures and microbial mats with mudcracks in the uppermost dolostone (Gu and Renaut, 1995). The presence of desiccation cracks in the shale directly overlying the surface also attests to subaerial exposure.

Similar surface paleokarsts were reported by Walkden (1974), Read and Grover (1977), Kobluk *et al.* (1977), Wright (1982), Kobluk (1984), Desrochers and James (1988), and Kahle (1988). However, the surface paleokarsts reported by Read and Grover (1977) were formed in intertidal environments, and were inhabited by algae and marine metazoans. Neither algal borings nor marine encrusting metazoans were found on the paleokarstic surface of the Second Red Bed Member in this study. The absence of marine hard-bottom fauna or algal borings, together with the smooth forms of the solution basins

and the widespread distribution of the paleokarst surface across the Canadian part of the Williston Basin, indicate that this surface formed in karst terrain distant from the contemporary shoreline. Similar modern karst surfaces with the small-scale basin-like forms are termed "kamenitzas" (Bogli, 1980; James and Choquette, 1984). They are usually developed on horizontal to slightly inclined substrates where dissolution by stagnant water forms pools and basins (Sweeting, 1973). This indicates that the Williston Basin probably had a widespread, subaerial flat surface before deposition of the Burr Member.

3.2.2 Paleokarsts at the Base of the Burr Member

In addition to the paleokarst surface at the top of the Second Red Bed Member, a paleokarst unit is also present at the base of the Burr Member. In central Saskatchewan, it is composed of only one carbonate horizon (Plate 3-2B & C), whereas in southeastern Saskatchewan, two superimposed karstified limestone horizons are present in most core sections (Plate 2-11A). In this thesis, the former is termed `Paleokarst A´ and the latter, `Paleokarst B´.

Paleokarst A

Paleokarst A is mainly found in central Saskatchewan. It is represented by *in situ* breccia, collapse breccia or massive dolostone with a highly irregular upper surface. It ranges from 2 to 20 cm in thickness and was termed as `halite-cemented breccia´ by Lane (1959) and Dunn (1982a, 1982b). In southeastern Saskatchewan, the paleokarst is characterized by fossil molds, vugs and fractures. However, collapse breccias have not been recognized in any cores. In the following sections, representative cores of Paleokarst A, from both central and southeastern Saskatchewan, are described.

In Core 3-30-37-2W3, from central Saskatchewan, a thin dolostone is present at the base of the Burr Member (Plate 3-2D). It is about 6 cm thick and has a highly undulating upper surface, with a relief of 2.5 cm. The dolostone is overlain by a thin, finely laminated black shale. The laminations in the black shale are completely conformable with the undulating surface of the dolostone. This suggests that the undulating surface had developed *before* deposition of the black shale. In addition, the dolostone contains abundant fractures, solution vugs and fossil molds, some of which are also filled with black shale that is characterized by fine laminations. The fossil molds are of gastropods,

brachiopods and probable crinoids (Plate 3-3A). Dunn (1982a) assigned the dolostone to the top of the Second Red Bed Member and placed the black shale directly above the dolostone in the lowermost part of the Burr Member. However, the presence of fossil molds in the dolostone shows that it may represent the lowermost part of the Burr Member because shelly macrofossils have never been confirmed in the Second Red Bed Member throughout Saskatchewan. This interpretation is supported by the presence of another thin black shale that directly underlies the dolostone (Plate 3-2D). Because no black shale intercalation is found in the Second Red Bed Member, the lower black shale is regarded here as the base of the Burr Member.

In Core 16-21-34-27W2, a matrix-supported breccia (Plate 3-3B), up to 10 cm thick, is present at the base of the Burr Member. The matrix is dark-grey to black, clay-rich siltstone and sandstone. The clasts are typically 1 to 20 mm long, and angular to subangular. Some clasts have a subvertical orientation. They are composed of brown dolostone, with minor anhydrite. They are extremely poorly sorted, oligomictic and are clearly derived from the same stratigraphic horizon. The breccia grades both upward and downward into a clast-supported breccia. Clasts in the latter are tightly sutured with a black bitumen-stained matrix. Similar breccias were reported by Kerans (1988) from the Lower Ordovician Ellenburger Group of West Texas. They were termed chaotic breccia (Kerans, 1988) or `collapse breccia´ (Esteban and Klappa, 1983) and interpreted as cave-fill deposits associated with cavern-roof collapse during karst development.

In Core 15-36-32-29W2, the base of the Burr Member is a massive, *in situ* brecciated dolostone, up to 6 cm thick (Plate 3-2C). The rock has a highly irregular upper surface with some sediment-filled fissures. These fissures are subvertical and up to 1.5 cm wide. The lower and middle parts of the fissures are filled with dolostone clasts and dark-grey, fine-grained internal sediment, whereas the upper part is normally filled with light grey carbonate sediment that is identical to the overlying sediment. The dolostone clasts in the fissures are sand- to pebble-sized, subangular to subrounded, and poorly sorted.

In Cores 8-20-33-20W2 and 13-11-33-23W2, the base of the Burr Member is composed of clast-supported breccia (Plate 3-3C & D). The breccia consists entirely of host dolostone clasts in a dark brown to black matrix. The clasts are poorly sorted, ranging in size from mm to >10 cm. They are randomly oriented, with many clasts being subvertical. Although angular clasts are present, most have embayed surfaces, which suggests that they were derived from a host rock that had highly developed solution vugs.

PLATE 3-3

Plate 3-3 A: Plane-light photomicrograph of karstic rock of Plate 3-2 D, showing solution vugs (v) and fossil molds (f). Lsd. 3-30-37-2W3. Scale bar is 0.5 mm.

Plate 3-3 B: Slabbed core photograph showing a paleokarst breccia composed of angular to subangular dolomitic clasts, cemented by dark grey to black argillaceous internal sediment. A large anhydrite clast (a) is present in the middle. Lsd. 16-21-34-27W2. Coin diameter is 1.7 cm.

Plate 3-3 C: Slabbed core photograph showing chaotic breccia composed of dolostone clasts in a dark brown to black matrix. Lsd. 13-11-33-23W2. Coin diameter is 1.7 cm.

Plate 3-3 D: Slabbed core photograph showing chaotic breccia composed of dolostone clasts in a dark brown to black matrix. The clasts show embayed surfaces. Lsd. 8-20-33-20W2. Coin diameter is 1.7 cm.


A
V
f
B
C
D

Additionally, fossil molds of gastropods and brachiopods are very common in the dolostone clasts. The breccia grades both upward and downward into the massive dolostone.

In Core 01-02-021-31W1, from southeastern Saskatchewan (Plate 3-4A), the base of the Burr Member is composed of a thin limestone bed about 7 cm thick. It is underlain by a thin black shale, that in turn rests on the slightly upward inclined surface of the Second Red Bed Member. The limestone contains abundant fossil molds and solution vugs. However, the chaotic breccia and sediment-filled fissures that are common in central Saskatchewan, are absent. The solution vugs and fossil molds are generally less than 0.5 cm long. Most fossil molds are left by dissolution of gastropod shells, but other shell molds are present, that cannot be identified with confidence. The fossil molds and solution vugs in the lower part of the limestone are filled with tobacco brown halite, whereas those in the upper part are filled with light grey to dark brown carbonate sediment. The dark brown carbonate sediment is identical to the overlying rock. This suggests that the vugs and fossil molds had developed before deposition of the overlying carbonate sediment. The contact between the limestone and the overlying rock is sharp, flat and smooth; the dissolution vugs directly beneath the contact are evidently truncated, indicating that this is an erosional surface.

Rocks Directly Overlying Paleokarst A

In central Saskatchewan, the rock directly overlying Paleokarst A is commonly a thin, finely laminated, black shale. The black shale is, in turn, overlain by a kerogen-laminated lime mudstone (Plates 3-4B, 2-9C). In southeastern Saskatchewan, the paleokarst is commonly overlain by a thin black shale or by a brown argillaceous limestone. The latter contains abundant small *Chondrites* (Plate 3-4A). These are overlain by bioturbated lime mudstone and argillaceous mudstone that lack dissolution vugs, fractures or pipes.

Interpretation

The carbonate rock at the base of the Burr Member is characterized by fossil molds, solution vugs, fractures, chaotic breccias and erosional surfaces. All these features are commonly associated with karstified rocks. Their presence shows that the carbonate rocks were once emergent and subjected to karstification. Although not all these features can be observed in a single core, and some cores may only contain one or two examples,

PLATE 3-4

Plate 3-4 A: Slabbed core photograph showing the single paleokarst horizon (p) at the base of the Burr Member in southeastern Saskatchewan that is characterized by fossil molds, solution vugs and a flat upper surface. The paleokarst is overlain by a dark brown argillaceous lime mudstone (m) that contains small *Chondrites*. Lsd. 01-02-021-31W1. Scale bar is 2 cm.

Plate 3-4 B: Core photograph showing the single paleokarst horizon (p) with a highly discordant upper surface at the base of the Burr Member in central Saskatchewan. The paleokarst was originally overlain by a 4 cm-thick black shale; see Plate 5 (1) of Dunn (1982a). Lsd. 3-30-37-2W3. (One core box is 0.76 m long and core diameter is 10.1 cm.)

Plate 3-4 C: Core photograph showing two superimposed paleokarst horizons (p) at the base of the Burr Member in southeastern Saskatchewan. Lsd.11-2-20-30W1. (One core box is 0.76 m long and core diameter is 10.1 cm.)

Plate 3-4 D: Slabbed core photograph showing the lower paleokarst horizon of Plate 3-4 C. It is composed of brown argillaceous limestone with solution pipes (s) that are filled with light grey fossiliferous carbonate sediment. Lsd. 11-2-20-30W1. Scale bar is 2 cm.

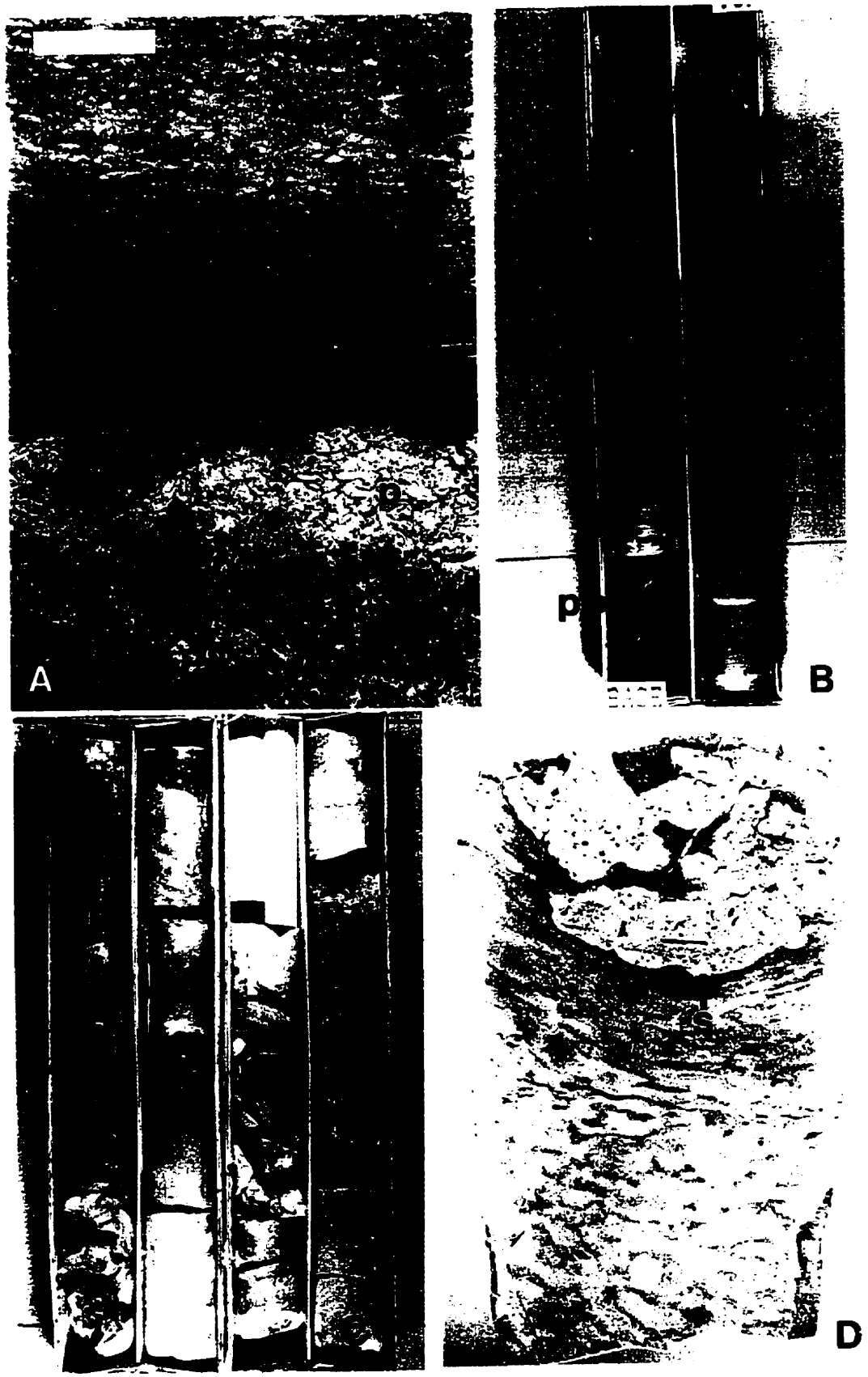
A
B
D

the carbonate rock with these features is consistently present at the base of the Burr Member.

This shows that the karstic rock is stratigraphically controlled and that karstification took place before the overlying sediments were deposited. This interpretation is supported by the fact that the sedimentary rocks above the paleokarst lack the features described above, and the vugs and fractures in the karstified rock are filled with sediments identical to the overlying rock.

Paleokarst B

Paleokarst B is present at the base of the Burr Member in southeastern Saskatchewan. It is comprised of two superimposed limestone horizons (Plate 3-1A). Each horizon ranges in thickness from cm to tens of cm. The limestones vary from light grey to dark grey or brown. In places, they are black. Both limestone horizons are characterized by solution vugs and/or pipes, fossil molds, fractures, and internal sediments. *In situ* breccia is common in the lower limestone horizon, but collapse breccia or chaotic breccia has never been observed. As for Paleokarst A, not all these features can be observed in a single core, thus the examples are described from several cores in the study area.

In Core 11-2-20-30W1, the lower limestone horizon is a brown argillaceous limestone that has abundant indistinct trace fossils. Solution pipes up to 4 cm long and 2 cm wide are present in the upper part of the limestone horizon (Plate 3-4C & D). These are now filled with light grey fossiliferous carbonate sediment identical to the upper limestone horizon. The upper limestone horizon is composed of light grey fossiliferous carbonate sediment and is characterized by fossil molds, fractures, solution vugs and channels, and *in situ* breccia (Plate 3-5A). Breccia clasts are commonly 1-2 cm in diameter, angular to subrounded, and most can be fitted back together, although some display minor rotation. The solution channels and fractures are filled with light yellow to dark brown argillaceous sediment. The former is probably terra rossa, whereas the latter is probably black shale. Where they occur in the same voids, the light yellow sediment always infills the lower part of the voids, whereas the black shale infills the upper part. This suggests that the black shale entered the voids later than the light yellow sediment. Anhydrite also fills some fractures, but it is unclear whether the anhydrite is primary or secondary.

In Core 41/09-22-23-06W2, the base of the Burr Member is an anhydrite layer, up to 2

PLATE 3-5

Plate 3-5 A: Slabbed core photograph showing the upper paleokarst horizon of Plate 3-4 C. It is composed of light grey fossiliferous limestone characterized by fossil molds, fractures, solution vugs, solution channels and *in situ* brecciation. The solution channels and fractures are filled by brown to black argillaceous sediments. Lsd. 11-2-20-30W1. Scale bar is 2 cm.

Plate 3-5 B: Core photograph showing two superimposed paleokarst horizons at the base of the Burr Member. The lower paleokarst (L) is underlain by a wedge-shape anhydrite (a) mass and is rich in fossil molds and solution vugs. Its upper surface is smooth and slightly undulating. The upper paleokarst (U) is characterized by fossil molds, but its solution vugs are less well developed than in the lower paleokarst. Additionally, the top of the upper paleokarst displays microkarren-like features (m). Lsd. 09-22-23-6W2. Scale bar is 3 cm.

Plate 3-5 C: Slabbed core photograph showing two superimposed paleokarst horizons at the base of the Burr Member. Lsd. 09-22-23-6W2. Scale bar is 3 cm.

Plate 3-5 D: Slabbed core photograph showing the lower paleokarst horizon (L) at the base of the Burr Member of Plate 3-1 A. It is characterized by fossil molds, solution vugs and small fractures. Its upper surface is flat and smooth. Black clasts (c), probably derived from the lower paleokarst, are present in the overlying sedimentary rock. Lsd. 8-14-20-30W1. Scale bar is 2 cm.

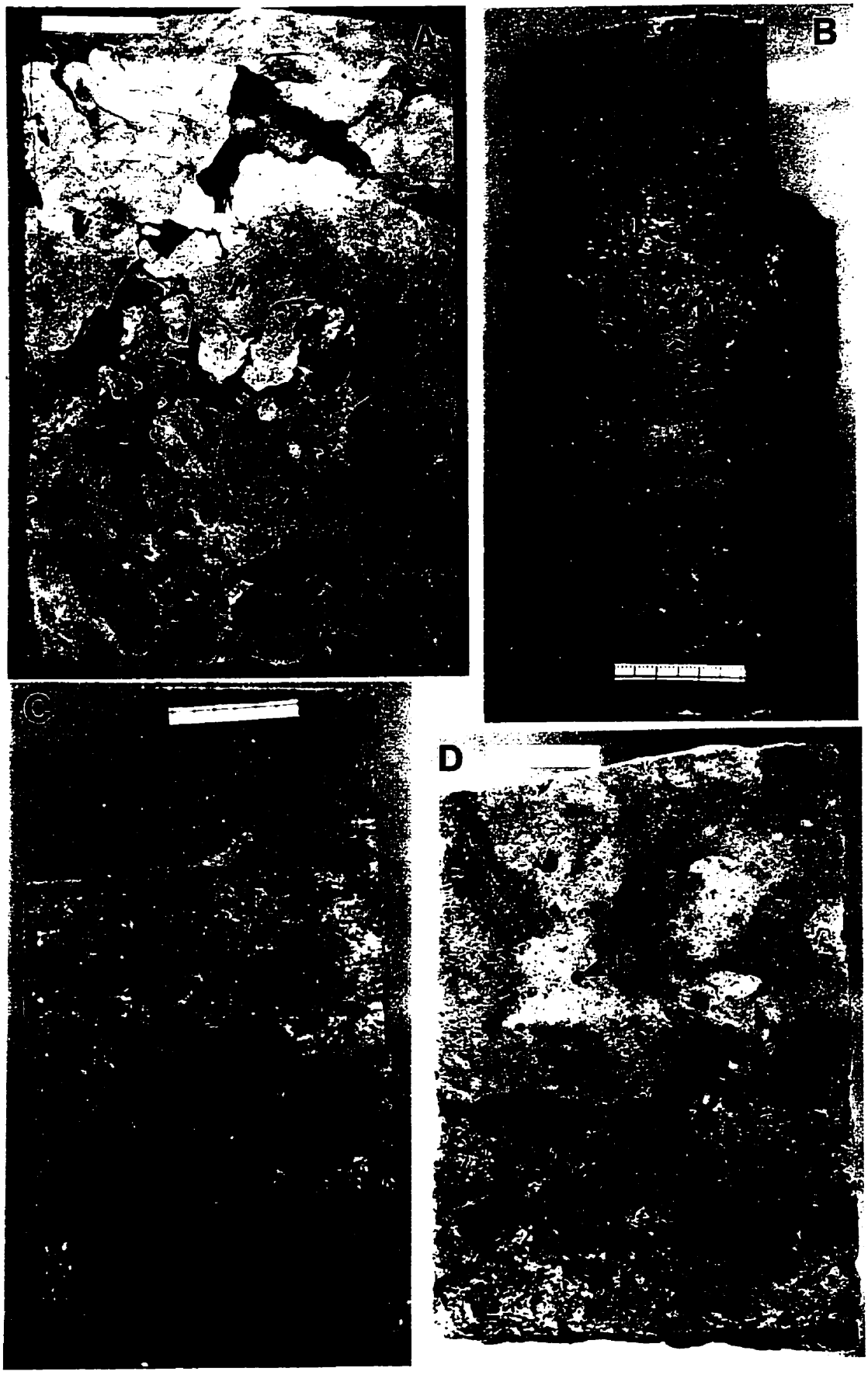
A
B
C
D

cm thick. The limestone unit above the anhydrite can be divided into lower and upper horizons (Plate 3-5B & C). The lower horizon is a dark grey to black limestone characterized by *in situ* microbreccia, fossil molds, solution vugs and small fractures. The contact between the lower and upper horizons is sharp and horizontal. At the contact, the solution vugs of the lower limestone horizon were evidently truncated, indicating physical erosion before the deposition of the upper horizon. The upper horizon contains fossil molds, vugs and small fractures, but *in situ* breccia is not developed. Its upper surface displays well-preserved microkarren-like features (Plate 3-5B) that in cross section have the form of a series of upwardly concave arcs with overhanging lips. The maximum relief observed on the surface is 1.5 cm, with a maximum diameter of 2 cm for microkarren-like features.

In Core 8-14-20-30W1, the lower limestone horizon is dark grey to black, with a mottled appearance. It is rich in solution vugs, fossil molds, fractures and *in situ* microbreccia (Plate 3-5D). The upper surface of the lower limestone horizon is sharp and worn smoothly. A relatively large solution vug, that was formerly present in the central part of the slabbed core section, is now filled with fossiliferous carbonate sediment identical to the upper limestone unit (Plate 3-5D). The upper horizon (Plates 3-5D, 3-6A) is composed of mottled limestone with slight colour discoloration. The rock is characterized by fossil moulds and solution vugs. It also contains black reworked clasts from the lower limestone horizon. The clasts range in size from coarse sand to small pebble and are well rounded. They are sparsely, but evenly, distributed in the limestone. The upper surface of the upper limestone horizon is undulating, with a relief up to 1 cm, and is covered by a thin black pyritic rind that is best developed in the concave part of the surface (Plate 3-6A). Petrographic examination reveals that it consists of euhedral crystals of pyrite (Plate 3-6B). The most significant feature in the upper limestone horizon is the relatively large solution vugs (up to 2 cm wide by 3.5 cm long) that lie directly below the upper surface (Plate 3-6B). They are subparallel to the bedding plane. The vugs are now filled with bioclasts. The wall of the host rock is characterized by pyritized microbial borings and filaments that are normally larger than 10 μm (Plate 3-6C). These features are similar to those in the phytokarst described by Folk *et al.* (1973) and Jones (1989) from the Cayman Islands.

In Core 16-11-21-31W1, both the lower and upper limestone horizons are composed of fossiliferous limestones (Plate 3-6D). The lower horizon is dark grey to black and up to 3 cm thick, with a brecciated appearance. Solution vugs and fractures are well developed,

PLATE 3-6

Plate 3-6 A: Slabbed core photograph showing the upper paleokarst horizon (U) at the base of the Burr Member of Plate 3-1 A. A relatively large solution vug (v), filled with carbonate sediment, is present directly below the upper surface of the paleokarst. The upper surface of the paleokarst is pyritized (p). Lsd. 8-14-20-30W1. Scale bar is 2.2 cm.

Plate 3-6 B: SEM photomicrograph showing that the pyritized upper surface of the paleokarst in Plate 3-6 A is composed of well-crystallized pyrite. Lsd. 8-14-20-30W1.

Plate 3-6 C: Photomicrograph showing pyritized microbial filaments (f) in the paleokarst. Lsd. 8-14-20-30W1. Scale bar is 0.5 mm.

Plate 3-6 D: Slabbed core photograph showing the brecciated appearance of the lower paleokarst (L) and the strongly mottled appearance of the upper paleokarst (U) at the base of the Burr Member. The latter is due to the presence of reworked clasts (c) from the lower paleokarst. Lsd. 16-11-21-31W1. Scale bar is 2 cm.


A
f
f
f
L

and are filled with halite or carbonate sediment. However, all these features are very small in scale. The upper limestone horizon is about 7 cm thick, with a mottled appearance. It contains fossil moulds, fractures and brown argillaceous internal sediment. Careful examination shows that the mottled appearance results from the presence of light- to dark-grey clasts in a light yellow matrix. The clasts consist of limestone similar to the lower limestone horizon. Some clasts have distinctive boundaries that distinguish them from the surrounding matrix. In others, however, the boundary is obscured. The clasts are highly variable in shape and generally range from coarse sand to small pebble in size; some are up to 1 cm in diameter. The upper surface of the limestone horizon is flat and a black pyritic rind is present at the surface. Small shallow borings are also present.

Rock Above the Paleokarsts

The rock directly above the upper limestone horizon is a brown argillaceous limestone, rich in small *Chondrites* (Plate 3-6D). In some core sections, small shell fossils are present at the base of the argillaceous limestone (Plate 3-6D). The fossils are small, fragmental and preserved as moulds, but could not be identified with confidence. Their small size may indicate that this is a dwarfed fossil assemblage, indicating a restricted environment.

Interpretation

Both the lower and upper limestone horizons are characterized by solution vugs, fossil moulds, fractures, *in situ* breccias and erosional surfaces. In places, solution pipes developed in the lower limestone, whereas the upper limestone is characterized by microkarren. All these features are common in modern and fossil karstic environments. Their presence in the Dawson Bay limestones supports an interpretation that they are karstified rocks.

It is appropriate, however, to question whether the limestones experienced one or two periods of karstification. The upper surface of the lower limestone horizon is almost everywhere sharp and smooth. Reworked clasts from this horizon are present in the upper limestone horizon. This shows that the lower limestone had already been lithified and experienced physical erosion *before* deposition of the upper limestone. Furthermore, the solution vugs and pipes are filled with carbonate sediments identical in composition to the upper limestone. This strongly suggests that the solution pipes and vugs had developed

before the upper limestone was deposited. Therefore, it can be concluded that two separate phases of karstification interrupted sedimentation in the early Burr time.

3.3 Discussion

3.3.1 Development of Paleokarsts

Karst is a common landscape on the earth's surface and is divided into surface karst forming at the land surface, and subsurface karst associated with meteoric groundwater processes (Wright, 1982). Most recognized paleokarsts are either associated with large unconformities or associated with cave sediments. They are relatively easy to recognize in outcrops. In contrast, small-scale surface karst of the type described in this chapter is difficult to recognize in the rock record (Choquette and James, 1988; Jones and Smith, 1988; Tucker and Wright, 1990), especially when only small core samples are available (Wright and Smart, 1994). This is probably one of the reasons why surface paleokarsts are rarely reported and to the best of my knowledge, the contact between the Second Red Bed Member and Burr Member described in this chapter is probably the first surface paleokarst to be recognized based solely on the examination of small core samples.

The paleokarsts at the base of the Burr Member are characterized by familiar karst features, but all are present at a very small scale. Such small-scale paleokarsts (microkarsts) could be easily eroded at localities where the wave energy was high in the subsequent transgressive environment (Jones and Smith, 1988; Ford and Williams, 1989), or they are commonly modified or destroyed by marine bioerosion (Rasmussen and Neumann, 1988). The smoothly worn surface of the lower limestone horizon in Paleokarst B indicates that the limestone had indeed suffered physical erosion before the upper limestone was deposited. Further evidence is provided by the presence of clasts from the lower paleokarst in the upper paleokarst. However, the upper surface of paleokarst A in central Saskatchewan and the upper surface of the upper paleokarst horizon in Paleokarst B of southeastern Saskatchewan are generally well preserved. This indicates that the karstic rock had been subjected to little or no physical erosion before burial by the overlying sediments. Additionally, except in rare cases, borings are absent in these karstic rocks. This suggests that biological modification was also very limited. There are two possible explanations. First, the paleokarst may have been rapidly covered by the overlying sediment. This normally occurs where karstic processes are overwhelmed by rapid terrigenous deposition and succeeded by prolonged subsidence

(Ford and Williams, 1989). This possibility is unsuitable for the preservation of the paleokarsts at the base of the Burr Member because their overlying sediment is black shale and limestone. Another possibility is that the paleokarst was rapidly submerged in a relatively deep water environment below wave base or in an environment which inhibited normal marine organisms. As described, the rock directly above the paleokarst is composed of black shale or brown argillaceous limestone. The black shale is finely laminated, indicating an anaerobic environment. The brown limestone contains exclusive *Chondrites*, and a dysaerobic sea floor is implied (Bromley and Ekdale, 1984). The presence of fine lamination in the black shale and *Chondrites* in the limestone indicates that the subsequent depositional environment following the development of the paleokarsts varied from anaerobic to dysaerobic. This may explain why the small-scale paleokarsts at the base of the Burr Member were preserved.

As described, there are normally two paleokarst horizons in the basal part of the Burr Member in southeastern Saskatchewan. In central Saskatchewan only one paleokarst horizon is present in some areas. However, in the rest of central Saskatchewan and entire northwestern Saskatchewan, the paleokarst(s) in the basal part of the Burr Member is absent. There are two possible explanations: either the paleokarst(s) was produced, but not preserved, or the paleokarst(s) did not form in these regions. If the first alternative is the case, the absence of the paleokarst(s) was due to complete erosion before the overlying sediment was deposited. However, this option can be excluded because the top of the Second Red Bed Member is an undulating surface that is characterized by solution basins and fractures. Even if the paleokarst(s) above the convex part of the surface was completely removed, some residuum should have been preserved in the concave part of the solution basins and fractures that penetrate the interior of the dolomitic rocks of the Second Red Bed Member. However, no paleokarst remains were recognized in the solution basins and fractures. On the contrary, the concave parts of the solution basins are filled with black shale that is parallel to the irregular surface of the Second Red Bed Member. Even the fractures in the dolomitic rocks of the Second Red Bed Member are exclusively filled with the black shale (e.g., in Core 4-18-35-8W3).

This evidence suggests that the black shale in Core 4-18-35-8W3 is the earliest sediment after the development of the paleokarstic surface at the top of the Second Red Bed Member. However, in the nearby Core 3-30-37-2W3, the same black shale lies above the paleokarst of the Burr Member (Fig. 3-1), which suggests that the black shale formed after the development of the paleokarst at the base of the Burr Member. This, in turn,

suggests that when the carbonate sediments that constitute the paleokarst(s) at the base of the Burr Member were accumulating in southeastern Saskatchewan and some areas of central Saskatchewan, the Second Red Bed Member in the rest of central and northwestern Saskatchewan was still subaerially exposed. A further line of evidence supporting this interpretation is that the paleosol profile in the Second Red Bed Member is more mature where the paleokarst(s) at the base of the Burr Member is absent.

As noted, in central Saskatchewan, only one paleokarst horizon is present at the base of the Burr Member, whereas there are normally two superimposed paleokarst horizons at the base of the Burr Member in southeastern Saskatchewan. There are two possible explanations: either one of the paleokarsts was produced but not preserved, or else one paleokarst was not formed. If the first alternative is correct, it is more likely that the lower paleokarst horizon was totally destroyed because in the cores with two superimposed paleokarst horizons, a sharp erosional surface is present at the top of the lower paleokarst (e.g., in Core 8-14-20-30W1). In contrast, the upper surface of the upper paleokarst is generally well preserved. This indicates that the top of the lower paleokarst experienced erosion before the deposition of the carbonate sediment of the upper paleokarst; and on the contrary, little erosion was taking place after the development of the upper paleokarst. This possibility is very likely to have occurred in southeastern Saskatchewan because, in Core 16-11-21-31W1, the lower paleokarst horizon was almost completely removed. In the core sections in which only one paleokarst is present, the upper surface of the Second Red Bed Member commonly shows a convex appearance.

However, several lines of evidence argue against the explanation that the lower paleokarst in central Saskatchewan was completely eroded. Firstly, as discussed earlier, the top of the Second Red Bed Member is a surface paleokarst that is characterized by solution basins. The karstic rock that filled the basins would have been preserved locally even if the erosion completely removed the karstic rock on the convex parts of the surface. Therefore, on a regional scale, some cores might contain two superimposed paleokarst horizons whereas others have only one paleokarst horizon. However, in central Saskatchewan, in the cores with solution basins at the top of the Second Red Bed Member, only one paleokarst horizon was observed at the base of the Burr Member. Secondly, if the paleokarst was destroyed, reworked clasts should be found in the overlying sediments, as shown by the presence of reworked intraclasts in the upper limestone horizon of Paleokarst B in southeastern Saskatchewan. However, no such reworked clasts have been observed. Moreover, in addition to fossil moulds, solution

vugs, fractures and discoloration, the paleokarst in central Saskatchewan is characterized by collapse breccias. In contrast, no collapse breccias were found in the paleokarsts of southeastern Saskatchewan. The absence of collapse breccias in southeastern Saskatchewan suggests that the single paleokarst horizon in central Saskatchewan was more mature and was subaerially exposed longer than the paleokarst(s) in southeastern Saskatchewan. Thus, it must have begun to develop during the same period as the lower paleokarst of Paleokarst B and during the deposition of the carbonate sediment that constitutes the upper paleokarst horizon, it was still subaerially exposed. Therefore, it can be concluded that the second paleokarst did not form in central Saskatchewan.

In summary, following the first transgression-regression in early Burr time, the Williston Basin became subaerially exposed, which led to the formation of the first paleokarst horizon. Then, another marine transgression took place, but this covered a smaller area than the first transgression, and resulted in the deposition of the second limestone horizon. However, during this time period, the area that was not covered by the sea was still experiencing karstification. This was followed by another regression, that led to the formation of the second paleokarst horizon in the area with the carbonate sediment that had formed during the second transgression. This means that paleokarst A in central Saskatchewan represents a condensed paleokarst B. The former was subaerially exposed longer than the latter. Therefore, it should have been more intensely weathered. This in indeed supported by the fact that paleokarst A is generally more intensely brecciated than Paleokarst B.

3.3.2 Direction of Marine Transgression

The direction of the marine transgression in the Williston Basin during the Devonian has long been a controversial issue. Most geologists have suggested that the Williston Basin was then an extensional part of the Elk Point Basin (e.g., Moore, 1993) and that the sea transgressed from Alberta southeastward to Saskatchewan (Fig. 3-2) (e.g., Porter *et al.*, 1982). Others have assumed that the open sea lay to the north, in the direction of the Canadian Shield (Edie, 1959; Dunn, 1982a). Still others believed that in addition to the water from the northwest, some marine waters must have come from the east (Braun and Mathison, 1986; Meijer Drees, 1994). However, no compelling evidence has ever been presented to support any of these suggestions.

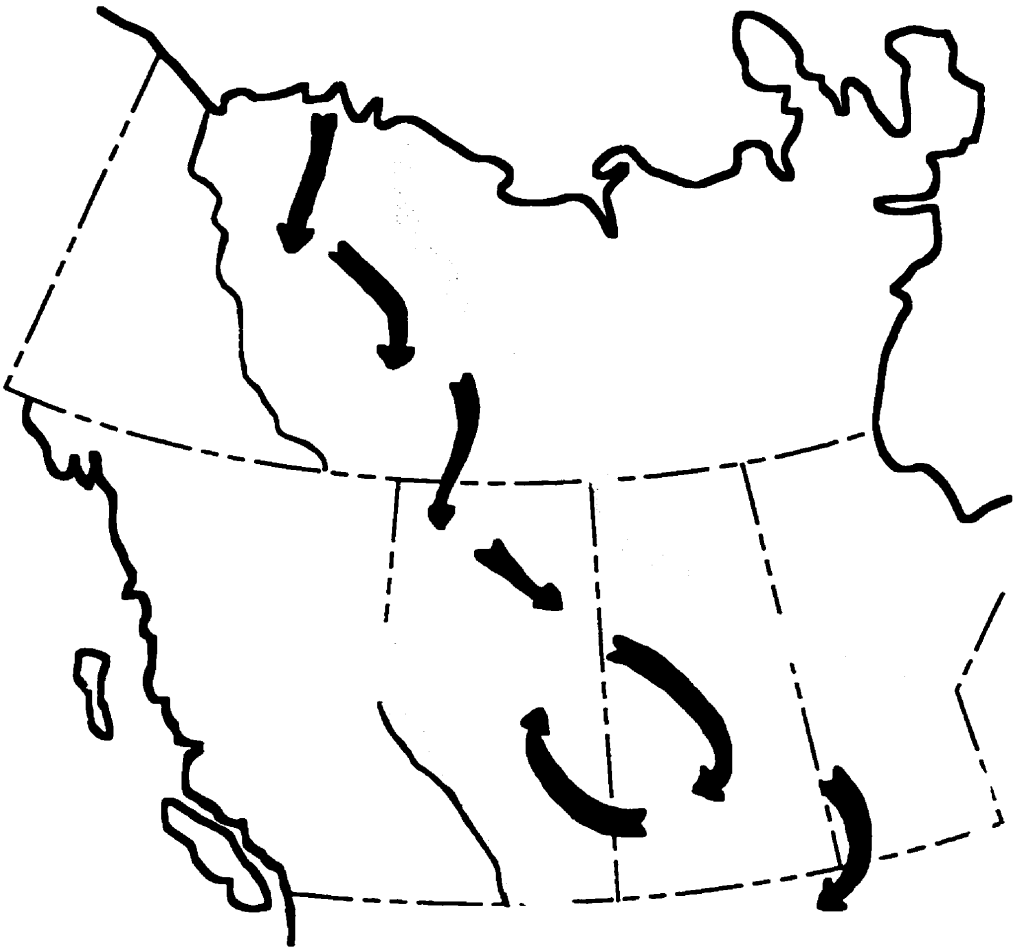

Fig. 3-2. Marine transgressive direction of the Williston Basin in the Middle Devonian (modified after Williams, 1984).

The distribution of the paleokarsts at the base of the Burr Member and the marked lateral variation in the degree of paleokarst development provide strong evidence for the direction of marine transgression in the Williston Basin during the deposition of the Dawson Bay Formation. As described, there are two superimposed paleokarst horizons at the base of the Burr Member in southeastern Saskatchewan; only one is present in some areas of central Saskatchewan, and none is present in northwestern Saskatchewan. This suggests that before the Williston Basin was completely flooded by a major transgression in the early Burr time, two minor marine transgressions took place in the basin. Both transgressions reached southeastern Saskatchewan, but only one was extensive enough to reach parts of central Saskatchewan. None reached northwestern Saskatchewan (Gu and Renaut, 1996) (Fig. 3-3). This shows that the marine waters came from the southeast. This conclusion is compatible with the fact that the unconformity between the Second Red Bed Member and Burr Member increases in time magnitude from southeastern to northwestern Saskatchewan, as evidenced by the higher maturity of the paleosol profile of the Second Red Bed Member in central Saskatchewan compared to that in southeastern Saskatchewan.

The Dawson Bay Formation has commonly been thought to have formed during single cycle of marine transgression and regression (Sandberg and Hammond, 1955; Johnson *et al.*, 1985; Peterson and MacCary, 1987). Johnson *et al.* (1985) suggested that it was formed during Cycle IIa of their sequence of Devonian transgressions and regressions. Furthermore, they suggested that this cycle was a long-sustained transgression, rather than a cluster of separate shorter events. However, the presence of the paleokarst horizons at the base of the Burr Member indicates the periodic emergence of the Williston Basin. Thus, it can be concluded that the deposition of the Dawson Bay Formation was marked by several shorter phases of marine trangressions and regressions, rather than a simple single cycle.

3.3.3 Paleoclimatic Inferences

Although karst develops under a variety of climatic conditions (e.g., Esteban and Klappa, 1983), the formation of subaerial solution basins on the top of the Second Red Bed Member requires a certain amount of rain and runoff undersaturated with respect to $CaCO_3$. This implies a moderately high precipitation -- extreme aridity could not have existed when the karst was developing. The paleokarsts at the base of the Burr Member are characterized by extensive mouldic and vuggy porosity, which also indicates

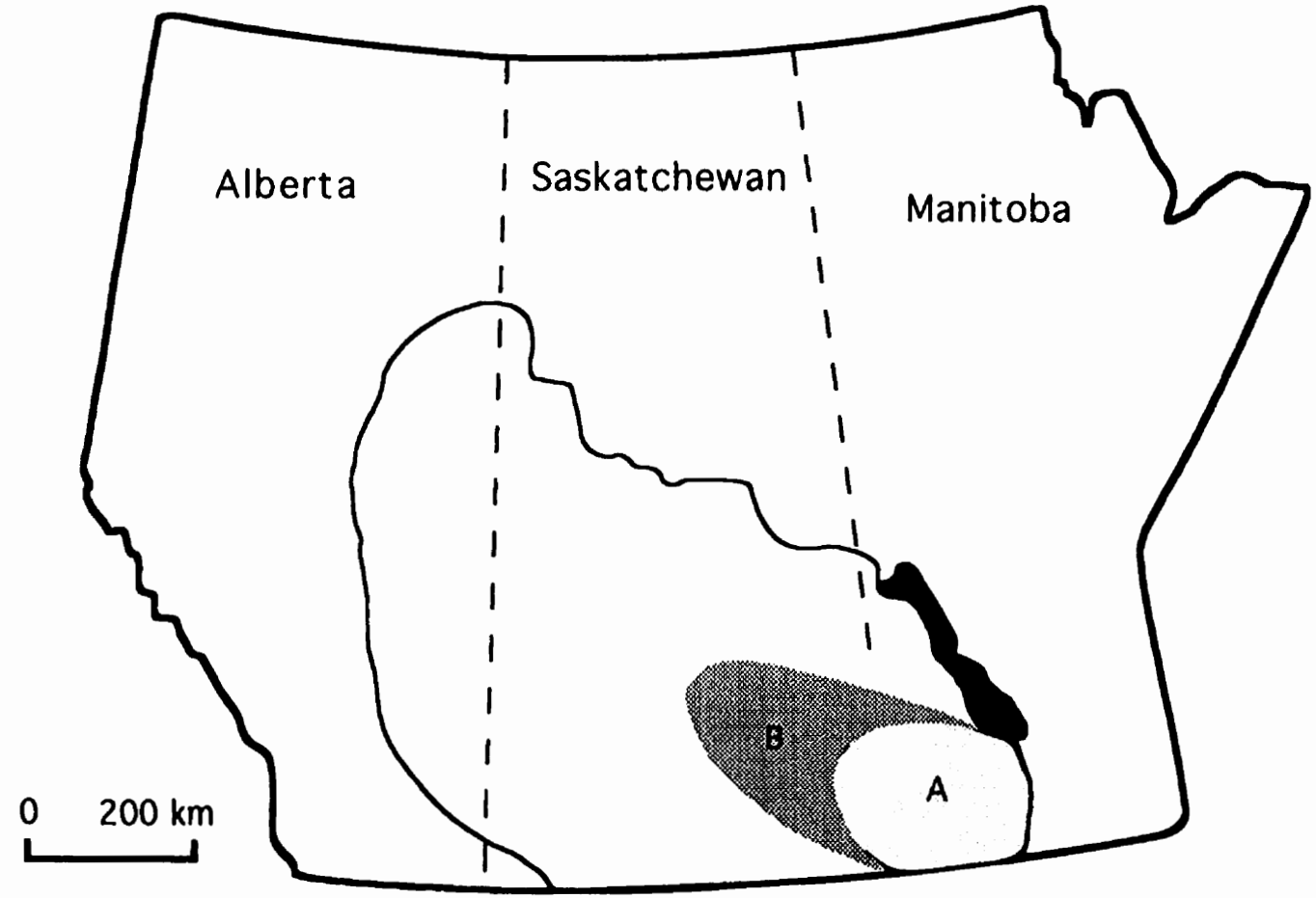

Fig. 3-3. Map showing the areas covered by two minor marine transgressions during early Burr times. A - area covered by both the marine transgressions; B - area covered by only one of the transgressions.

considerable percolation of meteoric waters and wet conditions (Wright and Smart, 1994). The presence of the probable phytokarst in Core 8-14-20-30W1 provides further evidence to support a humid climate because this type of karst probably forms only in humid tropical climates (Folk *et al.*, 1973). Further evidence includes the widespread presence of the collapse breccia and the absence of calcrete. The former is generally associated with humid climates (Choquette and James, 1988), whereas the latter, although variable, mainly develops in semi-arid subaerial settings (Wright and Smart, 1994). Therefore, although the Williston Basin was possibly dominated by arid climates in the Middle Devonian, as suggested by Witzke and Heckel (1988), periods of more humid climatic conditions were present.

3.4 The Black Shales at the Base of the Burr Member

Two thin black shales are present at the base of the Burr Member (Plate 3-7A). One lies above the top of the Second Red Bed Member; the other overlies the micro-paleokarstic horizon(s) of the Burr Member or rests on the top of the Second Red Bed Member where the paleokarst(s) is absent. For convenience, the former is termed *black shale A* and the latter *black shale B.*

3.4.1 Black Shale A

Black shale A is dark brown to black, finely laminated, and less than 1 cm thick (Plates 3-7A, 2-2C). It is widespread from central to southeastern Saskatchewan. The shale lies directly above the Second Red Bed Member and faithfully follows the undulating upper surface of the member (Plate 2-2B). No shell fossils or burrows are observed in the black shale. BSE photomicrographs show that the black shale consists of alternating organic-rich and organic-poor laminae, each with an average thickness of 150 μm (Plate 3-7B). The organic-rich laminae consist mainly of organic matter, pyrite and clastic grains (Plate 3-7C). The pyrite occurs as framboids, single crystals and irregular aggregates of crystals. Most framboids are less than 10 μm in diameter (Plate 3-7D). The clastic grains include potassium feldspar, quartz, calcite and dolomite. They are normally less than 10 μm in diameter and irregular in shape, indicating a detrital origin. The organic-poor laminae are composed predominantly of silt- and clay-grade grains, as above. Pyrite is present, but much less abundant than in the organic-rich laminae (Plate 3-7B).

The black shale has small, closely spaced polygonal mudcracks (Plate 2-2C). They are confined to the shale and do not extend vertically into the underlying dolostone of the Second Red Bed Member. The diameter of the mudcracks is less than 1 cm. Although the mudcracks have been observed in core samples, they are not present in every core.

3.4.2 Black Shale B

Black shale B is best developed in central Saskatchewan, where it is up to 4 cm thick. It either lies above the paleokarst in the basal part of the Burr Member (Plate 2-5D) or rests directly on the top of the Second Red Bed Member where the paleokarst at the base of the Burr Member is absent (Plates 2-9C, 3-8A). Black shale B also fills dissolution voids and fractures of the karstified rocks (Plates 2-5D, 3-8B). It is brown to dark brown and

PLATE 3-7

Plate 3-7 A: Core photograph showing black shale A (a) and B (b) at the base of the Burr Member, separated by a thin paleokarst horizon (p). Black shale A below the paleokarst is finely laminated. Black shale B above the paleokarst is massive and bioturbated by small *Chondrites*, with a thickness that varies significantly across the core. Lsd. 4-25-20-30W1. Scale bar is 2 cm.

Plate 3-7 B: BSE micrograph of black shale A in Plate 3-7 A, consisting of alternating organic-rich and organic-poor laminae. Lsd. 4-25-20-30W1.

Plate 3-7 C: BSE micrograph of black shale A showing an organic-rich lamina that is composed of organic matter, pyrite and detrital clasts. Lsd. 4-25-20-30W1.

Plate 3-7 D: BSE micrograph showing pyrite framboids in an organic-rich lamina of black shale A. Lsd. 4-25-20-30W1.

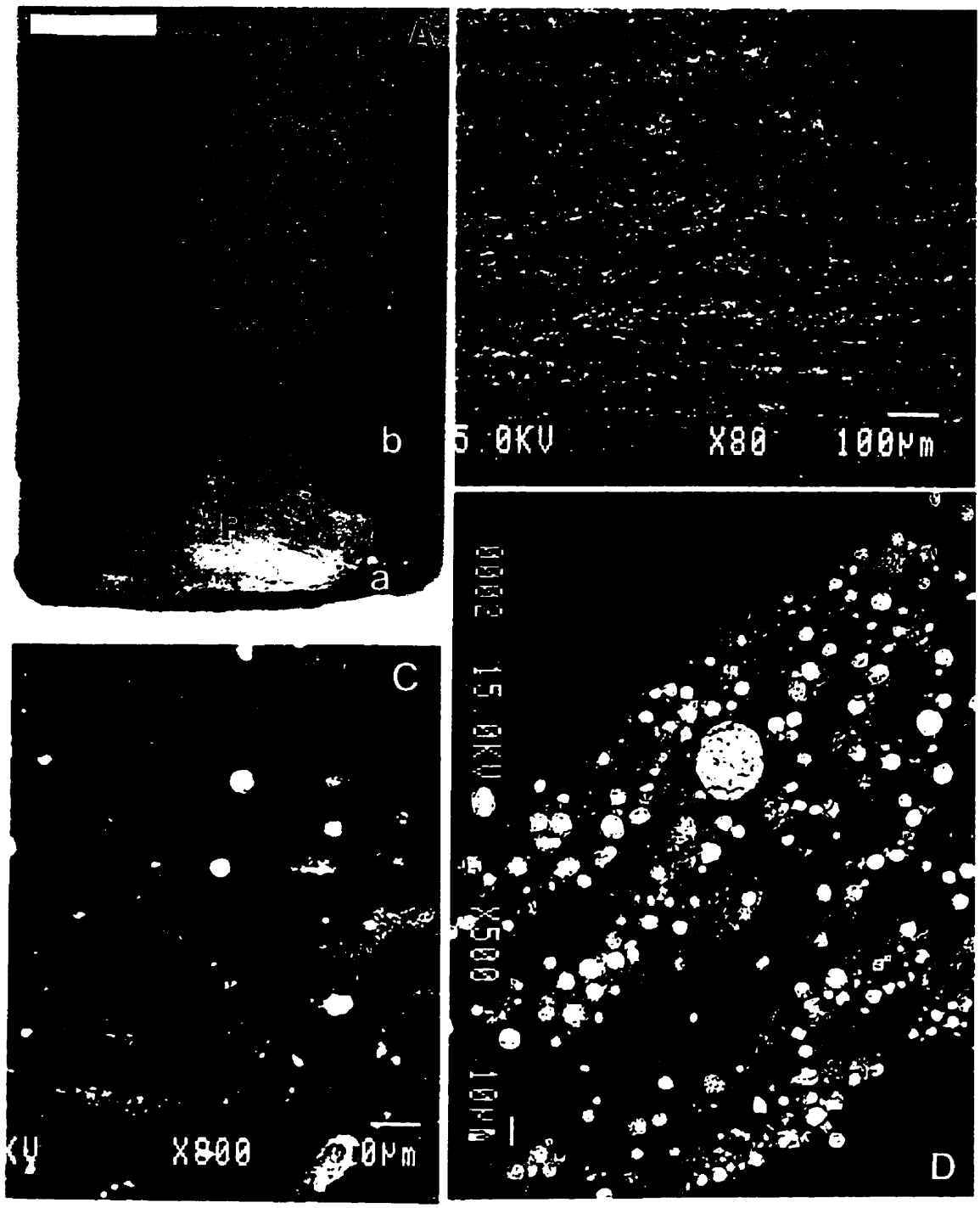
A
b
a
5.0KV X80 100μm
C
KV X800 10μm
D
X500 10μm

PLATE 3-8

Plate 3-8 A: Slabbed core photograph showing black shale B (b) at the base of the Burr Member in central Saskatchewan. It shows fine lamination. The black shale is in gradual transition with the overlying kerogen-laminated lime mudstone (k). Lsd. 4-18-35-8W3. Scale bar is 3 cm.

Plate 3-8 B: Slabbed core photograph showing fractures in the dolomitic conglomerate at the top of the Second Red Bed Member that are filled by black argillaceous sediment (s) that are identical to the overlying black shale B. Lsd. 4-18-35-8W3. Scale bar is 3 cm.

Plate 3-8 C: Plane-light photomicrograph of black shale B, composed of alternating organic-rich and organic-poor laminae. Lsd. 4-18-35-8W3. Scale bar is 0.5 mm.

Plate 3-8 D: Slabbed core photograph showing remains of black shale B (b) at the top of the paleokarst (p) of the Burr Member. Lsd. 13-12-22-32W1. Scale bar is 3 cm.

Plate 3-8 E: Slabbed core photograph showing pyritized crust (c) at the top of the paleokarst that is disrupted by boring and erosion. Lsd. 9-14-19-30W1. Coin diameter is 1.7 cm.

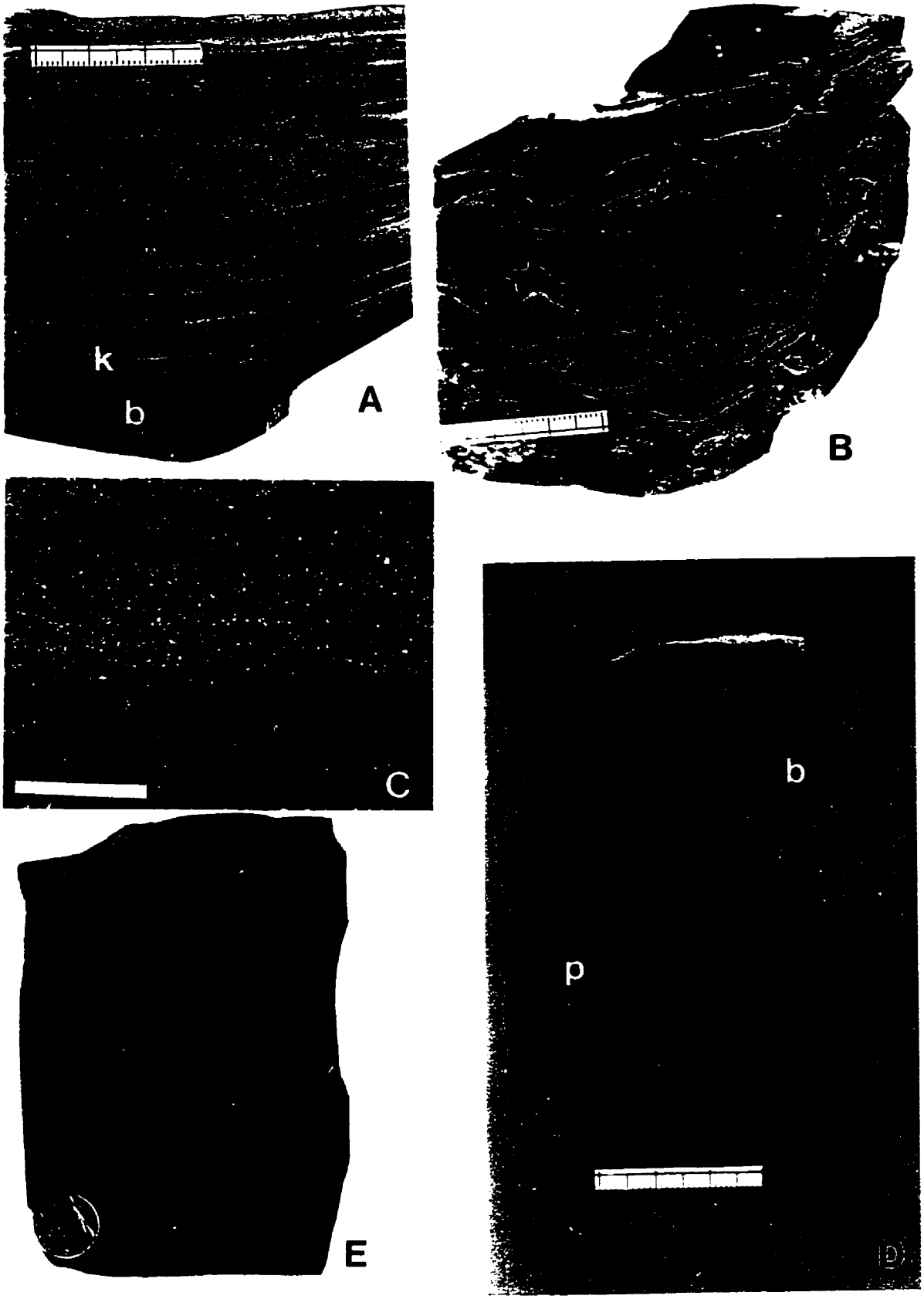
k
b
A
B
C
b
p
D
E

rich in organic matter. The black shale has uniformly fine and closely spaced laminae. The lamination results from a regular alternation of dark brown and black laminae, which are sub-millimeters in thickness. Where the underlying rock has a flat upper surface, the laminae are even and parallel. If the underlying rock has an undulating or irregular upper surface, the lamination is parallel to the irregular surface of the underlying rock. The black shale is completely undisturbed by burrowing organisms.

In thin section, black shale B appears orange in transmitted light and shows well-developed micro-laminations, which are composed of alternating organic-rich and organic-poor laminae (Plate 3-8C). The organic-rich laminae are relatively thin and are composed mainly of amorphous organic matter, pyrite and clastic grains. The thicker organic-poor laminae are composed predominantly of silt- to clay-grade clastic grains, which include potassium feldspar, quartz, dolomite and calcite. Pyrite is present throughout the black shale as disseminated microcrystals, with a diameter of about 1 μm. In places, pyrite framboids are observed.

In southeastern Saskatchewan, the discrete black shale B is generally absent except in Core 4-25-20-30W1, where it is present between the paleokarst of the Burr Member and the directly overlying marlstone (Plate 3-7A). The black shale is massive in appearance, with a thickness that varies significantly across the slabbed core, ranging from several mm up to 2 cm. Its boundary with the overlying marlstone is diffuse. Additionally, traces of small *Chondrites* are observed in the black shale, which penetrated from the overlying marlstone. In the portion where the black shale is relatively thin, the boundary between the black shale and the overlying marlstone is diffuse and the marlstone is speckled with a large amount of dark-brown argillaceous sediment. Where the black shale is relatively thick, the marlstone is significantly lighter in colour and contains fewer argillaceous specks. This suggests that the dark brown argillaceous specks in the marlstone are derived from black shale B by infaunal bioturbation.

Dark-brown argillaceous sediment, which appears identical to the black shale, is common in the voids of the underlying karstified rocks of the Burr Member in southeastern Saskatchewan (Plate 3-8D). The argillaceous sediment is also high in organic matter, pyrite and authigenic uranium. These features suggest that it was accumulated under reducing conditions, and that it is not a terra rossa soil, which develops under oxygenated conditions. The argillaceous sediment is mainly distributed in the voids near the top of the paleokarstic horizon(s). Most argillaceous sediment is massive in appearance. If the

paleokarst(s) at the base of the Burr Member is composed of two superimposed limestone horizons, the argillaceous sediment is generally confined to the voids in the upper limestone horizon.

The upper surface of the paleokarst(s) in southeastern Saskatchewan is commonly pyritized (Plate 3-8E). The thickness of the pyritized rind varies from less than 1 mm to 5 mm. In places, the pyritized rind was penetrated by borings, and fragments of the pyritized crust can be found in the overlying marlstone. This suggests that the pyritization took place in a synsedimentary environment. Where the underlying paleokarst is highly porous, a large amount of pyrite commonly formed in the porous parts of the karstic rock and gave them a black mottled appearance (Plate 3-4A). Because the pyritic crust cannot have formed in a (subaerial) oxygenated environment, it probably formed in the early marine transgressive stage after the development of the karstified rocks.

3.4.3 Geochemistry of the Black Shales

A total of 10 black shale samples was analyzed for trace metal elements by ICP-MS. Samples of both black shale A and B from central to southeastern Saskatchewan were selected. Their geochemical characteristics are strikingly similar and cannot be differentiated by the variation of the trace element contents. Both black shales are slightly to moderately enriched in uranium, ranging from 4.01 to 6.28 ppm (Table 3-1). Only one sample contains 3.25 ppm, which is close to the average U (3.7 ppm) content of black shale (Mielke, 1979). However, the content of thorium in all samples is very low, ranging from 2.89 to 4.82 ppm. These figures are significantly lower than the average Th content of black shales, which is 12 ppm (Mielke, 1979). Because Th is present mainly in the detrital clay fraction of mudrocks (Myers and Wignall, 1987), the low Th contents probably indicate that the detrital clay input was very low during black shale deposition. Like Th, U also is present in the detrital clay fraction, but is also carried partly in solution as uranyl carbonate complexes (Langmuir, 1978). Under reducing conditions it may be precipitated, enriching the sediment in "authigenic" (nondetrital) uranium. If the detrital component of U is known, the authigenic component can be calculated. The minimum Th/U ratio of normal mudstones, where U is assumed to be entirely detrital, is 3 (Wignall and Myers, 1988). Based on this assumption, the authigenic U was calculated for black shale A and B. They ranges from 2.03 to 5.20 ppm. This indicates that they are both enriched in authigenic U, which in turn suggests that they were deposited under reducing conditions.

Sample No.	U	Th	U - Th/3
3-30-37-2W3-1	6.28	3.25	5.20
3-30-37-2W3-2	3.25	3.67	2.03
4-18-35-8W3-3	4.45	4.80	2.85
1-2-39-8W3-1	4.01	2.89	3.05
4-25-20-30W1-1	6.09	4.13	4.61
4-25-20-30W1-2	4.59	3.69	3.36
8-14-20-30W1-4	6.24	4.33	4.80
16-11-21-31W1-2	5.92	4.02	4.58
1-12-34-1W3-1	4.62	4.42	3.15
1-12-34-1W3-2	4.43	4.82	2.83

Table 3-1. Showing contents of total uranium, thorium and authigenic uranium in the black shales at the bottom of the Burr Member (in ppm).

3.4.4 Wireline Log Response of the Black Shales

On gamma-ray logs, there is a radioactive peak at the base of the Burr Member in central Saskatchewan, registering 425 API units. Radioactivity decreases upwards for the next 2.5 m until it reaches a value of 80 API units. However, several subsidiary radioactive peaks appear in the generally decreasing curve. These peaks may represent the organic-rich layers in the kerogen-laminated lime mudstone, which lies directly above black shale B. In contrast, the gamma-ray logs from southeastern Saskatchewan show only one isolated radioactive peak at the base of the Burr Member (Fig. 2-4). This implies that the bottom of the Burr Member contains only one black shale and that the sedimentary rocks directly above the black shale are relatively low in radioactive elements.

3.5 Rocks Directly Below and Above Black Shale A and B

The rock directly below black shale A is the dolostone of the Second Red Bed Member. Directly above the black shale are the paleokarstic rocks of the Burr Member. In central Saskatchewan, if the karstified rock at the base of the Burr Member is present, black shale B lies above it; if the paleokarst is absent, the black shale rests on the top of the Second Red Bed Member. The rock above black shale B in central Saskatchewan is a kerogen-laminated lime mudstone. This, in turn, is overlain by a horizontally laminated lime mudstone. In southeastern Saskatchewan, the rock overlying black shale B is dark brown marlstone. The marlstone is rich in *Chondrites*, which is present to the exclusion of all other trace fossils. The *Chondrites* are about 1 mm in diameter and most of them are horizontal in orientation. The superabundance of *Chondrites* suggests a high organic concentration in the marlstone (Vossler and Pemberton, 1988).

3.6 Discussion

Black shales source the bulk of the world's hydrocarbons, thus intensive studies have been carried out on these rocks in recent years. However, they are still amongst the least understood of all sedimentary rock types. There are two major controversies. One concerns the deep-water versus shallow-water deposition of black shales, which is one of the longest running arguments in the history of geology (Cluff, 1980). It is well established that most black shales are relatively deep-water facies that formed in basin center locations in epicontinental settings (Wignall and Maynard, 1993; Heckel, 1991; Wignall and Hallam, 1991). However, some thin black shales are associated with shallow

water facies and this has led some authors to infer a shallow origin for these black shales (e.g., Zangerl and Richardson, 1963; Hallam, 1967; Hallam and Bradshaw, 1979; Nuhfer, 1981; Coveney and Shaffer, 1988, Leckie *et al.*, 1990; Schieber, 1994). The main evidence for the shallow-water model lies in the observation that the black shales are found in close association with shallow water facies, including coal (Cluff, 1980; Wignall and Maynard, 1993). This evidence was disputed by Heckel (1977), who suggested that "Although coals are non-marine to shoreline deposits, the overlying (black shale) beds do not necessarily have to be very shallow-water deposits..." Therefore, until now, no compelling evidence has been presented to support the shallow-water model for these black shales.

Black shales A and B in the Burr Member, although very thin, are commonly present in the cores that were examined by the author. They rest directly on the paleokarsts and no sediments belonging to transgressive system tracts are present between the black shales and karstic rocks. Additionally, they do not connect laterally with contemporary nearshore or shoreline facies. All these features suggest that both of the black shales resemble the basal transgressive black shales of Wignall and Maynard (1993).

As described previously, the black shales are finely laminated and are rich in organic matter, uranium and pyrite, all of which suggest that they were deposited under anoxic conditions. However, after the deposition of black shale A, the sediment was probably emergent briefly, as indicated by the presence of mudcracks. The possibility that these are syneresis cracks is rejected because the latter do not usually form a complete polygonal pattern (Tucker, 1991). This suggests that the cracks formed through desiccation associated with subaerial exposure. This, in turn, implies that black shale A was deposited in a very shallow water environment. Although no mudcracks are present in black shale B, its sedimentological, petrographic and geochemical characteristics are almost identical to those of black shale A, and it too probably was deposited in shallow water.

The stratigraphic position of black shale B, which lies directly above paleokarsts, suggests that it appears in the lowest part of the transgressive system tract, which is normally characterized by shallow water deposition (Nummedal and Swift, 1987). Furthermore, although very thin, the uniform thickness and widespread distribution of the black shales indicate that their formation did not need local topographic hollows, as proposed by Hallam and Bradshaw (1979), Dabard and Paris (1986) and Wignall (1994). This is further supported by the presence of the kamenitzas on the top of the Second Red

Bed Member, which suggests that the Williston Basin had a widespread flat bottom before the deposition of the Burr Member.

The exact depositional environments of the black shales remain unclear, but indirect evidence can shed light on this question. In southeastern Saskatchewan, black shale B is overlain by *Chondrites*-bearing marlstone. The *Chondrites*-producing organisms not only reworked the marlstone but also the black shale, which produced partial to complete mixing between the marlstone and the black shale. This indicates that the black shale was still soft when the marlstone was deposited. This, in turn, suggests that no significant sedimentary break is present between their deposition. Because *Chondrites* is a marine trace fossil (Bromley and Ekdale, 1984), its presence implies that the marlstone was deposited in a marine environment. This, in turn, suggests that black shale B was also deposited in a marine environment, or at least a transitional environment between non-marine and marine settings. Black shale A has similar geochemical, sedimentological and stratigraphic characteristics, and was probably deposited in a similar setting.

Another controversy concerning black shales is the factors that control the formation of organic-carbon-rich sediments and sedimentary rocks. It is one of the most contentious issues in current black-shale debates. The traditional view is that organic rich shales accumulate as a result of enhanced preservation in an anoxic environment. This model has received widespread support, but is disputed by some authors (e.g., Pedersen and Calvert, 1990), who have suggested that a high organic-carbon flux to the sediment caused by high surface water productivity may be the main mechanism for the formation of organic-rich sediments. The best example supporting this model is the Holocene sediments of the Black Sea, which are readily divisible into three units: unit 1, the coccolith limestone, which is currently accumulating; unit 2, an organic-rich sapropel, and unit 3, a claystone. Unit 2 is significantly enriched in organic matter, which was interpreted to have formed by increased production during a transition between the Pleistocene lacustrine conditions and the modern-day marine, euxinic basin. On the contrary, the modern marine facies are not particularly enriched in organic matter despite the presence of an anoxic water column (Pedersen and Calvert, 1990). The same interpretation has been used to explain the organic-rich unit of the Holocene sediments in Kau Bay, Indonesia (Middelburg *et al.*, 1991). Furthermore, Calvert (1990) has claimed that the entire water column was oxygenated during Unit 2 deposition in the Black Sea, by using evidence from I/Br ratios. This, in turn, led Pedersen and Calvert (1990) to propose that the fundamental control on the accumulation of carbon-rich facies is not the presence

or absence of anoxia. However, Wignall (1994) cast doubt on the reliability of I/Br ratios. The above-mentioned proposition is also in contradiction with the geological evidence observed from black shale B in the Burr Member.

As described, black shale B in central Saskatchewan is overlain by a kerogen-laminated lime mudstone. The presence of the well-preserved laminations indicates that the rock formed in an anoxic or very low oxygen environment, whereas in southeastern Saskatchewan, the black shale is normally not observed above the paleokarst(s) but in the voids of the karstic rocks. In addition, the top of the karstic rocks is commonly pyritized and the directly overlying marlstone is characterized by disseminated speckles of argillaceous sediment.

All these features suggest that a thin black shale was present above the paleokarst(s) of the Burr Member in southeastern Saskatchewan, but was almost completely removed by bioturbation during deposition of the directly overlying carbonate sediment. This conclusion is further supported by the presence of superabundant *Chondrites* in the dark brown marlstone, which suggests that an organic-rich sedimentary bed (black shale) was once present (Vossler and Pemberton, 1988) above the paleokarst(s). Because *Chondrites* is widely held as an indicator of low-oxygen conditions when it is the sole trace fossil encountered (Bromley and Ekdale, 1984; Savrda and Bottjer, 1986), the presence of these small *Chondrites* suggests that the depositional environment following the accumulation of black shale B was very low in oxygen. However, even under such low-oxygen conditions, organic-rich sediment could not be preserved. On the contrary, the same black shale is well preserved in central Saskatchewan due to persistence of anoxic conditions after accumulation of the black shale. Thus, it can be concluded that even if the absence of oxygen in bottom waters does not have any control on the accumulation of organic-rich sediments, it can enhance their preservation.

The exact mechanism that caused the deposition of the black shales is not clear at this time. It may have been due to high productivity caused by marine transgression on the paleokarstic surfaces, which were probably enriched in nutrients. When the nutrients were consumed, accumulation of organic-rich sediments stopped because no extra nutrients were provided. This is probably the reason that the black shales are so thin. The anoxic conditions during the deposition of the black shales may have been caused or enhanced by the extremely high productivity, especially during deposition of black shale B in southeastern Saskatchewan. After the deposition of the black shale, the anoxic conditions

were replaced by dysaerobic conditions. In central Saskatchewan, the anoxic conditions, however, seem not to have been caused by extremely high productivity because the anoxic conditions were still present during deposition of the overlying horizontally-laminated lime mudstone, which is low in organic content.

3.7 Summary

This study recognizes three, previously unrecorded paleokarst horizons in the contact zone between the Second Red Bed Member and the Burr Member. One is the contact between the Second Red Bed Member and the Burr Member, which has a widespread distribution in the subsurface of Saskatchewan. The two other paleokarst horizons are present at the base of the Burr Member, but their distribution is regionally limited. This study shows that there are two superimposed paleokarsts at the base of the Burr Member in southeastern Saskatchewan. However, only one of them is present in parts of central Saskatchewan and none is present in the rest of central Saskatchewan and northwestern Saskatchewan. New evidence also shows that in the area where the paleokarst(s) at the base of the Burr Member is present, the dolostone at the top of the Second Red Bed Member is well preserved. In contrast, in the area where the paleokarst(s) is absent, the dolostone is completely brecciated by pedogenesis. This indicates that the top of the Second Red Member was subaerially exposed longer in the area where the paleokarst(s) is absent. Moreover, the superimposed paleokarsts at the base of the Burr Member in southeastern Saskatchewan are characterized by well-developed solution vugs but lack the collapse breccia that typifies the single paleokarst horizon in central Saskatchewan. This suggests that before the Williston Basin was completely flooded by seawaters during early Burr time, two minor marine transgressions took place. Both reached southeastern Saskatchewan, but only one marine transgression reached parts of central Saskatchewan and none extended to northwestern Saskatchewan.

In addition, this study has shown that there are two thin black shales at the base of the Burr Member. One lies above the Second Red Bed Member; the other overlies the paleokarst(s) of the Burr Member or rests upon the Second Red Bed Member where the paleokarst(s) is absent. The black shales are finely laminated and are rich in organic matter, uranium and pyrite, indicating that they were deposited under anoxic conditions. The presence of the black shales that directly overlie the paleokarsts suggests that they may have been deposited in shallow water. This conclusion is supported by the local presence of mudcracks in the black shales.

CHAPTER 4

LOWER BURR MEMBER

4.1 Introduction

In order to understand better the role that increasing oxygen concentration may have had in the early Phanerozoic history of the Metazoa, Rhoads and Morse (1971) provided an excellent synthesis of data on extant oxygen-deficient basins and developed a model (Rhoads-Morse-Byers model) which divided marine benthic biofacies into three sub-biofacies based on dissolved oxygen content (Fig. 4-1). They are named aerobic, dysaerobic and anaerobic biofacies, respectively. In the Rhoads-Morse-Byers model, marine benthic environments with greater than 1.0 ml/l of dissolved oxygen typically produce a sedimentary record characterized by abundant and diverse macrofossils and heavily bioturbated fabrics. These conditions result in deposition of aerobic biofacies. A somewhat oxygen-deficient sea-floor environment, with oxygen concentration between 1.0 ml/l and 0.1 ml/l, is interpreted in the Rhoads-Morse-Byers model to lead to deposition of dysaerobic biofacies, which they described as characterized by a partially bioturbated sedimentary fabric with poorly calcified benthic faunas that are dominated by deposit feeders. The biofacies that represents the lowest oxygen concentrations, the anaerobic biofacies (oxygen concentrations lower than 0.1 ml/l), is defined as laminated sediment lacking all benthos. Later, Byers (1977) suggested that from the nearshore basinward, the aerobic biofacies passes through the dysaerobic biofacies into the anaerobic biofacies with increasing water depth (Fig. 4-1). Since then, this model has been widely used to interpret oxygen-deficient environments of ancient epeiric seas (e.g., Byers, 1977; Cluff, 1980; Davis and Byers, 1993).

Recently, some modifications to the model were proposed (Savrda *et al.*, 1984; Thompson *et al.*, 1985) and trace fossil assemblages have been added to detect subtle changes of dissolved oxygen level within the dysaerobic range (Savrda and Bottjer, 1986).

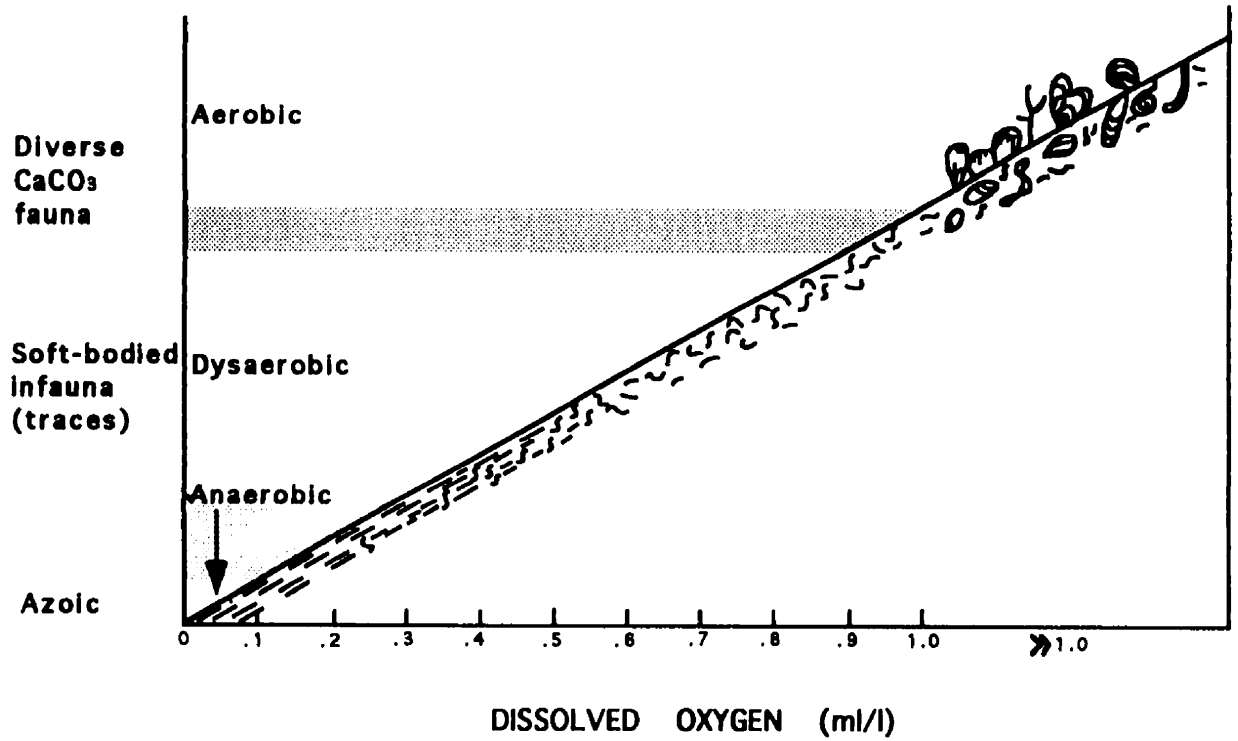

Fig. 4-1. Idealized cross-section of a Recent marine basin showing the relationship between levels of dissolved oxygen (X-axis) and the benthic fauna (Y-axis, left-hand side). (Modified after Rhoads and Morse, 1971).

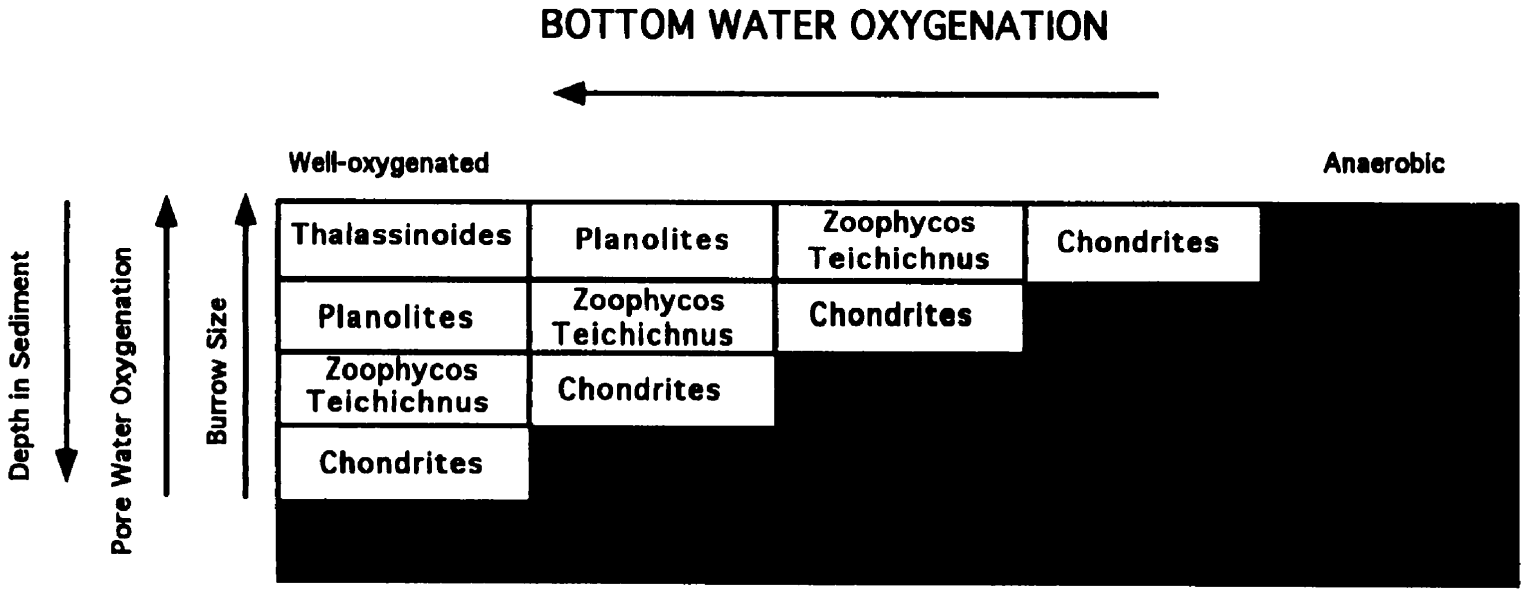

Fig. 4-2. Schematic diagram summarizing trace fossil associations in oxygen-depleted environments (modified after Pemberton et al., 1992).

It is now recognized that trace fossil diversity, burrow size and burrow penetration depth decrease with decreasing oxygen availability (Savrda *et al.*; 1984, Edwards, 1985). Four trace-fossil assemblages are now used to detect subtle changes of oxygen level within the dysaerobic range (Savrda and Bottjer, 1989) (Fig. 4-2). They are named the *Chondrites*, *Zoophycos/ Teichichnus*, *Planolites* and *Thalassinoides* assemblages. The *Chondrites* assemblage contains only small *Chondrites*. It represents an oxygen level slightly higher than that of the anaerobic biofacies (Bromley and Ekdale, 1984; Ekdale, 1985; Savrda and Bottjer, 1986). The *Zoophycos/Teichichnus* assemblage is composed of *Chondrites*, *Zoophycos* and *Teichichnus*, indicating an oxygen level higher than that represented by the *Chondrites* assemblage. Both *Zoophycos* and *Teichichnus* are typically present in the assemblage. However, one or the other may be absent in some cases. The *Planolites* assemblage indicates a further increase of oxygen level in a benthic environment. It contains *Planolites*, *Chondrites*, *Teichichnus* and *Zoophycos*. The *Thalassinoides* assemblage contains all trace fossils of the *Planolites* assemblage, in addition to *Thalassinoides*. It represents well-oxygenated conditions.

The Rhoads-Morse-Byers model was based on data compiled from modern marine environments, which are characterized by a steep shelf slope, with a rapid transition from shallow water shelf to deep basin setting. However, at times during geological record, epeiric seas covered extensive areas of cratons (Tucker and Wright, 1990), which were characterized by very broad shallow water areas, extremely low oceanward gradients and nearshore low-energy deposits due to the offshore dissipation of wave and current energy (Shaw, 1964; Irwin, 1965; Wilson, 1975). It has been suggested that these epeiric seas lacked normal astronomical tides and could be divided into marginal areas that were under the influence of tides, and interior regions that were unaffected by tidal action (Mazzullo and Friedman, 1975). Therefore, the landward areas of epeiric seas might have become stagnant more easily than the higher energy areas nearer to the open ocean. Thus, it is plausible that the depositional environment may have become progressively more oxygen-deficient from an offshore high energy area to a more nearshore low energy area.

In this chapter, an example from the lower Burr Member (the lower part of the Burr Member) is described, which shows that from more nearshore basinward, the benthic environment changed from less oxygenated to more oxygenated conditions.

PLATE 4-1

Plate 4-1 A, B, C and D: Detailed core photograph showing the lower Burr Member from southeastern Saskatchewan. **Plate 4-1 A** includes the uppermost part of the Second Red Bed Member, the paleokarsts (p) at the base of the Burr Member, the basal argillaceous lime mudstone unit, and the lower part of the lower unit. **Plate 4-1 B** shows the upper part of the lower unit. **Plate 4-1 C** includes the middle unit and the lower part of the upper unit. **Plate 4-1 D** shows the upper part of the upper unit. Lsd. 13-12-22-32W1. (One core box is 0.76 m long and core diameter is 10.1 cm.)

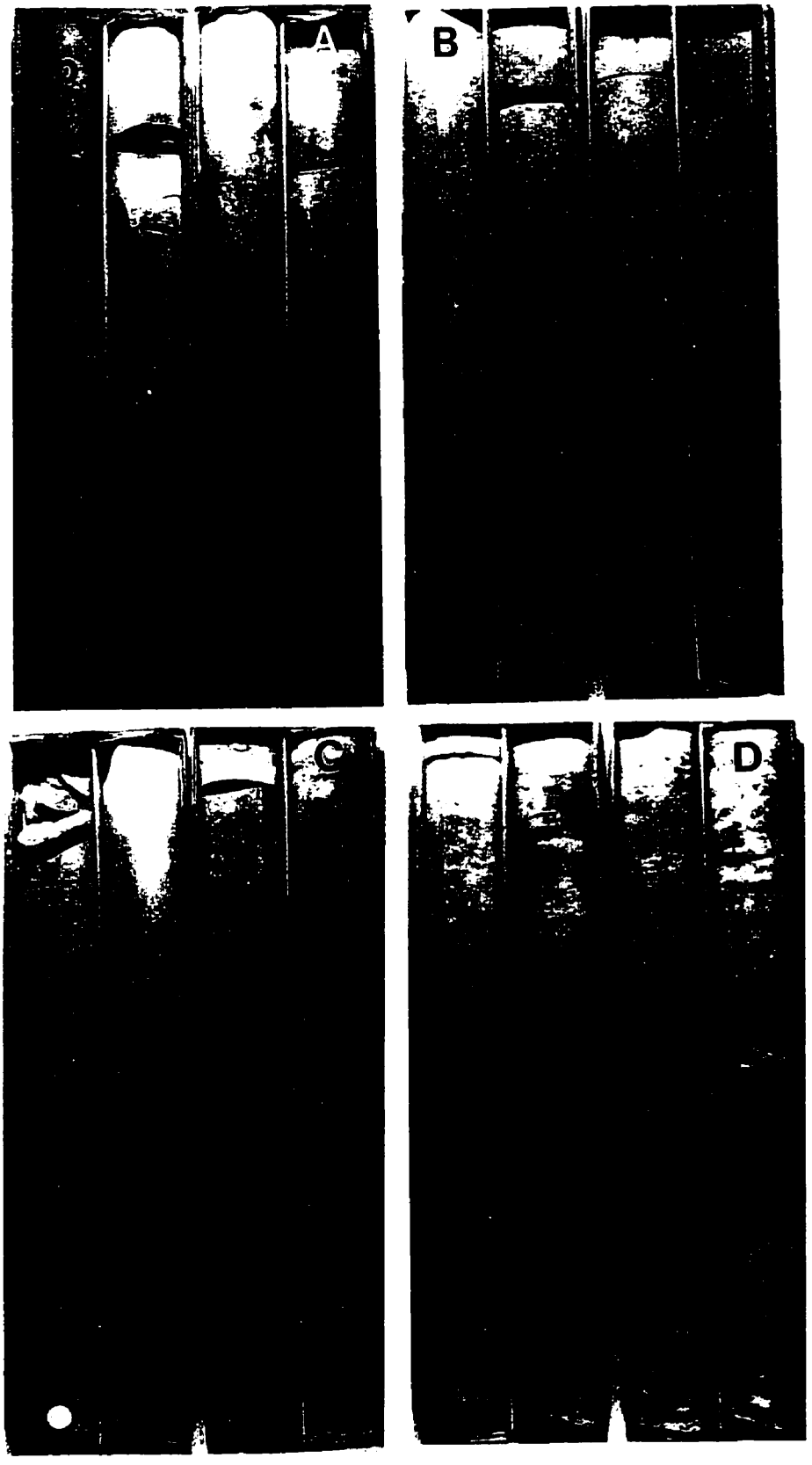
A
B
C
D

4.2 Biofacies in the lower Burr Member

4.2.1 Southeastern Saskatchewan

In southeastern Saskatchewan, the lower Burr Member is represented by a sedimentary succession in Core 13-12-22-32W1 (Plate 4-1A-D). There are two superimposed paleokarsts at the base of the Burr Member. The upper surface of the upper paleokarst is filled with black shale (Plate 3-8D). This, in turn, grades upward into a light grey to brown argillaceous lime mudstone unit, which is about 40 cm thick. Abundant microfossils are present at the base of this unit (Plate 4-2A). They are preserved as moulds and cannot be identified with confidence. In the lower part, the primary trace fossil in the argillaceous lime mudstone is composed exclusively of small *Chondrites* (Plate 4-2B). The *Chondrites* are about 1 mm in diameter. In the middle part, although still dominated by small *Chondrites*, trace fossils are more diverse and relatively large burrows begin to appear (Plate 4-2C). In the upper part, *Planolites* is the only distinct softground burrow (Plate 4-2D). A firmground is present at the top of this unit, which is penetrated by traces of *Glossifungites* ichnofacies (Plate 4-2D). Additionally, secondary *Skolithos* are observed penetrating the entire unit, which cross-cut all other softground burrows (Plate 4-2B). They are vertical in orientation, about 1 cm in diameter, and are filled with brown carbonate sediment.

However, this argillaceous lime mudstone unit is absent in Cores 09-24-21-30W1, 9-26-22-33W1 and 9-14-23-33W1. In these cores, the tops of the paleokarsts are flat and smooth, and are penetrated by borings. Most borings are straight, cylindrical *Trypanites* (Plate 4-3A & B), with one example of *Gastrochaenolites* (Plate 4-3A). These features indicate that the top of the paleokarsts was probably trimmed by wave action in a high energy environment.

The sedimentary succession above the argillaceous lime mudstone unit in Core 13-12-22-32W1 can be further divided into three units. The lower unit is about 4.4 m (14.5 ft.) thick and is composed mainly of lime mudstone, with a few argillaceous mudstone interbeds. The lime mudstone is light grey to brown, massive or mottled. The trace fossils are dominated by *Planolites*, with subordinate *Chondrites* (Plate 4-3C). Locally, *Chondrites* becomes the principal trace fossil in the rock. The *Planolites* are relatively large, about 6 mm in diameter (Plate 4-3C). Their distribution varies from sparsely to highly concentrated. Furthermore, medium sized, heavily calcified brachiopods are common in

PLATE 4-2

Plate 4-2 A: Slabbed core photograph showing the lowermost part of the argillaceous lime mudstone unit in Plate 4-1 A. It is rich in molds of microfossils. Lsd. 13-12-22-32W1. Scale bar is 3 cm.

Plate 4-2 B: Slabbed core photograph showing the lower part of the argillaceous lime mudstone in Plate 4-1 A. The primary trace fossil is composed exclusively of small *Chondrites* (c) that are cross-cut by secondary *Skolithos* (s). Lsd. 13-12-22-32W1. Scale bar is 3 cm.

Plate 4-2 C: Slabbed core photograph showing a more diverse trace-fossil assemblage in the middle part of the argillaceous lime mudstone unit in Plate 4-1 A. Lsd. 13-12-22-32W1. Scale bar is 3 cm.

Plate 4-2 D: Slabbed core photograph showing the upper part of the argillaceous lime mudstone unit in Plate 4-1 A that is characterized by firmground burrows (f). Lsd. 13-12-22-32W1. Scale bar is 3 cm.

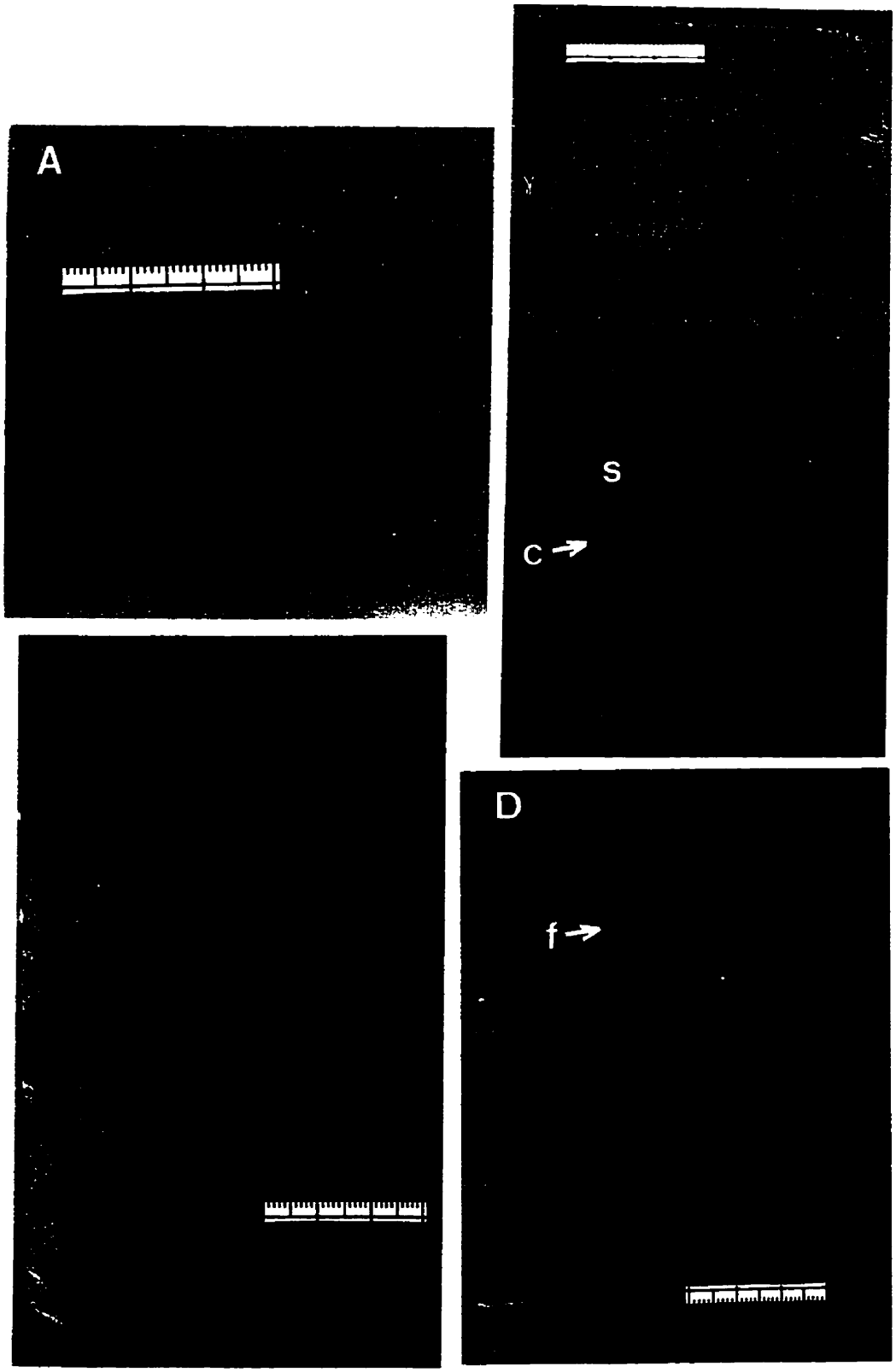
A
S
C
D
f

PLATE 4-3

Plate 4-3 A: Slabbed core photograph showing borings at the top of the paleokarst. Lsd. 09-24-21-30W1. Scale bar is 3 cm.

Plate 4-3 B: Plane-light photomicrograph of slabbed core in Plate 4-3 A that shows *Trypanites* (t) at the top of the paleokarst. Lsd. 09-24-21-30W1. Scale bar is 0.5 mm.

Plate 4-3 C: Core surface photograph showing relatively large *Planolites* (p) and smaller *Chondrites* (c) in the lower unit of the lower Burr Member. Lsd. 13-12-22-32W1. Scale bar is 3 cm.

Plate 4-3 D: Core surface photograph showing well-calcified brachiopods (b) in the lower unit of the lower Burr Member. Lsd. 13-12-22-32W1. Scale bar is 3 cm.

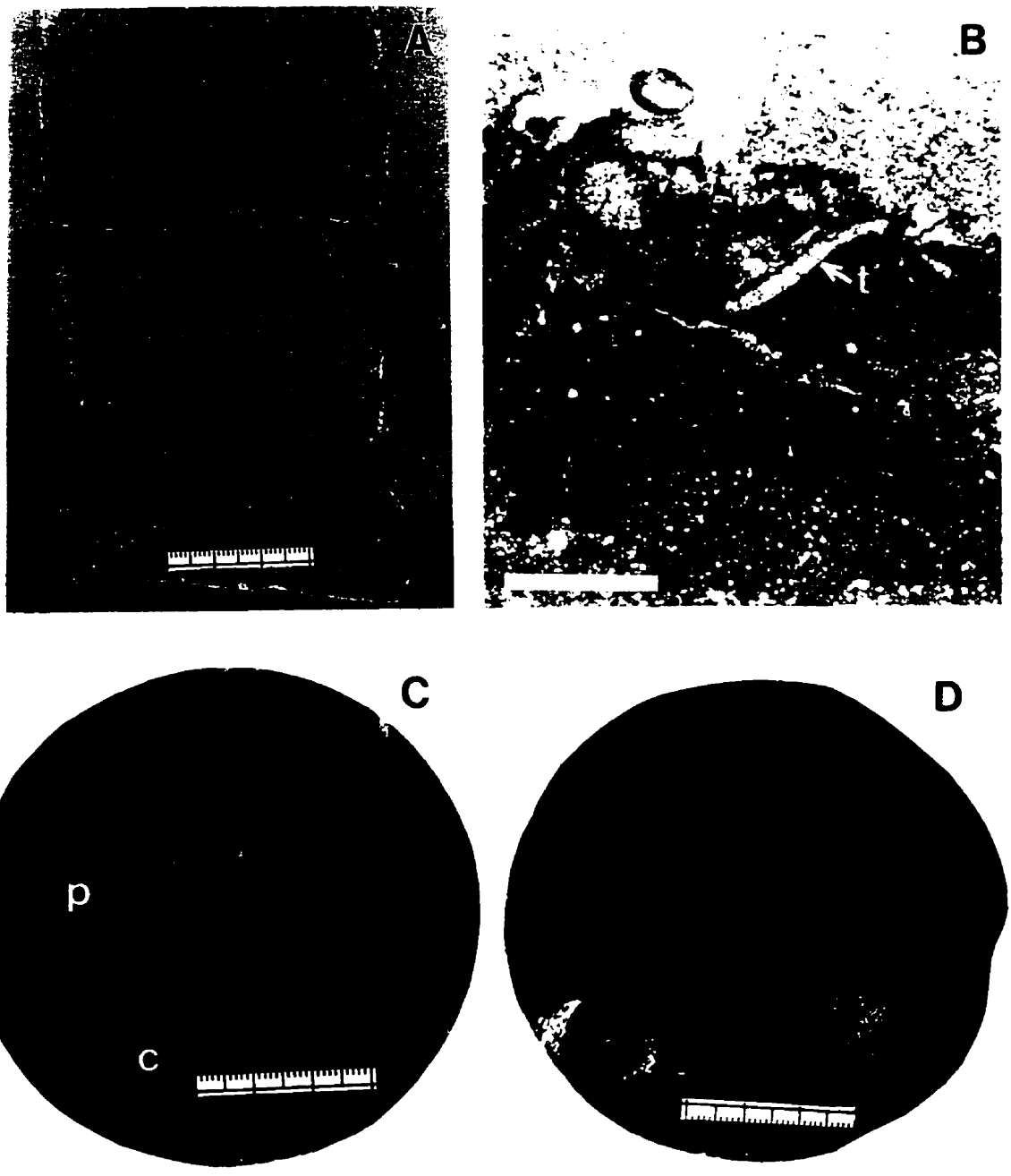
A
B
t
C
p
c
D

PLATE 4-4

Plate 4-4 A: Slabbed core photograph showing the dark brown argillaceous lime mudstone in the lower part of the lower unit. This is characterized by *Chondrites* and other burrows up to 1 cm in diameter. Lsd. 13-12-22-32W1. Scale bar is 3 cm.

Plate 4-4 B: Core bedding-surface photograph showing poorly calcified, thin-shelled brachiopods from the middle unit of the lower Burr Member. Lsd. 13-12-22-32W1. Scale bar is 3 cm.

Plate 4-4 C: Photograph showing small, thin-shelled and poorly calcified brachiopods from calcareous mudstone in the middle unit of the lower Burr Member. Lsd. 13-12-22-32W1. X 4.

Plate 4-4 D: Core bedding-surface photograph of the calcareous mudstone from the middle unit, which contains small tentaculitids (t). Lsd. 13-12-22-32W1. Scale bar is 3 cm.


A

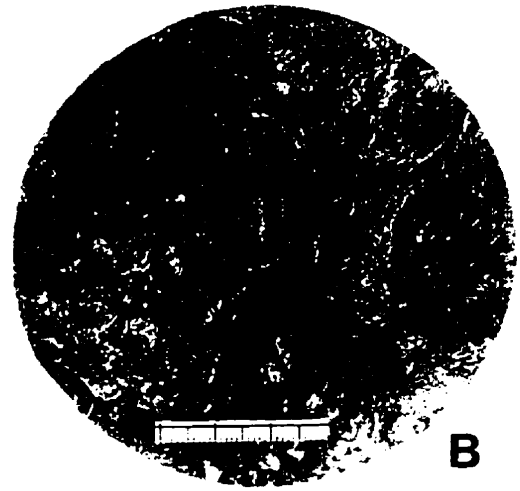
B

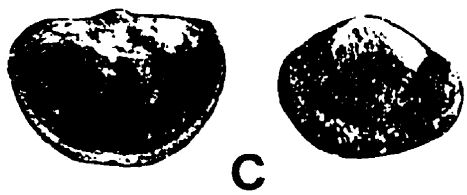
C

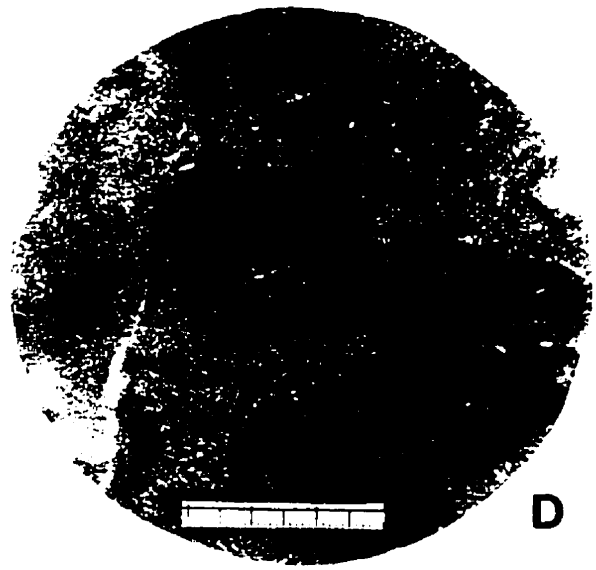
D

this unit (Plate 4-3D).

A dark brown argillaceous lime mudstone bed, up to 16 cm thick, is present in the lower part of the unit (Plates 4-1A, 4-4A). This bed is present throughout southeastern Saskatchewan. It contains a distinct trace-fossil assemblage dominated by *Chondrites* that are larger than 2 mm in diameter. They are sub-horizontal to sub-vertical in orientation. Additionally, irregular burrows with a diameter of up to 1 cm are present in the rock. They are filled with light grey carbonate sediment rich in small shell fragments. The top of the lime mudstone is eroded and overlain by a thin layer of light grey carbonate sediment, which contains sparsely to highly concentrated brachiopods. Locally, the brachiopods form a thin shell bed of 2 cm thick.

The middle unit, about 2 m thick, is composed of lime mudstone and calcareous mudstone (Plate 4-1C). The lime mudstone is massive and consists of fine-grained calcite, with a small amount of clay minerals and dolomite. Most calcite crystals are smaller than 2 μm and anhedral. Trace fossils are abundant, but they are generally smaller than 3 mm in diameter. They include *Planolites* and traces that have not been identified. Sparse, small brachiopods and tentaculites are present. The calcareous mudstone is brown to dark brown, massive, and well consolidated. SEM study indicates that the mudstone is composed of calcite, dolomite, clay minerals and abundant detrital quartz. It contains numerous small tentaculitids and brachiopods, in addition to few paper pectens. The brachiopods are thin-shelled, poorly calcified and range in length from 3 to 5 mm (Plate 4-4B & C). In a single hand specimen, normally only one or two species of brachiopods are present. However, different specimens may be dominated by different species of brachiopods. The tentaculitids are well preserved, randomly oriented and are up to 4 mm in length (Plates 4-4D, 4-5A). Paper pectens include mytiliform and dunbarelliform brachiopods (Plate 4-5B). They are up to 3 cm long and are scattered throughout the rock.

The upper unit, about 3.5 m (11.5 ft.) thick, is composed of alternating brown argillaceous lime mudstone and grey lime mudstone. The contact between them is diffuse (Plate 4-1D). Both rock types are generally less than 10 cm thick. The trace fossil assemblage in the brown lime mudstone is dominated by *Chondrites*, with subsidiary *Planolites* (Plate 4-5C & D). They are generally horizontal in orientation and about 1 mm in diameter. Very small *Zoophycos* are locally present. In addition, sparse and small, thin-shelled brachiopods and tentaculitids, as well as abundant carbonaceous debris, are present in the brown lime mudstone, but body fossils are less common than in the middle unit. The grey lime

PLATE 4-5

Plate 4-5 A: SEM photomicrograph showing a small tentaculitid from the middle unit of the lower Burr Member. Lsd. 13-12-22-32W1.

Plate 4-5 B: Core bedding-surface photograph showing dunbarelliform brachiopods (paper pectens) from the calcareous mudstone of the middle unit, the lower Burr Member. Lsd. 13-12-22-32W1. Scale bar is 3 cm.

Plate 4-5 C: Slabbed core photograph showing alternating brown and grey lime mudstones from the upper unit of the lower Burr Member. These are characterized by abundant small burrows. The brown lime mudstone is also very rich in carbonaceous remains. Lsd. 13-12-22-32W1. Scale bar is 3 cm.

Plate 4-5 D: Slabbed core photograph showing the bedding surface of the brown lime mudstone from the upper unit of the lower Burr Member. Lsd. 13-12-22-32W1. Scale bar is 3 cm.

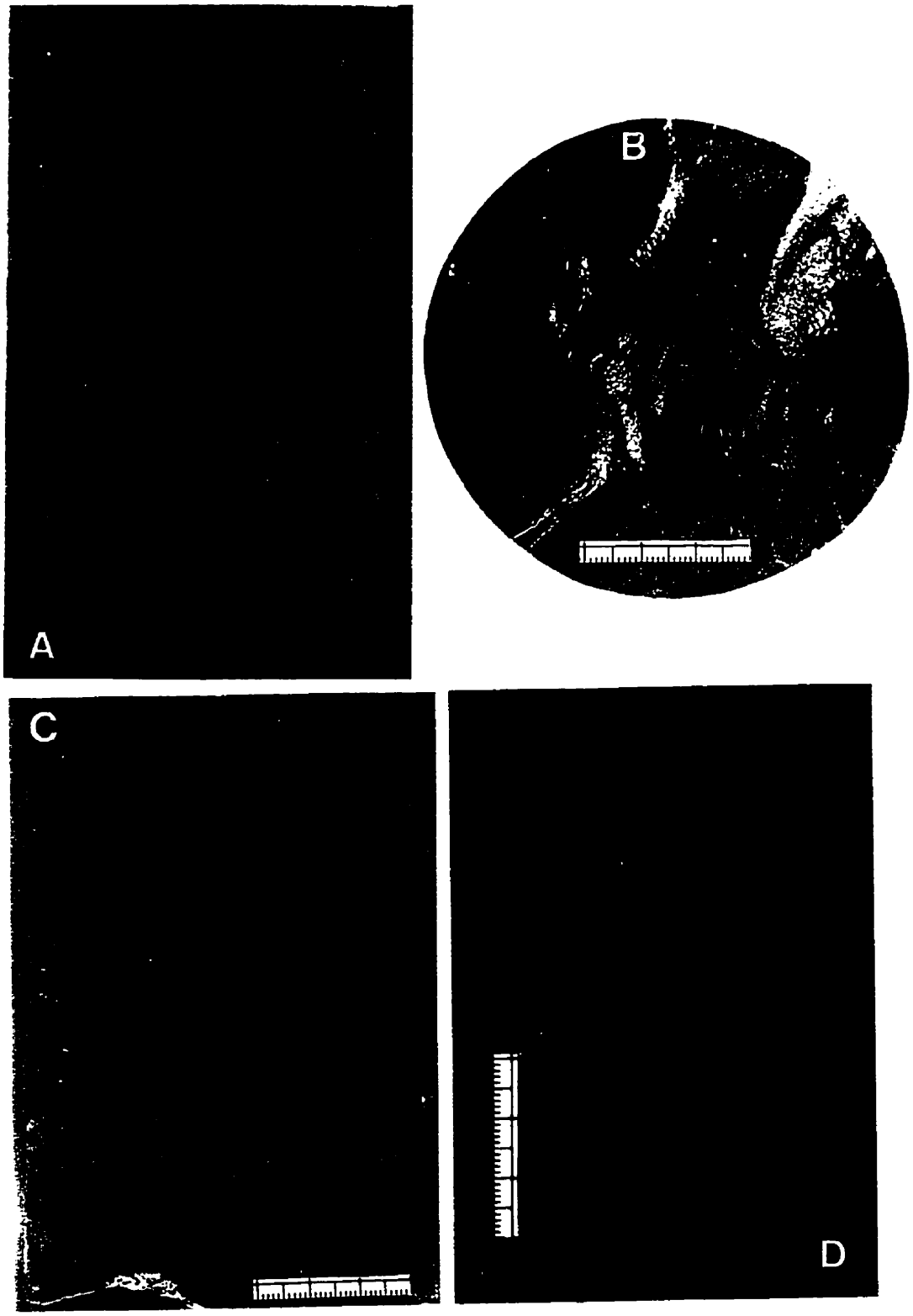
A
B
C
D

mudstone is strongly bioturbated. The burrows are composed predominantly of *Planolites*, but small *Chondrites* are also present. The *Planolites* are circular in cross-section, slightly to highly curved and rarely branched. Dimensions rarely vary within any given specimen. Most of the traces are inclined to bedding. The burrows are filled by structureless dark-grey halite. Close to the top of the upper unit, the rock changes from brown to olive-green, with sparse crinoid fragments present.

The top of the lower Burr Member is a brown lime mudstone, which contains superabundant *Chondrites* (Plate 4-6A). The original carbonate sediment seems to have been repeatedly burrowed by *Chondrites*-making organisms. The diameter of the *Chondrites* varies from 1 to 2 mm. Most are horizontal in orientation. No other distinct trace fossils are found, but sharp erosional structures are present. The contact between the lower and upper parts of the Burr Member is characterized by several superimposed firmgrounds.

Interpretation

The argillaceous lime mudstone unit directly above the paleokarsts in Core 13-12-22-32W1 contains a trace fossil assemblage that diversifies rapidly upward. In the lower part, the primary trace fossil is composed exclusively of small *Chondrites*, reflecting a low dysaerobic condition. In the middle part, besides small *Chondrites*, relatively large softground burrows begin to appear, indicating a more oxygenated environment. In the upper part, the trace fossils are composed of *Planolites* and firmground burrows. This indicates a bottom water environment with dissolved oxygen content very close to normal marine conditions. Furthermore, secondary *Skolithos* penetrated the entire unit. *Skolithos* is a vertical dwelling and feeding structure created by suspension feeding organisms. It is a representative trace fossil of the *Skolithos* ichnofacies, which is characteristic of relatively high-energy settings with well-oxygenated bottom waters (Seilacher, 1967; Beynon and Pemberton, 1992). Thus, it can be concluded that from the lower to the upper part, the bottom water environment changed from low dysaerobic to well-oxygenated conditions.

The argillaceous lime mudstone unit grades upward into a unit characterized by relatively large *Planolites* and *Chondrites*, as well as medium-sized, heavily calcified brachiopods. However, *Skolithos* are absent. This indicates that both energy level and oxygen content in the benthic environment had decreased. The presence of medium-sized, heavily calcified brachiopods shows that the oxygen level was close to normal marine conditions.

PLATE 4-6

Plate 4-6 A: Slabbed core photograph showing the top of the lower Burr Member, which is characterized by numerous small *Chondrites*. Lsd. 13-12-22-32W1. Scale bar is 3 cm.

Plate 4-6 B, C and D: Detailed core photograph showing the lower Burr Member of well 4-10-24-7W2 from base to top. **Plate 4-6 B** includes the top of the Second Red Bed Member (s), the paleokarsts (p) at the base of the Burr Member, the lower unit (l), and the lower part of the middle unit (m) of the lower Burr Member. **Plate 4-6 C** shows the middle and upper parts of the middle unit. **Plate 4-6 D** shows the upper unit of the lower Burr Member. (One core box is 0.76 m long and core diameter is 10.1 cm.)

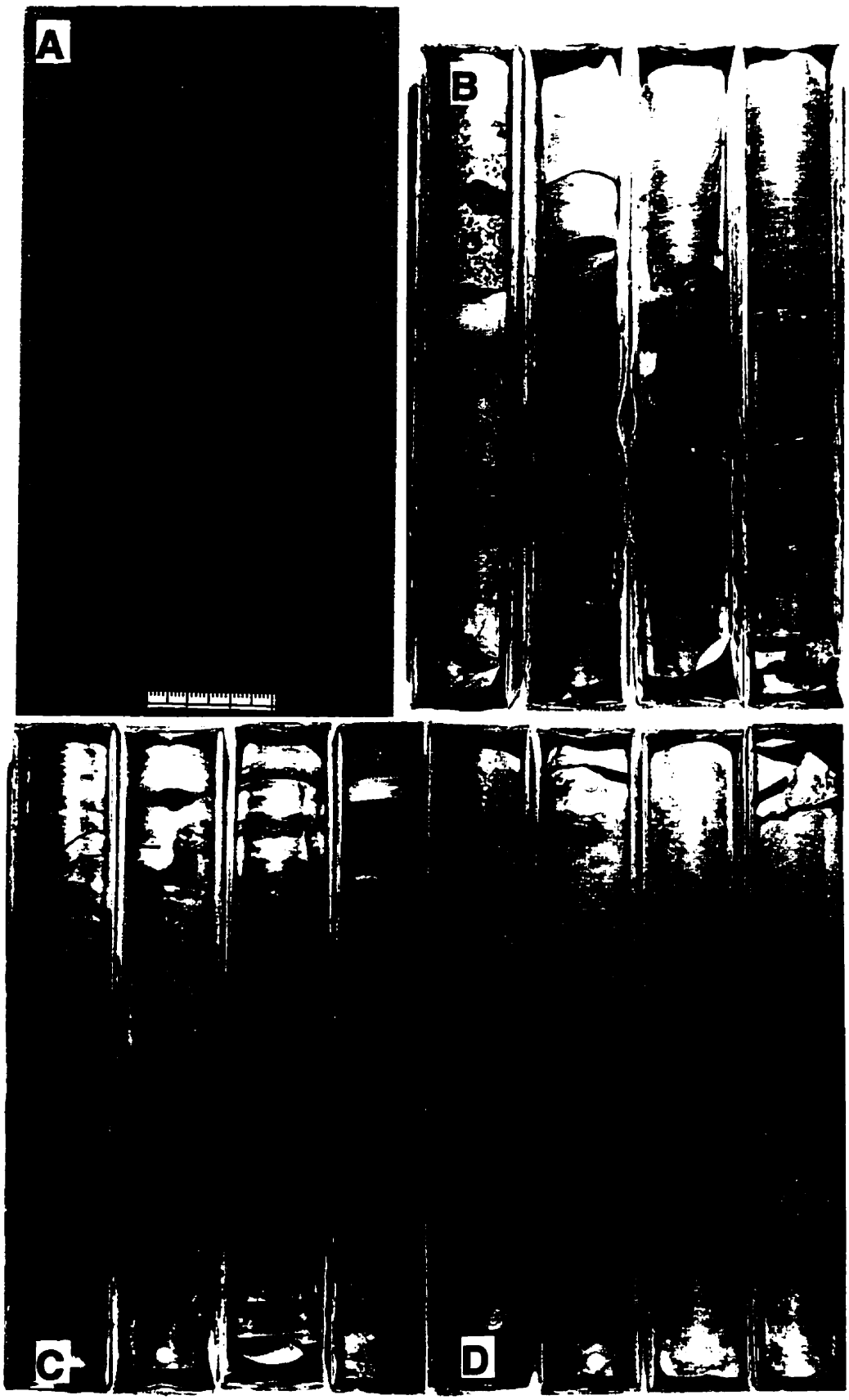
A
B
C
D

The argillaceous lime mudstone unit is overlain by a unit composed of lime mudstone and calcareous mudstone, that also contains *Planolites* and brachiopods. However, the size of both the *Planolites* and brachiopods has decreased significantly. In addition, abundant small tentaculitids are present. All these features suggest that the dissolved oxygen content in the depositional environment had further decreased. The abundant tentaculitids show that the deposits were formed by pelagic sedimentation, probably reflecting an increase in water depth.

The upper unit of the lower Burr Member is composed of alternating brown and grey lime mudstones that contain small *Chondrites* and *Planolites*. The *Chondrites* are the only type of burrow in some horizons. Small tentaculitids are still present, but brachiopods are rare. In contrast, abundant carbonaceous debris is present. This may indicate a further decrease in oxygen level. Therefore, it can be concluded that, from the base to the top of the lower Burr Member, the oxygen content in the benthic environment first increased rapidly, then gradually decreased upward.

4.2.2 Transitional Area between Southeastern and Central Saskatchewan

The lower Burr Member in the transitional area between southeastern and central Saskatchewan is represented by Core 4-10-24-7W2 (Plate 4-6B, C & D). The base of the Burr Member is composed of two superimposed paleokarsts (Plate 4-6B). The sedimentary succession above the paleokarsts can be subdivided into lower, middle and upper units.

The lower unit is about 0.8 m thick and is composed of brown marlstone (Plate 4-7A). It is massive and is characterized by abundant burrows of *Chondrites* that are 1-2 mm in diameter. In addition, very sparse, small, thin-shelled brachiopods are present.

The middle unit is about 4.6 m (15 ft) thick and is composed of brown marlstone. It has indistinct lamination (Plate 4-7B & C), which has a horizontal to slightly wavy appearance. In the lower part of the unit, the lamination is relatively well developed. Sparse, small burrows are present, but could not be identified. In the upper part, the lamination becomes more diffuse and indistinct. The trace fossils, however, are more abundant and include *Chondrites* and at least one other type of burrow. Additionally, sparse, small brachiopods are also present. The change of the lamination from relatively distinct and laterally more or less continuous in the lower part, to indistinct and laterally discontinuous in the upper part,

PLATE 4-7

Plate 4-7 A: Slabbed core photograph showing brown marlstone in the lower unit of Plate 4-6 B; this contains exclusively small *Chondrites*. Lsd. 4-10-24-7W2. Scale bar is 3 cm.

Plate 4-7 B: Slabbed core photograph showing brown marlstone from the middle unit of Plate 4-6 B, which is characterized by indistinct lamination. Lsd. 4-10-24-7W2. Scale bar is 3 cm.

Plate 4-7 C: Slabbed core photograph showing brown marlstone from the middle unit of Plate 4-6 C, showing indistinct lamination and small burrows. Lsd. 4-10-24-7W2. Scale bar is 3 cm.

Plate 4-7 D: Slabbed core photograph showing alternating brown and light grey lime mudstone from the lower part of the upper unit of Plate 4-6 D. Lsd. 4-10-24-7W2. Scale bar is 3 cm.

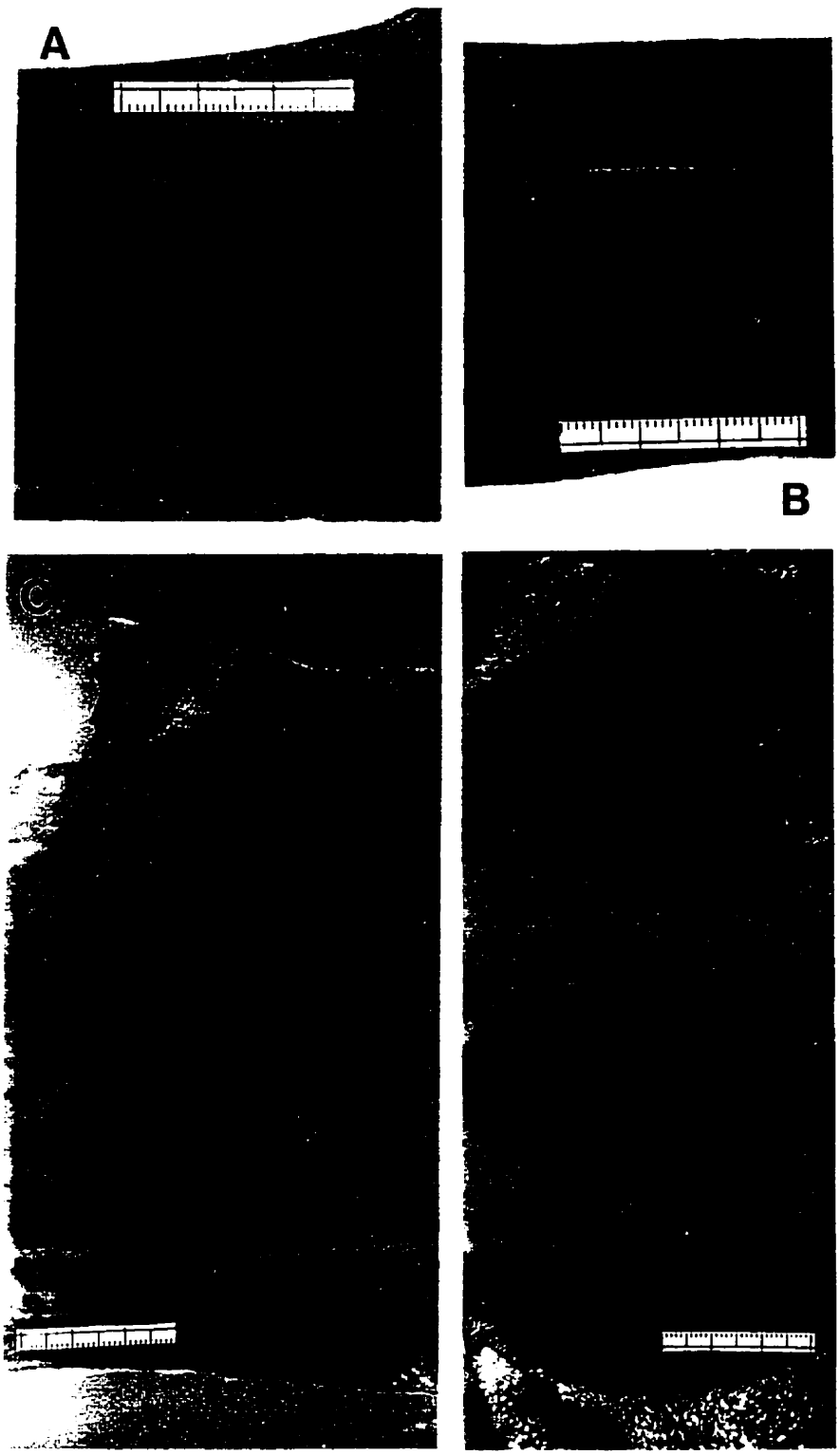
A
B
C

indicates an upward increase in bioturbation.

The upper unit is about 4 m thick. It is composed of thinly-bedded brown lime mudstone and light grey lime mudstone in the lower part (Plate 4-7D) and massive bioturbated lime mudstone in the upper part (Plate 4-6D). The argillaceous content is significantly less than the middle unit. In the lower portion of the upper unit, the rock contains trace fossils dominated by small *Chondrites* and *Planolites*, and some firmground burrows. Furthermore, well-preserved, small brachiopods and crinoid fragments are locally present. In the upper portion, the rock is intensely bioturbated and medium-sized brachiopods are abundant. Firmground burrows are highly developed (Plate 4-6D).

Interpretation

The exclusive presence of small *Chondrites* in the lower unit indicates low dysaerobic conditions. The preservation of indistinct lamination in the lower middle unit suggests a quasi-anaerobic condition. However, in the upper middle unit, the lamination becomes less distinct and bioturbation evidently increased, which suggests increasing oxygenation. The oxygen content further increased upward, as shown by the presence of large burrows and medium-sized brachiopods in the upper unit. Therefore, it can be concluded that the benthic environment was low dysaerobic during the deposition of the lower unit; it then passed through an almost anaerobic condition in the middle unit; then the oxygen content increased upward gradually. The vertical change of oxygenation was almost identical to that which happened in the lowest unit above the paleokarsts in southeastern Saskatchewan.

4.2.3 Central Saskatchewan

In central Saskatchewan, the sedimentary unit that directly overlies black shale B is a kerogen-laminated lime mudstone, with a thickness up to 70 cm (in Core 4-18-35-8W3) (Plate 4-8A). The contact between the black shale and the kerogen-laminated lime mudstone is transitional (Plate 3-8A). The lime mudstone is brown and lacks trace or body fossils. In the lower part of the unit, the rock is composed mainly of organic-rich laminae, with relatively few organic-poor laminae. The lamination is horizontal or slightly undulating (Plate 4-8D). In the upper part, the lime mudstone consists of alternating organic-rich and organic-poor laminae, with the organic-poor laminae increasing in proportion upward. The lamination changes from generally horizontal to strongly

PLATE 4-8

Plate 4-8 A, B and C: Detailed core photograph showing the lower Burr Member from central Saskatchewan. **Plate 4-8 A** includes the uppermost part of the Second Red Bed Member (s), the kerogen-laminated lime mudstone unit (k), and the horizontally-laminated lime mudstone unit (h) of the lower Burr Member. **Plate 4-8 B** includes the olive-green bioturbated lime mudstone unit (o) and the brown mottled lime mudstone-wackestone unit (b). **Plate 4-8 C** includes the uppermost unit of the lower Burr Member and the basal part of the upper Burr Member. These are separated by a distinct firmground (f). Lsd. 4-18-35-8W3. (One core box is 0.76 m long and core diameter is 10.1 cm.)

Plate 4-8 D: Slabbed core photograph showing the kerogen-laminated lime mudstone with a high concentration of organic-rich laminae that are more or less laterally horizontal. Lsd. 4-18-35-8W3. Scale bar is 3 cm.

Plate 4-8 E: Slabbed core photograph of the kerogen-laminated lime mudstone. The laminae have a wavy-crinkly appearance. Lsd. 4-18-35-8W3. Scale bar is 3 cm.

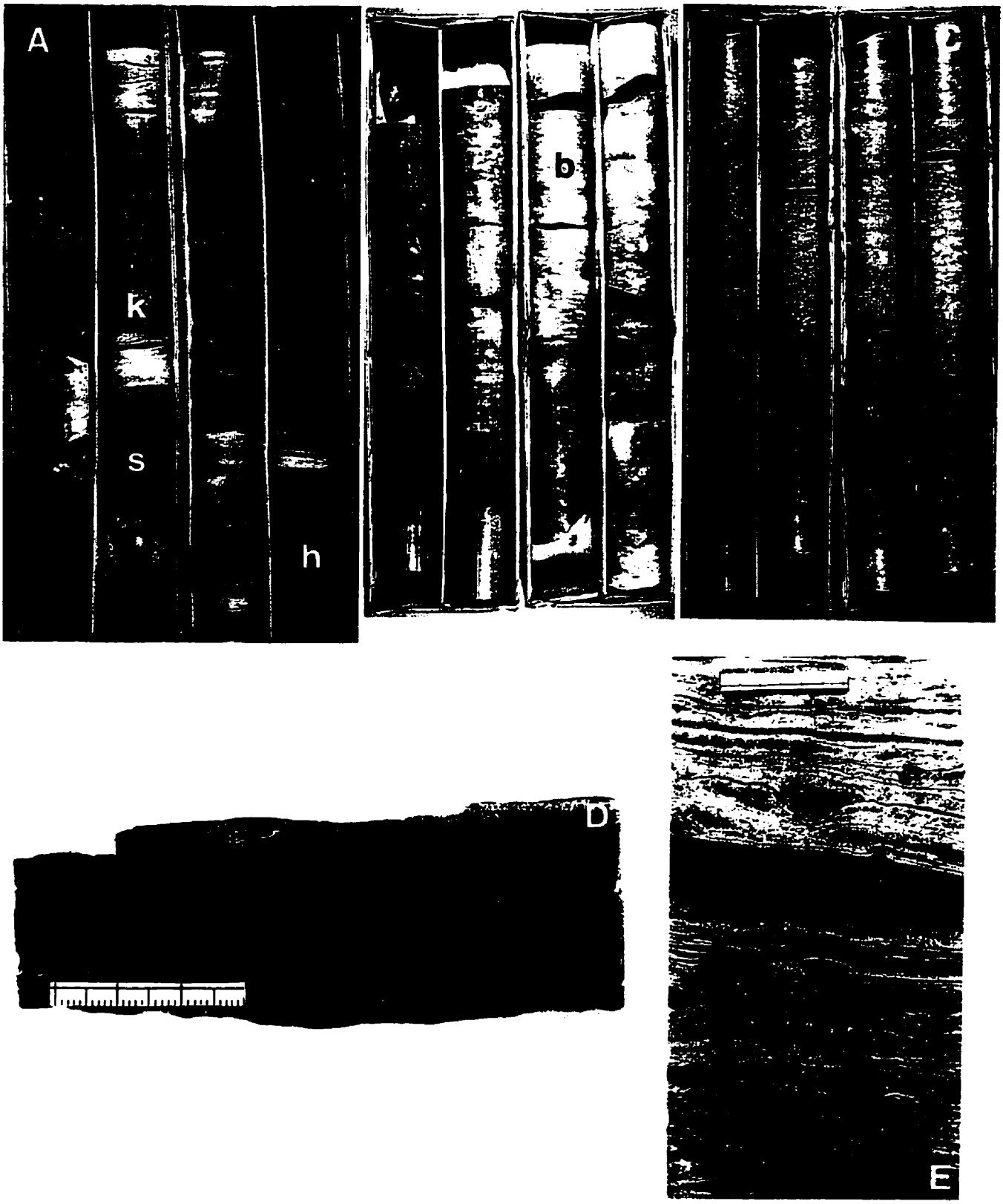
A
k
s
h
b
C
D
E

PLATE 4-9

Plate 4-9 A: Slabbed core photograph of the kerogen-laminated lime mudstone from the upper part of the unit. The organic-poor laminae appear lenticular and some organic-rich laminae are disrupted and eroded. Lsd. 4-18-35-8W3. Scale bar is 3 cm.

Plate 4-9 B: Plane-light photomicrograph of the organic-poor laminae in the kerogen-laminated lime mudstone. They are composed of peloids. Lsd. 4-18-35-8W3. Scale bar is 0.5 mm.

Plate 4-9 C: Slabbed core photograph of horizontally-laminated lime mudstone, characterized by fine parallel lamination. Lsd. 4-18-35-8W3. Scale bar is 3 cm.

Plate 4-9 D: Slabbed core photograph of horizontally-laminated lime mudstone that exhibits fine horizontal lamination and minor scour structures (s). Lsd. 4-18-35-8W3. Scale bar is 3 cm.

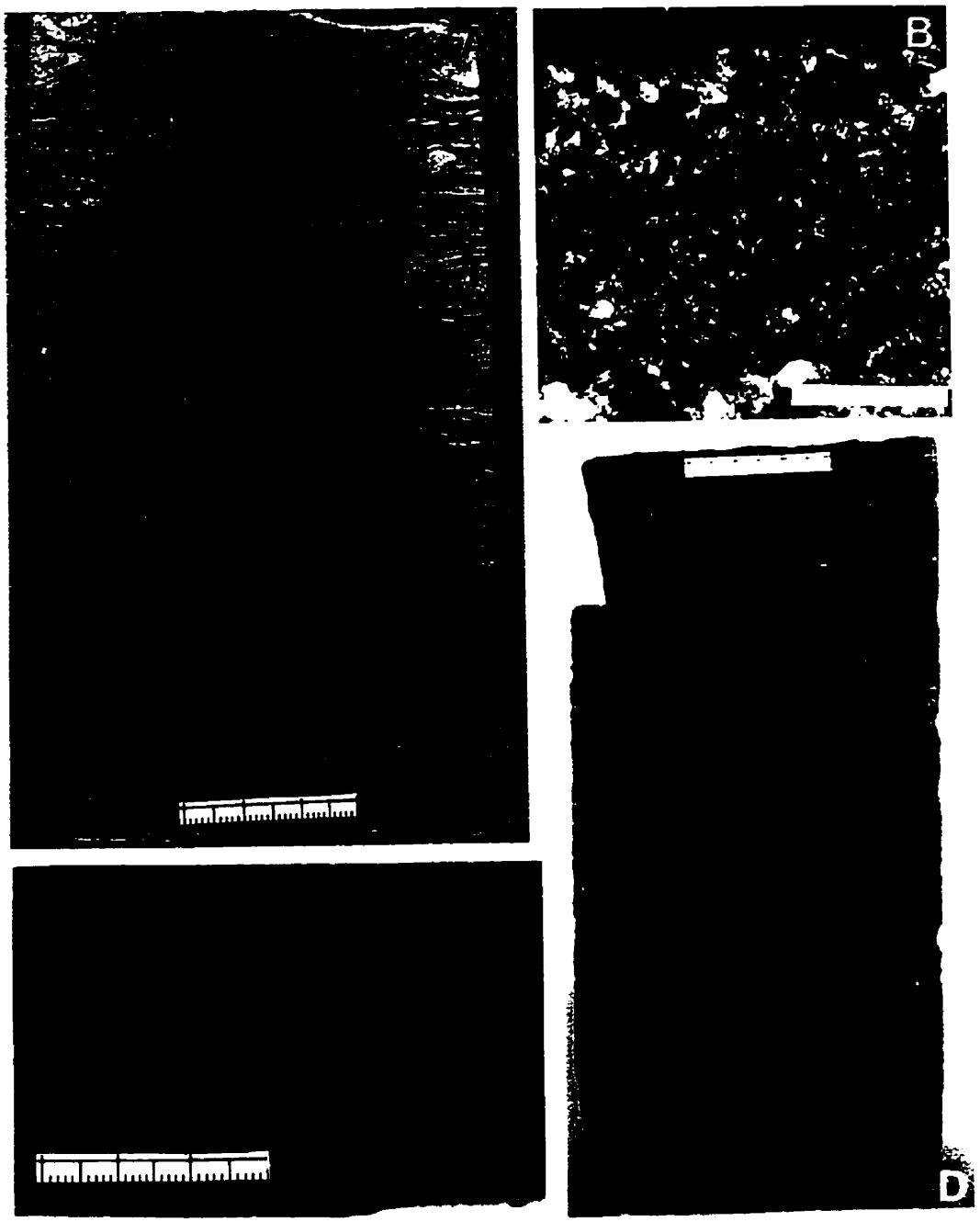
B
D

undulating (Plate 4-8E).

The organic-rich laminae are wavy-crinkly, discrete and sharply bounded, and 1 mm or less in thickness (Plate 4-8D). Normally, they are laterally continuous, but some kerogenous laminae are disrupted or eroded (Plate 4-9A), probably by current or storm activities. The organic-poor laminae (or beds) are composed of peloidal and micritic carbonate sediment, with a thickness ranging from submillimeters to several centimeters. Generally, they form laterally discontinuous carbonate lenses (Plate 4-9A) that are laterally elongated. In thin section, the carbonate lenses are composed of micrite or peloids (Plate 4-9B). The peloids are, in turn, composed of micrite. They have grain-supported to mud-supported fabrics. The peloids are irregular in shape; most are less than 2 mm in diameter.

The kerogenous laminae are significantly different from those laminae of the underlying black shale. The former are wavy-crinkly, and in places highly undulating whereas the latter are characterized by even and parallel lamination. This suggests that the mechanism that resulted in the formation of the kerogenous laminae is different from that for the black shale. The following features indicate that the kerogenous laminae may have a microbial origin:

(1) Crinkly laminae: the wavy-crinkly lamination is the most striking indication of a microbial origin. Many microbial laminae reported strongly resemble the kerogenous lamination of the lime mudstone. In contrast, black shales that are believed to have formed from the accumulation of detrital and planktonic organic matter under bottom reducing conditions show very even and parallel laminae (Schieber, 1986).

(2) The lateral continuity of the laminae: although most kerogenous laminae are continuous, some are discontinuous laterally. No evidence of physical disruption of these discontinuous laminae is observed. This precludes the possibility that the kerogenous laminae were accumulated as planktonic rain. In the case of a phytoplankton bloom, the deposition of organic matter should be widespread and the kerogenous laminae should be more laterally continuous.

(3) Further evidence in favour of a microbial origin is the mechanical behaviour of the kerogenous laminae during penecontemporaneous deformation. It appears that the kerogenous laminae behaved as a coherent layer, whereas the interlaminated carbonate sediment behaved more like a very viscous fluid during early soft-sediment deformation.

This can be illustrated by the mechanical behaviour of the kerogenous and carbonate laminae loaded with relatively large carbonate lenses. The kerogenous laminae directly underlying relatively large carbonate lenses are strongly deformed. However, the thickness of the individual kerogenous laminae remains almost unchanged laterally, indicating no significant lateral movement of the sediment. In contrast, the carbonate laminae underlying relatively large carbonate lenses decrease significantly in thickness, while the thickness has evidently increased at the margins of the lenses. This suggests that the kerogenous laminae behaved like a tough leathery membrane, rather than a soupy organic muck. This may indicate that the carbonate sediment below the lenses is largely squeezed out.

(4) Other evidence that supports a microbial origin of the kerogenous laminae includes the trapping of carbonate sediment and minor surface relief on the order of millimeters. Although the undulating appearance of the kerogenous laminae is mainly caused by differential compaction of organic matter around carbonate lenses, some minor positive relief cannot be ascribed to this origin. Some carbonate sediments are preserved on the tops of the minor relief whereas carbonate sediments are absent in the lows of the same laminae. Because these are preserved in a physically unstable position, this may be evidence for adhesion to the mucilage of cyanobacteria. Furthermore, some dark brown filamentous remnants are preserved in the kerogenous laminae. They are probably remnants of filamentous bacteria and cyanobacteria. Another feature that supports a microbial origin is the sharply bounded, discrete character of the laminae. It is unlikely that episodic seasonal rains of mineral grains, clay or carbonate would have retained such sharp boundaries if added to a layer of "putrescent ooze" (Fischer and Roberts, 1991).

It can be concluded that the organic-rich laminae are probably products of microbial mats. Because the lime mudstone lacks evidence of subaerial exposure, it must have been deposited subaqueously. In the Phanerozoic, the environments that mostly favour development and preservation of microbial mats are usually those characterized by high salinity or anoxia. Because no primary evaporites were discovered in the kerogen-laminated lime mudstone, a high salinity environment may be excluded. An alternative explanation is that the microbial mats might have developed in an oxygen-deficient environment and that the organic-rich layers were bacterial mats. Although no conclusive evidence is available, this alternative is supported by the gradational transition between the kerogen-laminated lime mudstone and both the underlying black shale and the overlying horizontally-laminated lime mudstone, both of which accumulated under anaerobic conditions. It is also supported by a lateral transition to a lime mudstone containing only

small *Chondrites*, which was deposited under low dysaerobic conditions in the transitional area between southeastern and central Saskatchewan. In modern environments, bacterial mats form in the absence of benthos and represent the lowest dysaerobic conditions (Wignall, 1994; Savrda *et al.*, 1991). Thus, it may be concluded that the kerogen-laminated lime mudstone was deposited under extremely low dysaerobic conditions. The common synsedimentary disruption of the kerogenous lamination, probably caused by current or storm activities, may indicate shallow water environments.

The kerogen-laminated lime mudstone grades upward into a horizontally-laminated lime mudstone unit. The latter is about 75 cm thick in Core 4-18-35-8W3 and is characterized by well-developed horizontal to slightly wavy lamination (Plates 4-8A, 4-9C & D). Shelly fauna is totally absent in the unit. However, sparse *Chondrites* (< 1 mm) are locally present and are confined to laminae up to 2 cm thick (Plate 4-10A).

The horizontally-laminated lime mudstone is composed of greenish-grey, brown and light grey laminae. Most laminae are on a scale of submillimeter to millimeters, but a few reach up to 2 cm thick. The greenish-grey and brown laminae are more or less parallel and laterally continuous whereas the light grey laminae locally show a lenticular shape. In general, the average thickness of the laminae increases from the base to top. In thin section, the brown laminae are enriched in argillaceous sediment (Plate 4-10B). SEM study reveals that they are composed of calcite, quartz, feldspar and clay minerals. The greenish-grey laminae consist of very fine calcite grains that are partially dolomitized (Plate 4-10B).

Scour structures and cross-bedding are locally present in the horizontally-laminated lime mudstone. Although most scour structures are 2-3 mm in amplitude (Plate 4-9D), a deeper scour structure, up to 2.5 cm in amplitude, was observed in Core 1-18-36-6W3 (Plate 4-10C). These scour structures are normally overlain by homogeneous fine-grained carbonate sediment. Locally, interbeds of laminated silty mudstone are observed in some core sections. The top of the horizontally-laminated lime mudstone unit is composed of dark grey massive limestone. It contains sparse small gastropods (Plate 4-10D) and is penetrated by small firmground burrows.

The unit directly above the horizontally-laminated lime mudstone is composed of olive-green bioturbated lime mudstone (Plate 4-8B). It is about 2.3 m in Core 4-18-35-8W3. Thin-section study reveals that the lime mudstone is composed of micrite. This unit can be subdivided into lower and upper parts:

PLATE 4-10

Plate 4-10 A: Slabbed core photograph of horizontally-laminated lime mudstone that has been partly bioturbated by small *Chondrites* (c) Lsd. 3-30-27-2W3. Scale bar is 3 cm.

Plate 4-10 B: Plane-light photomicrograph of horizontally-laminated lime mudstone, composed of alternating olive-green and brown laminae. The brown laminae are enriched in argillaceous sediment. Lsd. 4-18-35-8W3. Scale bar is 0.5 mm.

Plate 4-10 C: Slabbed core photograph of horizontally-laminated lime mudstone. The mudstone shows a relatively deep scour structure (s) that has been filled with homogeneous carbonate sediment. Lsd. 1-18-36-6W3. Scale bar is 3 cm.

Plate 4-10 D: Plane-light photomicrograph of lime mudstone from the top of the horizontally-laminated lime mudstone unit, showing a clotted fabric and small gastropods (g). Lsd. 4-18-35-8W3. Scale bar is 0.5 mm.

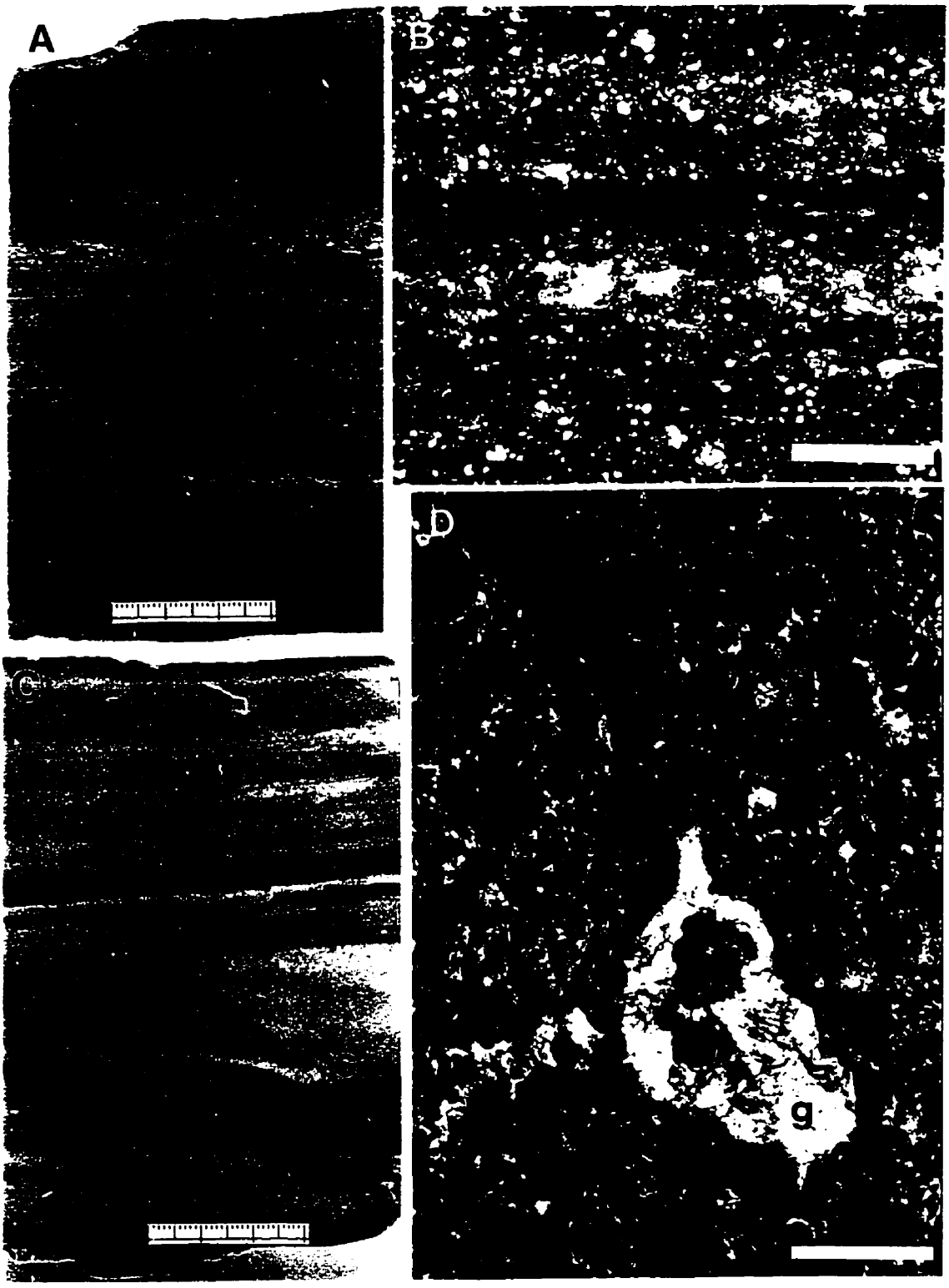
A
B
C
D
g

PLATE 4-11

Plate 4-11 A: Slabbed core photograph of olive-green bioturbated lime mudstone. It is characterized by remains of horizontal lamination, small *Chondrites* (c) and a few *Teichichnus* (t) Lsd. 4-18-35-8W3. Scale bar is 3 cm.

Plate 4-11 B: Slabbed core photograph of olive-green bioturbated lime mudstone. It shows indistinct horizontal lamination, horizons bioturbated exclusively by small *Chondrites* (c), and shell beds composed of small brachiopods (b) and their fragments. The Cominco potash mine. Scale bar is 3 cm.

Plate 4-11 C: Plane-light photomicrograph of the shell bed in Plate 4-11 B that shows well-preserved small, thin-shelled brachiopods and their fragments. The Cominco potash mine. Scale bar is 0.5 mm.

Plate 4-11 D: Slabbed core photograph of olive-green bioturbated lime mudstone that shows a trace fossil assemblage composed of *Chondrites* (c), *Teichichnus* (t), *Planolites* (p) and small *Skolithos*-like traces (s). A scour structure is probably present in the upper right part. Lsd. 4-18-35-8W3. Scale bar is 3 cm.

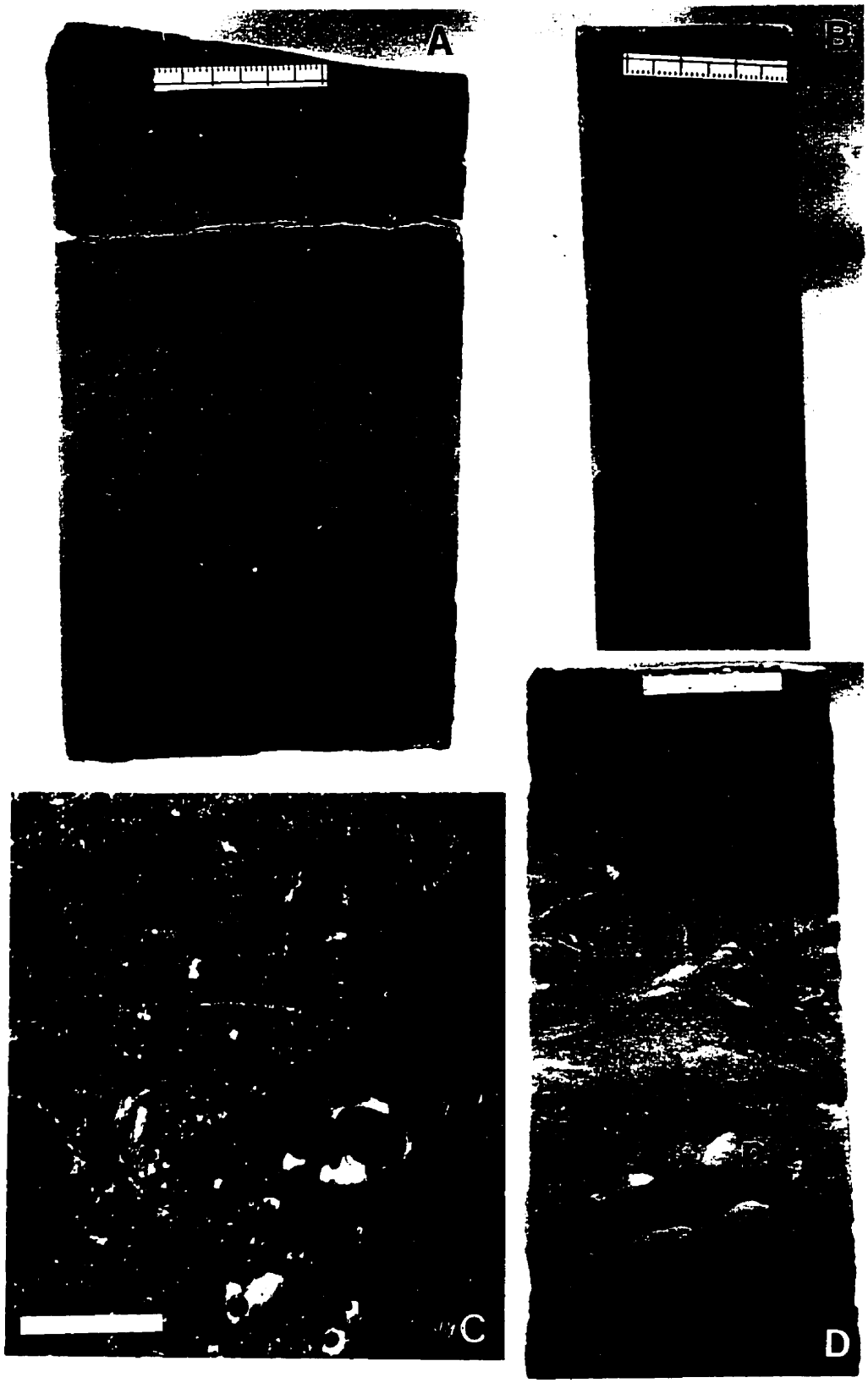
A
B
C
D

The lower part is dominated by small *Chondrites*, with a few *Teichichnus* (Plate 4-11A). The *Chondrites* are predominantly horizontal and less than 1 mm in diameter. Indistinct lamination can still be seen in this part (Plate 4-11A). Additionally, small, thin-shelled brachiopods are present (Plate 4-11B). In places, they even form discrete thin shell-beds. At least 13 shell beds were observed in one core from the Lanigan mine in central Saskatchewan although only two shell beds are present in Core 4-18-35-8W3. They are light grey and vary from a few mm up to 3 cm thick. These shell beds generally have sharp but non-erosional bases. The upper surface of the shell beds is generally flat and is in a gradational contact with the overlying sediment. Locally, it is characterized by an undulatory upper surface. The shell beds are dominated by small, thin-shelled brachiopods. These brachiopods are less than 6 mm long, preserved as whole- and half-valves, and as fragments (Plate 4-11C). They are oriented parallel to bedding and convex upward. Bedding style ranges from planar and laterally continuous to lenticular and less distinctly bedded. Grading is only developed in relatively thick shell beds and amalgamation is observed locally. The rock between the shell beds is composed of dark grey lime mudstone, varying from less than 1 cm up to 13 cm thick. Some lime mudstones are massive; others are burrowed by small *Chondrites*. They contain sparse, small, thin-shelled brachiopods, ostracods and foraminifera. Some lime mudstones have indistinct horizontal laminations.

The upper part of the unit is composed of more extensively bioturbated olive-green lime mudstone (Plate 4-11D). Lamination is generally absent, but sharp scour structures are present. The trace fossils are more diverse, but are still dominated by small *Chondrites*. However, some *Chondrites* are no longer horizontal in orientation and they are generally larger than those in the lower part, with a diameter of 1-2 mm. Additionally, *Planolites*, *Teichichnus*, *Zoophycos* and even small firmground burrows are present. These trace fossils are generally less than 5 mm in diameter. Furthermore, intraclasts are common in this part, where they are concentrated in layers. These intraclasts are highly irregular in shape and have not been rounded, indicating that they were not well lithified when reworked. Close to the top of this unit the diameter of the *Chondrites* and the abundance of large burrows both increase significantly. At the top of this unit, the burrows become less distinct. Additionally, abundant small, thin-shelled brachiopods are dispersed throughout the rock. Most are preserved as fragments.

The unit overlying the olive-green bioturbated lime mudstone consists of brown mottled lime mudstone and wackestone (Plate 4-8B). It is about 1.4 m (4.6 ft.) thick in Core 4-18-

PLATE 4-12

Plate 4-12 A: Slabbed core photograph showing the contact (c) between the olive-green bioturbated lime mudstone (o) and brown mottled limestone unit (b). Shell fragments of small body fossils and intraclasts are highly concentrated directly above the contact. The Cominco potash mine. Scale bar is 3 cm.

Plate 4-12 B: Slabbed core photograph showing wackestone from the upper part of the lower Burr Member. It is characterized by a strong mottled appearance, and diverse trace and body fossils. Lsd. 4-18-35-8W3. Scale bar is 3 cm.

Plate 4-12 C: Plane-light photomicrograph of wackestone in Plate 4-12 B. It is composed of bioclasts and micritic matrix. The bioclasts include brachiopods, crinoids, trilobites, tentaculitids and gastropods. Lsd. 4-18-35-8W3. Scale bar is 0.5 mm.

Plate 4-12 D: Slabbed core photograph showing the contact (c) between the lower and upper Burr Member. Lsd. 4-18-35-8W3. Scale bar is 3 cm.

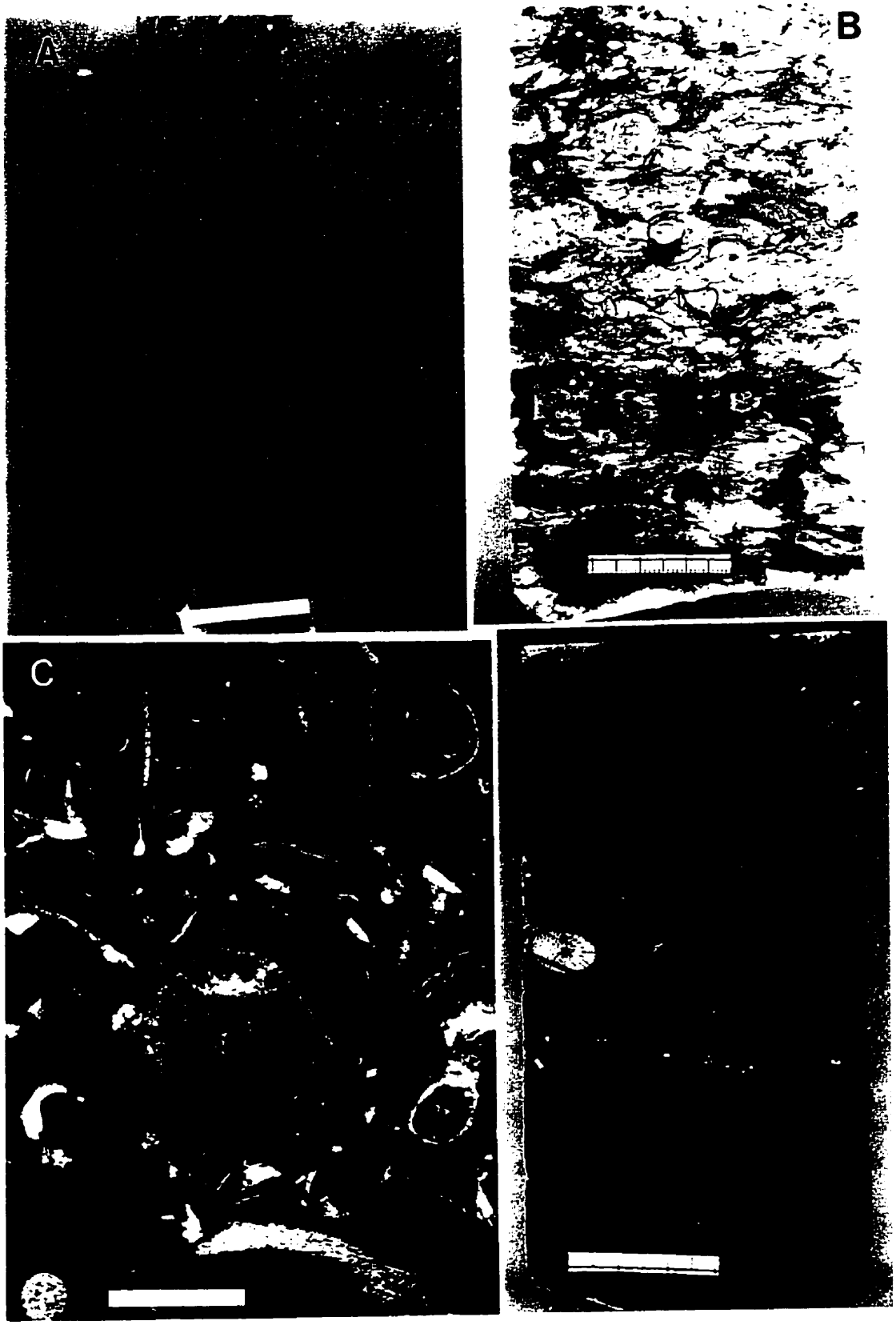
A
B
C

35-8W3. Its contact with the underlying unit is characterized by a firmground (Plate 4-12A) that is penetrated by relatively large burrows of *Glossifungites* ichnofacies (up to 1 cm in diameter). The wackestone within a few cm above the contact contains many intraclasts, and brachiopod and crinoid fragments. The intraclasts are highly irregular in shape and burrowed by a *Chondrites*-making organism, indicating that they were not well solidified when reworked. The brachiopods are thin-shelled and a few mm long. Most are preserved as single-valves.

The brown lime mudstone and wackestone have a mottled appearance. The burrows are still dominated by *Chondrites*, but they are about 2 mm in diameter and horizontal to subhorizontal in orientation. Additionally, at least one type of robust burrow, probably *Planolites*, is present. These are up to 1 cm in diameter and horizontal to sub-horizontal in orientation. Moreover, sparse but well-preserved brachiopods (up to 1.5 cm in length) and crinoid fragments are scattered throughout this unit. The colour of the unit changes from brown to light grey upward. The contact between the brown limestone and the overlying limestone unit is transitional.

The unit above the brown lime mudstone and wackestone is composed of grey to dark grey wackestone (Plate 4-8C). It is about 1.6 m (5.4 ft) thick in Core 4-18-35-8W3. The rock is heavily bioturbated and is rich in crinoid fragments. These are normally interspersed throughout the unit, but are locally concentrated as shell beds locally. Well-preserved brachiopods, their fragments and intraclasts are frequently encountered in this unit. The brachiopods are up to 12 mm long and have thicker shells (Plate 4-12B). Trace fossils are abundant and still dominated by *Chondrites*. Some relatively large burrows are also present, but are not sufficiently distinct to be identified. The top of the unit is a distinct firmground that is penetrated by large burrows, up to 1 cm in diameter, that are probably *Thalassinoides* (Plate 4-12D). They are filled with brown carbonate sediment rich in shell fragments and intraclasts. Microscopic study reveals that the wackestone contains abundant, but patchily distributed, shell fossils. These include brachiopods, gastropods, echinoderm debris, ostracods and trilobites (Plate 4-12C). The matrix of the rock is rich in silt-sized bioclasts.

Interpretation

As described above, the kerogen-laminated lime mudstone in the basal part of the Burr Member is characterized by organic-rich, wavy-crinkly laminae, that have a probable bacterial origin. This lime mudstone may have formed under extremely low dysaerobic conditions. The common disruption of the kerogenous laminae may imply a shallow water environment. The kerogen-laminated lime mudstone is overlain by a horizontally-laminated lime mudstone that is characterized by fine lamination and a general absence of body or trace fossils, suggesting that it accumulated in a predominantly anaerobic environment. The local presence of small-diameter, shallow *Chondrites* indicates that a dysaerobic benthic environment with extremely low levels of oxygen became established occasionally. Comparable interpretations have been put forward for similar bioturbated beds in Pleistocene, Miocene and Devonian laminate sequences (Anderson and Gardner, 1989; Savrda, 1992; Ozalas *et al.*, 1994). The common presence of scour structures shows that the depositional substrate may have been periodically affected by storms. The horizontally-laminated lime mudstone is, in turn, overlain by a bioturbated lime mudstone unit containing small *Chondrites*, *Teichichnus* and indistinct lamination. These features indicate that the dissolved oxygen level in the benthic environment increased slightly but still within dysaerobic range.

As described, the bioturbated lime mudstone unit also contains up to 13 thin shell beds. These are characterized by sharp but non-erosional bases, well-preserved *in situ* brachiopods, and extremely variable bed thickness and lateral discontinuity. These features show that these shell beds were formed by winnowing of fine sediment in place. This interpretation is strongly supported by the presence of the same fauna in the directly underlying lime mudstone. Because the small thin-shelled fossils are normally well preserved, this indicates that they were not exposed on the seafloor for a long time but were rapidly covered by the overlying sediment. Therefore, it can be concluded that these shell beds are probably storm deposits. Similar storm deposits are interpreted as distal tempestites (as defined by Aigner, 1982) and form in relatively deep water environments. However, they were also present in a Middle Devonian lagoonal environment (Leonard, 1996). The presence of up to 13 storm beds suggests that the depositional environment was frequently disrupted by storms.

The shell bed-bearing part is succeeded by an olive-green lime mudstone, which is more

intensely bioturbated. Besides small *Chondrites* and *Teichichnus*, *Zoophycos*, *Planolites* and large *Chondrites* (up to 2 mm in diameter) are present. The more diverse trace fossils suggest that the amount of oxygen content in the benthic environment had further increased.

The olive-green bioturbated lime mudstone, in turn, grades upward into brown lime mudstone-wackestone unit with a mottled appearance, reflecting intense bioturbation. It contains *Chondrites* and *Planolites*, with the latter up to 1 cm in diameter, reflecting a more oxygenated environment.

The uppermost part of the lower Burr Member is composed of grey to dark grey, bioturbated wackestone with abundant large burrows and diverse shell fossils. The latter include brachiopods, gastropods, crinoids, ostracods and trilobites. This fauna suggests that the depositional environment was very close to or at normal marine conditions.

From this evidence, it can be concluded that the lower Burr Member in central Saskatchewan formed in a predominantly oxygen-restricted environment. The oxygen level first decreased from extremely low dysaerobic to anaerobic, then gradually increased upward. This vertical trend in oxygen status is identical to that in the transitional area between central and southeastern Saskatchewan. However, the presence of the well-laminated lime mudstone in central Saskatchewan suggests that it was deposited in a more oxygen-restricted environment than the indistinctly-laminated marlstone in the area between central and southeastern Saskatchewan.

4.2.4 Northwestern Saskatchewan

In northwestern Saskatchewan, the Dawson Bay Formation can be represented by the stratigraphic succession in Core 14-19-41-23W3.

The sedimentary succession above the Second Red Bed Member is composed predominantly of dark grey to brown dolostone with yellow sandstone intercalations (Plate 4-13A) and a limestone unit in its uppermost part. The paleokarsts and black shales of the Burr Member are absent in this core (probably due to non-deposition), and are replaced by a dark grey sandstone less than 1 cm thick. The sandstone is overlain by a dark grey dolostone. It is about 0.37 m (1.2 ft.) thick and massive in appearance. Close core examination shows that the dark grey dolostone contains abundant small *Chondrites* and a

PLATE 4-13

Plate 4-13 A: Core photograph showing the basal part of the Burr Member from northwestern Saskatchewan. It is composed predominantly of dark grey to brown dolostone (d) with sandstone intercalations (s). Lsd. 14-19-41-23W3. (One core box is 0.76 m long and core diameter is 10.1 cm.)

Plate 4-13 B: Slabbed core photograph of the dolostone from the basal part of the Burr Member in northwestern Saskatchewan. The rock is characterized by abundant small *Chondrites* and a few small vertical burrows. Lsd. 14-19-41-23W3. Scale bar is 3 cm.

Plate 4-13 C: Slabbed core photograph showing dolostone with carbonaceous stripes (c). The dolostone contains the trace fossil *Chondrites*, and probable *Zoophycos* and *Teichichnus*. Lsd. 14-19-41-23W3. Scale bar is 3 cm.

Plate 4-13 D: Plane-light photomicrograph showing sandstone from the basal part of the Burr Member in northwestern Saskatchewan. It is composed of well-rounded dolomite grains. Lsd. 14-19-41-23W3. Scale bar is 0.5 mm.

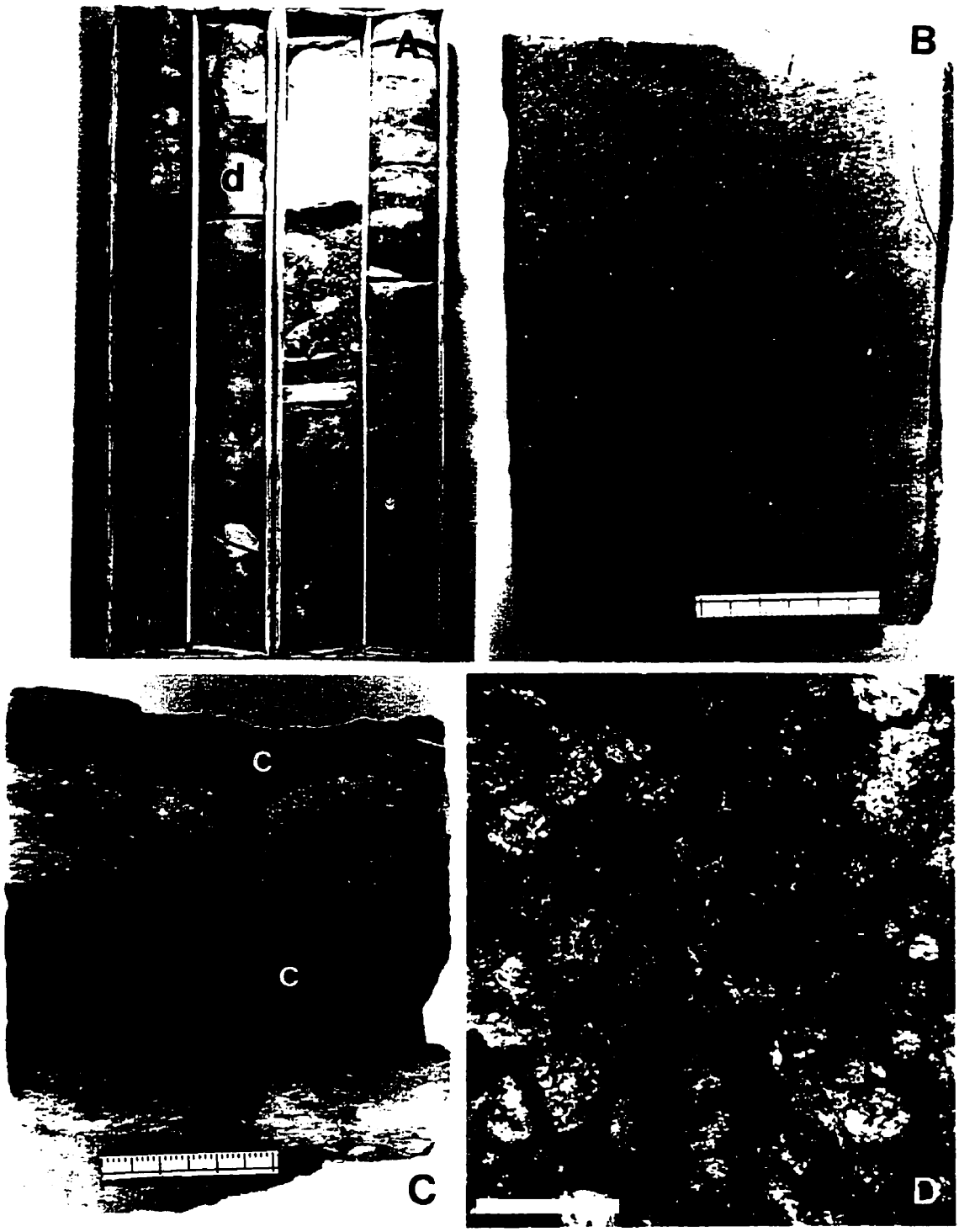
A
d
B
C
C
C
D

few small vertical burrows (Plate 4-13B). This, in turn, grades upward into a dark grey dolostone unit with black carbonaceous stripes (Plate 4-13C). The rock is heavily bioturbated and at least three types of trace fossils are present. The smaller examples are *Chondrites*, which are about 1 mm in diameter, horizontal in orientation, and are cross-cut by larger burrows. The larger burrows are light grey and up to 0.5 cm in diameter. They are probably *Zoophycos* and *Teichichnus*. Additionally, very sparse small brachiopods are locally present. The dark grey dolostone, in turn, is overlain by a unit of brown massive dolostone with sandstone interbeds that contains small *Chondrites* and a few small vertical burrows.

Sandstone interbeds, a few cm thick, are common in the core (Plate 4-13A). Two sandstones are up to 20 cm thick. One is present close to the bottom of the Burr Member; the other lies just below the limestone at the top. In hand specimen, the sandstone is loosely cemented and can be easily broken. In thin section, the sandstone is composed of dolomitic clasts, that are from subangular to subrounded in shape (Plate 4-13D). No pore-filling carbonate cement is present. The sandstones have both mud-supported and grain-supported fabrics.

Interpretation

Although most carbonate rocks in Core 14-19-41-23W3 are dolomitized, the original trace fossils can still be recognized. The low diversity of the trace fossil assemblage, dominated by small *Chondrites*, indicates that the carbonate rocks directly above the Second Red Bed Member were deposited under dysaerobic conditions. The absence of lamination shows that the general oxygen level was probably higher than that in central Saskatchewan. The common development of the terrigenous sandstone interbeds suggests that the area was located in a more nearshore environment.

4.3 Discussion

The lower Burr Member from northwestern to southeastern Saskatchewan is composed of fine-grained carbonate rocks with rare argillaceous mudstone and sandstone. The argillaceous content increases from central to southeastern Saskatchewan. The entire sedimentary succession is dominated by a low diversity of body fossils, which include small brachiopods, tentaculitids, gastropods, ostracods and foraminifera, with thin-shelled and poorly-calcified brachiopods as the principal body fossils. The trace fossils are

dominated by small *Chondrites*, with subsidiary *Planolites*, *Teichichnus*, *Zoophycos*, and rare *Thalassinoides* and *Skolithos*. In addition, fine-lamination is well developed in some rocks of central Saskatchewan. These indicate that the lower Burr Member was mainly deposited in a low energy, oxygen-deficient environment.

However, subtle changes in biofacies indicate that dissolved oxygen levels in the benthic environments varied both spatially and temporally during deposition of the lower Burr Member. In central Saskatchewan, the kerogen-laminated lime mudstone, with laminae probably produced by bacterial mats may have formed under extremely low dysaerobic conditions. As noted, there is a gradational transition between the kerogen-laminated lime mudstone and the underlying black shale and overlying horizontally-laminated lime mudstone, which formed under anaerobic conditions. This is also supported by the lateral transition of the kerogen-laminated lime mudstone into a lime mudstone with exclusive small *Chondrites* in the transitional area between central and southeastern Saskatchewan. The kerogen-laminated lime mudstone grades upward into a horizontally-laminated lime mudstone, suggesting an anaerobic condition. However, the common presence of scour structures, probably formed by storm activities, indicates a shallow water environment. The horizontally-laminated lime mudstone passes upward into an olive-green bioturbated lime mudstone unit, with progressively increasing ichnogeneric diversity and burrow diameters, reflecting a gradual upward increase in oxygenation. However, small, thin-shelled brachiopods are the only macrobenthic body fossils found in the unit. The presence of a low diversity assemblage of small, poorly calcified, macrobenthic body fossils indicates a dysaerobic environment.

Thus, it can be concluded that from the kerogen-laminated lime mudstone through the horizontally-laminated lime mudstone to the bioturbated lime mudstone and wackestone, the depositional environment changed from extremely low dysaerobic through anaerobic to dysaerobic condition with more dissolved oxygen content (Fig. 4-3).

A similar trend in oxygen level variation can be detected in the lower Burr Member in the transitional area between central and southeastern Saskatchewan. The exclusive presence of small *Chondrites* in the lower unit of the lower Burr Member suggests a low dysaerobic condition, but with oxygen levels slightly higher than the equivalent unit in central Saskatchewan, where the kerogen-laminated lime mudstone represents the lowest dysaerobic condition. The indistinct lamination in the middle unit reflects sedimentation in a quasi-anaerobic environment. Its dissolved oxygen level was lower than that during the

deposition of the lower unit, but was slightly higher than its equivalent in central Saskatchewan, which is composed of the well-laminated lime mudstone. The indistinctly laminated limestone, in turn, grades upward into bioturbated lime mudstone with a more diverse trace-fossil assemblage and relatively abundant brachiopods, that reflect a dysaerobic environment with higher dissolved oxygen content.

Thus, from the *Chondrites*-dominated lime mudstone through the indistinctly laminated lime mudstone to the bioturbated lime mudstone, the benthic environment changed from low dysaerobic, through quasi-anaerobic to dysaerobic with greater dissolved oxygen content. This trend is similar to that of the lower Burr Member in central Saskatchewan. However, the environment was generally less oxygen-restricted in the area between central and southeastern Saskatchewan than that in central Saskatchewan.

A similar trend of oxygenation can also be detected in the basal part of the Burr Member in southeastern Saskatchewan. However, the changes in oxygenation are condensed in a 40 cm-thick unit in Core 13-12-22-32W1, that lies directly above the paleokarsts of the Burr Member. The trace fossil assemblage changed from exclusive small *Chondrites* in the lower part to an assemblage composed of *Planolites* and firmground burrows in the upper part. These trace fossils, in turn, are cross-cut by secondary *Skolithos*. This suggests an environmental change from low dysaerobic in the lower part to a well-oxygenated condition at the top. This change of oxygen level is similar to that in central Saskatchewan and the transitional area between central and southeastern Saskatchewan. However, the thinness of the unit suggests that the upward increasing of the oxygen level was much more rapid than that in central Saskatchewan and the area between central and southeastern Saskatchewan.

In southeastern Saskatchewan, the sedimentary unit above the *Skolithos*-bearing lime mudstone is composed of brown lime mudstone with relatively large *Chondrites*, *Planolites*, medium-sized brachiopods and tentaculitids, but *Skolithos* is absent. This is overlain by a unit composed of lime mudstone and calcareous mudstone that contain small, poorly calcified brachiopods and pelagic tentaculitids. This unit is succeeded by a limestone unit containing trace fossil assemblages composed of small *Planolites* or *Chondrites*, but brachiopods are rare. All these features suggest that the oxygen level gradually decreased upward after deposition of the *Skolithos*-bearing lime mudstone (Fig. 4-3).

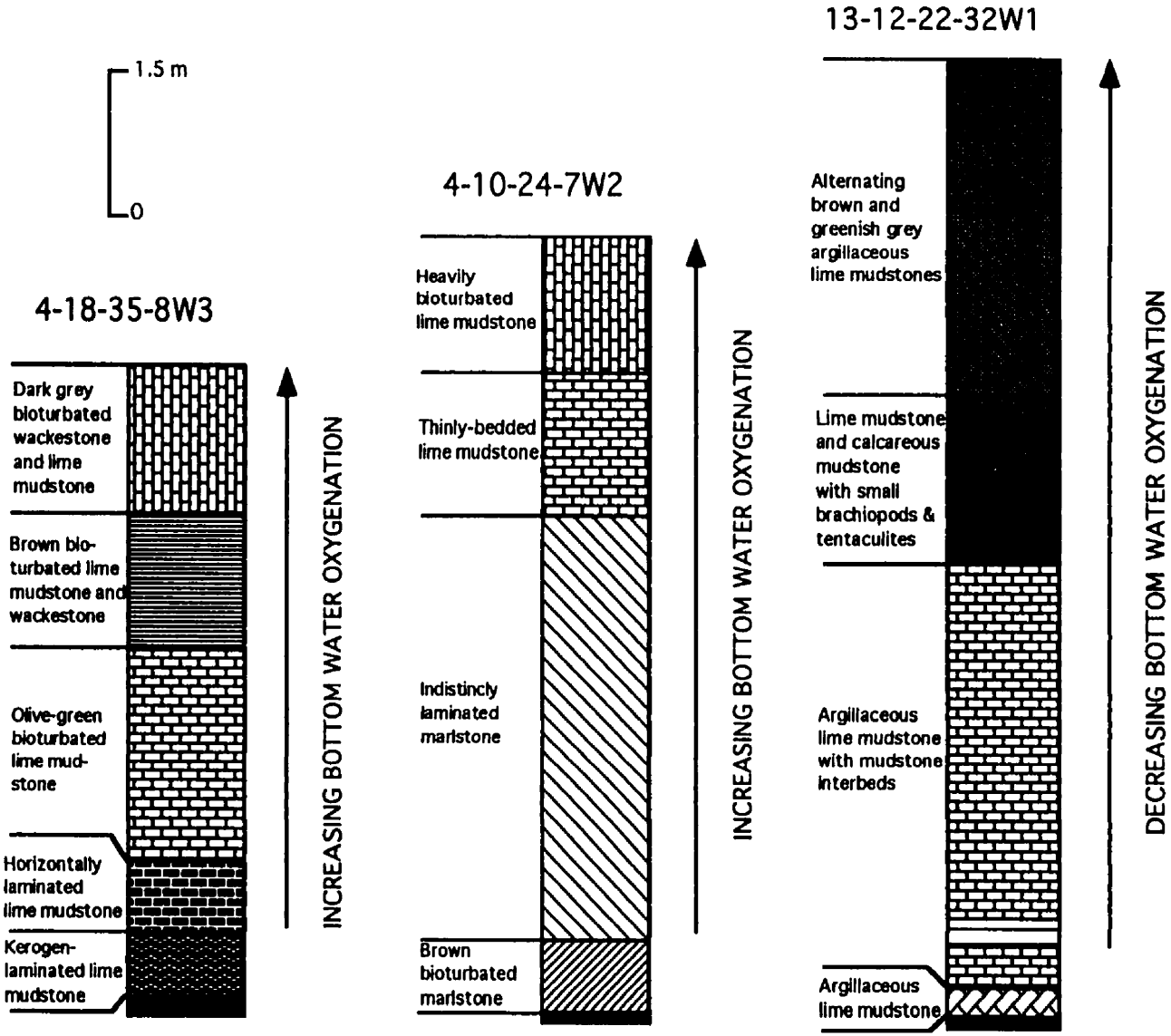

Fig. 4-3. Diagram showing oxygen variations during deposition of the lower Burr Member in central Saskatchewan, the transitional area between central and southeastern Saskatchewan, and southeastern Saskatchewan.

From this evidence, it can be concluded that the general oxygen level in the bottom water environment increased from central to southeastern Saskatchewan. However, as discussed in Chapter 3, before the Williston Basin was completely flooded by a large marine transgression in the early Burr time, two minor marine transgressions took place in the basin. Both reached southeastern Saskatchewan, but only one was extensive enough to reach parts of central Saskatchewan. However, none of the transgressions extended into northern Saskatchewan. This not only suggests that the marine waters came from the southeast, but also shows that the water depth increased southeastward. Thus, from central to southeastern Saskatchewan, the general oxygen level in the benthic environment gradually increased with increasing water depth. This trend is in contradiction with the prediction of the Rhoads-Morse-Byers model, which predicts that oxygen levels in bottom water environments decrease with increasing water depth.

A similar trend can also be detected in a transect from southeastern Saskatchewan to the outcrop belt of the Dawson Bay Formation in northwestern Manitoba. The Dawson Bay Formation in the latter region formed in a more near-shore environment (as discussed in the following chapter) than that in southeastern Saskatchewan. However, the lower Burr Member (Member B) in northwestern Manitoba is locally composed of laminated bituminous dolomite (Norris *et al.*, 1982), which indicates a more oxygen-restricted environment than the equivalent in southeastern Saskatchewan.

A similar trend of oxygen variation may have occurred during deposition of the Mowry Shale (Cretaceous) of Wyoming. Davis and Byers (1993) divided the sedimentary rocks of the Mowry Shale into a fine-grained lithofacies and a graded siltstone and mudstone lithofacies. The fine-grained lithofacies was deposited farther from the inferred western shoreline of the Mowry Sea than the graded siltstone and mudstone lithofacies. However, sharply defined fine-scale horizontal layering is notably rare in this lithofacies. Such layering, usually considered diagnostic of pelagic deposition in anoxic waters, may have been obliterated by very small-scale bioturbation in a low-oxygen environment (Davis and Byers, 1993). In contrast, the graded siltstone and mudstone lithofacies that formed in a more nearshore environment contains fine lamination. This probably reflects sedimentation of this lithofacies in a more oxygen-deficient environment than the fine-grained lithofacies. Thus, from nearshore basinward, the depositional environment contained more dissolved oxygen with increasing water depth.

This apparent anomaly poses a question as to why the oxygen level in the Canadian part of

the Williston Basin increased with increasing water depth, in contradiction to the Rhoads-Morse-Byers model. The Rhoads-Morse-Byers model was established based on data compiled from modern oxygen-deficient marine basins -- the California borderland and Black Sea -- which are characterized by steep slopes, with a rapid transition from shallow water shelf to deep basin setting. Such a rapid transition is unlikely to develop in ancient epicontinental settings, which are characterized by very extensive areas of negligible topography and a low tidal range, with the tidal energy dampened by frictional effects over the very extensive shallow seafloor.

In the much-cited model of Irwin (1965) for epicontinental seas (Fig. 4-4), a low-energy zone, below wave-base in the open sea, gives way to a relatively narrow zone of higher energy where waves impinge on the seafloor and there are strong tidal currents. Beyond this, in Zone Z, which is up to hundreds of kilometers wide, there is restricted circulation, tidal effects are minimal, and storm-wave action is only periodically significant. Hallam (1981) suggested that the restricted circulation in Zone Z would increase the tendency towards stagnation compared with the open sea. Thus, the oxygen-level is very likely to decrease from Zone Y to Zone Z. In other words, in ancient epicontinental seas, the dissolved oxygen content increased basinward within the range of Zone Y and Zone Z. This lateral oxygen-level variation is significantly different from that predicted by the Rhoads-Morse-Byers model, with the aerobic biofacies located between two oxygen-restricted biofacies, some distance from the nearshore environment. Furthermore the anaerobic and dysaerobic biofacies may have occurred both shoreward and basinward of the aerobic biofacies (Fig. 4-5).

During deposition of the lower part of the Burr Member in central Saskatchewan, the dissolved oxygen content first changed from extremely low or low dysaerobic to anaerobic or quasi-anaerobic condition. After that, the oxygen content gradually, but persistently, increased upward (Fig. 4-3). A similar oxygen-level change can also be detected during deposition of the lower part of the Burr Member in southeastern Saskatchewan. However, the entire oxygen-level change process happened in a sedimentary unit about 40 cm thick, suggesting that it happened much more quickly than that in central Saskatchewan. After that change, the oxygen level in the benthic environment of southeastern Saskatchewan decreased gradually upward (Fig. 4-3). This trend is significantly different from that in central Saskatchewan. Why should the oxygen level in central Saskatchewan have increased upward, while in southeastern Saskatchewan it decreased upward? This phenomenon can be explained as follows: southeastern Saskatchewan was located close to

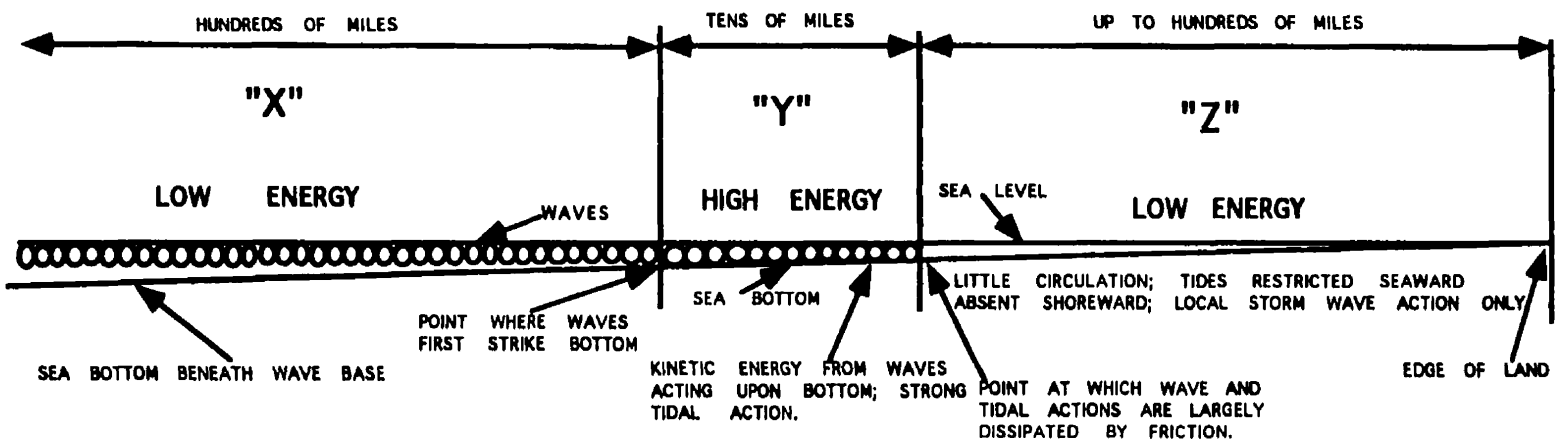

Fig. 4-4. Section showing energy zones in epeiric seas. Not to scale (from Irwin, 1965).

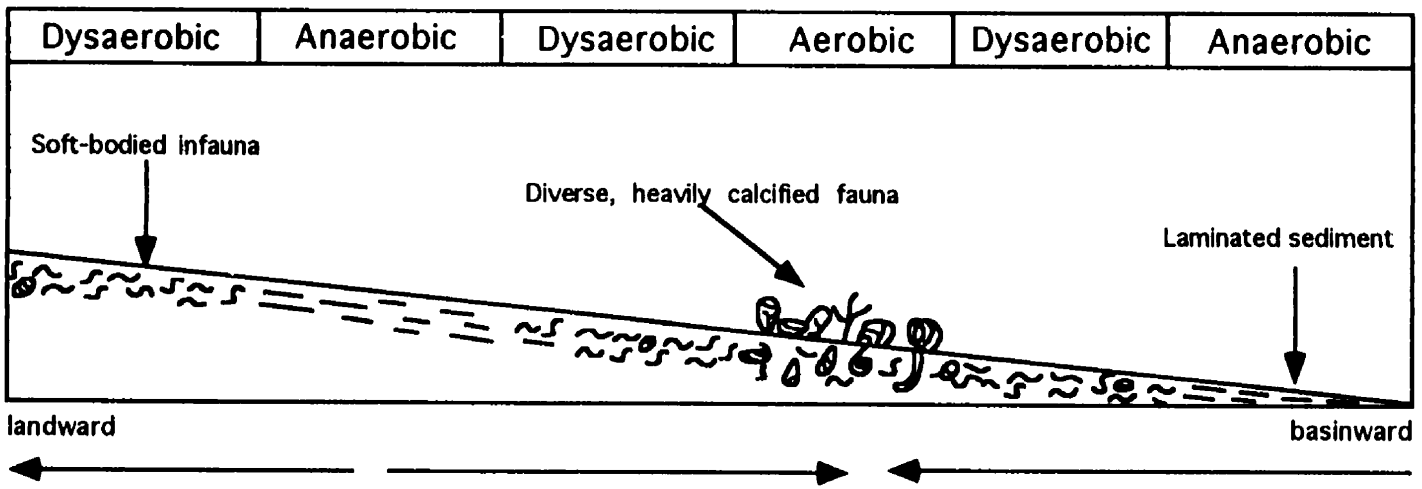

Fig. 4-5. Idealized cross-section of epeiric seas showing lateral biofacies changes.

the high energy zone of the epeiric sea model during the initial marine transgression, whereas central Saskatchewan was located in the low energy zone closer to the land. During the early transgression, the very shallow waters inhibited free water circulation and resulted in deposition of sediments under dysaerobic and anaerobic conditions (Hallam and Bradshaw, 1979). Freer circulation ensued as the sea deepened during the transgression: this gave rise to more aerated bottom conditions (Hallam and Bradshaw, 1979). Because southeastern Saskatchewan was located near the high energy zone, a high energy environment was rapidly established there. However, the high energy zone was still far away from central Saskatchewan at that time. The following high energy condition in southeastern Saskatchewan provided abundant oxygen to the bottom water environment and the environment changed sharply to well-oxygenated conditions. In some cores from southeastern Saskatchewan, the original sediment that formed in oxygen-restricted environment was eroded totally during this high energy phase. Even the paleokarstic surface at the base of the Burr Member was bored by organisms and trimmed by wave action. With further increase of water depth, the high energy zone migrated slowly and gradually to central Saskatchewan. The energy level in central Saskatchewan thus increased gradually, as did the oxygen level. During the same period, however, southeastern Saskatchewan began to enter the low energy zone, below-wave base. This resulted in decreasing energy level and consequently the oxygen level in the benthic environment.

4.4 Summary

As described and discussed previously, the lower Burr Member is composed predominantly of fine-grained carbonate rocks and the entire succession is dominated by a low diversity of small body fossils, which include brachiopods, tentaculitids, gastropods, ostracods and foraminifera, with small, thin-shelled, poorly-calcified brachiopods as the principal body fossils. The trace fossils in the lower Burr Member are dominated by small *Chondrites*, with subsidiary *Planolites*, *Teichichnus*, *Zoophycos*, and rare *Thalassinoides* and *Skolithos*. These indicate that the lower Burr Member was mainly deposited in a low energy, oxygen-restricted environment.

This study shows that the lower part of the lower Burr Member in central Saskatchewan consists of kerogen-laminated lime mudstone and horizontally laminated lime mudstone. They have fine laminations but lack body or trace fossils, reflecting anaerobic and extremely low dysaerobic conditions. In contrast, fine laminations are absent in the lower

Burr Member in southeastern Saskatchewan. This reflects that the overall dissolved oxygen level in central Saskatchewan was lower than that in southeastern Saskatchewan. Thus, from central to southeastern Saskatchewan, the depositional environment became less oxygen-restricted with increasing water depth. This trend contradicts with the Rhoads-Morse-Byers model, which predicts that oxygen level decreases with increasing water depth. This example shows that in the ancient epicontinental seas, the dissolved oxygen level in the benthic environments might increase from the landward low energy zone to the oceanward high energy zone of Irwin's model with increasing water depth.

CHAPTER 5

THE UPPER BURR MEMBER

5.1 Introduction

In contrast to the lower Burr Member, the upper Burr Member (upper part of the Burr Member) is composed of more pure and fossiliferous carbonate rocks. Its contact with the lower Burr Member is characterized by a distinct firmground in central Saskatchewan. In southeastern Saskatchewan, however, the contact is ambiguous, and is marked by several superimposed firmgrounds. The thickness of the upper Burr Member is about 9.5 m in central Saskatchewan, increasing gradually southeastward to reach a thickness of 12 m in southeastern Saskatchewan.

In this chapter, the stratigraphy, lithology, sedimentological features and depositional environments of the upper Burr Member from southeastern, central and northwestern Saskatchewan, as well as from northwestern Manitoba, are described and discussed, respectively. Emphasis is given to the origin of discontinuity surfaces (termed hardgrounds by previous authors) and storm deposits, which are distinctive features of this member. Detailed field, core and petrographic studies form the basis of this chapter.

5.2 Southeastern Saskatchewan

5.2.1 Stratigraphy

In southeastern Saskatchewan, the upper Burr Member is represented by Core 13-12-22-32W1 (Plate 5-1A-F). It is about 11.3 m (37 ft) thick and can be divided into lower, middle and upper parts. The lower part is composed of light grey to brown wackestone and lime mudstone, with a few thin packstone and grainstone interbeds. Additionally, several discontinuity surfaces are present close to the base of this part. The middle part is

PLATE 5-1

Plate 5-1 A-F: Detailed core photograph showing the upper Burr Member from southeastern Saskatchewan (b -- base of the upper Burr Member; t -- top of the upper Burr Member). Lsd. 13-12-22-32W1. (One core box is 0.76 m long and core diameter is 10.1 cm.)

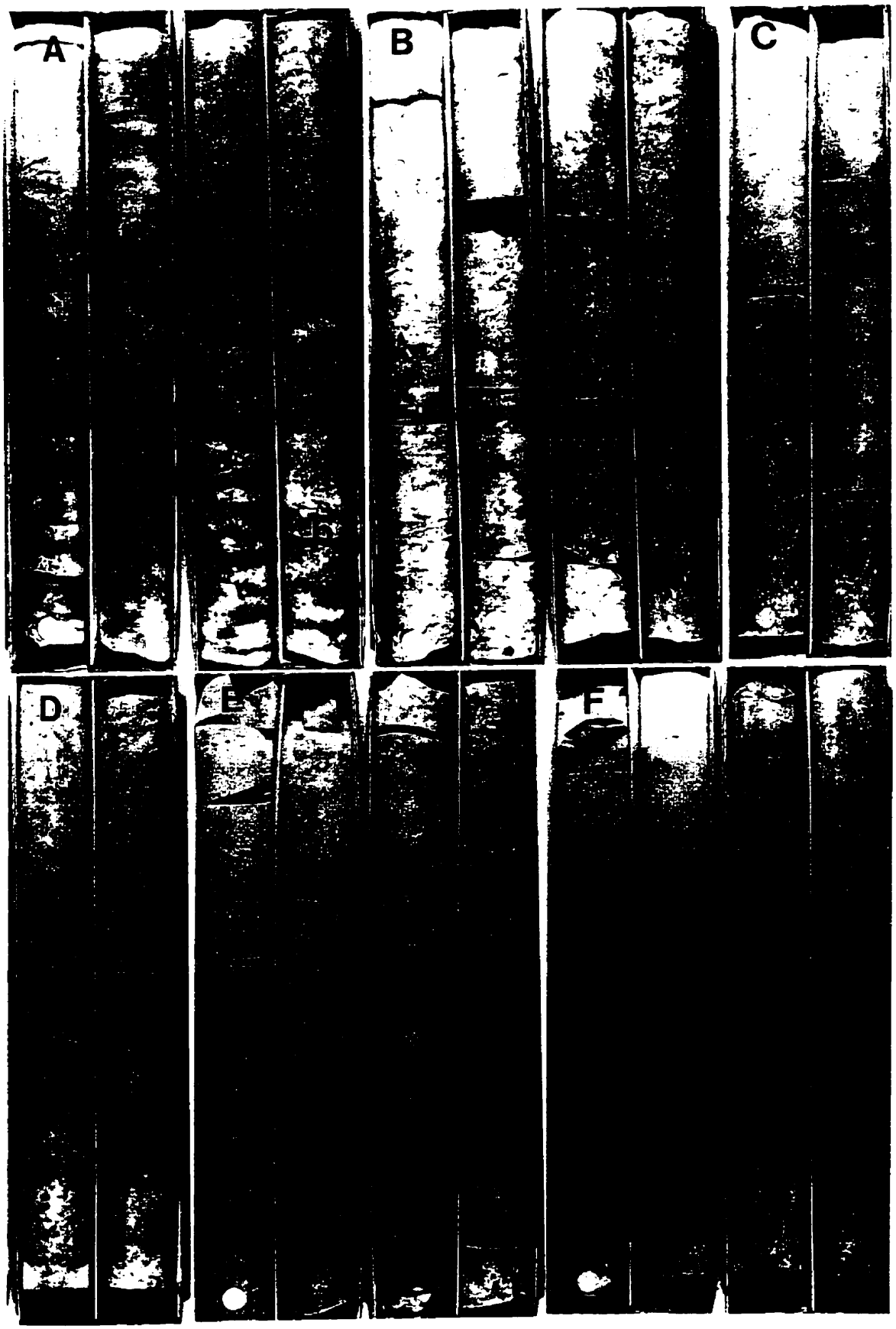
A
B
C
D
E
F

composed of lime mudstone and wackestone. No packstones, grainstones or discontinuity surfaces were observed. The upper part consists predominantly of wackestone and lime mudstone. Thin packstones and grainstones are present, but they are less common than those in the lower part. In addition, a few discontinuity surfaces are present. The contact between the upper Burr Member and overlying Neely Member is tentatively placed on a firmground that is characterized by intense mineralization (Plate 5-1F).

5.2.2 Lithology and Sedimentary Features

The carbonate rocks of the upper Burr Member in southeastern Saskatchewan can be divided into wackestone, lime mudstone, packstone and grainstone according to Dunham's classification (1962), with lime mudstone and wackestone as the dominant rock types.

Wackestone

Wackestone ranges from cm to tens of cm in thickness. This rock type can be divided into nodular wackestone and massive wackestone.

The nodular wackestone exhibits variable degrees of nodularity (Plate 5-2A & B). The nodules are present in irregular layers parallel or sub-parallel to bedding. Most nodules are lensoid and ovoid in shape and less than 1 cm in length. Black argillaceous seams are present around some nodules. The nodules are composed of micrite and bioclasts (Plate 5-3A). The bioclasts vary from moderately to highly concentrated. In the latter case, much allochthonous shell debris is present. The argillaceous seams contain rich, highly comminuted, shell debris of robust fossils (Plate 5-2D) that are dominated by brachiopods, with subordinate echinoderms, bivalves and trilobites. Coral fragments are locally present (Plate 5-2B).

The massive wackestone is interbedded with nodular wackestone (Plate 5-2B), lying below packstone or above lime mudstone. It is composed of micrite and shell fossils (Plate 5-2C). The amount of shell fossils in the wackestone varies from moderate to abundant. Where the wackestone contains a moderate amount of shell fossils, the fauna consists mainly of small gastropods, ostracods, tentaculitids, foraminifera and brachiopods, with a few fragments of robust brachiopods and crinoids. Most shell fossils are well preserved, indicating a predominant autochthonous fossil assemblage. Where the

PLATE 5-2

Plate 5-2 A: Slabbed core photograph showing interbedded nodular wackestone (n) and massive wackestone (m). The nodules of wackestone are surrounded by black argillaceous seams. Lsd. 16-29-22-30W1. Scale bar is 2 cm.

Plate 5-2 B: Slabbed core photograph showing nodular wackestone and massive wackestone in the upper Burr Member. A coral fragment (c) is present in the nodular wackestone. Lsd. 9-24-21-30W1. Scale bar is 2 cm.

Plate 5-2 C: Plane-light photomicrograph of massive wackestone. It is composed of micrite and bioclasts, which are dominated by small, thin-shelled fossils. Lsd. 9-24-21-30W1. Scale bar is 1 mm.

Plate 5-2 D: Plane-light photomicrograph showing abundant shell fragments in the black argillaceous seams of nodular wackestone. Lsd. 9-24-21-30W1. Scale bar is 1 mm.


A
B
C

PLATE 5-3

Plate 5-3 A: Plane-light photomicrograph of nodular wackestone. The carbonate nodule is composed of micrite and bioclasts. The latter contain both *in-situ* small, thin-shelled gastropods (g) and allochthonous brachiopod fragments (b). Lsd. 9-24-21-30W1. Scale bar is 1 mm.

Plate 5-3 B: Plane-light photomicrograph showing lime mudstone composed of micrite and scattered bioclasts. Scale bar is 1 mm.

Plate 5-3 C: Plane-light photomicrograph of packstone. It has a grain-support fabric, with gastropods (g) as predominant shell fossils. Lsd. 14-32-20-30W1. Scale bar is 1 mm.

Plate 5-3 D: Plane-light photomicrograph of packstone with bioclast dominated by fragments of small, thin-shelled brachiopods. Lsd. 14-32-20-30W1. Scale bar is 1 mm.

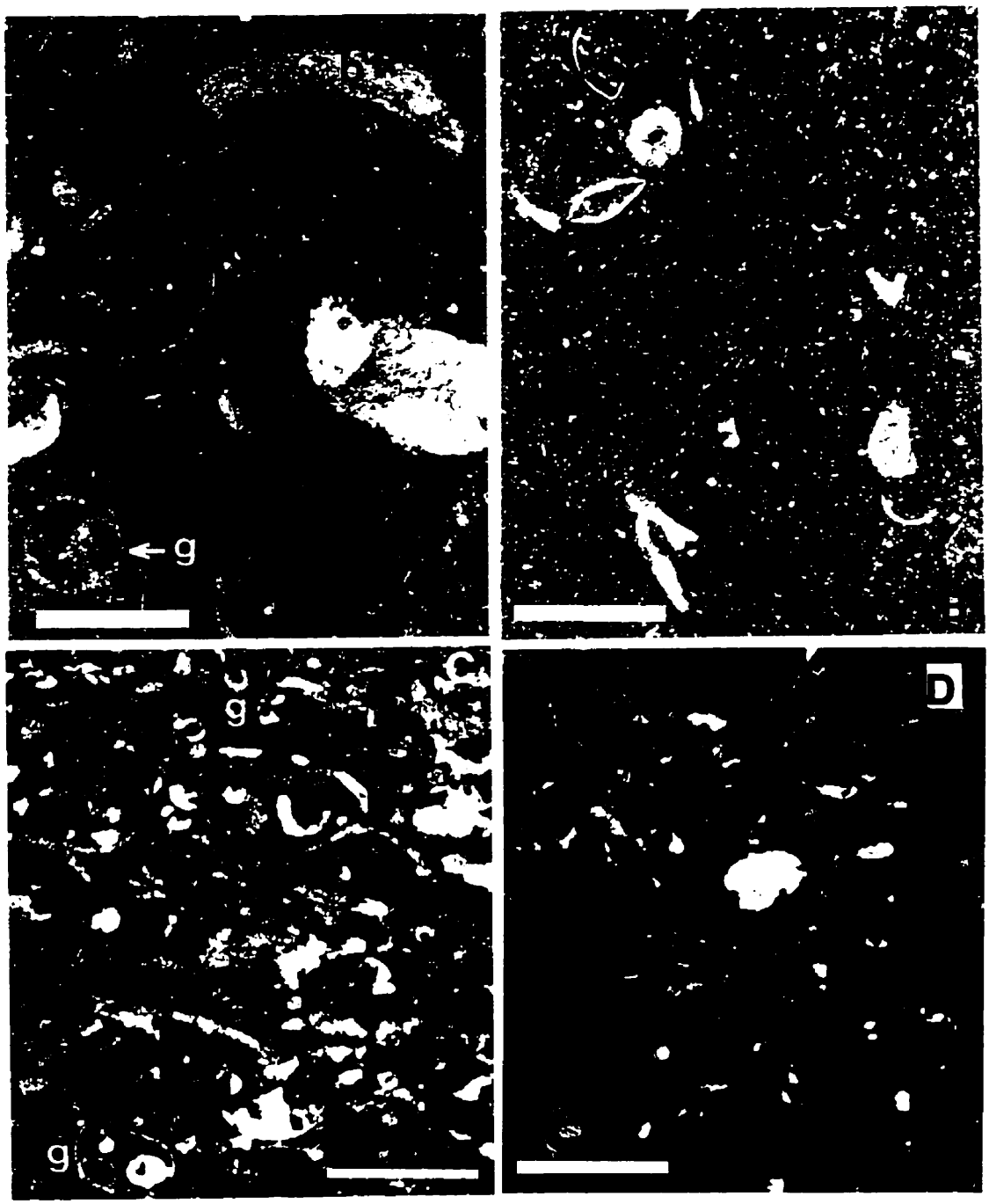
g
g
g
D

wackestone contains abundant shell fossils, they normally include many fragments of robust brachiopods and echinoderms, in addition to well-preserved *in situ* fauna. The presence of rich robust shell fragments suggests that some carbonate sediments may have been carried from adjacent shallow water areas. Additionally, trace fossils are abundant in the massive wackestone. They are dominated by a soft bottom ichnofauna, including *Planolites* and *Chondrites*. Other trace fossils are also present, but they cannot be identified with confidence.

Lime Mudstone

The lime mudstone has a thickness ranging from several to tens of centimetres. It is interbedded with wackestone or rests on packstone or grainstone. It is massive, grey to light brown, and composed of micrite and scattered shell fossils (Plate 5-3B). The shell fossils are dominated by small, thin-shelled ostracods, gastropods, tentaculitids, brachiopods and foraminifera. They are generally well preserved. Sparse debris of robust brachiopods and echinoderms are also present. In addition, abundant trace fossils are present in places. They are dominated by *Chondrites* and *Planolites*, which are 1-2 mm in diameter.

Packstone

The packstone is typically light grey and is composed of whole shells, their fragments and carbonate matrix (Plate 5-3C & D). Peloids are present locally. They constitute discrete shell beds, with a typical thickness ranging from a few millimetres to 2 cm (Plate 5-4A & C). Very rarely, the shell beds reach up to 4 cm thick. Their bedding ranges widely from planar and continuous to lenticular and less distinctly bedded. Individual packstone beds are characterized by sharp but non-erosive bases (Plate 5-4A). Although grading is only present locally (Plate 5-4C), planar and cross laminations are absent. Intraclasts are absent. Brachiopods, echinoderm, foraminifera, bryozoans and gastropods dominate the fauna. They show varying degrees of breakage, ranging from nearly *in situ* and unabraded accumulations to finer, comminuted and reworked accumulations. Most bioclasts are coarse-sand to small pebble in size.

The packstone can be divided into Type A and Type B. Type A packstone is composed mostly of parautochthonous or authochthonous shell deposits (Plate 5-4A & B). Whole-fossil valves are abundant. Most are parallel to bedding and convex-up. The thickness of

PLATE 5-4

Plate 5-4 A: Slabbed core photograph showing Type A packstone (p) in the centre of the core, which is composed mainly of parautochthonous and authochthonous brachiopods. Lsd. 9-24-21-30W1. Scale bar is 2 cm.

Plate 5-4 B: Plane-light photomicrograph of Type A packstone shown on Plate 5-4 A. Lsd. 9-24-21-30W1. Scale bar is 1 mm.

Plate 5-4 C: Slabbed core photograph showing Type B packstone (p), which is composed largely of well-sorted, coarse-sand sized shell debris. Lsd. 14-32-20-30W1. Scale bar is 2 cm.

Plate 5-4 D: Slabbed core photograph showing packstone composed of robust brachiopod fragments. The base of the upper Burr Member, southeastern Saskatchewan. Lsd. 13-12-22-32W1. Scale bar is 2 cm.

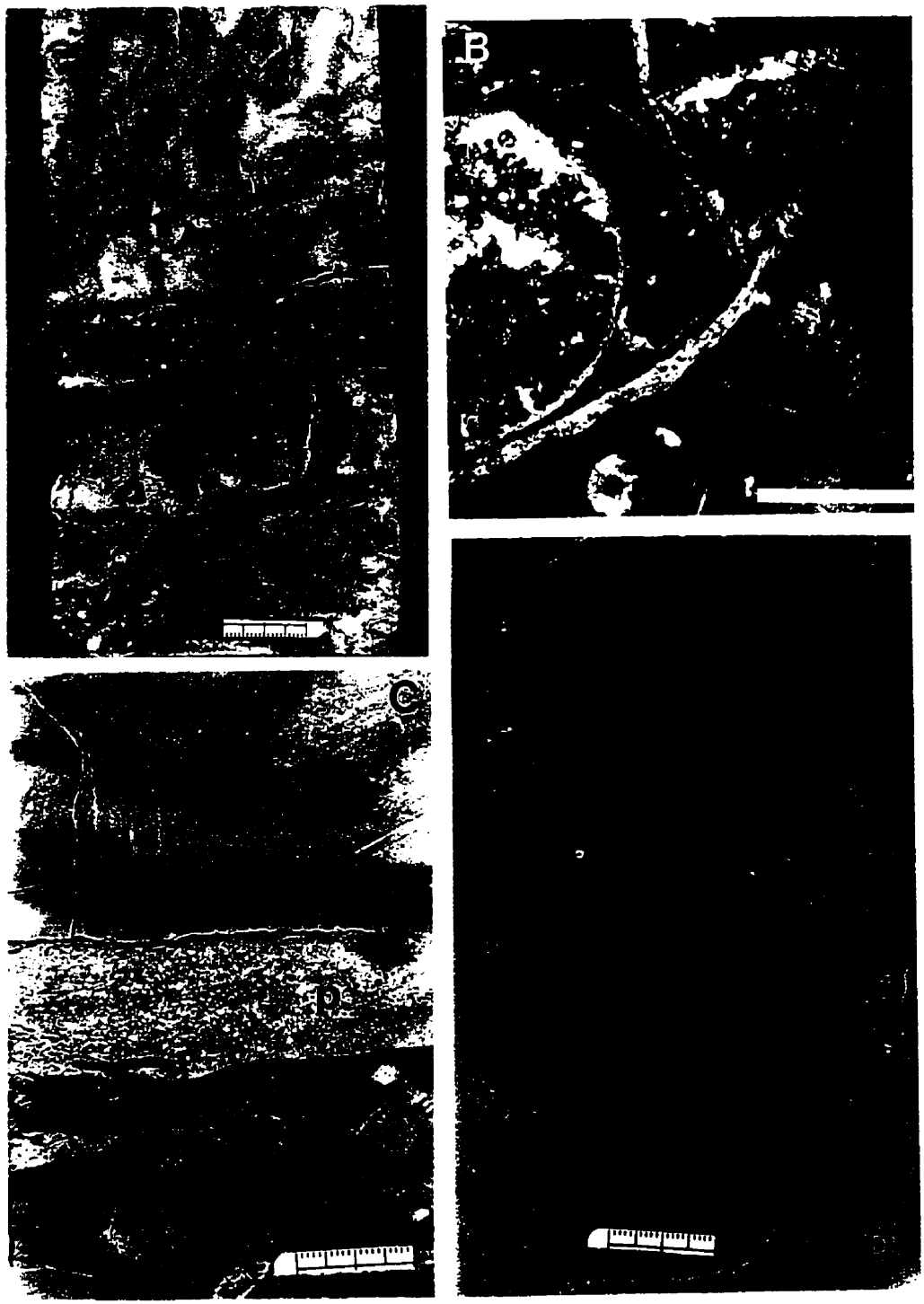
B
C
D

the packstones is highly variable laterally; some pinch out completely within the diameter of core samples. Small brachiopods, foraminifera, gastropods, tentaculitids and echinoderm fragments are the major skeletal constituents. Brachiopods are thin-walled and delicate, but excellently preserved and non-abraded (Plate 5-4B). Type B packstone has a relatively constant thickness within the diameter of core. It is composed of well-sorted, coarse-sand sized shell debris (Plate 5-4C). They are dominated by fragments of small, thin-shelled brachiopods, ostracods, tentaculites, gastropods and foraminifera (Plate 5-3C & D) although rare fragments of robust brachiopods and echinoderms are also present. Whole-shell fossils are present but rare. This type of packstone has a planar to irregular micro-scoured base (1-5 mm relief) (Plate 5-4C). The upper surface is planar or undulating. Both Type A and B packstones are underlain by wackestones or lime mudstones and are overlain by lime mudstones (Plate 5-4A & C).

Although most packstones in the upper Burr Member are composed predominantly of small, thin-shelled fossils and their fragments, a thin packstone composed of mainly robust shells is present at the base of the upper Burr Member. In Core 13-12-22-32W1, it is composed mainly of robust brachiopods, with subordinate echinoderm debris, thin-shelled brachiopods and gastropods (Plate 5-4D). Most elongate shells are parallel to bedding. The base of the packstone is sharp but non-erosive. It is underlain by a wackestone and overlain by a lime mudstone. The underlying wackestone contains abundant robust brachiopod shells that are randomly oriented. Some are even edgewise, probably indicating bioturbation. The overlying lime mudstone is massive and contains scattered shell fossils. The elongated shell fossils are parallel to bedding, suggesting no or very little bioturbation. The dominance of robust shell fossils and the presence of abundant shell fragments in the packstone suggest that it was deposited in relatively shallow water.

Grainstone

The grainstone is composed of bioclasts, peloids and sparry calcite (Plate 5-5A). The bioclasts are dominated by small, thin-shelled fossils, which include tentaculites, ostracods, foraminifera and brachiopods. Echinoderm debris and robust brachiopod fragments increase compared with the packstone described above. Although most shells in the grainstone are fragmentary, a few well-preserved ostracods and other microfossils are present. The peloids are well rounded. The grainstone is underlain by wackestone or lime mudstone and overlain by lime mudstone. The shell fossils from the underlying rocks are

PLATE 5-5

Plate 5-5 A: Photomicrograph of grainstone composed of crinoids, brachiopods, foraminifera, tentaculites and peloids that are cemented by sparry calcite. Lsd. 14-32-20-30W1. Scale bar is 1 mm.

Plate 5-5 B-D: Core photograph showing the lower and middle parts of the upper Burr Member in central Saskatchewan. C -- the contact between the lower and upper parts of the Burr Member. Lsd. 4-18-35-8W3. (One core box is 0.76 m long and core diameter is 10.1 cm.)

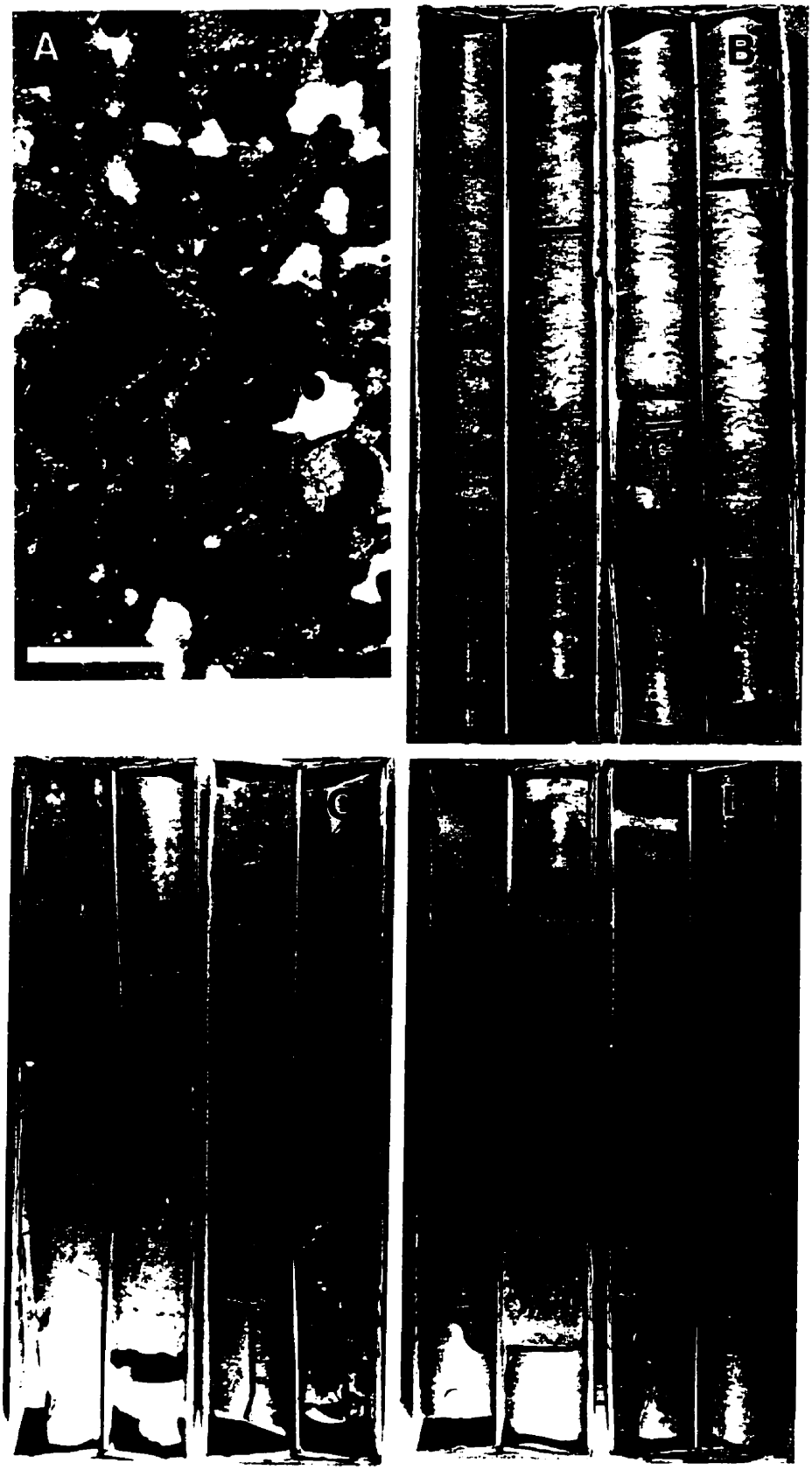
A
B
C

PLATE 5-6

Plate 5-6 A: Core photograph showing the upper part of the upper Burr Member in central Saskatchewan. Lsd. 4-18-35-8W3. (One core box is 0.76 m long and core diameter is 10.1 cm.)

Plate 5-6 B: Core photograph showing the top of the upper Burr Member and the contact (c) between the Burr and Neely Members. Lsd. 4-18-35-8W3. (One core box is 0.76 m long and core diameter is 10.1 cm.)

Plate 5-6 C: Slabbed core photograph showing shell beds (s) from Unit A of the upper Burr Member in central Saskatchewan. Lsd. 4-18-35-8W3. Coin diameter is 1.7 cm.

Plate 5-6 D: Slabbed core photograph showing a firmground (f) from Unit A of the upper Burr Member in central Saskatchewan. It is characterized by mineral impregnation. Lsd. 4-18-35-8W3. Coin diameter is 1.7 cm.

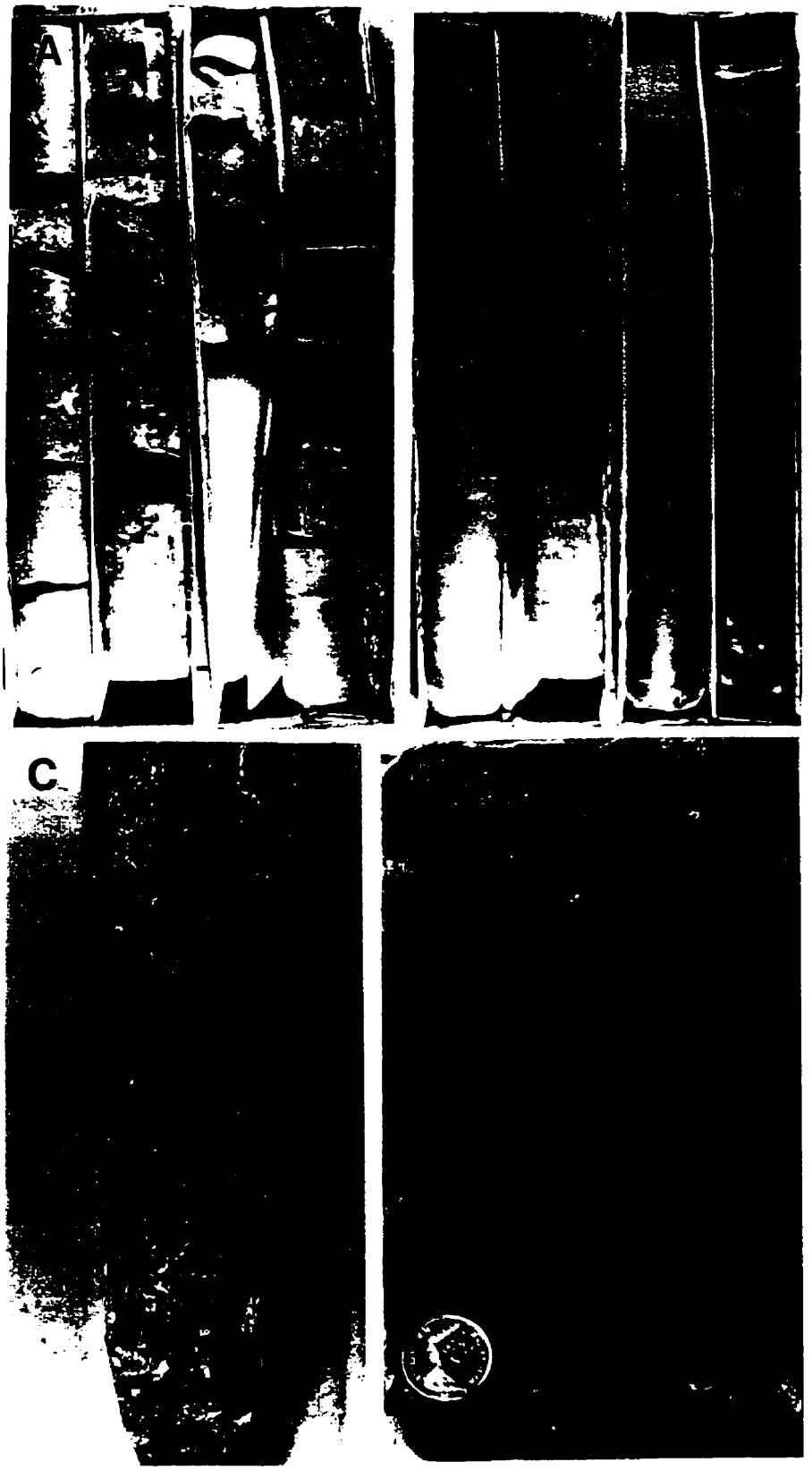
A
C

similar to those in the grainstone.

5.2.3 Interpretation

The upper Burr Member in southeastern Saskatchewan is dominated by wackestones and lime mudstones, with a few thin skeletal packstone and grainstone interbeds. This suggests that the sediments were mainly deposited in low energy, relatively deep water environments, with occasional high energy intervals. Most packstones and grainstones are less than 2 cm thick. They are characterized by sharp, non-erosive bases. Bedding ranges from planar and continuous to lenticular and less distinctly bedded. Some beds pinch out laterally in a few cm. Lateral discontinuity and extreme variability in thickness are recognized as important features of storm beds (Kreisa, 1981). This suggests that the packstones and grainstones were formed in place, probably by storm processes. This interpretation is supported by the presence of the same fauna in the wackestones or lime mudstones that underlie the packstones and grainstones. Furthermore, these packstones/grainstones are overlain by lime mudstones. They constitute characteristic packstone/grainstone-lime mudstone couplets formed by storm activities (Kreisa, 1981). Similar packstone/grainstone-lime mudstone couplets have been widely reported from storm deposits (e.g., Kreisa, 1981; Faulkner, 1988; Sami and Desrochers, 1992). Winnowing and suspension of finer sediment by storm turbulence resulted in the deposition of the upward-fining, but typically distinctly segregated, coarse (lag) and fine (suspended fraction) couplet (Kumar and Sanders, 1976; Kazmierczak and Goldring, 1978). The packstone/grainstone formed when high-energy storm waves scoured and suspended bottom sediments, then redeposited winnowed materials as storm lags. The lime mudstones are low-energy suspension deposits formed under waning storm-energy conditions. The thinness of the packstones/grainstones, and the general absence of erosive bases and amalgamated shell beds, suggest that they were deposited in distal environments according to the distality-proximality trends of Aigner (1982, 1985).

However, storm deposits are composed largely of well-preserved autochthonous or parautochthonous faunas (Aigner, 1985; Kreisa, 1981). This occurs because the shells are rapidly buried by storm-transported sediment and there is little opportunity for postmortem breakdown by biological and physical processes (Sami and Desrochers, 1992; Jones and Desrochers, 1992). In contrast, some packstones and grainstones in the upper Burr Member of southeastern Saskatchewan are rich in shell fragments. Locally, they even become the dominant component of the rocks. Although most shell fragments

are derived from small shell fossils similar to those present in the directly underlying limestones, the presence of abundant shell fragments implies relatively long periods of exposure on the sea floors. Such a feature cannot be attributed to storm action alone. Similar shell beds were referred to as TOP (or Top Of Parasequence) beds by Banerjee and Kidwell (1991) or as composite condensed shell beds associated with meter-scale upward-shallowing cycles by Li and Droser (1997). Such shell beds may form as a result of the shallowing of the sea floor into areas that are affected more frequently by the winnowing and scouring effects of storm waves (Brett, 1995). They are the product of erosional winnowing or dynamic bypass of finer grained sediments as the sea bottom approaches and then exceeds a threshold of higher energy conditions associated with average storm wave base. They are probably deposited in the fairweather wave base to storm-base region (Calvet and Tucker, 1988). Such deposits may have been formed by repeated storm events, in which bioclasts have accumulated and been winnowed over long time, but only the ultimate storm left a deposit of sedimentological significance (Fursich, 1971). TOP shell beds are typically well developed in carbonate-dominated parasequences where they may form extensive shell-rich caps up to several meters thick (Kidwell and Aigner, 1985; Aigner, 1985).

5.3 Central Saskatchewan

5.3.1 Stratigraphy and Lithology

In central Saskatchewan, the upper Burr Member is represented by Core 4-18-35-8W3 and can be divided into 4 units. From base to top, they are termed Unit A, B, C and D (Plate 5-5B-D & Plate 5-6A-B).

Unit A, about 3 m thick, can be divided into lower, middle and upper parts. The lower part (Plate 5-5B) is composed of light grey, nodular wackestone and lime mudstone, with at least 8 firmgrounds. Shell fossils and intraclasts are scattered throughout this part. The middle part (Plate 5-5C) consists of light grey lime mudstone, wackestone and packstone. More than ten shell beds are present in this part (Plate 5-6C). They are believed to be storm deposits, as described below. In addition, firmgrounds are also abundant in this part (Plate 5-6D). The upper part (Plate 5-5C) consists of light grey lime mudstone and wackestone, with a few shell beds. A single shell bed composed of large, *in situ* brachiopods is present locally. The contact between Unit A and B is a firmground.

Unit B (Plate 5-5D), about 1 m thick, is dominated by lime mudstone and wackestone, with thin packstone interbeds. The lime mudstone and wackestone are massive and contain small, thin-shelled brachiopods and sparse fragments of echinoderms and robust brachiopods (Plate 5-7A). Most thin-shelled brachiopods are less than 5 mm in length. They are unbroken, unabraded and scattered throughout the rocks (Plate 5-7C). Locally, they are highly concentrated but still have a wackestone fabric (Plate 5-7A). The lime mudstone locally contains *Chondrites* (Plate 5-7B). The *Chondrites* are consistently less than 1 mm in diameter. They are horizontal to subhorizontal in orientation. Packstone (Plate 5-7A), up to 1 cm thick, is composed of bioclasts and micritic matrix. The bioclasts are dominated by small, thin-shelled brachiopods. They are probably storm deposits and are described in next section. Close to the top of the unit, both the size and diversity of trace fossils appear to increase. The contact between Unit B and C is a firmground (Plate 5-5D), characterized by robust burrows, intraclasts, and shell fragments.

Unit C (Plate 5-5D), about 2.5 m thick, is composed of wackestone, lime mudstone and packstone. At least 10 firmgrounds are present in this unit. Intraclasts, robust brachiopods and solitary corals are scattered throughout the rocks. Most rocks have a mottled appearance, similar to those in the lower part of Unit A. A thin reefal rock composed of small corals is present in this unit.

Unit D, about 3 m thick, is made up of alternating brown and grey lime mudstones in the lower part (Plates 5-6A, 5-7D). The average thickness for both rock types is 6 cm. The brown lime mudstone appears mottled and is extensively dolomitized. It contains carbonaceous debris, crinoid fragments, small gastropods and thin-shelled brachiopods. Trace fossils are abundant and are dominated by *Chondrites* and *Planolites*. The grey lime mudstone is highly bioturbated and composed of micrite and shell fossils. Shell fossils are dominated by ostracods and small gastropods. The trace fossils include *Chondrites* and *Planolites*. Additionally, several firmgrounds are present in this part. The firmgrounds have irregular upper surfaces, which lack mineralization.

The upper part of Unit D is composed of massive grey to brown lime mudstone with thin packstone interbeds (Plates 5-6B, 5-8D). The packstones range from mm up to 2 cm thick. They are light grey and composed of small, thin-shelled brachiopods, echinoderm fragments and local tentaculites. They are probably formed by storm processes and are described in the following section.

PLATE 5-7

Plate 5-7 A: Core photograph of Unit B in the upper Burr Member of central Saskatchewan. The core is composed of lime mudstone, wackestone and thin packstone interbeds. The packstones have sharp, flat to undulating bases. The shell fossils in these rocks are dominated by small, thin-shelled brachiopods that are generally well preserved. Lsd. 13-21-29-20W2. Scale bar is 2 cm.

Plate 5-7 B: Core photograph of lime mudstone from Unit B of the upper Burr Member in central Saskatchewan. The rock is characterized by small *Chondrites* (c) and scattered, well-preserved, small brachiopods. Lsd. 13-21-29-20W2. Coin diameter is 1.7 cm.

Plate 5-7 C: Photomicrograph showing lime mudstone from Unit B of the upper Burr Member in central Saskatchewan. It is composed of micrite with well-preserved, small, thin-shelled brachiopods. Lsd. 13-21-29-20W2. Scale bar is 1 mm.

Plate 5-7 D: Slabbed core photograph showing alternating brown and grey lime mudstones in Unit D of the upper Burr Member in central Saskatchewan. The contact between them is a firmground (f). However, the surface of the firmground lacks mineralization. Lsd. 4-18-35-8W3. Scale bar is 2 cm.

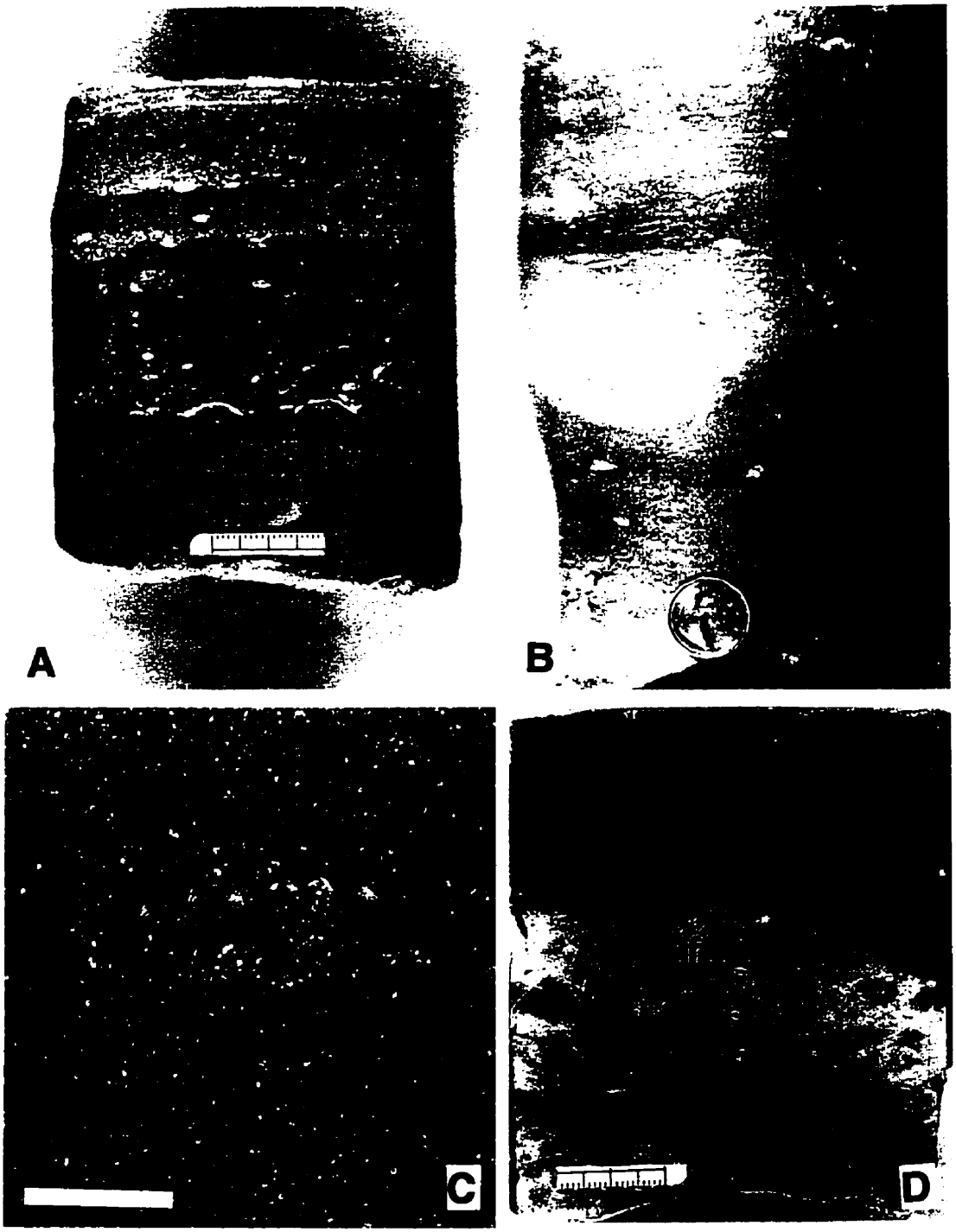
A
B
C
D

PLATE 5-8

Plate 5-8 A: Core photograph showing a high concentration of shell beds in Unit A of the upper Burr Member. The general thickness of the shell beds and the size of the shells decrease from the base to the top of the core. Lsd. 5-22A-34-1W3. Coin diameter is 1.7 cm.

Plate 5-8 B: Slabbed core photograph showing shell beds from Unit A of the upper Burr Member in central Saskatchewan. They are composed of mainly small to medium brachiopods, with some shell fragments subvertical to vertical in orientation in the lower middle part of the slabbed core. Lsd. 5-22A-34-1W3. Scale bar is 2 cm.

Plate 5-8 C: Slabbed core photograph showing that the shell beds from Unit A of the upper Burr Member are bioturbated. Lsd. 3-27-38-27W2. Scale bar is 2 cm.

Plate 5-8 D: Core photograph showing Type B shell beds (s) from Unit D of the Upper Burr Member, from the Cominco potash mine. Scale bar is 1 cm.

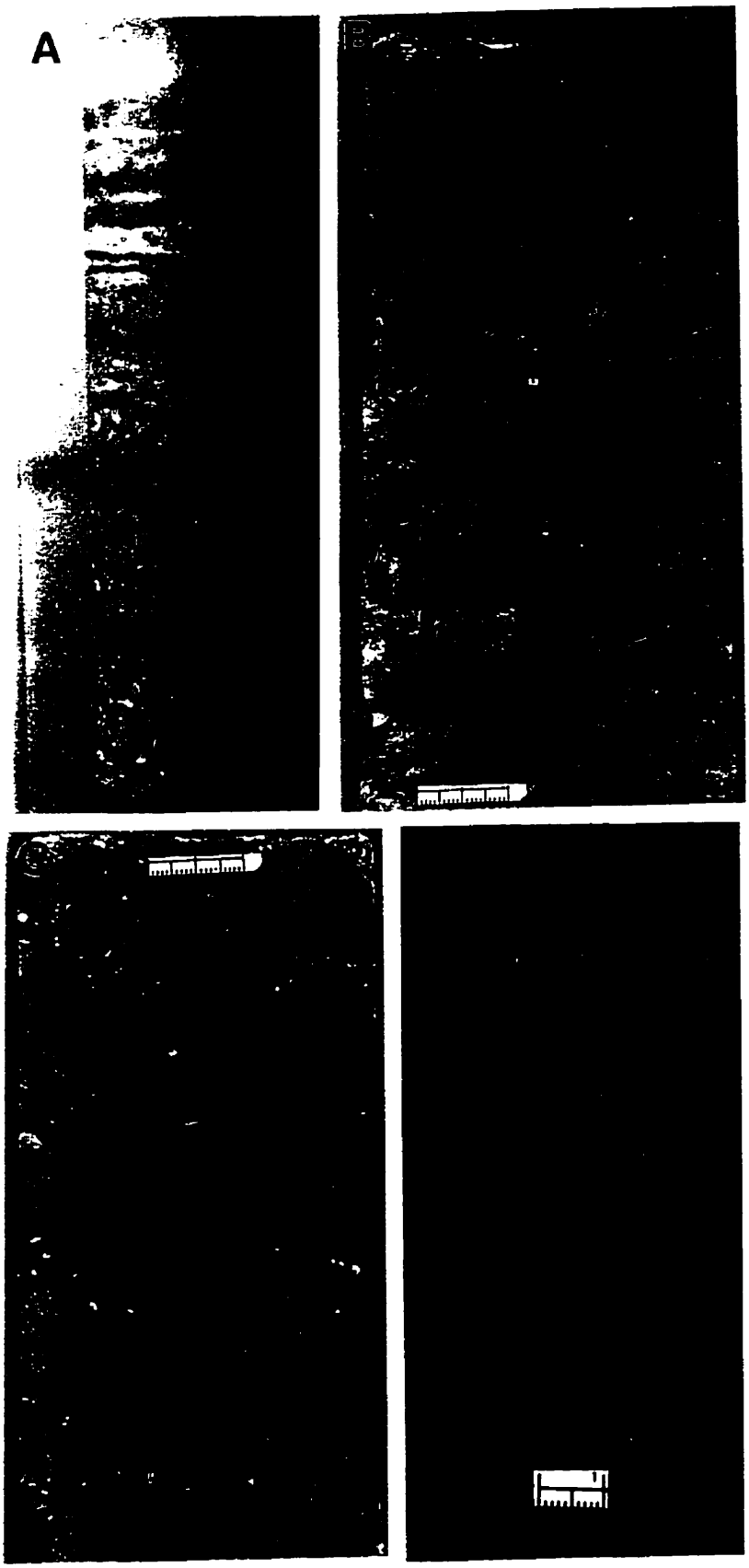
A

5.3.2 Storm Deposits in Central Saskatchewan

Shell beds that probably formed by storm processes are present throughout the upper Burr Member in central Saskatchewan. They are composed of shells and their fragments. Based on the size of shells, they can be divided into Type A and B shell beds.

Type A Shell Beds

Type A shell beds are highly concentrated in Units A and C of the upper Burr Member (Plate 5-8A), with a much higher frequency than those in southeastern Saskatchewan. These shell beds are composed of bioclasts, intraclasts, and carbonate matrix (Plate 5-8B). Most shell beds are between 2 and 4 cm thick, slightly thicker than those in southeastern Saskatchewan. However, the wackestones or lime mudstones between the shell beds are commonly less than 1 cm thick (Plate 5-8A). Generally, the thicker shell beds are tabular in appearance, whereas the thinner shell beds are lenticular.

The shell beds can be divided into those with distinct boundaries and those without distinct boundaries. The former are relatively thin, typically 1-2 cm thick, with sharp but non-erosive bases (Plate 5-8A & B). The latter do not have distinct boundaries (Plate 5-8C), but still have bedded appearance. These shell beds are relatively thick (> 2 cm). The shell fossils in these beds are randomly oriented. They are interlocked with irregular patches of lime mudstone. Burrows are abundant in these shell beds. The presence of burrows and the irregular patchy distribution of the shell fossils indicate that these shell beds were bioturbated. In the upper part of Unit A, the thickness of the shell beds and the size of the shell fossils decrease significantly.

Most bioclasts in the shell beds are medium to large robust brachiopods, with subordinate echinoderm debris, corals and small, thin-shelled brachiopods. Some shells are broken and abraded, but only moderately. Shell fossils lie preferentially parallel to bedding and are imbricated in a convex-up position. These indicate that they were reworked by currents after deposition. However, shell fossils in one shell bed are characterized by a dominant convex-down position, with some shells standing "end-on" (Plate 5-8 B). This suggests that the shell bed was immediately buried by sediment without subsequent current reworking (Jefferey and Aigner, 1982). The intraclasts are composed of lime mudstone. These intraclasts are typically rounded and have irregular shapes. Apparently they were weakly consolidated when reworked.

Type B Shell Beds

Type B shell beds are present in Units B and D (Plates 5-8D, 5-7A). They are thin and are composed of small, fragile shell fossils dominated by brachiopods. These shells are generally well preserved. They are oriented parallel to bedding. Sharp minor scoured bases, probably formed by erosion, are locally present. They vary from flat to slightly undulating, with a wavelength up to 2 cm and an amplitude up to 3 mm. They are overlain by a thin, light grey lime mudstone.

Interpretation

The brachiopod-rich shell beds in central Saskatchewan were first reported by Ahlstrom (1992), who interpreted them as high energy deposits on localized topographic highs. However, these shell beds are widely distributed in central Saskatchewan. They are present in every core that has been examined. Although shell fossils in most shell beds lie preferentially parallel to bedding and are convex-upward, shells with convex-downward orientation are present locally, a characteristic indicating immediate burial without subsequent current reworking (Jeffery and Aigner, 1982). This feature indicates that at least some shell beds were not formed by long exposure to high energy environments but were accumulated by sudden storm activities. This interpretation is supported by shell fossils showing only moderate breakage, which also suggests rapid burial by sediment.

In comparison with the shell beds in southeastern Saskatchewan, the shell beds in central Saskatchewan are characterized by larger shell size and greater shell thickness. Morphological trends toward greater shell size and thickness indicate habitation in a more agitated environment related to shallower depths (Jennette and Pryor, 1993). Additionally, intraclasts are common in the shell beds, and fine-grained carbonate sediments between shell beds are relatively thin. All these features suggest that these shell beds were deposited in more proximal environments. However, these shell beds commonly have sharp, but non-erosive bases. Additionally, the presence of carbonate matrix indicates that the storms were not strong enough to remove all fine-grained sediments between the shells, possibly indicating depositional environments with moderate water depths. The upward decrease in the shell bed thickness and in size of bioclasts from Unit A to Unit B, and from Unit C to Unit D, probably indicates increasing water depths.

5.4 Northwestern Saskatchewan

In northwestern Saskatchewan, the Dawson Bay Formation is represented by the stratigraphic sequence in Core 14-19-41-23W3. The strata above the Second Red Bed Member are composed of carbonate rocks, with thin sandstone interbeds. The brown carbonate rocks are almost completely dolomitized, and massive in appearance. They cannot be subdivided into the lower and upper Burr Member. In the middle of the carbonate succession, several former shell beds, now characterized by fossil moulds and filled with halite, are present (Plate 5-10A). Based on the sizes of the fossil moulds, it can be deduced that the former shell beds were composed mainly of sand-sized shell fragments with a few gravel-sized whole-shell fossils. At least three shell beds were originally present in a sedimentary unit less than 10 cm thick. Although they are only a few cm thick, one of them has a sharp, strong erosional base. This suggests that the shell beds were probably deposited in relatively high energy, shallow-water environments by storm processes.

5.5 Northwestern Manitoba

5.5.1 Stratigraphy

In northwestern Manitoba, the Burr Member, which is locally called Member B, consists of a lower argillaceous, in places bituminous, dolomite, succeeded by micritic limestone that grades up to a clean fossiliferous limestone, capped by an argillaceous limestone unit. It forms the cap rock of many domal structures in the southwestern part of the Dawson Bay area. The Burr Member is 7 to 10 m thick in the Dawson Bay area, but thickens markedly to the south (Norris *et al.*, 1982).

In contrast to the lower Burr Member, the upper Burr Member crops out well in a domal structure on Highway 10 directly north of the junction with the road leading to Pelican Rapids (Figs. 5-1, 5-2) (Plate 5-9A). The lowest part of the outcrop is composed of yellowish nodular lime mudstone (Plate 5-9B). It forms a recessive part of the domal structure and was believed to be part of the Mafeking Member (Second Red Bed Member) by Norris *et al.* (1982). However, some shell fossils were found in the rock, including ostracods, crinoid debris and brachiopods (Plate 5-10B). Because (1) no marine shell fossils have ever been observed in the dolostone of the Second Red Bed Member in Saskatchewan, and (2) the Mafeking Member (Second Red Bed Member) in northwestern

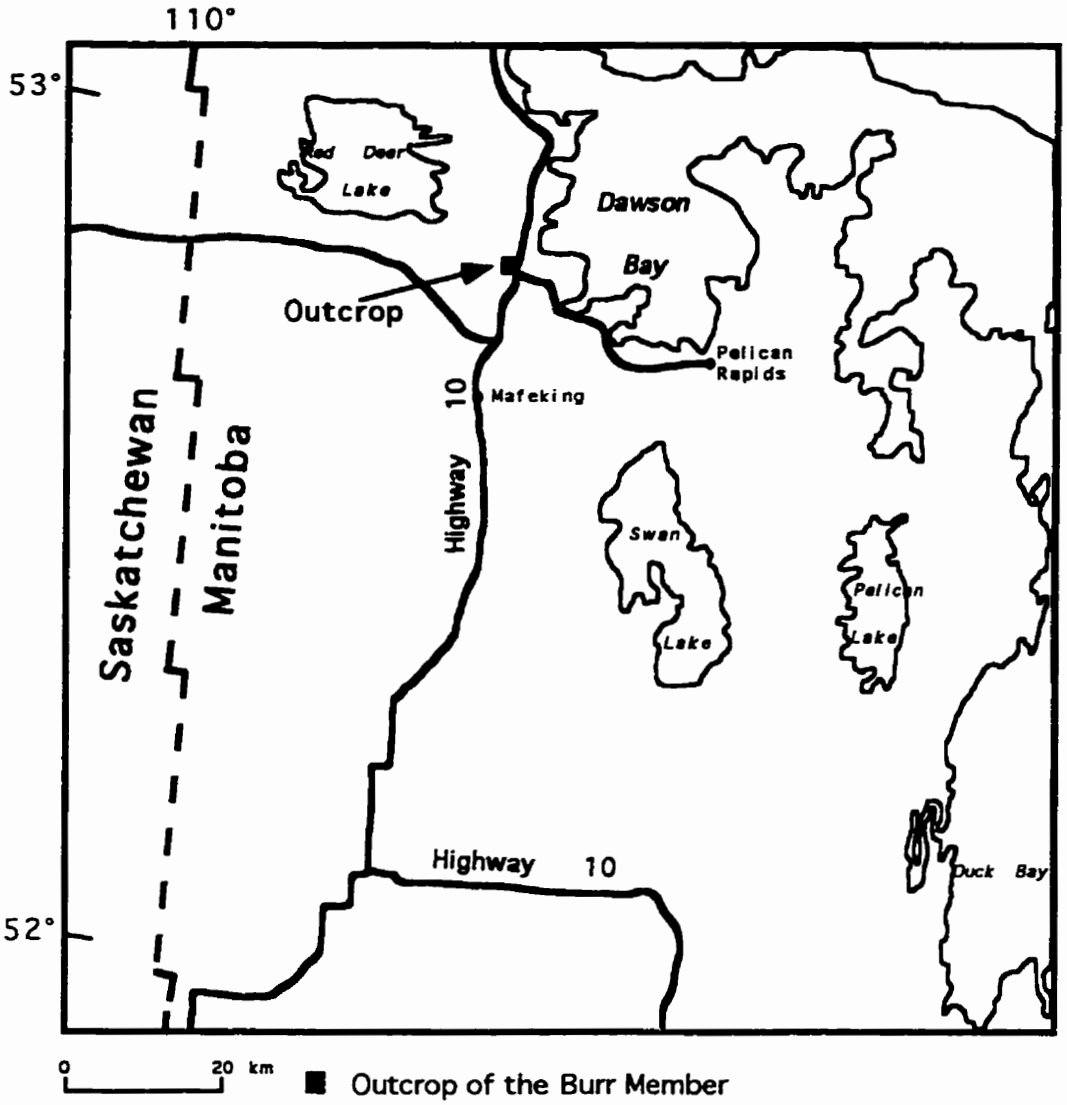

Fig. 5-1. Map showing the location of the Burr Member outcrop in this study.

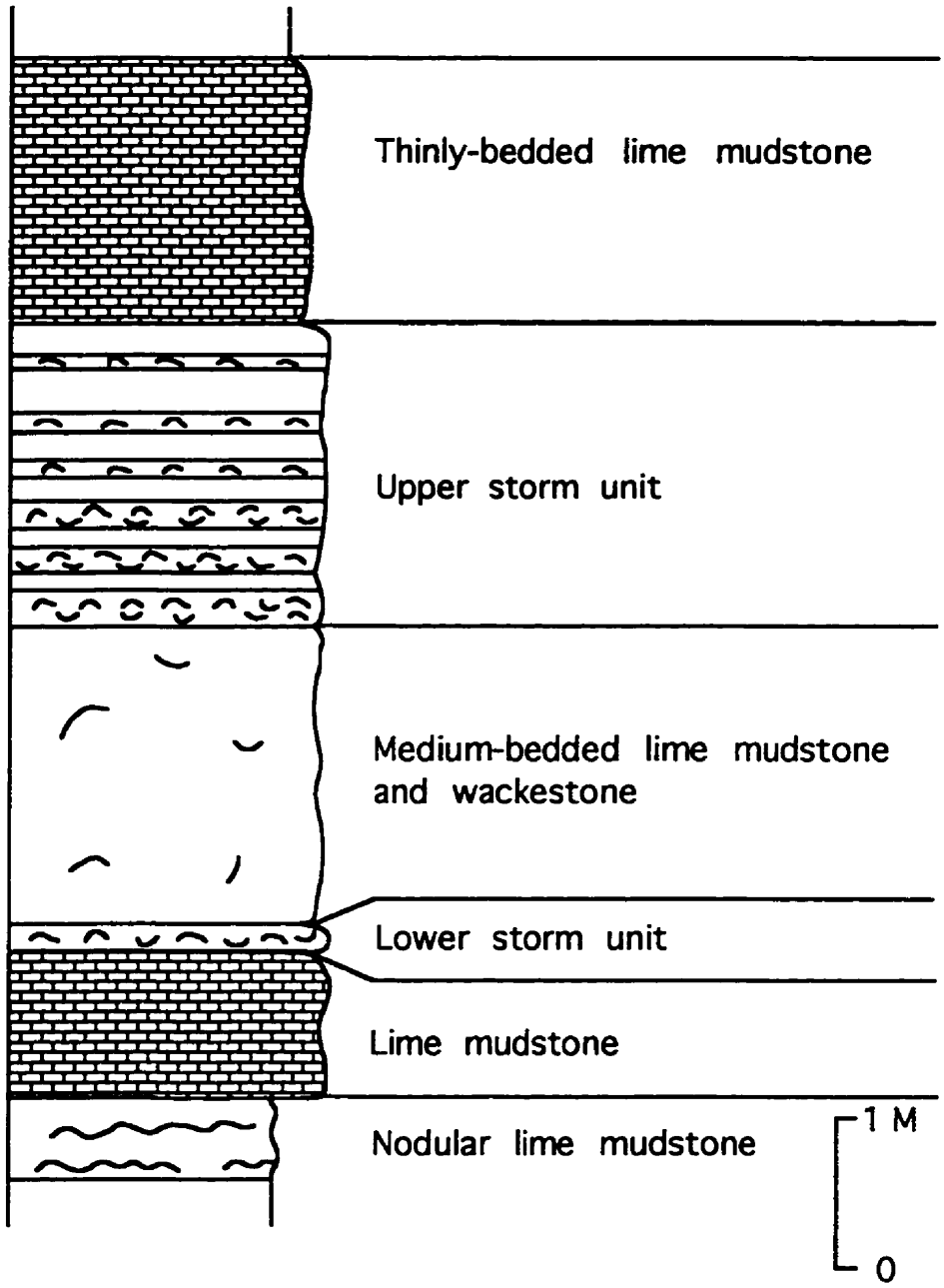

Fig. 5-2. Stratigraphic section of the Burr Member in the domal outcrop on Highway 10 directly north of the junction with the road leading to Pelican Rapids.

PLATE 5-9

Plate 5-9 A: Photograph showing an outcrop of the Burr Member on Highway 10 directly north of junction with the road leading to the Pelican Rapids, Dawson Bay, northwestern Manitoba.

Plate 5-9 B: Photograph showing yellowish nodular lime mudstone (Y) at the base of the outcrop on Highway 10 directly north of junction with the road leading to the Pelican Rapids. It forms the recessive part of the outcrop. Dawson Bay, northwestern Manitoba.

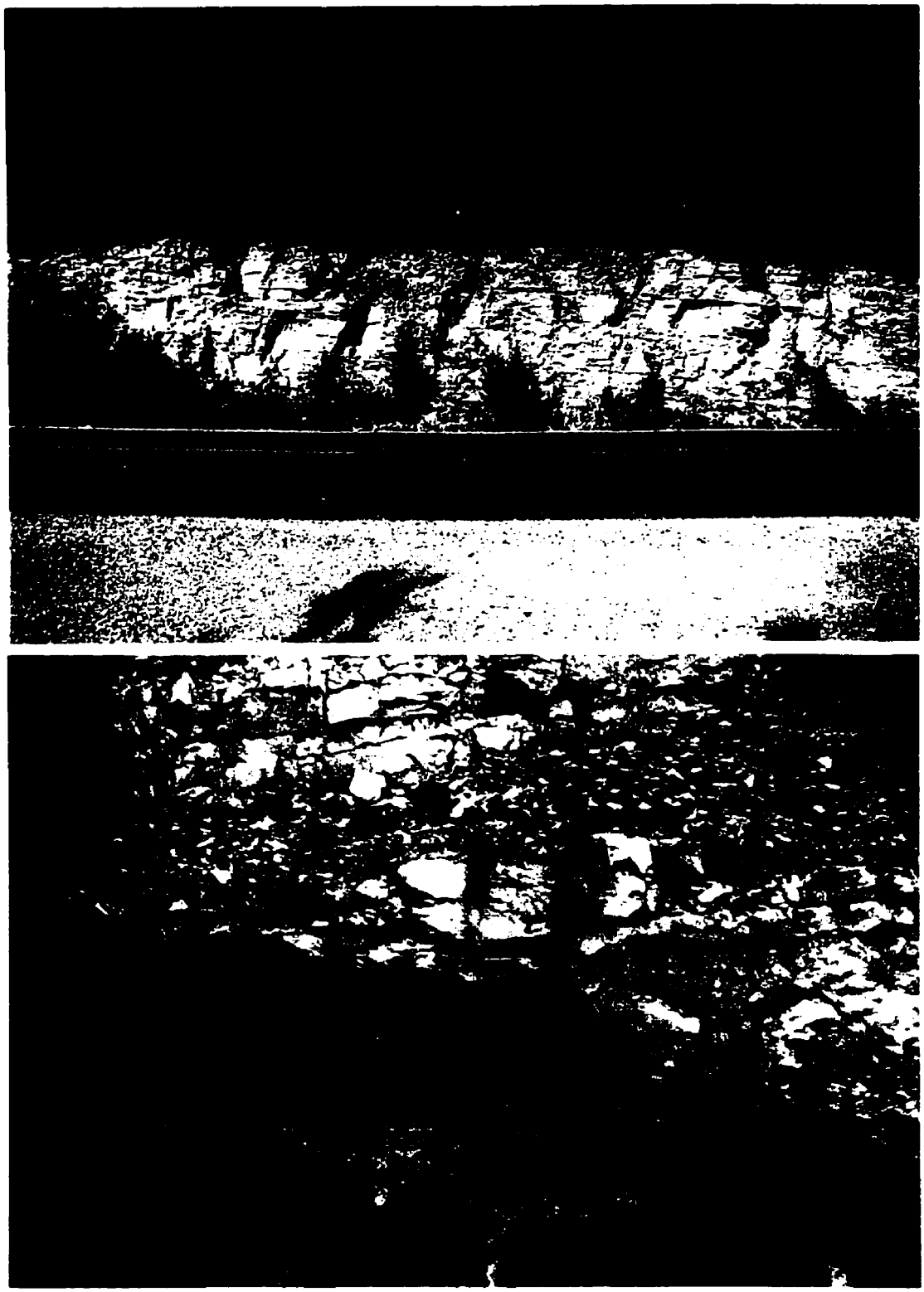

PLATE 5-10

Plate 5-10 A: Slabbed core photograph showing former shell beds, now characterized by fossil molds. One former shell bed in the upper part of the core has a sharp erosional base (b). The Burr Member, northwestern Saskatchewan. Lsd. 14-19-41-23W3. Scale bar is 2 cm.

Plate 5-10 B: Photomicrograph of the yellowish nodular lime mudstone from the outcrop on Highway 10 directly north of junction with the road leading to the Pelican Rapids. The rock is composed of micrite with scattered crinoids (c) and other shell fossils. Dawson Bay, northwestern Manitoba. Scale bar is 1 mm.

Plate 5-10 C: Sample photograph of lower storm unit from the outcrop on Highway 10 directly north of junction with the road leading to the Pelican Rapids, Dawson Bay, northwestern Manitoba. Scale bar is 2 cm.

Plate 5-10 D: Sample photograph of shell bed from the lower part of the upper storm unit. The shell bed (grainstone) is composed of highly comminuted debris of robust brachiopods and crinoids. It is underlain by a wackestone and overlain by a lime mudstone. The outcrop on Highway 10 directly north of junction with the road leading to the Pelican Rapids, Dawson Bay, northwestern Manitoba. Scale bar is 2 cm.

A
B
C

Manitoba appears to be barren of macrofossils (Norris *et al.*, 1982), the nodular lime mudstone may belong to the lower part of the Burr Member. Further evidence to support this interpretation includes the absence of the argillaceous bituminous dolostone in the outcrop, which is stratigraphically present between the Mafeking Member and the fossiliferous limestone of the Burr Member (Norris *et al.*, 1982).

Directly above the nodular lime mudstone is a brown lime mudstone (Plate 5-9B), which is about 40 cm thick and contains no shell fossils. It, in turn, is overlain by light grey medium-bedded lime mudstone of 1 m thick, that contains scattered shell fossils (Plates 5-9B, 5-11A). It grades upward into a shell bed, with a thickness up to 13 cm (Plate 5-11A & B). The strata overlying the shell bed are composed of medium-bedded lime mudstone with local argillaceous mudstone interbeds. This part is about 1.5 m thick. The upper part of the outcrop is composed of thinly bedded limestones, which include lime mudstone, wackestone, packstone and grainstone. Dozens of shell beds are present in this part (Plate 5-12A & B), varying from 6 cm to less than 1 cm thick and with thickness decreasing upward. The top of the domal structure is composed of medium-bedded limestone, which appears massive and unfossiliferous.

5.5.2 Storm Deposits in Northwestern Manitoba

Two storm units are present in the upper Burr Member in northwestern Manitoba, which are separated by a lime mudstone with sparse shell fossils.

Lower Storm Unit

The lower storm unit is composed of a single shell bed that is 13 cm thick (Plates 5-11A & B, 5-10C). The shell bed is underlain by a thin, light yellow lime mudstone and overlain by a lime mudstone with sparse shell fossils. It can be traced throughout the entire outcrop and has a tabular bedset. Low-angle cut-and-fill structures were observed at the base of the shell bed and the light yellow lime mudstone is evidently truncated (Plate 5-10C). The contact between the shell bed and the overlying lime mudstone is gradational (Plate 5-11B).

The shell bed can be divided into lower, middle and upper parts (Plate 5-10C). The lower part, varying from 1 to 3 cm thick, is composed largely of sand-grade debris of

PLATE 5-11

Plate 5-11 A: Photograph showing the lower storm unit (S) in the outcrop on Highway 10 directly north of junction with the road leading to the Pelican Rapids, Dawson Bay, northwestern Manitoba.

Plate 5-11 B: Photograph showing the lower storm unit (S) in the outcrop on Highway 10 directly north of junction with the road leading to the Pelican Rapids, Dawson Bay, northwestern Manitoba.

PLATE 5-12

Plate 5-12 A: Photograph showing the shell beds in the lower portion of the upper storm unit. They are composed of highly comminuted debris of robust brachiopods and crinoids, and are characterized by erosional bases (b). The outcrop on Highway 10 directly north of junction with road leading to the Pelican Rapids, Dawson Bay, northwestern Manitoba.

Plate 5-12 B: Photograph showing the shell beds (s) in the middle portion of the upper storm unit in the outcrop on Highway 10 directly north of junction with the road leading to the Pelican Rapids, Dawson Bay, northwestern Manitoba.


A

echinoderms and robust brachiopods, with intraclasts of lime mudstone. It has a grainstone texture. Locally, pockets of wackestone are present among the grainstone, suggesting that a wackestone bed was originally present below the grainstone.

The middle part (Plate 5-10C), about 4 cm thick, is a packstone composed largely of robust brachiopods and carbonate fines. Most shells are well preserved or broken into large fragments. They have a much better preservation than the shells in the lower part. Most shells are parallel to bedding. Finer-grained sediment interstitial to large shells consists of skeletal sand and silt, and fine carbonate matrix.

The upper part (Plate 5-10C), about 3 cm thick, is composed of large, robust brachiopods and their fragments. The shell fossils are less concentrated than those in the middle part and more carbonate matrix is present. The shell fossils at the top of the shell bed are chaotic in orientation; some are even subvertical to vertical (Plate 5-11B).

From this evidence, even though the storm unit seems to be composed of a single shell bed, the abrupt changes in the size and breakage of shell fossils within the shell bed suggest that it represents an amalgamated deposit.

Upper Storm Unit

The upper storm unit consists of dozens of shell beds that are separated by thin layers of lime mudstone or wackestone. In the lower portion of the storm unit, the shell beds are composed of grainstones and packstones, with thickness varying from 4 cm to 6 cm (Plates 5-12A, 5-10D). The lime mudstones or wackestones between shell beds are from several mm to 2 cm thick. Individual shell beds are tabular and can be traced throughout the domal outcrop. Petrographic study shows that the grainstone consists of predominantly coarse sand-sized bioclasts of robust, highly fragmented brachiopods and crinoids, with subordinate trilobite fragments (Plate 5-13A). These bioclasts are well rounded, abraded and cemented by sparry calcite. Some shell fragments have micrite envelopes. Close to the top of the shell bed, the carbonate matrix increases significantly and the grainstone is replaced by packstone (Plate 5-13B). This may have resulted from infiltration of fines at the top of the shell bed (Kreisa and Bambach, 1982). The upward increase in interstitial sediment within the rock supports the interpretation of infiltration (Kreisa, 1981). The abundance of crinoidal grains and the highly fragmented and abraded nature of the bioclasts indicate prolonged reworking and enrichment in abrasion-resistant

PLATE 5-13

Plate 5-13 A: Photomicrograph of shell bed from the lower portion of the upper storm unit. It has a grainstone fabric, with bioclasts dominated by debris of crinoids and robust brachiopods. Some bioclasts are characterized by micrite envelopes. The outcrop on Highway 10 directly north of junction with the road leading to the Pelican Rapids, Dawson Bay, northwestern Manitoba. Scale bar is 1 mm.

Plate 5-13 B: Photomicrograph showing that the top of the same shell bed in Plate 5-13 A has a packstone fabric. The outcrop on Highway 10 directly north of junction with the road leading to Pelican Rapids, Dawson Bay, northwestern Manitoba. Scale bar is 1 mm.

Plate 5-13 C: Photomicrograph showing that the shell bed from the middle portion of the upper storm unit is composed of packstone. A shelter void (s) is present in the lower central part of the photomicrograph. The outcrop on Highway 10 directly north of junction with the road leading to Pelican Rapids, Dawson Bay, northwestern Manitoba. Scale bar is 1 mm.

Plate 5-13 D: Photomicrograph of lime mudstone directly above the grainstone shown on Plate 5-13 A. It is composed of micrite and silt-sized skeletal fragments. The outcrop on Highway 10 directly north of junction with the road leading to Pelican Rapids, Dawson Bay, northwestern Manitoba. Scale bar is 0.5 mm.

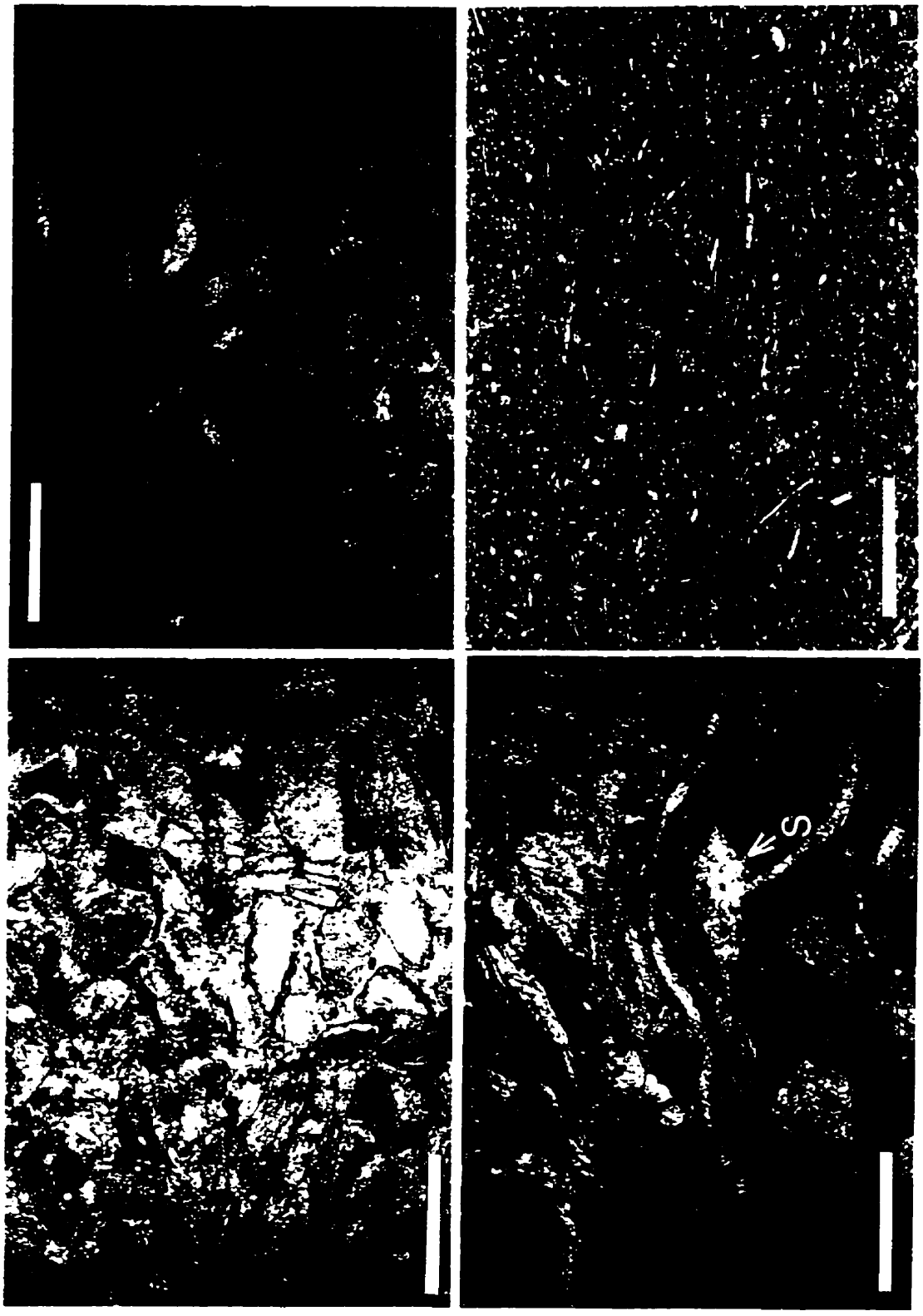
S

and dissolution-resistant grains (Holland, 1993; Holland *et al.*, 1997). Similar grainstone facies was believed by Holland *et al.* (1997) to represent a complex multi-event history of storm-induced erosion, winnowing and redeposition.

The packstones are also composed predominantly of brachiopods and echinoderm debris, with large robust brachiopods as the principal skeletal constituents. However, these fossils are poorly sorted with varying degrees of breakage, ranging from well-preserved half-valve shells to highly comminuted fragments.

The packstones and grainstones rarely show internal stratification or imbrication, but grading is present locally (Plate 5-10D). Intraclasts derived from the underlying lime mudstone are also found. They are normally less than 1 cm in length, angular to subangular in shape. Amalgamation is common; the amalgamated shell beds are separated by erosional surfaces, with no fine-grained fair-weather sediment between them (Plate 5-14B). The bioclasts above and below the erosional surfaces are characterized by widely different degrees of size, breakage and abrasion of shell fossils. In some amalgamated shell beds, the shell fossils in the lower part are clearly better preserved than those in the upper part (Plate 5-14B). This suggests that the shell fossils in the upper part experienced more reworking than those in the lower part.

The bases of the packstones and grainstones are sharp and erosional, with gutters locally present. In addition, isolated gutters are also present. These gutters are highly sculptured and irregular. They are up to 7 cm wide and 2 cm deep, and are encased in lime mudstone and filled with sand-sized bioclasts (Plate 5-14C). Very little sand was deposited outside these scours. Gutter casts are present either in arrays (i.e. many closely spaced and parallel-aligned gutter casts that project downward from a single bedding plane) or as isolated casts encased in lime mudstone. In cross-section, they have asymmetric shapes, with a gentle slope in one side and steep slope on the other (Plate 5-14C). The steep walls attest to the cohesive nature of the substrate. Gutters and gutter casts are common on storm bed bases and reflect the selective erosion of cohesive sediments by high-velocity currents (Johnson and Baldwin, 1985).

The lime mudstone directly overlying the packstone or grainstone appears massive (Plate 5-10D), with a significant amount of silt-sized skeletal fragments (Plate 5-13D). The elongate shell fragments are oriented parallel to bedding, and no whole-shell fossils are preserved *in situ*. Most silt-sized elongated bioclasts are fragments of small, thin-shelled

PLATE 5-14

Plate 5-14 A: Hand specimen photograph showing an amalgamated shell bed from the middle portion of the upper storm unit. The shell bed is composed dominantly of small to medium sized brachiopods, with a sharp undulating erosional surface in the middle of the shell bed. The outcrop on Highway 10 directly north of junction with the road leading to Pelican Rapids, Dawson Bay, northwestern Manitoba. Scale bar is 2 cm.

Plate 5-14 B: Hand specimen photograph showing an amalgamated shell bed from the lower portion of the upper storm unit. The shell bed is composed dominantly of debris of crinoids and robust brachiopods, with a sharp erosional surface in the lower central part of the shell bed. The outcrop on Highway 10 directly north of junction with the road leading to Pelican Rapids, Dawson Bay, northwestern Manitoba. Scale bar is 2 cm.

Plate 5-14 C: Hand specimen photograph showing gutter casts from the upper storm unit, the outcrop on Highway 10 directly north of junction with the road leading to Pelican Rapids, Dawson Bay, northwestern Manitoba. Scale bar is 2 cm.

Plate 5-14 D: Hand specimen photograph of two superimposed shell beds from the middle portion of the upper storm unit. Outcrop on Highway 10 directly north of junction with the road leading to Pelican Rapids, Dawson Bay, northwestern Manitoba. Scale bar is 2 cm.

fossils. Bioturbation is generally absent. These features suggest that the carbonate sediment was rapidly deposited from suspension.

Underlying the packstone and grainstone are lime mudstone or wackestone (Plate 5-10D), with packstone locally present. All have more carbonate matrix than the directly overlying packstone and grainstone. The wackestone and packstone are composed of brachiopods, echinoderms and carbonate matrix. The fauna is almost identical to that in the overlying packstone and grainstone, but the shell fossils are better preserved, larger, with proportionally less echinoderm debris (Plate 5-10D). These features suggest that the wackestone and packstone experienced less reworking processes than the shell fossils in the overlying packstone and grainstone. The lime mudstone appears homogeneous. There is little evidence of biogenic activity, and it is very similar to the lime mudstone directly above the packstones. Thus, the lime mudstone may be a part of underlying storm bed; the storm event may have completely eroded the wackestone beneath the packstone and reached the upper part of the underlying storm bed, a further line of evidence to support amalgamation.

The shell beds in the middle portion of the upper storm unit are 1 to 4 cm thick, with planar to wavy bedding appearance (Plates 5-12B, 5-14A & D). They are composed of packstone; grainstone is absent. Although some shell fossils are broken and abraded, others are well preserved. Shelter voids are common (Plate 5-13C) and are filled with equant calcite. Amalgamation is still evident. The size of the bioclasts changes abruptly below and above the erosional surface of amalgamated shell beds (Plate 5-14A). The erosional surfaces are sharp, but most are planar to slightly undulatory. Additionally, these packstones are characterized by normal grading. Intraclasts composed of lime mudstone are present. Shell fossils are dominated by medium to small, thin-shelled brachiopods, with subordinate echinoderms and trilobite fragments. However, the proportion of the echinoderms in the shell assemblage is significantly less than that in the shell beds in the lower portion of the upper storm unit. Above the packstone is a lime mudstone with abundant elongated silt-sized fragments of small, thin-shelled fossils that are oriented parallel to bedding. Below the packstone is wackestone or lime mudstone. The wackestone and lime mudstone are up to 2 cm thick, but still thinner than the packstone.

The shell beds in the upper portion of the upper storm unit are thinner, varying from mm to 2 cm thick (Plate 5-15 A). They are lenticular, some pinching out over a few cm. In

PLATE 5-15

Plate 5-15 A: Hand specimen photograph showing a shell bed from the upper portion of the upper storm unit. Outcrop on Highway 10 directly north of junction with the road leading to Pelican Rapids, Dawson Bay, northwestern Manitoba. Scale bar is 2 cm.

Plate 5-15 B: Photomicrograph of the shell bed shown on Plate 5-15 A. From the upper portion of the upper storm unit in the outcrop on Highway 10 directly north of junction with the road leading to Pelican Rapids, Dawson Bay, northwestern Manitoba. Scale bar is 1 mm.

Plate 5-15 C: Photomicrograph showing a hardground (H) in the upper Burr Member of central Saskatchewan. It is characterized by micro-borings of *Trypanites* and truncation of peloids. Lsd. 9-33-34-1W3. Scale bar is 0.5 mm.

Plate 5-15 D: Photomicrograph of an intraclast above a firmground. It has a packstone fabric, with many shell fossils and their fragments. Lsd. 9-14-23-33W1. Scale bar is 1 mm.

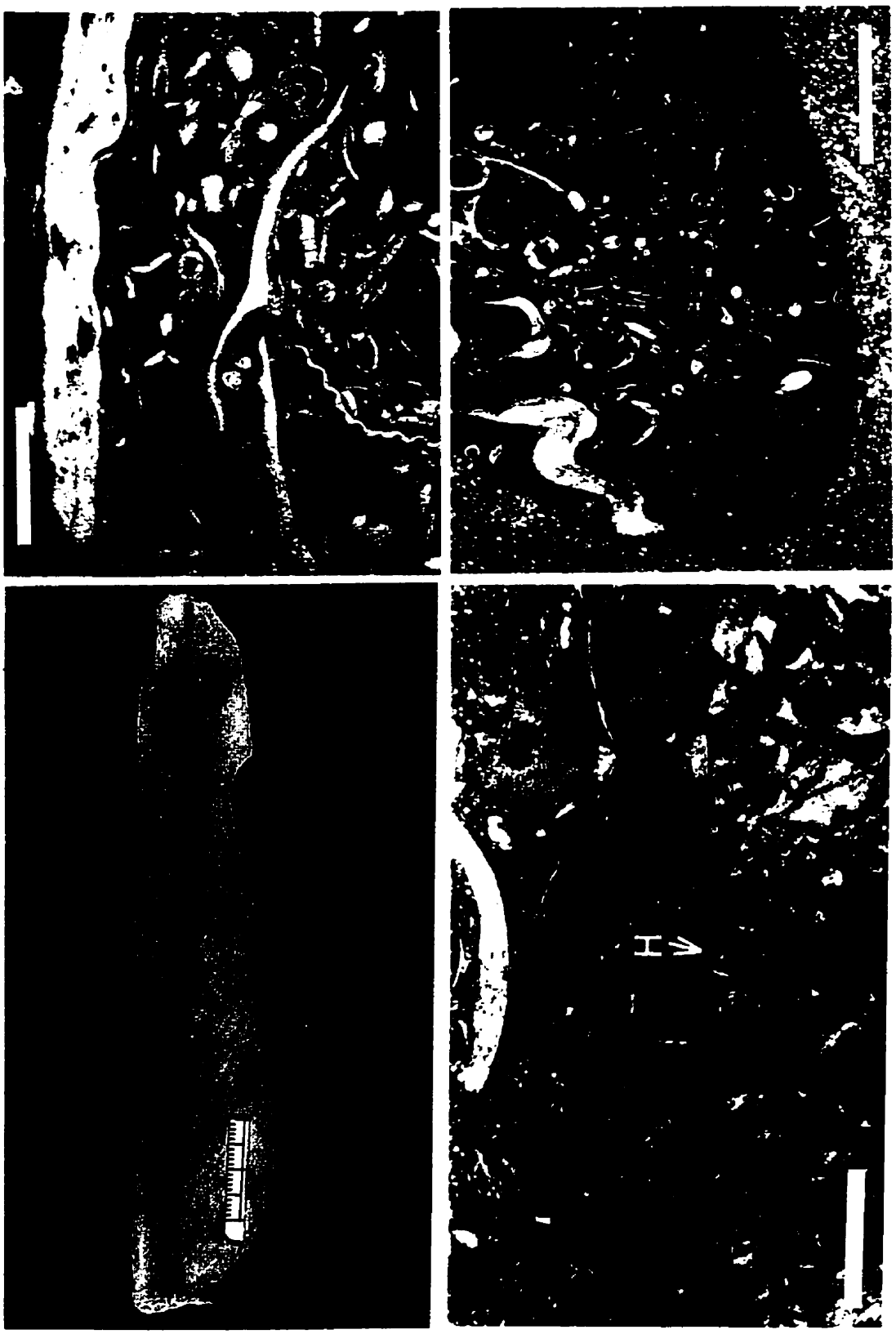
H

contrast, the interbedded lime mudstone and wackestone are significantly thicker. Small thin-shelled brachiopods (less than 5 mm in length) become a major component of the shell beds (Plate 5-15 A & B). They are non-abraded, oriented predominantly parallel to bedding and are convex-upward in general. Although sparse, medium-sized brachiopod shells are still present. The bases of shell beds are sharp but non-erosive. The shell beds are underlain by lime mudstone with sparse thin-shelled brachiopods, and overlain by lime mudstone. In contrast to the shell beds in southeastern Saskatchewan, sand-sized clasts derived from robust shells are rare. The poor lateral continuity and minor breakage of shell fossils suggest that these shell beds were more or less wave-winnowed *in situ* and buried immediately by fine-grained sediments.

Interpretation

The lower storm unit is dominated by robust brachiopod shells and their fragments. Thin-shelled brachiopods are rare. Most shell fossils are oriented parallel to bedding. The unit has an erosional base. These features suggest that the sediment is a storm deposit. However, most shell fossils are fragmental, with variable degrees of abrasion and breakage. This favors sedimentation in a relatively high energy and shallow water environment, where the deposit was reworked repeatedly by waves and currents. This storm bed grades upward into a limestone unit with sparse shell fossils, probably reflecting decreasing energy and increasing water depth.

In the lower portion of the upper storm unit, the shell beds are similar to those of the lower storm unit although individual shell beds are only up to 6 cm thick. They are composed predominantly of robust shell fossils and are characterized by tabular bedsets, erosional bases, and highly comminuted shells. In addition, amalgamation is very common. These suggest deposition in proximal environments. The sharp, erosive bases of shell beds are attributed to peak storm-wave surges that strongly agitated the sea bottom (Kreisa, 1981; Kreisa and Bumbach, 1982). Because grading is rare, many shell beds were probably deposited under relatively uniform, peak storm conditions rather than under waning conditions (Allen, 1982). In contrast to shell beds from the distal facies in southeastern Saskatchewan, the proximal shell beds in northwestern Manitoba show evidence of multiple episodes of relatively high energy reworking.

In the upper portion of the upper storm unit, both the thickness and abundance of the shell beds decrease, and thin-shelled brachiopods become major components of the storm

deposits. This suggests that they were deposited in more distal environments. Thus, from the lower to upper portion of the upper storm unit, the energy level in the depositional environment decreased, probably reflecting a relative rise in sea-level. The storm deposits grade upward into medium-bedded unfossiliferous limestones. Similar vertical variation of the sedimentary succession was recognized in the upper Burr Member of central Saskatchewan.

Compared to the storm deposits in southeastern Saskatchewan, those in the Manitoba outcrops are characterized by the dominance of large, robust shells, high fossil comminution and the presence of amalgamated storm beds. All these features suggest that they represent a more proximal facies. The upward progressive change in the thickness of the shell beds and the size of the shell fossils suggests a sequentially deepening facies assemblage.

5.6 Discontinuity Surfaces in the Upper Burr Member

As mentioned previously, there are many discontinuity surfaces in the upper Burr Member in central Saskatchewan (Plate 5-16A). They are most abundant in the Viscount district (Range 25, Townships 32-34) where twenty-five are present (Dunn, 1982a). These discontinuities were termed hardgrounds by Dunn (1982a, 1982b), Braun and Mathison (1982, 1986) and Ahlstrom (1992). Some discontinuity surfaces are easily recognizable in core, whereas others are less distinct. They are irregularly spaced, ranging from a few centimetres to several metres apart. Some discontinuity surfaces are eroded to a degree that one discontinuity surface merges with an earlier formed surface (Dunn, 1982a).

5.6.1 Features of the Discontinuity Surfaces

The discontinuity surfaces vary from flat and smooth to highly hummocky and irregular. They are characterized by mineralization, reworked clasts, undercut knobs, firmground burrows, borings and truncation of allochems.

Mineralization

Mineralization occurs in some discontinuities (Plate 5-16B & C), but is absent in others. The mineralization is in the form of mineral impregnation. The mineral impregnation not only happened at the surfaces of the discontinuities but also extended down to the walls of

PLATE 5-16

Plate 5-16 A: Core photograph showing at least three distinct firmgrounds (f). Unit A of the upper Burr Member. Lsd. 5-18-34-25W2. (One core box is 0.76 m long and core diameter is 10.1 cm.)

Plate 5-16 B: Slabbed core photograph showing two firmgrounds. The upper surfaces of the firmgrounds are mineralized. *Gastrochaenolites* (g) is present in the firmground in the lower part of the core. Lsd. 5-18-34-25W2. Scale bar is 2 cm.

Plate 5-16 C: Slabbed core photograph showing a firmground. The firmground is characterized by mineral impregnation and *Thalassinoides*-like burrows. Burrow skirting around a shell (s) can be seen directly below the firmground surface. The rock directly below the firmground surface is composed of lime mudstone that is rich in small *Chondrites*. Lsd. 8-14-20-31W1. Scale bar is 2 cm.

Plate 5-16 D: Slabbed core photograph showing a firmground that is truncated and overlain by intraclasts and shell fragments. Lsd. 14-32-20-30W1. Scale bar is 2 cm.

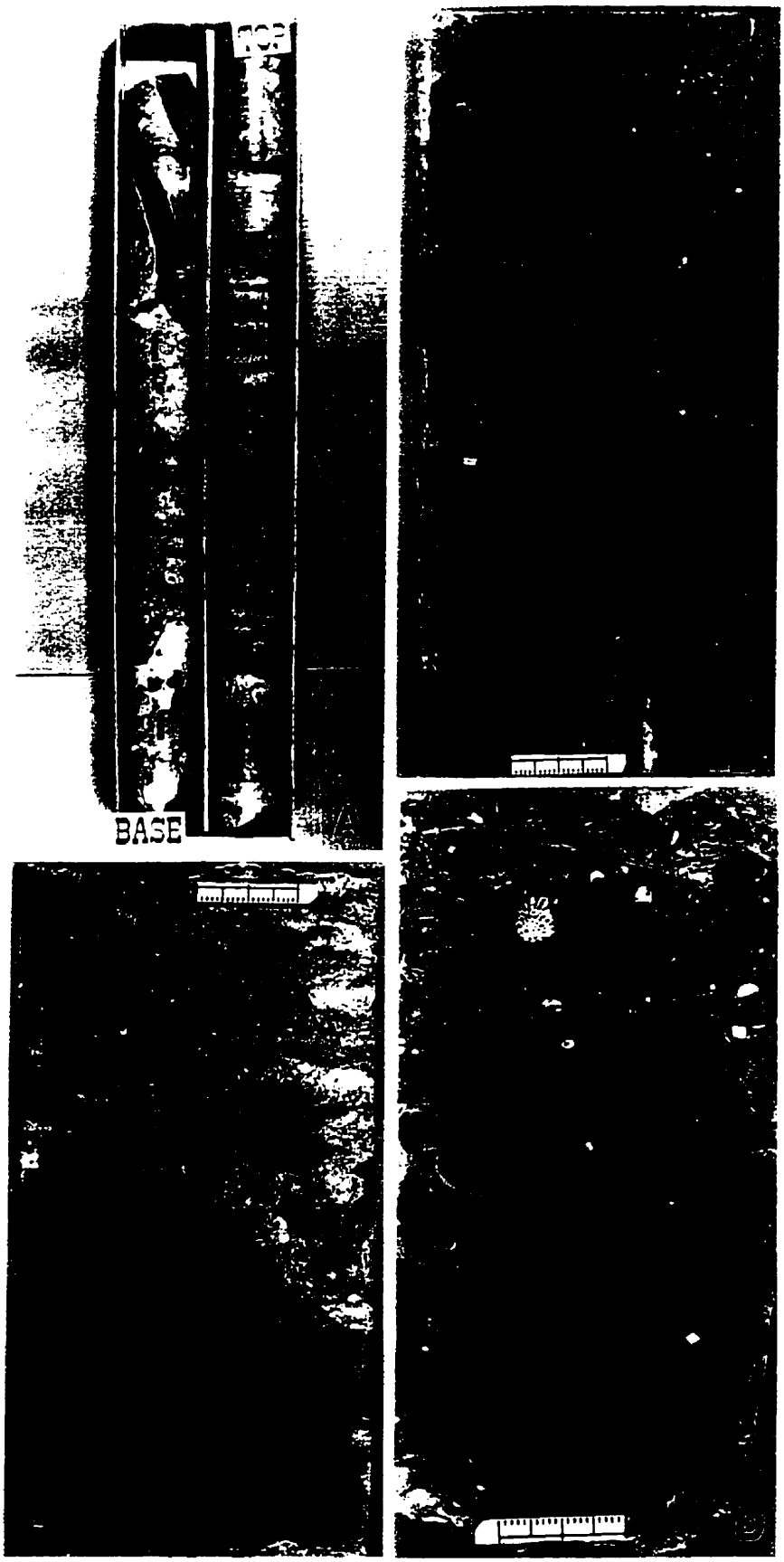
BASE

burrows. Some reworked intraclasts are also characterized by mineral impregnation (Plate 5-16D). The intensity of mineral impregnation fades gradually downward from the surface of the discontinuities and from the wall of a burrow. No significant difference of impregnation intensity was observed between the walls of the burrows and the surfaces of the discontinuities. This suggests that the mineral impregnation followed the development of the discontinuity surfaces rather than preceding or accompanying their development. The mineral impregnation normally displays a black colour, which is believed to be caused by the presence of disseminated pyrite or manganese oxides (Ahlstrom, 1992). However, microprobe scans by Ahlstrom failed to detect the presence of significant amounts of Fe or Mn. This may reflect low concentration of these elements rather than their absence (Ahlstrom, 1992).

Firmground Burrows

Burrows are well developed at the discontinuities. They extend from the discontinuity surfaces into the underlying sediments. Three types of burrows can be distinguished -- *Spongeliomorpha*, *Thalassinoides* and *Gastrochaenolites*. *Spongeliomorpha* and *Thalassinoides* are characterized by irregular network and variable diameter (Plate 5-17A & B). This burrow morphology most likely reflects the hardening of the substrate that prevented the development of a regular branching pattern (Fursich, 1979). These burrows are filled with shell fragments and intraclasts. Some burrows were strongly eroded, which resulted in the formation of intraclasts in the rock directly above the discontinuity surfaces (Plates 5-16D, 5-17D). Individual burrows are sharp and unlined, sub-vertical to steeply inclined, and up to 5 cm deep and 1-2 cm wide. A few burrows have smooth walls, but most have rough walls, which reflect the excavation process. If the burrows encountered shells, they did not cut across but skirted around them (Plates 5-16C, 5-17A). This suggests that the discontinuity surfaces were not hardgrounds but firmgrounds and the burrows belong to *Glossifungites* ichnofacies. *Gastrochaenolites* are only present locally (Plate 5-16B) and are associated with *Spongeliomorpha*. These burrows apparently remained open for a considerable span of time as the mineralization extends down the walls for some distance.

Borings and Truncation of Allochems

Micro-borings, *Trypanites*, and truncation of peloids are only observed at one discontinuity (Plate 5-15C). Truncation of bioclasts is found at the same discontinuity

PLATE 5-17

Plate 5-17 A: Hand specimen photograph showing a firmground. It is penetrated by *Thalassinoides*-like burrows, which skirted shell fragments (s). From the outcrop along winding road leading to Pelican Rapids, about 7.2 km east from Highway 10. Scale bar is 2 cm.

Plate 5-17 B: Slabbed core photograph showing a firmground that is penetrated by *Thalassinoides* (t) and overlain by shell fossils and intraclasts. Lsd. 10-32-20-30W1. Scale bar is 2 cm.

Plate 5-17 C: Slabbed core photograph of the hardground shown on Plate 5-15 C. It is characterized by truncation a crinoid debris. Lsd. 9-33-34-1W3. Scale bar is 2 cm.

Plate 5-17 D: Slabbed core photograph showing an intensely eroded firmground that is overlain by intraclasts and shell fragments. Lsd. 8-14-20-31W1. Scale bar is 2 cm.


A


B

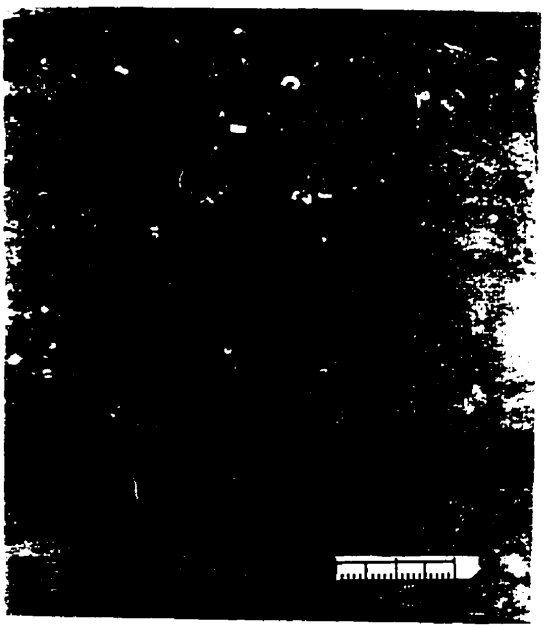

(Plate 5-17C). This was also reported by Ahlstrom (1992).

Intraclasts

Sparse to abundant reworked intraclasts are associated with the discontinuities. They occur in the burrows and in the sediment directly above the discontinuities. They are commonly associated with large amounts of shell fragments. In some cases, they even constitute a clast-supported conglomerate (Plates 5-16D, 5-17D), reaching a thickness of up to 4 cm. Most intraclasts are composed of lime mudstone or wackestone. Locally, intraclasts composed of packstone are present (Plate 5-15D). These intraclasts range from 2 to 15 mm in diameter and are highly variable in shape, but most have been rounded.

5.6.2 Carbonate Rocks Directly Below and Above the Discontinuities

Carbonate Rocks Below the Discontinuities

The carbonate rocks directly below the discontinuity surfaces are commonly lime mudstone or wackestone. These rocks are light grey to olive green, massive and are locally characterized by extensive bioturbation. Although no grainstone or packstone was observed by Ahlstrom (1992), they are present locally.

The lime mudstones and wackestones consist of fine-grained carbonate, with scattered to loosely packed shell fossils (Plates 5-18C, 5-19C & D). The body fossils are small and thin-shelled, up to a few mm long and are generally well preserved. They include ostracods, gastropods, foraminifera, pelecypods and brachiopods. In addition, sparse crinoid plates and robust brachiopod fragments are present. They are worn and broken. Locally, wackestone with a large amount of robust shell fragments can be observed directly underlying discontinuity surfaces. Burrows are also very rich in places. They are dominated by small, softground burrows, such as *Chondrites* (Plate 5-16C).

Packstones are present locally (Plate 5-18A). These rocks have a grain-supported fabric, with a fine carbonate matrix. The grains are composed exclusively of bioclasts or a mixture of bioclasts and peloids. The bioclasts include ostracods, gastropods, foraminifera, bivalves and unidentified microfossils. These fossils are small and thin-shelled. Both articulated and disarticulated shells are present; most are well preserved. A small amount of reworked robust brachiopod and crinoid fragments is also present. The

PLATE 5-18

Plate 5-18 A: Photomicrograph showing a packstone that lies directly below the firmground in the lower part of the core shown on Plate 5-16 B. The packstone is composed of small, thin-shelled fossils but has a grain-supported fabric. Lsd. 5-18-34-25W2. Scale bar is 1 mm.

Plate 5-18 B: Photomicrograph showing the rock directly below the firmground surface changing from lime mudstone to packstone, probably indicating upward shallowing and increase in water energy. Lsd. 4-18-35-8W3. Scale bar is 1 mm.

Plate 5-18 C: Photomicrograph of lime mudstone directly below a firmground surface. It is composed of micrite and scattered bioclasts. The latter include ostracods and crinoids. Lsd. 01-02-21-31W1. Scale bar is 0.5 mm.

Plate 5-18 D: Photomicrograph of grainstone directly below the hardground surface shown on Plate 5-17 C. Lsd. 9-33-34-1W3. Scale bar is 0.5 mm.

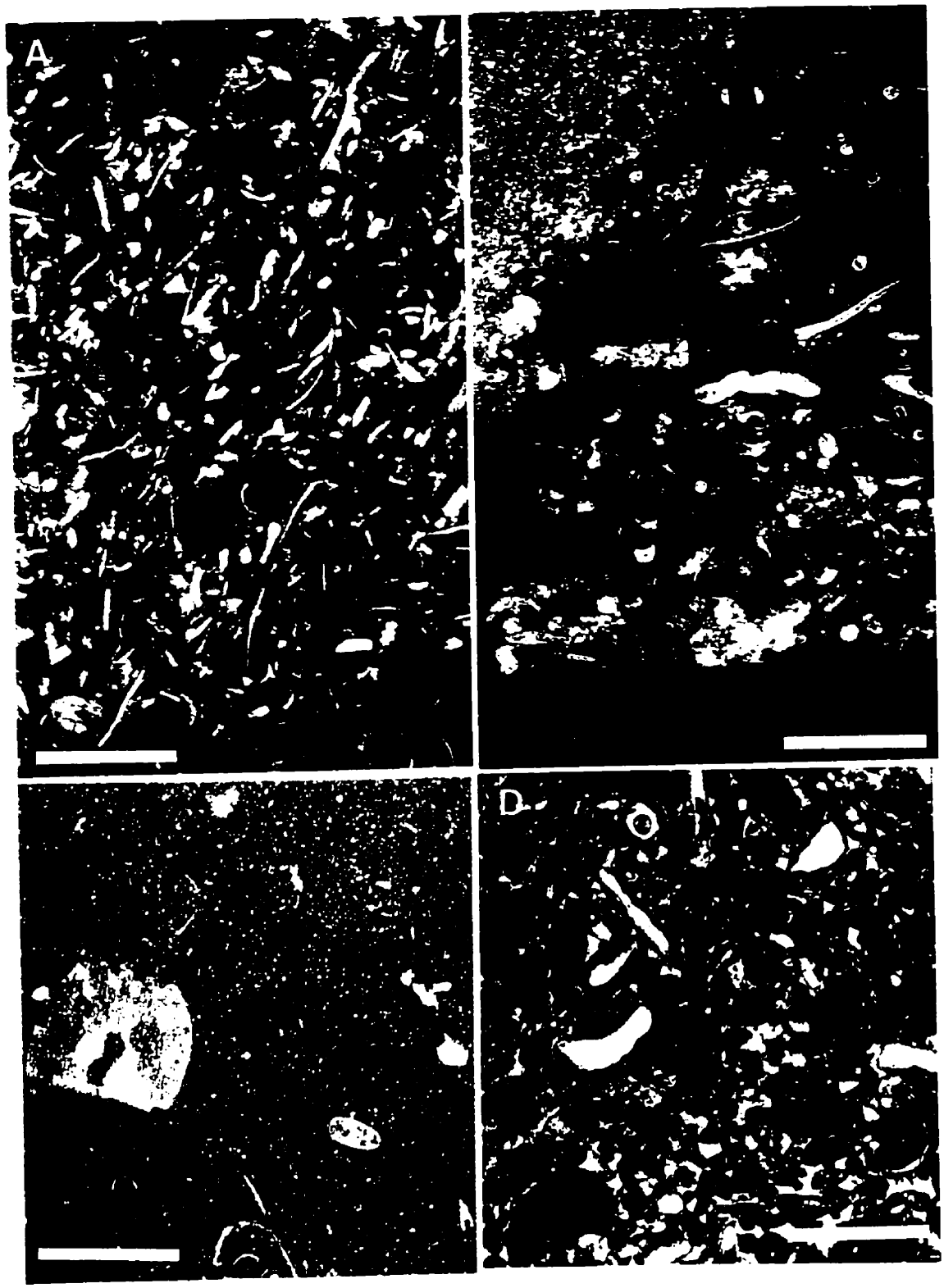
A
D

PLATE 5-19

Plate 5-19 A: Slabbed core photograph showing abundant fossil corals above a firmground. However, they are separated from the firmground by a thin layer of shell fossils dominated by brachiopods. Lsd. 3-27-38-27W2. Scale bar is 2 cm.

Plate 5-19 B: Slabbed core photograph showing a firmground from southeastern Saskatchewan. The firmground surface lacks mineralization. Lsd. 9-14-23-33W1. Scale bar is 2 cm.

Plate 5-19 C: Photomicrograph showing rocks directly below and above a firmground surface. The rock below the firmground surface is a lime mudstone with sparse small, thin-shelled fossils and their fragments. The rock directly above the firmground is a wackestone that is rich in robust shell fragments. Lsd. 01-02-21-31W1. Scale bar is 1 mm.

Plate 5-19 D: Photomicrograph showing rocks directly below and above a firmground surface. The rock below the firmground surface is a lime mudstone. The rock above the firmground is a packstone, characterized by highly comminuted shell fragments. Lsd. 01-02-21-31W1. Scale bar is 1 mm.

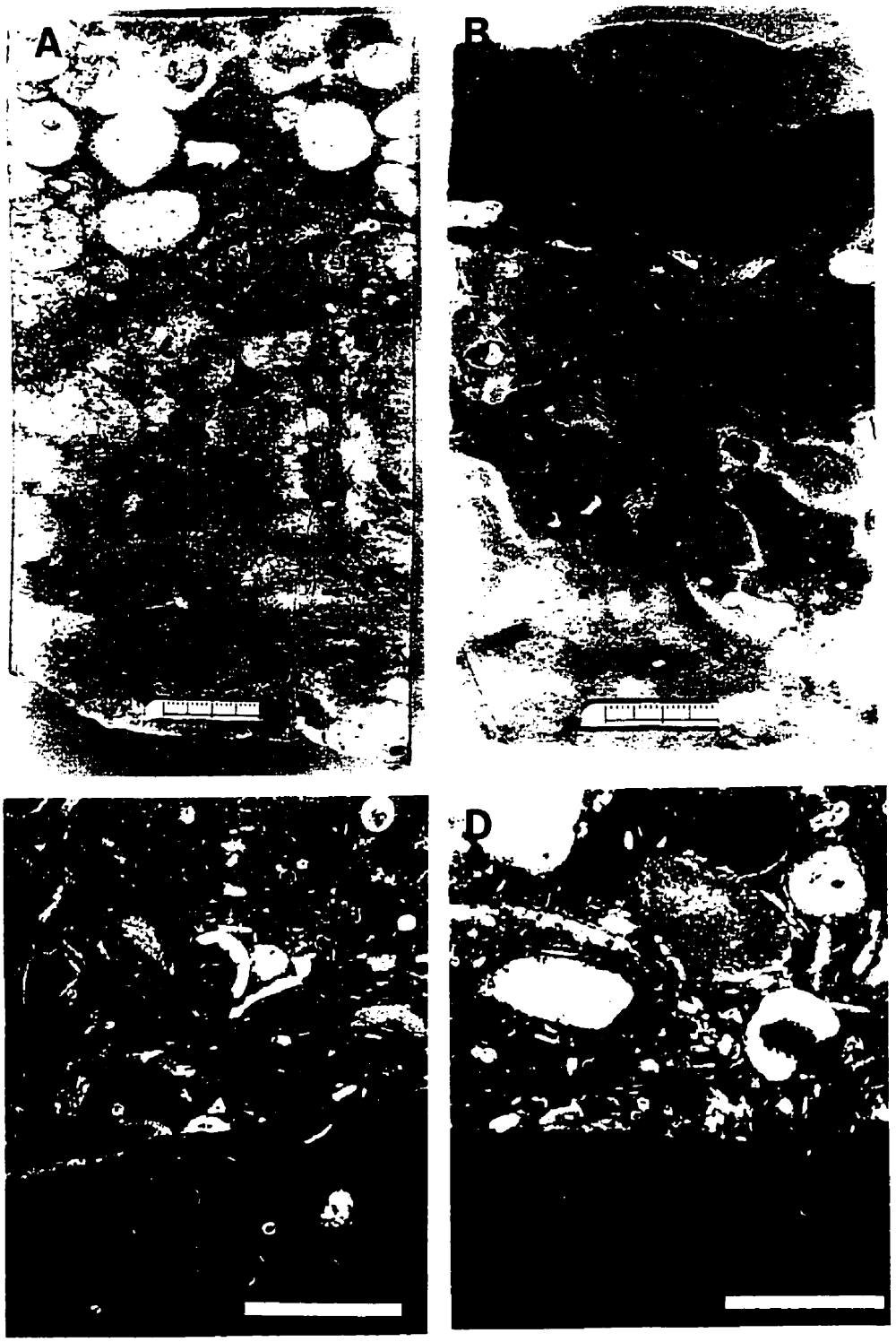
A
B
D

peloids are subrounded to rounded, ellipsoidal to spherical, and are internally structureless. An upward gradation from lime mudstone to packstone has been observed in one thin section (Plate 5-18B).

Grainstone is found only beneath one discontinuity surface in central Saskatchewan (Plates 5-15C, 5-18D). It has a grain-supported fabric and consists of peloids and bioclasts that are cemented by sparry calcite. Peloids are the dominant component and are well sorted, well rounded, spherical and ellipsoidal. Most are internally structureless, but a few contain shell fragments, suggesting that at least some peloids are sand-sized bioclasts. The bioclasts include shell fragments derived from robust brachiopods, echinoderms, bivalves and trilobites, gastropods and ostracods. Most shell fragments are characterized by micrite envelopes. Some contain micro-borings.

Carbonate Rocks Above the Discontinuities

The carbonate rocks directly above the discontinuity surfaces are normally wackestones or packstones (Plate 5-19C & D), with lime mudstones present locally (Plate 5-19B). The wackestones and packstones are characterized by rich, robust shell fragments. Vertically, they pass upward abruptly into lime mudstone or wackestone with small, thin-shelled fossils.

The wackestones above the discontinuity surfaces are only a few cm thick and are characterized by abundant, robust shell fragments (Plate 5-19C). These fossils are highly comminuted and rounded. Small, thin-shelled fossils are generally absent. Well-preserved, whole shells are present but rare. They range from coarse-sand to gravel sized. Elongate shell fragments are randomly oriented, varying from horizontal to subvertical. The wackestones directly above the discontinuity surfaces have the greatest amount of shell fragments, with the amount decreasing upward abruptly.

The packstones are composed of a mixture of shells and intraclasts with a carbonate matrix, or composed of shells alone, with a carbonate matrix (Plates 5-19D, 5-16D). These rocks rest abruptly on the discontinuities. They are only a few cm thick. The shells are dominated by robust fossils, which includes brachiopods, trilobites, echinoderms, bryozoans and tentaculites, with brachiopods dominant. These shell fossils are highly fragmented and rounded. Some are partly coated with carbonate matrix, indicating that they were reworked from previous sediment. Locally, encrusting corals and

stromatoporoids are also present. However, they are not in direct contact with the discontinuity surface but separated from it by a thin layer of broken shell fossils (Plate 5-19A). The corals and stromatoporoids form a biostrome resting on the shell bed, but with a thickness of only a few centimetres.

Both the wackestone and packstone described above are, in turn, overlain by lime mudstone or wackestone characterized by a well-preserved, small, thin-shelled fauna. These rocks have similar microfabrics to those of the lime mudstone and wackestone directly below the discontinuity surfaces and will not be further described here.

5.6.3 Vertical and Lateral Variations of Discontinuities

Numerous discontinuities are present in Units A and C in the upper Burr Member of central Saskatchewan. They are closely spaced, ranging from centimetres to dozens of centimetres. These discontinuities are normally characterized by mineralization and overlain by shell beds. In contrast, no discontinuity was observed in Unit B and very few discontinuities are present in Unit D of the upper Burr Member in central Saskatchewan. There are also very few discontinuities in the upper Burr Member of southeastern Saskatchewan. In the latter region, three discontinuity surfaces are found close to the base of the upper Burr Member and a few more are present in the upper part of the upper Burr Member. The latter have highly irregular surfaces. They are widely spaced and generally lack mineralization (Plate 5-19B). Concentrated shell beds are generally absent in the sediment directly above the discontinuity surfaces.

5.6.4 Interpretation

Almost all of discontinuity surfaces in the upper Burr Member are characterized by *Spongeliomorpha* and *Thalassinoides*. These are characteristic of *Glossifungites* ichnofacies, which is typical of firm unlithified substrates (Seilacher, 1967; Pemberton and Frey, 1985, 1992; Bromley and Asgaard, 1991). The *Glossifungites* assemblage demarcates discontinuity surfaces that reflect pauses in sedimentation, generally accompanied by erosion (MacEachern *et al.*, 1992). Such firmgrounds typically consist of dewatered muds (Pemberton and Frey, 1992). Dewatering occurs either due to subaerial exposure, or burial and subsequent exhumation (MacEachern *et al.*, 1992). Because the firmgrounds in the upper Burr Member lack evidence of subaerial exposure, they might have been formed by dewatering due to burial. Thus, these firmgrounds are

interpreted as previously buried and dewatered sediments that were exhumed following removal of their overlying sediments. While short-term storm events might have facilitated exhumation of sediment, storm action cannot have been the only agent responsible for the exhumation because post-storm deposition (settling of stirred-up fines) would cover the firmgrounds almost immediately and thus prevent burrowing (Fursich *et al.*, 1992). An essential agent involved in the exhumation of the firmgrounds, therefore, might have been bottom-currents that swept the sea floors (Fig. 5-3). Similar firmgrounds produced by erosional exhumation of compacted semi-consolidated substrates have been reported by Kennedy (1967), Dawson and Reaser (1985), Savrda (1991) and MacEachern *et al.* (1992).

As described, the carbonate rocks directly beneath the firmgrounds are commonly lime mudstones or wackestones. The presence of small thin-shelled fossils, the high percentage of micritic sediment, the lack of physical sedimentary structures, and the high degree of bioturbation by deposit-feeding organisms in these rocks indicate low energy, relatively deep water conditions. In contrast, the firmgrounds formed by the erosional exhumation of buried sediments, reflect high energy conditions (MacEachern *et al.*, 1992). Therefore, from the deposition of the lime mudstone or wackestone to the erosion of the sediment and exposure of the firmgrounds, the water energy in the depositional environments must have increased significantly. Such an increase in energy is most likely due to shallowing. This interpretation is supported by the presence of shell beds directly above the firmgrounds. Because these shell beds are composed of highly fragmented clasts of robust brachiopods and echinoderms, it indicates prolonged exposure in high energy conditions. Similar shell beds are referred to as BOP or Base of Parasequence shell beds (Banerjee and Kidwell, 1991). They occur during times of initial flooding following shallowing episodes, predictably at the bases of parasequences (Brett, 1995). This in turn suggests that firmground surfaces beneath the shell beds are flooding surfaces of parasequences.

The shell beds are, in turn, overlain by lime mudstone and wackestone, which contain small, thin-shelled fossils and indicate relatively low energy and deep water conditions. Thus, from the shell beds to the overlying lime mudstone and wackestone, an abrupt increase in water depth took place. This interpretation is supported by the local presence of encrusting corals and stromatoporoids directly above the shell beds. The corals and stromatoporoids constitute biostromes with a thickness of only a few cm centimetres. This suggests that the deepening event was sufficiently rapid that the biostromes failed to keep

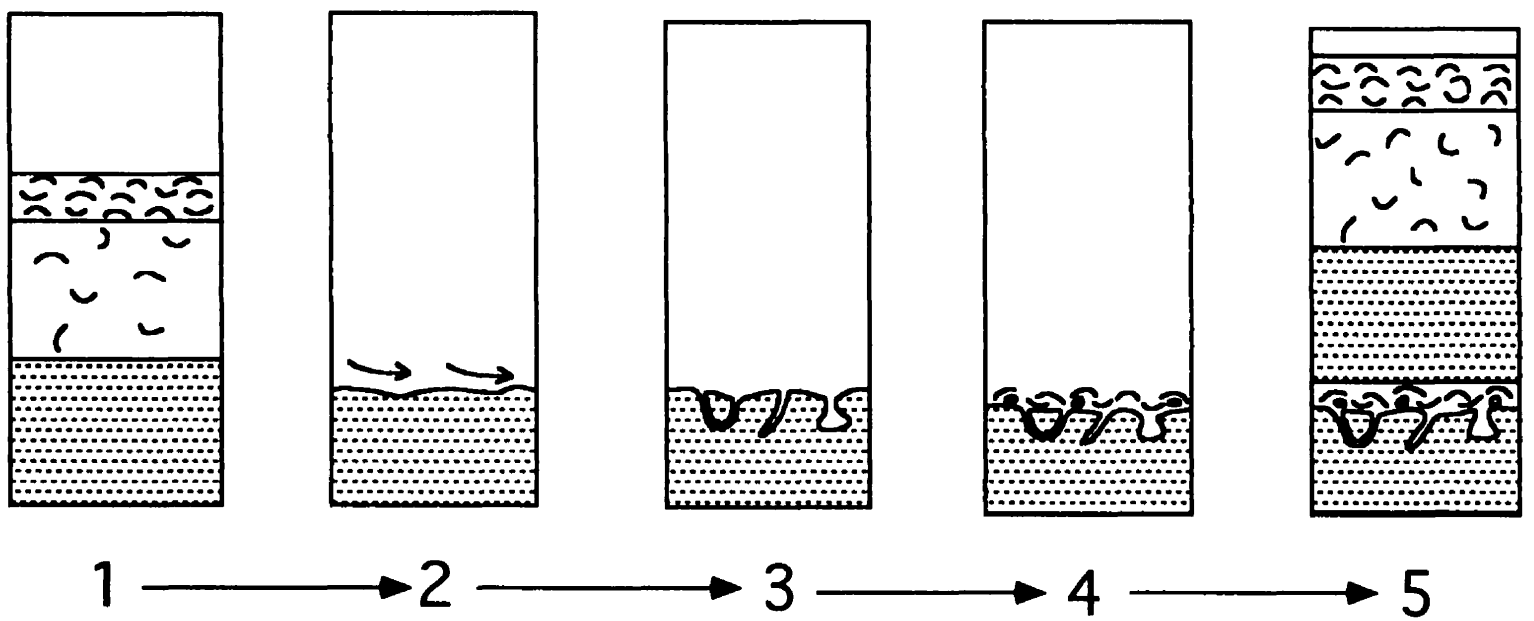

Fig. 5-3. Stage development of firmgrounds in the Dawson Bay Formation. 1 - burial, 2 - erosional exhumation, 3 - colonisation during depositional hiatus, 4 - deposition and passive infill, 5-preservation by burial. (modified after MacEachern et al., 1992).

up with deposition and became drowned and buried in fine grain carbonate sediment. This pattern holds true for many small bioherms and biostromes that developed at flooding surfaces of parasequences (Brett, 1995).

From this evidence, it is concluded that each firmground in the upper Burr Member probably represents a parasequence-scale flooding surface and that the sedimentary succession between two adjacent firmgrounds represents a parasequence. Similar firmgrounds that were interpreted as parasequence-scale flooding surfaces have been reported by Ghibaudo *et al.* (1996). Such parasequences result from fourth or fifth-order relative sea-level changes (Tucker, 1993).

5.7 Discussion

The upper Burr Member is composed of wackestones, lime mudstones and packstones. Grainstones are only well developed in northwestern Manitoba. Some packstones and grainstones were formed by storm activities. They are well developed in northwestern Manitoba, and are relatively well developed in central Saskatchewan. However, very few thin packstones formed in distal environments are present in southeastern Saskatchewan. Thus, the general depositional environments in northwestern Manitoba and central Saskatchewan were higher in energy and shallower in water depth, and the depositional environments in southeastern Saskatchewan had lower-energy and deeper-water conditions. Thus, from northwestern Manitoba to southeastern Saskatchewan and from central to southeastern Saskatchewan, the depositional environments changed from proximal or from more proximal conditions to distal conditions. This suggests that water depth increased from central to southeastern Saskatchewan and from northwestern Manitoba to southeastern Saskatchewan. This conclusion is therefore consistent with those reached from the distribution of the paleokarsts at the base of the Burr Member, and from the lateral variation in the maturity of the paleosols in the Second Red Bed Member.

Vertically, the depositional environments also underwent a significant change during the deposition of the upper Burr Member. In southeastern Saskatchewan, distal storm deposits are relatively abundant in the lower part of the upper Burr Member. However, no shell bed is present in the middle part of the upper Burr Member, probably indicating deeper water conditions. In the lower portion of the upper part, shell beds are present again, although less common than in the lower part, showing that the waters were shallowing again. This suggests that although within distal facies, sediments were often

reworked by storms. In contrast, distal storm layers are rare in the upper part of the upper Burr Member, probably indicating deeper water conditions. This suggests that the depositional environments became deepening upward.

Similar vertical changes can be also detected in the upper Burr Member of central Saskatchewan. Unit A of the upper Burr Member is characterized by abundant storm layers and many firmgrounds, suggesting deposition in shallow water environments characterized by frequent storm activities. Unit B is composed of lime mudstone and wackestone with small, thin-shelled brachiopods and *Chondrites*. Storm layers are very rare. This indicates that the energy levels during deposition of Unit B were much lower than those of Unit A, probably reflecting increasing water depth. The small, thin-shelled brachiopods and exclusive small *Chondrites* suggest that the sediments in Unit B were deposited under low energy dysaerobic conditions. Unit C, like Unit A, is characterized by abundant firmgrounds and shell beds. This may reflect increasing storm activity, probably associated with shallowing water. This is further supported by the presence of large robust shell beds and other marine fossils. Unit D is composed of intensely bioturbated limestone, with fewer firmgrounds than in Unit C, indicating deposition in relatively deep water environments. It can be concluded, therefore, that the depositional environments of the upper Burr Member in central Saskatchewan were characterized by two cycles of marine transgression-regression.

In the outcrop area of northwestern Manitoba, the upper Burr Member is also characterized by a carbonate succession that indicates two cycles of marine transgression-regressions. The lower storm unit at the base of the upper Burr Member suggests a shallow water, high energy environment. It is followed by a limestone unit with sparse shell fossils, probably reflecting deepening waters. The limestone unit is succeeded by the upper storm unit, and grades upward into a unfossiliferous limestone unit, which, in turn, is overlain by calcareous shale and argillaceous fossiliferous limestone of Member C.

The numerous firmgrounds are the distinguishing feature of the upper Burr Member of central Saskatchewan. They were regarded as hardgrounds by Dunn (1982a), Ahlstrom (1992), and Brown and Mathison (1986). However, this study shows that most discontinuity surfaces lack real borings. Instead, they are characterized by *Glossifungites* ichnofossils. This suggests that the sediments were firm but unlithified when organisms reworked them. The common presence of the firmgrounds in the upper Burr Member of central Saskatchewan shows that the sedimentary sequence contains many stratigraphic

breaks, whereas in southeastern Saskatchewan, firmgrounds are rare, reflecting an essentially continuous succession.

The origin of the firmgrounds (hardgrounds) in the Dawson Bay Formation was discussed by Dunn (1982a, 1982b), Braun and Mathison (1982, 1986), and Ahlstrom (1992). Dunn (1982a, 1982b) believed that the development of the firmgrounds was due to increasing restriction of marine conditions and cessation of sedimentation, or was due to periodical changes in the direction of bottom currents. Braun and Mathison (1982, 1986) related the development of the firmgrounds to upward movements of the Peace River Arch in northern Alberta. They suggested that this movement had a destabilizing influence on the basin and that the effect could be felt into Saskatchewan. They did not make it clear, however, how this movement could be responsible for the firmground formation (Ahlstrom, 1992). Ahlstrom (1992) suggested that the tectonic instability in northern Alberta could have caused a relative rise in sea level hindering sedimentation, and thus promoting a hiatus. In this chapter, the firmground surfaces are interpreted as marine flooding surfaces, and their development is due to erosion of their overlying sediments caused by relative fall in sea level. In addition, the strata between two adjacent firmgrounds are interpreted as parasequences. However, several questions concerning these firmgrounds and parasequences need to be further addressed here.

(1) A parasequence consists of a shallowing-upward cycle bounded above and below by marine flooding surfaces (Goodwin and Anderson, 1985; Van Wagoner *et al.*, 1990). They are best developed in nearshore and shallow marine setting in both siliciclastic and carbonate rocks (James, 1984; Pratt *et al.*, 1992). Although upward gradation from lime mudstone to packstone is indeed present in some firmground-bounded successions in the upper Burr Member of southeastern Saskatchewan and in Unit D of the upper Burr Member in central Saskatchewan, a succession that is strongly suggestive of increasing energy and shallowing-upward history (Handford, 1986), most carbonate rocks below the firmgrounds are lime mudstone and wackestone and no obvious upward-shallowing facies successions can be observed. The interpretation for this phenomenon is that the lime mudstone and wackestone were once covered by packstones or grainstones. Their absence now is due to erosion before deposition of the overlying sediments. They were usually completely removed during upward-shallowing processes. Only those parasequences that formed in relatively deep water environments or were exposed to relatively weak high-energy conditions during upward-shallowing processes may contain a coarsening-upward sedimentological signature. This interpretation is supported by the

presence of reworked intraclasts above firmground surfaces having a wackestone or packstone fabric, whereas the limestones directly below the firmground surfaces are characterized by mudstone fabric. This may also provide explanation why there are many reworked robust shell fragments in the carbonate rocks of the upper Burr Member in southeastern Saskatchewan.

(2) There are numerous firmgrounds in Unit A and C of the upper Burr Member in central Saskatchewan. They are closely spaced, characterized by mineralization, and commonly overlain by shell beds. In contrast, there are very few firmgrounds in Unit D and no firmgrounds in Unit B of the upper Burr Member in central Saskatchewan. There are also very few firmgrounds in the upper Burr Member of southeastern Saskatchewan. These phenomena can be interpreted as follows: the sediments in Unit B and D are characterized by thin shell beds formed by storms in distal environments; therefore these two units represent relatively deep water conditions. Because the parasequences are produced by small-scale rise and fall of sea levels, they can easily affect the sediments deposited in shallow water environments. For the sediments deposited in relatively deep water environments, most small-scale sea level falls were probably insufficient to result in bottom erosion of sediment and to expose potential firmgrounds. This explains why there are no firmgrounds in Unit B and very few firmgrounds in Unit D.

(3) The firmgrounds in Unit A and C are distinct, whereas the firmgrounds in Unit D of the upper Burr Member in central Saskatchewan and the firmgrounds in the upper Burr Member of southeastern Saskatchewan are generally indistinct. This is due to whether the firmground is characterized by mineral impregnation or not. Mineralization of the sea floor indicates a prolonged phase of non-deposition or at least an extremely low sedimentation rate allowing chemical reactions to take place at the depositional interface (Furish, 1979). The longer the sediment in direct contact with sea water, the stronger the mineralization. Because the sediments in Unit A and C were deposited in relatively shallow water environments, the relative fall of sea levels would easily expose the sediments well above fair weather wave bases. The high energy shallow water conditions would keep sediments from covering those firmgrounds for relatively long periods of time, which in turn prolonged the residence time span in which the firmgrounds were in direct contact with sea waters. Thus, mineralization happened on those firmgrounds. In contrast, for firmgrounds formed in relatively deep water environments, even if fall of sea levels could expose the firmgrounds above the fair weather wave bases, they were only slightly raised above it. In the subsequent sea level rise, they were rapidly falling below the fair-weather

wave base and buried by sediments. Therefore, the firmgrounds formed in relatively deep water conditions had relatively short periods of residence time to be in direct contact with sea waters. Probably for this reason, they lack mineralization.

5.8 Summary

The upper Burr Member in southeastern Saskatchewan is composed predominantly of wackestone and lime mudstone, with a few thin skeletal packstone and grainstone interbeds. These suggest sedimentation in a low energy, relatively deep water environment, with occasional high energy intervals. In contrast, the proportion of packstone and grainstone increases significantly in the upper Burr Member of central and northwestern Saskatchewan. The body fossils in these rocks are larger and have greater shell thickness. This indicates that the depositional environments in those regions were generally higher in energy with shallower water conditions. Therefore, from both northwestern Manitoba and central Saskatchewan to southeastern Saskatchewan, the depositional environments changed from more proximal to more distal conditions.

New evidence shows that the upper Burr Member in central Saskatchewan consists of two superimposed upward-deepening successions. Firmgrounds were highly developed in the lower part of each succession. These firmgrounds are interpreted as previously buried and dewatered sediments that were exhumed during phases of relative fall in sea level. The reason for the absence or paucity of firmgrounds in the upper parts of the successions is the relatively deep water conditions that existed in those environments. The same explanation can also be used to explain why there are very few firmgrounds in the upper Burr Member of southeastern Saskatchewan.

CHAPTER 6

NEELY MEMBER

6.1 Introduction

The Neely Member is underlain by the Burr Member and overlain by the Hubbard Evaporite Member of the Dawson Bay Formation or the First Red Bed of the Souris River Formation. It is widespread in the Canadian part of the Williston Basin, with an average thickness ranging from 15 m in central Saskatchewan to 18 m in southeastern Saskatchewan. In this chapter, the lithological and sedimentological features, as well as sequence stratigraphy of the Neely Member from southeastern and central Saskatchewan are described and discussed, respectively.

6.2 Neely Member in Southeastern Saskatchewan

6.2.1 The Contact Between Burr and Neely Members

In southeastern Saskatchewan, the contact between the Burr and Neely members is characterized by a distinct firmground (Plate 6-1A & B). The firmground has a smooth, flat upper surface that is penetrated by burrows. The burrows vary from regular to highly irregular in form. Transverse sections of the regular burrows are circular or elliptical. Burrows that connect to the surface of the firmground are truncated by erosion. The walls of the burrows are sharp, smooth and unlined, with rare indentations. These burrows range from a few mm to 2 cm in diameter, and are filled with bioclasts (most of which are of sand grade), anhydrite and halite. Additionally, sparse reworked intraclasts are present in the burrows and in the sediment directly overlying the firmground. The firmground is also characterized by intense mineral impregnation (Plate 6-1A & B). It is present not only at the surface of the firmground, but also extends some distance down on the walls of the burrows. The mineral impregnation exhibits a red to black colour. The impregnated area

PLATE 6-1

Plate 6-1 A: Slabbed core photograph showing the contact (c) between the Burr and Neely members in southeastern Saskatchewan. It is a firmground, characterized by an intense mineral impregnation. Lsd. 13-12-22-32W1. Scale bar is 1 cm.

Plate 6-1 B: Slabbed core photograph showing the contact between the Burr and Neely members in southeastern Saskatchewan. It is a firmground (f) with strong mineral impregnation. Lsd. 9-24-21-30W1. Scale bar is 2 cm.

Plate 6-1 C: BSE micrograph of same sample as Plate 6-1 B. It shows that the top of the firmground is composed of a thin pyritic film. Pyrite is also scattered in the rock below the firmground surface, but is absent in the rock directly above the firmground. Lsd. 9-24-21-30W1.

Plate 6-1 D: Slabbed core photograph showing lime mudstone with packstone interbeds from the lower part of Unit A of the Neely Member. The bioclasts in the packstone are composed of crinoids and small, thin-shelled brachiopods. Lsd. 13-12-22-32W1-26. Scale bar is 2 cm.

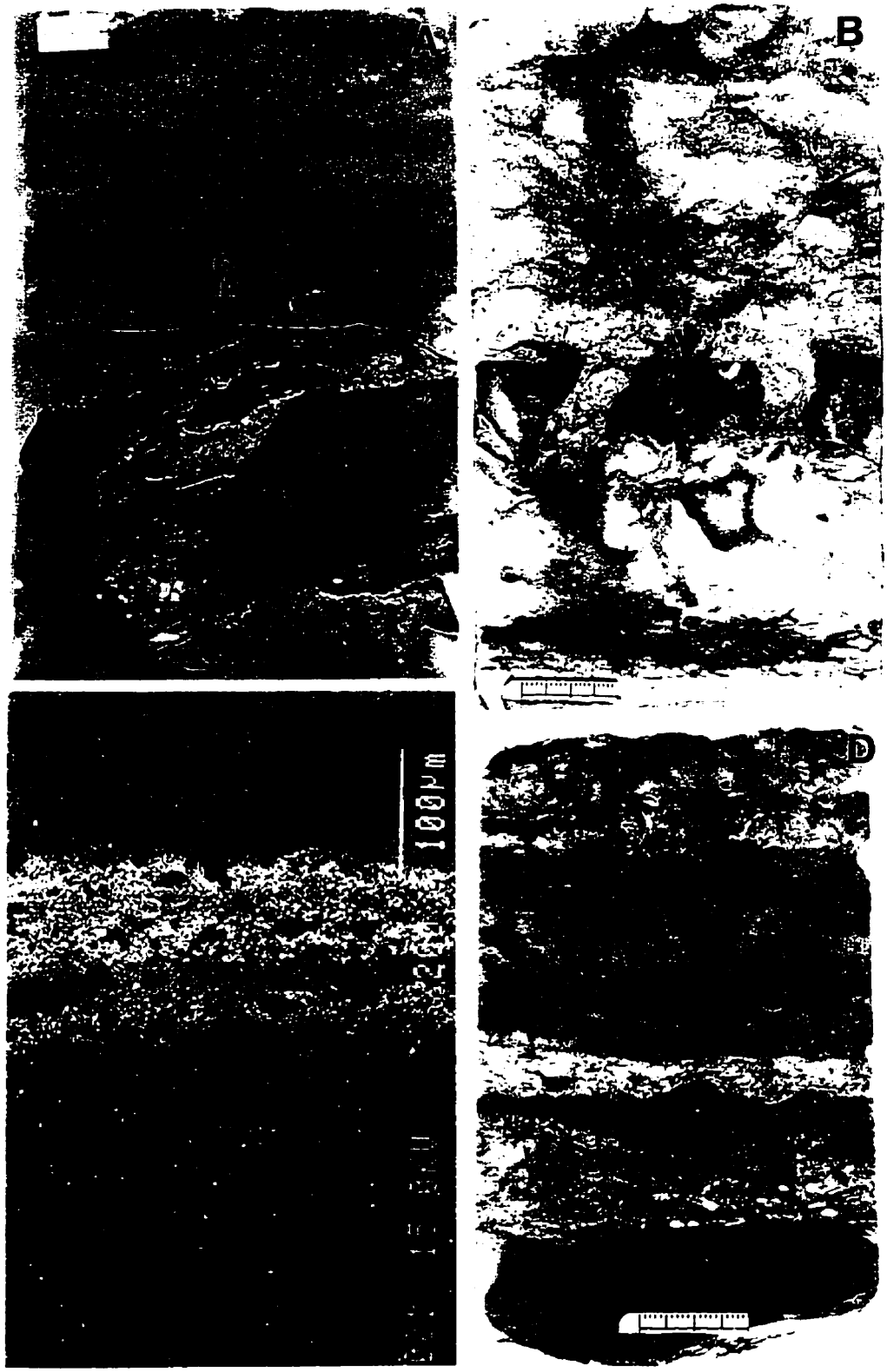
B
100μm
D

varies from a few mm up to 1 cm thick, with the colour intensity fading downward from the surface of the firmground and outward from the walls of the burrows. However, the walls of the burrows that are located relatively deep in the sediment lack mineral impregnation (Plate 6-1A).

Microprobe study reveals that the top of the firmground is composed of a film of pyrite (Plate 6-1C). The pyritic film is about 150 μm thick, with pyrite crystals ranging from 1 to 2 μm in diameter. However, pyrite crystals are absent in the rock overlying the firmground. Below the firmground, scattered pyrite is present. This coincides with the fading of the black or red hue of the rock. Therefore, it can be concluded that the rock is blackened by pyrite. The red colour is probably due to hematite, which formed by oxidation of earlier pyrite.

Interpretation

The presence of the firmground and reworked intraclasts indicates that the contact between the Burr and Neely members is an omission surface. The development of the firmground reflects erosional exhumation of subjacent sediments by current winnowing or by sedimentary lithification due to very slow sedimentation or non-deposition (Savrda, 1995). The presence of intense mineral impregnation at the surface of the firmground and on the walls of the burrows suggests a prolonged phase of non-deposition or, at least, an extremely low sedimentation rate to allow chemical reactions to take place at the depositional interface (Fursich, 1979). Because such intense mineral impregnation is absent in the other firmgrounds in the Dawson Bay Formation, it may be concluded that the firmground between the Neely and Burr members probably represents the longest phase of non-deposition during the accumulation of the carbonates above the paleokarsts at the base of the Burr Member. Such surfaces are often associated with maximum water depth during the deposition of a sedimentary sequence (Loutit *et al.*, 1988); therefore, it probably represents the maximum flooding surface of the Dawson Bay Formation. This interpretation is supported by the fine-grained limestone that forms the uppermost part of the Burr Member, which was deposited in a relatively deep offshore environment. It is also supported by the sediment that directly overlies the firmground, which also formed in a relatively deep water environment (see below).

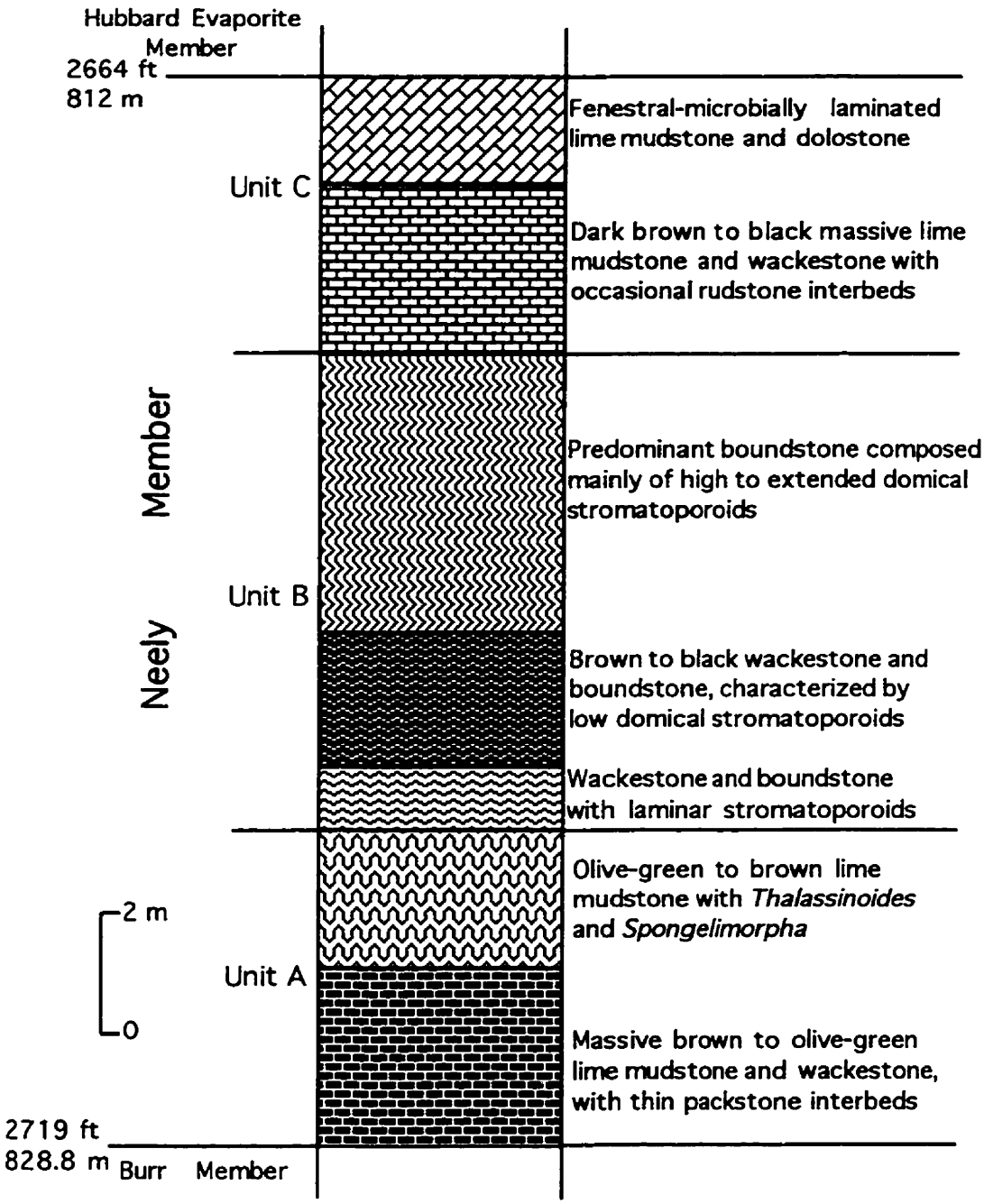

Fig. 6-1. Stratigraphic section of the Neely Member from Well 13-12-22-32W1 in southeastern Saskatchewan.

PLATE 6-2

Plate 6-2 A - Plate 6-3 D: Detailed core photograph showing an entire vertical succession of the Neely Member in southeastern Saskatchewan. Lsd. 13-12-22-32W1.

Plate 6-2 A: Core photograph showing the uppermost part of the Burr Member, the contact between the Burr and Neely members (c), and the lowermost part of the Neely Member. Lsd. 13-12-22-32W1. (One core box is 0.76 m long and core diameter is 10.1 cm.)

Plate 6-2 B: Core photograph showing the lower part of Unit A of the Neely Member. It is composed of olive-green lime mudstone with thin packstone interbeds. The lime mudstone is partly mottled. Additionally, several indistinct firmgrounds are present in this part. Lsd. 13-12-22-32W1. (One core box is 0.76 m long and core diameter is 10.1 cm.)

Plate 6-2 C: Core photograph showing the upper part of Unit A and the lower part of Unit B of the Neely Member. The lower portion of the upper part of Unit A is composed of olive-green lime mudstone with local packstone interbeds. The lime mudstone was strongly bioturbated by *Thalassinoides*-making organisms. The upper portion of the upper part of Unit A is composed of brown lime mudstone that is characterized by *Spongeliomorpha* (see Plate 6-4 D). The lower part of Unit C is composed of brown to black wackestone and boundstone. The boundstone consists of laminar stromatoporoids. Lsd. 13-12-22-32W1. (One core box is 0.76 m long and core diameter is 10.1 cm.)

Plate 6-2 D: Core photograph showing the middle and upper parts of Unit B of the Neely Member. The middle part is composed of wackestone and boundstone. The latter is dominated by low domical stromatoporoids. The upper part consists of wackestone and boundstone, with stromatoporoids characterized by high domical types. Lsd. 13-12-22-32W1. (One core box is 0.76 m long and core diameter is 10.1 cm.)

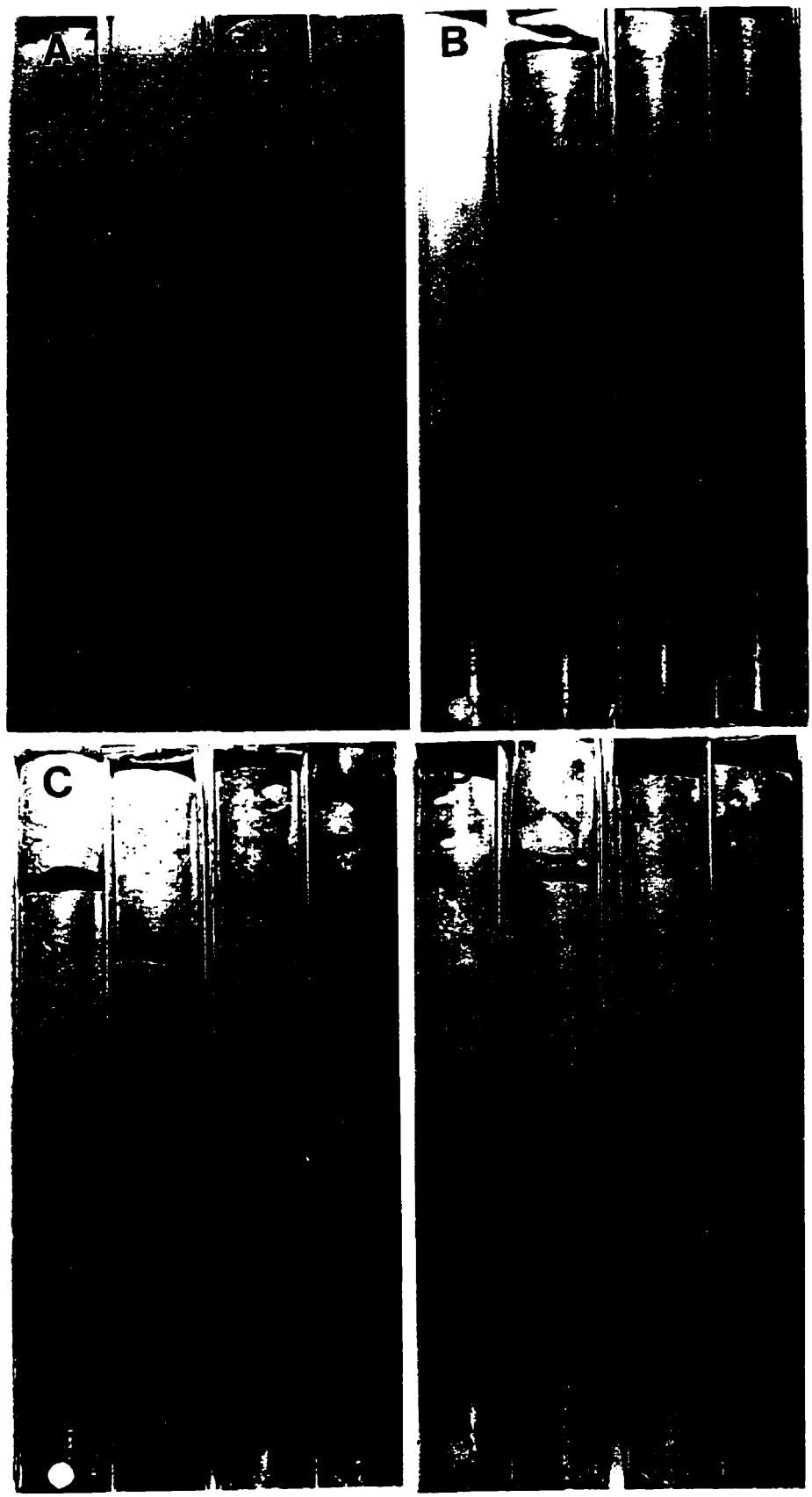
A
B
C

PLATE 6-3

Plate 6-3 A: Core photograph showing the upper part of Unit B of the Neely Member. It is composed of wackestone and boundstone. The latter is characterized by high domical stromatoporoids. Lsd. 13-12-22-32W1. (One core box is 0.76 m long and core diameter is 10.1 cm.)

Plate 6-3 B: Core photograph showing the upper part of Unit B and the lower part of Unit C of the Neely Member. The former is composed almost completely of stromatoporoid boundstone. Most stromatoporoids were toppled and lie on their sides. The lower part of Unit C consists of dark brown to black massive lime mudstone and wackestone, and stromatoporoid rudstone. Lsd. 13-12-22-32W1. (One core box is 0.76 m long and core diameter is 10.1 cm.)

Plate 6-3 C: Core photograph showing the lower and upper parts of Unit C of the Neely Member. The lower part consists of dark brown to black massive lime mudstone and wackestone. The upper part is composed of fenestral and microbially laminated dolostone. Lsd. 13-12-22-32W1. (Core diameter is 0.76 m long and core diameter is 10.1 cm.)

Plate 6-3 D: Core photograph showing the transition between the Neely and Hubbard Evaporite members. The base of the core is composed of fenestral dolostone of the Neely Member, which is overlain by laminated anhydrite of the Hubbard Evaporite Member. Lsd. 13-12-22-32W1. (Core diameter is 0.76 m long and core diameter is 10.1 cm.)


A
B
C

6.2.2 The Neely Member

The Neely Member in southeastern Saskatchewan is represented by a sedimentary succession from Core 13-12-22-32W1 (Plate 6-2A to Plate 6-3D). It can be divided into three units (Fig. 6-1), which are termed here units A, B and C from base to top, respectively.

Unit A

Lower Part of Unit A

Unit A can be divided into lower and upper parts. The lower part of Unit A is composed of massive brown to olive-green lime mudstone and wackestone, with a few thin packstone interbeds (Plates 6-1D, 6-2A & B). The lime mudstone and wackestone have a mottled appearance locally (Plate 6-2B), and consist largely of micritic calcite, with variable amount of bioclasts, that include crinoids, brachiopods, ostracods and foraminifera. The brachiopods are small and thin-shelled. The packstones are less than 2 cm thick and laterally more or less continuous (Plate 6-1D). Some display a pinch-and-swell bedform. The shell fossils in the packstones show variable degrees of breakage, ranging from nearly *in situ* and unabraded accumulations to finer, comminuted and reworked accumulations. They are mainly small, thin-shelled species. The contact between the packstone and the underlying lime mudstone or wackestone is sharp but non-erosional. In places, the contact is undulating.

Additionally, there are at least two firmgrounds in this part (Plate 6-2B). The firmgrounds are penetrated by burrows with a diameter up to 1 cm. These burrows are vertical to sub-horizontal. The upper surface of the firmgrounds has a hummocky appearance, and is covered by reworked intraclasts and bioclasts. The bioclasts are dominated by crinoid and brachiopod debris, with lesser solitary rugose corals, bryozoans and trilobites. The rock directly below the firmground surface is composed of lime mudstone. Sparse shell fossils, including crinoid debris, trilobites and well-preserved brachiopods, are present. However, these firmgrounds lack mineral impregnation. This suggests that the firmgrounds are similar to those in the Burr Member, but are significantly different from the mineral-stained firmground at the Burr-Neely contact.

Interpretation

The lower part of Unit A is dominated by lime mudstone and wackestone, with local thin packstone interbeds. This suggests that these carbonate sediments mainly accumulated in a low energy, relatively deep water environment, with occasional high energy conditions. This interpretation is supported by the fragile fauna in the packstone, dominated by small and thin-shelled brachiopods. These fossils are generally well preserved, and are identical to the fauna in the directly underlying lime mudstone or wackestone. Additionally, the packstones are characterized by sharp but non-erosive bases. Intraclasts are rare. Bedding ranges widely from planar to lenticular. Some beds even pinch out laterally in a few cm. Lateral discontinuity and extreme variability in bed thickness are recognized as important features of storm beds (Kreisa, 1981); consequently, the packstone beds are believed to have been deposited by storm processes. Because the packstones are very thin and lack erosional bases or amalgamation, they may represent a distal storm facies.

Upper part of Unit A

The upper part of Unit A is about 2.3 m (7.5 ft) thick in Core 13-12-22-32W1. It is composed predominantly of olive-green to brown bioturbated lime mudstones (Plate 6-2C), with very rare packstone interbeds. The lime mudstone in the lower portion of the upper part of Unit A is *Thalassinoides*-dominated and has a mottled appearance (Plates 6-2C, 6-4A & B). The *Thalassinoides* are highly developed. The matrix surrounding the burrows is olive-green whereas the burrow fills are brown, highlighting their presence. The burrows are 8 to 12 mm in diameter, with cylindrical to elliptical cross sections. They are smooth-walled and unlined. Horizontal and inclined parts of burrow systems are predominant, with fewer vertical branches. Branching is evident in two-dimensional view. However, because of their limited areal extent in core slabs, regular branching with Y- or T-shaped bifurcations are rarely observed. Burrows swell at branch junctions. Side branches off the main trunk of a burrow may have smaller diameters than the main trunk. In thin section (Plate 6-5C), the non-bioturbated part of the rock is composed of micrite, with sparse crinoids, brachiopods, ostracods and trilobite fragments. Sparse dolomite crystals are also present. The burrow-fills consist of finely crystalline dolomite. Small shell fragments can also be observed in the filling material.

PLATE 6-4

Plate 6-4 A: Slabbed core photograph showing lime mudstone from the upper part of Unit A of the Neely Member in southeastern Saskatchewan. It contains abundant *Thalassinoides* and scattered crinoid debris. Lsd. 13-12-22-32W1-11. Scale bar is 2 cm.

Plate 6-4 B: Slabbed core photograph showing a high concentration of *Thalassinoides*. *Spongeliomorpha* is probably also present. The upper part of Unit A of the Neely Member. Lsd. 9-14-19-30W1. Scale bar is 1 cm.

Plate 6-4 C: Slabbed core photograph showing lime mudstone intercalated with a thin packstone. The upper part of Unit A of the Neely Member. Lsd. 13-6-22-30W1-3. Scale bar is 1 cm.

Plate 6-4 D: Slabbed core photograph showing *Spongeliomorpha* from the upper part of Unit A of the Neely Member. Lsd. 13-12-22-32W1. Scale bar is 1 cm.

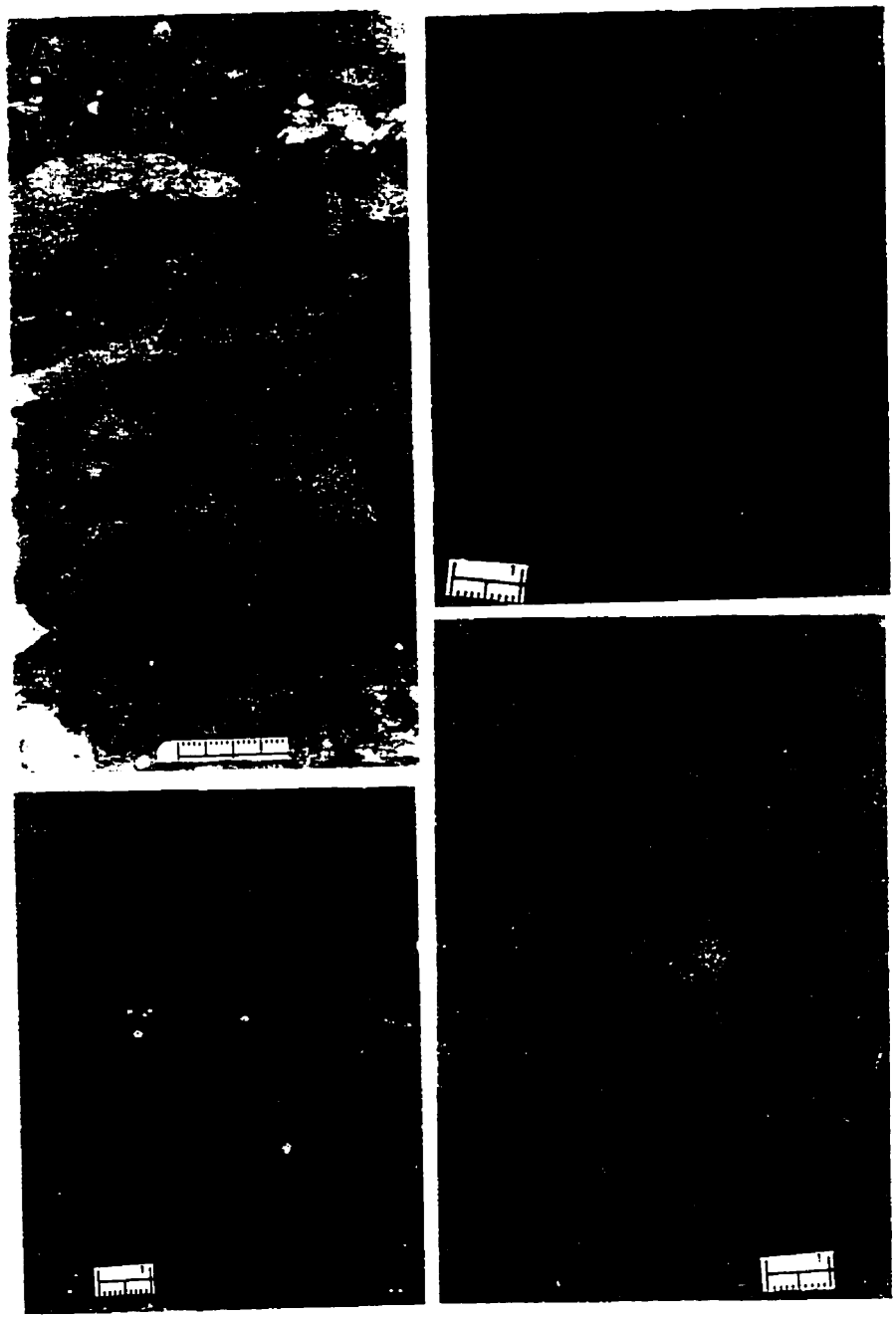

PLATE 6-5

Plate 6-5 A: Slabbed core photograph showing the top (T) of Unit A of the Neely Member. The sediment was highly bioturbated and is rich in crinoid debris. Lsd. 13-12-22-32W1. Scale bar is 1 cm.

Plate 6-5 B: Slabbed core photograph showing the top of Unit A of the Neely Member. It is bioturbated by firmground burrows. Lsd. 13-12-22-32W1. Scale bar is 1 cm.

Plate 6-5 C: Plane-light photomicrograph showing *Thalassinoides*-bearing lime mudstone from the upper part of Unit A of the Neely Member. The non-bioturbated part is composed of micrite. The burrow-fills consist of dolomite. Lsd. 09-24-21-30W1-11A. Scale bar is 1 mm.

Plate 6-5 D: Slabbed core photograph showing laminar stromatoporoids from the lower part of Unit B of the Neely Member. Lsd. 13-12-22-32W1. Scale bar is 1 cm.

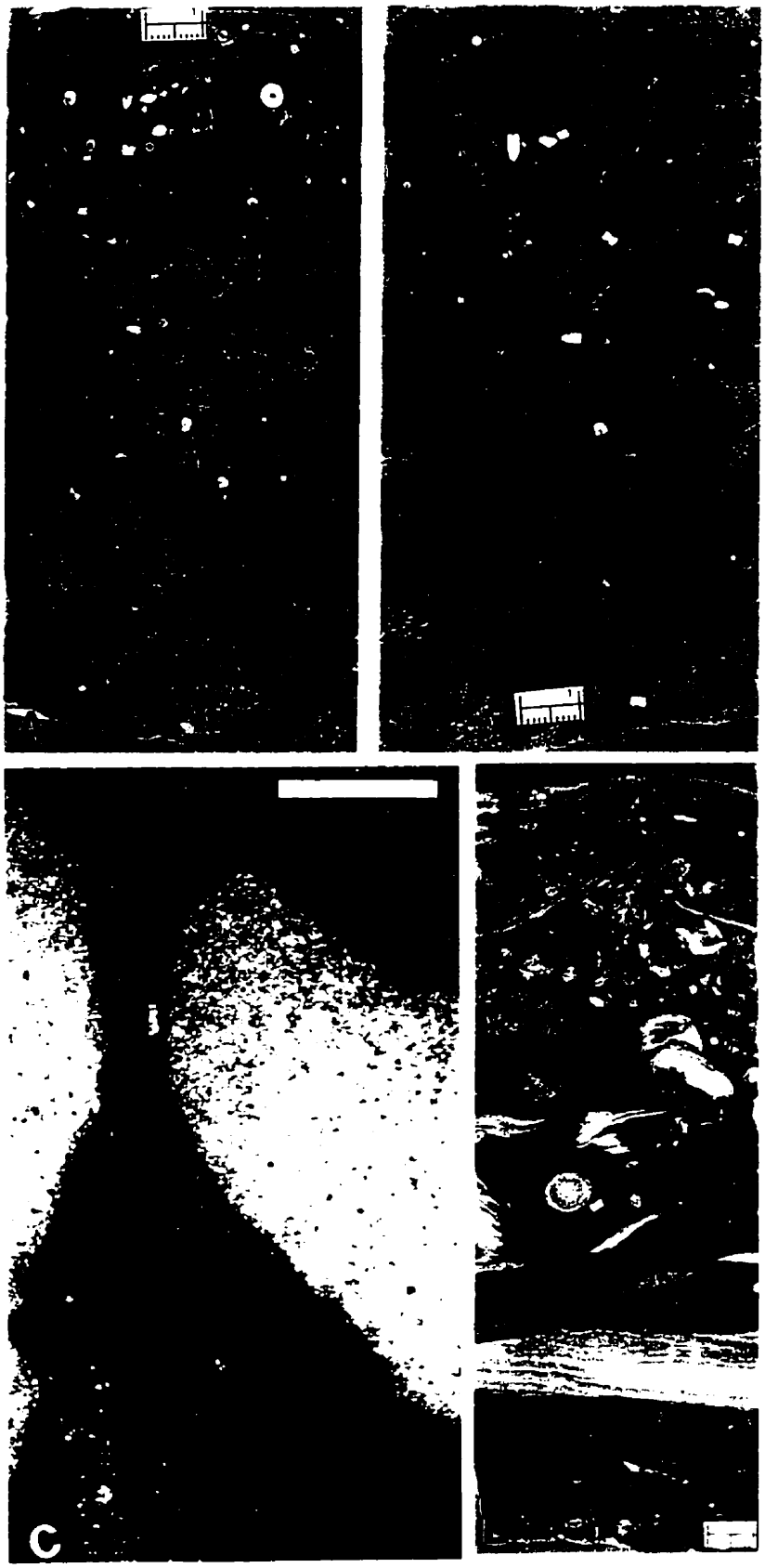
C

In the upper portion, the rock colour changes from olive-green to brown, and the burrows become less distinct (Plate 6-2C). The burrows are larger (up to 4 cm in diameter) and more irregular (Plate 6-4D). Vertical shafts are more common, with superimposed tunnels. Individual burrow systems overall are less discrete, due to excessive overprinting and reduced colour contrast between the burrow fill and surrounding sediments. Furthermore, the surrounding matrix is much less abundant than that in the olive-green lime mudstone in the lower portion, suggesting more extensive bioturbation. The walls of the burrows are no longer smooth and scratch marks are common (Plate 6-4D). Thus, this type of trace fossil is more appropriately assigned to the ichnogenus *Spongeliomorpha* (Myrow, 1995).

Additionally, there are at least two packstone beds in the upper part of Unit A. They are less than 2 cm thick and comprise intraclasts, crinoids, foraminifera, ostracods and brachiopod fragments (Plate 6-4C). The intraclasts are irregular in shape and are penetrated by soft-sediment burrows, indicating that they were not fully lithified when reworked. The contact between the packstone and the underlying lime mudstone is sharp and erosional.

At the top of the unit, the amount of crinoid debris increases significantly (Plate 6-5A & B). However, the crinoids are loosely packed and are floating in a carbonate matrix, suggesting that the crinoid debris was not concentrated by wave or storm activity. The increase in the crinoid debris may indicate a decreasing sedimentation rate. Some burrows, which display well-defined shapes of brachiopods or bivalves, are also found. The contact between units A and B is characterized by a firmground (Plate 6-2C).

Interpretation

Thalassinoides is a common branching burrow system in marine sediments of Cambrian to Recent age (Sheehan and Schiefelbeiw, 1984). It is generally considered the dwelling structure of decapod crustaceans (Myrow, 1995), with paleoenvironmental distribution ranging from tidal flat to outer shelf facies, and even to deep sea fan facies (Myrow, 1995). They are found both within the *Zoophycos* ichnofacies, a soft-ground assemblage, and within the *Glossifungites* ichnofacies, a firmground assemblage (Frey and Seilacher, 1980). The exclusive presence of *Thalassinoides* in the lower portion of upper Unit A shows that these burrows developed in a firm, at least semi-consolidated, substrate. This was probably due to a relatively slow sedimentation rate. A similar interval of dense

Thalassinoides in the Silurian Racine Formation at Milwaukee, Wisconsin (USA), was interpreted to represent development of a firmground during a time of minimal sedimentation (Watkins and Coorough, 1997).

The upward change from *Thalassinoides* to *Spongeliomorpha* burrows may signify a further increase in the firmness of the substrate, probably associated with a decreasing sedimentation rate. This is supported by a more pervasive bioturbation in the upper part. The intensity of bioturbation is related to sedimentation rates such that the slower the rate of sedimentation, the more intense is the bioturbation (Simpson and Eriksson, 1990), and a higher degree of bioturbation indicates a decrease in sedimentation rate (Strasser, 1991). The presence of a large amount of crinoid fragments at the top of Unit A reflects a further decrease in sedimentation rate. However, no conclusive evidence has been found to show the absolute water depth of the paleoenvironment in which the *Thalassinoides*- and *Spongeliomorpha*-dominated carbonate sediments were deposited. Given their stratigraphic position between the underlying lime mudstone- and wackestone-dominated lithofacies and the overlying stromatoporoid-dominated lithofacies (see below), and the general continuity of sedimentation between them, it is likely that the depositional environment was located between those of these two lithofacies. Similar *Thalassinoides*-dominated lithofacies were described from the Silurian Racine Formation of Wisconsin and from the Upper Ordovician sediments of the eastern Great Basin. The former was interpreted as an offshore deposit (Watkins and Coorough, 1997), whereas the latter was believed to represent deposition near or below wave base (Sheehan and Schiefelbein, 1984).

Unit B

Unit B, which is separated from Unit A by a firmground, is composed of wackestone, stromatoporoid boundstone, floatstone and rudstone. It is about 9.9 m (32.5 ft) thick in Core 13-12-22-32W1 from southeastern Saskatchewan (Plates 6-2C & D, 6-3A & B). Overall the rocks appear massive. Dark bituminous wisps are common, becoming more abundant close to the top of the unit.

The base of Unit B is a brown wackestone that is 0.4 m (1.2 ft) thick (Plate 6-2C). It is massive and contains *Thamnopora* and crinoid debris, with sparse brachiopods and stick-like stromatoporoids.

PLATE 6-6

Plate 6-6 A: Plane-light photomicrograph showing matrix of wackestone from the lower part of Unit B of the Neely Member, which is composed of dolomite and dark brown organic wisps. Lsd. 13-12-22-32W1. Scale bar is 0.25 mm.

Plate 6-6 B: Plane-light photomicrograph showing a stromatoporoid fragment embedded in a dolomitic matrix. The lower part of Unit B of the Neely Member. Lsd. 13-12-22-32W1. Scale bar is 0.25 mm.

Plate 6-6 C: Slabbed core photograph showing laminar and low domical stromatoporoids from the middle part of Unit B of the Neely Member. Lsd. 14-32-020-30W1-56. Scale bar is 1 cm.

Plate 6-6 D: Slabbed core photograph showing a low domical stromatoporoid from the middle part of Unit B of the Neely Member. Lsd. 13-12-22-32W1-30. Scale bar is 1 cm.

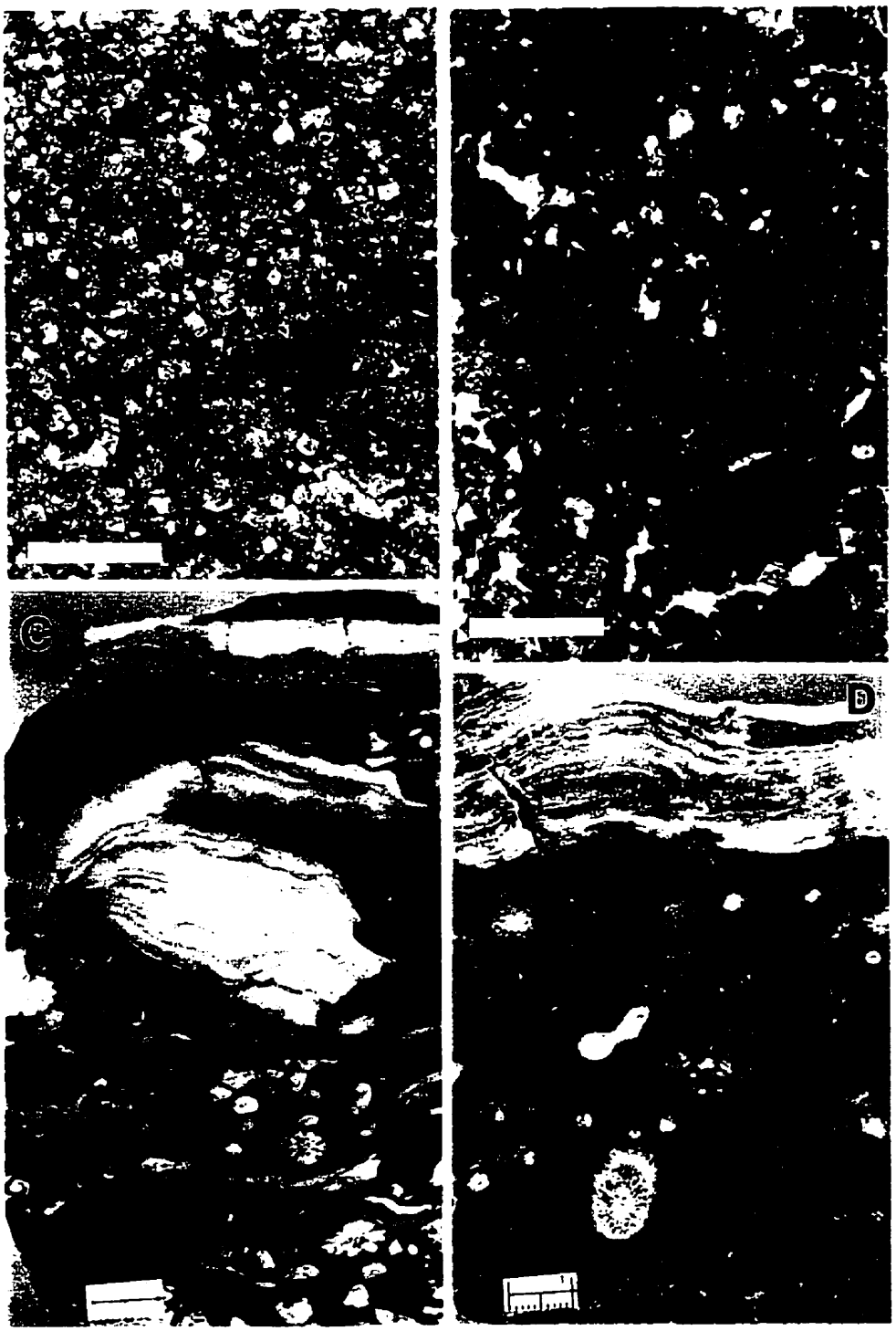
C
D

The lower part of Unit B is composed of wackestone and boundstone with laminar stromatoporoids, rugose corals and *Thamnopora* (Plates 6-2C, 6-5D). The laminar stromatoporoids are up to 4 cm thick and are preserved in life position. Usually they form slightly wavy layers, resting directly on lime mud or silt (Plate 6-6D). This type of stromatoporoid is believed to develop below wave base, encrusting or binding micrite matrix, and was formed consistently downslope of buildups (Wilson, 1975). The sediment between the laminar stromatoporoids is composed of fine-grained carbonate matrix and bioclasts. The bioclasts include solitary rugose corals, brachiopods, trilobites, crinoids and stromatoporoid fragments. They are angular to subangular, poorly sorted and randomly oriented, ranging from silt- to gravel-size. The black carbonate matrix is rich in organic matter. Thin section study reveals that the matrix is composed mainly of dolomite rhombs (Plate 6-6A & B). The non-dolomitized part of the matrix comprises micrite and organic wisps. Additionally, small anhydrite nodules are present locally.

The middle part of Unit B comprises stromatoporoid boundstone and brown to black wackestone (Plate 6-2D). The boundstone consists of stromatoporoids that are mainly low domical types, with sparse high domical types. The low domical stromatoporoids are only a few cm in height and preserved in life position (Plate 6-6C). The diameter of the high domical stromatoporoids is generally smaller than the core diameter (Plate 6-7A). The wackestone appears massive, consisting of carbonate matrix and randomly oriented bioclasts. The sediment is poorly sorted and bioclasts are angular to subrounded. The size of the bioclasts varies from medium silt to gravel. They include both fragmented and whole skeletal grains, which are dominated by stromatoporoids, crinoids and brachiopods. Petrographic study shows that like the lower part, the matrix is almost completely dolomitized, but the shell fossils are only partially dolomitized or non-dolomitized. The overall depositional texture of the wackestone and the lack of physical sedimentary structures, such as cross-bedding, indicate that these sediments were deposited in a predominantly quiet-water environment.

The upper part of Unit B is mainly boundstone composed of high to extended domical stromatoporoids (Plates 6-2D, 6-3A & B). They are densely packed and usually exceed the core diameter, their size being significantly larger than the stromatoporoids in the middle part. Some are up to 25 centimeters high. Although a few are preserved in growth position, most stromatoporoids were toppled and lie on their sides (Plate 6-3B). A similar phenomenon was found in the Silurian stromatoporoid reefs of Gotland, Sweden, where it was attributed to storm processes (Kershaw, 1993; Kershaw and Keeling, 1994).

PLATE 6-7

Plate 6-7 A: Slabbed core photograph showing a toppled domical stromatoporoid (t) from the middle part of Unit B of the Neely Member. Lsd. 1-12-34-1W3-4-B. Scale bar is 1 cm.

Plate 6-7 B: Slabbed core photograph showing boundstone composed of highly packed stromatoporoids. The stromatoporoid in the lower part of the slabbed core section has two growth centres. The upper part of Unit B of the Neely Member. Lsd. 13-12-22-32W1. Scale bar is 1 cm.

Plate 6-7 C: Slabbed core photograph showing a stromatoporoid boundstone, which is partially cemented by sparry calcite (c). The upper part of Unit B of the Neely Member. Lsd. 9-24-21-30W1. Scale bar is 1 cm.

Plate 6-7 D: Slabbed core photograph showing a stromatoporoid rudstone from the lower part of Unit C of the Neely Member. Lsd. 4-2-21-30W1-1. Scale bar is 1 cm.


A
t
B
C
C

The toppled stromatoporoids, however, are not abraded. Some stromatoporoids have more than one growth centre (Plate 6-7B). These forms can be explained by the coalescence of several specimens that happened to grow near each other and merged as they grew. The interskeletal sediment is brown to black and has depositional textures varying from wackestone to packstone (Plate 6-7B). It consists predominantly of coarse sand-sized bioclasts and micrite. The bioclasts are angular, randomly oriented and poorly sorted, and include crinoids, stromatoporoids, bryozoans, gastropods, brachiopods, and tabulate and rugose corals. Some elongated shells were compressed and are oriented parallel to the outlines of stromatoporoids.

Furthermore, throughout Unit B of the Neely Member, framework structures are absent and sparry calcite cements are only locally observed (Plate 6-7C). These cements are composed of coarse, equant sparry calcite. Some voids among the stromatoporoids are filled with anhydrite.

Stromatoporoid rudstone and floatstone are well developed at the top of Unit B and in the lower part of Unit C. These rocks are poorly sorted (Plate 6-7D) with grain- to mud-supported textures. The grain size of the bioclasts varies from fine sand- to pebble-sized. These bioclasts are disoriented and sub-angular to subrounded. They are composed largely of stromatoporoid fragments. Brachiopod fragments are locally present. The sediment between the bioclasts is black massive micrite with a high organic content.

Interpretation

The vertical zonation from laminar stromatoporoids in the lower part, through low domical stromatoporoids in the middle part, to high and extended domical stromatoporoids in the upper part, shows a broad change from deep to shallow water conditions, accompanied by a trend from quiet to turbulent water (Bjerstedt and Feldmann, 1985; Watts, 1988). Kershaw (1988), however, suggested that energy alone is not the only factor affecting stromatoporoid morphology. A similar vertical zonation of stromatoporoid buildups was found in the Lucas Dolostone (Middle Devonian) on Kelley Island, Ohio (Bjerstedt and Feldmann, 1985), and in the Lower Silurian Hogklint patch reefs of Gotland, Sweden (Kershaw, 1993). They were interpreted to have been influenced by an increasingly stabilized substrate, accompanied by an increase in turbulence, and in the frequency of episodic, high sedimentation events or water column turbidity (Bjerstedt and Feldmann, 1985; Watts, 1988). The relatively fine-grained texture of the matrix and the general lack

of current- or wave-generated features show that the buildups did not act as wave-resistant barriers or reefs, but rather they formed low-relief biostromes (Elrick, 1996).

Unit C

Unit C is about 3 m thick in Core 13-12-22-32W1 (Plate 6-3B & C). It is composed of dark brown to black, massive lime mudstone, wackestone and laminated lime mudstone in the lower part, and fenestral and microbially laminated lime mudstone and dolostone in the upper part.

Lower Part of Unit C

Dark brown to black massive lime mudstone and wackestone

The dark brown to black, massive lime mudstone and wackestone in the lower part of Unit C are slightly to extensively bioturbated, with remains of black laminae and variable amounts of trace and body fossils (Plates 6-8C & D, 6-9A). Usually, trace fossils are exclusively *Chondrites* (Plate 6-9B & C). They are less than 2 mm in diameter and predominantly horizontal. Relatively large burrows, probably *Planolites*, are locally present (Plate 6-8C). The body fossils include both allochthonous and *in situ* shell fossils. The former include sand- to pebble-sized fragments of stromatoporoids and robust brachiopods (Plates 6-8A, 6-9B, 6-10A), whereas the latter comprise small, thin-shelled brachiopods, ostracods and gastropods, that are characterized by high individual numbers but low species diversity (Plate 6-8C & D). Where the *Chondrites* are found alone, only allochthonous shell fragments are present. Where the sediment was extensively bioturbated, both allochthonous and *in situ* shells are present. Additionally, scattered anhydrite nodules, up to a few mm long, are found in these rocks (Plate 6-9A). Thin section study shows that the matrix of the lime mudstone and wackestone is composed of micrite, argillaceous sediment and organic wisps. The micrite is partially dolomitized (Plate 6-8B). Burrow fills are generally more intensely dolomitized than the surrounding matrix (Plate 6-9D). Vertically, the lime mudstone and wackestone are in direct contact with the black laminated lime mudstone (Plate 6-10B).

Black laminated lime mudstone

The black laminated lime mudstone is present in Cores 16-29-22-30W1 and 4-2-22-31W1. It is composed of alternating carbonate- and organic-rich laminae (Plate 6-10B, C & D). The carbonate-rich laminae are white to brown whereas the organic-rich laminae are black. They are predominantly horizontal or slightly wavy. Although local minor bioturbation can be observed, neither scours nor current sedimentary structures have been found. Fragments of robust brachiopods and stromatoporoids are occasionally observed embedded within the laminae (Plate 6-10C). The carbonate-rich laminae range from less than 1 to 5 mm thick. They are more or less laterally continuous. They are composed predominantly of foraminifera (?) (Plate 6-11A). The organic-rich laminae comprise amorphous organic matter, foraminifera (?) and argillaceous stripes (Plate 6-11B). Additionally, terrigenous carbonate clasts are present locally in the laminated lime mudstone (Plate 6-11C & D). These clasts are predominantly polycrystalline, and have internal textures that range from aphanitic to coarsely crystalline. Some clasts are well rounded. The black laminated lime mudstone is commonly interbedded with dark brown to massive lime mudstone and wackestone (Plate 6-10B).

Interpretation

The presence of a low diversity, *in situ* fauna in the massive lime mudstone and wackestone suggests that they formed under low energy, restricted conditions. This interpretation is supported by the presence of remains of fine laminations and the exclusive presence of *Chondrites* in some examples. The *Chondrites* and general absence of *in situ*, preserved shell fossils in the lime mudstone may indicate that it was deposited in a more restricted environment than the wackestone. The presence of well-preserved lamination in the black laminated lime mudstone indicates a more restricted setting. Such a setting could be present both in a basinal environment and in a subtidal lagoonal environment landward of the stromatoporoid biofacies. The lack of *in situ* open-marine fossils and the stratigraphic position of these rocks between the stromatoporoid facies and intertidal-supratidal facies (as discussed in the following section) argue strongly against a basinal environment. Therefore, it can be concluded that the sedimentary rocks in the lower part of Unit C were deposited in a lagoon landward of the stromatoporoid facies. Similar facies were also interpreted to have accumulated in a shallow-subtidal, restricted,

PLATE 6-8

Plate 6-8 A: Plane-light photomicrograph of lime mudstone from the lower part of Unit C. It is composed of dolomite, micrite and organic wisps, with a robust brachiopod fragment (b) in the middle. Lsd. 13-12-22-32W1-32. Scale bar is 0.5 mm.

Plate 6-8 B: Plane-light photomicrograph of lime mudstone from the lower part of Unit C. It consists of dolomite, micrite and organic wisps (o). Lsd. 13-12-22-32W1-32. Scale bar is 0.5 mm.

Plate 6-8 C: Slabbed core photograph showing a black mottled lime mudstone and an overlying wackestone. The lime mudstone is bioturbated by *Chondrites* and other relatively large burrows, but it lacks body fossils. The wackestone is massive and contains many medium-sized brachiopods. The lower part of Unit C of the Neely Member. Lsd. 13-12-20-32W1-34. Scale bar is 1 cm.

Plate 6-8 D: Slabbed core photograph showing a wackestone from the lower part of Unit C of the Neely Member. It is bioturbated, with bioclasts composed of small gastropods, thin-shelled brachiopods and relatively large brachiopod fragments. 14-32-020-30W1-60. Scale bar is 1 cm.

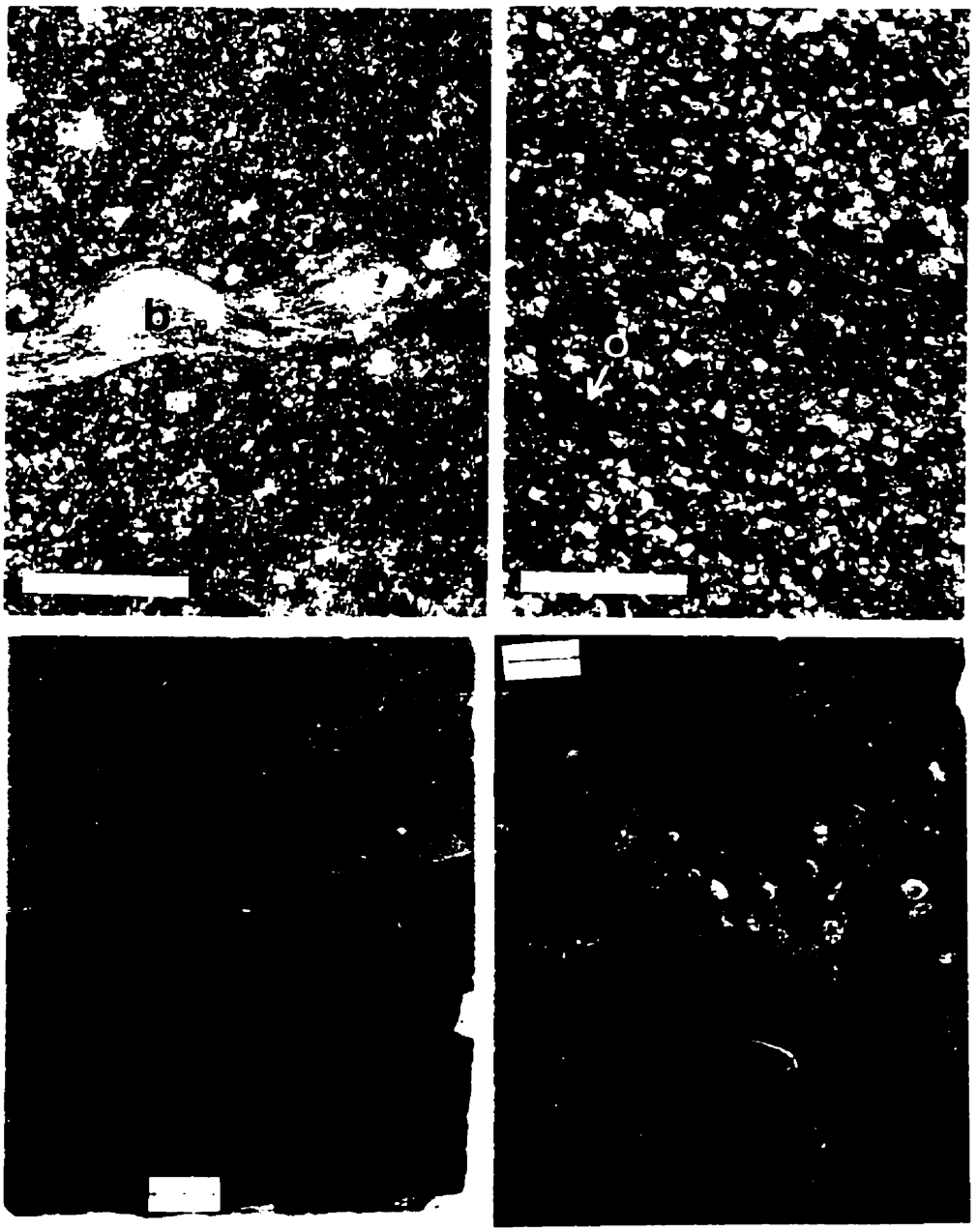
b
c

PLATE 6-9

Plate 6-9 A: Slabbed core photograph showing lime mudstones from the lower part of Unit C of the Neely Member. The upper part of the slabbed core is a dark brown, massive lime mudstone with sparse brachiopod fragments. The lower part of the slabbed core consists of black lime mudstone, which contains small *Chondrites* and remains of fine laminations. Additionally, very small anhydrite nodules (a) are present in both the black and dark brown lime mudstones. Lsd. 14-32-020-30W1-62. Scale bar is 1 cm.

Plate 6-9 B: Slabbed core photograph showing black lime mudstone from the lower part of Unit C of the Neely Member. It contains exclusively small *Chondrites*, with a stromatoporoid debris (s) close to the base of the slabbed core. Lsd. 13-12-22-32W1-32. Scale bar is 1 cm.

Plate 6-9 C: Slabbed core photograph showing small *Chondrites* in a black lime mudstone, from the lower part of Unit C of the Neely Member. Lsd. 4-2-22-31W1-7. Scale bar is 1 cm.

Plate 6-9 D: Plane-light photomicrograph of black lime mudstone from the lower part of the Neely Member. It shows some *Chondrites* burrows that are filled with dolomite. Lsd. 4-2-22-31W1. Scale bar is 1 mm.

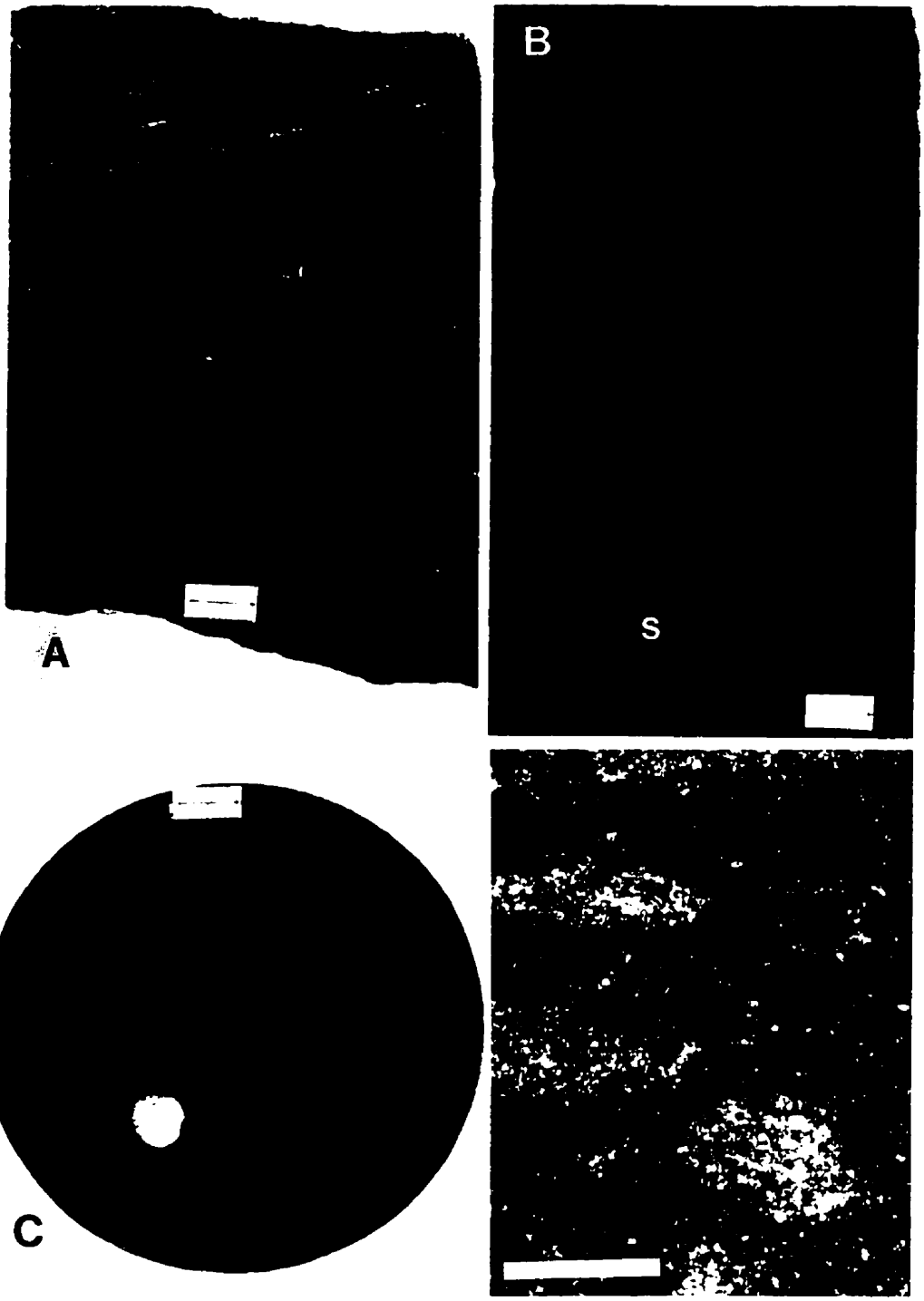
A
B
S
C

PLATE 6-10

Plate 6-10 A: Plane-light photomicrograph of black lime mudstone from the lower part of Unit C of the Neely Member. It is composed of micrite, dolomite and organic matter, with a large stromatoporoid fragment (s). Lsd. 13-12-22-32W1-32. Scale bar is 1 mm.

Plate 6-10 B: Slabbed core photograph showing contact between massive brown lime mudstone and black laminated lime mudstone. The latter is characterized by alternation of carbonate- and organic-rich laminae. Lsd. 16-29-22-30W1-3A. Scale bar is 3 cm.

Plate 6-10 C: Slabbed core photograph showing a black laminated lime mudstone from the lower part of Unit C of the Neely Member. Fragments of stromatoporoid (s) and robust brachiopods (b) are embedded within the laminae. Lsd. 4-2-22-31W1-6. Scale bar is 3 cm.

Plate 6-10 D: Plane-light photomicrograph of black laminated lime mudstone from the lower part of Unit C of the Neely Member. It is characterized by alternation of carbonate- and organic-rich laminae. Lsd. 4-2-22-31W1-6. Scale bar is 1 mm.

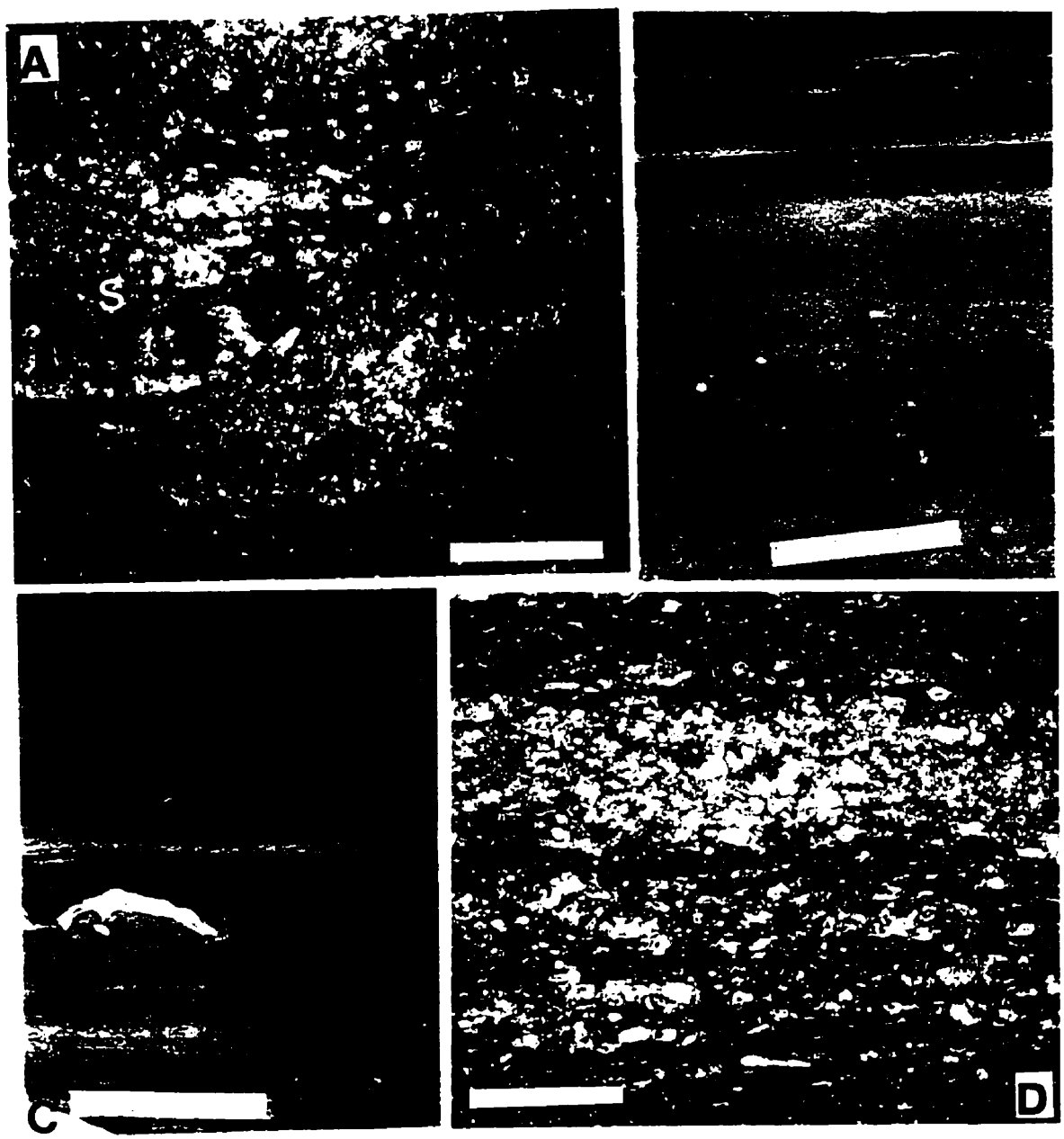
A
S
C
D

PLATE 6-11

Plate 6-11 A: Plane-light photomicrograph showing a carbonate-rich lamina in a black laminated lime mudstone from the lower part of Unit C of the Neely Member. It is composed predominantly of foraminifera (?). Lsd. 4-2-22-31W1-6. Scale bar is 0.5 mm.

Plate 6-11 B: Plane-light photomicrograph showing an organic-rich lamina in a black laminated lime mudstone from the lower part of Unit C of the Neely Member. It is composed of organic matter, micrite and foraminifera (?). Lsd. 4-2-22-31W1-6. Scale bar is 0.5 mm.

Plate 6-11 C: Plane-light photomicrograph of the same black laminated lime mudstone as Plate 6-11 B. In the lower part of the photomicrograph there are abundant dolomitic clasts, which are probably of terrigenous origin. Lsd. 4-2-22-31W1-6. Scale bar is 0.5 mm.

Plate 6-11 D: Crossed-polarized photomicrograph showing terrigenous dolomitic clasts in the black laminated lime mudstone from the lower part of Unit C of the Neely Member. Some dolomitic clasts are polycrystalline (p) and well rounded. Lsd. 4-2-22-31W1-6. Scale bar is 0.25 mm.

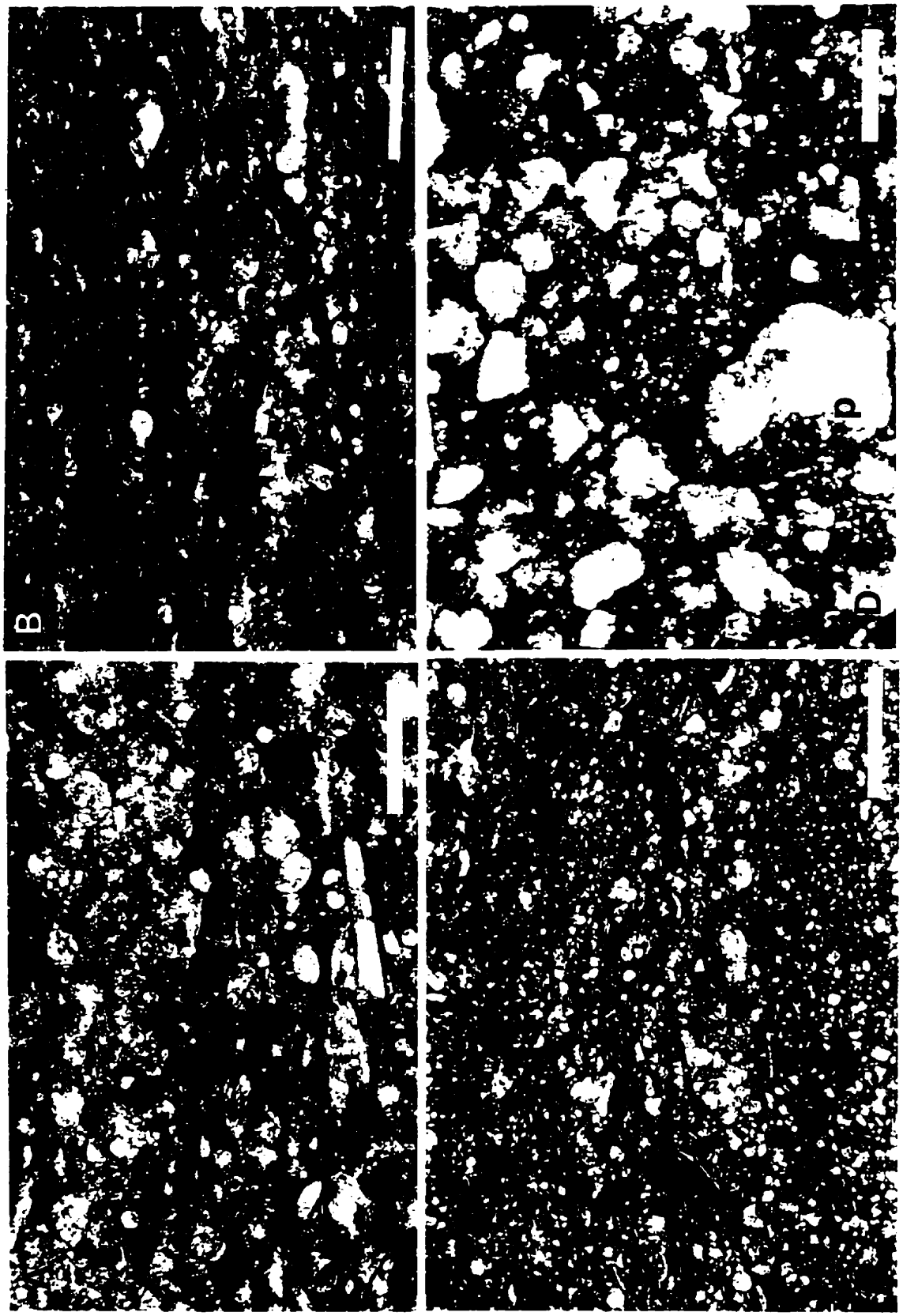
B
D

PLATE 6-12

Plate 6-12 A: Slabbed core photograph showing a gastropod wackestone (w) in the lower part, a microbially-laminated dolostone (m) in the middle, and a nodular anhydrite (a) layer at the top. Unit C of the Neely Member. Lsd. 4-2-21-30W1-7. Scale bar is 1 cm.

Plate 6-12 B: Slabbed core photograph showing a fenestral dolostone from the upper part of Unit C of the Neely Member. It is characterized by fenestral fabrics, with porosity filled by anhydrite. Additionally, black carbonaceous wisps are present at the top of the slabbed core. Lsd. 14-32-020-30W1-69. Scale bar is 1 cm.

Plate 6-12 C: Slabbed core photograph showing fenestral lime mudstone from the upper part of Unit C of the Neely Member. Some fenestral pores are partly filled or remain open. Lsd. 09-22-023-06W2-12. Scale bar is 1 cm.

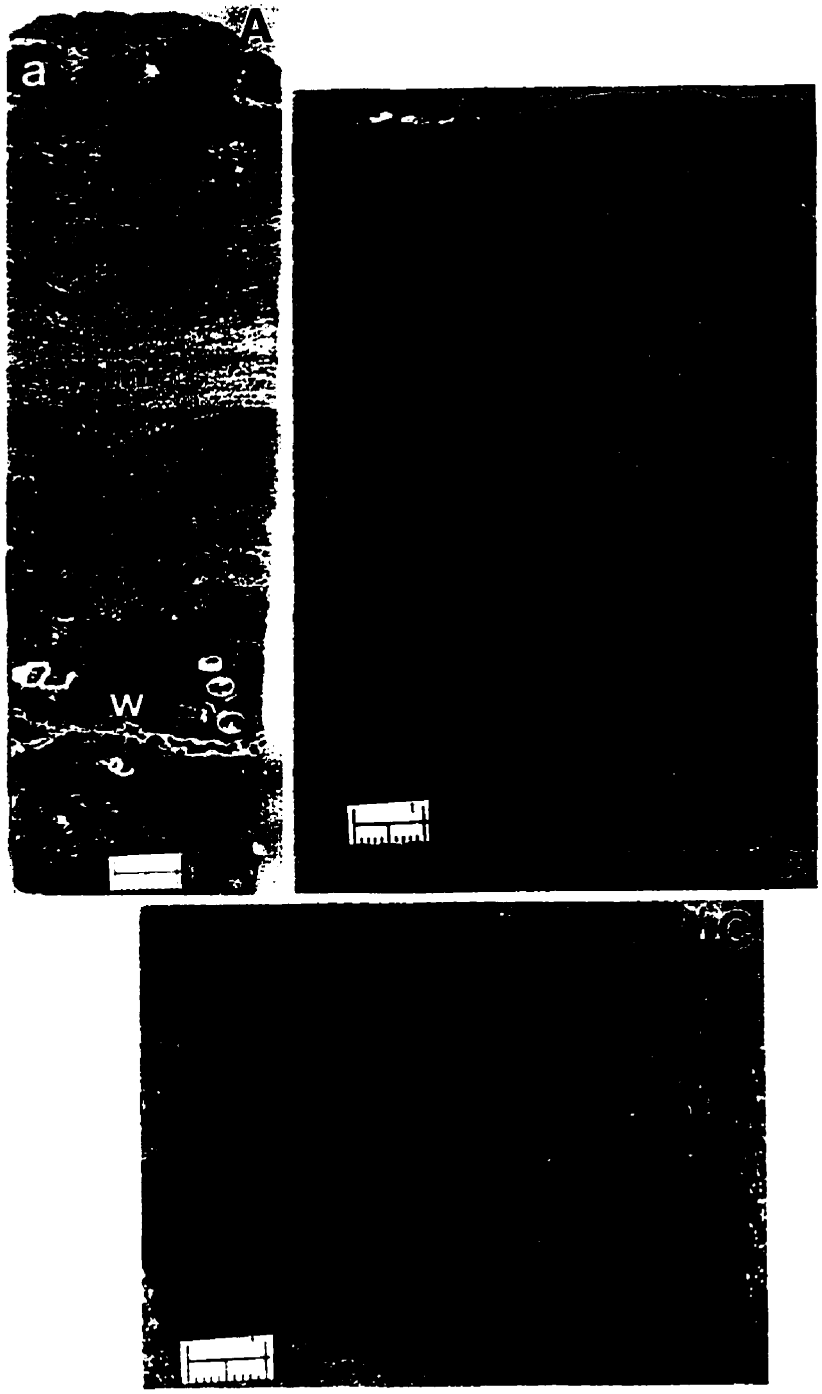
A
a
W

low energy lagoon by Goldhammer *et al.* (1993). The presence of small anhydrite nodules suggests the possibility of hypersaline conditions in the lagoon.

Upper Part of Unit C

Fenestral lime mudstone and dolostone

Fenestral lime mudstone

The fenestral lime mudstone is dark brown and massive (Plate 6-12C). Microbial laminations and desiccation structures are either absent or strongly disrupted. However, these rocks have well-developed fenestral fabrics. The fenestral fabrics display mm-sized, isolated, more or less, bubble-like shapes. Most voids remained unfilled. Some are partially to completely filled with sparry calcite or anhydrite. Microscopic study shows that the rock is composed of micritic calcite with a clotted fabric. It contains abundant remains of microbial filaments, that resemble the radial filament fabric of *Scytonema* (Plate 6-13A & B). In addition, sparse ostracods are present (Plate 6-13C). The presence of fenestrae is a fairly reliable indicator of upper intertidal to supratidal conditions (Shinn, 1968; Shinn *et al.*, 1969) although caution is needed in interpreting environments based mainly upon these distinctive features (Choquette and Pray, 1970). They are most useful as depositional environment indicators when they occur with stromatolites, mudcracks, and storm layers (Shinn, 1983a, 1983b).

Fenestral dolostone

The fenestral dolostone is composed of extremely fine-grained dolomite. It commonly contains irregular black organic wisps (Plate 6-12B). Microbial laminations are normally absent. In contrast, fenestral fabrics are common and are filled with anhydrite (Plates 6-12B, 6-13D). They display isolated, approximately, bubble-like shapes. These fenestral fabrics are concentrated in layers parallel to bedding.

Microbially laminated dolostone

The microbially-laminated dolostone is present at the top of the Neely Member. It contains rare mudcracks and is characterized by well-developed microbial laminations (Plates 6-12A, 6-14 B). These laminations are on a millimetre to centimetre scale. Additionally, no

PLATE 6-13

Plate 6-13 A: Photomicrograph of fenestral lime mudstone that contains abundant remains of microbial filaments. Upper part of Unit C of the Neely Member. Lsd. 09-22-023-06W2-12. Scale bar is 0.5 mm.

Plate 6-13 B: Photomicrograph showing remains of microbial filaments from a fenestral lime mudstone from the upper part of Unit C of the Neely Member. Lsd. 09-22-023-06W2-12. Scale bar is 0.25 mm.

Plate 6-13 C: Photomicrograph of fenestral lime mudstone from the upper part of Unit C of the Neely Member, which has a clotted fabric, with a well-preserved ostracod (o) in the right side of the photograph. Lsd. 09-22-023--06W2-12. Scale bar is 0.5 mm.

Plate 6-13 D: Photomicrograph showing a fenestral fabric (f), with pores filled by anhydrite. The upper part of the Neely Member. Lsd. 14-32-020-30W1-69. Scale bar is 1 mm.

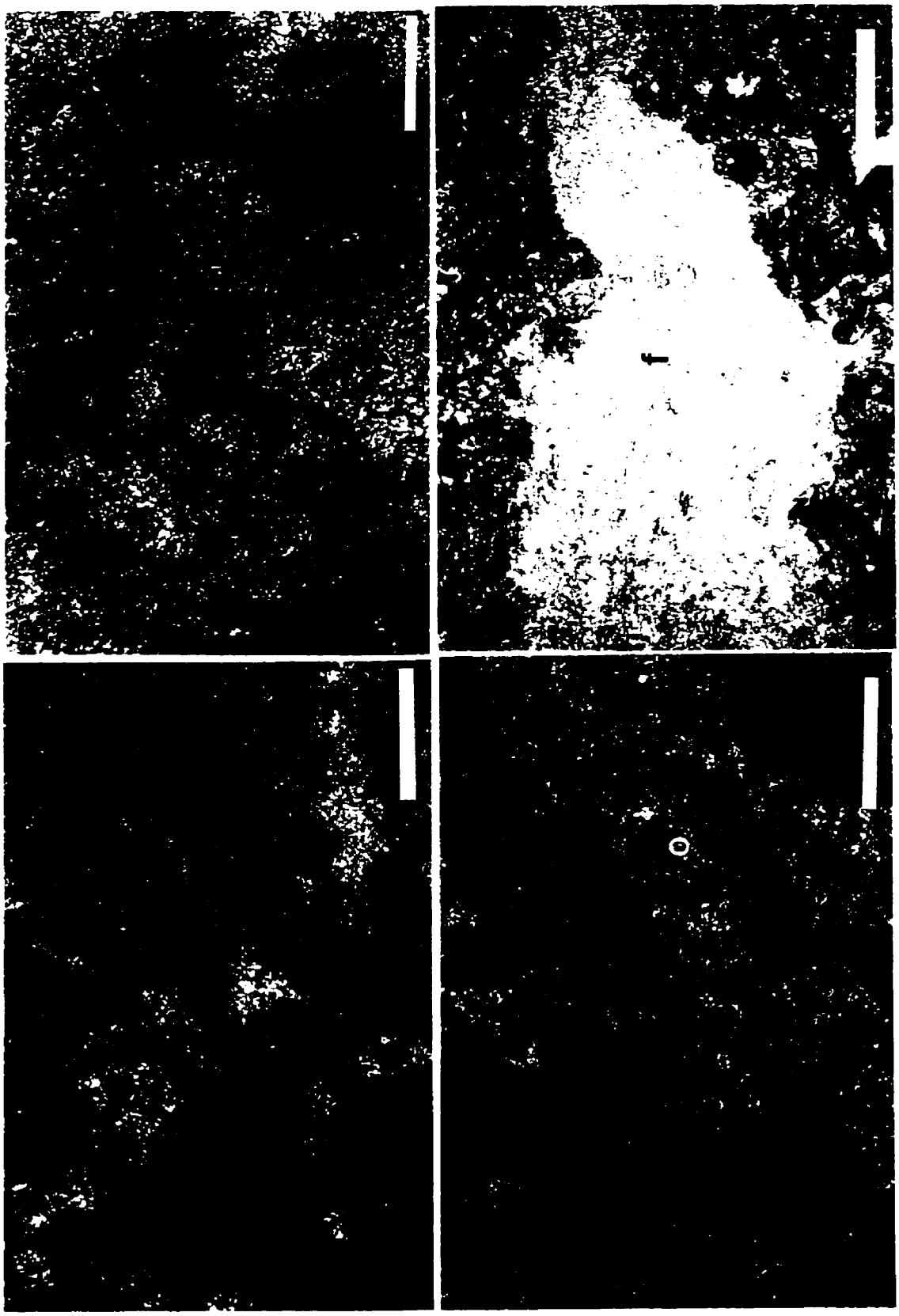

PLATE 6-14

Plate 6-14 A: Slabbed core photograph showing microbially laminated lime mudstone from the upper part of Unit C of the Neely Member. Lsd. 7-10-25-6W2-10. Scale bar is 2 cm.

Plate 6-14 B: Slabbed core photograph showing microbially laminated dolostone from the upper part of Unit C of the Neely Member. It is characterized by wavy, crinkly laminae, which were partially disrupted at the base of the slabbed core. Lsd. 01-02-021-31W1-5A. Scale bar is 1 cm.


A

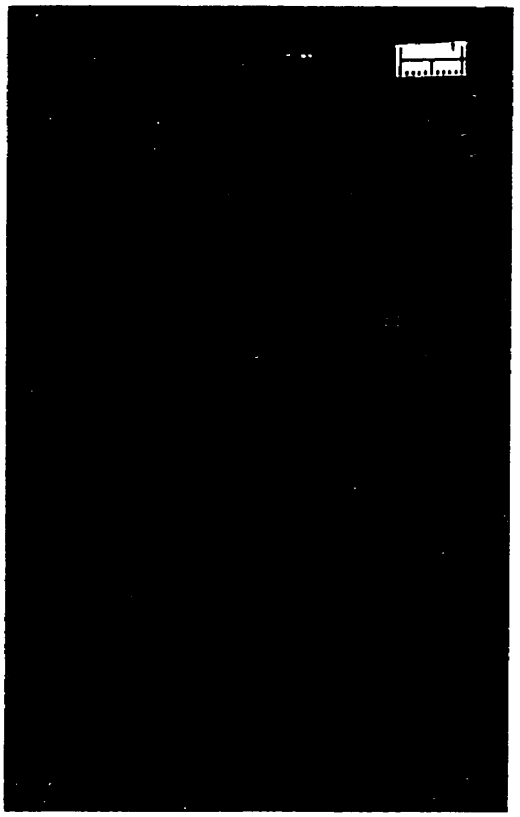

PLATE 6-15

Plate 6-15 A: Plane-light photomicrograph of microbially laminated dolostone from the upper part of Unit C, which displays fan-shaped tufts of elongate anhydrite crystals with probable remains of microbial filaments. Lsd. 01-02-021-31W1-5A. Scale bar is 0.5 mm.

Plate 6-15 B: Plane-light photomicrograph of microbially laminated lime mudstone from the upper part of Unit C of the Neely Member. It is composed mainly of micrite, with dolomite rhombs and anhydrite needles (n) scattered throughout the rock. Lsd. 7-10-25-6W2-10. Scale bar is 1 mm.

Plate 6-15 C: Plane-light photomicrograph of microbially laminated lime mudstone from the upper part of Unit C of the Neely Member. Lsd. 7-10-25-6W2-10. Scale bar is 0.5 mm.

Plate 6-15 D: Slabbed core photograph showing a microbially laminated dolostone (la) that grades upward into an anhydrite layer composed of mosaic of anhydrite nodules (a). The upper part of Unit C of the Neely Member. Lsd. 3-27-38-27W2. Coin diameter is 1.7 cm.

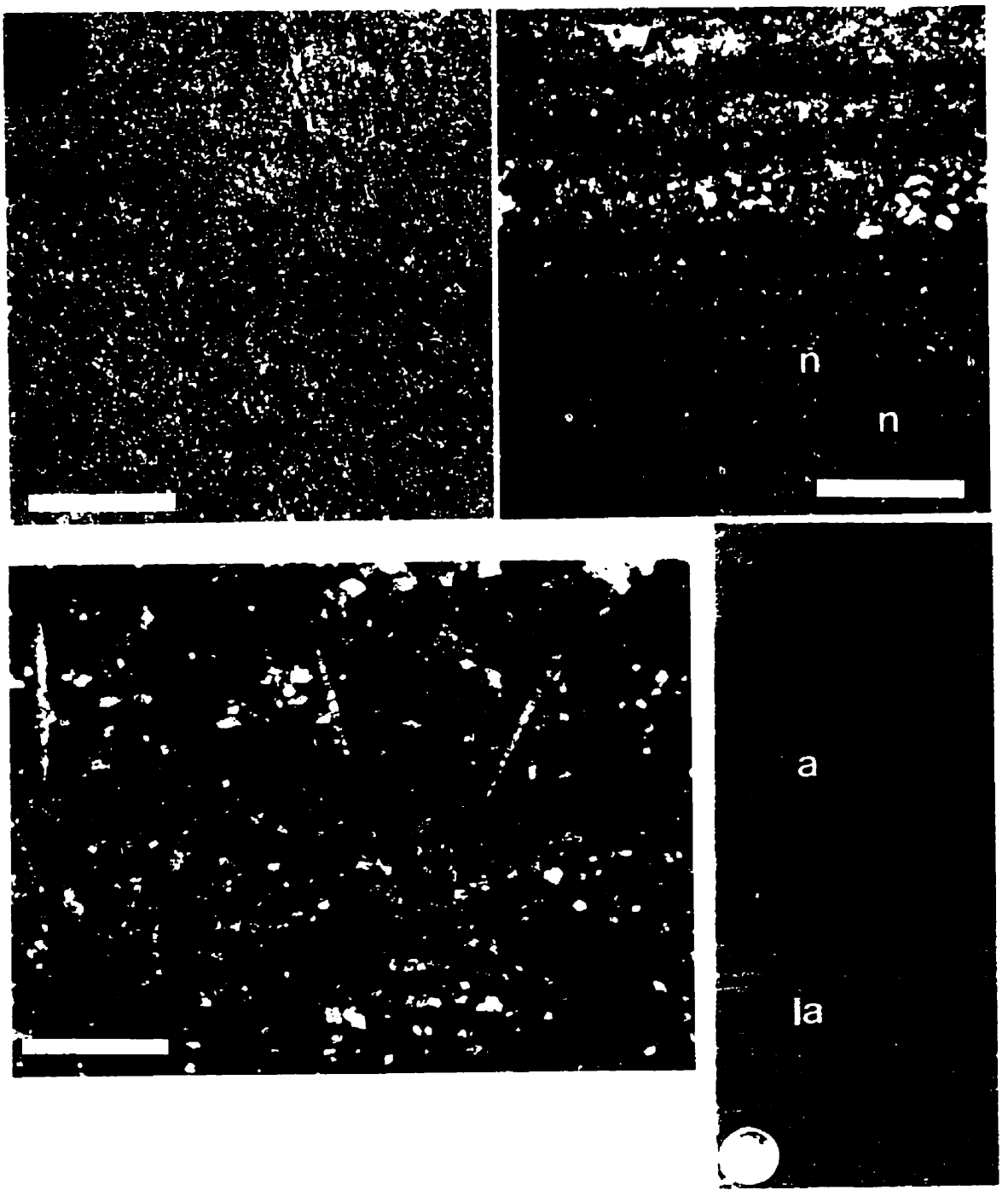
n
n
a
la

skeletal or trace fossils were observed. Petrographic study shows that the dolostone is composed of extremely fine-grained dolomite and fan-shaped tufts of elongate anhydrite crystals with remains of microbial filaments (Plate 6-15A).

Anhydrite nodules are also common in the microbially laminated dolostone (Plate 6-12A). They are bluish and surrounded by carbonate matrix. The nodules are delicately preserved, and grew displacively within the dolomitic sediment. Some anhydrite nodules form coalescing beds. Additionally, thin wavy laminae of anhydrite can be observed in the laminated dolostone. They are normally found in dolomitic sediments that are overlain by anhydrite beds. Microscopically, the anhydrite nodules consist of felted masses of anhydrite needles.

Microbially laminated lime mudstone

The microbially laminated lime mudstone is present in Core 7-10-25-6W2 (Plate 6-14A). This rock has similar colour and lamination to those of the microbially laminated dolostone. However, it is composed mainly of micritic calcite, with dolomite rhombs and anhydrite crystals scattered throughout the rock (Plate 6-15B & C). The dolomite rhombs are evenly distributed in individual laminae, but their amount varies from the laminae to laminae, from sparsely distributed to highly concentrated. The anhydrite forms small elongated, euhedral crystals (Plate 6-15C) that cross-cut the microbial laminae, and are, in turn, cross-cut by dolomite rhombs. This may indicate that the dolomite rhombs postdate the anhydrite formation.

Interpretation

The upper part of Unit C is dominated by microbially laminated lime mudstone and dolostone, and fenestral lime mudstone and dolostone. The former are characterized by fine laminations. Although these laminations are mainly smooth and flat, with little evidence of tufting or convolution, petrographic study shows the common presence of remains of microbial filaments. This suggests that these laminations have a microbial origin. The presence of microbial laminations and paucity of shell fossils suggest a restricted upper intertidal or supratidal environments (Pratt *et al.*, 1992) because in subtidal and lower intertidal areas the lamination may be destroyed by bioturbation (Tucker and Wright, 1990). However, the smoothness of the microbial mats and general

absence of mudcracks in these carbonate rocks indicate that submergence was frequent and exposure was fleeting (Davies, 1970).

The fenestral lime mudstone and dolostone are massive in appearance. Microbial laminations and body fossils are generally absent in these rocks, but they contain well-developed birdseye structures. The birdseye structures are a fairly reliable indicator of supratidal conditions when they are present in predominantly muddy rocks (Shinn, 1983) or are characteristic of the upper intertidal and supratidal zones (Tucker and Wright, 1990). Thus, these rocks probably formed in upper intertidal to supratidal conditions. This interpretation is further supported by the presence of nodular anhydrite and black carbonaceous bands.

Nodular anhydrite

Microbially laminated and fenestral lime mudstones and dolostones are normally overlain by nodular anhydrite. Small scattered nodules are set in a dolomitic matrix or are tightly packed (Plate 6-12A). In some places nodules coalesced to form mosaic and massive anhydrite (Plate 6-15D). Nodular anhydrite is well known from the Trucial Coast (Kinsman, 1966; Shearman, 1966; Butler, 1969) and has been frequently cited as a key toward recognition of ancient, arid sabkha environments (Fuller and Porter, 1969; Wood and Wolfe, 1969; Wilson, 1975).

6.3 Neely Member in Central Saskatchewan

6.3.1 The Contact Between Burr and Neely Members

In central Saskatchewan, the contact between the Neely and Burr members is at the top of a thin limestone bed up to 10 cm thick (Plate 6-16A). The limestone bed is bounded at its top and base by firmgrounds. It contains many shell fragments that are dominated by coarse sand-grade fragments of crinoids, trilobites and brachiopods (Plate 6-17A). Subordinate shell fossils include solitary corals and stick-like stromatoporoids. Rare whole-shelled robust brachiopods are present locally. These shell fragments are intensely corroded and cemented by phosphorite (Plate 6-17A & B).

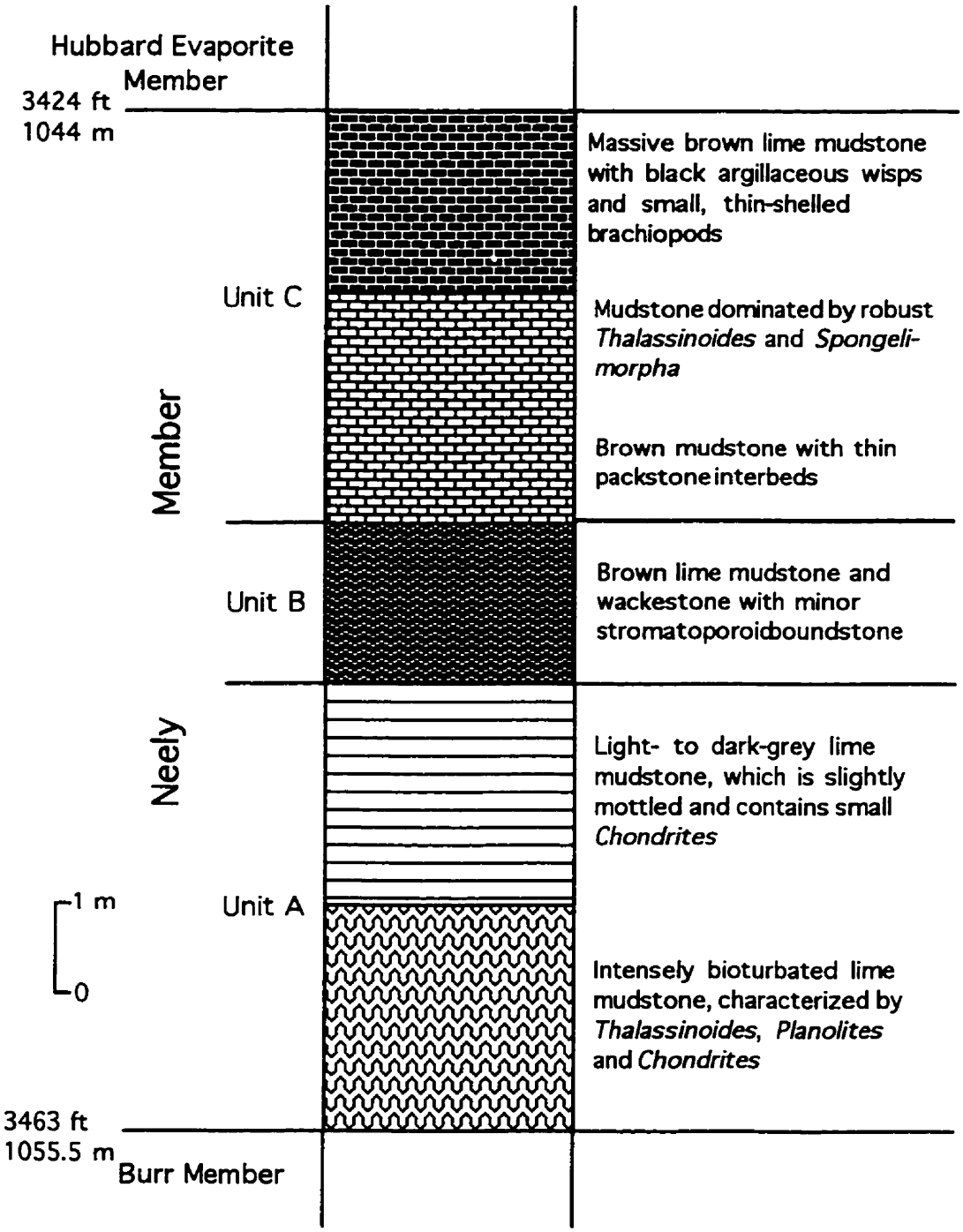

Fig. 6-2. Stratigraphic section of the Neely Member from Well 4-18-35-8W3 in central Saskatchewan.

PLATE 6-16

Plate 6-16 A: Slabbed core photograph showing the contact between the Burr and Neely members in central Saskatchewan. It is a thin limestone bed (b) at the top of the slabbed core that is rich in crinoid debris. It is bounded by firmgrounds (f) at both the top and base. Core was donated by the Cominco potash mine (DDH17). Scale bar is 1 cm.

Plate 6-16 B: Core photograph of lime mudstone from the lower part of Unit A of the Neely Member in central Saskatchewan. It contains robust burrows of *Thalassinoides* (t) Core was donated by the Cominco potash mine (DDH17). Scale bar is 1 cm.

Plate 6-16 C: Slabbed core photograph of lime mudstone from the lower part of Unit A of the Neely Member. It contains *Thalassinoides*, *Planolites* and scattered crinoid debris. Core was donated by the Cominco potash mine (DDH17). Scale bar is 1 cm.

Plate 6-16 D: Slabbed core photograph of lime mudstone from the lower part of the Neely Member. It contains *Thalassinoides*, *Planolites* and *Chondrites*. Both the *Thalassinoides* and *Planolites* are crosscut by *Chondrites*. Core was donated by the Cominco potash mine (DDH17). Scale bar is 1 cm.

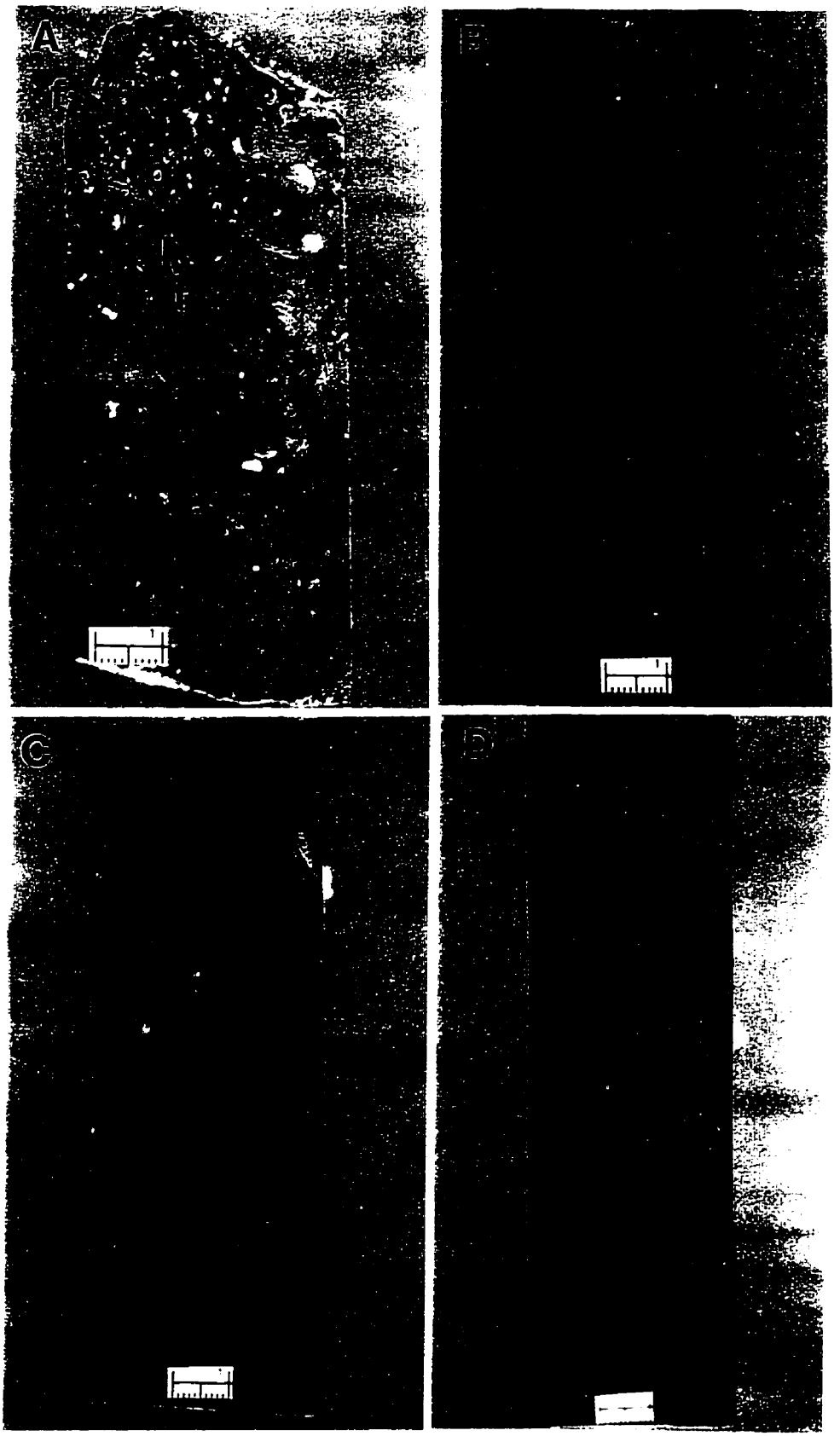
A
B
C
D

PLATE 6-17

Plate 6-17 A: Photomicrograph of the thin limestone at the contact between Burr and Neely members in central Saskatchewan. It is composed predominantly of crinoid and other robust shell fragments. These shell fragments display corroded features and are cemented by phosphorite. Core was donated by the Cominco potash mine (DDH17). Scale bar is 1 mm.

Plate 6-17 B: Photomicrograph of the thin limestone at the contact between the Burr and Neely members in central Saskatchewan (from the same specimen as Plate 6-17 A but different portion of the sample). It is composed predominantly of peloids that are cemented by phosphorites. These peloids display corroded margins. They are probably micritized shell fragments. Core was donated by the Cominco potash mine (DDH17). Scale bar is 1 mm.

Plate 6-17 C: Photomicrograph of lime mudstone from the lower part of Unit A of the Neely Member. It shows burrows of *Chondrites* (c) that are filled with dolomite. Core was donated by the Cominco potash mine (DDH17). Scale bar is 1 mm.

Plate 6-17 D: Photomicrograph of lime mudstone from the upper part of Unit A of the Neely Member. The rock contains sparse but well-preserved ostracods (o). Core was donated by the Cominco potash mine (DDH17). Scale bar is 0.5 mm.

A
C
C
C
C
D
O

Interpretation

The presence of phosphorite, the domination of robust shell fragments, and the intense corrosion of fossil shells indicate a prolonged period of slow sedimentation or non-deposition. Thus, this thin limestone bed represents a condensed section. These characteristics, together with the mid-cycle position of the limestone bed, match the expected attributes of maximum flooding surfaces as defined by Loutit *et al.* (1988). This limestone bed is therefore interpreted to represent the maximum flooding surface of the Dawson Bay Formation, separating the underlying transgressive deposits from the overlying highstand deposits. However, condensed sections are normally thin marine stratigraphic units consisting of pelagic to hemipelagic sediments containing microfossils (Loutit *et al.*, 1988), but microfossils are almost absent in this limestone bed. The interpretation for this phenomenon may be very slow sedimentation rate and intense corrosive water that eventually dissolved all microfossils.

6.3.2 The Neely Member

In central Saskatchewan, the Neely Member has an average thickness of 15 m and varies from 9 to 18 m thick. It is about 11.5 m thick in Core 4-18-35-8W3 and can be divided into three units, termed here Unit A, B and C, from base to top (Fig. 6-2).

Unit A

Unit A lies directly above the Burr-Neely contact. It was called argillaceous carbonate by Dunn (1982) and Ahlstrom (1992). They suggested that it contains a greater argillaceous content than the underlying carbonate rocks. Unit A is divided into lower and upper parts.

Lower Part of Unit A

The lower part of Unit A ranges from 1.5 to 4.5 m thick. It is about 2.5 m thick in Core 4-18-35-8W3. It is composed of intensely bioturbated lime mudstone that includes *Thalassinoides*, *Planolites* and *Chondrites*, with *Thalassinoides* as the principal traces (Plate 6-16B, C & D).

Thalassinoides are primarily horizontal and appear to have undergone slight to moderate compaction (Plate 6-16B & C). Most *Thalassinoides* are 8 to 12 mm in diameter. Some

are up to 2 cm in diameter. They show cylindrical to elliptical cross sections. However, the three-dimensional geometry of *Thalassinoides* is difficult to evaluate, owing to the lack of large bedding plane exposures. Branching is evident in two-dimensional view afforded by vertical core surfaces (Plate 6-16B). This feature distinguishes them from *Planolites*. Regular branching with Y- or T-shaped bifurcations is locally observed. Burrows swell at branch junctions. Some are composed of superimposed tunnels. The walls of the burrows are smooth and unlined. The *Thalassinoides* may be present alone or associated with *Planolites* and *Chondrites*. Where the *Thalassinoides* are found alone, they are discrete, with distinct boundaries. If they are present with *Planolites* and *Chondrites*, the *Thalassinoides* have diffuse boundaries, and are cross-cut by *Planolites* and *Chondrites* (Plate 6-16D).

Chondrites appear as isolated horizontal to subhorizontal blebs on vertical surfaces (Plate 6-16D). Branching is evident in both horizontal and vertical planes. The burrow boundaries are typically smooth. Burrow fills appear structureless and are lighter than surrounding sediment. The diameter of the *Chondrites* ranges from 1 to 2 mm. They are subhorizontal to subvertical. Although *Chondrites* are predominant in some horizons, they are not found alone but associated with *Planolites* and *Thalassinoides*.

Planolites are normally less than 5 mm in diameter and are characterized by simple, unbranched burrows (Plate 6-16C). These burrows are primarily horizontal to subhorizontal, but steeply inclined forms are also present. They are light grey and accompany *Thalassinoides* and *Chondrites*, but most commonly with *Chondrites*. Where they occur with *Thalassinoides*, they are generally distinct and cross-cut the latter. Where they are associated with *Chondrites*, they are normally less distinct than the *Chondrites*. These relationships suggest that the *Planolites* were produced after the *Thalassinoides*, but before the *Chondrites*.

In places, the lime mudstone was extensively bioturbated. It displays a homogeneous to faintly burrow-mottled appearance. Detailed core examination reveals the exclusive presence of *Chondrites*, but these are larger than 1 mm in diameter.

Microscopic study shows that the lime mudstone in the lower part of Unit A is composed of micrite (Plate 6-17C), with scattered thin-shelled brachiopods and crinoid fragments. It is partially to almost completely dolomitized. The dolomitization in the fills of the burrows is generally more pervasive than the surrounding matrix (Plate 6-17C). It is noteworthy

that in some horizons, although only *Chondrites* are present, dolomite not only occurs in the fills of the burrows but also in the surrounding matrix. This may indicate that the surrounding matrix had also been pervasively burrowed. Therefore, the exclusive presence of the *Chondrites* may represent deep-penetrating secondary traces, but not dysaerobic conditions.

Interpretation

The presence of *Thalassinoides*, *Planolites* and *Chondrites* indicates a *Cruziana* ichnofacies. This ichnofacies is most characteristic of moderate energy levels in shallow waters below fair weather wave base but above storm wave base, to low energy levels in deeper, quieter waters (Pemberton *et al.*, 1992). Because the lime mudstone is composed of micrite and is characterized by small, thin-shelled fossils, a relatively deep and quiet water environment is suggested for this part. The intensive bioturbation indicates slow sedimentation, which is also characteristic of *Cruziana* ichnofacies. However, the presence of *Thalassinoides* throughout the unit may indicate that the sediment was deposited in a well-oxygenated environment. The absence of discontinuity surface suggests a more or less continuous deposition with little change of depositional conditions.

Upper Part of Unit A

The upper part of Unit A is about 2.5 m thick in Core 4-18-35-8W3. It is composed of light- and dark-grey lime mudstones, which are massive or slightly mottled (Plate 6-18A). However, careful examination shows that they contain small *Chondrites* (Plate 6-18B). They are about 1 mm in diameter and are found exclusively in some horizons. In places, sparse, relatively large burrows, probably *Thalassinoides* or *Planolites*, are observed, but they are not distinct enough to be identified. Furthermore, sparse, thin-shelled brachiopods, ostracods and crinoid debris are found in the lime mudstones (Plate 6-17D). The brachiopods are generally well preserved, with a length of 2-4 mm. They are scattered throughout the rocks. Close to the top of this part, several indistinct firmgrounds appear. The top of Unit A is characterized by a distinct firmground, which is penetrated by large burrows. The burrows are filled with brown carbonate sediment, intraclasts, crinoid debris and medium-sized brachiopods.

PLATE 6-18

Plate 6-18 A: Slabbed core photograph showing the lime mudstone from the upper part of Unit A of the Neely Member in central Saskatchewan. The rock is only slightly bioturbated. Core was donated by the Cominco potash mine (DDH17). Scale bar is 1 cm.

Plate 6-18 B: Photomicrograph of lime mudstone from the upper part of Unit A of the Neely Member in central Saskatchewan. It shows sparse ostracods (o) and *Chondrites* (c) burrows. Core was donated by the Cominco potash mine. Scale bar is 1 mm.

Plate 6-18 C-D: Detailed core photograph showing Unit C of the Neely Member from central Saskatchewan. **Plate 6-18 C**: Its lower part, composed of lime mudstone with thin packstone interbeds, is overlain by lime mudstone characterized by robust burrows of *Thalassinoides* and *Spongeliomorpha*, and firmgrounds. This, in turn, grades upward into lime mudstone with argillaceous wisps and small, thin-shelled brachiopods. **Plate 6-18 D**: The lower part is composed of lime mudstone with black argillaceous wisps and small, thin-shelled brachiopods. The upper part consists of microbially laminated dolostone and anhydrite layers composed of an anhydrite mosaic that, in turn, grades upward into laminated anhydrite of the Hubbard Evaporite Member. Lsd. 4-18-35-8W3. (One core box is 0.76 m long and core diameter is 10.1 cm.)

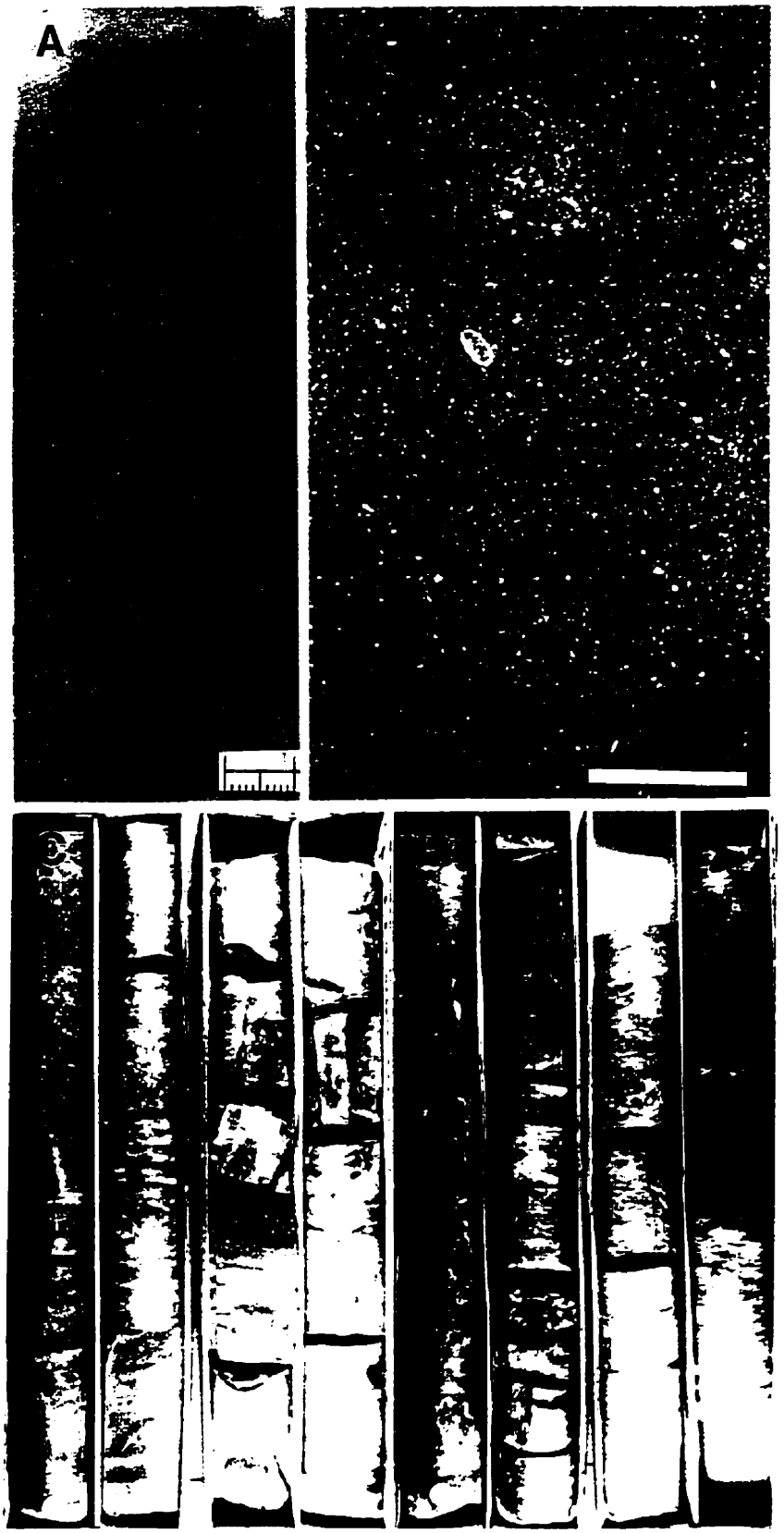
A

Interpretation

In contrast to the lime mudstone in the lower part of Unit A, the lime mudstone in the upper part is dominated by trace fossil *Chondrites*, with possible *Planolites* and *Thalassinoides* present only locally. This may indicate an oxygen-restricted, relatively deep water environment. However, the appearance of indistinct firmgrounds close to the top of the unit indicates an overall shallower water condition. The presence of a distinct firmground at the top of the unit further supports this interpretation.

Unit B

Like Unit B of the Neely Member in southeastern Saskatchewan, Unit B of the Neely Member in central Saskatchewan is also composed of stromatoporoid wackestone, floatstone and boundstone. It is about 1.8 m thick in Core 4-18-35-8W3, but stromatoporoids are not abundant in this core. In contrast, they are well developed in a core donated by the Cominco potash mine (both cores are from the same locality). The base of Unit B is a wackestone that is composed of bioclasts and black carbonate matrix. The bioclasts are dominated by solitary rugose corals and *Thamnopora*, with subordinate medium-sized brachiopods, small dendroid and irregular encrusting stromatoporoids, and crinoid debris. The matrix is micrite, which is partially dolomitized and rich in bituminous matter. Additionally, small *Chondrites* are abundant in the matrix.

This part is followed by a carbonate bed composed mainly of laminar stromatoporoids, solitary rugose corals and *Thamnopora* (Plate 6-19A). The stromatoporoids are 1 to 2 cm thick and are preserved *in situ*. Accessory fossils include crinoid debris, brachiopods and gastropods. The sediment surrounding the shell fossils is composed of sand- to pebble-sized bioclasts and micrite. In the middle part, the boundstone is composed of low domical stromatoporoids (Plate 6-19B & C). In the upper part, stromatoporoids are dominated by high domical forms (6-19D) up to 20 cm high. These stromatoporoids often used corals as substrates. Toppled stromatoporoids are locally present. Additionally, reworked stromatoporoid fragments were found in the matrix surrounding the stromatoporoids. The surrounding matrix is composed of dark brown to black dolomitized micrite. Sparry calcite cement is absent and no framework structure has ever been observed.

PLATE 6-19

Plate 6-19 A-D: Core photograph showing representative types of stromatoporoids from the lower, middle and upper parts of Unit B of the Neely Member in central Saskatchewan. **Plate 6-19 A**: Core photograph showing laminar stromatoporoids from the lower part of Unit B. **Plate 6-19 B & C**: Core photograph showing low domical stromatoporoids from the middle part of Unit B. **Plate 6-19 D**: Core photograph showing high domical stromatoporoids from the upper part of Unit B. Core was donated by the Cominco potash mine. Scale bar is 1 cm.

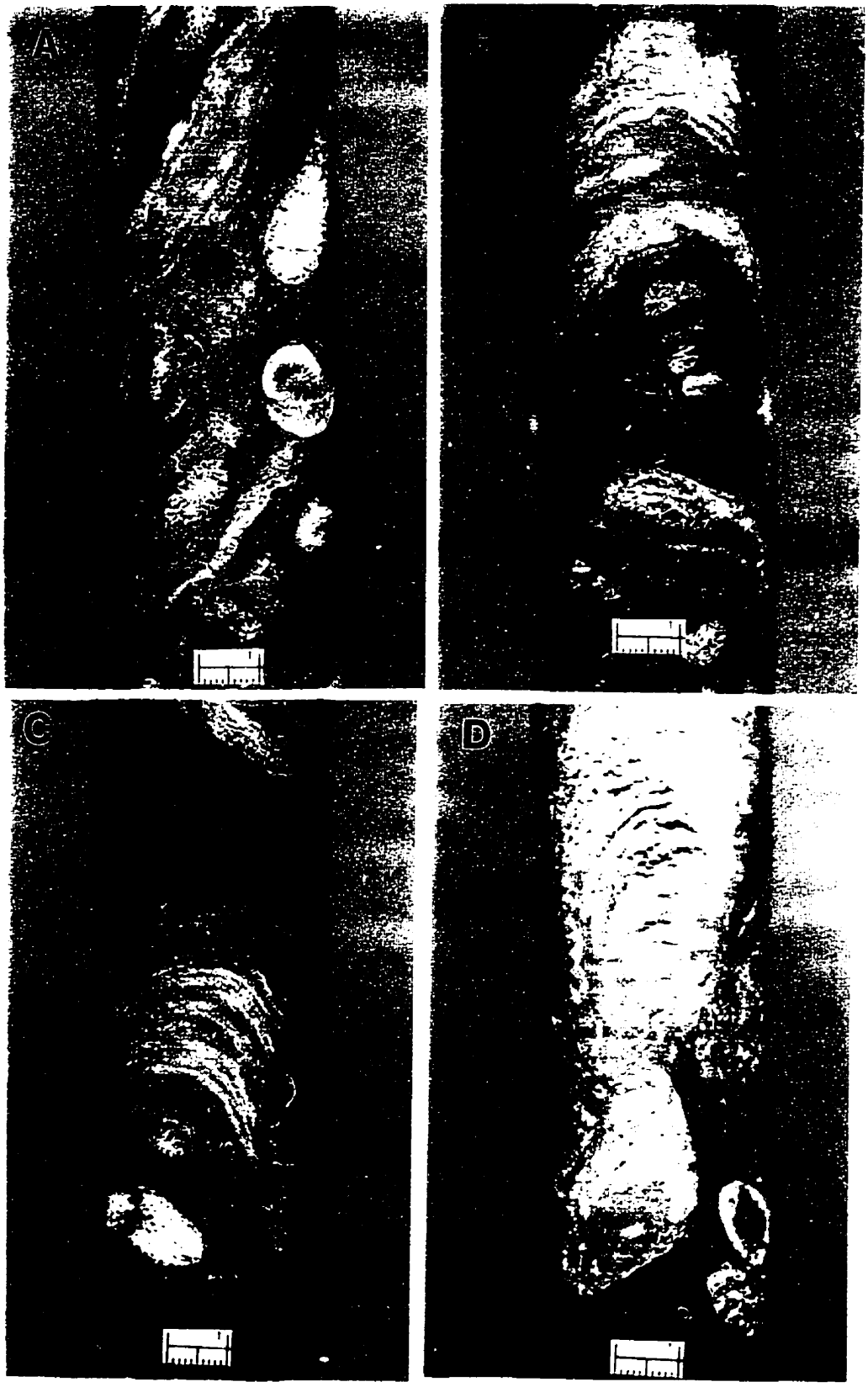
A
C
D

Interpretation

Despite being much thinner, Unit B of the Neely Member in central Saskatchewan is also characterized by an upward transition of stromatoporoid types from dendroid through laminar to high domical stromatoporoids, which is similar to that in southeastern Saskatchewan. This vertical transition indicates an upward-shallowing depositional environment.

Unit C

Unit C is separated from Unit B by a distinct firmground. It is about 4.6 m thick in Core 4-18-35-8W3, which is composed of lime mudstone, bioclastic wackestone and packstone. It can be subdivided into lower and upper parts.

The Lower Part

The lower portion of the lower part of Unit C is composed of brown lime mudstones, with light grey packstone interbeds (Plate 6-18C). The lime mudstone contains small, thin-shelled brachiopods, foraminifera and crinoid debris, which are scattered throughout the rock. Indistinct trace fossils are abundant and are dominated by small *Chondrites*. The packstone is only several mm thick and is composed of skeletal grains and carbonate matrix. The skeletal grains are small, thin-shelled brachiopods, gastropods, foraminifera and crinoid fragments. The upper portion of the lower part consists of light grey to brown lime mudstone with abundant *Thalassinoides* (Plates 6-18C, 6-20A, C & D). Most are horizontal burrows with vertical connections; some burrows show distinct wall scratchings that indicate that those burrows are *Spongeliomorpha*.

Interpretation

The dominance of the lime mudstone with small body and trace fossils in the lower portion of the lower part of Unit C indicates an overall quiet, relatively deep water environment. The thin packstones reflect occasional higher energy intervals. The appearance of robust *Thalassinoides* and *Spongeliomorpha* in the upper portion signifies a general increase in water energy, probably linked to decreasing water depth. This is supported by the presence of the firmground at the top of the lower part. Therefore, it can

PLATE 6-20

Plate 6-20 A: Slabbed core photograph showing lime mudstone from the lower part of Unit C of the Neely Member in central Saskatchewan, which is characterized by robust burrows of *Thalassinoides*. Lsd. 4-18-35-8W3-11. Scale bar is 1 cm.

Plate 6-20 B: Slabbed core photograph showing a firmground (f) from the lower part of Unit C of the Neely Member in central Saskatchewan. Lsd. 4-18-35-8W3-12. Scale bar is 1 cm.

Plate 6-20 C: Photomicrograph of slabbed core shown in Plate 6-20 A. It displays a non-bioturbated part of the lime mudstone that is composed of micrite and sparse shell fossils. Lsd. 4-18-35-8W3-11. Scale bar is 1 mm.

Plate 6-20 D: Photomicrograph of slabbed core shown in Plate 6-20 A. It shows a bioturbated part of the lime mudstone. The burrow is filled with dolomite. Lsd. 4-18-35-8W3-11. Scale bar is 1 mm.

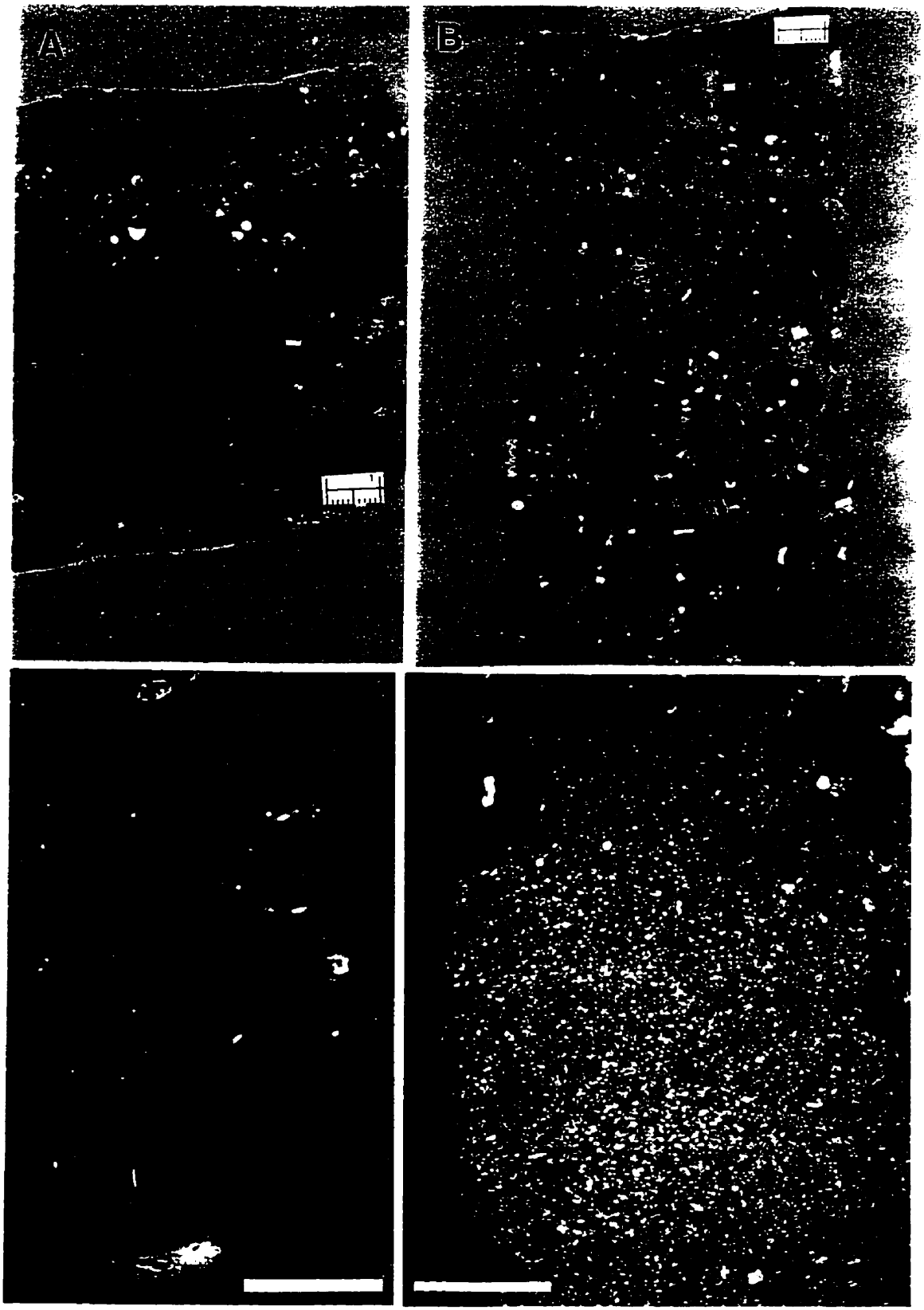
A
B

PLATE 6-21

Plate 6-21 A: Slabbed core photograph showing a lime mudstone from the top of Unit C of the Neely Member. It contains small, thin-shelled brachiopods and argillaceous wisps. Lsd. 4-18-35-8W3. Coin diameter is 1.7 cm.

Plate 6-21 B: Slabbed core photograph showing a microbially laminated dolostone from the top of Unit C of the Neely Member. Lsd. 4-3-12-34-1W3-7. Scale bar is 1 cm.

Plate 6-21 C & D: Photomicrograph showing small, thin-shelled brachiopods from the lime mudstone in the upper part of Unit C of the Neely Member. Brachiopods are normally the only body fossils in the rock. Thin-section made from core donated by the Cominco potash mine (DDH17). Scale bar is 1 mm.

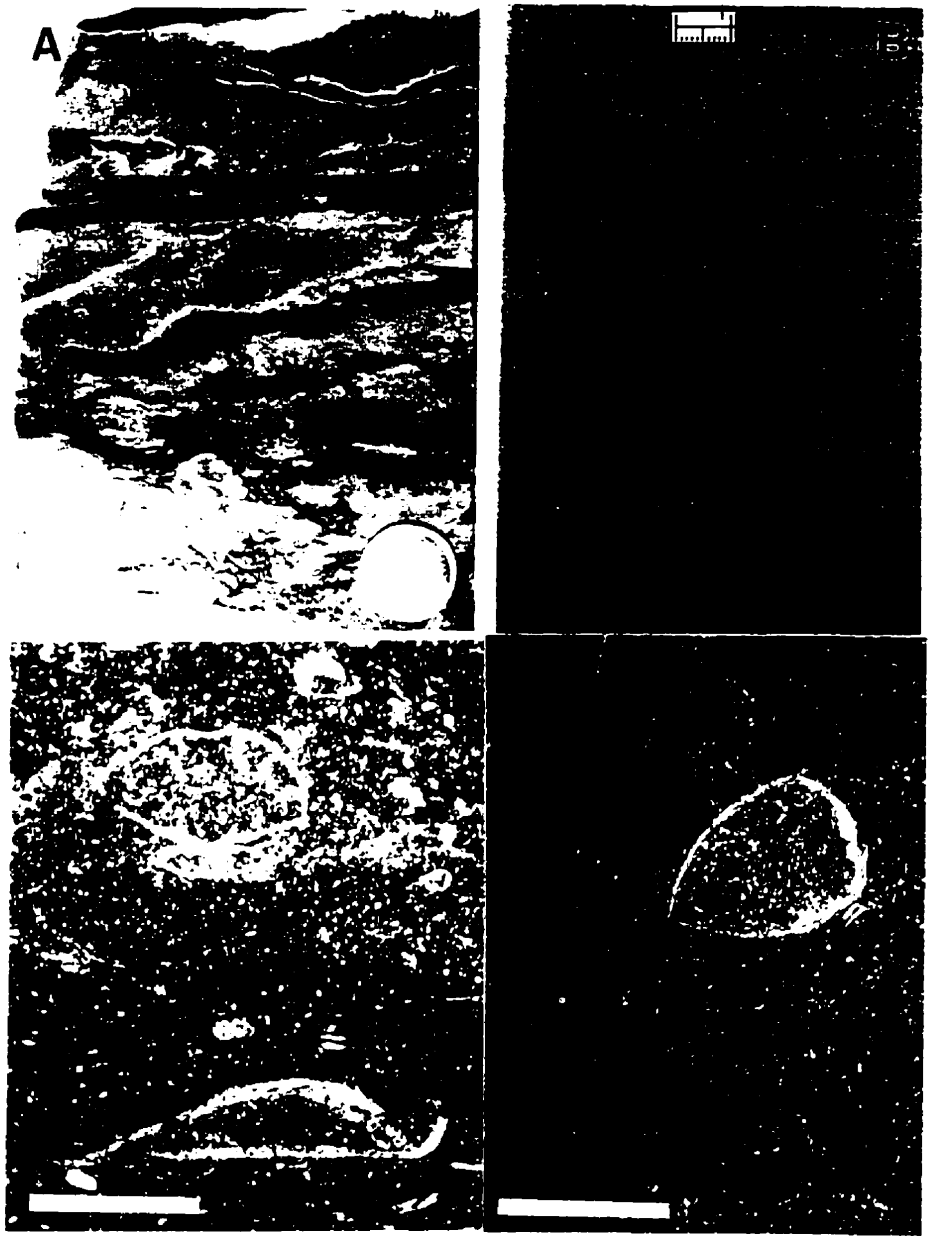
A

be concluded that the lower part of Unit C represents an upward-shallowing succession bounded by a marine flooding surface.

The Upper Part

The upper part of Unit C is composed of massive brown lime mudstones and black argillaceous wisps (Plates 6-18D, 6-21A). The latter increase in abundance at the top of the unit. The lime mudstone comprises micrite with scattered bioclasts, which are dominated by brachiopods with lesser foraminifera and crinoid debris. The brachiopods are extremely small and thin-shelled, only 1 to 2 mm in length. They are well preserved (Plate 6-21C & D).

Interpretation

The massive appearance of the lime mudstone and total lack of any physical sedimentary structures, the predominance of micrite and the restricted small, thin-shelled fossil assemblage suggest a protected low-energy environment for the upper part of Unit C. The presence of argillaceous sediment also indicates that the depositional environment was strongly influenced by terrigenous deposits, probably signifying a decrease in water depth. A similar brachiopod-dominated lithofacies from the Middle Devonian Muscatatuck Group in southeastern Indiana was interpreted as restricted marine or lagoonal facies (Leonard, 1996).

The Top of the Neely Member

The top of the Neely Member consists of microbially laminated dolostone, which is overlain by massive anhydrite composed of a mosaic of nodular anhydrite (Plate 6-18 D). These facies indicate upper intertidal to supratidal environments.

6.4 Discussion

The contact between the Neely and Burr members in southeastern Saskatchewan is one of the most pronounced discontinuity surfaces in the Dawson Bay Formation. Previous workers (Dunn, 1982a, 1982b; Ahlstrom, 1992) suggested that this contact was a hardground, but the present study shows that it is penetrated only by firmground burrows. This indicates that it is not a hardground but a firmground. Additionally, the

mineral impregnation at the surface of the firmground and on the burrow walls suggests a prolonged phase of non-deposition, or at least an extremely low sedimentation rate, which allowed chemical reactions to take place at the depositional interface (Fursich, 1979). Because such intense mineral impregnation is absent in the other firmgrounds in the Dawson Bay Formation, the firmground between the Neely and Burr members probably represents the longest phase of non-deposition during the deposition of the formation. Such surfaces are commonly associated with maximum water depth during deposition of a sedimentary sequence (Loutit *et al.*, 1988), which suggests that the firmground may represent the maximum flooding surface of the Dawson Bay Formation. This interpretation is supported by the fact that the uppermost part of the Burr Member and lowest part of the Neely Member were deposited in a relatively deep, distal environment.

This interpretation also gains support from the nature of the contact between the Neely and Burr members in central Saskatchewan. Unlike that in southeastern Saskatchewan, the Burr-Neely contact in central Saskatchewan is represented by a condensed section, delimited by two firmgrounds. It is characterized by highly concentrated shell fragments, which are dominated by dissolution-resistant echinoderm debris (Walter, 1985; Brett, 1995). This is typical of maximum marine flooding surfaces (Brett, 1995). These shell fragments are characterized by corrosion pitting, indicative of biogeochemical dissolution processes, and cementation by phosphate. These features all suggest a prolonged phase of non-deposition.

The Burr-Neely contact in central Saskatchewan is characterized by a sharp increase in gamma-ray response (Dunn, 1982a) (Fig. 6-3). The precise cause of the gamma-ray peak is unclear. It is probably due to the presence of uranium in the phosphate cement. U^{4+} may substitute for calcium^{2+} in the carbonate-fluorapatite generally found in marine phosphorites (Durrance, 1986). The chemical conditions required for this type of reaction may be very localised, such as those that exist in hardgrounds (Rider, 1996). A sharp increase in gamma-ray response in sedimentary successions is commonly associated with condensed sections (Loutit *et al.*, 1988), and is often considered synonymous with the maximum flooding surface (Rider, 1996). The gamma ray spike supports the interpretation that the Burr-Neely contact is a condensed section that marks the maximum flooding surface of the Dawson Bay Formation.

The lower part of Unit A of the Neely Member in southeastern Saskatchewan was deposited in a relatively deep, low energy environment, with occasional short phases of

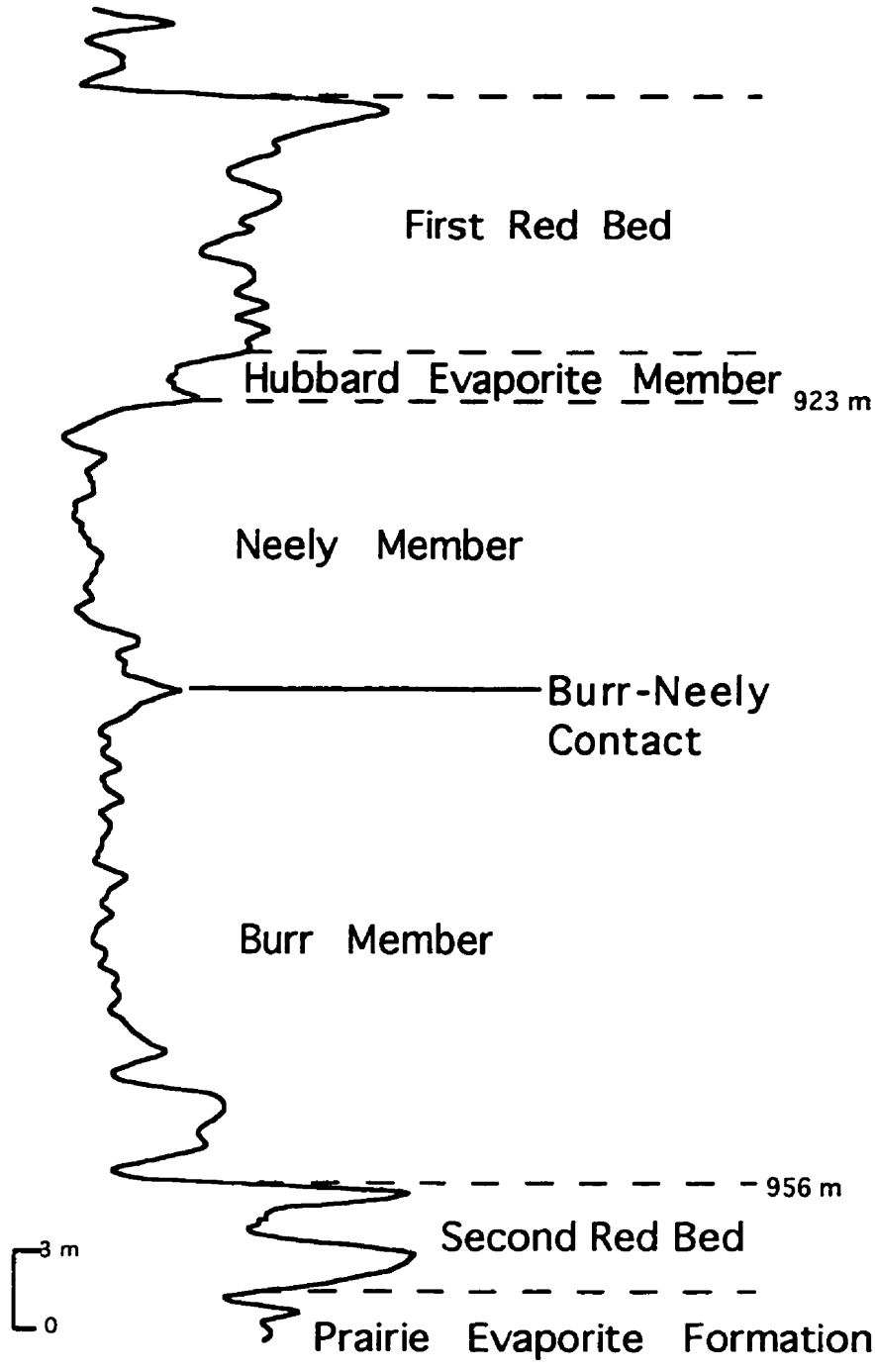

Fig. 6-3. Gamma ray log showing a spike at the Burr-Neely contact, Well 4-18-35-23W2.

higher energy conditions. The upper part of Unit A consists predominantly of bioturbated lime mudstone with well-developed firmground burrows that reflect a slow sedimentation rate. From the lower to the upper portion of the upper part of Unit A, the firmground burrow, *Thalassinoides*, is replaced by *Spongeliomorpha*, and at the top of the unit, the amount of crinoid debris increases abruptly. These features suggest a further decrease in sedimentation rate. This is consistent with sediments deposited during early part of the highstand systems tract, that are characterized by slow sedimentation. A smooth transition between early and late highstand phases has been predicted by most sequence models. Moreover, a gradually increasing rate of sedimentation rate would also be anticipated (Brett, 1995). However, the firmground at the top of Unit A in the Neely Member of southeastern Saskatchewan suggests a phase of non-deposition, in contradiction to the general model of highstand systems tract. A similar phenomenon has been described by Brett (1995) from the Paleozoic sediments of the Appalachian Basin. In the latter example, careful examination of many sequences revealed the development of a distinct discontinuity and a condensed shell bed between the earlier and later parts of the highstand systems tract. These features appear to have developed during an initial rapid phase of sea level fall. It is unclear why sedimentary starvation or condensation should occur during initial regressive events. One possibility is that during forced regression, shallowing brings portions of seafloor within storm base, causing submarine erosion (Brett, 1995).

The succeeding unit of the Neely Member is a stromatoporoid buildup. From base to top, the stromatoporoid types change from laminar stromatoporoids through low domical stromatoporoids to high and extended domical stromatoporoids. A similar vertical zonation of stromatoporoid buildups was found in the Lucas Dolostone (Middle Devonian) on Kelley Island, Ohio (Bjerstedt and Feldmann, 1985) and in the Lower Silurian Hogklint patch reef of Gotland, Sweden (Watts, 1988). It was interpreted to be associated with a change from deep to shallow water conditions, accompanied by a trend from quiet to turbulent water. The fact that from the lower to the upper parts of the stromatoporoid buildup, the toppled stromatoporoids increase significantly and the sediment between the stromatoporoids changes from mud- to coarse sand-size bioclasts, supports this interpretation. It can be concluded that the stromatoporoid unit represents an upward-shallowing facies.

The stromatoporoid unit is, in turn, overlain by dark brown to black carbonate rocks that formed in a shallow, restricted subtidal lagoonal environment. These grade upward into dolomitic limestone and dolostone of intertidal and supratidal environments.

From this evidence, it can be concluded that the Neely Member in southeastern Saskatchewan represents an overall upward-shallowing succession. From base to top, the depositional environment changed from quiet, relatively deep, offshore settings above the maximum flooding surface, through higher energy, shallower water conditions represented by high domical stromatoporoids, to intertidal and supratidal environments. This vertical variation is characteristic of a highstand systems tract. Thus, the Neely Member represents a highstand systems tract deposit.

Although the vertical sedimentary succession of the Neely Member in central Saskatchewan is slightly different from that in southeastern Saskatchewan, its vertical facies change also reflects an overall upward-shallowing trend. The highly bioturbated lime mudstone unit in the lower part of Unit A indicates slow sedimentation. The same trace fossil assemblage occurs throughout the unit, which suggests little change in water depth. It may represent sediment formed by aggradation in the early part of the highstand systems tract. This interpretation is strongly supported by the presence of a maximum marine flooding surface at the base of this unit.

The intensely bioturbated lime mudstone is overlain by a lime mudstone that contains trace fossils which are less distinct. The depositional setting for this part is unclear at this point. It may represent a less oxygenated environment, probably signifying an increase in water depth, or may represent an increased sedimentation rate, reflecting a depositional change from aggradation to progradation. The firmground at the top of the unit indicates shallower water. As noted, it is followed by a stromatoporoid unit that is characterized by an upward change from laminar to high domical stromatoporoids. This biofacies change reflects upward-shallowing. However, in contrast to the sedimentary facies directly overlying the stromatoporoid unit in southeastern Saskatchewan, which was deposited in a restricted lagoonal environment landward of the stromatoporoid facies, the lower part of Unit C in central Saskatchewan seems to have been deposited in an open marine environment. From the base to the top of the lower part of Unit C, the sedimentary rock changes from predominant lime mudstone with thin packstone interbeds, which was deposited in a relatively deep, distal environment, to lime mudstone characterized by robust firmground burrows, which indicates relatively shallow water. Like the lower part, the upper part of Unit C is also composed mainly of lime mudstone. However, its argillaceous content increases significantly, particularly near the top of Unit C. This indicates shallower waters because if other factors remain unchanged, regression usually

leads to an increase flux of clastic sediment. This upward-shallowing interpretation is supported by the presence of microbially-laminated dolostone and nodular anhydrite layers at the top of the unit, which represent depositional settings that range from upper intertidal to supratidal environments.

In conclusion, the Neely Member in central Saskatchewan is composed of two upward-shallowing successions that are separated by a distinct firmground at the top of Unit B. The upper succession was deposited in shallower water than the lower succession. This suggests that they are progradational parasequences. It remains unclear why the Neely Member in southeastern Saskatchewan is composed of a relatively simple upward-shallowing succession, whereas that in central Saskatchewan provides evidence of more sea-level fluctuations.

6.5 Summary

New geological evidence shows that the contact between the Neely and Burr members represents the maximum flooding surface of the Dawson Bay Formation. New evidence also shows that the Neely Member in southeastern Saskatchewan represents an overall upward-shallowing succession. From base to top, the depositional environment changed from quiet, relatively deep, offshore settings, through higher energy, shallower water conditions represented by high domical stromatoporoids, to intertidal and supratidal environments. This vertical variation is typical of a highstand systems tract. Thus, the Neely Member represents a highstand systems tract deposit. In central Saskatchewan, however, the Neely Member is composed of two superimposed upward-shallowing successions. The explanation for this is unclear.

CHAPTER 7

HUBBARD EVAPORITE MEMBER AND FIRST RED BED

7.1 Introduction

The Hubbard Evaporite Member and the First Red Bed are each assigned to different formations. The former is present at the top of the Dawson Bay Formation, whereas the latter forms the lowest part of the Souris River Formation. Although the latter is technically beyond the scope of this study, it is closely related to the Hubbard Evaporite Member, as discussed below.

7.2 The Hubbard Evaporite Member

The Hubbard Evaporite Member was named by Lane (1959), who described it as being the uppermost member of the Dawson Bay Formation, with a thickness of up to 19 m in Core 1-28-24-20W2. The contacts between the Hubbard Evaporite Member and both the underlying Neely Member and overlying First Red Bed are transitional. The distribution of the Hubbard Evaporite Member is much more restricted than the other members of the Dawson Bay Formation. It is present over an area of some 10,000 square miles in central-southeastern Saskatchewan. In northwestern Saskatchewan, the Hubbard Evaporite Member is absent due to non-deposition (Ahlstrom, 1992). In the area where the Hubbard Evaporite Member is absent, the top of the Neely Member is in conformable contact with the First Red Bed of the Souris River Formation.

The depositional environment of the Hubbard Evaporite Member was briefly discussed by Lane (1959), Dunn (1982) and Ahlstrom (1992). Lane (1959) suggested that it was deposited in a barred basin. Ahlstrom (1992) believed that during deposition of the Hubbard Evaporite Member the basin was cut off from normal marine water circulation, but continued to receive a supply of water that was capable of precipitating the evaporites.

In the following sections, the stratigraphic, lithological and sedimentological features of the Hubbard Evaporite Member are described, and its depositional environment is discussed.

7.2.1 Stratigraphy of the Hubbard Evaporite Member

The Hubbard Evaporite Member in southeastern Saskatchewan is represented by the cored section in Well 13-12-22-32W1 (Plate 7-1A to D). It is about 10 m thick at this location. Based on its vertical lithological variation, the Hubbard Evaporite Member is divided here into Units A, B and C, from base to top. Unit A (810.6-812 m) (2659.5-2664.5 ft.) is composed of alternating laminated anhydrite and dolostone (Plate 7-1A). Unit B comprises chaotic mudstone-halite. Some cores from this unit are missing. Geophysical well logs show that the total thickness of the unit is about 2.3 m (808.3-810.6 m) (2652-2659.5 ft.). Unit C consists of massive halite and chaotic mudstone-halite. It is about 6.3 m thick (802-808.3 m) (2632-2652 ft) (Plate 7-1B to D).

The Hubbard Evaporite Member in central Saskatchewan is represented by the cored section in Well 1-2-39-8W3 (Plate 7-2A). There it is composed of clastic anhydrite and laminated anhydrite-dolostone, with a thickness of 1.8 m. No halite rock is present.

7.2.2 Major Rock Types of the Hubbard Evaporite Member

Based on an examination of the core samples, and petrographic study, five lithofacies are recognized in the Hubbard Evaporite Member. They are laminated anhydrite, laminated to thinly bedded dolostone, clastic anhydrite, chaotic mudstone-halite and massive halite.

Laminated Anhydrite

Laminated anhydrite (Plates 7-1A, 7-3C) is present in Unit A of the Hubbard Evaporite Member in southeastern Saskatchewan, where it is interbedded with laminated to thinly bedded dolostone. The rock is olive- to dark-green, and is characterized by wavy laminae. Although most anhydrite laminae are slightly wavy, in places they are completely disrupted by growth of anhydrite nodules. The laminated anhydrite is underlain by supratidal nodular anhydrite and microbially laminated dolostone of the Neely Member, and is overlain by chaotic mudstone-halite of the Hubbard Evaporite Member.

PLATE 7-1

Plate 7-1 A-D: Detailed core photograph showing entire vertical succession of the Hubbard Evaporite Member from Well 13-12-22-32W1. **Plate 7-1 A**: Core photograph showing the uppermost part of the Neely Member and Unit A of the Hubbard Evaporite Member. The latter is composed of laminated anhydrite and dolostone. **Plate 7-1 B**: Core photograph showing Unit B and the lower part of Unit C of the Hubbard Evaporite Member. Unit B is composed of chaotic mudstone-halite (c). Some cores are probably missing in this Unit. The lower part of Unit C consists of massive halite (h). **Plate 7-1 C**: Core photograph showing the middle part of Unit C of the Hubbard Evaporite Member. It is composed of massive halite (h) and chaotic mudstone-halite (c). **Plate 7-1 D**: Core photograph showing the upper part of Unit C of the Hubbard Evaporite Member and the lower part of the First Red Bed. The upper part of Unit C is composed of chaotic mudstone-halite and massive halite. The lower part of the First Red Bed consists of chaotic mudstone-halite and massive mudstone. **Plate 7-1 E**: Core photograph showing the First Red Bed. It consists of massive dolomitic mudstone (m) and brecciated dolomitic mudstone (b), with a thin chaotic, mudstone-halite interbed (c). Lsd. 13-12-22-32W1. (One core box is 0.76 m long and core diameter is 10.1 cm.)


A
B
C
D
E

PLATE 7-2

Plate 7-2 A: Core photograph showing the uppermost part of the Neely Member and the Hubbard Evaporite Member in central Saskatchewan. The uppermost part of the Neely Member is composed of dark brown massive dolostone. The Hubbard Evaporite Member consists of clastic anhydrite and laminated anhydrite-dolostone. Lsd. 1-2-39-8W3. (One core box is 0.76 m long and core diameter is 10.1 cm.)

Plate 7-2 B-D: Core photograph showing the entire vertical succession of the First Red Bed in Well 1-2-39-8W3 of central Saskatchewan. (One core box is 0.76 m long and core diameter is 10.1 cm.)

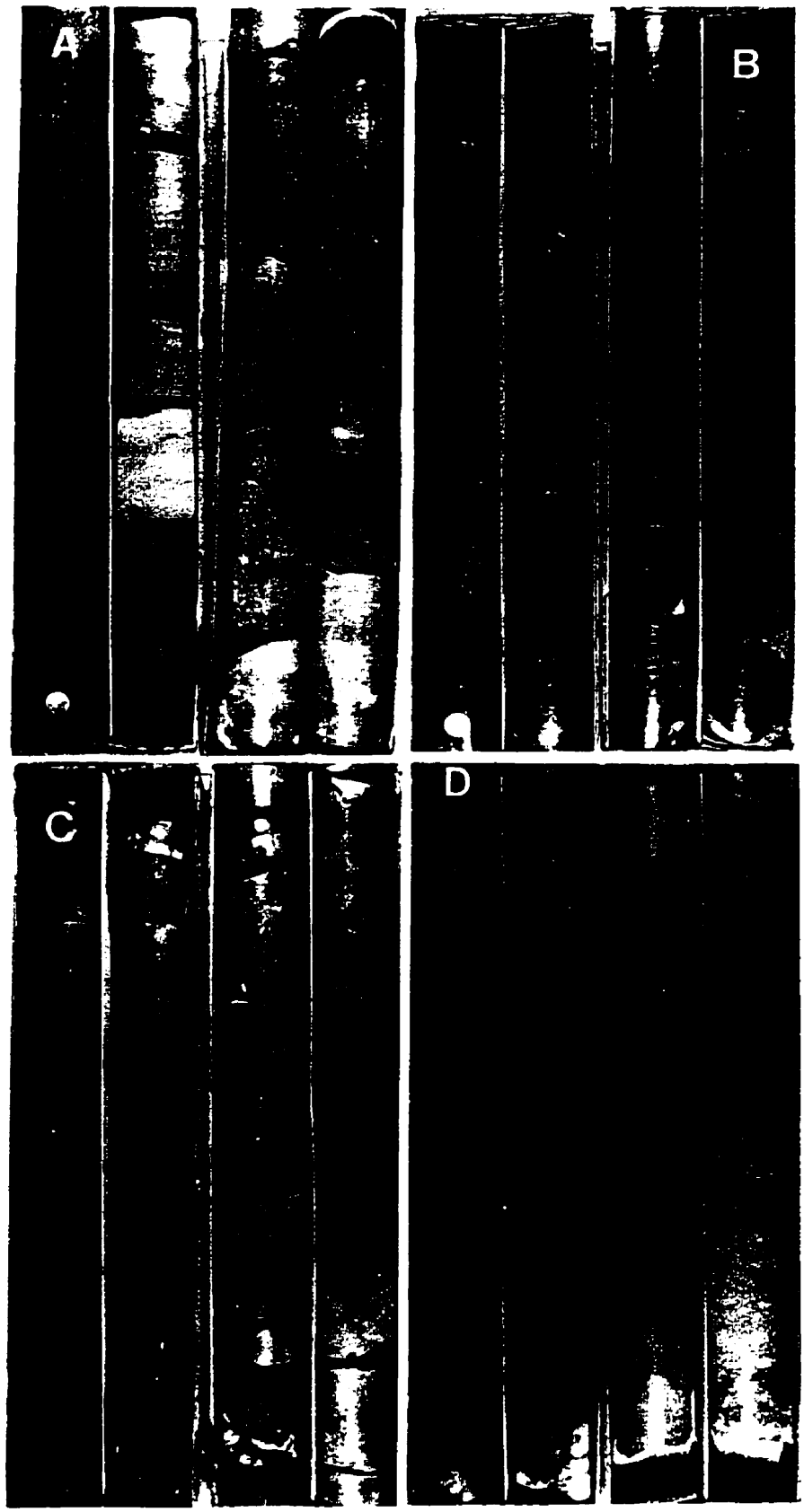
A
B
C
D

PLATE 7-3

Plate 7-3 A & B: Core photograph showing interbedded dolostone (d) and anhydrite (a) from the lower part of the Hubbard Evaporite Member in southeastern Saskatchewan. The dolostone is generally massive, with intraclasts scattered throughout the rock. Fine wavy, crinkly laminations are locally preserved. Anhydrite is characterized by wavy laminations, with laminae disrupted locally. Lsd. 13-12-22-32W1-6. Scale bar is 1 cm.

Plate 7-3 C: Slabbed core photograph showing anhydrite from the lower part of the Hubbard Evaporite Member in southeastern Saskatchewan. It is characterized by horizontal to slightly wavy laminations. Lsd. 14-32-020-30W1-72. Scale bar is 1 cm.

Plate 7-3 D: Slabbed core photograph showing a clastic anhydrite from the Hubbard Evaporite Member in central Saskatchewan, which also contains rich dolomitic intraclasts. Lsd. 1-2-39-8W3-2. Scale bar is 1 cm.

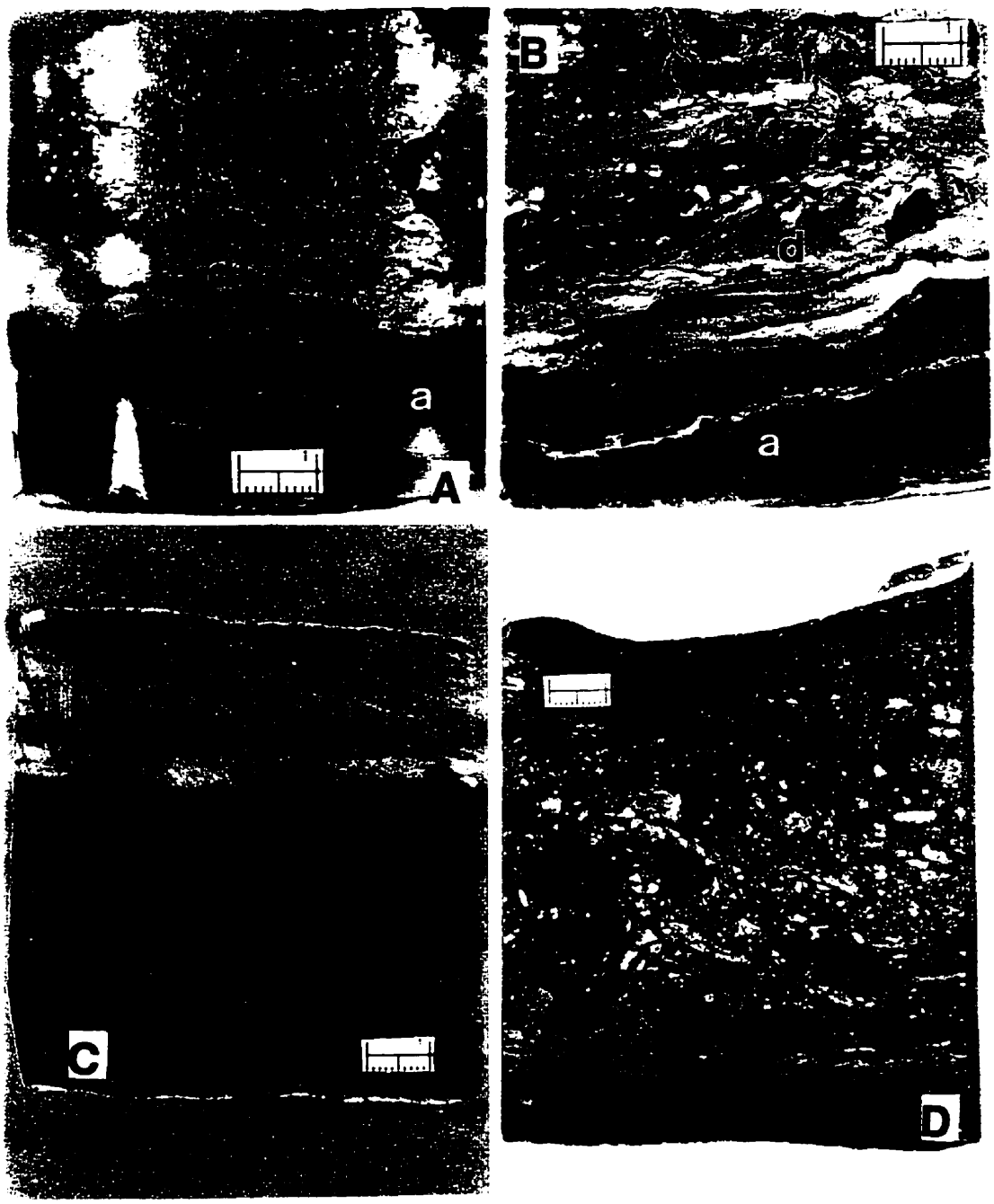
a
A
B
d
a
C
D

Interpretation

The presence of lamination in the anhydrite rock indicates a subaqueous environment. Kendall (1976) has described similar laminated to thinly bedded anhydrites from the Ordovician Bighorn Group. He believed that this form of anhydrite was most likely deposited subaqueously in very shallow waters of calm lagoons. Subaqueous evaporites generally have been characterized as having laminated structures, whereas sabkha evaporites are typically nodular (e.g., Schreiber *et al.*, 1982; Warren and Kendall, 1985). The stratigraphic position of the laminated anhydrite above the sabkha sediment of the Neely Member suggests that its deposition occurred in hypersaline ponds or around the seaward fringes of shallow, inner-sabkha salt pans that lay leeward of a marginal sabkha environment.

Laminated to Thinly Bedded Dolostone

The brown laminated to thinly bedded dolostone is interbedded with laminated anhydrite and characterized by wavy laminae of probable microbial origin (Plate 7-3A). The laminae range in thickness from mm to cm. The thicker dolostone beds are commonly massive, with microbial laminations partially to completely disrupted by mud-cracks, which in turn produced abundant intraclasts (Plate 7-3B). Petrographic study shows that the dolostone has a clotted fabric. Some laminae are rich in remains of microbial filaments. The voids between the filaments are filled with anhydrite. Additionally, acicular, randomly-distributed anhydrite crystals are common in the dolostone.

Interpretation

Like the laminated anhydrite, the presence of the laminated to thinly bedded dolostone directly above the supratidal sediments of the Neely Member suggests a very shallow water environment. This is further supported by the presence of the mudcracks in the dolostone. The depositional environment of the dolostone, however, was probably less saline than that of the laminated anhydrite.

Clastic Anhydrite

In Core 1-2-39-8W3 of central Saskatchewan, the Hubbard Evaporite Member is composed predominantly of clastic anhydrite, that is interbedded with laminated anhydrite-dolostone. The rock is generally massive, but current bedding, which is defined by inclined laminae, is locally present (Plate 7-2A). In the lower part of the Hubbard Evaporite Member, anhydrite clasts are mixed with carbonate intraclasts (Plates 7-3D, 7-4A), whereas in the upper part, anhydrite clasts are found alone (Plate 7-4D). Most anhydrite clasts are of coarse sand- to pebble-size. They are poorly sorted, angular to well rounded, and have a loosely packed grain-supported fabric. Microscopic study shows that these anhydrite clasts are composed of aggregates of small crystals (Plate 7-4B). The carbonate intraclasts are dolomitic and are characterized by wavy microbial laminations, suggesting that they were originally fragments of microbial mats. Some intraclasts have sharp and angular margins, and adjacent intraclasts can be fitted back together, reflecting *in situ* brecciation (Plate 7-4C). The matrix is composed of a mixture of dolomicrite and acicular anhydrite (Plate 7-4A & B). In addition, a small-scale, tepee-like structure is present in the clastic anhydrite. The associated laminated anhydrite and dolostone are characterized by wavy microbial laminations. These laminations, however, are commonly disrupted and laterally discontinuous.

Interpretation

The presence of the clastic anhydrite lying directly above the supratidal sediment of the Neely Member suggests a very shallow water environment. This is supported by the presence of interbedded laminated anhydrite-dolostone, which is characterized by microbial laminae. The local presence of tepee structure in the clastic anhydrite provides further support to this interpretation. Similar anhydrite clasts have been reported by Logan (1987) from the MacLeod Evaporite Basin in western Australia, where they are a facies of the phreatic majanna environment.

Chaotic Mudstone-Halite

Chaotic mudstone-halite is present in units B and C of the Hubbard Evaporite Member in southeastern Saskatchewan, but is best developed in Unit C, where it is up to 1.5 m (5 ft) thick (Plate 7-1C & D). The rock is massive, ranges from grey, green to slightly red, and

PLATE 7-4

Plate 7-4 A: Photomicrograph of the slabbed core shown in Plate 7-3 D. It is composed of dolomitic intraclasts (d), with an anhydrite matrix. Lsd. 1-2-39-8W3-2. Scale bar is 1 mm.

Plate 7-4 B: Photomicrograph of clastic anhydrite from the Hubbard Evaporite Member in central Saskatchewan. It is composed of anhydrite (a) and dolomitic intraclasts (d), and an anhydrite matrix. Lsd. 1-2-39-8W3. Scale bar is 1 mm.

Plate 7-4 C: Slabbed core photograph showing massive to microbially laminated dolostone from the Hubbard Evaporite Member in central Saskatchewan. It contains irregular layers and wisps of anhydrite. The microbial laminae are disrupted. Lsd. 1-2-39-8W3-5. Scale bar is 1 cm.

Plate 7-4 D: Slabbed core photograph of clastic anhydrite (a) from the Hubbard Evaporite Member in central Saskatchewan. Lsd. 1-2-39-8W3-5. Scale bar is 1 cm.

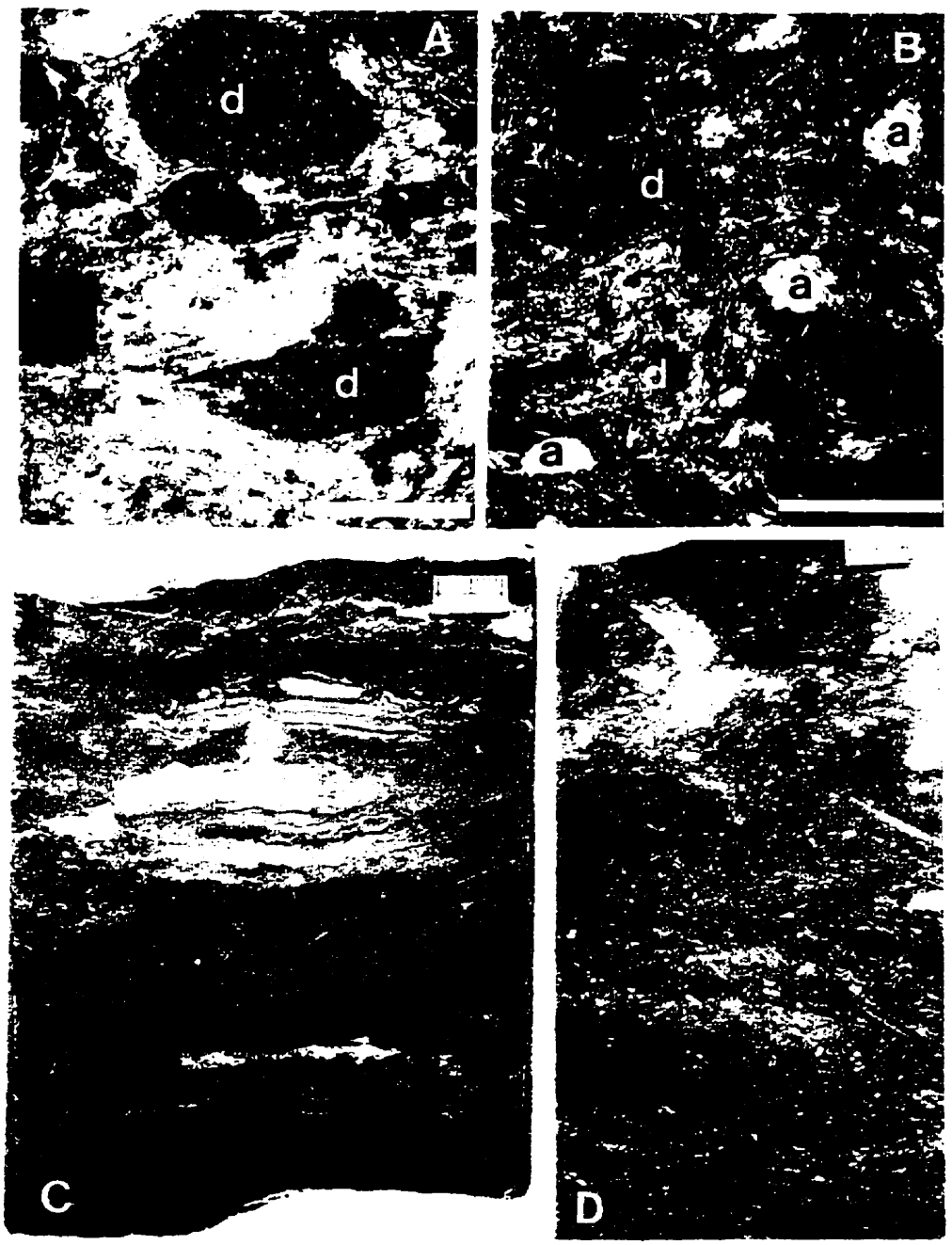
A
d
d
B
a
d
a
d
a
C
D

PLATE 7-5

Plate 7-5 A: Slabbed core photograph showing a chaotic mudstone-halite from Unit B of the Hubbard Evaporite Member in southeastern Saskatchewan. Lsd. 13-12-22-32W1-7. Scale bar is 1 cm.

Plate 7-5 B: Slabbed core photograph showing a chaotic mudstone-halite from Unit C of the Hubbard Evaporite Member in southeastern Saskatchewan. Lsd. 13-12-22-32W1-14. Scale bar is 1 cm.

Plate 7-5 C: Slabbed core photograph showing clear halite rock from Unit C of the Hubbard Evaporite Member in southeastern Saskatchewan. Lsd. 13-12-2-32-W1-8. Scale bar is 1 cm.

Plate 7-5 D: Slabbed core photograph showing cloudy halite from Unit C of the Hubbard Evaporite Member in southeastern Saskatchewan. Lsd. 13-12-22-32W1-11. Scale bar is 1 cm.

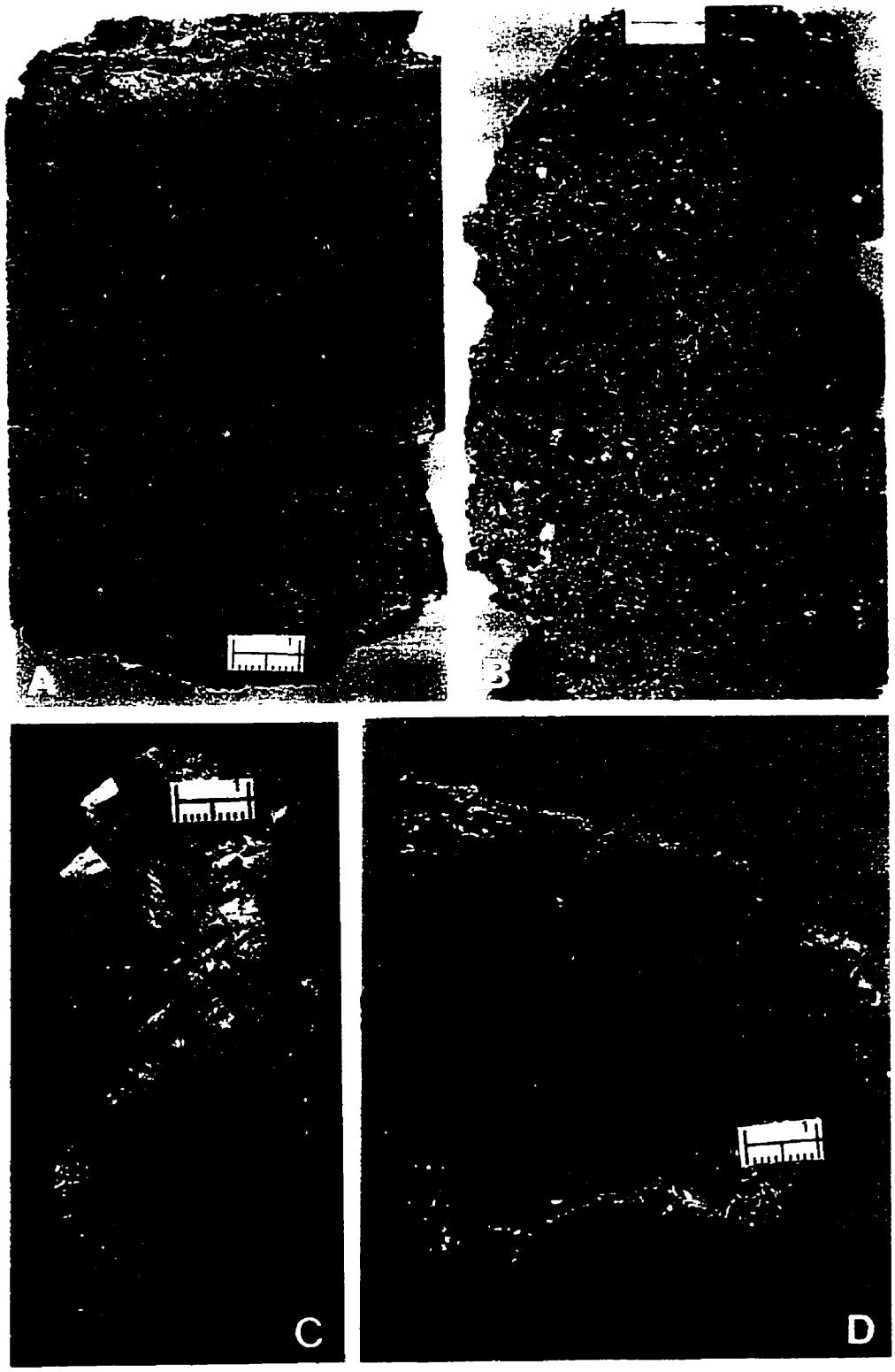
A
B
C
D

lacks physical sedimentary structures. In vertical section, the chaotic mudstone-halite lies directly below, above or interbedded with massive halite. Where the chaotic mudstone-halite is overlain by halite, the contact between them is sharp. Where the chaotic mudstone-halite lies above the halite, a transitional contact is present.

The chaotic mudstone-halite is a disorganized mixture of halite crystals and mudstone (Plate 7-5A & B). Mudstone forms irregularly shaped masses between the halite crystals. The halite crystals are typically euhedral to subhedral in shape, and have no preferred crystal orientation, growth direction or elongation with respect to bedding, which indicates displacive growth. The amount of displacive halite is highly variable, ranging from individual crystals that are isolated by mud, to halite crystal aggregates in mud matrix, to displacive halite in excess of mudstone. Some halite crystals are rimmed by mudstone matrix that was displaced during recrystallization. Jones (1965) noted that the Permian massive salt in Kansas consists of large, anhedral, transparent crystals that are colorless without inclusions, but which contain abundant matrix surrounding the crystals, that may have been expelled during recrystallization.

Interpretation

In a review of saline lacustrine subenvironments, Hardie *et al.* (1978) observed a common association of saline mudflats flanking a central salt pan. The sediments of saline mudflats are saturated with interstitial brines from which salts precipitate, forming a crowded mass of crystals in a mud matrix. Because of the remarkable similarity of this lithofacies to the chaotic mudstone-halite of the Hubbard Evaporite Member, the latter is interpreted to be deposited in a saline mudflat. Similar lithofacies were reported by Handford (1981, 1982), Smith (1971) and Poborski (1970) from other saline mudflats. This facies is also present in Unit D of the Second Red Bed Member (see Chapter 2).

Massive halite

Massive halite is present in Unit C of the Hubbard Evaporite Member in southeastern Saskatchewan (Plate 7-1B to D), where it is divided into lower and upper beds. These halite beds are separated by chaotic mudstone-halite. The halite is typically granoblastic and coarsely crystalline, consisting of an interlocking mosaic of translucent to transparent, anhedral to subhedral, equant to elongate, halite crystals that range up to 2.5 cm in length. The halite is either light or dark colour-banded (Plate 7-5 C &D). The dark

colour-banded halite is due to the presence of argillaceous sediment along crystal boundaries. The halite rock is structureless and massive. The absence of recognizable bedding may indicate that these rocks have experienced extensive diagenesis. Repeated dissolution and reprecipitation of halite, at or just below the surface, would tend to destroy primary fabrics and textures (Handford, 1981; Lowenstein and Hardie, 1985; Smoot and Lowenstein, 1991).

Interpretation

It is difficult to make a precise environmental interpretation for the halite because its primary features have been masked by recrystallization. However, the variation in colour banding may define original bedding, a feature diagnostic of a subaqueous origin. Furthermore, the halite is interbedded, overlain or underlain by the chaotic mudstone-halite, which is interpreted as sediment that formed in saline mudflat sub-environment. Thus, it is very likely that the massive halite was deposited in a saline pan subenvironment.

7.3 The First Red Bed

The First Red Bed belongs to the Davidson Member of the Souris River Formation in the subsurface of Saskatchewan (Lane, 1964), or the Point Wilkins Member of the Souris River Formation in western Manitoba (Norris *et al.*, 1982). It is composed predominantly of dolomitic mudstones with relatively high radioactivity as demonstrated by gamma ray logs. The First Red Bed is usually 3-15 m thick, with a maximum thickness of 21 m.

7.3.1 The First Red Bed in Central Saskatchewan

In central Saskatchewan, the First Red Bed is represented by the cored section in Well 1-2-39-8W3, where it is about 7.6 m thick (885.7-893.3m) (2906-2931 ft) (Plate 7-2B to D). It is composed of dolomitic mudstones that are characterized by a brick-red colour in the lower part and brown to olive-green colour in the upper part. The lower boundary lies conformably upon the Hubbard Evaporite Member. The upper boundary is marked by the presence of fossiliferous limestones. Based on an examination of core samples and petrographic study, three facies of dolomitic mudstones -- chaotic mudstone, mud-

PLATE 7-6

Plate 7-6 A: Slabbed core photograph showing a chaotic dolomitic mudstone from the First Red Bed in central Saskatchewan. Lsd. 1-2-39-8W3-11. Scale bar is 1 cm.

Plate 7-6 B: Photomicrograph of chaotic dolomitic mudstone from the First Red Bed in central Saskatchewan. It is characterized by highly irregular distribution of anhydrite, and argillaceous patches and wisps. Lsd. 1-2-39-8W3-11. Scale bar is 1 mm.

Plate 7-6 C: Slabbed core photograph showing a mud-cracked dolomitic mudstone from the First Red Bed in central Saskatchewan. Lsd. 1-2-39-8W3-7. Scale bar is 1 cm.

Plate 7-6 D: Slabbed core photograph showing a root-disrupted dolomitic mudstone from the First Red Bed in central Saskatchewan. Lsd. 1-2-39-8W3-10. Scale bar is 1 cm.

Plate 7-6 E: Slabbed core photograph showing a mud-cracked dolomitic mudstone from the First Red Bed in southeastern Saskatchewan. Lsd. 13-12-22-32W1-15. Scale bar is 1 cm.

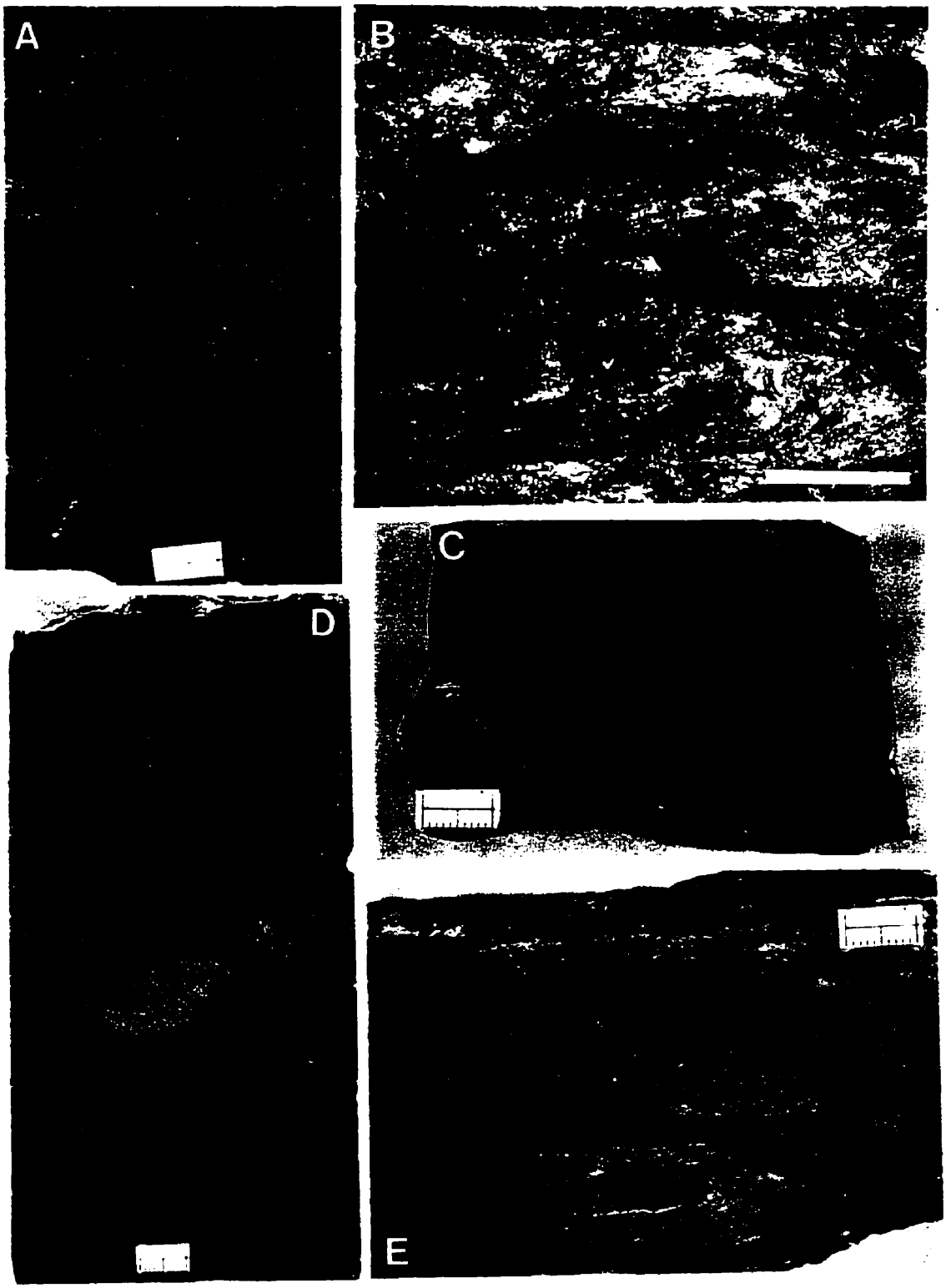
A
B
C
D
E

cracked mudstone, and root-disrupted massive mudstone -- are recognized from the lower part of the First Red Bed.

Chaotic Dolomitic Mudstone

Chaotic dolomitic mudstone is present in the lower part of the First Red Bed, and is locally found in the middle part of the First Red Bed. It is brick-red, massive and mottled, and lacks sedimentary structures (Plate 7-6A). However, irregular patches and stringers of anhydrite are common. The sediment shows evidence of soft deformation, but mud-cracks and brecciated mudstone blocks are absent. Petrographic study shows that the chaotic mudstone is composed of clay, silt-sized quartz, dolomite and anhydrite. The anhydrite is present as isolated acicular crystals or irregular aggregates of anhydrite needles that are randomly oriented (Plate 7-6B).

Interpretation

The absence of sedimentary structures in the chaotic dolomitic mudstone suggests that the original sediment was disrupted by displacive growth of evaporites. This is confirmed by the presence of abundant acicular anhydrite crystals and irregular anhydrite nodules. By analogy with the chaotic mudstone-halite facies in the Hubbard Evaporite Member, it can be concluded that the chaotic dolomitic mudstone of the First Red Bed was deposited in a saline mudflat environment.

Mud-cracked Dolomitic Mudstone

Mud-cracked dolomitic mudstone directly overlies the chaotic dolomitic mudstone. It is brick-red and composed of dolomite, silt-sized quartz, anhydrite and clay minerals. Horizontal laminations can be seen in the mudstone. The dense mud-cracks (Plate 7-6C) form a polygonal pattern, which separates blocks of mudstone. Most mudstone blocks are only a few mm thick and less than 1 cm long. They are laterally elongated and are characterized by sharp, angular margins. Mudstone blocks that are thinly bedded internally show no evidence of displacement or rotation. The mud-cracks are normally only a few millimeters deep. Their cross-sections are commonly not simple V-shaped, sediment-filled structures, but complex, jagged to sinuous features that may bifurcate. The cracks are filled with olive-green dolomitic sediment and anhydrite.

Interpretation

The fine lamination in the mud-cracked dolomitic mudstone shows that the sediment was little influenced by displacive growth of evaporites. This may, in turn, indicate that the groundwater table was too deep for the formation and preservation of significant amounts of evaporites. The presence of abundant small mudcracks shows that during the period of deposition, the sediments were subaerially exposed repeatedly. All these features indicate that the mud-cracked mudstone was probably deposited in a dry mudflat environment. Because dry mudflats are located landward of saline mudflats, this suggests that from the chaotic dolomitic mudstone to the mud-cracked dolomitic mudstone, the depositional environment became shallower upward.

Root-disrupted Dolomitic Mudstone

Root-disrupted dolomitic mudstone is present in the middle part of the First Red Bed. It is characterized by downward bifurcating and tapering tubes that range in diameter from submillimetre to several centimeters (Plate 7-6D). These characteristics are believed to be diagnostic of roots and root traces. The relatively large tubes are mainly oriented perpendicular to bedding. Smaller examples are generally parallel to bedding, forming patterns that radiate from larger vertical tubes. The larger tubes are filled with olive-green to brown argillaceous mud, but small red mudstone clasts are also very common. Petrographic study shows that the mudstone is composed of silt-size quartz, dolomite and clay minerals, but with very few evaporite minerals.

Interpretation

The root-disrupted mudstone either formed in a floodplain or formed along the edges of marginal marine salinas. It may also be an indicator of climatic changes, from an arid to a relatively less arid condition.

7.3.2 The First Red Bed in Southeastern Saskatchewan

The First Red Bed in southeastern Saskatchewan is represented by the cored section in Well 13-12-22-32W1. However, only the lower part of the First Red Beds is cored in this well, where it is about 4.5 m thick (Plate 7-1E). It lies conformably upon the

Hubbard Evaporite Member and is composed of massive- and brecciated dolomitic mudstones.

Massive Dolomitic Mudstone

The massive dolomitic mudstone is olive-green to dark grey and is composed of clay minerals, dolomite and evaporites. Fine powdery evaporites are common in the mudstone. They are whitish, massive and porous. They are present as powdery aggregates of anhydrite crystals, disseminated single crystals, or massive irregular beds. The latter are laterally discontinuous, ranging from mm to cm in thickness. However, no laminations are present in the anhydrite beds, which preclude the possibility of subaqueous deposition. The amount of anhydrite in the mudstone is very variable, ranging from sparsely distributed to highly concentrated.

Interpretation

The massive appearance of the mudstone and the abundant anhydrite suggest that the rock was disrupted by the displacive growth of the abundant evaporites. Thus, it is very likely that the mudstone was deposited in a saline mudflat environment.

Brecciated Dolomitic Mudstone

The brecciated dolomitic mudstone is light-grey to olive-green, and consists of brecciated mudstone blocks (Plates 7-1E, 7-6E). In vertical section it is both underlain and overlain by massive dolomitic mudstone. The mudstone has abundant narrow, jagged, sinuous cracks, similar to those that Smoot and Lowenstein (1991) described from dry mudflat environments. The mudstone blocks are generally 1-2 cm high by up to several cm long, with their long axes parallel or subparallel to bedding. They are subangular to angular. Most adjacent blocks can be refitted and show no evidence of displacement and rotation, indicating *in situ* brecciation. Sheet cracks, filled with olive-green mud and sand clasts, are also well developed in the mudstone.

Interpretation

The presence of abundant, narrow, jagged and sinuous cracks in the brecciated dolomitic mudstone suggests that the rock was deposited in a dry mudflat that experienced repeated flooding and desiccation.

7.4 Discussion

As described, the Hubbard Evaporite Member is conformably underlain by the Neely Member and overlain by the First Red Bed of the Souris River Formation. Because the top of the Neely Member was deposited in a supratidal setting and the lower part of the First Red Bed formed in a saline mudflat-dry mudflat environment, the sediments of the Hubbard Evaporite Member were therefore deposited in a setting located between supratidal setting and dry mudflat. Such an environment was termed a marginal marine salina by Handford (1981, 1982, 1991). A marginal marine salina is an evaporite system that is partially to completely isolated from the open ocean, and is covered by water for brief to long periods of time. A salina is usually marked by the presence of a dry mudflat that passes into a saline mudflat and eventually into a standing body of water.

The lithofacies deposited in such environments have been described from the Lower Clear Fork Formation (Permian) in Texas and from Bristol Dry Lake, California (Handford, 1981, 1982). The major lithofacies and their environments of deposition change laterally, in a seaward direction from (1) red terrigenous clastics--wadi or desert alluvial-eolian plain and dry mudflat, to (2) chaotic mudstone-halite--saline mud flat, to (3) banded to massive halite-inner-sabkha salt pan, to (4) laminated to massive anhydrite--salt pan to marginal-sabkha hypersaline pond, to (5) nodular anhydrite--marginal sabkha.

The major lithofacies from the top of the Neely Member, through the Hubbard Evaporite Member, to the lower part of the First Red Bed are almost identical to the example described above. Although no lateral facies distribution map is available (this needs further research), the vertical lithofacies changes from the laminated dolostone and nodular anhydrite at the top of the Neely Member, through the laminated anhydrite-dolomite, clastic anhydrite, massive halite, chaotic mudstone-halite in the Hubbard Evaporite Member, to the chaotic mudstone, mud-cracked mudstone and root-disrupted mudstone in the lower part of the First Red Bed, reflect a clear lateral lithofacies

distribution similar to that of the Permian Lower Clear Fork Formation. Thus, it can be concluded that the uppermost part of the Neely Member, the Hubbard Evaporite Member and the lower part of the First Red Bed were deposited in an upward-shallowing coastal salina complex.

Although the First Red Bed is assigned to the Souris River Formation, its lithofacies and depositional environments are closely related to those of the Hubbard Evaporite Member. Additionally, no significant stratigraphic break is present between the Hubbard Evaporite Member and the First Red Beds. Moreover, the mudstones in the lower part of the First Red Bed were deposited in environment that ranged from saline to dry mudflats, whereas the halite and chaotic mudstone-halite in the Hubbard Evaporite Member formed in environment that varied from salt pans to saline mudflats. It is very likely, therefore, that the mudstones of the First Red Bed, especially those in the lower part of the First Red Bed, are coeval with the sediments of the Hubbard Evaporite Member and that they are laterally adjacent facies. This conclusion is strongly supported by a restricted distribution of the Hubbard Evaporite Member, and a much more extensive distribution of the First Red Bed in the subsurface of Saskatchewan. It would thus seem appropriate to include the First Red Bed with the Dawson Bay Formation, as suggested by Dunn (1982a).

As to the reason why the salt pan sediment in Well 1-2-39-8W3 is composed of anhydrite without halite rock, whereas in Well 13-12-22-32W1, the Hubbard Evaporite Member is composed predominantly of halite, a probable explanation is that during the deposition of the Hubbard Evaporite Member, central Saskatchewan was located close to the margin of the extensive coastal salina. With its shallow water conditions, the brine had completely evaporated before subaqueous halite began to precipitate. Therefore, only gypsum (now anhydrite) was formed and preserved. In contrast, southeastern Saskatchewan had a lower topography, as discussed in Chapters 2 and 3. Thus, a more perennial subaqueous environment was present in that area, which lasted long enough for halite to precipitate.

7.5 Summary

Although the First Red Bed was assigned to the Souris River Formation, new evidence shows that its lithofacies and depositional environments are closely related to those of the Hubbard Evaporite Member. Both were deposited in a marine marginal salina complex. The Hubbard Evaporite Member was deposited in a salt pan to saline mudflat environment, and the lower part of the First Red Bed formed in environments that ranged

from saline mudflat, dry mudflat to distal floodplain. Thus, the top of the Neely Member, the Hubbard Evaporite Member and the First Red Bed belong to a single upward-shallowing succession. It would seem appropriate to include the First Red Bed with the Dawson Bay Formation, as suggested by Dunn (1982a). New evidence also shows that no significant stratigraphic break is present between the Hubbard Evaporite Member and the First Red Bed.

CHAPTER 8

CONCLUSIONS AND IMPLICATIONS

As demonstrated throughout this thesis, it is evident that the Dawson Bay Formation is much more complicated than originally thought. In this chapter, the main conclusions from each chapter of the thesis will be emphasized.

The Second Red Bed Member

The Second Red Bed Member is significantly different from the rest of the Dawson Bay Formation by its predominant dolomitic argillaceous mudstone. Although previous geologists suggested that its contact with the underlying Prairie Evaporite Formation is a disconformity, this study shows that the lower part (Unit D) of the Second Red Bed Member was deposited in a setting that ranged from saline-mudflat to dry-mudflat, which was environmentally related to the saline-pan evaporites of the uppermost part of the Prairie Evaporite Formation. This implies that no disconformity is present between the Second Red Bed Member and the Prairie Evaporite Formation, and that the sediments deposited at the latest stage of the Prairie Evaporite Formation period and the earliest stage of the Second Red Bed period are laterally adjoining facies, belonging to a single upward-shallowing succession. This conclusion differs from that of Dunn (1982a), who suggested that the Second Red Bed Member was deposited during a new marine transgression.

This study supports Dunn's viewpoint that the top of the Second Red Bed Member is an unconformity, but it disagrees with his interpretation that it was formed by tectonic disturbance. New evidence shows that the unconformity is a paleokarstic surface.

In southeastern Saskatchewan and parts of central Saskatchewan, the dolostone directly below the paleokarstic surface is well preserved. In the rest of central Saskatchewan,

however, the dolostone has extensive solution vugs or is completely brecciated, indicating that the paleokarst is more mature in those areas. This suggests that the development of the paleokarst was terminated earlier in southeastern Saskatchewan than that in central Saskatchewan. This, in turn, suggests that the paleorelief in central Saskatchewan was higher than that in southeastern Saskatchewan, and the marine waters entered the Williston Basin from the southeast. This conclusion differs from the prevailing viewpoints that the seawater came from the northwest or from the north.

New geological evidence shows that Unit D of the Second Red Bed Member formed in a setting ranging from saline mudflat to dry mudflat. Unit C was probably deposited in a distal alluvial-eolian plain. Units A and B consist of dolostone and argillaceous dolostone, which were probably deposited in a Coorong-like environment. Like dolomite in the Coorong region, the abundant evidence for subaerial exposure and paucity of evaporites indicate that the basin had a seasonally alternating, arid and humid climate. The common presence of black argillaceous grains in the dolostone, which were introduced by upward movement of groundwater, suggests that groundwater played a significant role in the formation of the dolomite. The local presence of pyritic films between dolostone beds is regarded as evidence of marine incursion. This suggests that seawater may also have played a role in the formation of the dolomite.

New evidence also shows that the Second Red Bed Member is rich in paleosol features, of which slickensides are prominent. Previous workers believed that the formation of the slickensides was due to tectonic disturbance. However, the widespread distribution of the slickensides from northwestern Saskatchewan to northwestern Manitoba and their restriction to the Second Red Bed Member indicate a pedogenic origin. This suggests that parts of the Second Red Bed Member are a paleovertisol. The development of the paleovertisol also indicates that the Williston Basin then had a seasonally alternating arid and humid climate. However, pedogenic slickensides are normally found between 0.3 and 1.3 m below the land surface. In some cored sections of the Second Red Bed Member, however, the strata that contain slickensides are more than 1.3 m thick. This implies that the paleovertisol is probably cumulative.

Paleokarsts and Black Shales at the Base of the Burr Member

As described in Chapter Three, two superimposed micro-paleokarsts are present at the base of the Burr Member in southeastern Saskatchewan. However, only one of them is

present in parts of central Saskatchewan and none is present in the rest of central Saskatchewan and northwestern Saskatchewan. Previous geologists described them as brecciated carbonates, formed by boring of hardgrounds. However, new geological evidence shows that the carbonate rocks are characterized by karstic features, that include solution vugs and pipes, fossil molds, terra rossa, *in situ* breccias and collapse breccias. All these features suggest that the carbonate rocks are paleokarsts.

New geological evidence also shows that in the area where the paleokarsts at the base of the Burr Member are present, the dolostone at the top of the Second Red Bed Member is well preserved. In contrast, in the area where the paleokarsts are absent, the dolostone contains extensive solution vugs or is completely brecciated. This indicates that the top of the Second Red Bed Member was subaerially exposed longer in the area where the paleokarsts are absent. Moreover, the superimposed paleokarsts in southeastern Saskatchewan contain well-developed solution vugs but lack the collapse breccia, that typifies the single paleokarst in central Saskatchewan. This implies that the latter was subaerially exposed longer than the former. This evidence suggests that marine transgression during the early Burr time took place in stages. Before the Williston Basin was completely flooded by seawaters, two minor marine trangressions took place. Both reached southeastern Saskatchewan, but only one marine incursion reached parts of central Saskatchewan and none extended to northwestern Saskatchewan.

Additionally, there are two thin black shales at the base of the Burr Member. One lies above the Second Red Bed Member; the other overlies the paleokarst(s) of the Burr Member or rests upon the Second Red Bed Member where the paleokarst(s) is absent. The black shales are finely laminated and are rich in organic matter, uranium and pyrite, indicating that they were deposited under anoxic conditions. The presence of the black shales that directly overlie the paleokarsts suggests that they may have been deposited in shallow. This conclusion is supported by the local presence of mudcracks in the black shales.

The Lower Burr Member

The lower Burr Member, which is composed of fine-grained carbonate sediment, was deposited in a predominantly oxygen-deficient environment. New evidence shows that during the deposition of the lower Burr Member, the dissolved oxygen level in the benthic environment varied both temporally and spatially. In central Saskatchewan, the

oxygen level increased gradually upward, but in southeastern Saskatchewan, the oxygen level first increased rapidly, then gradually decreased upward. This contrast is believed to be caused by a gradual increase in water depth. During the initial transgression, the very shallow water inhibited free circulation, and resulted in dysaerobic and anaerobic conditions. Because southeastern Saskatchewan was located near the high energy zone of Irwin's epeiric sea model, a high energy environment was rapidly established. The high energy condition provided abundant oxygen to the bottom waters, and consequently the oxygen-deficient conditions were rapidly replaced by well-oxygenated conditions. However, central Saskatchewan was then located in the landward low-energy zone of Irwin's model, where the oxygen-deficient environments were dominant. With progressive increase of water depth, the high energy zone migrated slowly to central Saskatchewan. The energy level thus increased gradually upward, as did the oxygen level. During the same time, southeastern Saskatchewan entered the oceanward low energy zone of Irwin's model, which resulted in decreasing energy, and consequently the oxygen level.

The lower part of the lower Burr Member in central Saskatchewan consists of kerogen-laminated lime mudstone and horizontally laminated lime mudstone. These have fine laminations but lack body or trace fossils, reflecting anaerobic and extremely low dysaerobic conditions. In contrast, fine laminations are absent in the lower Burr Member in southeastern Saskatchewan. This reflects that the overall oxygen level in central Saskatchewan was lower than that in southeastern Saskatchewan. Thus, from central to southeastern Saskatchewan, the environment became less oxygen-restricted with increasing water depth. This trend contradicts with the Rhoads-Morse-Byers model, which suggests that the oxygen level decreases with increasing water depth. This example shows that in the ancient epicontinental seas, the dissolved oxygen level in the benthic environments might increase from the landward low energy zone to the oceanward high energy zone with increasing water depth.

The Upper Burr Member

In southeastern Saskatchewan, the upper Burr Member is composed predominantly of wackestone and lime mudstone, with a few thin skeletal packstone and grainstone interbeds. These indicate sedimentation in a low energy, relatively deep water environment, with occasional high energy intervals. In contrast, the proportion of skeletal packstone and grainstone increases significantly in the upper Burr Member of central

Saskatchewan and northwestern Manitoba. The fossil shells in these rocks are larger and have greater shell thickness. This suggests that the depositional environments in those areas were higher in energy with shallower waters. Thus, from both northwestern Manitoba and central Saskatchewan to southeastern Saskatchewan, the depositional environments changed from more proximal to more distal conditions.

New geological evidence also shows that the upper Burr Member in central Saskatchewan consists of two superimposed upward-deepening successions. Firmgrounds were highly developed in the lower part of each succession. Although the carbonate rocks directly below the firmground surfaces are commonly lime mudstones or wackestones, packstones are present in places, and an upward transition from lime mudstone to packstone was observed locally. This vertical transition indicates an upward-shallowing succession. The firmgrounds are commonly overlain by a thin packstone, that is composed of fragments of robust shells, and overlain by lime mudstones. The upward change from packstone to lime mudstone implies an abrupt increase in water depth. Thus, the firmgrounds are interpreted as marine flooding surfaces and the strata between two adjacent firmgrounds are interpreted as parasequences. The reason for the absence or paucity of firmgrounds in the upper parts of the successions is the relatively deep water conditions that existed in those environments.

The Neely Member

New geological evidence shows that the contact between the Neely and Burr members in southeastern Saskatchewan is a firmground. It is characterized by intense mineral impregnation, which suggests a prolonged phase of non-deposition or, at least, an extremely low sedimentation rate that allowed chemical reactions to take place at the depositional interface. In central Saskatchewan, the contact is composed of a thin limestone bed that contains abundant fragments of crinoids, trilobites and brachiopods, all of which are intensely corroded and cemented by phosphorite. Considering these features and its mid-cycle position, the Burr-Neely contact is interpreted as the maximum flooding surface of the Dawson Bay Formation.

In southeastern Saskatchewan, from the lower to the upper parts of the Neely Member, the lithofacies change from predominant lime mudstone, through stromatoporoid boundstone, massive lime mudstone and wackestone, and laminated lime mudstone, to microbially laminated and fenestral lime mudstone and dolostone. This succession

suggests an upward-shallowing succession. In central Saskatchewan, however, the Neely Member is composed of two superimposed upward-shallowing successions. The explanation for this is not clear.

The Hubbard Evaporite Member and the First Red Bed

Although the First Red Bed was assigned to the Souris River Formation, new geological evidence shows that it is closely related to the Hubbard Evaporite Member. Both were deposited in a marine marginal salina complex. The Hubbard Evaporite Member formed in a salt pan to saline mudflat environment, whereas the First Red Bed was deposited in saline mudflat, dry mudflat to distal flood plain environments. Therefore, the top of the Neely Member, the Hubbard Evaporite Member and the First Red Bed of the Souris River Formation belong to a single upward-shallowing succession.

REFERENCES

Ahern, J. L. and Mrkvicka, S. R. 1984. A mechanical and thermal model for the evolution of the Williston Basin. *Tectonics*, v. 3, p. 79-102.

Ahlstrom, J. H. 1992. Geology and diagenesis of the Dawson Bay Formation in the Saskatoon potash mining district, Saskatchewan. *MSc thesis*, University of Saskatchewan, Saskatoon, Saskatchewan, 250 p.

Ahmad, N. 1983. Vertisols. In: *Pedogenesis and Soil Taxonomy. II. The Soil Orders* (Ed. by L. P. Wilding, N. E. Smeck and G. F. Hall). Elsevier, New York, p. 91-123.

Aigner, T. 1982. Calcareous tempestites: storm-dominated stratification in upper Muschelkalk limestone (Middle Trias, SW-Germany). In: *Cyclic and Event Stratification* (Ed. by G. Einsele and A. Seilacher). Springer-Verlag, New York, p. 180-198.

Aigner, T. 1985. Storm depositional systems: dynamic stratigraphy in modern and ancient shallow marine sequences. In: *Lecture Notes in Earth Sciences 3*. Springer-Verlag, New York, 174 p.

Aitken, J. D. 1993. Tectonic evolution and basin history. In: *Sedimentary Cover of the Craton in Canada* (Ed. by D. F. Stott and J. D. Aitken). Geological Survey of Canada, Ottawa, p. 485-502.

Allen, J. R. L. and Banks, N. L. 1972. An interpretation and analysis of recumbent-folded deformed cross-bedding. *Sedimentology*, v. 19, p. 257-283.

Allen, J. R. L. 1982. Sedimentary structures, their character and physical basis. *Developments in Sedimentology*. 30B, 663 p.

Allen, J. R. L. 1986. Pedogenic calcretes in the Old Red Sandstone facies (Late Silurian-Early Carboniferous) of the Anglo-Welsh area, southern Britain. In: *Paleosols: Their Recognition and Interpretation* (Ed. by V. P. Wright). Princeton University Press, Princeton, New Jersey. p. 58-86.

Amiri-Garroussi, K. 1988. Eocene spheroidal dolomite from the western Sirte Basin, Libya. *Sedimentology*, v. 35, p. 577-585.

Anderson, R. Y., Gardner, J. V. and Hemphill-Haley, E. 1989. Variability of the late Pleistocene-Holocene oxygen-minimum zone off northern California. In: *Aspects of Climate Variability in the Pacific and Western Americas* (Ed. by D. H. Peterson). American Geophysical Union, Washington, D.C., p. 75-84.

Andrichuk, J. M. 1951. Regional stratigraphic analysis of the Devonian System in Wyoming, Montana, Southern Saskatchewan and Alberta. *Bulletin of the American Association of Petroleum Geologists*, v. 35, p. 2368-2408.

Arthurton, R. S. 1973. Experimentally produced halite compared with Triassic layered halite-rock from Cheshire, England. *Sedimentology*, v. 20, p. 145-160.

Baillie, A. D. 1951. Devonian geology of Lake Manitoba - Lake Winnipegosis area, Manitoba. *Manitoba Mines Branch, Publication* 49-2, 74 p.

Baillie, A. D. 1953. Devonian System of the Williston Basin area, Manitoba. *Manitoba Mines Branch, Publication* 52-5, 105 p.

Baillie, A.D. 1955. Devonian System of Williston Basin. *Bulletin of the American Association of Petroleum Geologists*, v. 39, p. 575-629.

Banerjee, I. and Kidwell, S. M. 1991. Significance of molluscan shell beds in sequence stratigraphy: an example from the Lower Cretaceous Mannville Group of Canada. *Sedimentology*, v. 38, 913-934.

Bannatyne, B. B. 1975. High-calcium limestone deposits of Manitoba. *Manitoba Mineral Resources Division, Exploration and Geological Survey Branch, Publication* 75-1, 103 p.

Bassett, H. G. and Stout, J. G. 1968. Devonian in western Canada. In: *International Symposium on the Devonian System* (Ed. by D. H. Oswald). Alberta Society of Petroleum Geologists, v. 1, p. 717-752.

Beynon, B. M. and Pemberton, S. G. 1992. Ichnological significance of a brackish water deposit: an example from the Lower Cretaceous Grand Rapids Formation, Cold Lake Oil Sands area, Alberta. In: *Applications of Ichnology to Petroleum Exploration* (Ed. by S. G. Pemberton). Society of Economic Paleontologists and Mineralogists, Core Workshop, No. 17, p. 199-221.

Birkeland, P. W. 1984. Soils and Geomorphology. Oxford University Press, New York, 372 p.

Bjerstedt, T. W. and Feldmann, R. M. 1985. Stromatoporoid paleosynecology in the Lucas Dolostone (Middle Devonian) on Kelleys Island, Ohio. *Journal of Paleontology*, v. 59, p. 1033-1061.

Blokhuis, W. A., Kooistra, M. J. and Wilding, L.P. 1990. Micromorphology of cracking clayey soils (Vertisols). In : *Soil Micromorphology: A Basic and Applied Science* (Ed. by L. A. Douglas). Elsevier, New York. p. 123-148.

Bögli, J. 1980. Karst hydrology and physical speleology. Springer-Verlag, Berlin, 285 p.

Braun, W. K. and Mathison, J. E. 1982. Ostracods as a correlation tool in Devonian studies of Saskatchewan and adjacent areas. In: *4th International Williston Basin Symposium* (Ed. by J. E. Christopher, J. Kaldi, C. E. Dunn, D. M. Kent and J. A. Lorsong). Saskatchewan Geological Society Special Publication 6, p. 43-49.

Braun,W. K. and Mathison, J. E. 1986. Mid-Givetian events in western Canada: the Dawson Bay-Watt Mountain-Slave Point interlude. *Bulletin of Canadian Petroleum Geology*, v. 34, p. 426-451.

Braun, W. K., Norris, A. W. and Uyeno, T. T. 1988. Late Givetian to early Frasnian biostratigraphy of western Canada: the Slave Point-Waterways boundary and related events. In: *Devonian of the World* (Ed. by N. J. McMillan, A. F. Embry and D. J. Glass). Canadian Society of Petroleum Geologists, Calgary, v. 3, p. 93-111.

Brett, C. E. 1995. Sequence stratigraphy, biostratigraphy, and taphonomy in shallow

marine environments. *Palaios*, v. 10, p. 597-616.

Brewer, R. 1976. Fabric and mineral analysis of soils. 2nd Edition, Robert E. Krieger Publishing Co., New York, 482 p.

Brindle, J. E. and Lane, D. M. 1963. Saskatchewan Stringocephalids. *Bulletin of Canadian Petroleum Geology*, v. 11, p. 59-63.

Bromley, R. G. and Ekdale, A. A. 1984. *Chondrites*: a trace fossil indicator of anoxia in sediments. *Science*, v. 224, p. 872-874.

Bromley, R. G. and Asgaard, U. 1991. Ichnofacies: a mixture of taphofacies and biofacies. *Lethaia*, v. 24, p. 153-163.

Buol, S. W., Hole, F. D. and McCracken, R. J. 1980. Soil genesis and classification (second edition). Iowa State University Press, Ames, 404 p.

Butler, G. P. 1969. Modern evaporite deposition and geochemistry of coexisting brines, the sabkha, Trucial Coast, Arabian Gulf. *Journal of Sedimentary Petrology*, v. 39, p. 70-89.

Byers, C. W. 1977. Biofacies patterns in euxinic basins: a general model. In: *Deep-Water Carbonate Environments* (Ed. by H. E. Cook and P. Enos). Society of Economic Paleontologists and Mineralogists Special Publication 25, p. 5-17.

Calvet, F. and Tucker, M. E. 1988. Outer ramp cycles in the Upper Muschelkalk of the Catalan Basin, northeast Spain. *Sedimentary Geology*, v. 57, p. 185-198.

Calvet, S. E. 1990. Geochemistry and origin of the Holocene sapropel in the Black Sea. In: *Facets of Modern Biogeochemistry* (Ed. by V. Ittekkot, S. Kempe, W. Michaelis and A. Spitzy). Springer-Verlag, Berlin, p. 326-352.

Carballo, J. D., Land, L. S. and Miser, D. E. 1987. Holocene dolomitization of supratidal sediments by active tidal pumping, Sugarloaf Key, Florida. *Journal of Sedimentary Petrology*, v. 57, p. 153-165.

Carlson, C. G. 1960. Stratigraphy of the Winnipeg and Deadwood Formations in North Dakota. *North Dakota Geological Survey Bulletin* 35, 149 p.

Carlson, C. G. and Anderson, S. B. 1965. Sedimentary and tectonic history of the North Dakota part of the Williston Basin. *Bulletin of the American Association of Petroleum Geologists*, v. 49, p. 1833-1846.

Choquette, P. W. and Pray, L. C. 1970. Geologic nomenclature and classification of porosity in sedimentary carbonates. *Bulletin of the American Association of Petroleum Geologists*, v. 54, p. 207-250.

Choquette, P. W. and James, N. P. 1988. Introduction, In: *Paleokarst* (Ed. by N. P. James and P. W. Choquette). Springer-Verlag, New York. p. 1-21.

Cluff, R. M. 1980. Paleoenvironment of the New Albany Shale Group (Devonian-Mississippian) of Illinois. *Journal of Sedimentary Petrology*, v. 50, p. 767-780.

Coveney, R. M. Jr. and Shaffer, N. R. 1988. Sulfur-isotope variations in Pennsylvanian shales of the midwestern United States. *Geology*, v. 16, p. 18-21.

Crickmay, C. H. 1954. Paleontological correlation of Elk Point and equivalents. In: *Western Canada Sedimentary Basin* (Ed. by L. M. Clark). The American Association of Petroleum Geologists, Tulsa, Oklahoma. p. 143-158.

Crickmay, C. H. 1960. Studies of the Western Canada Stringocephalinae. *Journal of Paleontology*, v. 34, p. 874-890.

Crickmay, C. H. 1961. The misinterpreted Middle Devonian of Saskatchewan. *Journal of the Alberta Society of Petroleum Geologists*, v. 9, p. 10-14.

Dabard, M.-P. and Paris, F. 1986. Palaeontological and geochemical characteristics of Silurian black shale formations from the central Brittany Domain of the Amorican Massif (northwest France). *Chemical Geology*, v. 55, p. 17-29.

Davis, G. R. 1970. Algal laminated sediments, Gladstone Embayment, Shark Bay, Western Australia. In: *Carbonate Sedimentation and Environments, Shark Bay,*

Western Australia (Ed. by B. W. Logan, G. R. Davis, J. F. Read and D. E. Cebulski). American Association of Petroleum Geologists Memoir 13, p. 169-205.

Davis, H. R. and Byers, C. W. 1993. The role of bottom currents and pelagic settling in the deposition of shale in an oxygen-stratified basin: case study of the Mowry Shale (Cretaceous) of Wyoming. In: *Evolution of Western Interior Basin* (Ed. by W. G. E. Caldwell and E. G. Kauffman). Geological Association of Canada Special Paper 39, p. 177-188.

Dawson, W. C. and Reaser, D. F. 1985. Trace fossils in middle and upper Austin Chalk near Dallas, Texas: paleoecologic and economic significance. *Bulletin of the American Association of Petroleum Geologists*, v. 69, p. 143.

Day, J., Uyeno, T., Norris, W., Witzke, B. J. and Bunker, B. J. 1996. Middle-Upper Devonian relative sea-level histories of central and western North American interior basins. In: *Paleozoic Sequence Stratigraphy: Views from the North American Craton* (Ed. by B. J. Witzke, G. A. Ludvigson and J. Day). Geological Society of America Special Paper 306, p. 259-275.

Dean, K. 1982. Devonian Dawson Bay Formation in northwestern North Dakota. In: *Fourth International Williston Basin Symposium* (Ed. by J. E. Christopher, J. Kaldi, C. E. Dunn, D. M. Kent and J. A. Song). Saskatchewan Geological Society Special Publication 6, p. 89-92.

De Deckker, P. and Last, W. M. 1988. Modern dolomite deposition in continental, saline lakes, western Victoria, Australia. *Geology*, v. 16, p. 29-32.

Deffeyes, K. S., Lucia, F. J. and Weyl, P. K. 1965. Dolomitization of Recent and Plio-Pleistocene sediments by marine evaporite waters on Bonaire, Netherlands Antilles. In: *Dolomitization and Limestone Diagenesis - a Symposium* (Ed. by L. C. Pray and R. C. Murray). Society of Economic Paleontologists and Mineralogists Special Publication 13, p. 71-88.

Desrochers, A. and James, N. P. 1988. Early Paleozoic surface and subsurface paleokarsts: Middle Ordovician carbonates, Mingan Islands, Quebec. In: *Paleokarst* (Ed. by N. P. James and P. W. Choquette). Springer-Verlag, New York, p. 183-210.

Dickson, J. A. D. 1965. A modified staining technique for carbonates in thin section. *Nature*, v. 205, p. 587.

Driese, S. G. and Foreman, J. L. 1992. Paleopedology and paleoclimatic implications of Late Ordovician vertic paleosols, Juniata Formation, southern Appalachians. *Journal of Sedimentary Petrology*, v. 62, p. 71-83.

Driese, S. G., Mora, C. I., Cotter, E. and Foreman, J. L. 1992. Paleopedology and stable isotope chemistry of Late Silurian vertic paleosols, Bloomsburg Formation, central Pennsylvania. *Journal of Sedimentary Petrology*, v. 62, p. 825-841.

Dudal, R. and Eswaran, H. 1988. Distribution, properties and classification of Vertisols. In: *Vertisols: Their Distribution, Properties, Classification and Management* (Ed. by L. P. Wilding and R. Puentes). Texas A & M University Printing Center, College Station, Texas, p. 1-22.

Dunham, R. J. 1962. Classification of carbonate rocks according to depositional texture. In: *Classification of Carbonate Rocks* (Ed. by W. E. Ham). American Association of Petroleum Geologists Memoir 1, p. 108-121.

Dunn, C. E. 1982a. Geology of the Middle Devonian Dawson Bay Formation in the Saskatoon potash mining district, Saskatchewan. *Saskatchewan Energy and Mines Report 194*, 117 p.

Dunn, C. E. 1982b. Geology of the Middle Devonian Dawson Bay Formation in the northern part of the Williston Basin. In: *Fourth International Williston Basin Symposium* (Ed. by J. E. Christopher, J. Kaldi, C. E. Dunn, D. M. Kent and J. A. Song). Saskatchewan Geological Society Special Publication 6, p. 75-78.

Durrance, E. M. 1986. Radioactivity in geology: principles and applications. Halsted Press, New York, 441 p.

Edie, R. W. 1958. Middle Devonian Elk Point Group and Dawson Bay Formation, Central Saskatchewan (abstract). In: *2nd International Williston Basin Symposium*. North Dakota Geological Society and Saskatchewan Geological Society.

Edie, R. W. 1959. Middle Devonian sedimentation and oil possibilities, central Saskatchewan, Canada. *Bulletin of the American Association of Petroleum Geologists*, v. 43, p. 1026-1057.

Edwards, B. D. 1985. Bioturbation in a dysaerobic, bathyal basin: California borderland. In: *Biogenic Structures: Their Use in Interpreting Depositional Environments* (Ed. by H. A. Curran). Society of Economic Paleontologists and Mineralogists Special Publication 35, p. 309-331.

Ekdale, A. A. 1985. Trace fossils and mid-Cretaceous anoxic events in the Atlantic Ocean. In: *Biogenic structures: Their Use in Interpreting Depositional Environments* (Ed. by H. A. Curran). Society of Economic Paleontologists and Mineralogists Special Publication 35, p. 333-342.

Elrick, M. 1996. Sequence stratigraphy and platform evolution of Lower-Middle Devonian carbonates, eastern Great Basin. *Geological Society of America Bulletin*, v. 108, p. 392-416.

Esteban, M. and Klappa, C. F. 1983. Subaerial exposure environment. In: *Carbonate Depositional Environments* (Ed. by P. A. Scholle, D. G. Bebout and C. H. Moore). American Association of Petroleum Geologists Memoir 33, Tulsa, OK., p. 1-54.

Ettensohn, F. R., Dever, G. R. Jr. and Grow, J. S. 1988. A paleosol interpretation for profiles exhibiting subaerial exposure "crusts" from the Mississppian of the Appalachian Basin. In: *Paleosols and Weathering Through Geologic Time: Principles and Applications* (Ed. by J. Reinhardt and W. R. Sigleo). Geological Society of America Special Paper 216. p. 49-79.

Fanning, D. S. and Fanning, M. C. B. 1989. Soil, morphology, genesis and classification. John Wiley & Sons, New York. 395 p.

Faulkner, T. J. 1988. The Shipway Limestone of Gower: sedimentation on a storm-dominated Early Carboniferous ramp. *Geological Journal*, v. 23, p. 85-100.

Fischer, A. G. and Roberts, L. T. 1991. Cyclicity in the Green River Formation

(lacustrine Eocene) of Wyoming. *Journal of Sedimentary Petrology*, v. 61, p. 1146-1154.

Ford, D. C. and Williams, P. W. 1989. Karst Geomorphology and Hydrology. Unwin Hyman, London, 601 p.

Folk, R. L., Roberts, H. H. and Moore, C. H. 1973. Black phytokarst from Hell, Cayman Islands, British West Indies. *Geological Society of America Bulletin*, v.84, p. 2351-2360.

Foth, H. D. and Schafer, J. W. 1980. Soil geography and land use. John Wiley & Sons, New York, 484 p.

Fowler, C. M. R. and Nisbet, E. G. 1985. The subsidence of the Williston Basin. *Canadian Journal of Earth Sciences*, v. 22, p. 408-415.

Frey, R. W. and Seilacher, A. 1980. Uniformity in marine invertebrate ichnology. *Lethaia*, v. 13, p. 183-207.

Fuller, J. G. C. M. and Porter, J. W. 1969. Evaporite formations with petroleum reservoirs in Devonian and Mississippian of Alberta, Saskatchewan, and North Dakota. *Bulletin of the American Association of Petroleum Geologists*, v. 53, p. 909-926.

Fürsich, F. T. 1979. Genesis, environments, and ecology of Jurassic hardgrounds. *Neues Jahrbuch für Geologie und Paläontologie Abhandlungen*, v. 158. p. 1-63.

Fürsich, F. T., Oschmann, W., Singh, I. B. and Jaitly, A. K. 1992. Hardgrounds, reworked concretion levels and condensed horizons in the Jurassic of western India: their significance for basin analysis. *Journal of the Geological Society, London*. v. 149, p. 313-331.

Fuzesy, L. M. 1982. Petrology of potash ore in the Esterhazy Member of the Middle Devonian Prairie Evaporite in the Esterhazy - Rocanville area. In: *Summary of Investigations 1982, Saskatchewan Geological Survey* (Ed. by R. F. Davie). Miscellaneous Report - Saskatchewan Mineral Resources, 82-4, p. 144-151.

Gerhard, L. C., Anderson, S. B., Lefever, J. A. and Carlson, C. G. 1982. Geological development, origin, and energy mineral resources of Williston Basin, North Dakota. *Bulletin of the American Association of Petroleum Geologists*, v. 66, p. 989-1020.

Gerhard, L C., Fischer, D. W. and Anderson, S. B. 1990. Petroleum geology of the Williston Basin. In: *Interior Cratonic Basins* (Ed. by M. W. Leighton, D. R. Kolata, D. F. Oltz and J. J. Eidel). American Association of Petroleum Geologists Memoir 51, p. 507-559.

Ghibaudo, G., Grandesso, P., Massari, F. and Uchman, A. 1996. Use of trace fossils in delineating sequence stratigtraphic surfaces (Tertiary Venetian Basin, northeastern Italy). *Palaeogeography, Palaeoclimatology, Palaeoecology*, v. 120, p. 261-279.

Goebel, K. A., Bettis, E. A. and Heckel, P. H. 1989. Upper Pennsylvanian paleosol in Stranger Shale and underlying Iatan Limestone, southwestern Iowa. *Journal of Sedimentary Petrology*, v. 59, p. 224-232.

Goldhammer, R. K., Lehmann, P. J. and Dunn, P. A. 1993. The origin of high-frequency platform carbonate cycles and third-order sequences (Lower Ordovician El Paso Gp, West Texas): constraints from outcrop data and stratigraphic modeling. *Journal of Sedimentary Petrology*, v. 63, p. 318-359.

Goodwin, P. W. and Anderson, E. J. 1985. Punctuated aggradational cycles: a general hypothesis of episodic stratigraphic accumulation. *Journal of Geology*, v. 93, p. 515-533.

Gray, M.B., and Nickelsen, R.P. 1989. Pedogenic slickensides, indicators of strain and deformation processes in redbed sequences of the Appalachian foreland. *Geology*, v. 17, p. 72-75.

Graystone, L. D., Sherwin, D. F. and Allan, J. R. 1964. Middle Devonian. In: *Geological History of Western Canada* (Ed. by R. G. McCrossan and R. P. Glaister). Alberta Society of Petroleum Geologists, Calgary, p. 49-59.

Green, A. G., Weber, W. and Hajnal, Z. 1985. Evolution of Proterozoic terrains beneath the Williston basin. *Geology*, v. 13, p. 624-628.

Gu Chenggao and Renaut, R. W. 1995. Depositional environment of the dolostones in the Second Red Bed Member of the Devonian Dawson Bay Formation, Saskatchewan. In: *7th International Williston Basin Symposium, 1995 Guidebook* (Ed. by L. D. V. Hunter and R. A. Schalla). North Dakota & Saskatchewan Geological Societies and the Fort Peck Tribes, Montana. p. 373-382.

Gu Chenggao and Renaut, R. W. 1996. Validity of the Rhoads-Morse-Byers model in interpreting oxygen-related environments of ancient epeiric seas (abstr.). In: *30th International Geological Congress, Meeting Abstracts*, Beijing, v. 2, p. 199.

Gu Chenggao and Renaut, R. W. 1997. Depositional environments and pedogenesis of the Second Red Bed Member, Middle Devonian Dawson Bay Formation, Saskatchewan (abstr.). In: *1997 CSPG - SEPM Joint Convention, Program with Abstracts*, Calgary, p. 117.

Gu Chenggao and Renaut, R. W. 1997. Firmgrounds in the Middle Devonian Dawson Bay Formation and their significance for sequence stratigraphy (abstr.). In: *1997 CSPG - SEPM Joint Convention, Program with Abstracts*, Calgary, p.118.

Gunatilaka, A., Saleh, A., Al-Temeemi, A. and Nasser, N. 1984. Occurrence of subtidal dolomite in a hypersaline lagoon, Kuwait. *Nature*, v. 311, p. 450-452.

Gustavson, T. C. 1991. Buried vertisols in lacustrine facies of the Pliocene Fort Hancock Formation, Hueco Bolson, West Texas and Chihuahua, Mexico. *Geological Society of America Bulletin*, v. 103, p. 448-460.

Hallam, A. 1967. The depth significance of shales with bituminous laminae. *Marine Geology*, v. 5, p. 481-493.

Hallam, A. and Bradshaw, M. J. 1979. Bituminous shales and oolitic ironstones as indicators of transgressions and regressions. *Journal of the Geological Society, London*, v, 136, p. 157-164.

Hallam, A. 1981. Facies interpretation and the stratigraphic record. W. H. Freeman & Co. Ltd., Oxford, 291 p.

Handford, C. R. 1981. Coastal sabkha and salt pan deposition of the lower Clear Fork Formation (Permian), Texas. *Journal of Sedimentary Petrology*, v. 51, p. 761-778.

Handford, C. R. 1982. Sedimentology and evaporite genesis in a Holocene continental-sabkha playa basin-Bristol Dry Lake, California. *Sedimentology*, v. 29, p. 239-253.

Handford, C. R. 1986. Facies and bedding sequences in shelf-storm-deposited carbonates-Fayetteville Shale and Pitkin Limestone (Mississppian), Arkansas. *Journal of Sedimentary Petrology*, v. 56, p. 127-137.

Handford. C. R. 1991. Marginal marine halite: sabkhas and salinas. In: *Evaporites, Petroleum and Mineral Resources* (Ed. by J. L. Melvin). Developments in Sedimentology 50. Elsevier, Amsterdam, p. 1-66.

Hardie, L. A., Smoot, J. P. and Eugster, H. P. 1978. Saline lakes and their deposits: a sedimentological approach. In: *Modern and Ancient Lake Sediments* (Ed. by A. Matter and M. E. Tucker). International Association of Sedimentologists Special Publication 2, Oxford. p. 7-41.

Heckel, P. H. 1977. Origin of phosphatic black shale facies in Pennsylvanian cyclothems of Mid-Continent North America. *Bulletin of the American Association of Petroleum Geologists*, v. 61, p. 1045-1068.

Heckel, P. H. 1991. Thin widespread Pennsylvanian black shales of Midcontinent North America: a record of a cyclic succession of widespread pycnoclines in a fluctuating epeiric sea. In: *Modern and Ancient Continental Shelf Anoxia* (Ed. by R. V. Tyson and T. H. Pearson). Geological Society Special Publication 58, p. 259-273.

Holland, S. M. 1993. Sequence stratigraphy of a carbonate-clastic ramp: The Cincinnatian Series (Upper Ordovician) in its type area. *Geological Society of America Bulletin*, v. 105, p. 306-322.

Holland, S. M., Miller, A. I., Dattilo, B. F., Meyer, D. L. and Diekmeyer, S. L. 1997. Cycle anatomy and variability in the storm-dominated type Cincinnatian (Upper Ordovician): coming to grips with cycle delineation and genesis. *Journal of Geology*, v.

105, p. 135-152.

Holter, M. E. 1969. The Middle Devonian Prairie Evaporite of Saskatchewan. *Sask. Dept. Min. Res., Report* 123, 134 p.

Hovorka, S. 1987. Depositional environments of marine-dominated bedded halite, Permian San Andres Formation, Texas. *Sedimentology*, v. 34, p. 1029-1054.

Inden, R. A. and Burke, R. B. 1995. Fault control on late stage diagenetic creation and enhancement of reservoirs. In: *7th International Williston Basin Symposium* (Ed. by L. D. V. Hunter and R. A. Schalla). North Dakota & Saskatchewan Geological Societies and the Fort Peck Tribes, Montana. p. 351-366.

Illing, L. V., Wells, A. J. and Taylor, J. C. M. 1965. Penecontemporaneous dolomite in the Persian Gulf. In: *Dolomitization and Limestone Diagenesis: A Symposium* (Ed. by L. C. Pray and R. C. Murray). Society of Economic Paleontologists and Mineralogists Special Publication 13, p. 89-111.

Irwin, M. L. 1965. General theory of epeiric clear water sedimentation. *Bulletin of the American Association of Petroleum Geologists*, v. 49. p. 445-459.

James, N. P. 1984. Shallowing-upward sequences in carbonates. In: *Facies Models* (Ed. by R. G. Walker). Geoscience Canada. p. 213-228.

James, N. P. and Choquette, P. W. 1984. Diagenesis 9-. Limestones - the meteoric diagenetic environment. *Geoscience Canada*, v. 11, p. 161-194.

Jeffery, D. and Aigner, T. 1982. Storm sedimentation in the Carboniferous limestones near Weston-Super-Mare (Dinantian, SW - England). In: *Cyclic and Event Stratification* (Ed. by G. Einsele and A. Seilacher). Springer-Verlag, Berlin, p. 240-247.

Jenner, G. A., Longerich, H. P., Jackson, S. E. and Fryer, B. J. 1990. ICP-MS - a powerful tool for high-precision trace-element analysis in Earth sciences: evidence from analysis of selected U.S.G.S. reference samples. *Chemical Geology*, v. 83, p. 133-148.

Jennette, D. C. and Pryor, W. A. 1993. Cyclic alternation of proximal and distal storm facies: Kope and Fairview formations (Upper Ordovician), Ohio and Kentucky. *Journal of Sedimentary Petrology*, v. 63, p. 183-203.

Joeckel, R. M. 1989. Geomorphology of a Pennsylvanian land surface: pedogenesis in the Rock Lake Shale Member, southeastern Nebraska. *Journal of Sedimentary Petrology*, v. 59, p. 469-481.

Joeckel, R. M. 1991. Paleosol stratigraphy of the Eskridge Formation, Early Permian pedogenesis and climate in southeastern Nebraska. *Journal of Sedimentary Petrology*, v. 61, p. 234-255.

Joeckel, R. M. 1995. Paleosols below the Ames marine unit (Upper Pennsylvanian, Conemaugh Group) in the Appalachian Basin, U.S.A.: variability on an ancient depositional landscape. *Journal of Sedimentary Reserach*, v. 65, p. 393-407.

Johnson, J. G., Klapper, G. and Sandberg, C. A. 1985. Devonian eustatic fluctuations in Euramerica. *Geological Society of America Bulletin*, v. 96, p. 567-587.

Jones, B. and Smith, D. S. 1988. Open and filled karst features on the Cayman Islands: implications for the recognition of paleokarst. *Canadian Journal of Earth Sciences*, v. 25, p. 1277-1291.

Jones, B. 1989. The role of microorganisms in phytokarst development on dolostones and limestones, Grand Cayman, British West Indies. *Canadian Journal of Earth Sciences*, v. 26, p. 2204-2213.

Jones, B. and Desrochers, A. 1992. Shallow platform carbonates. In: *Faices Models: Response to Sea Level Change* (Ed. by R. G. Walker and N. P. James). Geoscience Canada. p. 277-301.

Jones, C. L. 1965. Petrography of evaporites from the Wellington Formation near Hutchison, Kansas. *U. S. Geological Survey Bulletin 1201-A*, 70 p.

Kahle, C. F. 1988. Surface and subsurface paleokarst, Silurian Lockpot, and Peeble Dolomites, western Ohio. In: *Paleokarst* (Ed. by N. P. James and P. W. Choquette).

Springer-Verlag, New York. p. 229-255.

Kazmierczak, J. and Goldring, R. 1978. Subtidal flat-pebble conglomerate from the Upper Devonian of Poland: a multiprovenant high-energy product. *Geological Magazine*, v. 115, p. 359-366.

Kendall, A. C. 1976. The Ordovician carbonate succession (Bighorn Group) of southeastern Saskatchewan. *Saskatchewan Geological Survey Report No.* 180. Regina. 185 p.

Kendall, A. C. 1992. Evaporites. *In: Facies Models: Response to Sea Level Change* (Ed. by R. G. Walker and N. P. James). Geoscience Canada. p. 375-409.

Kennedy, W. J. 1967. Burrows and surface traces from the lower Chalk of southern England. *Bulletin of the British Museum, Natural History, Geology Series*, v. 15, p. 127-167.

Kent, D. M. 1987. Paleotectonic controls on sedimentation in the northern Williston Basin, Saskatchewan. In: *Williston Basin: Anatomy of a Cratonic Oil Province* (Ed. by M. W. Longman). The Rocky Mountain Association of Geologists, Denver, p. 45-56.

Kerans, C. 1988. Karst-controlled reservoir heterogeneity in Ellenburger Group Carbonates of West Texas. *Bulletin of the American Association of Petroleum Geologists*, v. 72, p. 1160-1183.

Kershaw, S. 1993. Sedimentation control on growth of stromatoporoid reefs in the Silurian of Gotland, Sweden. *Journal of the Geological Society, London*, v. 150, p. 197-203.

Kershaw, S. and Keeling, M. 1994. Factors controlling the growth of stromatoporoid biostromes in the Ludlow of Gotland, Sweden. *Sedimentary Geology*, v. 89, p. 325-335.

Kidwell, S. M. and Aigner, T. 1985. Sedimentary dynamics of complex shell beds: implications for ecologic and evolutionary patterns. In: *Sedimentary and Evolutionary Cycles* (Ed. by U. Bayer and A. Seilacher). Springer-Verlag, Berlin, p. 382-395.

Kindle, E. M. 1914. The Silurian and Devonian section of western Manitoba. *Canada Geological Survey Summary Report 1912*, p. 247-261.

Kinsman, D. J. J. 1966. Gypsum and anhydrite of recent age, Trucial Coast, Persian Gulf. In: *Second Symposium on Salt, Volume 1*. Northern Ohio Geological Society, Cleveland, Ohio. p. 302-306.

Kinsman, D. J. J. 1969. Modes of formation, sedimentary association, and diagnostic features of shallow-water and supratidal evaporites. *Bulletin of the American Association of Petroleum Geologists*, v. 53, p. 830-840.

Klingspor, A. M. 1969. Middle Devonian Muskeg Evaporites of western Canada. *Bulletin of the American Association of Petroleum Geologists*, v. 53, p. 927-948.

Kobluk, D. R., Pemberton, S. G., Karolyi, M. and Risk, M. J. 1977. The Silurian-Devonian disconformity in southern Ontario. *Bulletin of Canadian Petroleum Geology*, v. 25, p. 1157-1186.

Kobluk, D. R. 1984. Coastal paleokarst near the Ordovician-Silurian boundary, Manitoulin Island, Ontario. *Bulletin of Canadian Petroleum Geology*, v. 32, p. 398-407.

Kramers, J. W. and Lerbekmo, J. F. 1967. Petrology and mineralogy of Watt Mountain Formation, Mitsue - Nipisi area, Alberta. *Bulletin of Canadian Petroleum Geology*, v. 15, p. 346-378.

Kumar, N. and Sanders, J. E. 1976. Characteristics of shoreface storm deposits: modern and ancient examples. *Journal of Sedimentary Petrology*, v. 46, p. 145-162.

Kreisa, R. D. 1981. Storm-generated sedimentary structures in subtidal marine facies with examples from the Middle and Upper Ordovician of southwestern Virginia. *Journal of Sedimentary Petrology*, v. 51. p. 823-848.

Kreisa, R. D. and Bambach, R. K. 1982. The role of storm processes in generating shell beds in Paleozoic shelf environments. In: *Cyclic and Event Stratification* (Ed. by G.

Einsele and A. Seilacher). Springer-Verlag, Berlin, p. 200-207.

Lane, D. M. 1959. Dawson Bay Formation in the Quill Lakes-Qu'Appelle area, Saskatchewan. *Saskatchewan Department of Mineral Resources Report No. 38*, 51 p.

Lane, D. M. 1964. Souris River Formation in southern Saskatchewan. *Saskatchewan Department of Mineral Resources Report No. 92*, 72 p.

Lane, D. M. 1987. The Dawson Bay Formation (Devonian) in southern Saskatchewan (update). In: *Summary of Investigations 1987, Saskatchewan Geological Survey* (Ed. by R. Macdonald). Miscellaneous Report - Saskatchewan Mineral Resources 87-4, p. 170-175.

Langmuir, D. 1978. Uranium solution-mineral equilibria at low temperatures with applications to sedimentary ore deposits. *Geochimica et Cosmochimica Acta*, v. 42, p. 547-569.

Leckle, D. A., Singh, C., Goodarzi, F. and Wall, J. H. 1990. Organic-rich, radioactive marine shale: a case study of a shallow-water condensed section, Cretaceous Shaftesbury Formation, Alberta, Canada. *Journal of Sedimentary Petrology*, v. 60, p. 101-117.

Leonard, K. W. 1996. Sequence stratigraphy of the lower part of the Muscatatuck Group (Middle Devonian) in southeastern Indiana. In: *Paleozoic Sequence Stratigraphy: Views from the North American Craton* (Ed. by B. J. Witzke, G. A. Ludvigson and J, Day). Geological Society of America Special Paper 306, p. 243-257.

Li, X. and Droser, M. L. 1997. Nature and distribution of Cambrian shell concentrations: evidence from the Basin and Range Province of the western United States (California, Nevada, and Utah). *Palaios*, p, 111-126.

Lockman-Balk, C. and Wilson, J. L. 1967. Stratigraphy of Upper Cambrian-Lower Ordovician subsurface sequence in Williston Basin. *Bulletin of the American Association of Petroleum Geologists Bulletin*, v. 51, p. 883-917.

Logan, B. W. 1987. The MacLeod evaporite basin, western Australia. *The American Association of Petroleum Geologists Memoir* 44, 140 p.

Longerich, H. P., Janner, G. A., Fryer, B. J. and Jackson, S. E. 1990. Inductively coupled plasma-mass spectrometric analysis of geological samples: a critical evaluation based on case studies. *Chemical Geology*, v. 83, p. 105-118.

Loutit, T. S., Hardenbol, J., Vail, P. R. and Baum, G. R. 1988. Condensed sections: the key to age determination and correlation of continental margin sequences. In: *Sea-Level Changes: An Integrated Approach* (Ed. by C. K., Wilgus, B. S. Hastings, C. G. St. C. Kendall, H. W. Posamentier, C. A. Ross and J. C. Van Wagoner). Society of Economic Paleontologists and Mineralogists Special Publication 42, p. 183-213.

Love, L. G. 1967. Early diagenetic iron sulphide in Recent sediments of the Wash (England). *Sedimentology*, v. 9, p. 327-352.

Lowe, D. R. 1975. Water escape structures in coarse-grained sediments. *Sedimentology*, v. 22, p. 157-204.

Lowe, D. R. and LoPiccolo, R. D. 1974. The characteristics and origins of dish and pillar structures. *Journal of Sedimentary Petrology*, v. 44, p. 484-501.

Lowenstein, T. K. and Hardie, L. A. 1985. Criteria for the recognition of salt-pan evaporites. *Sedimentology*, v. 32, p. 627-644.

MacEachern, J. A., Raychaudhuri, I. and Pemberton, S. G. 1992. Stratigraphic applications of the *Glossifungites* ichnofacies: delineating discontinuities in the rock record. In: *Applications of Ichnology to Petroleum Exploration: A Core Workshop* (Ed. by S. G. Pemberton). Society of Economic Paleontologists and Mineralogists Core Workshop No. 17, p. 169-198.

Maltman, A. 1987a. Shear zones in argillaceous sediments - an experimental study. In: *Deformation of Sediments and Sedimentary Rocks* (Ed. by M. E. Jones and R. M. F. Preston). Geological Society Special Publication No. 29, p. 77-87.

Maltman, A. 1987b. A laboratory technique for investigating the deformation microstructures of water rich sediments. In: *Deformation of Sediments and Sedimentary Rocks* (Ed. by M. E. Jones and A. M. F. Preston). Geological Society

Special Publication No. 29, p. 71-76.

Marriott, S. B. and Wright, V. P. 1993. Palaeosols as indicators of geomorphic stability in two Old Red Sandstone alluvial suits, South Wales. *Journal of the Geological Society, London*, v. 150, p. 1109-1120.

Mazzullo, S. J. and Friedman, G. M. 1975. Conceptual model of tidally influenced deposition on margins of epeiric seas: Lower Ordovician (Canadian) of eastern New York and southwestern Vermont. *Bulletin of the American Association of Petroleum Geologists*, v. 59, p. 2123-2141.

Meijer Drees, N. C. 1994. Devonian Elk Point Group of the Western Canada Sedimentary Basin. In: *Geological Atlas of Western Canada Sedimentary Basin* (Ed. by G. Mossop and I. Shetsen). Canadian Society of Petroleum Geologists and the Alberta Research Council, Calgary, p. 129-147.

Middelburg, J. J., Calvert, S. E. and Karlin, R. 1991. Organic-rich transitional facies in silled basin: response to sea-level changes. *Geology*, v. 19, p. 679-682.

Mielke, J. E. 1979. Composition of the Earth's crust and distribution of the elements. In: *Review of Research on Modern Problems in Geochemistry* (Ed. by F. R. Siegel). Earth Science, v. 16, p. 13-37.

Moore, P. F. 1989. The Lower Kaskaskia Sequence - Devonian. In: *Western Canada Sedimentary Basin - A Case History* (Ed. by B. D. Ricketts). Canadian Society of Petroleum Geologists, Calgary, p. 139-164.

Moore, P. F. 1993. Devonian. In: *Sedimentary Cover of the Craton in Canada* (Ed. by D. F. Stott and J. D. Aitken). Geological Survey of Canada, Ottawa, p. 150-201.

Muir, M., Lock, D. and von der Borch, C. 1980. The Coorong model for penecontemporaneous dolomite formation in the Middle Proterozoic McArthur Group, Northern Territory, Australia. In: *Concepts and Models of Dolomitization* (Ed. by D. H. Zenger, J. B. Dunham and R. L. Ethington). Society of Economic Paleontologists and Mineralogists Special Publication 28, p. 51-67.

Myers, K. J. and Wignall, P. B. 1987. Understanding Jurassic organic-rich mudrocks - new concepts using gamma ray spectrometry and palaeoecology: examples from the Kimmeridge Clay of Dorset and the Jet Rock of Yorkshire. In: *Marine Clastic Sedimentology: Concepts and Case Studies* (Ed. by J. K. Leggett and G. G. Zuffa). Graham & Trotman, London, p. 172-189.

Myrow, P. M. 1995. *Thalassinoides* and the enigma of early Paleozoic open-framework burrow systems. *Palaios*, v. 10, p. 58-74.

Norris, A. W., Uyeno, T. T. and McCable, H. R. 1982. Devonian rocks of the Lake Winnipegosis - Lake Manitoba outcrop belt, Manitoba. *Geological Survey of Canada, Memoir* 392, 280 p.

Nuhfer, E. B. 1981. Mudrock fabrics and their significance - discussion. *Journal of Sedimentary Petrology*, v. 51, p. 1027-1029.

Nummedal, D. and Swift, D. J. P. 1987. Transgressive stratigraphy at sequence-bounding unconformities: some principles derived from Holocene and Cretaceous examples. In: *Sea-level Fluctuation and Coastal Evolution* (Ed. by D. Nummedal, O. H. Pilkey and J. D. Howard). Society of Economic Paleontologists and Mineralogists Special Publication 41, p. 241-260.

Owen, G. 1987. Deformation processes in unconsolidated sands. In: *Deformation of Sediments and Sedimentary Rocks* (Ed. by M. E. Jones and R. M. F. Preston). Geological Society Special Publication No. 29, p. 11-24.

Ozalas, K., Savrda, C. E. and Fullerton, R. R. Jr. 1994. Bioturbated oxygenation-event beds in siliceous facies: Monterey Formation (Miocene), California. *Palaeogeography, Palaeoclimatology, Palaeoecology*, v. 112, p. 63-83.

Pedersen, T. F. and Calvert, S. E. 1990. Anoxia vs. productivity: what controls the formation of organic-carbon--rich sediments and sedimentary rocks? *Bulletin of the American Association of Petroleum Geologists*, v. 74, p. 454-466.

Peterson, J. A. and MacCary, L. M. 1987. Regional stratigraphy and general petroleum geology of the U.S. portion of the Williston Basin and adjacent areas. In: *Williston*

Basin: Anatomy of a Cratonic Oil Province (Ed. by M. W. Longman). The Rocky Mountain Association of Geologists, Denver. p. 9-43.

Pemberton, S. G. and Frey, R. W. 1985. The *Glossifungites* ichnofacies: modern examples from the Georgia coast, U.S.A. In: *Biogenic Structures: Their Use in Interpreting Depositional Environments* (Ed. by H. A. Curran). Society of Economic Paleontologists and Mineralogists Special Publication 35, p. 237-259.

Pemberton, S. G., Frey, R. W., Ranger, M. J. and MacEachern, J. A. 1992. The conceptual framework of ichnology. In: *Applications of Ichnology to Petroleum Exploration: A Core Workshop* (Ed. by S. G. Pemberton). Society of Economic Paleontologists and Mineralogists Core Workshop No. 17, p. 1-32.

Pettijohn, E. J. 1975. Sedimentary rocks. Harper & Row Publishers, New York. 628 p.

Platt, N. H. and Keller, B. 1992. Distal alluvial deposits in a foreland basin-setting - the Lower Freshwater Molasse (Lower Miocene), Switzerland: sedimentology, architecture and paleosols. *Sedimentology*, v. 39, p. 545-565.

Poborski, J. W. 1970. The Upper Permian Zechstein in the eastern province of Central Europe. In: *Third Symposium on Salt* (Ed. by J. L. Raw and L. F. Dellwig). Northern Ohio Geological Society, Cleveland, Ohio. p. 24-29.

Porter, J. W. and Fuller, J. G. C. M. 1959. Lower Paleozoic rocks of northern Williston Basin and adjacent areas. *Bulletin of the American Association of Petroleum Geologists*, v. 43, p. 124-189.

Porter, J. W., Price, R. A. and McCrossan, R. G. 1982. The Western Canada Sedimentary Basin. *Philosophical Transactions of the Royal Society of London, Series A: Mathematical and Physical Sciences*, v. 305, p. 169-193.

Pound, W. R. 1985. The geology and hydrocarbon potential of the Dawson Bay carbonate unit (Middle Devonian), Williston Basin, North Dakota. *MSc thesis*, University of North Dakota. 320 p.

Powley, D. E. 1951. Devonian stratigraphy of central Saskatchewan. *MSc thesis*,

University of Saskatchewan, Saskatoon, Saskatchewan, 98 p.

Pratt, B. R. and James, N. P. 1986. The St. George Group (Lower Ordovician) of western Newfoundland: tidal flat island model for carbonate sedimentation in shallow epeiric seas. *Sedimentology*, v. 33, p. 313-343.

Pratt, B. R., James, N. P. and Cowan, C. A. 1992. Peritidal carbonates. In: *Facies Models: Response to Sea Level Change* (Ed. by R. G. Walker and N. P. James). Geoscience Canada. p. 303-322.

Pratt, B. R. 1994. Seismites in the Mesoproterozoic Altyn Formation (Belt Supergroup), Montana: a test for tectonic control of peritidal carbonate cyclicity. *Geology*, v. 22, p. 1091-1094.

Pratt, B. R., Bernstein, L. M., Kendall, A. C. and Haidl, F. M. 1996. Occurrence of reefal facies in Red River Strata (Upper Ordovician), subsurface Saskatchewan. In: *Summary of Investigations 1996, Saskatchewan Geological Survey*. Saskatchewan Energy and Mines, Miscellaneous Report 96-4. p. 147-152.

Rasmussen, K. A. and Neumann, A. C. 1988. Holocene overprints of Pleistocene paleokarst: Bight of Abaco, Bahamas. In: *Paleokarst* (Ed. by N. P. James and P. W. Choquette). Springer-Verlag, New York. P. 132-148.

Reineck, H.-E. and Singh, I. B. 1980. Depositional sedimentary environments: with reference to terrigenous clastics. Springer-Verlag, Berlin, 549 p.

Read, J. F. and Grover, G. A. Jr. 1977. Scalloped and planar erosion surface, Middle Ordovician limestones, Virginia: analogues of Holocene exposed karst or tidal rock platforms. *Journal of Sedimentary Petrology*, v. 47, p. 956-972.

Renaut, R.W., and Long, P. R. 1989. Sedimentology of the saline lakes of the Cariboo Plateau, Interior British Columbia, Canada. *Sedimentary Geology*, v. 64, p. 239-264.

Renaut, R. W. 1994. Carbonate and evaporite sedimentation at Clinton Lake, British Columbia, Canada. In: *Paleoclimate and Basin Evolution of Playa Systems* (Ed. by M. R. Rosen). Geological Society of America Special Paper 289, p. 49-68.

Retallack, G. J. 1988. Field recognition of paleosols. In: *Paleosols and Weathering Through Geologic Time: Principles and Applications* (Ed. by J. Reinhardt and W. R. Sigleo). Geological Society of America Special Paper 216, p. 1-20.

Rhoads, D. C. and Morse, J. M. 1971. Evolutionary and ecologic significance of oxygen-deficient marine basins. *Lethaia*, v. 4, p. 413-428.

Rider, M. H. 1996. The geological interpretation of well logs. Gulf Publishing Company, Houston. 280 p.

Rizzi, G. and Braithwaite, C. J. R. 1996. Cyclic emersion surfaces and channels within Dinantian limestones hosting the giant Navan Zn-Pb deposit. Ireland. In: *Recent Advances in Carboniferous Geology* (Ed. by P. Strogen, I. D. Sommerville and G. Ll. Jones). Geological Society Special Publication No. 107, p. 207-219.

Rosen, M. R. and Coshell, L. 1992. A new location of Holocene dolomite formation, Lake Hayward, Western Australia. *Sedimentology*, v. 39, p. 161-166.

Rosen, M. R., Miser, D. E. and Warren, J. K. 1988. Sedimentology, mineralogy, and isotopic analysis of Pellet Lake, Coorong region, South Australia. *Sedimentology*, v. 35, p. 105-122.

Sami, T. and Desrochers, A. 1992. Episodic sedimentation on an early Silurian, storm-dominated carbonate ramp, Becscie and Merrimark formations, Anticosti Island, Canada. *Sedimentology*, v. 39, p. 355-381.

Sandberg, C. A. and Hammond, C. R. 1958. Devonian System in Williston Basin and central Montana. *Bulletin of the American Association of Petroleum Geologists*, v. 42. p. 2293-2334.

Savrda, C. E., Bottjer, D. J. and Gorsline, D. S. 1984. Development of a comprehensive oxygen-deficient marine biofacies model: evidence from Santa Monica, San Pedro, and Santa Barbara basins, California continental borderland. *Bulletin of the American Association of Petroleum Geologists*, v. 68, p. 1179-1192.

Savrda, C. E., and Bottjer, D. J. 1986. Trace fossil model for reconstruction of paleo-oxygenation in bottom waters. *Geology*, v. 14, p. 3-6.

Savrda, C. E. and Bottjer, D. J. 1989. Trace-fossil model for reconstructing oxygenation histories of ancient marine bottom waters: application to Upper Cretaceous Niobrara Formation, Colorado. *Palaeogeography, Palaeoclimatology, Palaeoecology*, v. 74, p. 49-74.

Savrda, C. E. 1991. Ichnology in sequence stratigraphic studies: an example from the Lower Paleocene of Alabama. *Palaios*, v. 6, p. 39-53.

Savrda, C. E., Bottjer, D. J. and Seilacher, A. 1991. Redox-related benthic events. In: *Cycles and Events in Stratigraphy* (Ed. by G. Einsele, W. Ricken and A. Seilacher). Springer-Verlag, Berlin, p. 524-541.

Savrda, C. E. 1992. Trace fossils and benthic oxygenation. In: *Trace Fossils* (Ed. by C. Maples and R. West), Paleontological Society Short Course Notes 5, p. 172-196.

Savrda, C. E. 1995. Ichnologic applications of paleoceanographic. paleoclimatic, and sea-level studies. *Palaios*, v. 10, p. 565-577.

Schieber, J. 1986. The possible role of benthic microbial mats during the formation of carbonaceous shales in shallow Mid-Proterozoic basins. *Sedimentology*, v. 33, p. 521-536.

Schieber, J. 1994. Reflection of deep vs shallow water deposition by small scale sedimentary features and microfabrics of Chattanooga Shale in Tennessee. In: *Pangea: Global Environments and Resources* (Ed. by A. F. Embry, B. Beauchamp and D. J. Glass). Canadian Society of Petroleum Geologists Memoir 17, p. 927-947.

Schrieber, B. C., Roth, M. S. and Helman, M. L. 1982. Recognition of primary facies characteristics of evaporites and the differentiation of these forms from diagenetic overprints. In: *Depositional and Diagenetic Spectra and Evaporites - A Core Workshop* (Ed. by C. R. Handford, R. G. Loucks and G. R. Davies). Society of Economic Paleontologists and Mineralogists Core Workshop No. 3. p. 1-32.

Seilacher, A. 1967. Bathymetry of trace fossils. *Marine Geology*, v. 5, p. 413-428.

Shaw, A. B. 1964. Time in stratigraphy. McGraw-Hill, New York, 365 p.

Shearman, D. J. 1966. Origin of marine evaporites by diagenesis. *Transactions of the Institution of Mining Metallurgy, Section B: Applied Earth Science*, v. 75, p. 208-215.

Sheehan, P. M. and Schiefelbein, D. R. J. 1984. The trace fossil *Thalassinoides* from the Upper Ordovician of the eastern Great Basin: deep burrowing in the early Paleozoic. *Journal of Paleontology*, v. 58, p. 440-447.

Shinn, E. A., Ginsburg, R. N. and Lloyd, R. M. 1965. Recent supratidal dolomite from Andros Island, Bahamas. In: *Dolomitization and Limestone Diagenesis: A Symposium* (Ed. by L. C. Pray and R. C. Murray). Society of Economic Paleontologists and Mineralogists Special Publication 13, p. 112-123.

Shinn, E. A. 1968. Selective dolomitization of recent sedimentary structures. *Journal of Sedimentary Petrology*, v. 38, p. 612-616.

Shinn, E. A., Lloyd, R. M. and Ginsburg, R. N. 1969. Anatomy of a modern carbonate tidal flat, Andros Island, Bahamas. *Journal of Sedimentary Petrology*, v. 39, p. 1202-1228.

Shinn, E. A. 1983a. Tidal flat environment. In: *Carbonate Depositional Environments* (Ed. by P. A. Scholle, D. G. Bebout and C. H. Moore). American Association of Petroleum Geologists Memoir 33, p. 171-210.

Shinn, E. A. 1983b. Birdseyes, fenestrae, shrinkage pores and loferites: a reevaluation. *Journal of Sedimentary Petrology*, v. 53, p. 619-628.

Simpson E. L. and Eriksson, K. A. 1990. Early Cambrian progradational and transgressive sedimentation patterns in Virginia: an example of the early history of a passive margin. *Journal of Sedimentary Petrology*, v. 60, p. 84-100.

Smith, D. B. 1971. Possible displacive halite in the Permian Upper Evaporite Group of

northeast Yorkshire. *Sedimentology*, v. 17, p. 221-232.

Smoot, J. P. 1981. Subaerial exposure criteria as seen in modern playa mudcracks. *Bulletin of the American Association of Petroleum Geologists*, v. 65, p. 530.

Smoot, J. P. and Katz, S. B. 1982. Comparison of modern playa mudflat fabrics to cycles in the Triassic Lockatong Formation of New Jersey. *Geological Society of America, Abstracts with Programs*, v. 14, p. 83.

Smoot, J. P. and Olsen, P. E. 1988. Massive mudstones in basin analysis and paleoclimatic interpretation of the Newark Supergroup. In: *Triassic-Jurassic Rifting* (Ed. by W. Manspeizer). Elsevier, Amsterdam, p. 249-274.

Smoot, J. P. and Lowenstein, T. K. 1991. Depositional environments of non-marine evaporites. In: *Evaporites, Petroleum and Mineral Resources* (Ed. by J. L. Melvin). Developments in Sedimentology 50. Elsevier, Amsterdam, p. 189-347.

Soil Survey Staff, 1992. Keys to Soil Taxonomy, 5th Edition, Soil Management Support Services Technical Monograph 19. Pocahontas Press, Blacksburg, Virginia, 541 p.

Sweeting, M.M. 1973. Karst landforms. Macmillan, London. 362 p.

Strasser, A. 1991. Lagoonal-peritidal sequences in carbonate environments: autocyclic and allocyclic processes. In: *Cycles and Events in Stratigraphy* (Ed. by G. Einsele, W. Ricken and A. Seilacher). p. 709-721.

Thompson, J. B., Mullins, H. T., Newton, C. R. and Vercoutere, T. L. 1985. Alternative biofacies model for dysaerobic communities. *Lethaia*, v. 18, p. 167-179.

Tucker, M. E. 1990. Dolomites and dolomitization models. In: *Carbonate Sedimentology* (Ed. by M. E. Tucker and V. P. Wright). Blackwell Scientific Publications, Oxford, p. 365-400.

Tucker, M. E. 1991. Sedimentary petrology: an introduction to the origin of sedimentary rocks. Blackwell Scientific Publications, Oxford. 260 p.

Tucker, M. E. 1993. Carbonate diagenesis and sequence stratigraphy. In: *Sedimentology Review 1* (Ed. by V. P. Wright). Blackwell Scientific Publications, London. p. 51-72.

Tucker, M.E. and Wright, V.P. 1990. Carbonate sedimentology. Blackwell Scientific Publications, Oxford, 482 p.

Tyrell, J. B. 1892. Report on north-western Manitoba with portions of the adjacent districts of Assiniboia and Saskatchewan. Geological Survey of Canada, Annual Report 1889-91, pt. E, p. 1-240.

Utha-aroon, C. 1990. Sedimentary depositional environments of the Prairie Evaporite Formation, Saskatoon region, Saskatchewan. *MSc thesis*, University of Saskatchewan, Saskatoon, Saskatchewan,152 p.

van Hees, H. 1956. Elk Point Group: notes on a subsurface cross section extending from east central Alberta through Saskatchewan to western Manitoba. *Journal of the Alberta Society of Petroleum Geologists*, v. 4, p. 29-37.

Vanstone, S. D. 1991. Early Carboniferous (Mississippian) paleosols from southwest Britain: influence of climatic change on soil development. *Journal of Sedimentary Petrology*, v. 61, p. 445-457.

Van Wagoner, J. C., Mitchum, R. M., Campion, K. M. and Rahmanian, V. D. 1990. Siliciclastic sequence stratigraphy in well logs, cores, and outcrops: concepts for high-resolution correlation of time and facies. *American Association of Petroleum Geologists, Methods in Exploration Series*, No. 7, 55 p.

von der Borch, C. C. 1965. The distribution and preliminary geochemistry of modern carbonate sediments of the Coorong area, South Australia. *Geochimica et Cosmochimica Acta*, v. 29, p. 781-799.

von der Borch, C. C. and Lock, D. 1979. Geological significance of Coorong dolomites. *Sedimentology*, v. 26, p. 813-824.

Vossler, S. M. and Pemberton, S. G. 1988. Superabundant *Chondrites*: a response to storm buried organic material ? *Lethaia*, v. 21, p. 94.

Walkden, G. M. 1974. Palaeokarstic surfaces in Upper Visean (Carboniferous) limestones of the Derbyshire Block, England. *Journal of Sedimentary Petrology*, v. 44, p. 1232-1247.

Walker, C. T. 1957. Correlations of Middle Devonian rocks in western Saskatchewan. *Saskatchewan Department of Mineral Resources Report No. 25*, 59 p.

Walter, L. M. 1985. Relative reactivity of skeletal carbonates during dissolution: implications for diagenesis. In: *Carbonate Cements* (Ed. by N. Schneidermann and P. M. Harris). Society of Economic Paleontologists and Mineralogists Special Publication 36, p. 3-16.

Warren, P. S. and Stelck, C. R. 1956. Devonian faunas of western Canada. Geological Assoiciation of Canada Special Paper No. 1, p. 1-15.

Warren, J. K. and Kendall, C. G. St. C. 1985. Comparison of sequences formed in marine sabkha (subaerial) and salina (subaqueous) settings - modern and ancient. *Bulletin of the American Association of Petroleum Geologists*, v. 69, p. 1013-1023.

Warren, J. K. 1988. Sedimentology of Coorong dolomite in the Salt Creek Region, South Australia. *Carbonates and Evaporites*, v. 3, p. 175-199.

Warren, J. K. 1990. Sedimentology and mineralogy of dolomitic Coorong lakes, South Australia. *Journal of Sedimentary Petrology*, v. 60, p. 843-858.

Watkins, R. and Coorough, P. J. 1997. Silurian *Thalassinoides* in an offshore carbonate community, Wisconsin, USA. *Palaeogeography, Palaeoclimatology, Palaeoecology*, v. 129, p. 109-117.

Watts, N. R. 1988. Carbonate particulate sedimentation and facies within the Lower Silurian Hogklint patch reefs of Gotland, Sweden. *Sedimentary Geology*, v. 59, p. 93-113.

Whiteaves, J. F. 1891. Description of some previously unrecorded species of fossils from the Devonian rocks of Manitoba. *Transactions of the Royal Society of Canada*, v.

8, p. 93-110.

Wignall, P. B. and Myers, K. J. 1988. Interpreting benthic oxygen levels in mudrocks: a new approach. *Geology*, v. 16, p. 452-455.

Wignall, P. B. and Hallam, A. 1991. Biofacies, stratigraphic distribution and depositional models of British onshore Jurassic black shales. In: *Modern and Ancient Continental Shelf Anoxia* (Ed. by R. V. Tyson and T. H. Pearson). Geological Society Special Publication 58, p. 291-309.

Wignall, P. B. and Maynard, J. R. 1993. The sequence stratigraphy of transgressive black shales. In: *Source Rocks in a Sequence Stratigraphic Framework* (Ed. by B. J. Katz and L. M. Pratt). American Association of Petroleum Geologists Studies in Geology No. 37, p. 35-47.

Wignall, P. B. 1994. Black shales. Clarendon Press, Oxford, 127 p.

Willams, G. E. 1970. Origin of disturbed bedding in Torridon Group Sandstones. *Scotish Journal of Geology*, v. 6, p. 409-411.

Williams, G. K. 1984. Some musings on the Devonian Elk Point Basin, Alberta. *Bulletin of Canadian Petroleum Geology*, v. 32, p. 216-232.

Wilson, J. L. 1975. Carbonate facies in geologic history. Springer-Verlag, Berlin, 471 p.

Witzke, B. J. and Heckel, P. H. 1988. Paleoclimatic indicators and inferred Devonian paleolatitudes of Euramerica. In: *Devonian of the World* (Ed. by N. J. McMillan, A. F. Embry and D. J. Glass). Canadian Society of Petroleum Geologists, Calgary. v. 1, p. 49-63.

Wood, G. V. and Wolfe, M. J. 1969. Sabkha cycles in the Arab-Darb Formation off the Trucial Coast of Arabia. *Sedimentology*, v. 12, p. 165-191.

Wright, V. P. 1982. The recognition and interpretation of paleokarsts: two examples from the Lower Carboniferous of South Wales. *Journal of Sedimentary Petrology*, v. 52, p. 83-94.

Wright, V. P. 1986. Pyrite formation and the drowing of a palaeosol. *Geological Journal*, v. 21, p. 139-149.

Wright, V. P. and Robinson, D. 1988. Early Carboniferous floodplain deposits from South Wales: a case study of the control on palaeosol development. *Journal of the Geological Society, London*, v. 145. p. 847-857.

Wright, V. P., Vanstone, S. D. and Robinson, D. 1991. Ferrolysis in Arundian alluvial paleosols: evidence of a shift in the early Carboniferous monsoonal system. *Journal of the Geological Society, London*, v. 148, p. 9-12.

Wright, V. P. and Smart, P. L. 1994. Paleokarst (dissolution diagenesis): its occurrence and hydrocarbon exploration significance. In: *Diagenesis, IV. Development in Sedimentology* 51 (Ed. by K. H. Wolf and G. V. Chilingarian). Elsevier, Amsterdam, p. 477-517.

Wright, V. P., Vanstone, S. D. and Marshall, J. D. 1997. Contrasting flooding histories of Mississippian carbonate plateforms revealed by marine alteration effects in paleosols. *Sedimentology*, v. 44, p. 825-842.

Yaalon, D. H. and Kalmar, D. 1978. Dynamics of cracking and swelling clay soils, displacement of skeletal grains, optimum depth of slickensides, and rate of intra-pedonic turbation. *Earth Surface Processes*, v. 3, p. 31-42.

Zangerl, R. and Richardson, E. S. Jr. 1963. The paleoecological history of two Pennsylvanian black shales. *Fieldiana Geological Memoirs 4*, p. 1-352.

APPENDIX I

CORE LOCATIONS AND DESCRIPTIONS

Well 14-19-41-23W3

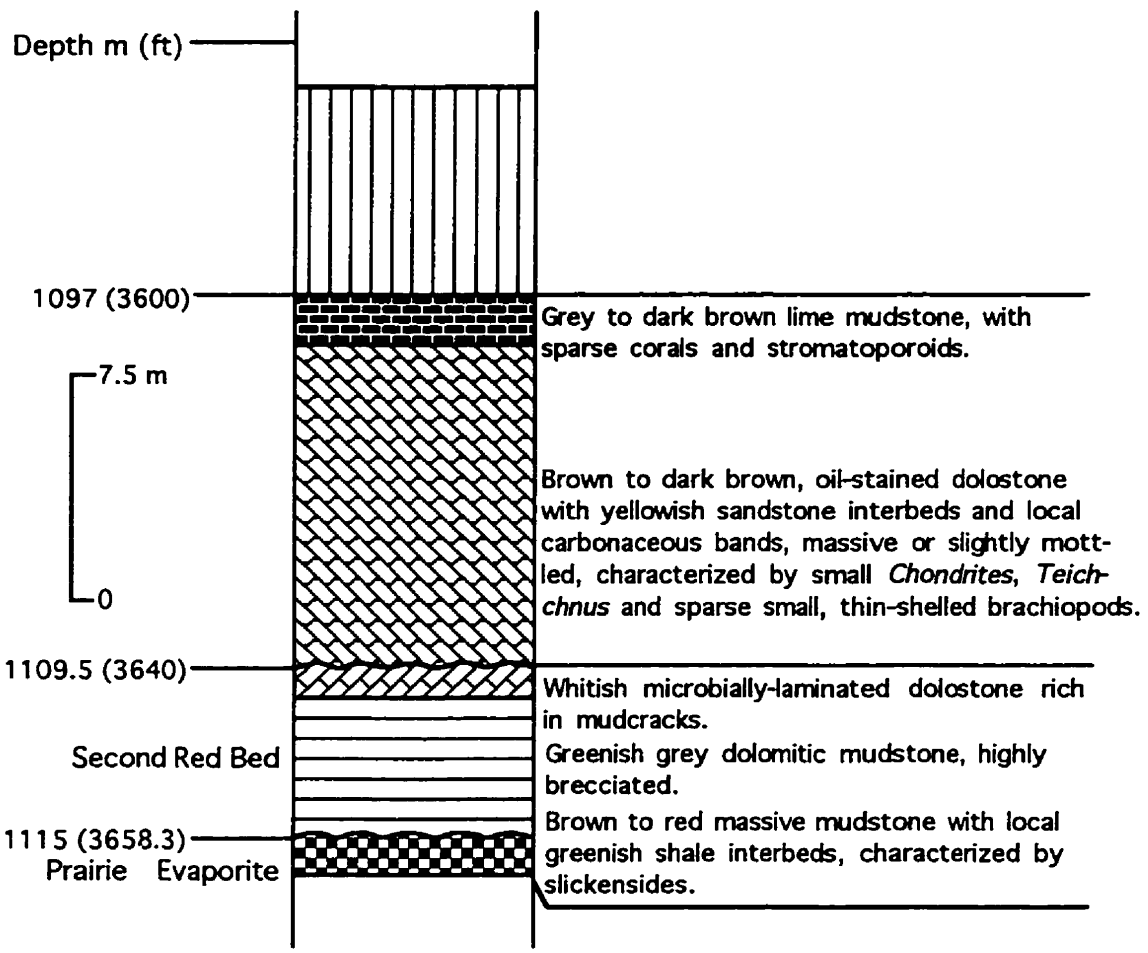

Well 4-18-35-8W3

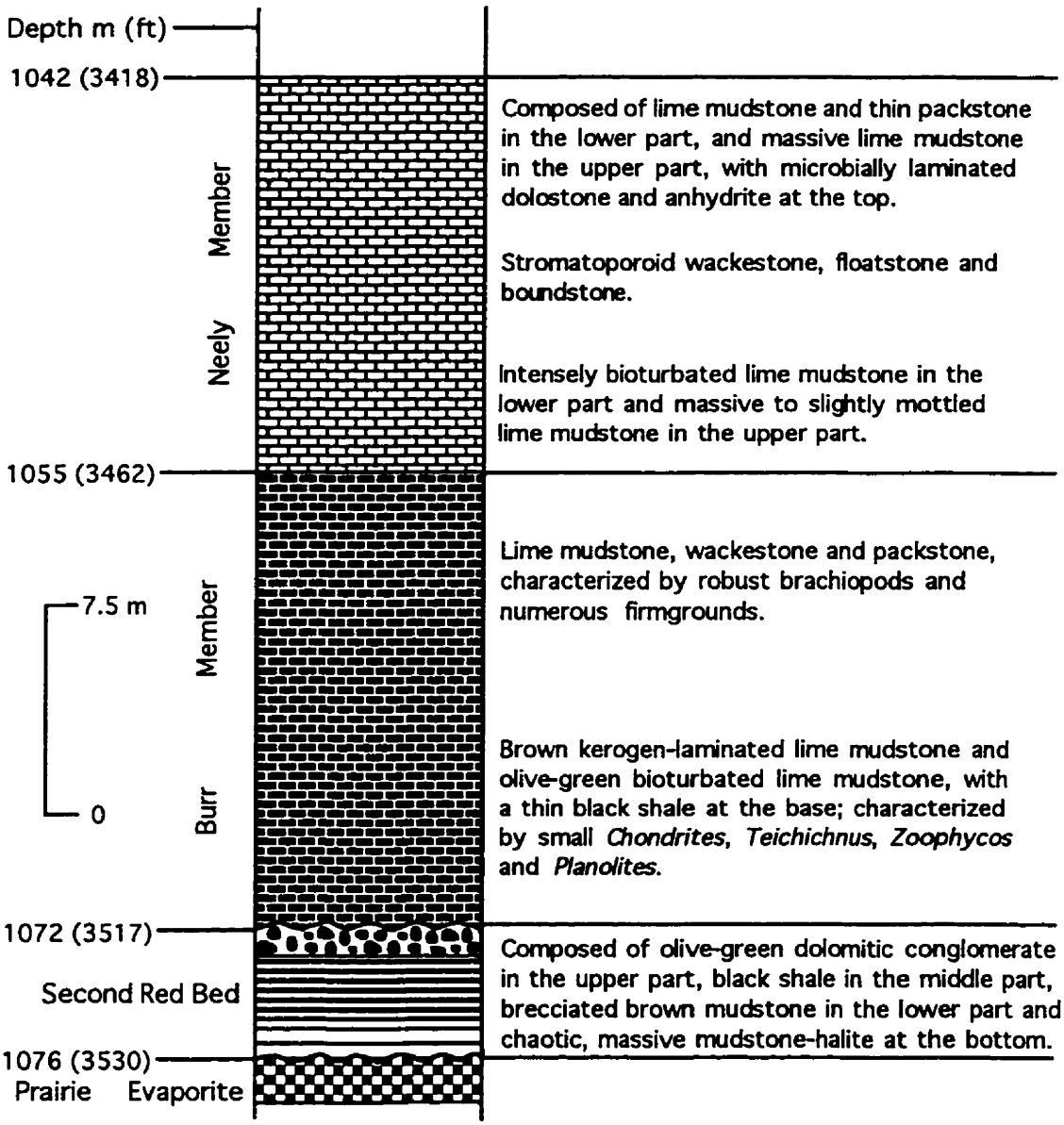

Well 1-2-39-8W3

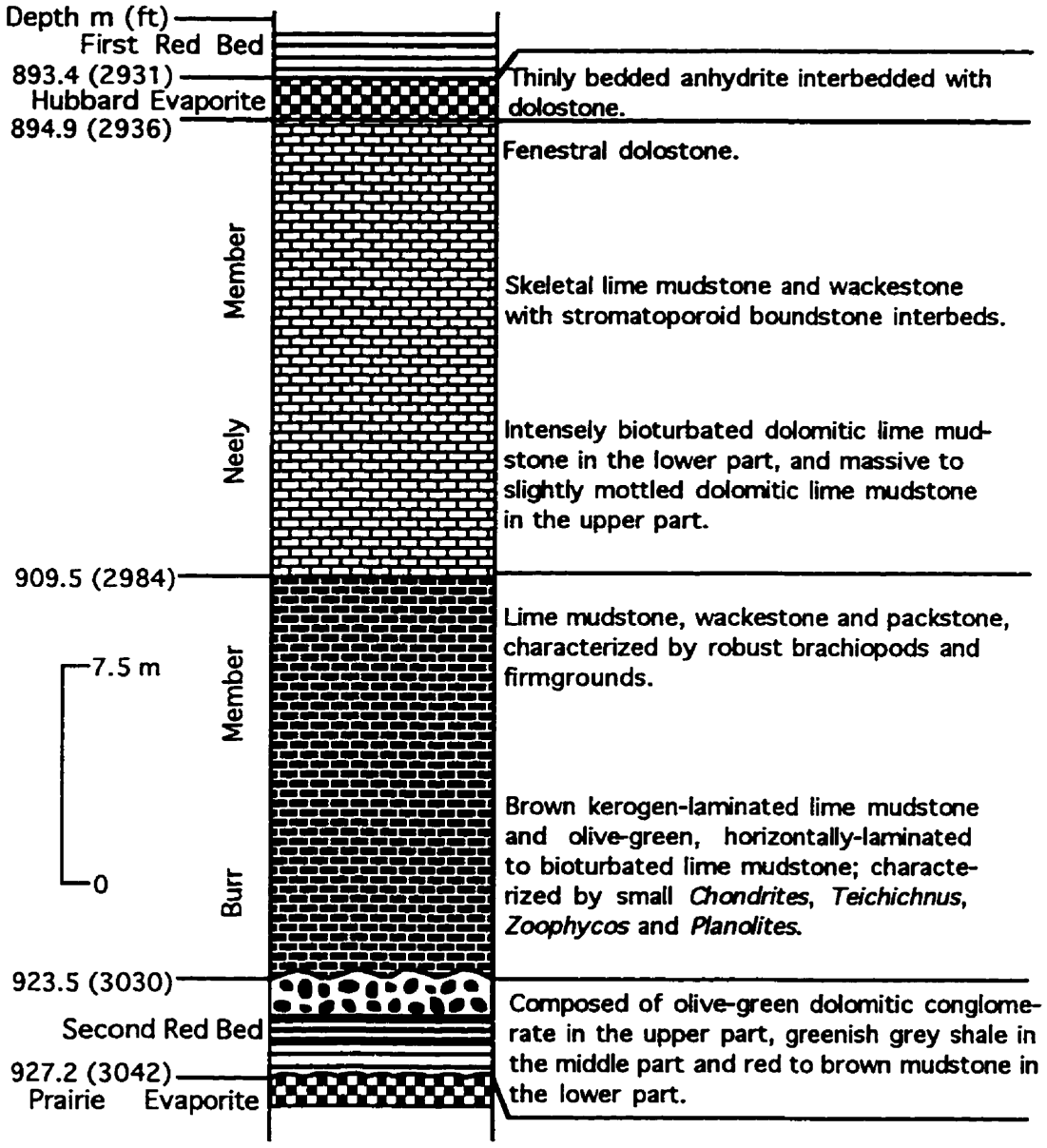

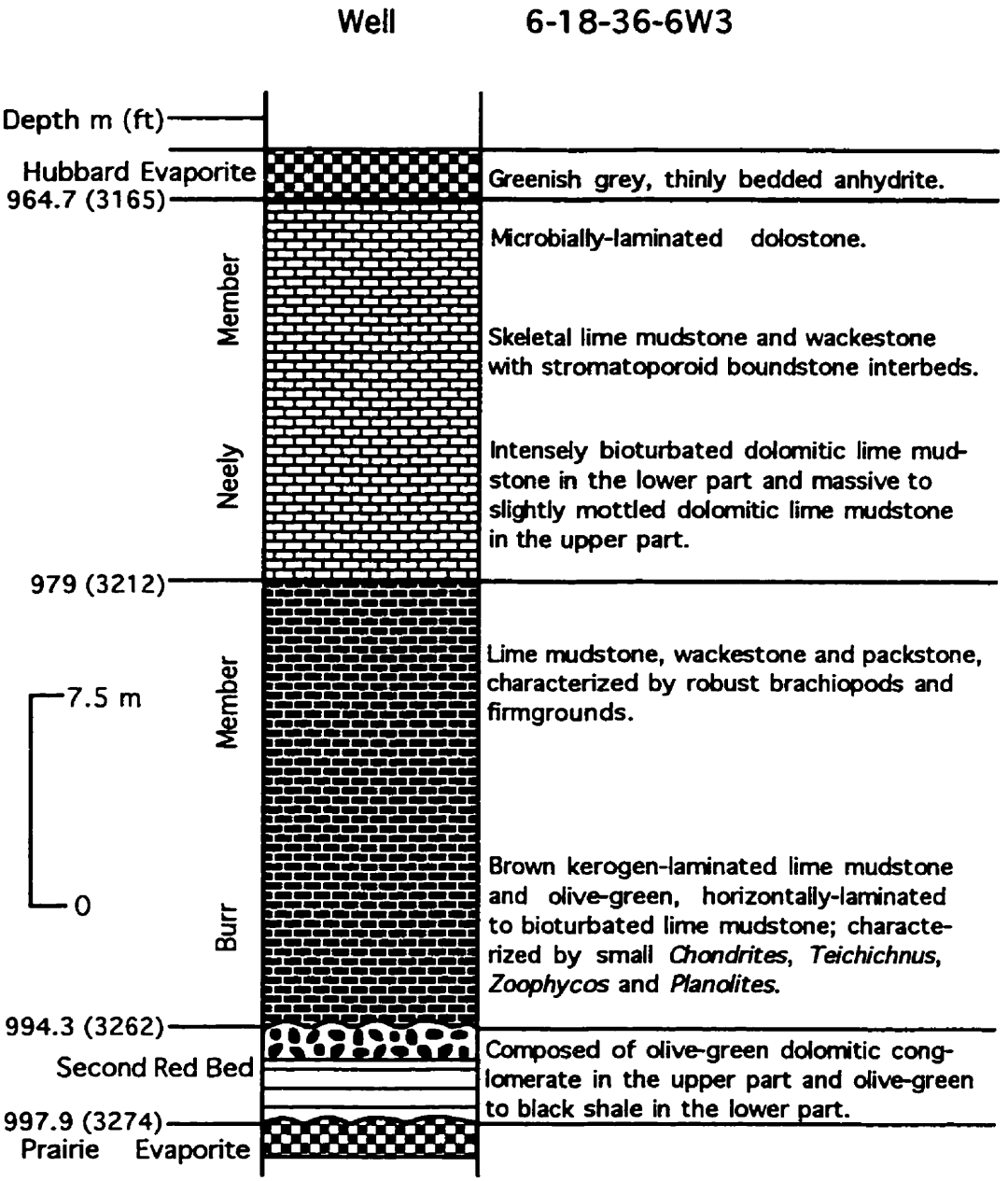
Well 6-18-36-6W3
Depth m (ft)
Hubbard Evaporite
964.7 (3165)
Member
Neely
979 (3212)
7.5 m
0
Member
Burr
994.3 (3262)
Second Red Bed
997.9 (3274)
Prairie Evaporite
Greenish grey, thinly bedded anhydrite.
Microbially-laminated dolostone.
Skeletal lime mudstone and wackestone with stromatoporoid boundstone interbeds.
Intensely bioturbated dolomitic lime mudstone in the lower part and massive to slightly mottled dolomitic lime mudstone in the upper part.
Lime mudstone, wackestone and packstone, characterized by robust brachiopods and firmgrounds.
Brown kerogen-laminated lime mudstone and olive-green, horizontally-laminated to bioturbated lime mudstone; characterized by small Chondrites, Teichichnus, Zoophycos and Planolites.
Composed of olive-green dolomitic conglomerate in the upper part and olive-green to black shale in the lower part.

Well 10-7-32-5W3

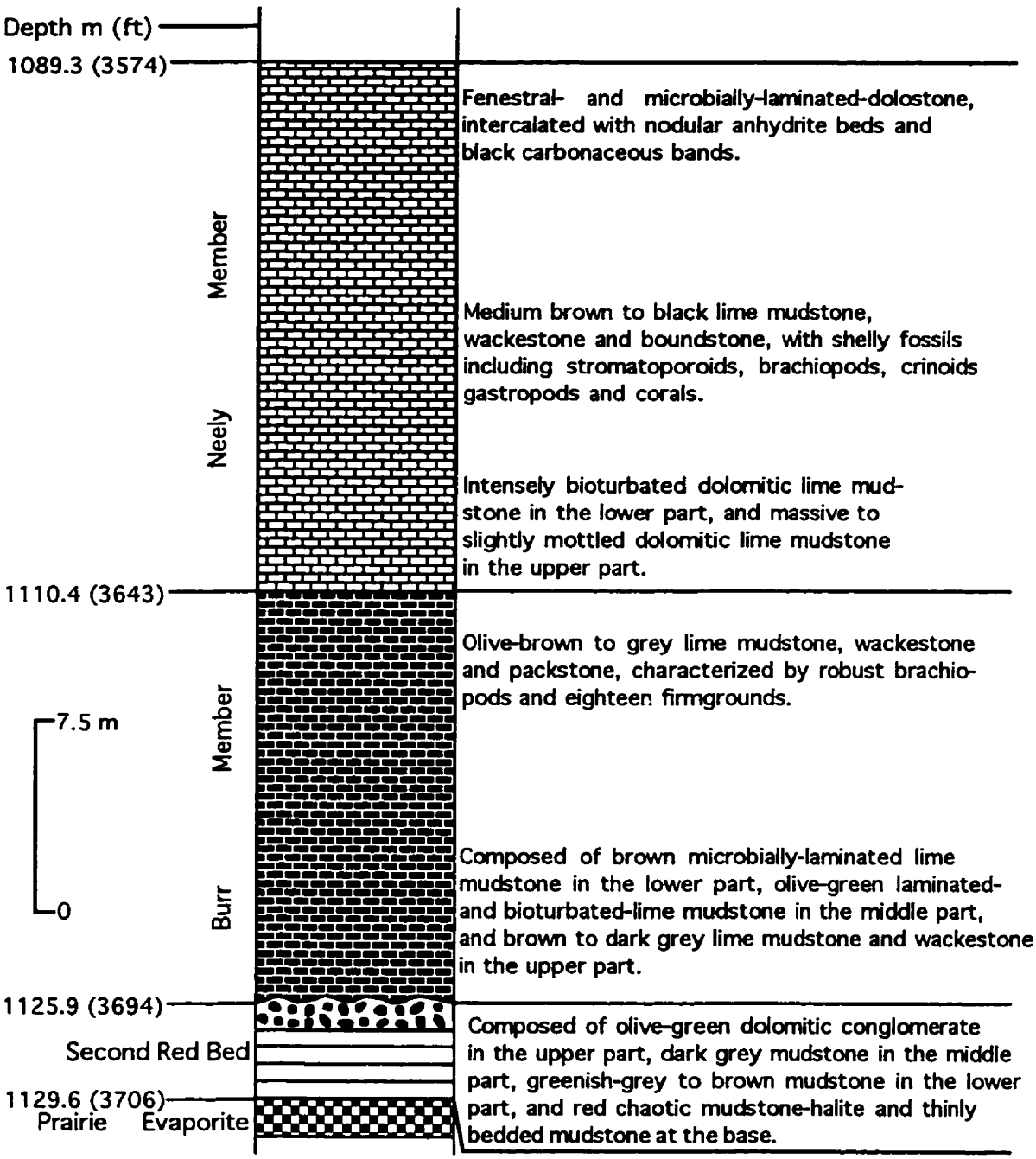

Well 3-30-37-2W3

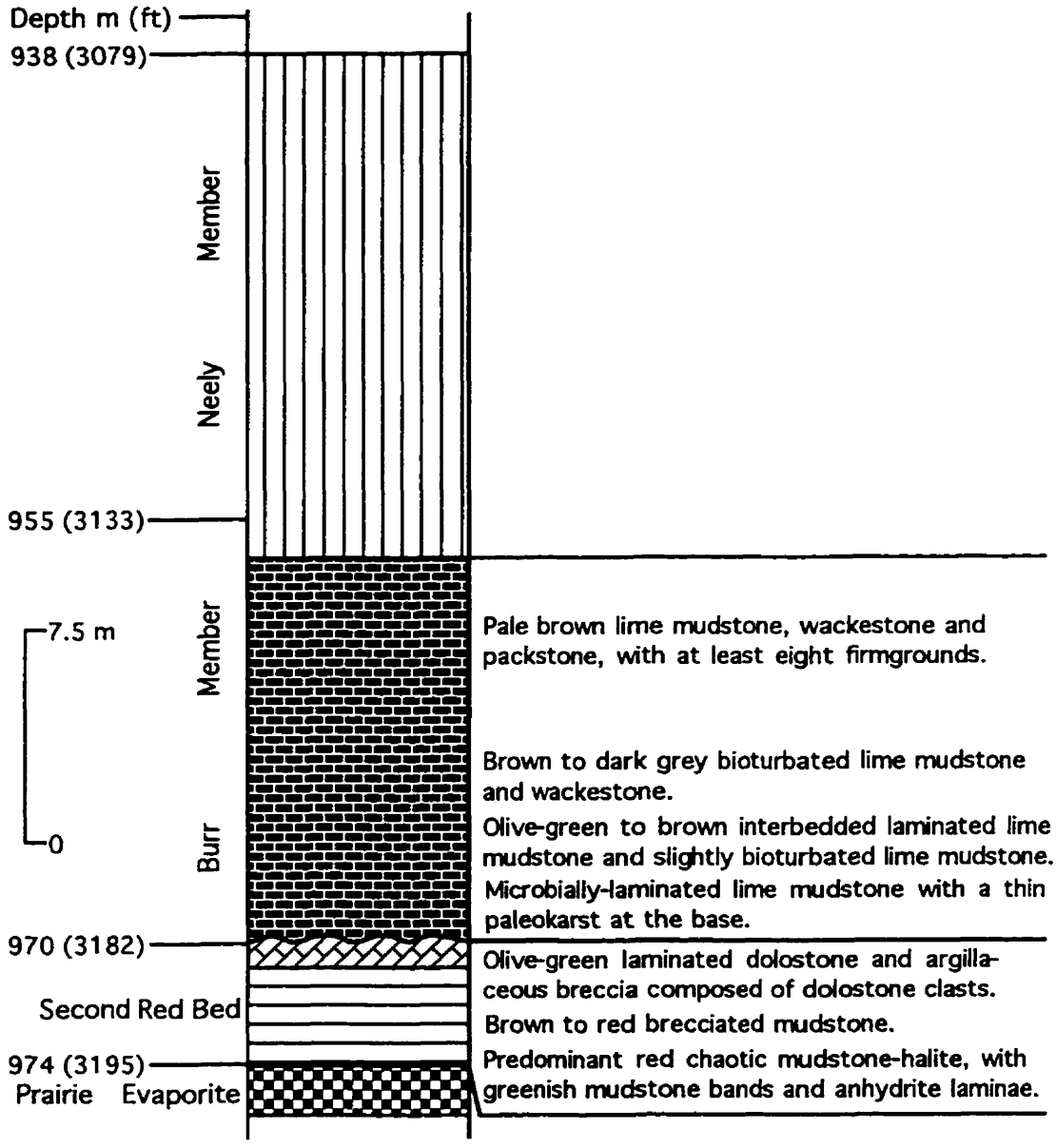

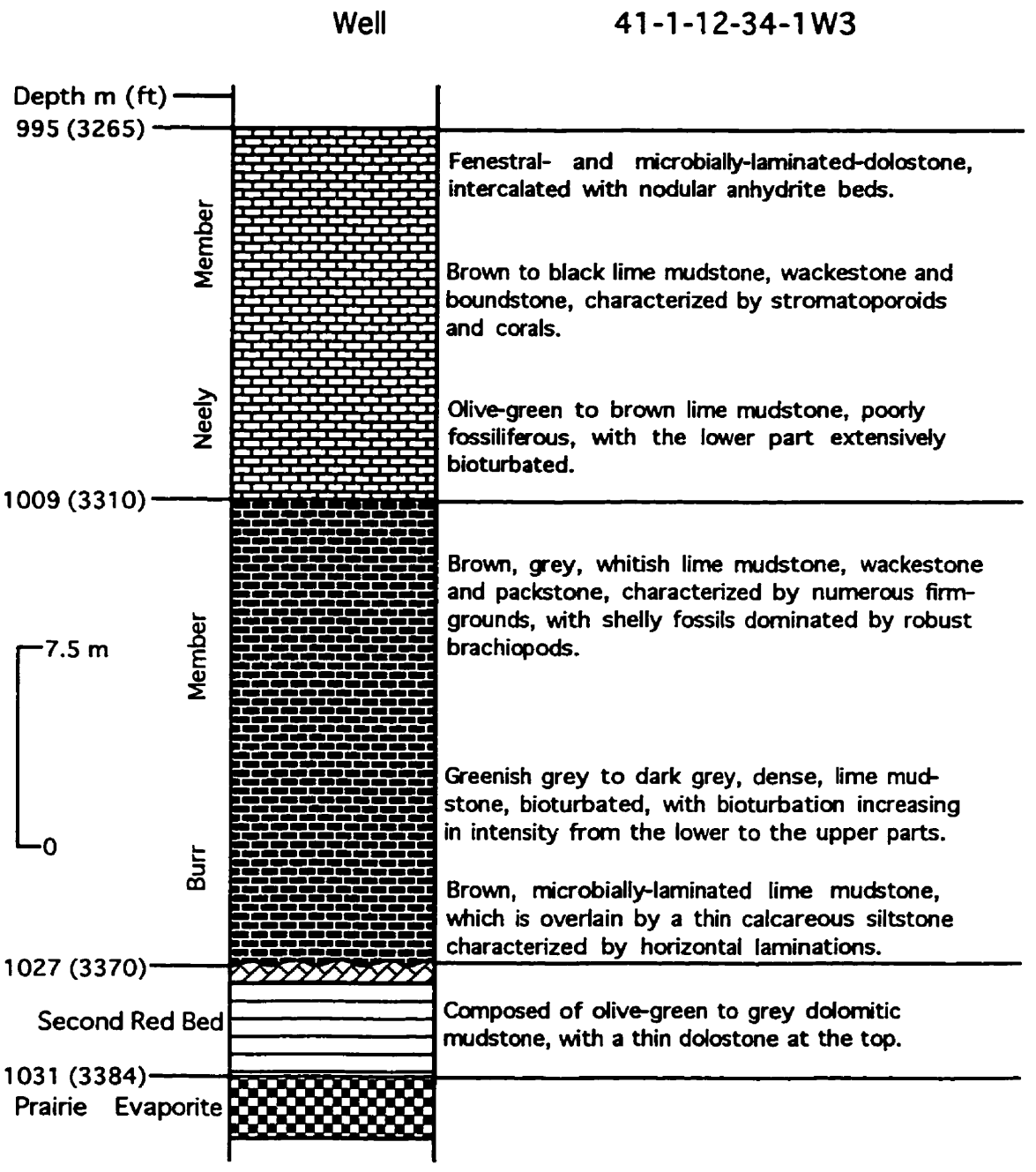
Well 41-1-12-34-1W3
Depth m (ft)
995 (3265)
Member
Neely
Fenestral- and microbially-laminated-dolostone, intercalated with nodular anhydrite beds.
Brown to black lime mudstone, wackestone and boundstone, characterized by stromatoporoids and corals.
Olive-green to brown lime mudstone, poorly fossiliferous, with the lower part extensively bioturbated.
1009 (3310)
Member
Brown, grey, whitish lime mudstone, wackestone and packstone, characterized by numerous firm-grounds, with shelly fossils dominated by robust brachiopods.
7.5 m
0
Burr
Greenish grey to dark grey, dense, lime mud-stone, bioturbated, with bioturbation increasing in intensity from the lower to the upper parts.
Brown, microbially-laminated lime mudstone, which is overlain by a thin calcareous siltstone characterized by horizontal laminations.
1027 (3370)
Second Red Bed
Composed of olive-green to grey dolomitic mudstone, with a thin dolostone at the top.
1031 (3384)
Prairie Evaporite

Well 15-36-32-29W2

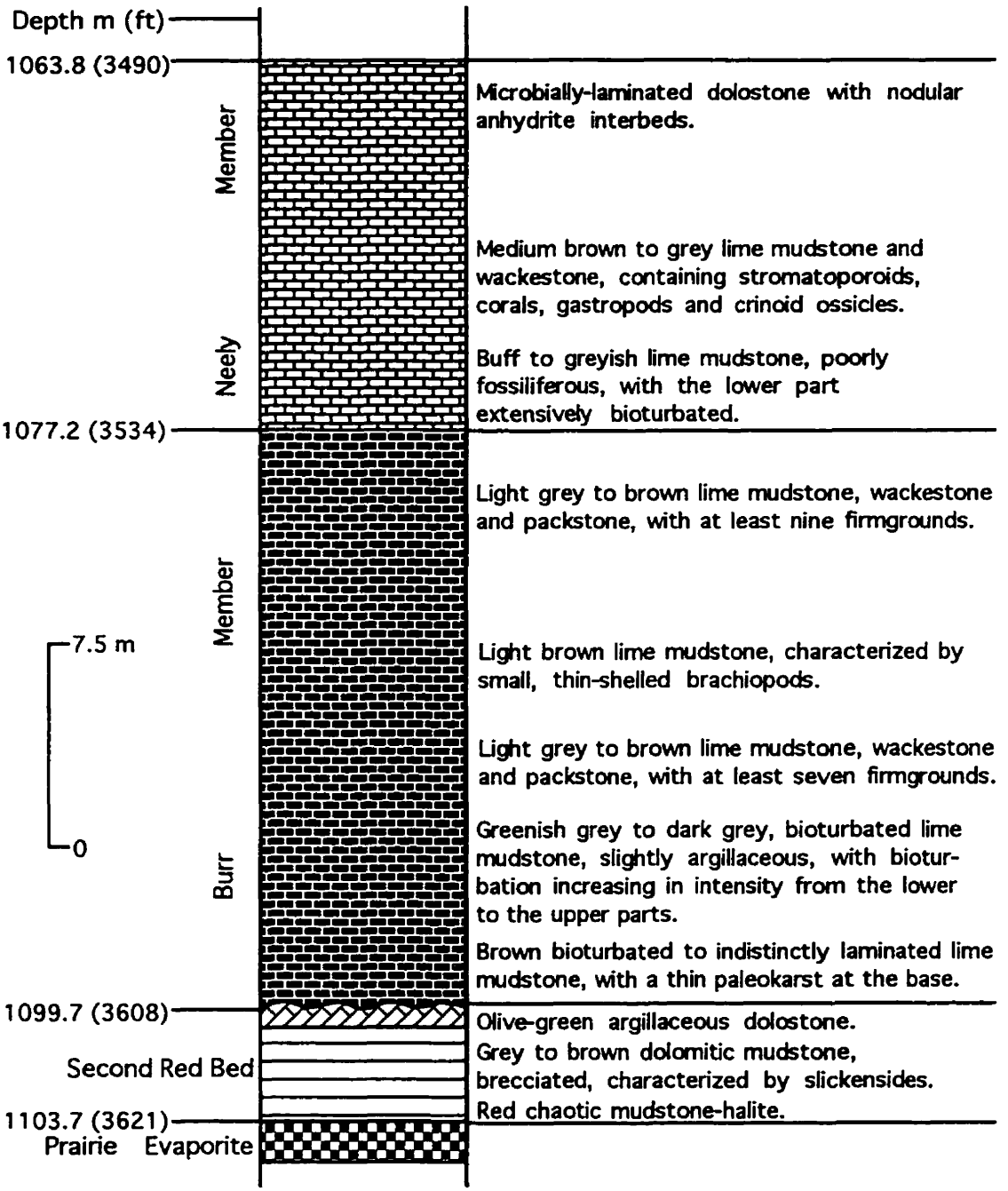

Well 3-27-38-27W2

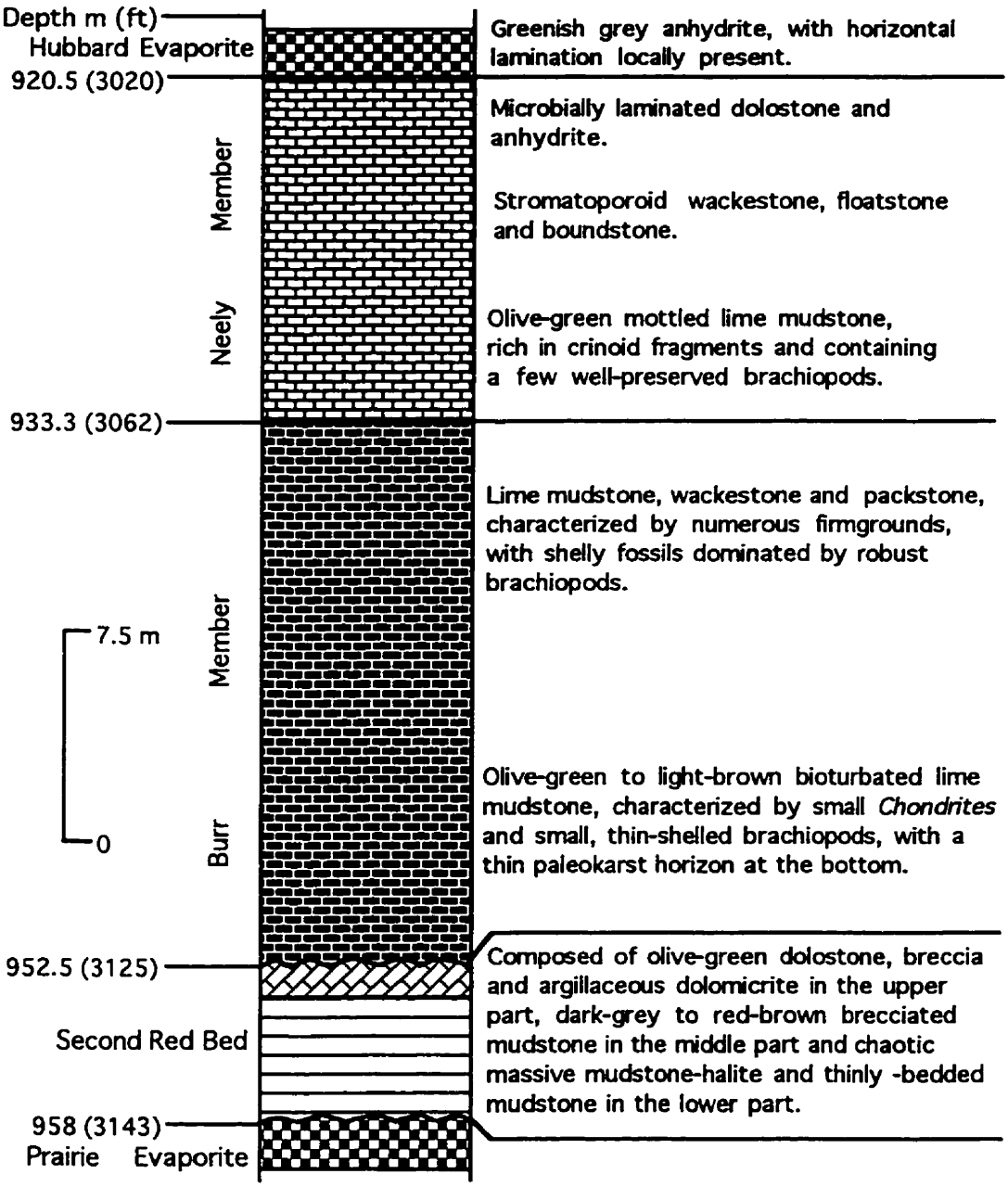

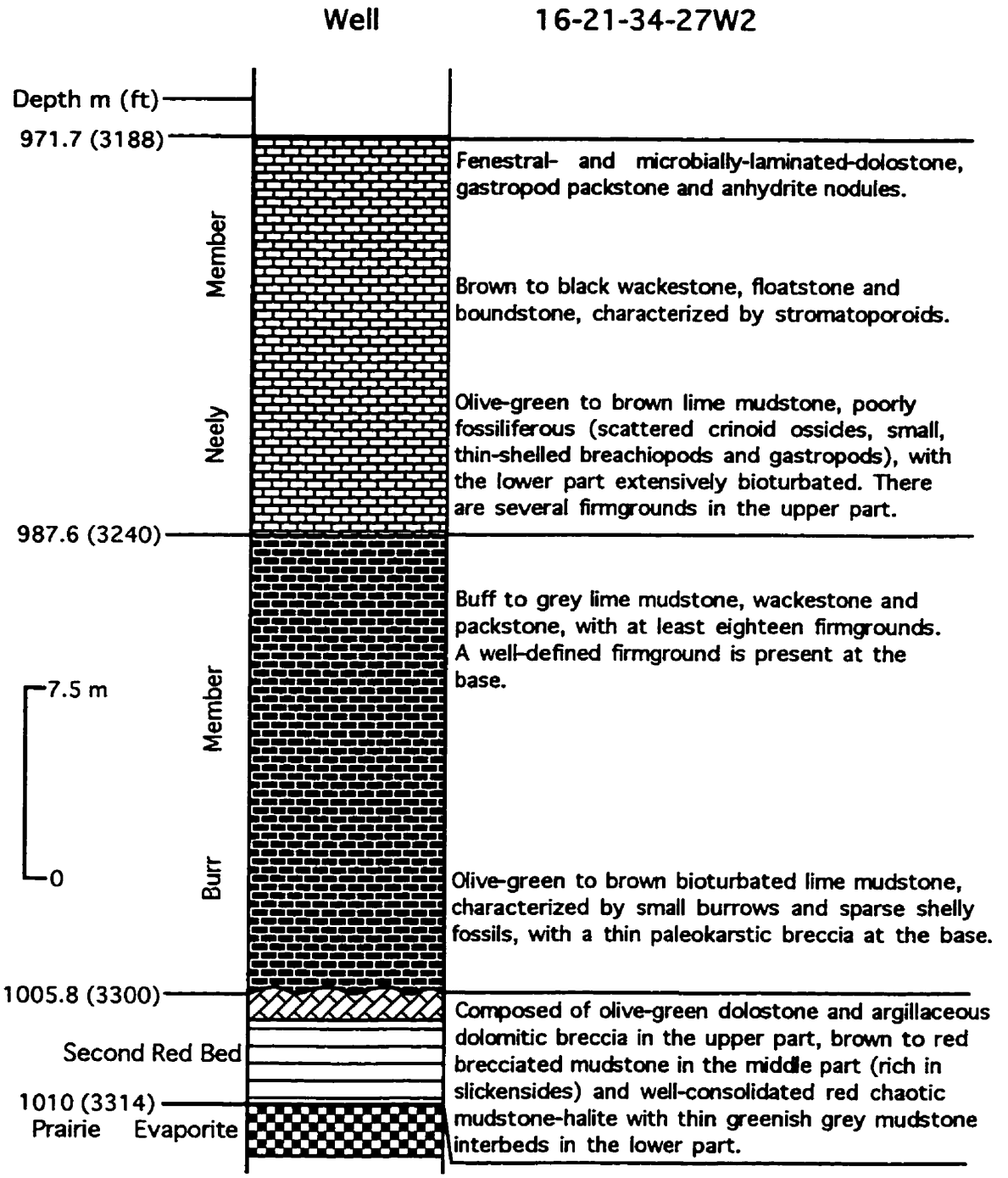
Well 16-21-34-27W2
Depth m (ft)
971.7 (3188)
Member
Neely
Fenestral- and microbially-laminated-dolostone, gastropod packstone and anhydrite nodules.
Brown to black wackestone, floatstone and boundstone, characterized by stromatoporoids.
Olive-green to brown lime mudstone, poorly fossiliferous (scattered crinoid ossicles, small, thin-shelled breachiopods and gastropods), with the lower part extensively bioturbated. There are several firmgrounds in the upper part.
987.6 (3240)
7.5 m
0
Member
Burr
Buff to grey lime mudstone, wackestone and packstone, with at least eighteen firmgrounds. A well-defined firmground is present at the base.
Olive-green to brown bioturbated lime mudstone, characterized by small burrows and sparse shelly fossils, with a thin paleokarstic breccia at the base.
1005.8 (3300)
Second Red Bed
1010 (3314)
Prairie Evaporite
Composed of olive-green dolostone and argillaceous dolomitic breccia in the upper part, brown to red brecciated mudstone in the middle part (rich in slickensides) and well-consolidated red chaotic mudstone-halite with thin greenish grey mudstone interbeds in the lower part.

Well 4-19-48-24W2

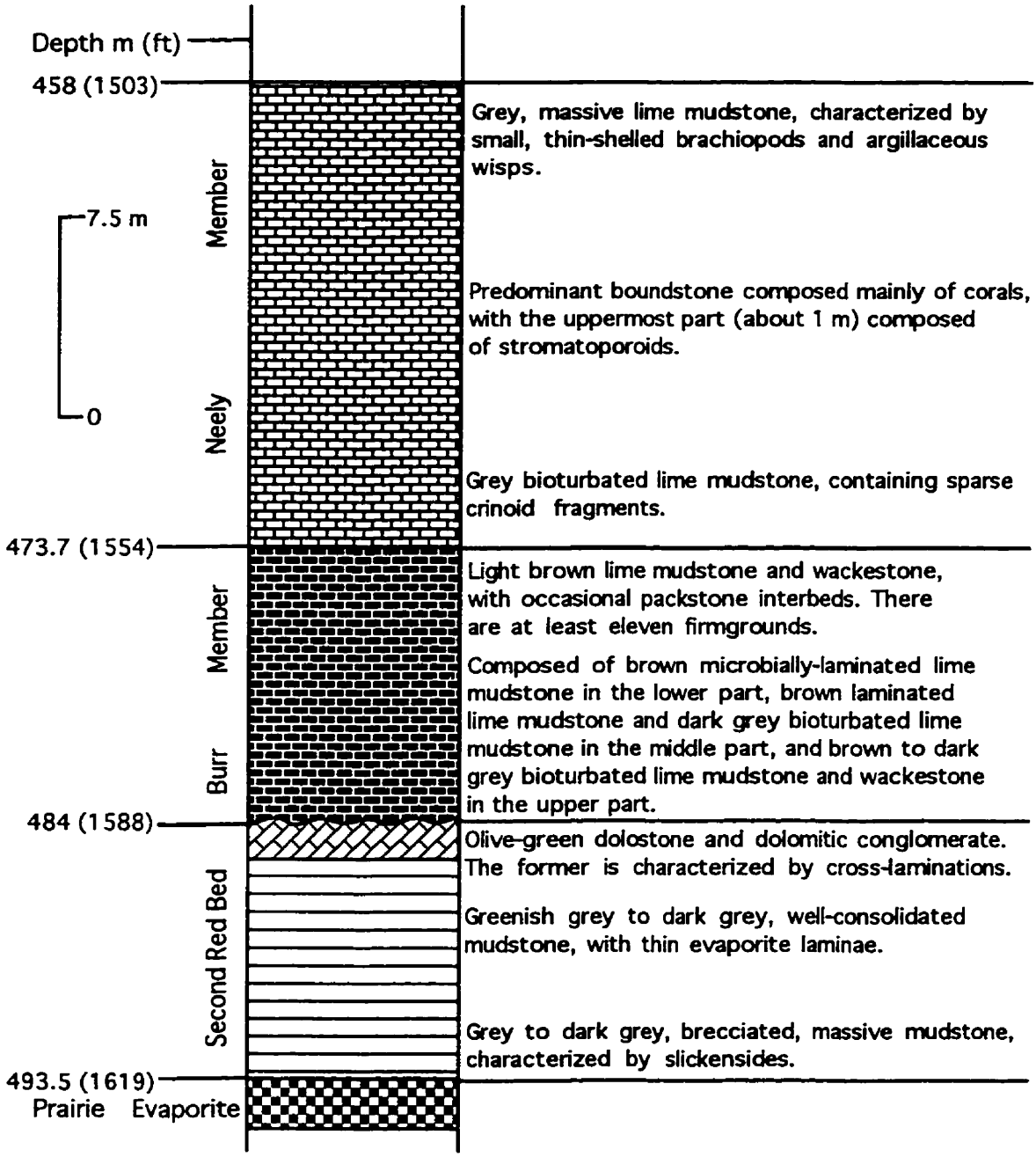

Well 8-20-33-20W2

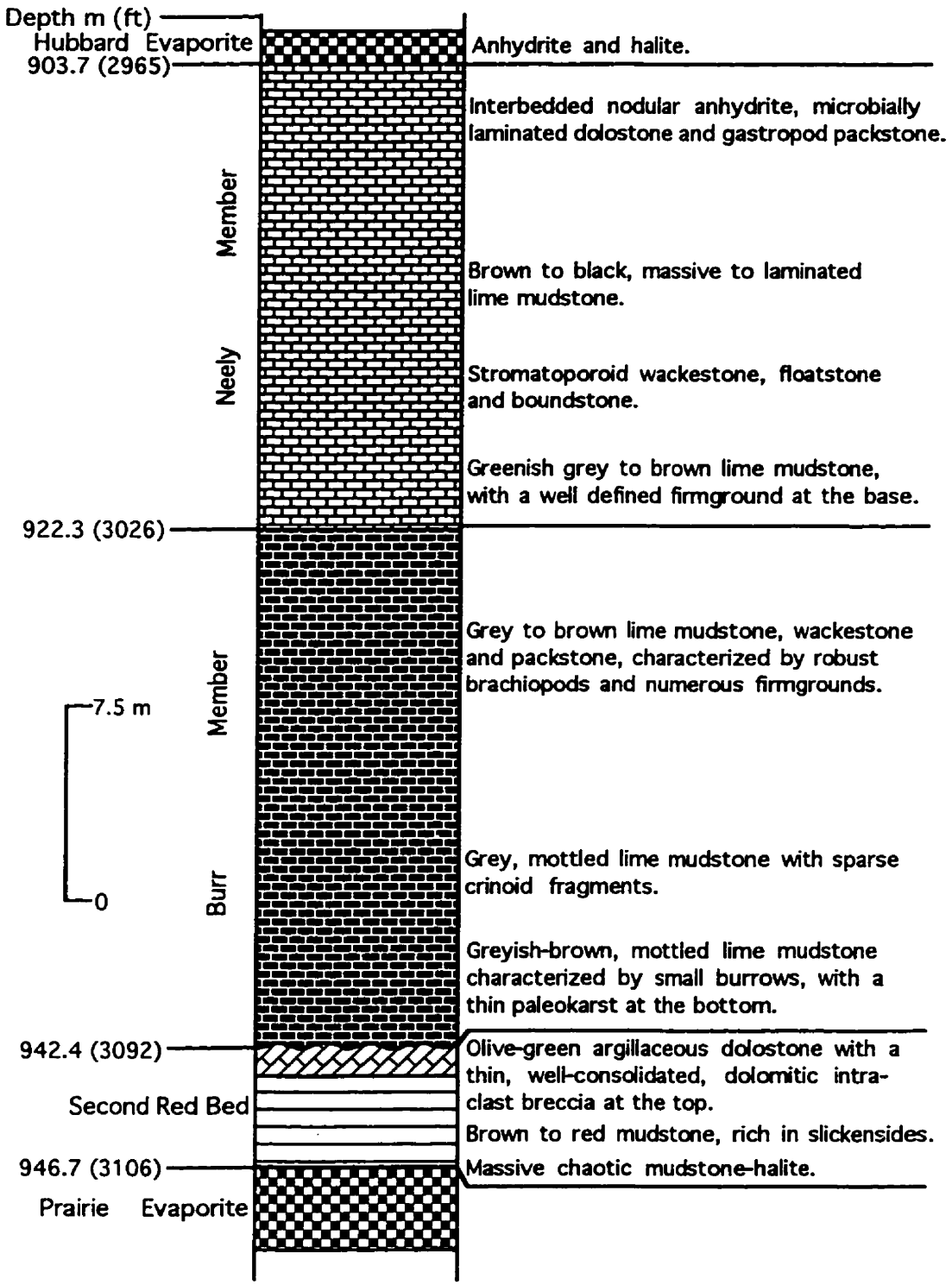

Well 13-21-29-20W2

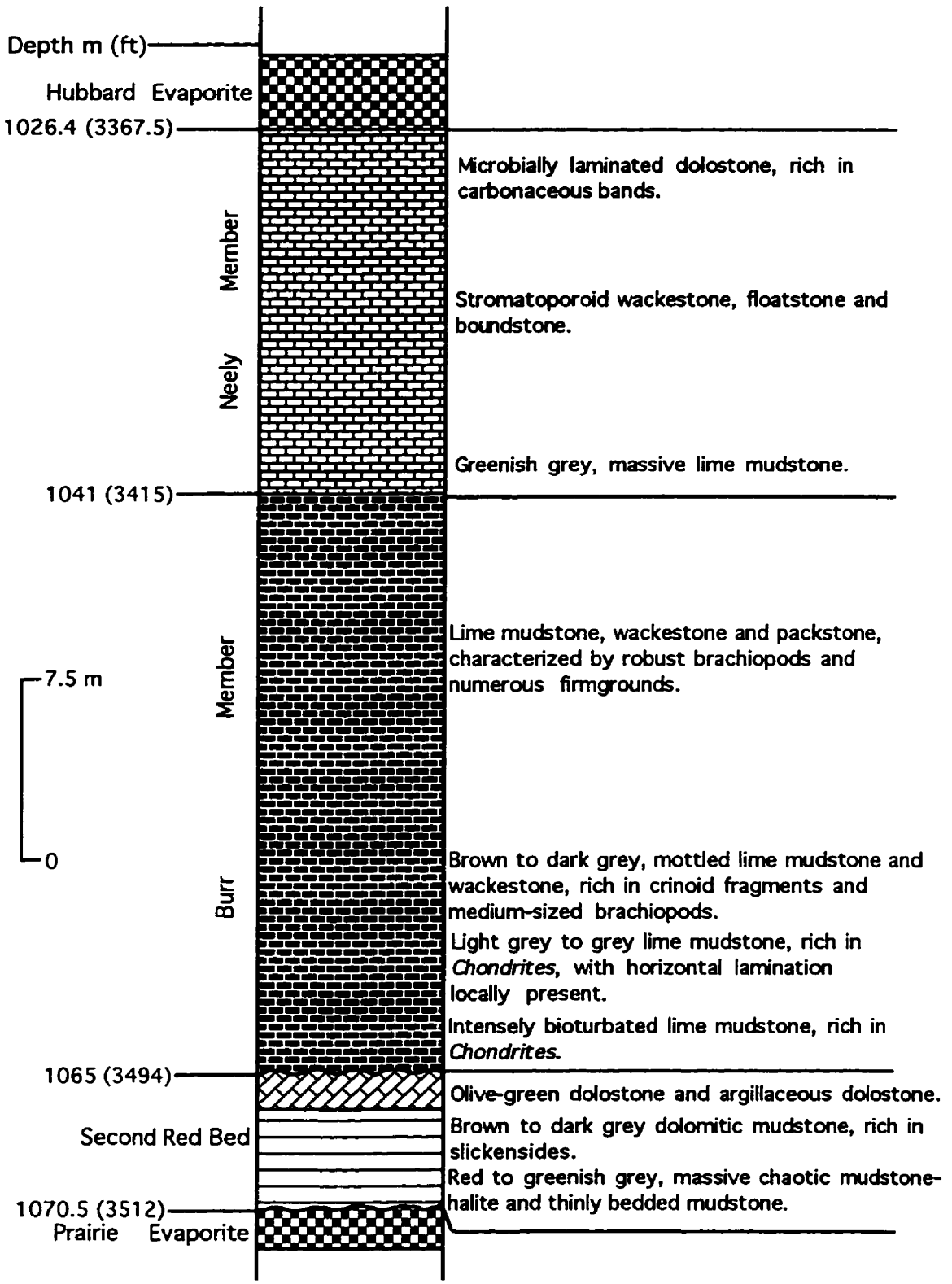

Well 1-27-31-16W2

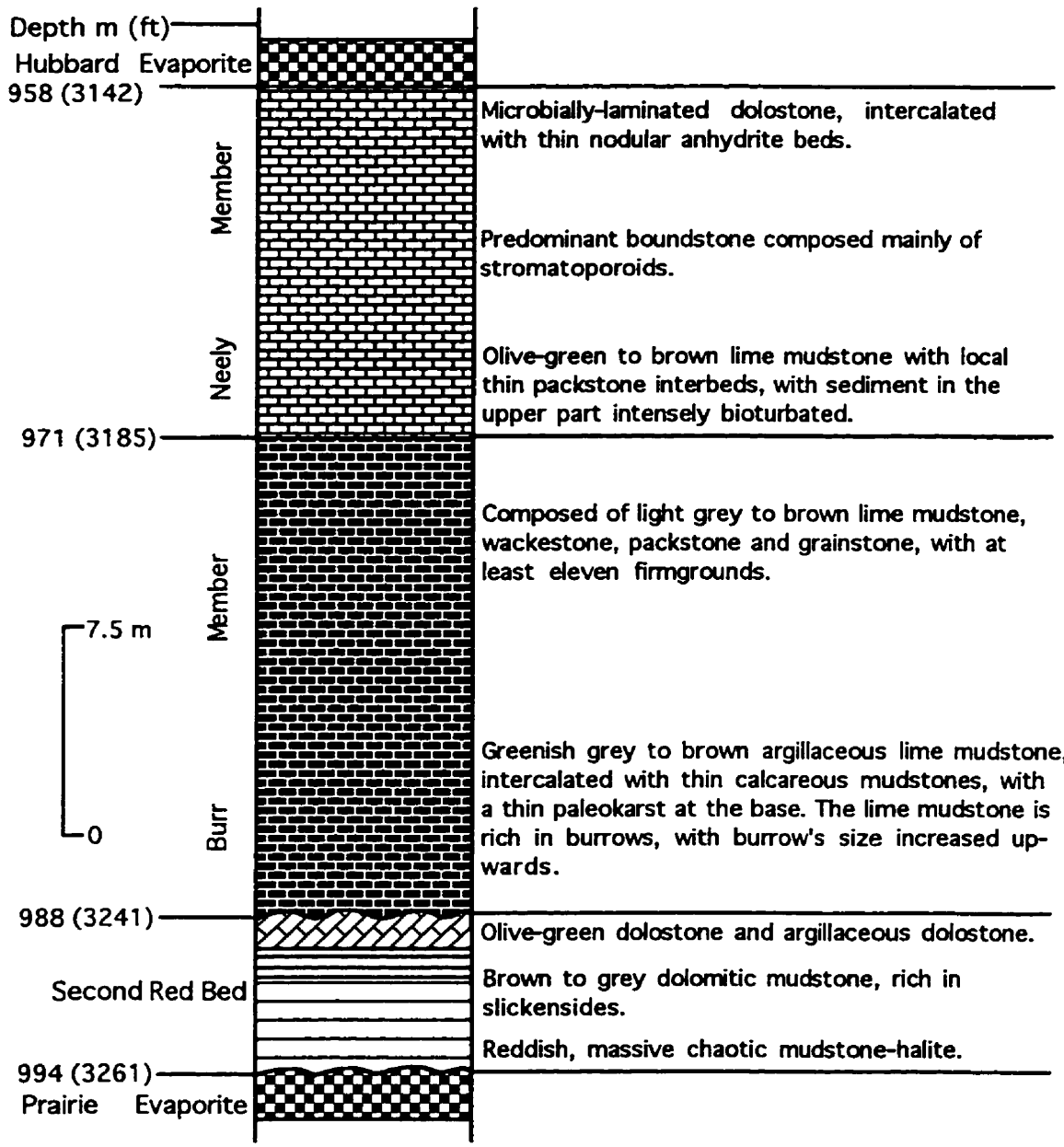

Well 41/09-022-023-06W2

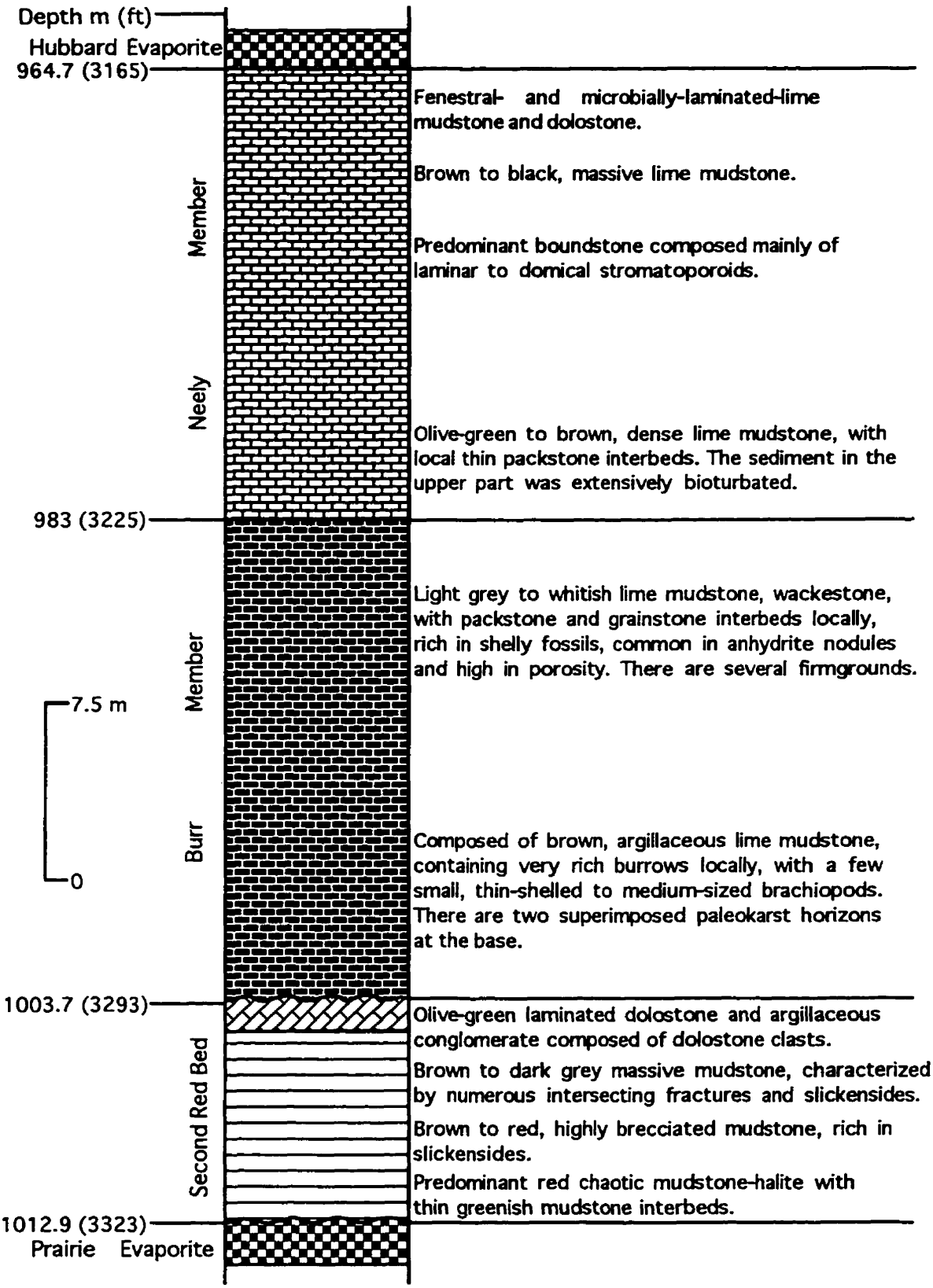

Well 13-12-22-32W1

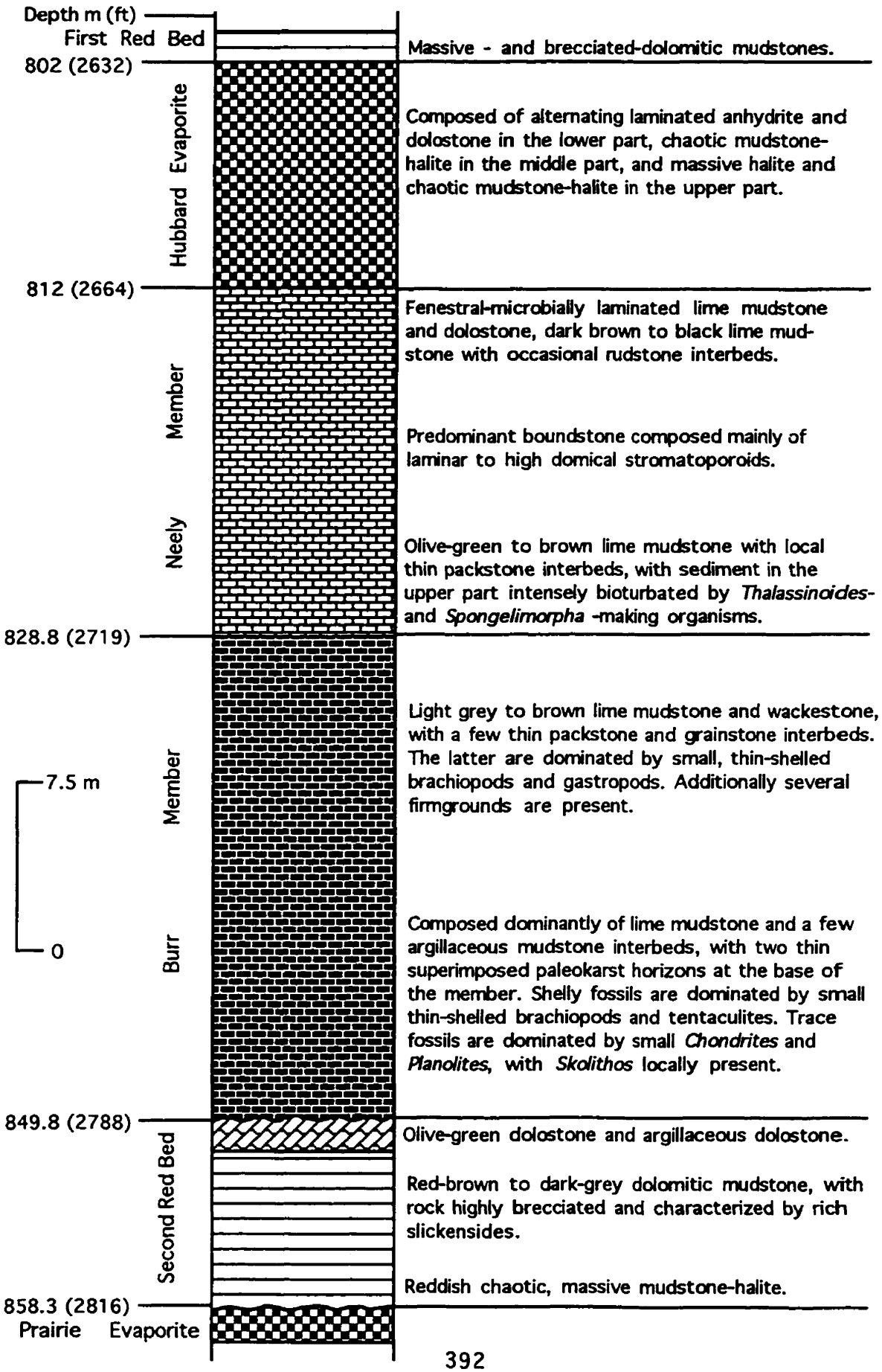

Well 4-2-22-31W1

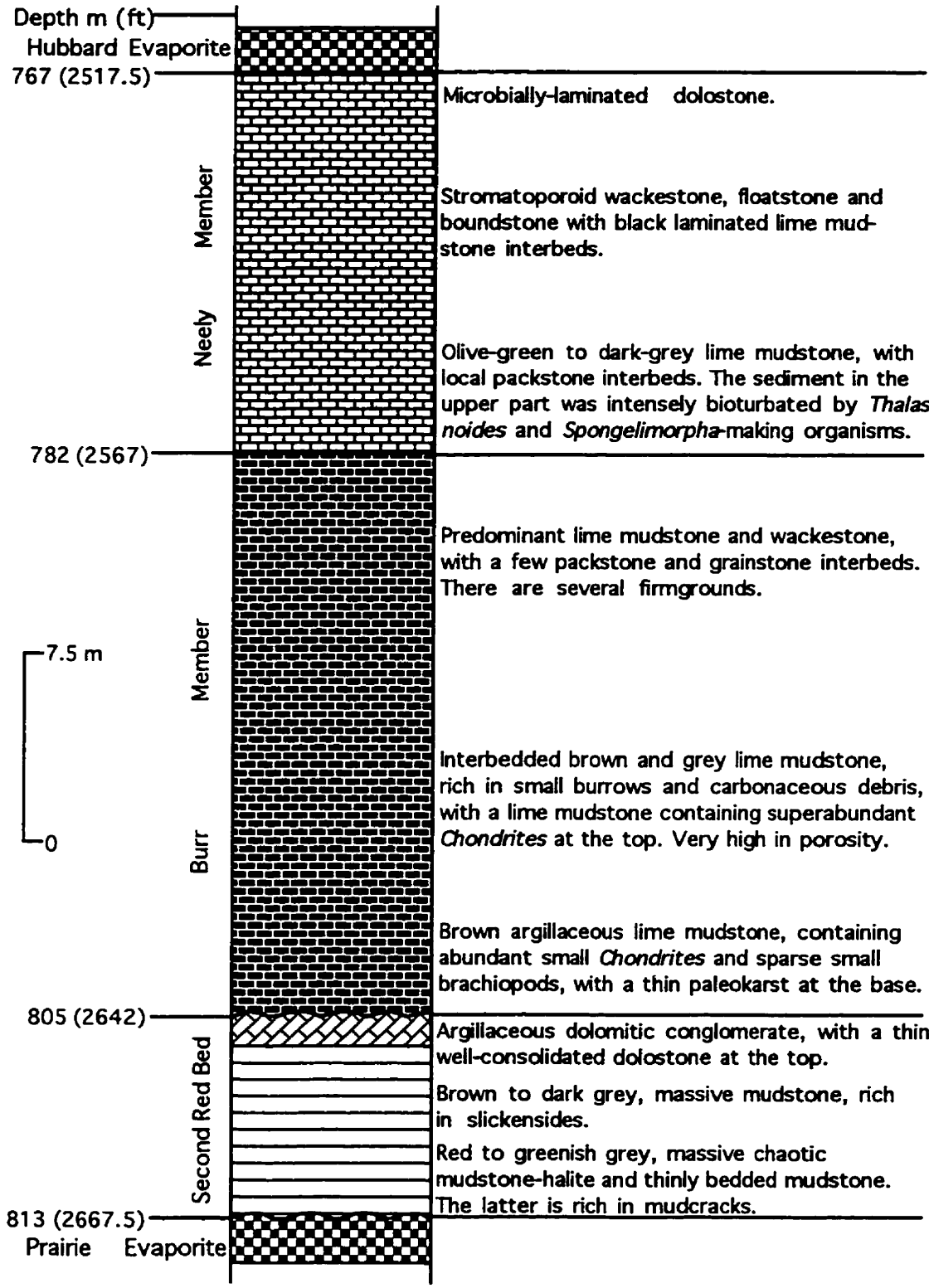

Well 9-24-21-30W1

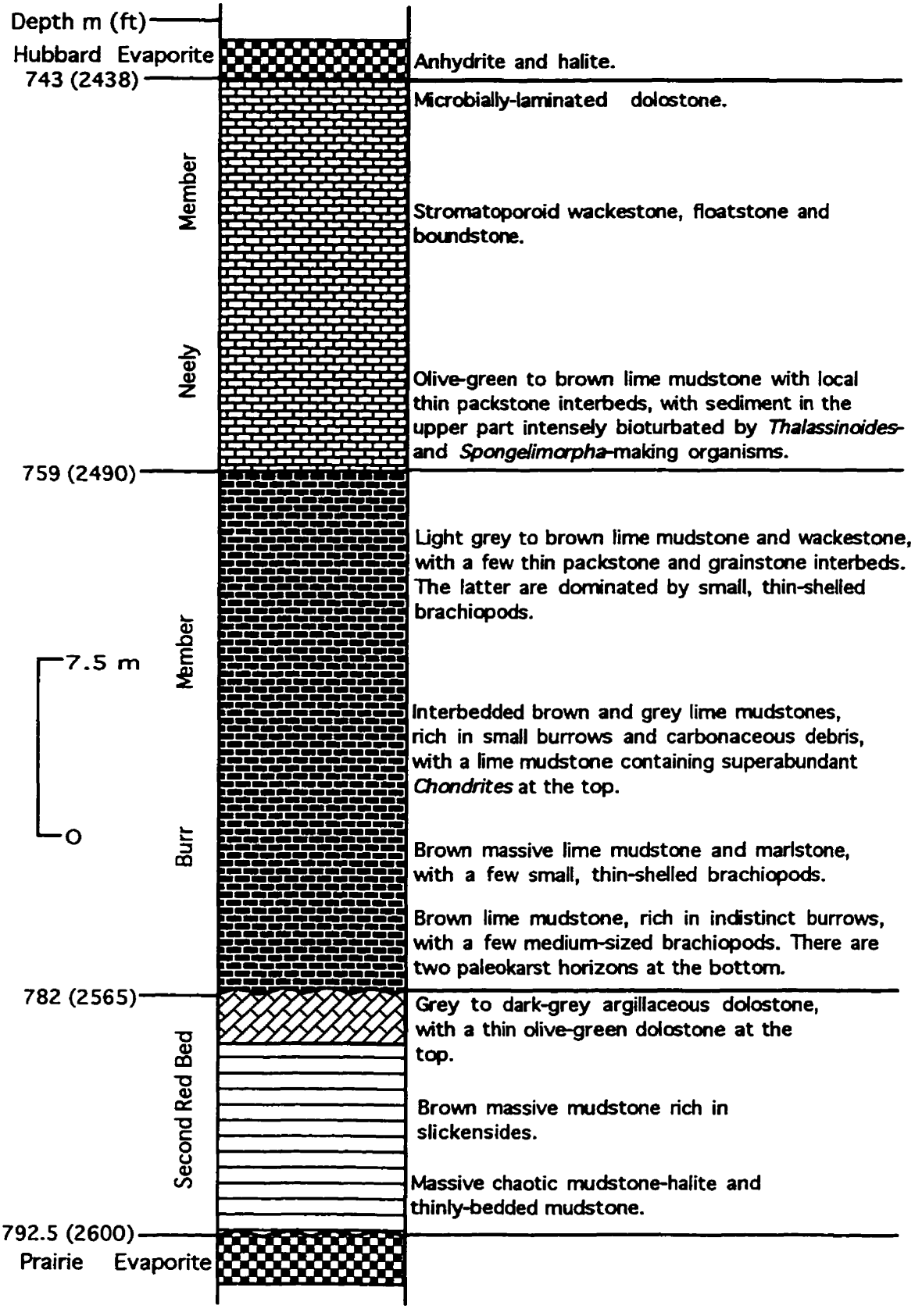

Well 14-32-20-30W1

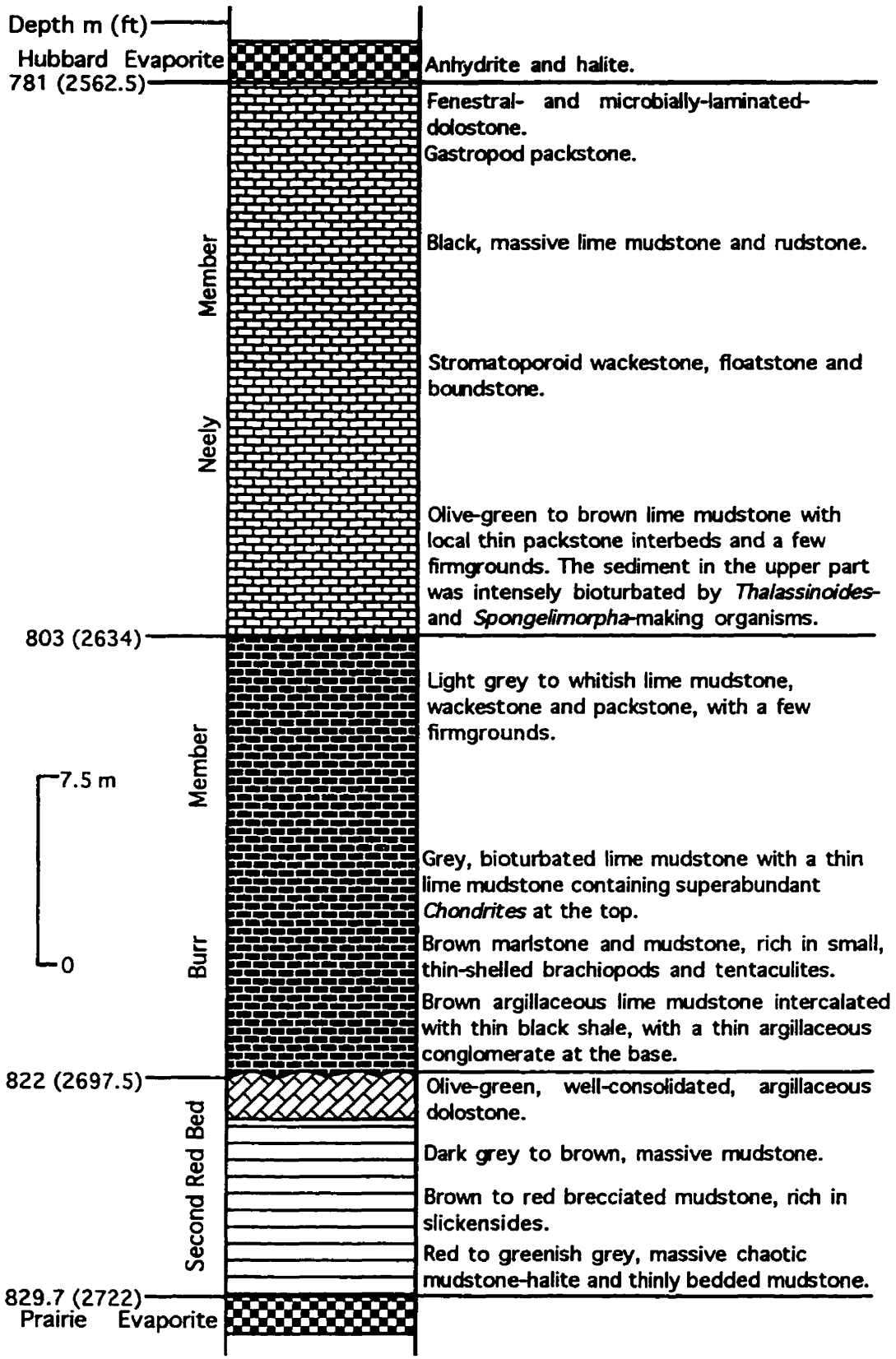

Well 14-22-20-30W1

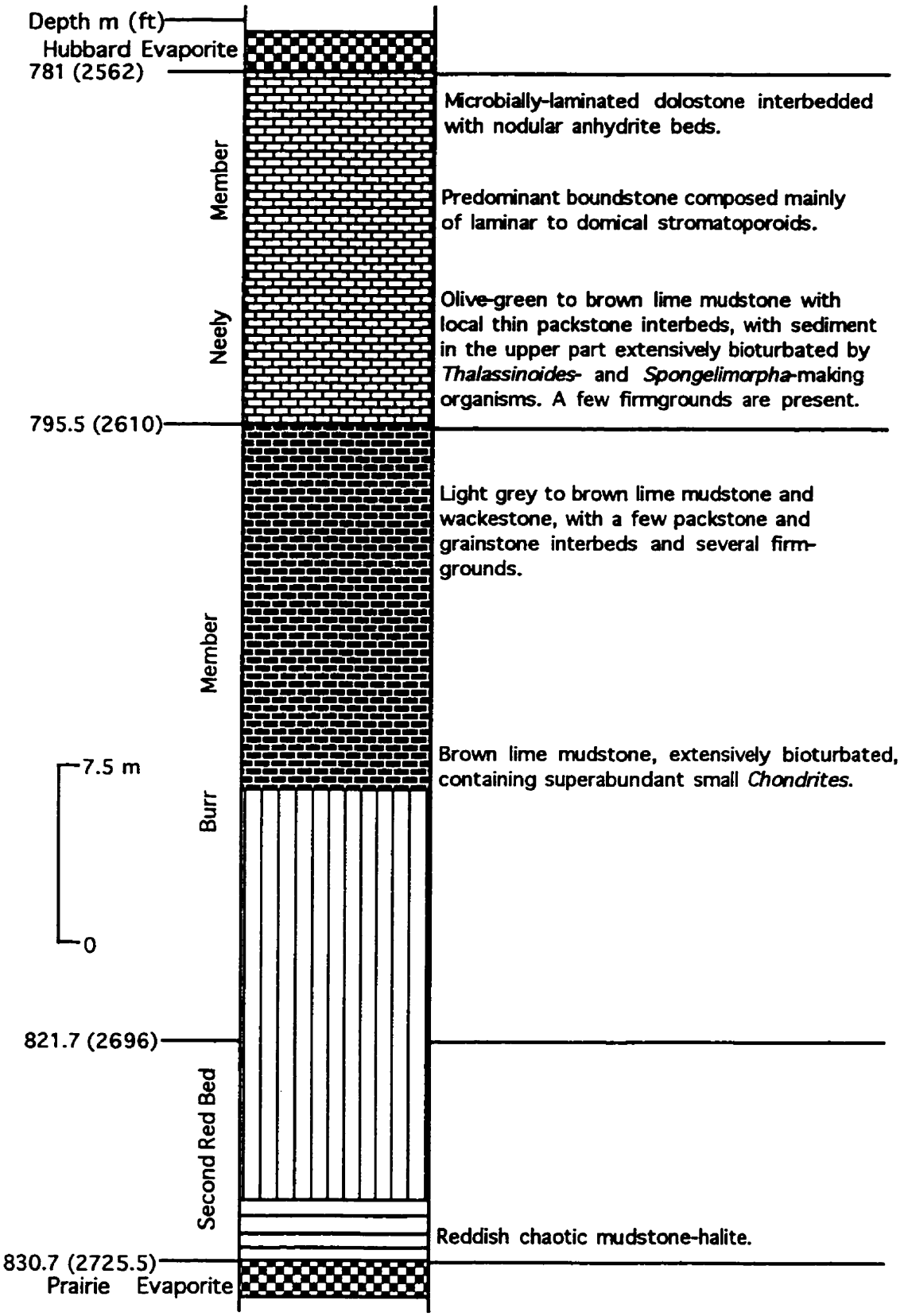

APPENDIX II

LATERAL THICKNESS AND LITHOLOGICAL FACIES CHANGES OF THE SECOND RED BED MEMBER AND PALEOKARST DISTRIBUTION AT THE BASE OF THE BURR MEMBER ACROSS SASKATCHEWAN

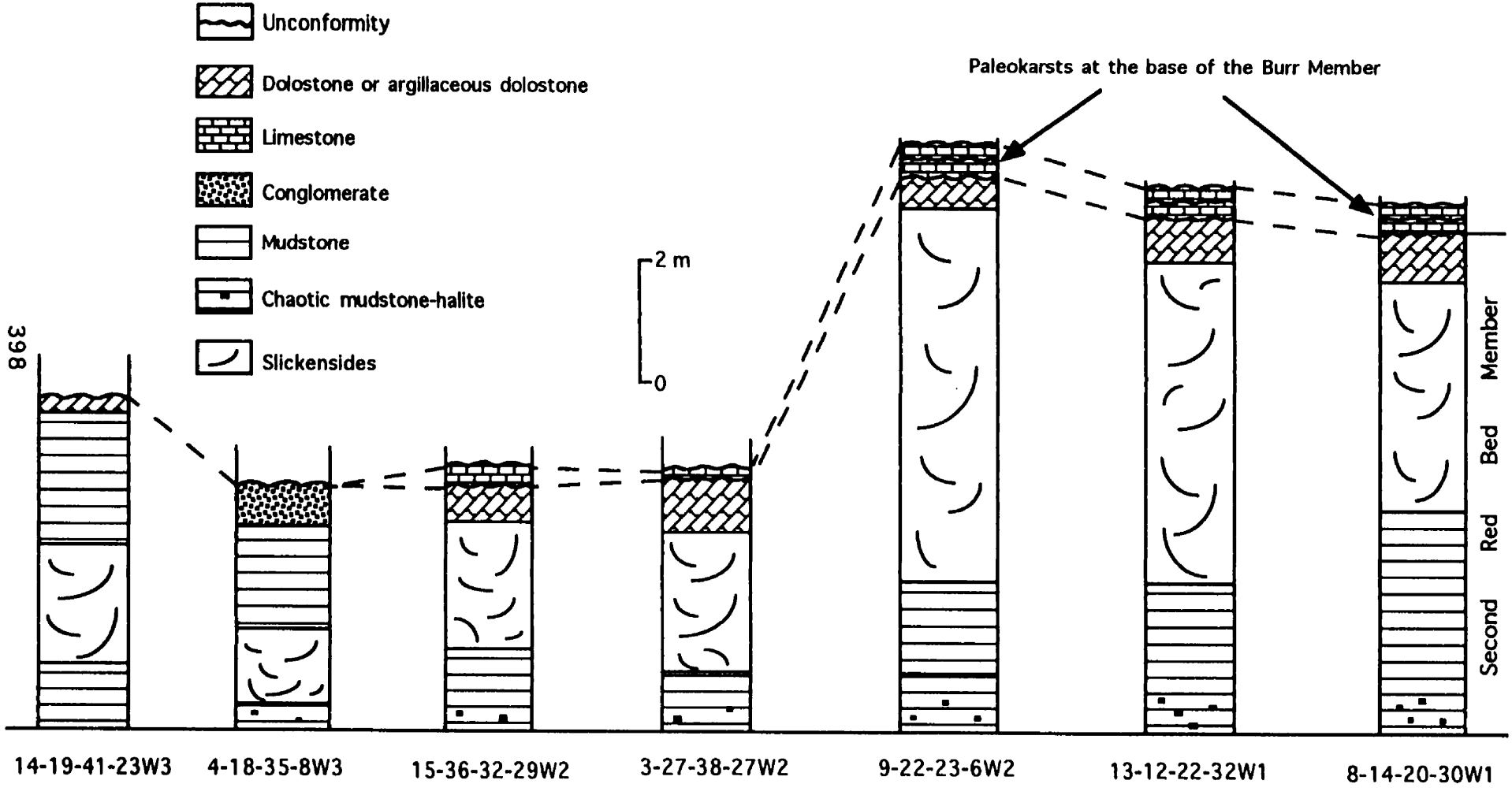

Lateral thickness and lithological facies changes of the Second Red Bed Member and paleokarst distribution at the base of the Burr Member across Saskatchewan.

PUBLICATIONS

Gu Chenggao (1996) Tibetan uplift and Asian monsoon circulation. *Meeting Abstracts, 30th International Geological Congress*, Beijing, China, v. 1, p. 84.

Gu Chenggao and Renaut, R.W. (1996) Validity of the Rhoads-Morse-Byers model in interpreting oxygen-related environments of ancient epeiric seas. *Meeting Abstracts, 30th International Geological Congress*, Beijing, China, v. 2, p. 199.

Gu Chenggao and Renaut, R.W. (1995) Depositional environment of the dolostones in the Second Red Bed Member of the Devonian Dawson Bay Formation, Saskatchewan. In: Hunter, L.D.V. and Schalla, R.A. (eds.), *Seventh International Williston Basin Symposium Guidebook*, Montana Geological Society, p. 373–382.

Gu Chenggao and Renaut, R.W. (1995) Petroleum potential of the sedimentary basins of the Chinese continental shelf. Abstracts of the Annual Meeting, American Association of Petroleum Geologists, p. 36.

Gu Chenggao and Renaut, R.W. (1994) The effect of Tibetan uplift on the formation and preservation of Tertiary lacustrine source rocks in eastern China. *Journal of Paleolimnology*, v. 11, p. 31–40.

Guo Shuang-xing and Gu Chenggao (1993) Fossil plants from calcareous tufa and palaeoenvironments in Ruoqiang, Xinjiang. *Acta Palaeontologica Sinica*, v. 32, p. 82–87.

Zhang Qingsong, Tao Jurong, Huang Cixuan and Gu Chenggao (1990) A discovery of Late Cenozoic fossil plants in Kunlun Mountains. *Chinese Science Bulletin*, v. 35, p. 1204–1208.

Gu Chenggao (1988) Characteristics and significance of Lower Tertiary caliches in the Pingyi Basin, Shandong Province. *Acta Sedimentologica Sinica*, v. 6, p. 89–95.

Gu Chenggao (1988) The characteristics, origin and palaeoclimatic significance of the Early Eocene lacustrine deposits in the Pingyi Basin, Shandong Province, China. *Abstracts, IAS International Symposium on Sedimentology Related to Mineral Deposits*, Academica Sinica, Inst. Geol., Beijing, China, p. 69–70.

Gu Chenggao (1988) An excursion guide to the Pingyi Basin. *In: Guide Book: Excursion B3--Tertiary Lacustrine Deposits, Shandong Province, IAS International Symposium on Sedimentology Related to Mineral Deposits*, Academica Sinica, Inst. Geol., Beijing, China, p. 29–42.

Gu Chenggao (1985) The age and terrestrial carbonates' depositional environments of Guanzhuang Formation in the Pingyi Basin, eastern China. M.Sc. thesis, unpublished.

UNIVERSITY OF SASKATCHEWAN

College of Graduate Studies and Research

SUMMARY OF DISSERTATION

Submitted in partial fulfillment

of the requirements for the

DEGREE OF DOCTOR OF PHILOSOPHY

by

Gu Chenggao

Department of Geological Sciences

University of Saskatchewan

Spring, 1998

Examining Committee:

Dr. T. Steele	Dean's Designate, Chair College of Graduate Studies and Research
Dr. J.F. Basinger	Chair of Advisory Committee, Department of Geological Sciences
Dr. R.W. Renaut	Supervisor, Department of Geological Sciences
Dr. K. Ansdell	Department of Geological Sciences
Dr. B. Pratt	Department of Geological Sciences
Dr. D. DeBoer	Department of Geography

External Examiner:

Dr. B. Jones
Department of Earth and Atmospheric Sciences
University of Alberta,
Edmonton, Alberta, T6G 2E3

Depositional Environments and Diagenesis of the Devonian Dawson Bay Formation in Saskatchewan and Northwestern Manitoba

The Devonian Dawson Bay Formation has been divided into the econd Red Bed, Burr, Neely and Hubbard Evaporite members from ase to top. The Second Red Bed Member (SRBM) comprises mudstone nd dolostone. New evidence indicates that the SRBM was affected by edogenesis, with the paleosol better developed in central Saskatchewan ian in southeastern Saskatchewan. This suggests that the paleorelief in ie former part of the basin was higher than in the latter, and that the iarine waters came from the southeast.

Three paleokarst horizons have been recognized in the contact zone etween the SRBM and the Burr Member. The presence of the aleokarsts indicates that before the Williston Basin was completely looded by seawater during early Burr time, two minor marine ransgressions took place in the basin.

New evidence shows that in central Saskatchewan parts of the lower Burr Member contain fine laminations, but the equivalent units in outheastern Saskatchewan lack these laminations. This shows that the nvironment in central Saskatchewan was more oxygen-restricted. Thus, rom central to southeastern Saskatchewan the environment became less oxygen-restricted with increasing water depth. This contradicts the rediction of the Rhoads-Morse-Byers model.

In southeastern Saskatchewan, the upper Burr Member consists mainly of wackestone and lime mudstone, with a few thin packstone and grainstone interbeds. This reflects a low energy, relatively deep water environment. In contrast, the proportion of packstone and grainstone increases significantly in the upper Burr Member of central Saskatchewan and northwestern Manitoba. This suggests that the depositional environments in those regions had higher energy and shallower water conditions.

From base to top, the depositional environment of the Neely Member changed from relatively deep, offshore settings through higher energy, shallower water conditions represented by domical stromatoporoids, to intertidal and supratidal conditions.

The Hubbard Evaporite Member was deposited in salt pan to saline mudflat environments. The overlying First Red Bed formed in environments that ranged from saline mudflat to dry mudflat to distal floodplain. New evidence also shows that no significant sedimentary break is present between the Hubbard Evaporite Member and the First Red Bed, and that they belong to a single upward-shallowing succession.

BIOGRAPHICAL

June, 1958	Born in Nanjing, China
February, 1982	B.Sc. equivalent (4-year), Department of Geology, Nanjing University
October, 1985	M.Sc., Nanjing Institute of Geology and Palaeontology, Chinese Academy of Sciences

HONOURS

Scholarship, College of Graduate Studies and Research, University of Saskatchewan, September 1993 -- March 1997

Student Excellence and Development Award, SEPM (Society for Sedimentary Geology) --1994

IMAGE EVALUATION
TEST TARGET (QA-3)

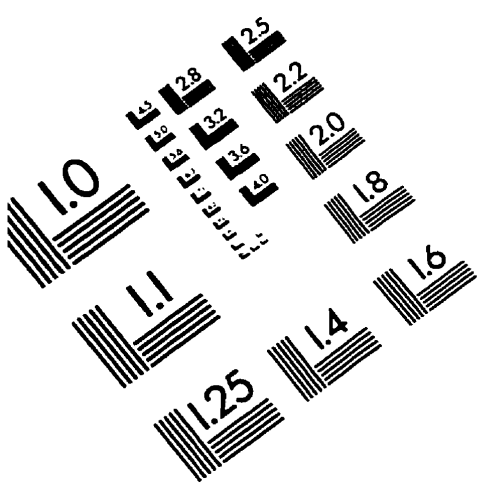

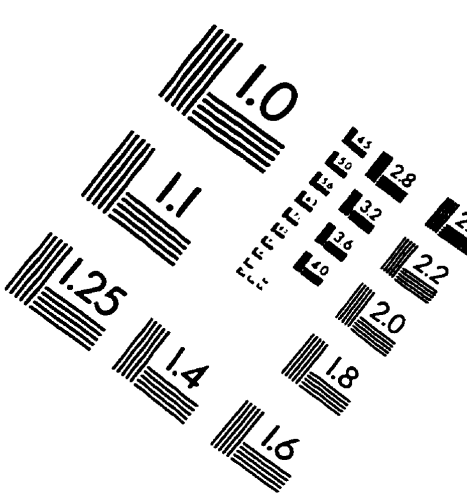

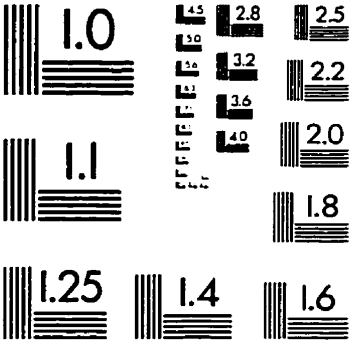

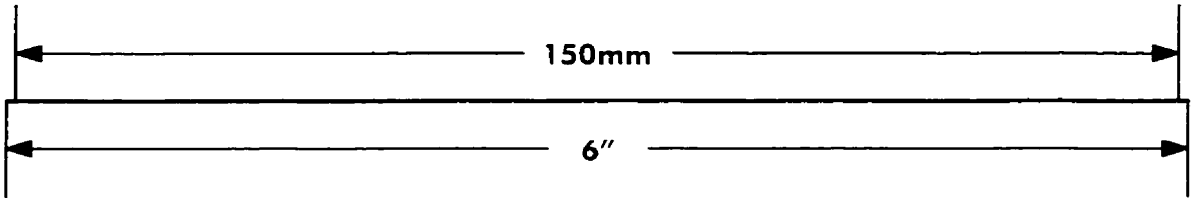

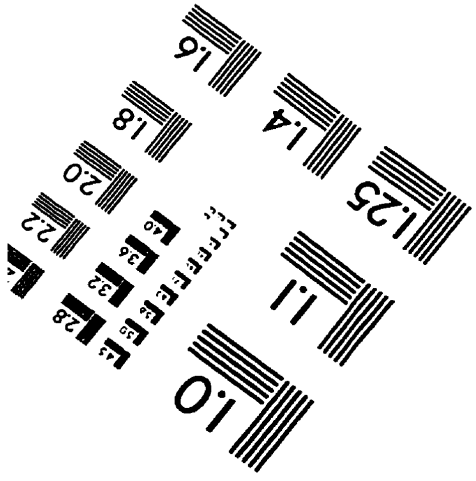

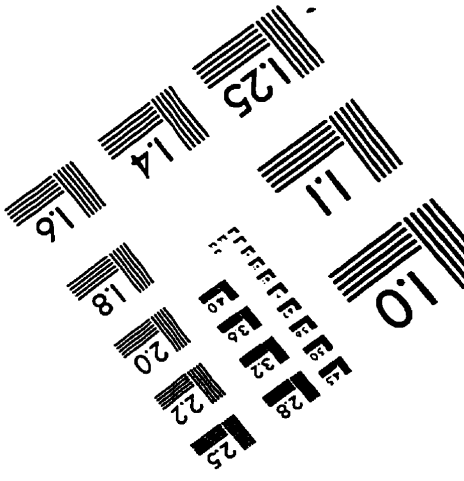

APPLIED IMAGE, Inc
1653 East Main Street
Rochester, NY 14609 USA
Phone: 716/482-0300
Fax: 716/288-5989

© 1993, Applied Image, Inc., All Rights Reserved